Universität Bremen

Resting-state brain connectivity in the LPS-rat model of schizophrenia

Dissertation

Zur Erlangung des Grades eines
Doktors der Naturwissenschaften (*Dr. rer. nat.*)
im Fachbereich 2 (Biologie/Chemie) der Universität Bremen

vorgelegt von

Andreas Coors

Bremen, Dezember 2023

1. Gutachter: Prof. Dr. Michael Koch

2. Gutachter: Dr. Ekkehard Küstermann

Tag des öffentlichen Kolloquiums: 29.01.2024

Versicherung an Eides Statt

Ich, Andreas Coors, versichere an Eides Statt durch meine Unterschrift, dass ich die vorstehende Arbeit selbständig und ohne fremde Hilfe angefertigt und alle Stellen, die ich wörtlich dem Sinne nach aus Veröffentlichungen entnommen habe, als solche kenntlich gemacht habe, mich auch keiner anderen als der angegebenen Literatur oder sonstiger Hilfsmittel bedient habe.

Ich versichere an Eides Statt, dass ich die vorgenannten Angaben nach bestem Wissen und Gewissen gemacht habe und dass die Angaben der Wahrheit entsprechen und ich nichts verschwiegen habe.

Die Strafbarkeit einer falschen eidesstattlichen Versicherung ist mir bekannt, namentlich die Strafandrohung gemäß § 156 StGB bis zu drei Jahren Freiheitsstrafe oder Geldstrafe bei vorsätzlicher Begehung der Tat bzw. gemäß § 161 Abs. 1 StGB bis zu einem Jahr Freiheitsstrafe oder Geldstrafe bei fahrlässiger Begehung.

_____ _____

Ort, Datum Unterschrift

Zusammenfassung

Schizophrenie ist eine schwere psychische Erkrankung, bei der die Patienten ein breites Spektrum an Symptomen sowie verschiedene Hirnanomalien aufweisen. Sowohl genetische als auch umweltbedingte Faktoren werden mit der Ätiologie der Schizophrenie in Verbindung gebracht. Nach der neurobiologischen Entwicklungshypothese könnten mehrere störende Ereignisse während der Gehirnentwicklung für das Auftreten der Krankheit verantwortlich sein. Die Vermutung, dass Entzündungsprozesse während der Schwangerschaft zum Risiko der Entwicklung von Schizophrenie beitragen, hat zur Entwicklung von Nagetiermodellen geführt, bei denen die so genannte maternale Immunaktivierung eingesetzt wird. Das Nager LPS-Modell löst durch die Injektion von bakteriellen Lipopolysacchariden mütterliche Immunreaktionen aus, die bei den Nachkommen zu einer Reihe von neuropathologischen, verhaltensbezogenen und pharmakologischen Anomalien führen, die denen von schizophrenen Patienten ähneln.

Mehrere Studien haben über eine veränderte funktionelle Konnektivität bei schizophrenen Patienten berichtet, die mittels funktioneller Magnetresonanztomographie (fMRI) im Ruhezustand gemessen wurde. Es fehlen jedoch Untersuchungen der funktionellen Konnektivität in Tiermodellen der Schizophrenie. Das Ziel dieser Studie war es daher, die funktionelle Konnektivität im Ruhezustand im Ratten LPS-Modell für Schizophrenie im Langzeitverlauf von der juvenilen Phase (PD~30) über die Pubertät (PD~45) und die späte Adoleszenz (PD~66) bis zum Erwachsenenalter (PD~94) zu untersuchen.

Eine Unabhängigkeitsanalyse (Independent Component Analysis, ICA) ergab sieben Ruhezustandsnetzwerke, darunter das so genannte Default-Mode-Netzwerk, somatosensorische und motorische Netzwerke, ein striatales Netzwerk sowie ein Kleinhirn Netzwerk. Es konnten Auswirkungen des Alters auf die Konnektivität im Kleinhirn Netzwerk und in den somatosensorischen Netzwerken beobachtet werden, die nicht mit der Behandlung zusammenhängen, aber es konnten keine Auswirkungen der LPS-Behandlung auf die Konnektivität der identifizierten Ruhezustandsnetzwerke gezeigt werden.

Da die Ergebnisse aus ergänzenden Verhaltensexperimenten zur Beurteilung schizophrenieähnlicher Symptome bei den Tieren jedoch auf methodische Probleme

bei der Umsetzung des LPS-Modells hindeuten, sollten weitere Untersuchungen zur Erforschung der funktionellen Konnektivität von Ratten mit einer verfeinerten Umsetzung des LPS-Modells durchgeführt werden, um die Ergebnisse dieser Studie zu ergänzen.

Abstract

Schizophrenia is a serious mental disease in which patients are showing a wide array of symptoms as well as several brain abnormalities. Both genetic and environmental factors have been implicated in the etiology of schizophrenia. According to the neurodevelopmental hypothesis, several disrupting events during brain development may be responsible for the onset of the disease. The implication of inflammatory processes during pregnancy contributing to the risk of developing schizophrenia has lead to the development of rodent animal models using the so called maternal immune activation. The rodent LPS model induces maternal immune responses by the injection of bacterial lipopolysaccharides, resulting in offspring showing a variety of neuropathological, behavioral and pharmacological abnormalities, similar to schizophrenic patients.

Several studies have reported an altered functional connectivity of schizophrenic patients, as measured by resting-state functional magnetic resonance imaging (fMRI). However, investigations of functional connectivity in animal models of schizophrenia are lacking. Therefore, the aim of this study was to investigate resting-state functional connectivity in the rat LPS model of schizophrenia on a longitudinal scale from the juvenile stage (PD~30), over puberty (PD~45) and late adolescence (PD~66) until adulthood (PD~94).

Independent component analysis (ICA) revealed seven resting-state networks including the so called default mode network, somatosensory and motor networks, a a striatal network as well as a cerebellar network. Effects of age on connectivity in the cerebellar network and somatosensory networks unrelated to the treatment could be observed, but no effects of LPS treatment on connectivity of the identified resting-state networks could be shown.

However, as the results from complementary behavioral experiments for the assessment of schizophrenia-like symptoms in the animals hint towards methodological problems in the implementation of the LPS model, further investigations exploring the functional connectivity of rats with a more refined implementation of the LPS model should be carried out in order to complement the results of this study.

Table of Contents

1. Introduction

1.1. Schizophrenia

Schizophrenia is a serious mental disease, often resulting in a lifelong disability of the affected individuals (for review see Lewis and Levitt, 2002; Schultz et al., 2007; Keshavan et al., 2008; Tandon et al., 2008a, 2008b; Hyman and Cohen, 2013). On average, around 1% of all people worldwide are diagnosed with schizophrenia, with a male:female ratio of 1.4:1 (McGrath et al., 2008). The first onset of symptoms mainly occurs after puberty and early adolescence, around an age of 20 years (Koch, 2006; Schultz et al., 2007). However, the onset is usually slightly later in women, and there is also a higher incidence of late-onset schizophrenia (after an age of 40 years) in females, presumably due to protective effects of estrogen (Hafner, 1998; Häfner et al., 1998).

The symptoms of schizophrenia are usually divided into at least three categories, namely positive, negative and cognitive (disorganized) symptoms (Tamminga and Holcomb, 2005). Positive symptoms are those phenomena that usually do not occur in healthy people, for example hallucinations and delusions. Accordingly, negative symptoms are those that result from an impairment of normal functions, and include blunted emotional responses, social withdrawal, poverty of thought and speech, as well as a lack of motivation symptoms (Tamminga and Holcomb, 2005). In the prodromal phase and preceding psychotic relapses, increased anxiety can be observed as well (Temmingh and Stein, 2015; Hall, 2017). Finally, cognitive dysfunctions include impairments in attention, working memory and executive functions (Tamminga and Holcomb, 2005; Hyman and Cohen, 2013). Actually, schizophrenia is a very heterogeneous disease, maybe even representing several different diseases with similar clinical manifestations (Tandon et al., 2008a). Since schizophrenia shares its symptoms with other psychiatric diseases like depression or bipolar disorder, it is typically diagnosed by confirming the presence of a number of symptoms and simultaneously ruling out other diseases (Silverstein et al., 2006; Schultz et al., 2007). In fact, the diagnosis of a relatively high portion of patients is changed to schizophrenia after the initial diagnosis of another disease (~30%), but the other way round happens as well (Chen et al., 1996; Schultz et al., 2007). The heterogeneity of schizophrenia is also reflected by the individual course of the

disease. Typically, a prodromal period of on average 5 years, consisting mainly of negative symptoms, precedes the first psychotic episode (Hafner, 1998; Bäuml et al., 2012). Those psychotic episodes are characterized by the positive symptoms, in which (mainly auditory) hallucinations and delusions may transfer the patient into a distorted reality (Hyman and Cohen, 2013). Following the first psychotic episode, periods of psychosis can alternate with periods of remission or residual symptoms, but some cases show chronic psychosis as well (Bäuml et al., 2012; Hyman and Cohen, 2013). Finally, full recovery to normal functioning is only seen in around 20% of patients, provided that a proper treatment took place (Silverstein et al., 2006).

1.1.1. Etiology and Neuropathology

Schizophrenic patients show several brain abnormalities, including differences in gray matter volumes (Shenton et al., 2001; Harrison et al., 2003; Olabi et al., 2011; Bakhshi and Chance, 2015), alterations in white matter (Höistad et al., 2009; Olabi et al., 2011; Skudlarski et al., 2013; Caprihan et al., 2015) or the enlargement of ventricles (Wright et al., 2000; Shenton et al., 2001; Olabi et al., 2011). The neuropathology and etiological factors underlying schizophrenia are still not clearly elucidated. However, there are several studies indicating the involvement of genetic as well as environmental factors.

Twin studies revealed that in monozygotic twins, if one sibling was diagnosed with the disease, the risk of the second sibling having schizophrenia is about 40-50%. This risk is lower for dizygotic twins, but still amounts to 10-15% (Gottesman et al., 1987; Sullivan et al., 2003; Tandon et al., 2008a). Together with studies of adopted children, showing that the risk of schizophrenia was related to the presence of the disease in biological parents but not in the adoptive parents (Heston, 1966; Kety et al., 1968; Tandon et al., 2008a), these results suggested a strong genetic contribution to the risk of having schizophrenia. There are several genes with a strong etio-pathogenetic relevance for schizophrenia research, including NRG1 (neuroregulin 1), DTNBP1 (dysbindin), DRD1-4 (dopamine receptors D1–D4), DISC1 (disrupted in schizophrenia 1), COMT (catechol-O-methyl-transferase) and GRM3 (metabotropic glutamate receptor) (Duan et al., 2007; Lewandowski, 2007; Li and He, 2007; Munafo et al., 2007; Nicodemus et al., 2007; Tan et al., 2007; Chubb et al., 2008; Tandon et al., 2008a; Hänninen et al., 2008; Schwab et al., 2008; Talkowski et al., 2008). However, the discovery of a specific single genetic marker has yet to be

confirmed. A common view sees schizophrenia as a heterogeneous, polygenic and multi-factorial disease with multiple common genetic polymorphisms, from which each of these contributes to a small extent to disease susceptibility (Risch, 1990; Chakravarti, 1999; Lichtermann et al., 2000; Tandon et al., 2008a). Another perspective considers schizophrenia as a highly heterogeneous genetic entity, caused by multiple, highly penetrant and individually very rare mutations, that may be specific to single cases or individual families (McClellan et al., 2007; Tandon et al., 2008a). In addition, further opinions suggest a strong contribution of heritable epigenetic factors (e.g. DNA methylation) instead of variations in the DNA sequence itself (DeLisi et al., 2002; Costa et al., 2006; Crow, 2007; Tandon et al., 2008a).

Despite the strong genetic contribution, several environmental factors have been implicated in the etiology of schizophrenia as well. Those include both biological and psychosocial risk factors during the pre- and postnatal periods, childhood, adolescence and early adulthood (Mäki et al., 2005). For example, maternal infections (e.g. influenza) during the first and second trimesters of pregnancy have been linked to an increased risk of developing schizophrenia (Mednick et al., 1988; Brown et al., 2001a, 2005; Meyer et al., 2007; Penner and Brown, 2007; Tandon et al., 2008a), probably mediated through the effects of cytokines and an aberrant immune response, which interfere with normal fetal brain development during this period (Ashdown et al., 2006). These observations have led to the development of animal models based on this so called maternal immune activation (MIA) (Patterson, 2009; see chapter 1.1.3). Furthermore, maternal malnutrition (Susser et al., 1996; St Clair et al., 2005; Penner and Brown, 2007) or the experience of severe adverse life events (Khashan et al., 2008) during the first trimester of pregnancy, as well as several obstetric complications (Geddes and Lawrie, 1995; Cannon et al., 2002; Byrne et al., 2007) have additionally been reported to increase the risk for schizophrenia. And finally, among various other environmental factors, the season of birth (Torrey et al., 1997; McGrath and Welham, 1999; Davies et al., 2003), urbanicity and migration (McGrath et al., 2008) or substance abuse (e.g. cannabis use) during adolescence (Bowers et al., 2001; Semple et al., 2005; Moore et al., 2007) have all been implicated in acting as risk factors for the development of schizophrenia, once again demonstrating the large heterogeneity of this disease.

Several neurotransmitter systems have been implicated in the pathogenesis of schizophrenia. Among these, the dopamine system has probably received most attention, leading to the strong influential dopamine hypothesis of schizophrenia (Silverstein et al., 2006; Keshavan et al., 2008; Howes and Kapur, 2009). The initial hypothesis stated an excess of dopamine in the brain of schizophrenic patients (van Rossum, 1966; Carlsson, 1977; Carlsson and Carlsson, 2006). However, most evidence for this theory was of indirect nature, based on the positive effects of dopamine blockade by antipsychotic medication (e.g. chlorpromazine or haloperidol), and the psychotomimetic effect of dopamine agonists such as amphetamine or cocaine (Silverstein et al., 2006; Guillin et al., 2007; Schultz et al., 2007; Keshavan et al., 2008). Furthermore, its explanatory power covered only one aspect of the disease, namely the positive symptoms (Keshavan et al., 2008). Therefore, and following the suggestion of a relationship between cognitive impairment and prefrontal dopamine D1 receptors (Weinberger, 1987), as well as the observation that increased D1 receptor availability has been found to correlate with impaired working memory in schizophrenia (Abi-Dargham et al., 2002), the dopamine hypothesis was reformulated. This modified dopamine hypothesis postulates a hypoactive mesocortical dopamine system responsible for the negative and cognitive symptoms, and a hyperactive mesolimbic dopamine system responsible for the positive symptoms (Weinberger, 1987; Davis et al., 1991; Keshavan et al., 2008).

Furthermore, the emergence of psychotic symptoms following the administration of drugs like lysergic acid diethylamide (LSD) or mescaline, known to increase serotonergic activity, suggested an involvement of serotonin in schizophrenia (Silverstein et al., 2006). However, the positive therapeutic effects of serotonin antagonists (e.g. clozapine and risperidone), which are actually increasing brain serotonin, shifted the attention on the interaction between serotonin and dopamine systems (Kapur and Remington, 1996). Even though direct evidence of serotonergic dysfunction in the pathogenesis of schizophrenia is lacking, there is still a significant interest in exploring the role of different serotonin receptors (e.g. 5-HT_3 and 5-HT_6 receptors) in schizophrenia (Abi-Dargham, 2007; Keshavan et al., 2008).

Another hypothesis emerged following the observations of reduced glutamate in the cerebrospinal fluid of patients with schizophrenia (Kim et al., 1980). However, studies failed to replicate this finding (Perry, 1982), and the initial glutamate hypothesis of

schizophrenia was later reformulated, postulating an insufficient glutamate mediated excitatory neurotransmission via N-methyl-D-aspartate (NMDA) receptors (Olney and Farber, 1995; Moghaddam, 2003; Keshavan et al., 2008). The emergence of psychotic symptoms following administration of NMDA antagonists like phencyclidine (PCP) and ketamine are supporting this hypothesis (Javitt and Zukin, 1991; Keshavan et al., 2008).

Moreover, there are also some findings implicating the role of an altered GABAergic (Gamma amino butyric acid) activity, e.g. reduced levels of GABA expression in the prefrontal cortex (measured by mRNA levels of glutamic acid decarboxylase, the major determinant of GABA synthesis) revealed in post-mortem studies (Lewis et al., 2005), or the up-regulation of $GABA_a$ receptors (Jarskog et al., 2007), affecting especially the chandelier subtype of GABA neurons (Keshavan et al., 2008).

1.1.2. Neurodevelopmental Hypothesis of Schizophrenia

As mentioned before, a lot of environmental risk factors for schizophrenia may occur during the pre- or postnatal periods of life. However, the onset of the characteristic psychotic symptoms happens several years later in late adolescence or early adulthood. This long delay between the occurrence of risk factors and the onset of the diagnostic symptoms brought up the idea that schizophrenia may be a disorder of neurodevelopment (Lewis and Levitt, 2002). First proposed by Jakob and Beckmann, 1986, as well as by Weinberger, 1987, this neurodevelopmental hypothesis of schizophrenia, which suggests a multi-step process of etiopathogenesis, is now widely accepted (Koch, 2006). According to the two-hit model, two or more ‘hits’ of disrupting events during early and late brain development may add up, and finally lead to the onset of the disease (Bayer et al., 1999; Koch, 2006; Giovanoli et al., 2013; Feigenson et al., 2014). The first hit(s) could be represented by a genetic susceptibility or by disrupting events like inflammatory processes during pregnancy or obstetric complications, as mentioned before. These may lead to an altered brain development (e.g. altered migration, differentiation and apoptosis of neurons), making the brain susceptible for adverse events later in life (e.g. stress, drugs or trauma during puberty) which finally cause the onset of the full clinical syndrome (Jakob and Beckmann, 1994; Beckmann, 1999; Kalus et al., 1999; Church et al., 2002; Lewis and Levitt, 2002; Caruncho et al., 2004; Arnold et al., 2005; Koch, 2006; Feigenson et al., 2014). Ideally, any of those hits should not produce larger brain

damage or behavioral impairment for itself, so that only the combination of multiple hits induces the full behavioral symptomatology and neuropathology (Koch, 2006).

1.1.3. Rodent Inflammation Models

Because schizophrenia is such a heterogeneous disease, it is not possible to model all aspects of the disease in one single animal model. Furthermore, the core symptoms of psychiatric disorders (like disrupted thoughts or verbal learning and memory) are uniquely human traits, and therefore difficult to assess in animals (Powell and Miyakawa, 2006). The fact that there is no current 'gold standard' medication (treating all the symptoms) available, which can be used as a definitive positive control in preclinical studies, further complicates the problem (Jones et al., 2011). Therefore, several different animal models have been developed, trying to address specific pathophysiological or etiological aspects of the disease (for review see Koch, 2006; Jones et al., 2011).

Comprehensive findings showed that cytokines and the immune system can influence and shape the development of the brain and behavior (Bauer et al., 2007; Deverman and Patterson, 2009; Yirmiya and Goshen, 2011; Bilbo and Schwarz, 2012; Feigenson et al., 2014). Due to the relevance of inflammatory processes (e.g. maternal infections during pregnancy) in the etiology of schizophrenia, this has lead to the development of rodent models based on the so called maternal immune activation (MIA) (Mednick et al., 1988; Brown et al., 2001a, 2005; Ashdown et al., 2006; Meyer et al., 2007; Penner and Brown, 2007; Tandon et al., 2008a; Patterson, 2009; Feigenson et al., 2014). In these models, prenatal immune activation is induced by injecting pregnant rats or mice with different pathogenic agents at different gestational stages (Wischhof et al., 2015b). A critical mid-gestation window between gestational days (GD) 15-19 is often chosen for the time of injection, which approximates to the human second to third trimester (Bayer et al., 1993; Clancy et al., 2001; Jones et al., 2011).

One pathogenic agent that is often used in MIA models is polyribosinic:polyribocytidylic acid (Poly(I:C)), a synthetic double-stranded RNA that mimics viral infections (Reisinger et al., 2015; Haddad et al., 2020b). Poly(I:C) is binding to Toll-like receptor 3 (TLR3) and thereby inducing a pro-inflammatory signal chain via nuclear factor kappa-light-chain-enhancer of activated B cells (NF-κB) and

Interferon Regulatory Factor (IRF) 3, finally leading to distribution of pro-inflammatory cytokines like interleukin (IL) 6, IL-10 and TNF-α (tumor necrosis factor α) in addition to type I interferons (IFN) IFN-α and IFN-β (Alexopoulou et al., 2001; Takeda and Akira, 2005; Gandhi et al., 2007; Takeuchi and Akira, 2007; Deverman and Patterson, 2009; Meyer et al., 2009b; Haddad et al., 2020b).

Besides the use of Poly(I:C), many studies are using lipopolysaccharides (LPS) as an immune stimulus in rodent experiments (Borrell et al., 2002; Koch, 2006; Feigenson et al., 2014; Wischhof et al., 2015b). LPS is found in the cell membrane of gram negative bacteria (e.g. *Escherichia coli*), and mimics the immunological effects of gram negative infections (Feigenson et al., 2014). It is well established that it stimulates monocytes and macrophages via TLR4, and thereby, via the MyD88-dependent (Myeloid differentiation primary response protein 88) and the Toll-IL-1 receptor domain-containing adapter-inducing interferon β (TRIF)-dependent downstream pathways, produces a range of proinflammatory cytokines like IL-1, IL-6 or TNF-α , which can have a variety of neurobehavioral effects (Medzhitov et al., 1997; Dantzer et al., 2008; Engel et al., 2011; Hayden and Ghosh, 2012; Feigenson et al., 2014; García Bueno et al., 2016; Bao et al., 2022). The notion that cytokines may be the common mediator responsible for the various effects seen after several viral, bacterial or other stressors during pregnancy, was first suggested by Gilmore and Jarskog, 1997.

Comparing the effects of Poly(I:C) with those of LPS, there are both similarities and differences depending on the behavior evaluated or the measurements made (Bao et al., 2022). A more detailed overview of the different outcome of Poly(I:C) and LPS on some specific behaviors is presented in section 1.3. Generally, studies using MIA in rodents described a variety of neuropathological, behavioral and pharmacological abnormalities that resemble at least partially the neuropathology and symptomatology of schizophrenia (Fortier et al., 2004a; Fatemi et al., 2005; Meyer et al., 2008a, 2008b; Fatemi and Folsom, 2009; Wischhof et al., 2015a), including deficits in sensorimotor gating, social interaction and cognition (e.g. working memory), abnormalities in the sensitivity to psychostimulant drugs, or alterations in the dopamine system (Borrell et al., 2002; Shi et al., 2003; Zuckerman et al., 2003; Fortier et al., 2004a, 2007; Golan et al., 2005; Romero et al., 2007; Boksa, 2010; Meyer and Feldon, 2010; Williamson et al., 2011). Furthermore, following the two-hit

model of schizophrenia, studies have shown that postnatal exposure to psychogenic stressors or cannabinoid receptor agonists in MIA offspring produces more dramatic behavioral deficits than those seen due to maternal infection alone (Dalton et al., 2012; Giovanoli et al., 2013; Feigenson et al., 2014). Interestingly, in contrast to viral or bacterial activation of TLR3 or 4 receptors, the activation of other TLR receptors (e.g. TLR7) might induce different (even opposite) patterns of behavioral or neural dysfunctions (Missig et al., 2019).

Considering the recent pandemic of the coronavirus disease 2019 (COVID-19), which also did not spare pregnant women (Dashraath et al., 2020; Narang et al., 2020; Wenling et al., 2020; Wastnedge et al., 2021; Zimmer et al., 2021), the topic of the connection between inflammation and schizophrenia is actually more up to date than ever. Considering that both TLR3 and TLR4 receptors are involved in the pathogenesis of COVID-19 (Khanmohammadi and Rezaei, 2021), and considering the hypothesis that the specific type of infection may play a secondary role in the development of schizophrenia (Meyer et al., 2009b), one may postulate a rise in schizophrenic patients in around 20 years, i.e. when the typical age-onset of schizophrenia is seen.

1.1.3.1. Behavioral Tests

Although the main task of this study was to assess resting-state connectivity in LPS model offspring on a longitudinal time scale, the study was complemented by contemporary behavioral experiments for the assessment of schizophrenia-like symptoms in the animals. In order to cover the whole range of positive, negative and cognitive symptoms observed in human schizophrenia, a test battery consisting of four tests was included, consisting of prepulse inhibition (reflecting positive symptoms / sensory motor gating deficits), elevated plus maze and open field tasks (reflecting negative symptoms / increased anxiety) and the novel object recognition task (reflecting cognitive symptoms / impairments in memory) (Young et al., 2009).

1.1.3.1.1. Elevated Plus Maze

The elevated plus maze (EPM) task is a test that can be utilized to measure unconditioned anxiety in rodents (Walf and Frye, 2007). Animals are placed on an plus shaped maze, elevated ~70 cm above the floor, consisting of two open arms without any walls, and two closed arms enclosed by walls. Each equivalent pair of

arms are positioned opposite to each other and are interconnected by a central open platform (Handley and Mithani, 1984; Walf and Frye, 2007). The animals behavior like time spent in the open and closed areas of the maze, or number of times the animals peak with their head over the edge of the open part of the maze (head-dipping) are measured and used to calculate different indices of anxiety (Walf and Frye, 2007). Small ledges can be attached to the open arms, but may change the interpretation of anxiety indices like the risk-assessment behavior of head-dipping (Fernandes and File, 1996).

The novel stimulation by placing the animal in the new environment of the EPM evokes a fear drive as well as an exploratory drive. Generally, the strength of the fear drive decreases with time of exposure. However, the elevated open alleys arouse a greater strength of fear than enclosed alleys (Montgomery, 1955). Thus, the EPM task is based on this approach-avoidance conflict, related to the unconditioned aversion to heights and open spaces, leading to a preference for the enclosed arms of the maze (Montgomery, 1955; Barnett, 1975; Rodgers and Dalvi, 1997). Based on the early experiments by Montgomery, Handley and Mithani hypothesized that anxiolytic drugs should increase the exploration of the open arms, whereas anxiogenic drugs should decrease it. By showing a clear preference for enclosed arms under standard conditions while open arm entries increased after giving the anxiolytic drug Diazepam, they redefined the EPM task into the test as it is known today (Handley and Mithani, 1984), which was shortly after validated for rats (Pellow et al., 1985) and mice (Lister, 1987). Within the last decade, the EPM was even translated into a virtual-reality test for humans, showing cross-species validity of the measured anxiety indices (Biedermann et al., 2017).

Early experiments have shown that re-testing the animals on consecutive days or after seven to eight days seem to evoke similar responses as in the first test (Pellow et al., 1985; Griebel et al., 1993; Schrader et al., 2018). Although the total number of arm entries may increase, the anxiety indices seem to be unaffected by re-testing (Lister, 1987). However, later experiments suggest that there might be a so called “one-trial tolerance” leading to a shift of measured construct from anxiety to fear when retesting with short (24h) intervals (Carobrez and Bertoglio, 2005; Schneider et al., 2011). But longer re-test intervals and the change of the room where the maze is placed seem to improve the re-test reliability (Schneider et al., 2011).

The illumination of the open areas of the maze is playing a role in the task, as high illumination reduces the entries and time spent in the open arms (Griebel et al., 1993; Schrader et al., 2018).

Younger animals seem to be less fearful than older animals (Imhof et al., 1993; Rodgers and Dalvi, 1997). Also, there may be differences between rat and mice in the EPM behavior (Rodgers and Dalvi, 1997), although a large meta review suggests the inter-species differencies are minor compared to the overall variance present in the test (Mohammad et al., 2016). Part of a general variability seen in the EPM test may actually be related to the presence of a temporal pattern present in rat behavior in the EPM over a 24 h cycle (Andrade et al., 2003).

The elevated zero maze (EZM) is an alternative measuring a comparable construct of approach-avoidance conflict, but removing the ambiguity associated with time spent on the central platform and increasing the number of locations with an approach-avoidance conflict, the phenomenon the EPM is intended to measure, by using a circular “maze” where open and closed compartments alternate (Shepherd et al., 1994).

Although the EPM test was controversially discussed in the past (Ennaceur, 2014; Ennaceur and Chazot, 2016), it is still one of the most widely used tests for measuring anxiety in the laboratory setting (Castanheira et al., 2018).

1.1.3.1.2. Open Field

The open field (OF) test is another test that may be used to measure anxiety related behaviours in rodents (Carola et al., 2002; Prut and Belzung, 2003). The OF test was initially developed by Hall in 1934 who studied defecation and urination as measures of individual differences in emotionality (Hall, 1934), and is nowadays one of the most used tests for measuring locomotion and anxiety related behaviors in mice and rats (Carola et al., 2002; Prut and Belzung, 2003; Seibenhener and Wooten, 2015). Animals are placed in an open circular, square or rectangular arena, and the movement as well as additional behaviors like rearings (i.e. the animals are standing upright on two paws with the front paws in the air or leaned against a wall) are measured over a time span of usually 5 to 20 minutes (Prut and Belzung, 2003; Seibenhener and Wooten, 2015). Due to the tendency of rodents to stay near the walls (i.e. thigmotaxis), the arena is usually divided into a central square and the

outer surrounding area, and increased movement in the central square are interpreted as indications of anxiolysis, while increased thigmotaxis is interpreted as higher anxiety (Prut and Belzung, 2003; La-Vu et al., 2020).

A study by Carola et al. suggests that the data obtained by the EPM and the OF test are more or less comparable (Carola et al., 2002), although others are suggesting both tests are assessing different underlying psychobiological phenomenon's and thus are complementing each other (Ramos, 2008).

1.1.3.1.3. Novel Object Recognition

The novel object recognition (NOR) test was first introduced by (Ennaceur and Delacour, 1988), and led to an advancement in recognition memory research. Most previously used paradigms testing recognition memory involved the learning of a response rule, and those tests might actually be assessing only a specific kind of recognition memory, namely the recalling of a rule, and not the recognition of a previously examined item. The novel object recognition test, on the other hand, is based on the spontaneous exploratory behavior of rats towards unknown objects, and therefore not relied on the learning of a rule (Ennaceur and Delacour, 1988; Steckler et al., 1998).

Before subjecting the animals to the NOR test, one should include a habituation session to the testing environment, as the approach or avoidance of a novel stimulus depends on the familiarity of the environment (Sheldon, 1969). In the first phase (sample phase) of the test, animals are placed in the test environment (usually an open field, similar as described in section 1.1.3.1.2) with two identical copies of an object A present for a short period of time (Bevins and Besheer, 2006). The exposure time of this first phase should be kept in the range of one to two minutes, as longer test periods seem to only add noise (Dix and Aggleton, 1999). Afterwards, the animals are returned to their home cage for an inter-trial interval (ITI) that can range from minutes, for assessing short term recognition memory, sometimes up to 24 hours or more, in order to assess long term recognition memory (Bevins and Besheer, 2006; Dere et al., 2007), although male wistar rats seem not to be able to discriminate between novel and familiar object anymore after a 24 h ITI (Akkerman et al., 2012). In the second phase (test phase), the animals are again placed in the test environment with another identical copy of the initial object A' and a new unknown

object B for 2-5 minutes (Bevins and Besheer, 2006). Afterwards, different discrimination indices can be calculated, although the discrimination ration, sometimes called recognition index (RI), might be more suited for comparing recognition memory in different studies between labs as the main index of object retention than the other indices (Bevins and Besheer, 2006; Akkerman et al., 2012; Antunes and Biala, 2012).

The test was initially denoted a ‘pure working memory test’, however later this statement was corrected by one of the original authors stating recognition memory does not involve working memory at all (Ennaceur, 2010). The reasoning was that working memory was previously wrongly equated with short-term memory. As working memory is the process of actively holding the information for later use in memory, but the animal does not know it will be retested after the initial exploration phase of the test and notwithstanding this it is not possible to predict which information of an object needs to be kept in memory in order to detect novelty, working memory cannot be involved in the NOR test (Ennaceur, 2010). Instead, object recognition memory is more related to episodic memory (Ennaceur, 2010). Since a novel object can’t be recognized, as it is not stored in memory, some authors recommended to use the term spontaneous object recognition (SOR) instead (Dix and Aggleton, 1999; Winters et al., 2008; Lyon et al., 2012; Cohen and Stackman, 2015).

There are many contradictory findings in the literature using the NOR test, however, these may be merely due to variations in the used task parameters (Cohen and Stackman, 2015). Generally, there is a lack of standardization of used items, resulting in nearly each lab using different sets of items. One common methodological problem that may arise depending on the used items is called object affordances, meaning the relations between the animals natural abilities and the objects properties. For example, if in the test phase an item which can be climbed on is compared to an item which can’t be climbed onto, this can influence the test and the recognition indices due to the animals natural tendency of interaction with such items (Chemero and Heyser, 2005; Ennaceur, 2010; Heyser and Chemero, 2012). Generally, it is recommended using different objects made of the same material (e.g., glass, plastic, porcelain, ceramic, metal) but which are different in terms of height, color, shape and surface texture (Dere et al., 2007). One problem arising when trying

to compare different studies is the lack of given information in the materials and methods section. For example one study reviewing 116 articles reports that with 44% nearly half of the publications gave little or no information concerning the specific objects which were used, and from the 56% which provided information, 28% used sets of objects with non-equivalent affordances, making the results difficult to interpret and making it virtually impossible to generalize across experiments (Chemero and Heyser, 2005). Statistically, although many studies are using differences in magnitude as evidence for stronger or weaker memory performance in different groups of animals, these differences alone may not be sufficient to draw a conclusion based solely on memory per se (Heyser and Chemero, 2012). One must assume that the RI-magnitude is reflective of how well the animals encoded the sample object, which is not supported e.g. by the study of Gaskin et al., 2010. Instead, it may be more appropriate to evaluate the rodents memory based on whether a groups average RI significantly differs from chance or not (Gaskin et al., 2010; Cohen and Stackman, 2015).

When testing recognition memory in human schizophrenic patients, they showed significantly lower recognition rates for previously presented objects, and significant impairment in the ability to recognize fragmented objects (Heckers et al., 2000; Doniger et al., 2002; Pelletier et al., 2005; Lyon et al., 2012).

1.1.3.1.4. Prepulse Inhibition

Prepulse inhibition (PPI) is related to the acoustic startle response (ASR), which is a sensorimotor response to a sudden acoustic stimulus with an intensity of about 90 dB sound pressure level (SPL) or higher that leads to a fast twitch of body muscles (Davis and File, 1984; Pilz et al., 1987; for review see: Koch, 1999). It probably has a protective function against attacks, and is mediated by a pathway located in the ponto-medullary brainstem, consisting of the auditory nerve, the ventral cochlear nucleus, the dorsal nucleus of the lateral lemniscus, the caudal pontine reticular nucleus (PnC), spinal interneurons and spinal motor neurons (Davis et al., 1982; Koch, 1999). The PnC neurons, especially the subpopulation of giant reticulospinal PnC neurons, seem to play a key role in this pathway (Koch et al., 1992). The magnitude and latency of the ASR depend on several different factors like stimulus intensity or interstimulus interval, and could be modulated by many different drugs (Koch, 1999). An important effect on the ASR is seen when the startling stimulus is

immediately preceded by a non-startling stimulus (prepulse), which leads to a decrease in the magnitude of the ASR. This phenomenon is called prepulse inhibition and is used as an operational measure for sensorimotor gating mechanisms (Hoffman and Ison, 1980). The extent of PPI strongly depends on the prepulse intensity and prepulse-pulse interval, weakly depends on the prepulse duration and modality, and is mostly independent of the properties of the startle-eliciting stimulus (Stitt et al., 1976; Fendt et al., 2001). In rats, PPI works best with an interstimulus interval of 100 ms between the prepulse and the startling pulse (Hoffman and Ison, 1980; Koch, 1999), is increased with increasing prepulse intensity, and is maximal at prepulse durations of 10-20 ms (Reijmers and Peeters, 1994). Apparently, the ASR and PPI are mediated by different brain pathways (Ison et al., 1997; Fendt et al., 2001).

Because PPI is reduced in human schizophrenic patients (Swerdlow and Geyer, 1998; Braff et al., 1999), the reduction of PPI for example by dopamine infusion into the nucleus accumbens of rats was used as an animal model for studying the sensorimotor gating deficits of schizophrenia (Swerdlow et al., 1994). The reduction of PPI was also shown in MIA rodent models of schizophrenia (e.g. Borrell et al., 2002; Fortier et al., 2007; Wischhof et al., 2015b; see section 1.3.4 for a detailed overview), underpinning their validity, as reduced PPI is often used as a benchmark test for the validity of animal models for schizophrenia (Swerdlow and Geyer, 1998; Van den Buuse et al., 2003; Zuckerman et al., 2003; Wolff and Bilkey, 2008; Wolff et al., 2011; Fendt and Koch, 2013; Swerdlow and Light, 2015; Swerdlow et al., 2016).

1.2. Resting-State Connectivity

Before delving into the topic of resting-state connectivity, which is usually measured via functional magnetic resonance imaging (fMRI), one may first need to explain the basics of (f)MRI for a better understanding. Readers already familiar with the basics of MRI and fMRI may skip the next sections and continue with section 1.2.2.

1.2.1. Functional Magnetic Resonance Imaging

Magnetic Resonance Imaging (MRI), including functional MRI (fMRI), is a noninvasive method that can be used to generate images from biological tissues, including the brain of humans and other mammals such as rodents. The basic

principle behind MRI, or nuclear magnetic resonance (NMR) in general, is the excitation of atomic nuclei in a strong magnetic field. During this process, energy is first absorbed and later emitted by the atomic nuclei, which then can be measured. The amount of emitted energy and therefore the signal depends on number and types of nuclei in the excited tissue. Because different tissues show different properties, depending on imaging parameters like the time point of signal reception, one can then conclude which types of tissue make up the imaged sample (Huettel et al., 2009). The following 3 sub-chapters (1.2.1.1 - 1.2.1.3) are, if not stated otherwise, a compilation of the books “Functional Magnetic Resonance Imaging” by Huettel et al., 2009, “Magnets, Spins, and Resonances: An introduction to the basics of Magnetic Resonance“ and “Magnets, Flows, and Artifacts: Basics, Techniques, and Applications of Magnetic Resonance Tomography” by Hendrix, 2003, 2004, as well as the introductory part of the doctoral thesis “Functional connectivity of the rat brain in magnetic resonance imaging“ by Kalthoff, 2011. For a more comprehensive description of the following, the reader is referred to any of these mentioned works. Since the notation of variables is sometimes different between those sources, all used formulas are adopted from Kalthoff, 2011.

1.2.1.1. Basics of NMR

1.2.1.1.1. Nuclear Spins

All material on earth is made up of atoms. These in turn are composed of electrons, protons and neutrons, with the latter two making up the atomic nucleus. Each of the atomic constituents possesses a spin of ½, a property from quantum mechanics. The net nuclear spin of the atomic nucleus is the combined spin of all its protons and neutrons. For the hydrogen atom ^{1}H, which nucleus consists only of one single proton, this net nuclear spin is simply ½.

In the classical model (for a quantum mechanical perspective, the reader is referred to chapter 5 of Brown et al., 2014), the proton is described as a rotating positive charge (see figure 1) with angular momentum $\vec{S}$. The rotation of the charge leads to a circulating electric current, which in turn gives rise to the magnetic moment $\vec{\mu}$ via

$$\vec{\boldsymbol{\mu}} = \boldsymbol{\gamma} \cdot \vec{\boldsymbol{S}} \tag{1}$$

where γ is a proportionality factor called the gyromagnetic ratio. Besides the hydrogen atom with its single proton, other atomic nuclei could be studied with MRI as well. However, they need both angular momentum as well as the magnetic moment in order to be useful for MRI. For example, in nuclei with an even number of protons and neutrons, the magnetic moment is cancelled out by distributing the same amount of charges in opposite directions, what makes them invisible for MRI. Other nuclei than ^{1}H with NMR property are for example ^{13}C or ^{19}F. However, since hydrogen atoms make up by far the most of all atoms with NMR property in biological tissues, the following description concentrates on the nuclei of hydrogen atoms, further simply referred to as protons or spins.

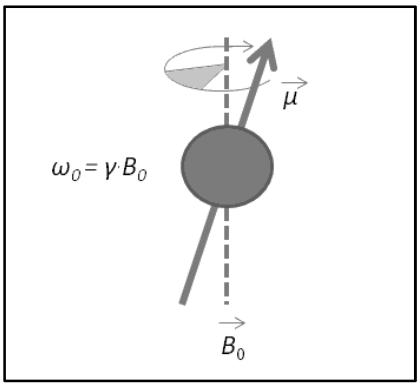

Figure 1: Classical Model of a Spin in a Magnetic Field
The proton or spin is typically viewed as a positive rotating charge, which gives rise to the magnetic moment $\vec{\mu}$. Located in an external magnetic field B_0, the spin precesses with the Larmor frequency ω_0 around the axis of the magnetic field. γ is a proportionality factor called the gyromagnetic ratio. Recreated after Kalthoff, 2011.

1.2.1.1.2. Spins in an External Magnetic Field

When located in an external magnetic field B_0, a spin sort of aligns with the magnetic field. However, since the conservation of angular momentum stands against alignment of the magnetic moment to the magnetic field, the magnetic moment of the proton follows an equation of motion:

$$\frac{d\vec{\mu}}{dt} = \gamma \cdot \vec{\mu} \times \boldsymbol{B_0} \tag{2}$$

This results in a precessing motion around the magnetic axis, which is often compared with a gyroscope that is tipped out of its original rotation. This precession occurs with a characteristic frequency, called the Larmor frequency ω_0, which depends on the magnetic field strength as well as the gyromagnetic ratio of the nucleus:

$$\boldsymbol{\omega_0 = \gamma \cdot B_0} \quad (3)$$

For the hydrogen protons, this frequency is 42.58 MHz/T.

1.2.1.1.3. Magnetization of a Spin Ensemble

The signal of a single proton is not detectable using MRI. Instead, all protons in the imaging volume are viewed as a pooled spin ensemble, or spin system. A typical volume element (voxel) in an MRI experiment consists of ~10^{18} protons of a living organism. In a space without a magnetic field (or only a very weak one), the spins of a spin ensemble are oriented randomly and the magnetic moments of the individual protons cancel out each other. Therefore, the voxel appears non magnetic to the outside. However, when placed in an external magnetic field, each individual spin of the spin ensemble can take one of two different orientations, either parallel or antiparallel to the magnetic axis. Because the parallel orientation is the state of lower energy, this orientation is slightly preferred. According to Boltzmann statistics, there is an excess of about 10 protons in the parallel position per one million protons in the antiparallel position at a magnetic field strength of 1.5 T and a body temperature of 37 °C, which resembles the typical clinical condition. Because of this slight excess, the spin ensemble inside a voxel gives rise to a net magnetization vector M_Z in longitudinal direction of the magnetic field B_0.

1.2.1.1.4. Excitation of a Spin Ensemble and Signal Reception

The net magnetization of a spin ensemble follows the same equation of motion as the magnetic moment of a single proton (equation 2). Therefore, in order to simplify the description of excitation and signal reception, the spin ensemble is viewed from a rotating reference frame. The coordinate system of this reference frame rotates with ω_0 around the axis of the magnetic field B_0, which leads to the fact that the magnetic moment of a proton stands still in this new reference frame. This can be compared with watching a child on a rotating carousel. When standing in front of the carousel, one can see the child rotating. However, when standing on the carousel (the reference frame), one rotates with the same velocity as the child, and therefore the child seems to stand still.

The excess of protons in the parallel orientation to the magnetic axis can be transferred into the antiparallel orientation by delivering energy in form of

radiofrequency (RF) pulses, which are transmitted by RF coils. The delivered electromagnetic waves are adjusted to oscillate in resonance with the Larmor frequency of the nuclei of interest, e.g. 42.58 MHz/T for the hydrogen protons, and this process of delivering energy is called excitation. The more of the excess protons in the parallel orientation switch to the antiparallel orientation, the more flips the net magnetization vector M_Z from the longitudinal towards the transverse plane (see figure 2 a). The degree of flipping is called the flip angle α, and depends on the amplitude as well as duration of the RF pulse. As soon as the whole excess of protons in the parallel orientation has switched to the antiparallel orientation, meaning there are equal numbers of protons in each state, there is no net magnetization along the longitudinal axis, because the net magnetization vector has been fully transferred into the transverse plane. The RF pulse that is able to accomplish this state is called the 90° pulse.

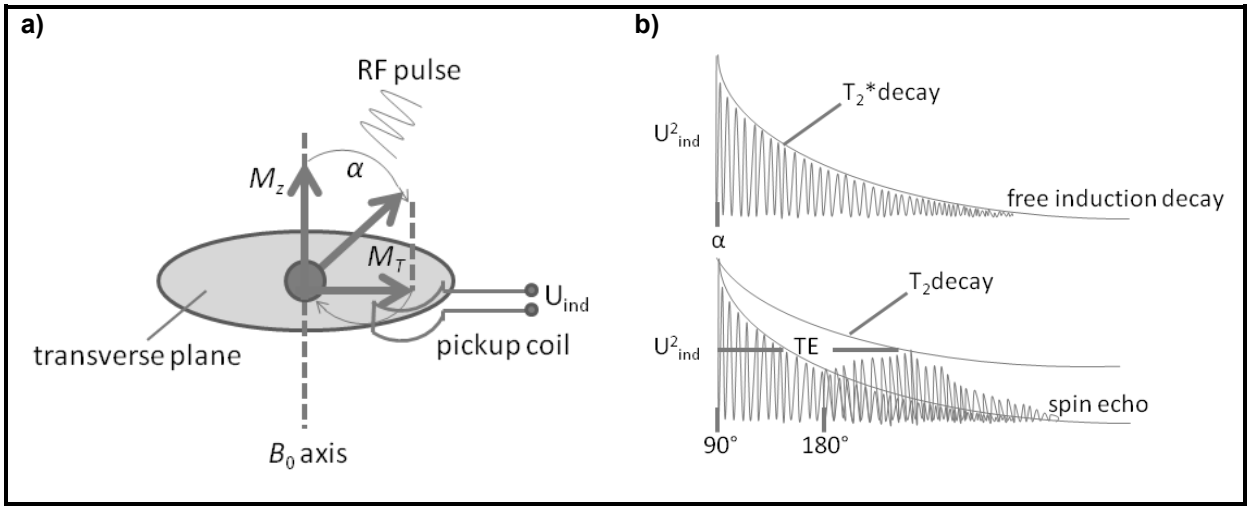

Figure 2: MR Signal Generation
a) By delivering a radiofrequency (RF) pulse with flip angle α (e.g. 90°), the longitudinal net magnetization vector M_Z (which is parallel to the axis of the magnetic field B_0) is flipped towards the transverse plane, generating the transverse net magnetization vector M_T. The precession of M_T in the transverse plane can be recorded by a pickup coil, due to the induction of a voltage U_{ind}. b) The MR signal recorded by the pickup coil oscillates with the Larmor frequency and decays exponentially with the characteristic time constant $T_2{}^*$, forming the so called free induction decay (FID, top). Delivering a 180° RF pulse after the 90° RF pulse induces an echo of the FID after the echo time (TE). Even though the echo is still decaying with $T_2{}^*$, its maximum amplitude is solely limited by the time constant T_2 (bottom, spin echo). Recreated after Kalthoff, 2011.

The magnetization in the transverse plane arises due to phase coherence of the spins. Before transmission of the RF pulse, the phases of all spins of the spin ensemble are randomly distributed. However, the RF pulse disturbs and sort of resets the phase of the spins. Therefore, afterwards all spins are precessing with the same phase. This transverse component M_T of the net magnetization vector is now

precessing with ω_0 in the transverse plane, and this precession can be recorded by a pickup coil (which is often the same coil that is used for the delivery of RF pulses) that is tuned to the same frequency ω_0. The changing magnetic flux of the precessing net magnetization vector M_T induces a corresponding voltage in the pickup coil, which is the basis signal of NMR or MRI (see figure 2 a).

1.2.1.1.5. Relaxation Mechanisms of the MR Signal

After the delivery of the RF pulse and the following flipping of the net magnetization vector from the longitudinal into the transverse plane, the measurable MR signal starts to decay due to different relaxation mechanisms.

First, some spins of the spin ensemble emit the previously absorbed energy and thereby switch back from the antiparallel to the parallel orientation, rebuilding the excess of parallel spins. After some time, the original state with an excess of 10 spins in the parallel orientation per one million spins in the antiparallel position (at a magnetic field strength of 1.5 T and a body temperature of 37 °C) has recovered, and therefore the net magnetization vector M_Z in the longitudinal direction of the magnetic field is back at its original value as well. This is an exponential process that occurs with a specific time constant T_1, and is called longitudinal (T_1) relaxation or longitudinal (T_1) recovery.

Second, the magnitude of the transverse magnetization M_T decays exponentially with a time constant $T_2{}^*$, and shapes what is known as the free induction decay (FID) (see figure 2 b, top). This second relaxation is called transverse ($T_2{}^*$) relaxation or transverse ($T_2{}^*$) decay, and is the additive result of two different processes. On the one hand, the magnetic moments of electrons translate and rotate together with their atoms and molecules due to Brownian motion, what leads to a rapidly varying magnetic environment of spins on a molecular scale. This slightly changes the magnetic field at each position. Because the Larmor frequency depends on the magnetic field (see equation 3), each spin experiences a Larmor frequency that is slightly different from ω_0, and this leads to a dephasing of the spins over time. This intrinsic part of the transverse relaxation is known as spin-spin relaxation, and could be seen as the “real” T_2 decay. On the other hand, spatial and time-constant field inhomogeneities of the external magnetic field B_0 add up to the T_2 decay, resulting in the faster $T_2{}^*$ decay.

Even though the FID is decaying with T_2^* instead of T_2, the T_2 decay can still be measured using echoes of the FID (see figure 2 b, bottom). In order to produce an echo, a 180° pulse can be played at time τ after the excitation with a 90° pulse. This 180° pulse will reverse the phase of the spins, which will now traverse backwards. After another time τ, they will be at the same phase as after the initial 90° pulse. Since the spins are now precessing with the same phase again, they give rise to a measurable spin echo of the FID. This echo is still decaying with T_2^*, however, its maximum amplitude is solely limited by T_2. An often used illustration is that of sprinters running on a circuit. They are all starting on the same start (i.e. with the same phase), but after some time τ, each will have travelled a different distance depending on the speed of the individual sprinters. However, when they are now getting the command to turn round and run back, and each one keeps its original speed, they will all be at the start again after the same time τ. Actually, most of the different imaging protocols these days are using those echoes in order to measure the MR signal. Besides producing a spin echo with a 180° pulse, a gradient echo can be produced as well. This is done by switching two consecutive magnetic field gradients (the frequency encoding gradient, see 1.2.1.2.1). Because the first gradient is dephasing the spins, the second gradient is switched with inverted polarity. This rephases the spins giving rise to a gradient echo.

The echo time (TE) is simply twice the time τ, at which the 180° refocusing pulse is played, and is an important parameter that changes the contrast of MRI images. Another important imaging parameter is the repetition time (TR). In order to visualize images, for which more than one voxel has to be measured, or for the purpose of averaging, an FID or spin echo experiment is usually repeated several times, separated by the TR. Because the TR is the time between the consecutive excitation of the same tissue, the length of it determines to what extend the longitudinal net magnetization M_Z can regrow, and therefore to what extend M_Z is available for the next excitation.

1.2.1.1.6. MR Signal Contrasts

Different tissues show different relaxation times, depending on the amount of hydrogen atoms, as well as the molecular environment of the spins. Because of these different relaxation times, different tissues will have different MR signal amplitudes when measured at the same time. Depending on the tissue of interest,

one can change the imaging parameters TR and TE in order to achieve different contrasts.

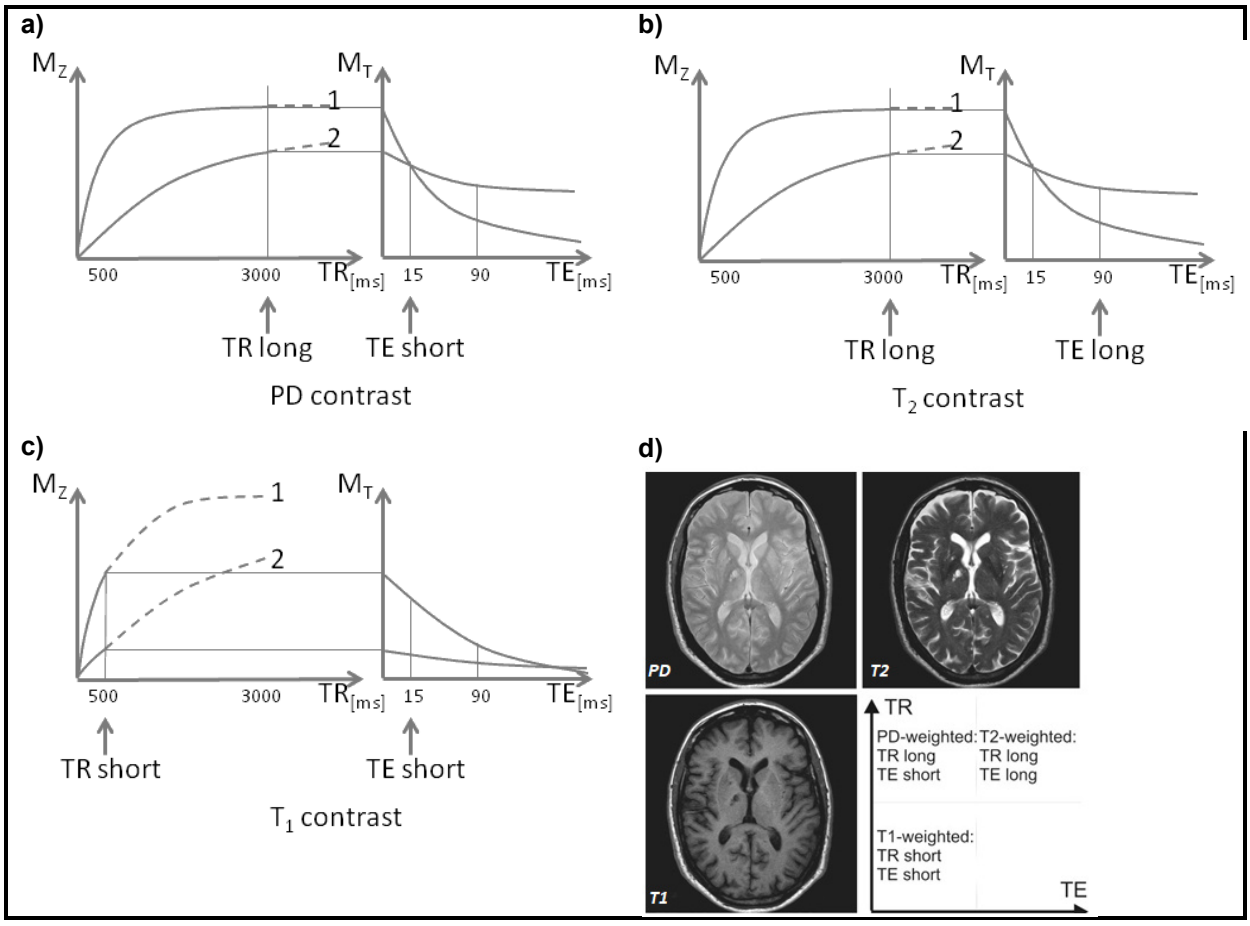

Figure 3: MR Signal Contrasts
a) Proton density (PD) contrast (TR long / TE short), b) T_2 contrast (TR long / TE long) and c) T_1 contrast (TR short / TE short), showing the differences in the longitudinal (M_Z) and transversal (M_T) net magnetization for 2 different tissues. Recreated after Hendrix, 2003**.**
d) Example images for the 3 different contrasts showing human brain slices (Jung and Weigel, 2013, reproduced with permission from John Wiley and Sons).

The longitudinal net magnetization M_Z recovers with the tissue specific time constant T_1, and its maximum value corresponds to the tissues proton density (i.e. number of protons per voxel). If a repeated 90° pulse is delivered after a sufficiently long TR, M_Z has recovered to its maximum value, and the MR signal difference of two or more tissues depends mainly on the proton densities. Therefore, by choosing a long TR together with a short TE, one obtains a proton density-weighted image (PD contrast, see figure 3 a).

By keeping a long TR and also selecting a long TE, one looses the proton density contrast, since the MR signals are decreasing with the tissue specific time constant T_2^* / T_2. Because the MR signal difference of two or more tissues are now mainly

depending on T_2^* / T_2, one obtains a T_2^*- / T_2-weighted image (T_2^* / T_2 contrast, see figure 3 b). The optimal TE is the mean value of the T_2^* / T_2 constants of the imaged tissues.

Finally, by selecting a short TR together with a short TE, the MR signal difference of two or more tissues mainly depends on the previous longitudinal net magnetization M_Z. And as mentioned before, this depends on the tissue specific time constant T_1. This means, with a short TR together with a short TE one obtains a T_1-weighted image (T_1 contrast, see figure 3 c).

1.2.1.2. MRI

A complex image (e.g. of a brain) is made up of several voxels. Due to their spatially differing proton densities and relaxation constants, the amount of transverse magnetization M_T, and therefore also the magnitude of the MR signal, depends on the location inside the measured sample. Omitting the transverse relaxation (for the sake of simplicity), the precession with frequency ω and phase φ in the transverse plane can be written as:

$$\boldsymbol{M_T(x,y,z,t) = M_{T0}(x,y,z) \cdot e^{-i\omega t} \cdot e^{-i\varphi}} \tag{4}$$

However, the measured MR signal includes contributions from the whole measured sample:

$$\boldsymbol{S(t) = \iiint M_T(x,y,z,t)dV} \tag{5}$$

Therefore, in order to form an image using MRI, one has to encode the spatial location into the measured MR signal. This is achieved using 3 magnetic field gradients G_x, G_y and G_z, which change the magnetic field strength linearly along the gradient axes (e.g. x-axis). Accordingly, the Larmor frequencies of the spins are changing depending on their position:

$$\boldsymbol{\omega(x) = \gamma \cdot (B_0 + G_x x) = \omega_0 + \gamma G_x x} \tag{6}$$

1.2.1.2.1. Spatial Encoding Gradients

First, a slice selection Gradient G_z is switched on during RF excitation. Since the Larmor frequency of the spins thus changes depending on the position, only those spins are excited, whose Larmor frequencies are covered by the RF pulse. Therefore, by adjusting the bandwidth of the RF pulse, one can select different slices of the whole sample. Using a small bandwidth results in relatively thin slices, whereas

with growing bandwidth the slice thickness increases (see figure 4). The selection of a single slice reduces further encoding to two dimensions, since the dz Integral in formula 5 is now set to well defined limits.

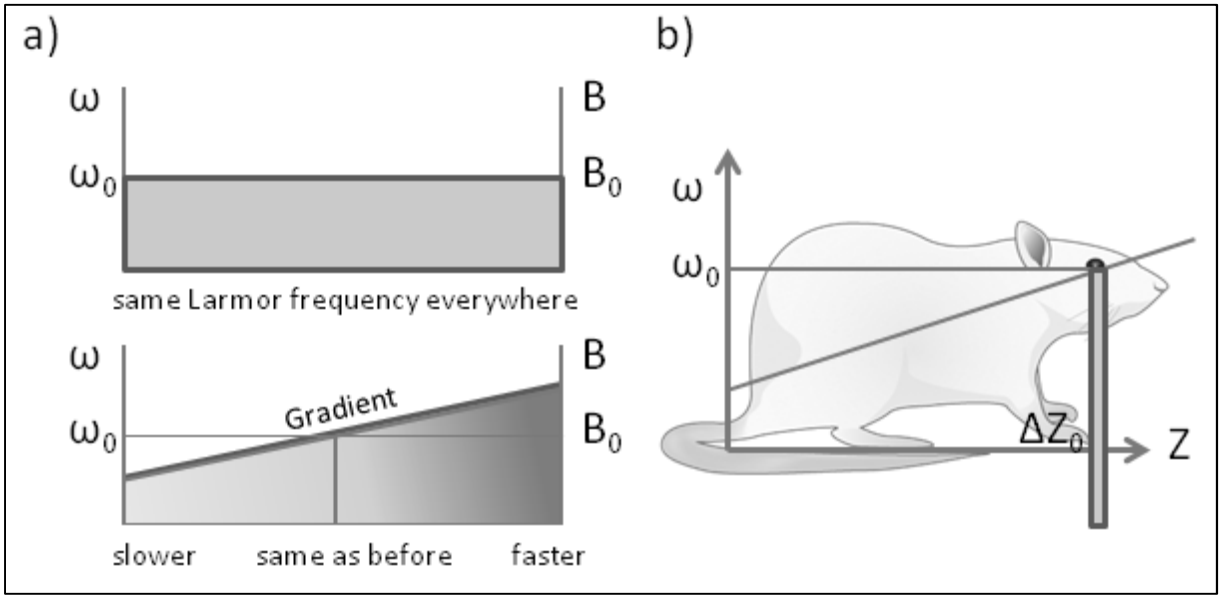

Figure 4: Slice Selection
a) When using a homogeneous magnetic field B_0, all hydrogen spins are having the same Larmor frequency ω_0 (top). However, after adding a gradient G_z which changes the field strength linearly along the magnetic axis, the spins are precessing with different Larmor frequencies, depending on their position (bottom). b) By using a radiofrequency (RF) excitation pulse with the bandwidth $\Delta\omega_0$, a slice with the thickness ΔZ_0 is selected, which includes only those spins whose Larmor frequency is included in $\Delta\omega_0$. Recreated after Hendrix, 2003; Cartoon rat image © DBCLS 統合 TV (CC BY 4.0).

Second, a frequency encoding gradient G_x (readout gradient) is switched on during signal reception, which changes the Larmor frequency of the spins along the x-axis of the selected slice. The slice is therefore divided into columns with different frequencies (see figure 5 a, b). Following formulas 4 and 6, their magnitude of transverse magnetization (viewed from the rotating reference frame) in x direction is:

$$\boldsymbol{M_T(x, G_x, t) = M_{TO}(x) \cdot e^{-i\gamma x \cdot G_x t}} \tag{7}$$

Third, in order to divide the columns of the slice into rows (and therefore into individual voxels), the phase of the spins is manipulated using a phase encoding gradient G_y (see figure 5 a). Depending on the amplitude G_y and duration T_y, the phase accumulates to

$$\boldsymbol{\varphi = \gamma y \cdot G_y T_y} \tag{8}$$

resulting in the magnitude of transverse magnetization in y direction:

$$\boldsymbol{M_T\left(y, G_y, T_y\right) = M_{TO}(y) \cdot e^{-i\gamma y \cdot G_y T_y}} \tag{9}$$

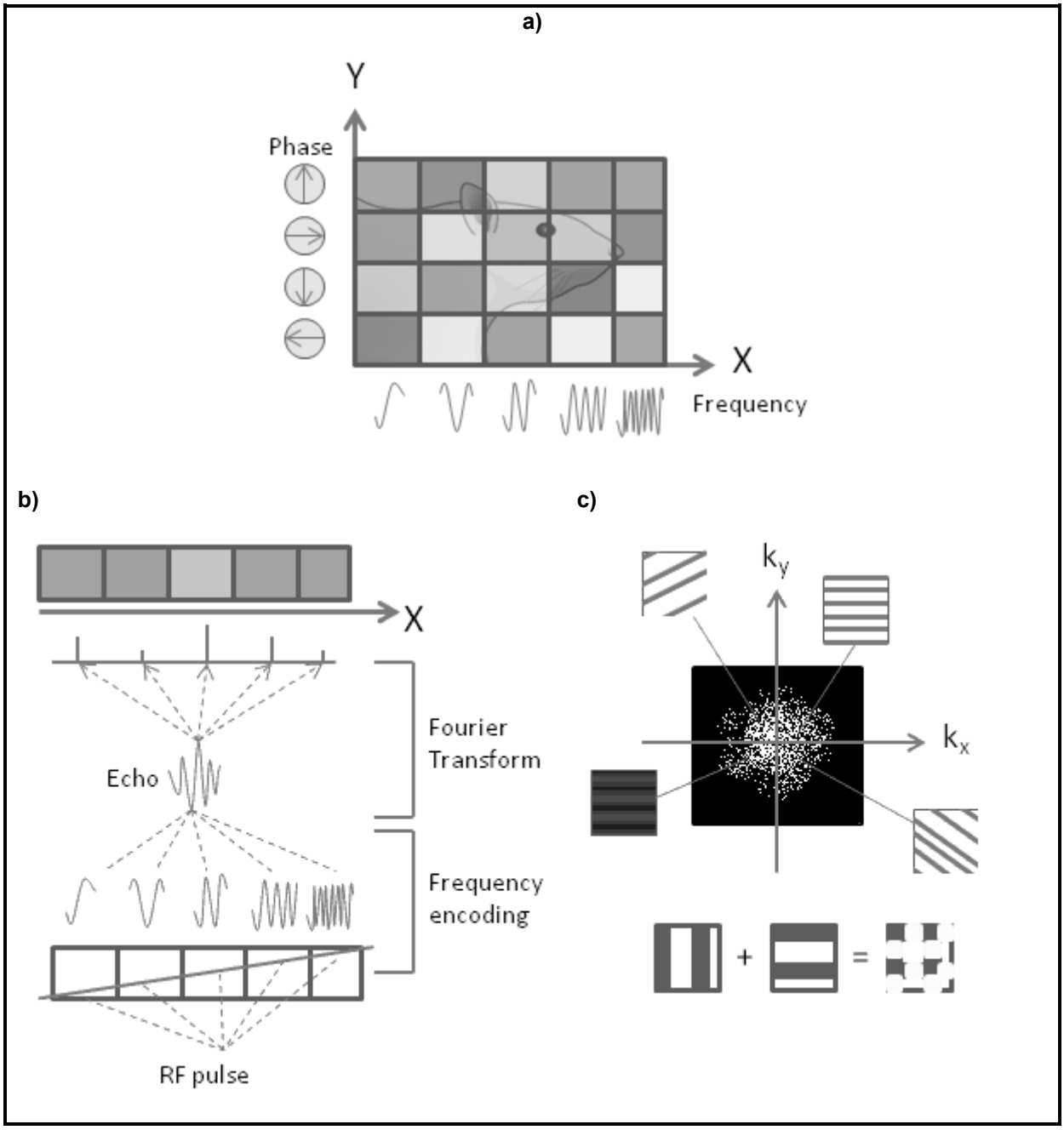

Figure 5: Frequency-, Phase Encoding and the Concept of K-Space
a) By using a frequency encoding gradient G_x, the selected slice is divided into columns with different frequencies. The phase encoding gradient G_y further divides the columns into rows. b) The RF pulse excites all spins that are included in its bandwidth. Due to the frequency encoding, each column of the slice has a slightly different Larmor frequency. All of those frequencies together form the FID MR signal (or echoes of it), which is recorded in k-space. The k-space data can be decoded into the underlying magnitudes of magnetization by using the Fourier Transform of it. c) The k-space contains information regarding the contribution of different components (stripe patterns) in the spatial-frequency domain to the MRI image (top). The combination of those components is forming the more complex image (bottom). Recreated after Hendrix, 2003; Cartoon rat image © DBCLS 統合 TV (CC BY 4.0).

1.2.1.2.2. The Concept of K-Space and MR-Sequences

The consideration of frequency and phase encoding can be simplified by using a notation scheme known as k-space. By introducing the new variables

$$\boldsymbol{k_x = -\gamma G_x t} \quad \text{and} \quad \boldsymbol{k_y = -\gamma G_y T_y} \tag{10}$$

the MR signal can be written as a function of k_x and k_y, which is the Fourier transform of the underlying spatial distribution of transverse magnetization M_{TO}:

$$\boldsymbol{S(k_x, k_y) \propto \iint_A M_{TO}(x,y) \cdot e^{-ik_x x} \cdot e^{-ik_y y} \cdot dxdy} \tag{11}$$

In analogy to a signal that changes over time (e.g. a piece of music), which can be constructed from a series of simpler frequencies, any image can be constructed from a series of simpler components in the so called spatial-frequency domain. The mathematical tool for this reconstruction process is the Fourier transform, which can be used to decode the k-space representation of the MR signal into the magnetization and therefore signal amplitude at each spatial location (see figure 5 b, c).

The number and range of k_x and k_y determine the resolution and the field-of-view of the image that can be reconstructed from the MR signal. Typically, one line of k-space is filled after excitation using an RF pulse. In order to reconstruct an image with a matrix size of for example 128x128 (i.e. 16384 voxels), the k-space has to be filled sufficiently by repeated imaging of the same slice using 128 different phase encoding gradients, since the decoding is comparable to solving a linear system of equations.

The repeated sequence of RF pulses and gradient switches is usually displayed using a sequence diagram as seen in figure 6 a.

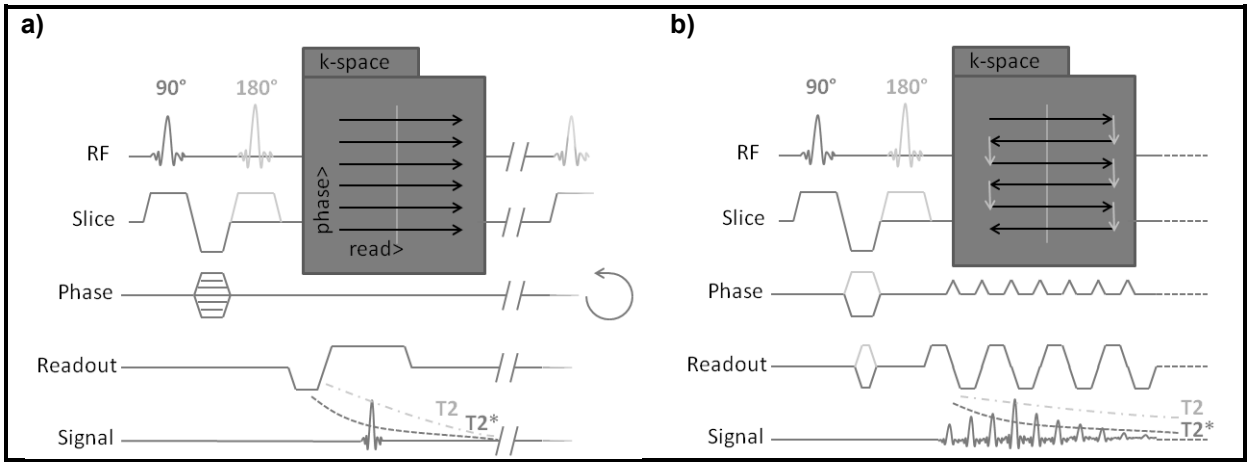

Figure 6: Typical MR and EPI Sequence Diagrams
a) Shown is a Typical MR sequence diagram. During RF excitation, a slice selection gradient is switched, followed by a gradient with inverted polarity to undo the dephasing from the slice selection gradient. During the second (inverted) slice selection gradient, a phase encoding gradient is switched whose amplitude is varied in every repetition of the sequence. For spin echo sequences, a 180° refocusing pulse is now played. A dephasing readout gradient is switched, followed by the actual readout gradient. This sequence is repeated with varied phase encoding gradients, separated by the repetition time TR, in order to fill the entire k-space with data. The k-space trajectory is illustrated in the inset image. b) Shown is an echo planar imaging (EPI) pulse sequence diagram. Instead of repeating the whole sequence with varying phase encoding gradients, the readout and phase encoding gradients are switched repeatedly, giving rise to a train of echoes. Modifications and additions for spin echo EPI sequences are shown in light grey color. The k-space trajectory is illustrated in the inset image. Recreated after Kalthoff, 2011.

1.2.1.2.3. Echo Planar Imaging

Echo planar imaging (EPI) is a technique that enables one to cover a full set of k-space lines following a single RF excitation pulse. Therefore it has also the name single shot EPI. Instead of reading out one k-space line using one phase gradient per RF pulse excitation, a whole echo train is read out. From echo to echo, the readout gradient is repeatedly inverted, and in-between the echoes, different phase encoding gradients (the so called blips) are switched. These result in a zigzag trajectory during which the k-space is traversed (and filled) back and forth (see figure 6 b).

Using EPI, one is able to carry out a rapid image acquisition (< 100 ms), which allows full brain coverage with repetition times on the order of a few seconds. Even though there are some drawbacks, for example possible spatial distortions due to field inhomogeneities (e.g. close to air cavities like the ear canals) or artifacts like Nyquist ghosting (the shifting of parts of the image by half the field of view), this fast acquisition technique is the basis of fMRI used to investigate brain function. EPI images are always $T_2{}^*$-weighted.

1.2.1.3. fMRI – The BOLD Contrast

The basis of fMRI is the BOLD (Blood oxygenation level-dependent) contrast, introduced by Ogawa et al. in 1990, which reflects the neuronal activity due to neurovascular coupling.

Hemoglobin, the key protein for oxygen transport, has different magnetic properties depending on its state of oxygen loading. Oxygenated hemoglobin is diamagnetic, whereas deoxygenated hemoglobin is paramagnetic, and therefore disturbs the magnetic field in its environment. This disruption leads to a shortening of T_2^*, and since fMRI EPI images are measuring T_2^*-weighted signals, to a corresponding signal drop.

The connection between neural activity and the BOLD signal is achieved by neurovascular coupling (for a schematic overview, see figure 7). Neural activity (e.g. synaptic signal transmission) is an energy demanding process, which includes the restoration of the membrane potential of neurons after firing or the reuptake of released neurotransmitters using transport-proteins. These processes increase the cerebral metabolic rate of oxygen, which in turn increases the amount of deoxygenated hemoglobin in the surrounding blood supplying vessels. Thus, the BOLD signal from the vasculature near active neurons is decreased. However, the synaptic transmission also triggers a hemodynamic response through the interplay of the neurovascular unit, which is comprised of neurons, astrocytes and microvessels. When neurotransmitters are released, this is not only detected by the subsequent neurons, but as well by surrounding astrocytes. These astrocytes in turn are releasing vaso-active substances (e.g. NO, K^+ or Adenosine) at their endfeet, which are in contact with arterioles and capillaries. This leads to vasodilatation of those vessels, and therefore to an increase in the regional cerebral blood volume (CBV) as well as a higher cerebral blood flow (CBF), in order to supply both oxygen and glucose (the main energy source of the brain). The increased CBV adds up to the decreasing BOLD signal, since the amount of deoxygenated hemoglobin will rise along with the total blood volume. Nevertheless, the dominating process is the increase of CBF, which lowers the amount of deoxygenated hemoglobin due to washout and dilution with oxygenated arterial blood. This increase in CBF occurs in an amount that exceeds the demands, leading to a net decrease of deoxygenated

blood, and therefore to an increase of the BOLD signal. Even though the increase is only a few percent, it is still measurable.

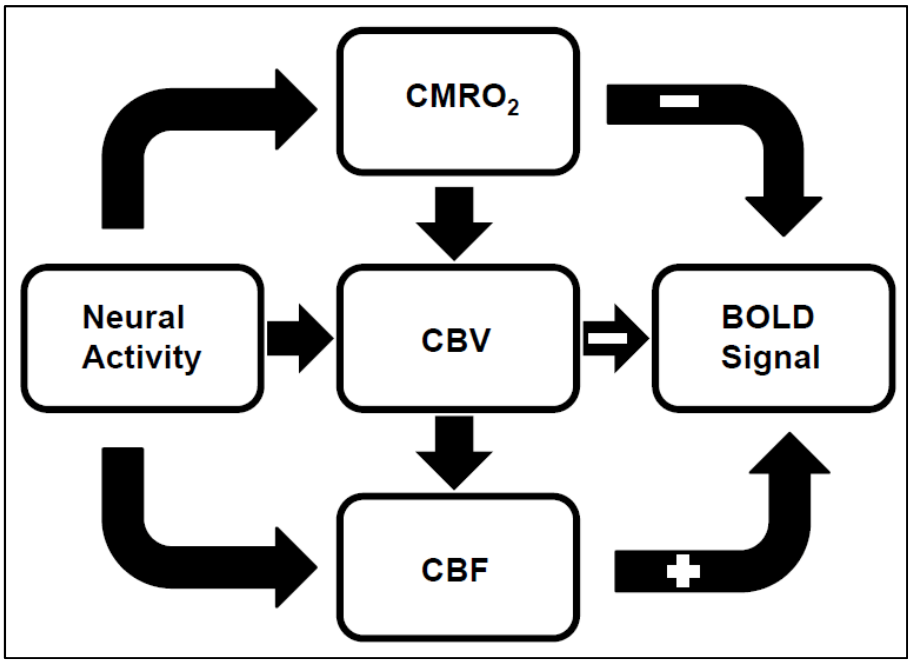

Figure 7: Simplified Model of Neurovascular Coupling
Neural activity leads to an increase of the cerebral metabolic rate of oxygen (CMRO2) and through a triggered hemodynamic response to increases in cerebral blood volume (CBV) and cerebral blood flow (CBF). Increases in CMRO2 and CBV have a negative effect on the BOLD (Blood oxygen level-dependent) signal. In contrast, the increase in CBF has a positive effect, as it lowers the amount of deoxygenated hemoglobin through the supply of oxygenated arterial blood. Normally, the CBF increase is the dominating effect, leading to a net increase of the BOLD signal. Recreated after Kalthoff, 2011.

The hemodynamic response lags the neuronal events initiating it by about 2 s, and so does the BOLD signal. It reaches a peak about 6 s after e.g. presentation of a stimulus, followed by a sustained plateau if the neuronal activity is extended in time. After cessation of the neuronal activity, the BOLD signal drops below the baseline (the so called undershoot) before recovering back to baseline values. Typical hemodynamic responses for both short and sustained events are shown in figure 8.

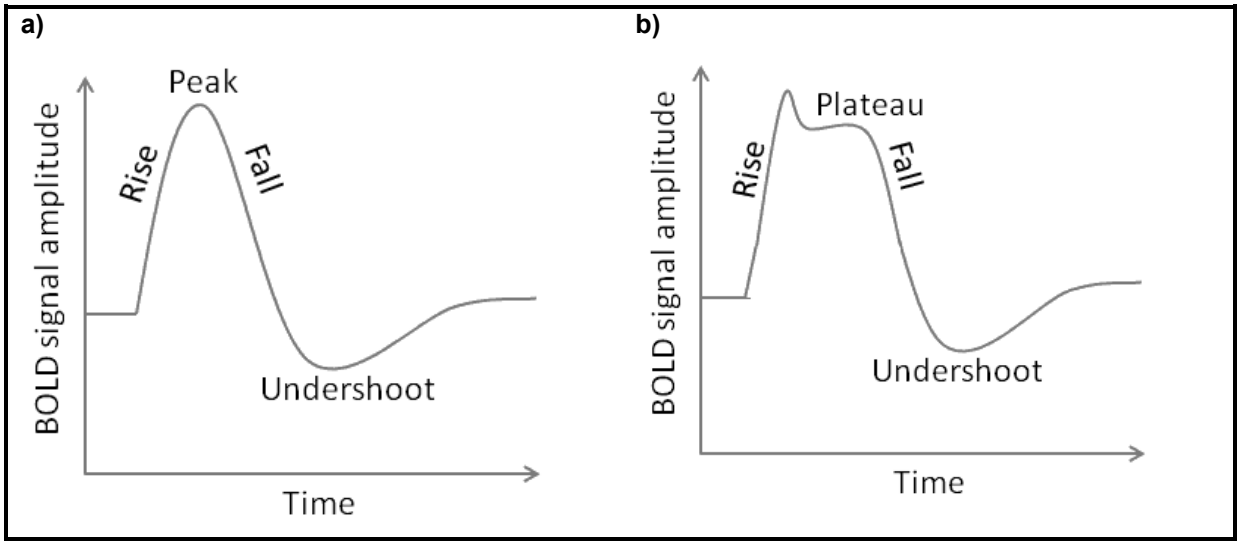

Figure 8: Schematic BOLD Hemodynamic Response
Shown are representative waveforms of for the hemodynamic response to a single short duration event (A) and to a block of multiple consecutive events or a sustained event (B). Recreated after Huettel et al., 2009.

Simultaneous intracortical recordings of neural signals and fMRI responses in monkeys showed that the BOLD signal had most agreement with low frequency potentials (LFPs), which reflect the neuronal input and intracortical processing rather than the spiking output of neurons (Logothetis et al., 2001; Logothetis, 2002).

1.2.1.4. Preprocessing of fMRI Data

In a typical fMRI experiment, the whole brain (or parts of it) is sampled consecutively several hundred times, resulting in a time series of signals for every brain voxel. Before those time series are analyzed, they are typically passed through a preprocessing pipeline, often including corrections for different artifacts, the registration of images into a common space (i.e. normalization), as well as spatial and temporal filtering (for review see Strother, 2006; Chen and Glover, 2015). All these steps are carried out in order to increase the functional signal to noise ratio (Chen and Glover, 2015). The exact chronological order, which steps to include, and the specific parameters for each step can differ between studies. Those choices should depend on the experimental design of the study (Strother, 2006). Nevertheless, most studies are using a typical preprocessing pipeline as shown in figure 9. Besides the acquisition of functional images in the experiment, a structural image with a higher resolution is often acquired as well, providing an anatomical reference for some of the preprocessing steps (Strother, 2006).

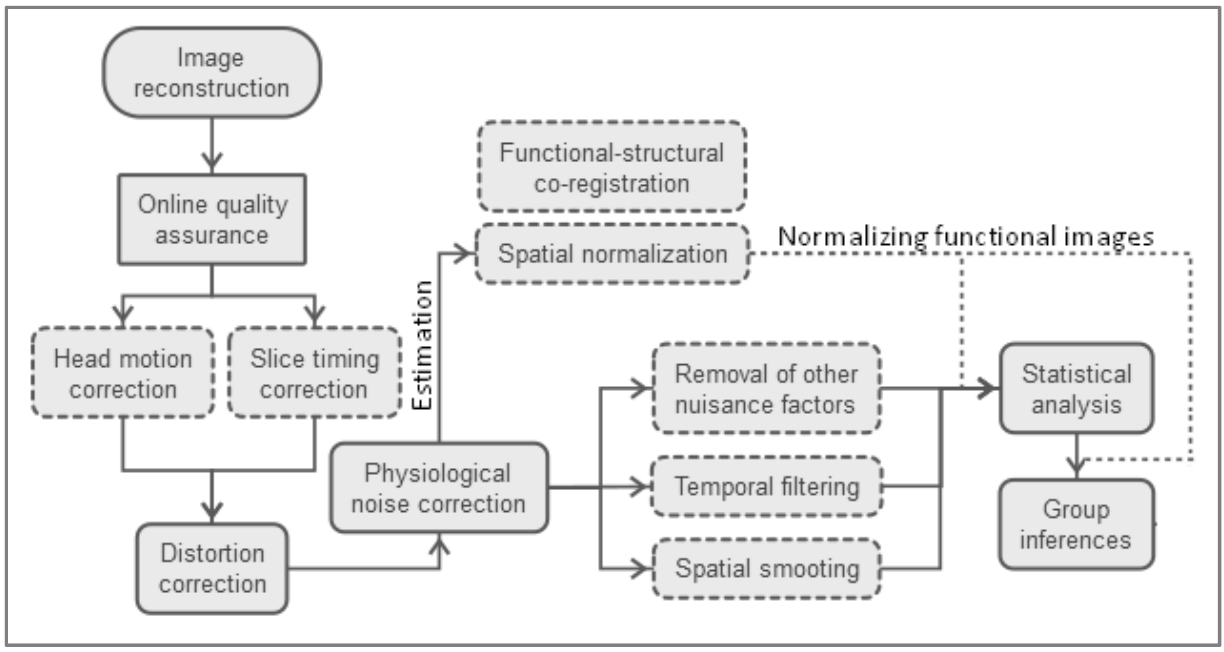

Figure 9: Typical Preprocessing Pipeline
Quality assurance after image reconstruction should always precede the actual preprocessing. Then, slice timing correction and head motion correction are carried out first. The sequential order of those two processes depends on the experimental protocol. Next, a correction for geometric distortions due to magnetic field inhomogeneities is applied, often followed by physiological noise correction (e.g. noise due to heart-rate or respiration). The functional images are co-registered to the structural images, followed by a spatial normalization of both (e.g. to a template brain). Finally, removal of other nuisance factors, temporal filtering and spatial smoothing can be applied as well. Afterwards, the data is provided to a statistical analysis, for example in order to make group inferences. Recreated after Chen and Glover, 2015.

The preprocessing of studies working with MRI data from rodents is sometimes differing in some aspects from human studies. The main big software packages for the analysis of fMRI data were originally designed for human MRI data, introducing translational problems ranging from data formats over brain dimensions up to biophysical priors when used for rodent data. Because of this, additional steps like increasing the brain size (typically, the edge lengths of voxels are multiplied by 10, i.e. the volume is increased by a factor of 1000) are often added to the preprocessing pipeline (Kalthoff, 2011).

An important but sometimes neglected element of data preprocessing is the quality control between consecutive steps, for example by visual inspection using image viewing tools. Despite standard image viewers, the major software packages have also implemented cine viewers. These are allowing the rapid viewing of many slices using the eyes sensitivity to dynamic changes, in order to detect anomalous slices (Strother, 2006). The absolute identification of left and right hemispheres (i.e. image orientation) should also be included, e.g. by testing the preprocessing pipeline with a phantom containing absolute left-right labels (Strother, 2006). There are two

conventions for displaying MRI data. The radiological convention swaps the left-right orientation (i.e. displays the left hemisphere on the right and the right hemisphere on the left side of the image), due to the way in which radiologists typically interact with their patients (generally facing them or lying in the scanner with their feed towards them). In contrast to this, the neurological convention keeps the normal left-right orientation (i.e. left is left and right is right), based on the way a surgeon is looking from the head to the feed of the patient (Huettel et al., 2009).

1.2.1.4.1. Slice Timing Correction

The TR (i.e. the time to collect one full brain volume) ranges between some hundreds of milliseconds to several seconds, depending on the experimental protocol. A lot of studies today are using TR's of 2-3 s. Due to the sequential acquisition of slices using EPI, the time point when each slice of one volume is sampled varies nearly a full TR of 2-3 s between the first slice and the last one. Even when using an interleaved acquisition scheme (i.e. all odd slices are collected first, followed by all even slices), this delay between the sampling of slices is still the TR/2 (Strother, 2006). The slice timing correction uses temporal interpolation in order to correct this acquisition delay (Calhoun et al., 2000). These corrections are estimating the signal amplitudes of each slice at a reference time point by interpolating information from neighboring TRs (i.e. previous and following volumes; Chen and Glover, 2015), which has been shown to be beneficial for parameter estimation (Sladky et al., 2011).

There is an interaction between the slice timing effect and motion, which raised the question if one should apply the slice timing correction before or after motion correction. There are different opinions regarding this issue. For example, Huettel et al., 2004 proposed that slice timing correction should precede motion correction for an interleaved slice acquisition with a long TR, whereas it should follow motion correction with sequential acquisitions or short TRs. Some years later, Sladky et al., 2011 proposed to perform the slice timing correction before motion correction, if the subjects motion is only moderate, whereas to perform it after motion correction, if there is a pronounced inter-slice motion. Combined algorithms, performing slice timing and motion correction simultaneously, are showing potential for solving this interaction problem (Bannister et al., 2007; Roche, 2011). However, those algorithms are not yet implemented in the major fMRI software packages.

1.2.1.4.2. Motion Correction

Most motion correction procedures used in fMRI studies are rigid-body realignment strategies. These corrections are assuming that a volume (i.e. a full stack of slices) is collected instantaneously, and therefore only rigid movement of the entire volume occurs across the sequentially collected volumes (Strother, 2006). These movements are corrected by properly aligning all volumes of the scan session to each other. This is usually done using a cost function, which measures the similarity of each volume to a reference volume (usually the first or the middle volume of the whole scan), and spatial interpolation. First, an algorithm estimates the optimal rigid-body movement variables (three rotations and three translations in direction and around the x-, y- and z-axis) for each volume by minimizing this cost function. Afterwards, spatial interpolation is carried out using this six movement variables, i.e. each volume is resampled according to the determined transformation parameters (Strother, 2006). This interpolation step is necessary, because the voxels discrete integer coordinates will usually turn into float coordinates after the transformation. Therefore, in order to map the data back onto a discrete grid, this interpolation is used (Kalthoff, 2011).

For rodent experiments, where the animal is first of all anesthetized or sedated, and second tightly fixed in the scanner (e.g. by a bite bar and ear rods), the motion does not stem from slow, physical head movements like in human studies. Instead, it results mainly from the rather fast respiratory cycle. Therefore, the displacement can differ between slices, which were possibly acquired in different respiratory phases (Kalthoff, 2011). Because of this, Kalthoff, 2011 developed a slice-wise motion correction, which realigns each slice to a reference slice, instead of using the full volumes. For this correction, transformations are restricted to in-plane translation (x- and y-direction) and rotation (around the z-axis).

1.2.1.5. Correction for Geometric Distortions

EPI images are prone to geometric or intensity distortions, due to magnetic field inhomogeneities, primarily caused by air- and bone-tissue magnetic susceptibility gradients (Strother, 2006). These distortions can be corrected by the acquisition of a field map, and the following so-called unwarping of the EPI images (Jezzard, 2012). The field-map is calculated using two gradient echo images with different TE’s, and is

representing the phase evolution between those two echo times, yielding the deviation from B_0 in every voxel (Kalthoff, 2011).

1.2.1.6. Normalization

In order to directly compare the data of different subjects, a voxel in one subject must represent the same underlying tissue (e.g. brain region) as the voxel at this position in all other subjects. This is not immediately given due to the different sizes and shapes of the individual brains. Therefore, in order to achieve this, all individual brains are normalized to a template brain (Chen and Glover, 2015). This template could be either one single brain (e.g. one representative brain from the study), or an "average brain" reconstructed from several brain images. For humans, the Talairach atlas (Talairach and Tournoux, 1988) or the MNI template (Fonov et al., 2009, 2011) are mostly used, but there are different templates available for rats as well (Schwarz et al., 2006; Valdés-Hernández et al., 2011; Nie et al., 2013; Lancelot et al., 2014).

This normalization can either be done using surface-based landmarks or voxel-based intensities (Strother, 2006). For example, the normalization routine from SPM (Statistical Parametric Mapping, Wellcome Trust Centre for Neuroimaging, London, UK; http://www.fil.ion.ucl.ac.uk/spm/), one of the major fMRI analysis software packages, uses tissue probability maps (TPM's, representing gray matter, white matter, cerebrospinal fluid and remaining tissues) in order to normalize the individual brains to the template brain (Ashburner and Friston, 1997, 1999, 2005). The individual brains are matched to the template brain by estimating an optimum 12-parameter affine transformation and the following warping of the volumes (Ashburner and Friston, 1997). The functional EPI volumes could either be directly normalized to the template brain, or one could use a high resolution structural MRI image for the estimation of the transformation parameters. These could be applied to the functional EPI volumes afterwards, given that the structural MRI image and the EPI images are aligned to each other (Chen and Glover, 2015). The latter approach using a high resolution structural MRI image for the estimation of the transformation parameters allows for a more accurate normalization, because the structural images usually have less noise and more structural information than the functional images (Ashburner and Friston, 1999).

1.2.1.7. Spatial and Temporal Filtering

The spatial filtering (i.e. spatial smoothing) of functional EPI images is mainly carried out, because it has been shown that this step can enhance the signal-to-noise ratio, and increase the significance of the BOLD activations (Lowe and Sorenson, 1997). Additionally, it can also help to reduce the anatomical or functional variations among the different subjects (Chen and Glover, 2015), to match the spatial scale of hemodynamic responses, or to improve the validity of inferences based on parametric tests (Scouten et al., 2006). Spatial smoothing is usually done by convolving the data with a Gaussian kernel. Because the optimal full width at half maximum (FWHM) of this kernel depends on several factors, it is a often difficult to choose an appropriate one. When using fixed smoothing kernels, a smaller kernel (~ 4 mm) is suggested for single subject analysis, while a wider kernel size (6-8 mm) may be applied for a group-level analysis, in order to compensate for differences between the individual subjects (Chen and Glover, 2015). However, there are also methods existing which are utilizing adaptive smoothing kernel sizes (Penny et al., 2005; Yue et al., 2010).

Temporal filtering using high-pass filters with small cut-offs (~ 0.01 Hz) is carried out in order to remove low frequency noise like slow scanner drifts (Holmes et al., 1997; Friston et al., 2000). However, for resting-state studies, additional low-pass filtering (or the use of a band-pass filter) is often carried out, in order to remove high-frequency artifacts due to cardiac rhythm, respiration, as well as thermal noise (Sierakowiak et al., 2015).

1.2.2. Functional Connectivity

Functional connectivity, including resting-state connectivity, is used to describe the temporal coherence of neural activity of anatomically separated brain regions, forming the so called resting-state networks (RSN's; for review see (Gusnard and Raichle, 2001; Raichle, 2010; van den Heuvel and Hulshoff Pol, 2010; Barkhof et al., 2014; Pan et al., 2015). The term functional connectivity was formerly used to describe the temporal coherence among the activity of different neurons, measured by cross-correlating their spike trains, resulting in the so called correlograms (Aertsen et al., 1989; Friston et al., 1993). In the early 90's, this concept was transferred to positron emission tomography (PET) data (Friston et al., 1993), but functional

magnetic resonance imaging (fMRI) is usually the method of choice today (see chapter 1.2.1 for an introduction into fMRI and the nuclear magnetic resonance mechanisms). Especially the application of resting-state fMRI (rs-fMRI) gained particular attention in the examination of functional connectivity between brain regions, measured as the level of co-activation of fMRI time-series during rest (van den Heuvel and Hulshoff Pol, 2010). The co-activation is believed to reflect the functional communication between those brain regions (Biswal et al., 1995; Greicius et al., 2003; Salvador et al., 2005a; Damoiseaux et al., 2006; van den Heuvel and Hulshoff Pol, 2010).

1.2.3. Brain Activity During Rest

Despite the fact that the human brain represents only 2% of the total body weight, it still accounts for around 20% of all the energy consumed (Clarke and Sokoloff, 1999; Gusnard and Raichle, 2001; Raichle, 2010). Remarkably, most of this energy consumption is present even during the resting-state, while the additional energy consumption associated with task related changes in brain activity is often less than 5%, i.e. the brain's enormous energy consumption is little affected by task performance (Sokoloff et al., 1955; Raichle, 2010). This raised the question of why the brain consumes all this energy in the resting state (Gusnard and Raichle, 2001). In fact, according to the assessments of brain energy metabolism using a variety of approaches, the majority of this brain energy consumption is likely devoted to functionally significant intrinsic activity (Raichle and Mintun, 2006; Raichle, 2010).

Biswal et al., 1995 were the first to describe an example of resting-state functional connectivity, when they demonstrated that the spontaneous fluctuations of the BOLD fMRI signal (see chapter 1.2.1.3) in the primary sensory motor cortex of the left and right hemisphere show a high correlation between their BOLD time-series (Biswal et al., 1995, 1997). This finding of functional connectivity between left and right motor cortex was replicated by several studies, and extended by findings of correlations between regions of other known functional networks, e.g. the primary visual network, auditory network and higher order cognitive networks (Lowe et al., 1998, 2000; Xiong et al., 1999; Cordes et al., 2000, 2002; Greicius et al., 2003; Beckmann et al., 2005; De Luca et al., 2005; Vincent et al., 2006; Damoiseaux et al., 2006; Fox and Raichle, 2007; Biswal et al., 2010; van den Heuvel and Hulshoff Pol, 2010; see chapter 1.2.6.2). Among the higher order cognitive networks, the default mode network

(DMN) has received by far the most attention (Gusnard and Raichle, 2001; Raichle et al., 2001; Rosazza and Minati, 2011; Raichle, 2015; see chapter 1.2.6.1).

Since the spontaneous BOLD fluctuations during rest are mainly dominated by lower frequencies (< 0.1 Hz) (Cordes et al., 2000, 2001), these low frequency oscillations (~0.01-0.1 Hz) of resting-state fMRI time-series are the main focus of resting-state functional connectivity studies (Biswal et al., 1995, 1997; Lowe et al., 2000; Cordes et al., 2001; van den Heuvel and Hulshoff Pol, 2010). There has been an ongoing discussion about the origin of these low frequency fluctuations, i.e. if these resting-state BOLD signals stem from physiological processes like respiratory and cardiac oscillations (Wise et al., 2004; Birn et al., 2006, 2008; Shmueli et al., 2007; Chang et al., 2009; van den Heuvel and Hulshoff Pol, 2010), or whether they really represent co-activations of brain regions due to correlated spontaneous neuronal activity (Gusnard and Raichle, 2001; Greicius et al., 2003; Buckner and Vincent, 2007). Due to the low temporal resolution of typical resting-state studies (using acquisition rates of 2-3 s per scan, i.e. 0.5 Hz), high frequency respiratory and cardiac oscillations (in the range of 0.25 Hz) are usually undersampled and therefore aliased into the lower resting-state frequencies (0.01–0.1 Hz), what might shape the BOLD time-series of anatomically separate brain regions in a similar way, introducing artificial correlations between the time-series of these regions (Wise et al., 2004; Birn et al., 2006, 2008; Shmueli et al., 2007; Chang et al., 2009; van Buuren et al., 2009; van den Heuvel and Hulshoff Pol, 2010). However, it was demonstrated that cardiac and respiratory oscillations (> 0.25 Hz) contributed only minimally to the correlation of brain areas (Cordes et al., 2001). Furthermore, the observation that most of the resting-state connectivity tends to occur between brain regions that are overlapping both in function and neuroanatomy (Biswal et al., 1995; Lowe et al., 2000; De Luca et al., 2005; Salvador et al., 2005a; Damoiseaux et al., 2006; van den Heuvel et al., 2008a; van den Heuvel and Hulshoff Pol, 2010), as well as studies showing a strong association between spontaneous BOLD fluctuations and simultaneous measured fluctuations in neuronal spiking (Shmuel et al., 2002; Shmuel and Leopold, 2008) are both in favor of a neuronal basis of the resting-state fMRI signal (van den Heuvel and Hulshoff Pol, 2010). In addition to this, a study demonstrated the abolishment of interhemispheric functional connectivity following the resection of the corpus callosum (Johnston et al., 2008). Nevertheless, non-neuronal fluctuations are still able to influence and corrupt the resting-state signal, which is why methods to reduce

the influence of these signals, e.g. monitoring physiological parameters during scanning and regressing those non-gray matter signals out of the fMRI signal (Weissenbacher et al., 2009), are becoming more and more standard in the preprocessing of resting-state fMRI signals (Birn et al., 2008; Chang et al., 2009; van Buuren et al., 2009; van den Heuvel and Hulshoff Pol, 2010).

1.2.4. Analysis Methods for Resting-State Data

During the typical acquisition time of resting-state studies of 5-10 minutes (Barkhof et al., 2014), the patients are instructed to relax and not to think of something in particular (van den Heuvel and Hulshoff Pol, 2010). Even though 5 minutes seem to be enough to investigate resting-state connectivity (Van Dijk et al., 2010; Whitlow et al., 2011), the reliability increases with longer acquisition times (Birn et al., 2013). Because no task is needed for resting-state studies, the method is suitable for investigating populations such as children, subjects with dementia, or patients with reduced consciousness (coma or sedation), where performing task-based fMRI might be problematic (Cole et al., 2010; Barkhof et al., 2014). Furthermore, it can be applied to animals like rodents as well, opening opportunities for translational studies (Pan et al., 2015). However, one has to keep in mind that altered states of consciousness, e.g. due to anesthesia (Greicius et al., 2008; Boveroux et al., 2010; Noirhomme et al., 2010; Williams et al., 2010; Magnuson et al., 2014) or sleep (Larson-Prior et al., 2009, 2011; Koike et al., 2011; Sämann et al., 2011), are able to alter the resting-state connectivity (Barkhof et al., 2014). There are different methods available for the investigation of resting-state data.

1.2.4.1. Seed-based Region of Interest Correlation Analyis (Seed ROI)

In seed-based correlation analyses, one or more regions of interest (ROI) are selected a priori, and the fMRI signal of the seed ROI is then compared to the signal of all other brain regions, using correlation or general linear model techniques (Cole et al., 2010; Van Dijk et al., 2010; Barkhof et al., 2014). This univariate method (analyzing the correlation of the seed ROI with each other data point separately, while ignoring the relationships between multiple data points) is the most straightforward way for the analysis of resting-state data, especially for hypothesis-driven studies (McKeown et al., 1998; van den Heuvel and Hulshoff Pol, 2010; Barkhof et al., 2014). The results are easy to interpret, since one is asking a simple

question about the connectivity (“which region is functionally connected with the ROI”) and receiving a direct answer (Cole et al., 2010; van den Heuvel and Hulshoff Pol, 2010). However, there are also disadvantages, e.g. the susceptibility for structured spatial confounds, such as structured noise (head motion effects, scanner-induced artifacts, or influences from the cardiac and respiratory cycle; Cole et al., 2010). Furthermore, the results may strongly depend on the choice of the seed region (including the choice of the specific voxel), which can result in a large amount of variability in results and subsequent interpretations (Cole et al., 2010).

1.2.4.2. Independent Component Analysis (ICA)

Another method that gained more and more popularity during the last two decades is the independent component analysis (ICA; see chapter 1.2.4.2.1). In contrast to seed based correlation techniques, the ICA is a multivariate technique (taking relationships between multiple data points into account; Barkhof et al., 2014). In short, the ICA decomposes the fMRI data into a set of spatially independent components (ICs), where each component is consisting of a collection of brain regions with an internally consistent temporal signal (i.e. the regions within a component are functionally connected; Barkhof et al., 2014). However, the voxel values of the component do not represent the gray values of the fMRI measurements. Instead, these values represent the relative amount a given voxel is modulated by the time course of that component (McKeown et al., 1998). Therefore, if two voxels in the spatial map of a component (which are thought to be functionally connected due to the sharing of the components associated time course) are having the same values, this does not mean that the fMRI signals of both voxels have to be correlated (which would be the case for voxels in the maps of seed-correlation analyses). The fact that the ICA is a model free technique, requiring no prior assumptions (e.g. which brain region to choose as a seed ROI), is a great benefit especially for explorative studies (van den Heuvel and Hulshoff Pol, 2010). However, there are some disadvantages as well. For example, the independent components are often perceived as more difficult to understand than traditional seed-based connectivity maps, as they contain a more complex representation of the data (Fox and Raichle, 2007; van den Heuvel and Hulshoff Pol, 2010). Additionally, the choice of dimensionality (i.e. one has to tell the ICA algorithm how many components to estimate) is somewhat arbitrary (Cole et al., 2010).

1.2.4.2.1. ICA explained

For the interested readers, this chapter explains how ICA is functioning more precisely. If not stated otherwise, it is a compilation of the book “Independent Component Analysis - A Tutorial Introduction” by Stone, 2004, and the following journal papers: McKeown et al., 1998; Hyvärinen and Oja, 2000; Brown et al., 2001b; Stone, 2002; Beckmann and Smith, 2004. For a more comprehensive description of the following, the reader is referred to any of these mentioned works. Readers familiar with the theory behind ICA may skip this section and continue with section 1.2.4.3.

The independent component analysis (ICA) is a blind source separation (BSS) technique, and therefore related to other BSS techniques like the principal component analysis (PCA) or factor analysis (FA). The basic idea of ICA is to extract a set of underlying source signals $s_1, s_2, \dots, s_n = S$ from a set of signal mixtures $x_1, x_2, \dots, x_n = X$, that were produced by an unknown mixing process M:

$$\begin{pmatrix} \boldsymbol{s_1} \\ \boldsymbol{s_2} \\ \dots \\ \boldsymbol{s_n} \end{pmatrix} \times \begin{pmatrix} \boldsymbol{m_1} \\ \boldsymbol{m_2} \\ \dots \\ \boldsymbol{m_n} \end{pmatrix} = \begin{pmatrix} \boldsymbol{x_1} \\ \boldsymbol{x_2} \\ \dots \\ \boldsymbol{x_n} \end{pmatrix} \tag{12}$$

$$\boldsymbol{S \times M = X}$$

This is done by finding an unmixing matrix W (which is actually the inverse of the mixing matrix, i.e. M'), that can be used to reconstruct a set of underlying independent components (ICs) $c_1, c_2, \dots, c_n = C$ from the signal mixtures $x_1, x_2, \dots, x_n = X$:

$$\begin{pmatrix} \boldsymbol{x_1} \\ \boldsymbol{x_2} \\ \dots \\ \boldsymbol{x_n} \end{pmatrix} \times \begin{pmatrix} \boldsymbol{w_1} \\ \boldsymbol{w_2} \\ \dots \\ \boldsymbol{w_n} \end{pmatrix} = \begin{pmatrix} \boldsymbol{c_1} \\ \boldsymbol{c_2} \\ \dots \\ \boldsymbol{c_n} \end{pmatrix} \tag{13}$$

$$\boldsymbol{X \times W = C}$$

The classical example is the so called “cocktail party problem”. Imagine two (or more) people talking at a party, whose voices are recorded by two (or more) microphones (in order to extract n sources, at least n different signal mixtures are needed). Each microphone is recording a time-varying audio signal that is a mixture (weighted sum)

of the voices of both speakers. The ICA can then be used to find an unmixing matrix (the inverse of the mixing process), that can be used to reconstruct two (or more) audio signals from which each comprises the voice of one of the two (or more) speakers (see figure 10).

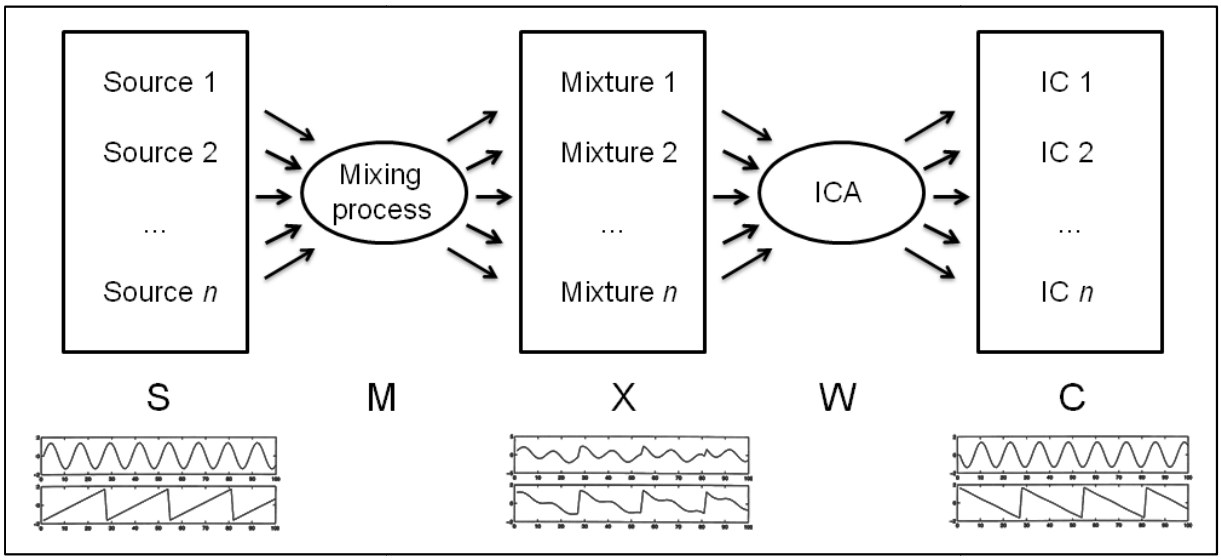

Figure 10: Independent Component Analysis Scheme
A set of source signals $s_1, s_2, \dots, s_n = S$ is mixed by an unknown mixing process M, resulting in a set of signal mixtures $x_1, x_2, \dots, x_n = X$. The independent component analysis (ICA) is finding an unmixing matrix W, that can be used to reconstruct the independent components (ICs) $c_1, c_2, \dots, c_n = C$ from the set of signal mixtures (top). A classical example is the reconstruction of audio signals, e.g. extracting individual voices from mixture recordings of those voice signals (bottom). Note that the ICA is unable to preserve the sign or scale of the signals, which is why the inverse of the source signals may be recovered as well. Furthermore, the number of components to be extracted could be specified in advance (e.g. set to 2 like in this example), or the algorithms might estimate the number of components by themselves. In the latter case, the extraction of components is usually stopped when the extraction of further components would not explain much more of the data's variance. The illustrations of audio signals (waveforms) are reprinted from Hyvärinen and Oja, 2000 with permission from Elsevier.

Unfortunately, the ICA is unable to preserve the sign or scale of the signals, which is why the inverse of the source signals may be recovered as well. However, this is no problem for most applications. Additionally, there is not only one solution of the unmixing matrix W. Because of this, running an ICA several times on the same data might in theory produce several different outcomes. In order to overcome this problem, algorithms like *ICASSO* have been introduced, that evaluate the consistency of estimated ICs over several runs (Himberg et al., 2004). Even though if the ICs extracted by two consecutive ICAs on the same data set might be identical, their ordering might still be different. Therefore, the algorithms are usually ordering the independent components by their amount of explained variance to the data (Beckmann and Smith, 2004). It is also worth noting the problem of dimensionality

when using ICA. The number of components to be extracted could be specified in advance, or the algorithms might estimate the number of components by themselves. In the latter case, the extraction of components is usually stopped when the extraction of further components would not explain much more of the data's variance.

While for example PCA assumes that the source signals are uncorrelated, ICA is based on the assumption that the source signals are not only uncorrelated, but statistically independent (hence the name). If two signals are statistically independent, then knowing the value of one signal provides absolutely no information about the corresponding value of the other signal, which is not always the case for uncorrelated signals. For example, if one defines $x = \sin z$ and $y = \cos z$ (where $z = 0 \ldots 2\Pi$) then x and y are uncorrelated. However, $x^2 = \sin^2 z$ and $y^2 = \cos^2 z$ are negatively correlated, which is why knowing the value of x still provides information about the value of y (indirectly via the square of the values). Now, the ICA algorithms are trying to find an unmixing matrix that maximizes the independence of the extracted components. It is usually assumed that the underlying source signals are less Gaussian than mixtures of those source signal. Therefore, by maximizing a measure of non-Gaussianity, one is able to extract the source signals. There are different approaches to counter this problem, and the exact method can differ between different algorithms. For example, the *infomax* algorithm by Bell and Sejnowski, 1995 maximizes the entropy of the signals extracted by the unmixing matrix, whereas the *FastICA* algorithm as used by Beckmann and Smith, 2004 maximizes the neg-entropy. However, other measures of non-Gaussianity like the kurtosis are possible as well.

Instead of using ICA to derive the source signals of audio signals, it can also be applied to fMRI data (see figure 11). The fMRI data is representing a temporal sequence of images, with each image consisting of a set of pixels. In general, each column of the data array X is an image at one timepoint, whereas each row of X is the temporal sequence of one pixel over time. Because of this, for fMRI data the ICA may maximize independence either over time (rows) or space (columns). Temporal ICA (tICA) is finding mutually independent temporal sequences and a corresponding set of unconstrained images. However, for fMRI data, spatial ICA (sICA) is usually the method of choice. In Contrast to tICA, sICA is finding mutually independent images and a corresponding set of unconstrained temporal sequences. The temporal

sequence can be viewed as a weight factor, which determines how much a spatially independent component contributes to the overall observed mixture signal at any given point of time. This means that the signal observed at a given voxel is modeled as a sum of the contributions of all the independent components.

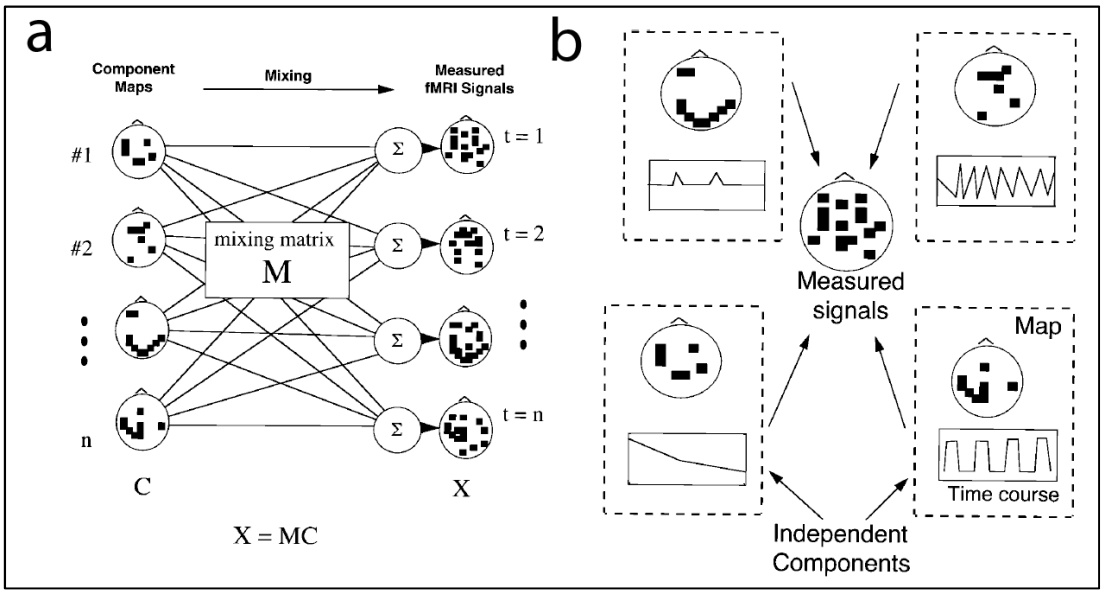

Figure 11: Independent Component Analysis of fMRI Data
a) The source signals of the fMRI signal, i.e. the brain areas covered by the different voxels, could be represented as a mixture of independent components. The mixing matrix M specifies the relative contribution of each component C to the measured fMRI signal X at each time point. The ICA finds an unmixing matrix that separates the observed component mixtures into the independent components. b) Each independent component consists of a component map, representing the spatial distribution of voxel values, and an associated time course of activation. The signal observed at a given voxel is modeled as a sum of the contributions of all the independent components. Note that the active areas of the statistically independent maps may be partially overlapping. McKeown et al., 1998, reproduced with permission from John Wiley and Sons.

There are two major analysis tools for the analysis of group fMRI data using ICA (Schöpf et al., 2010). The first one is GIFT (Group ICA Toolbox, http://icatb.sourceforge.net/) introduced by Calhoun et al., 2001, and the second one is the MELODIC (Multivariate Exploratory Linear Optimized Decomposition into Independent Components) tool of FSL (Beckmann and Smith, 2004). In order to analyze group data, these tools are usually using a concatenation approach, i.e. concatenating the fMRI runs of all subjects in the temporal domain. This means, the ICA algorithm virtually acts as if it is analyzing a very long run of one subject, instead of multiple runs of several subjects, and thereby extracts the underlying components that are shared by all or most of the subjects. However, MELODIC offers two different ways of performing an ICA on the data of multiple subjects. One can either run a 3 dimensional (3D) Tensor-ICA, where individual data sets will be represented as a time x space x subjects tensor of data (Beckmann and Smith, 2005), or one can

concatenate the data of all individuals in the temporal domain, and run a single 2D ICA on the concatenated data matrix (Calhoun et al., 2001; Beckmann et al., 2005). But since the 3D Tensor-ICA assumes that the temporal response pattern is the same across the population, which cannot be assumed for resting-state data, the 2D temporal concatenation approach is more appropriate for the analysis of functional connectivity in the resting-state.

After extracting spatially independent component maps from the fMRI data, MELODIC uses a Gaussian/Gamma mixture model in order to distinguish meaningful signals from the overall noisy signal (Hartvig and Jensen, 2000; Beckmann and Smith, 2004; see figure 12). The noise is modeled by a Gaussian distribution, and the intensity values of the independent component maps are transformed to Z-scores by dividing them by the estimate of the voxel-wise noise standard deviation. In contrast to raw IC estimates, the Z-score maps depend on the amount of variability explained by the entire decomposition at each voxel location. Finally, a Gaussian/Gamma mixture model is fitted to the individual maps in order to infer voxel locations that are significantly modulated by the associated time course. Voxels whose Z-scores are included in the Gaussian part of this model are assumed to represent noise, whereas voxels whose Z-scores are covered by one of the two Gamma curves are assumed to be “activated” voxels (i.e. their intensity value is some standard deviations different from the overall noise). Finally, the component maps can be thresholded appropriately, displaying only “activated” voxels (Beckmann and Smith, 2004).

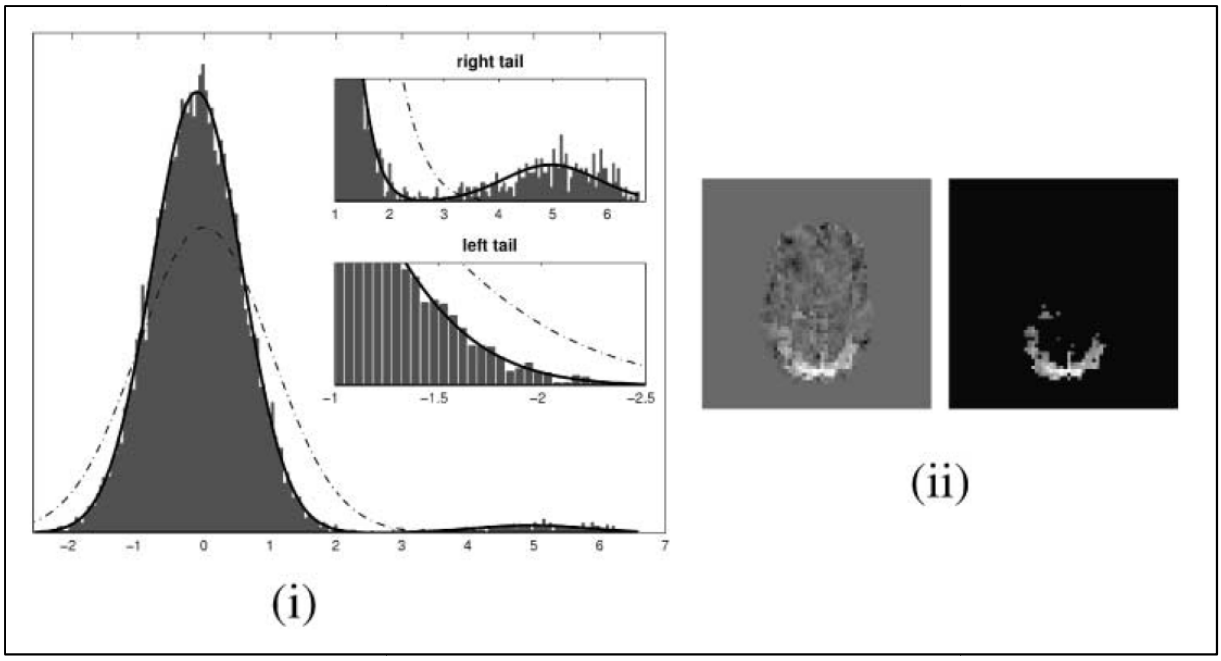

Figure 12: Gaussian/Gamma Mixture Model
(i) In order to distinguish meaningful signal from the overall noisy signal, the voxels intensity values are first transformed to Z-scores. Afterwards, a Gaussian and two Gamma curves are fitted to the intensity values, where the Gaussian curve is assumed to include the noise, and the Gamma curves are assumed to include the "activated" voxels, which are significantly modulated by the components associated time course. (ii) The left picture shows the raw IC map, and the right picture the thresholded IC map after Gamma/Gaussian mixture modeling. Beckmann and Smith, 2004, reprinted with permission © 2004 IEEE.

1.2.4.3. Dual Regression

At least two different methods have been developed for comparing the independent components of different groups, e.g. comparing an experimental group with a control group. For example, GIFT uses a back-projection approach which returns subject-specific maps and time courses after running ICA on the temporally concatenated group data (Calhoun et al., 2001; Schöpf et al., 2010). However, MELODIC uses a somewhat different approach called dual regression (Beckmann et al., 2009; Filippini et al., 2009). This approach uses the group-level spatial maps (from the multi-subject ICA components) as a set of spatial regressors in a General Linear Model (GLM) for the individual subject data, in order to get subject specific time courses for the multi-subject components. These subject specific time courses are normalized to unit variance, and then used as temporal regressors in a GLM for the individual subject data, in order to find subject specific maps which are still associated with the group-level spatial maps (Beckmann et al., 2009). Finally, the individual spatial maps are compared statistically, for example using nonparametric permutation testing (Nichols and Holmes, 2003; Beckmann et al., 2009; Winkler et al., 2014). This approach has

turned out to be an effective and reliable approach for the exploratory analysis of resting state fMRI data, with a moderate-to-high short- and long-term test-retest reliability (Zuo et al., 2010).

1.2.5. Seed ROI and ICA compared

Fortunately, comparing seed ROI with ICA, both methods tend to show a strong overlap between their results, supporting the existence of several functionally connected resting-state networks (Biswal et al., 2010; van den Heuvel and Hulshoff Pol, 2010). For example, functional connectivity in the primary motor network, which was originally revealed by seed based analyses (Biswal et al., 1995; Xiong et al., 1999; Cordes et al., 2001), has been replicated using ICA (Beckmann et al., 2005; Damoiseaux et al., 2006). And the DMN has been consistently found both using ICA (Beckmann et al., 2005; Damoiseaux et al., 2006) or seed-correlation techniques (Greicius et al., 2003; Whitfield-Gabrieli et al., 2009). There are some additional methods for the analysis of resting-state data as well, e.g. the principal component analysis (PCA) (Friston et al., 1993), clustering methods (Cordes et al., 2002; Thirion et al., 2006; van den Heuvel et al., 2008a), or graph analysis (Salvador et al., 2005b; Achard, 2006; Achard and Bullmore, 2007; Liu et al., 2008; van den Heuvel et al., 2008b). But seed based correlation and the application of ICA seem to be the most common used techniques for the analysis of resting-state data.

The test-retest reproducibility of resting-state fMRI studies seems to be variable (Barkhof et al., 2014), from low (Wang et al., 2011) to moderate to high (Van Dijk et al., 2010; Zuo et al., 2010; Chou et al., 2012; Guo et al., 2012; Seibert et al., 2012; Patriat et al., 2013). In a study using the pooled data of 1414 subjects from 35 different centers, and using both seed correlation as well as ICA analyses, Biswal et al., 2010 demonstrated that there is indeed a center-related variation present in the rs-fMRI data. But nevertheless, their study still provided evidence for a universal intrinsic functional architecture, and revealed consistent effects of age and sex on rs-fMRI measurements, that were detectable across centers despite the presence of center-related variability (Biswal et al., 2010). Therefore, rs-fMRI has proven to be a useful tool for the investigation of brain connectivity, for example in order to examine possibly altered functional connectivity in neurologic and psychiatric brain disorders, such as dementia (Rombouts et al., 2009), Alzheimer's disease (Greicius et al., 2004; Rombouts et al., 2005), depression (Greicius et al., 2007), and of course

schizophrenia (Bluhm et al., 2007; Garrity et al., 2007; Liu et al., 2008; Whitfield-Gabrieli et al., 2009; Karbasforoushan and Woodward, 2012; see chapter 1.2.7).

1.2.6. Resting-State Networks

1.2.6.1. Default Mode Network

In the late 90's, researchers started to notice that some specific areas in the human brain consistently reduced their activity while performing various novel, non-self-referential, goal-directed tasks, when these tasks were compared with the resting-state (Shulman et al., 1997; Binder et al., 1999; Raichle, 2015). Using PET measurements of regional blood flow and oxygen consumption, Raichle and colleagues concluded that these brain areas were not "activated" in the resting-state (e.g. caused by experimentally uncontrolled cognition) but rather were indicative of a "heretofore-unrecognized organization within the brain's intrinsic or ongoing activity" (Gusnard and Raichle, 2001; Raichle et al., 2001; Raichle, 2015). They titled their paper "A Default Mode of Brain Function", and thereby shaped the term "default mode network". Furthermore, together with the findings of Biswal et al., 1995, this laid the foundation for the investigations of other resting-state networks as well (Raichle et al., 2001; Raichle, 2015). In contrast to other resting-state networks, the regions of the DMN are known to show an elevated level of neuronal activity during rest, and diminish their activity during the performance of goal-directed tasks. This is suggesting that the activity of this network is reflecting a default state of the human brains neuronal activity (Raichle et al., 2001; van den Heuvel and Hulshoff Pol, 2010). According to the sentinel hypothesis, which views the DMN as a network for monitoring the external environment, this seems to be of great importance (Buckner et al., 2008). For example, the detection of predators should not require the intentional allocation of attentional resources. Instead, these resources should be allocated automatically and be continuously available, except if focused attention is needed for a successful task performance (Raichle et al., 2001). However, there are alternative hypotheses as well, e.g. the internal mentation hypothesis, which states that the DMN contributes directly to cognitive performances such as internal mentation (for review see Buckner et al., 2008).

1.2.6.1.1. Human DMN

The human DMN is comprised of three major subdivisions, namely the ventral medial prefrontal cortex (vmPFC), the dorsal medial prefrontal cortex (dmPFC), and the posterior cingulate cortex (PCC) including adjacent precuneus and the lateral parietal cortex (Raichle, 2015; see figures 13 and 14). Another area that has been associated with the DMN is the entorhinal cortex (Raichle, 2015).

The vmPFC seems to be a key structure in a network of areas which receive sensory information from the external world and the body via the orbital frontal cortex, and relay that information to structures such as the hypothalamus, the amygdala, and the periaqueductal gray of the midbrain (Rolls and Baylis, 1994; Carmichael and Price, 1995; Ongür and Price, 2000; Raichle et al., 2001; Barbas, 2007; Raichle, 2015). It seems to be involved in important components of an individual's personality, such as social behavior, mood control, and motivational drive (Raichle et al., 2001; Raichle, 2015). For example, it has been shown that the emotional state of the subject has a direct effect on the activity level in the vmPFC component of the default mode network (Simpson et al., 2001a, 2001b; Raichle, 2015). In contrast to the vmPFC, the dmPFC has been associated with self-referential judgments (Gusnard et al., 2001; Raichle, 2015).

Due to a significant relationship between the hippocampal formation and the posterior elements of the DMN (Vincent et al., 2006), these areas (i.e. the posterior cingulate cortex and the adjacent medial precuneus, together with the lateral parietal components of the DMN) have been consistently associated with the successful recollection of memory (Vincent et al., 2006; Raichle, 2015).

In summary, the DMN seems to be involved in emotional processing (vmPFC), self-referential mental activity (dmPFC), and the recollection of prior experiences (posterior elements of the DMN; Raichle, 2015). The individual parts of the DMN can be differentially affected during the performance of different tasks (Gusnard et al., 2001; Andrews-Hanna et al., 2010), but the available evidence indicates that the functions of the default mode network are never completely turned off. Instead, they seem to be carefully modulated (i.e. enhanced or attenuated), depending on the current demands (Raichle, 2015).

1.2.6.1.2. Rat DMN

As fMRI and especially rs-fMRI can also be measured in other species such as rodents, it is an ideal tool to bridge between animal models and research in human diseases like schizophrenia due to the direct translational value, meaning the same test can be done both in an animal model and in human patients (Gorges et al., 2017).

Lu et al., 2012 were the first to describe a network in the rat that is homologous to the human DMN, even though some aspects of DMN-like functional connectivity in rats were reported one year earlier by Upadhyay et al., 2011. This rat DMN is mainly comprised of frontal areas and areas along the central midline, including the ventral, lateral and rostral medial orbital frontal cortex (OFC, VO, LO, rMO), the rostral dorsal prelimbic cortex (PrL), the cingulate cortex (Cg1 and Cg2), the retrosplenial cortex (RSC; both granular and dysgranular retrosplenial cortex RSG/RSD), the rostral and dorsal posterior parietal cortex (PtPR, PtPD) as well as the medial secondary visual cortex (V2M). Furthermore, the primary and secondary auditory cortex (Au1, AuD, AuV) and the temporal association cortex (TeA), as well as the dorsal hippocampus (CA1) also appear to be involved (Lu et al., 2012; see figure 13). Another group also reported the involvement of the infralimbic cortex (IL), septal and thalamic nuclei, as well as the bilaterally anticorrelated sensorimotor region (Sierakowiak et al., 2015). But it should be mentioned that the latter group was using a seed correlation approach, placing their seed ROI in the rostral anterior cingulate cortex (ACC), whereas the former group was using an ICA approach.

As can be seen in figure 13, the DMNs of rats and humans are similar, but not identical. For example, the connectivity between anterior and posterior cingulate cortices includes the entire midline in the rat brain, whereas it remains more focal in the human (Lu et al., 2012). The orbital areas (VO, LO, rMO), PrL, and ACC are components of the rat prefrontal cortex, whereas the RSG and RSD are homologous to the human posterior cingulate cortex (Kolb, 1990; Price, 2007; Lu et al., 2012). Furthermore, the posterior parietal cortex (PPC) and the V2M are part of the rat parietal association cortex (Torrealba and Valdés, 2008; Lu et al., 2012).

The frontal orbital areas are part of the so called orbital medial prefrontal cortex (OMPFC), which can be divided into a medial “emotional motor” network, and into a

orbital “viscerosensory” network, receiving inputs from several sensory modalities (Floyd et al., 2000, 2001; Lu et al., 2012). In general, all the structures involved in the rat DMN seem to receive high-order information from virtually all sensory modalities, and are having direct or indirect connections with core limbic structures such as the hippocampus or amygdala, suggesting the involvement of memory and emotional behavior (Lu et al., 2012). Therefore, Lu et al., 2012 proposed that the main function of the rat DMN might be the evaluation of the internal and external milieu of the body by the integration of interoceptive and exteroceptive information.

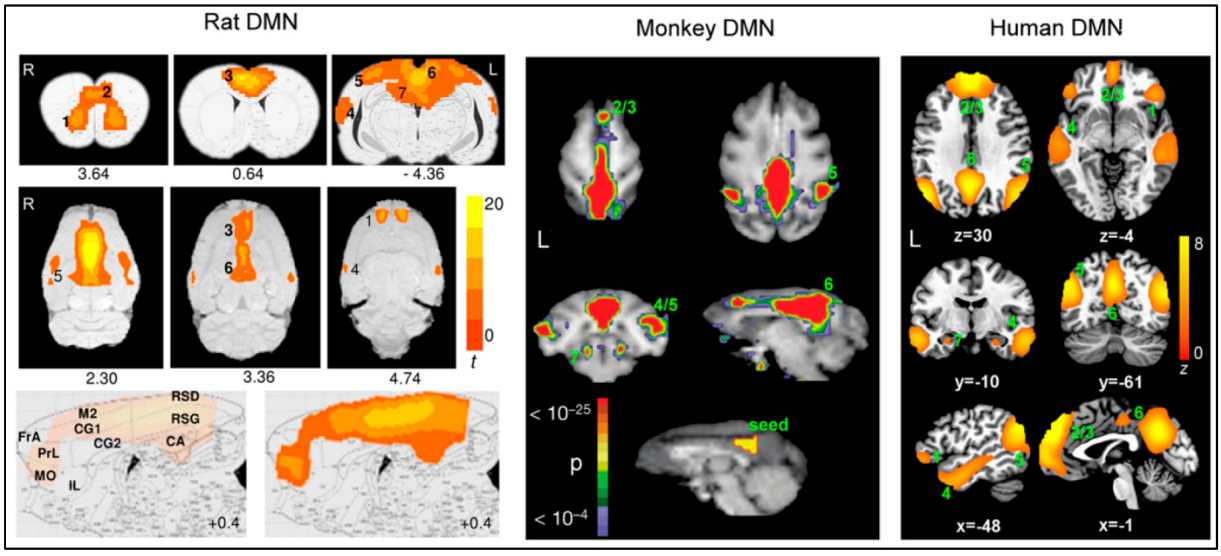

Figure 13: Comparison of the DMN in Rats, Monkeys and Humans.
The rat DMN (left) mainly included (1) the orbital cortex, (2) prelimbic cortex (PrL), (3) cingulate cortex (Cg1, Cg2), (4) auditory/temporal association cortex (Au1, AuD, AuV, TeA), (5) posterior parietal cortex (PPC), (6) retrosplenial cortex (corresponding to the human posterior cingulate cortex, PCC) and (7) the hippocampus (CA1). The monkey DMN (middle) included (2/3) the dorsal medial prefrontal cortex, (4/5) the lateral temporoparietal cortex, (6) the posterior cingulate/precuneus cortex and (7) the posterior parahippocampal cortex. The human DMN (right) included (1) the orbital frontal cortex, (2/3) the medial prefrontal cortex/anterior cingulate cortex, (4) the lateral temporal cortex, (5) the inferior parietal lobe, (6) the posterior cingulate/retrosplenial cortex, and (7) the hippocampus/parahippocampal cortex. Reprinted from Lu et al., 2012, reproduced with permission from the National Academy of Sciences (PNAS); The monkey DMN (middle) was adapted by Lu et al., 2012 from (Vincent et al., 2007) and is reproduced with permission from Springer Nature.

1.2.6.2. Other known Resting State Networks

In addition to the DMN, some other resting-state networks have been found to date (see figure 14). For example, Fox et al., 2005 noted the presence of anticorrelations (i.e. opposing activity) in the resting state between the default mode network and a “task-positive network” during the performance of novel, attention-demanding tasks (Raichle, 2015). This “task-positive network” may be better divided into the dorsal attention network (DAN; Corbetta and Shulman, 2002; Fox et al., 2006; Vincent et al.,

2008; Raichle, 2015), the salience network (SLN; Seeley et al., 2007; Day et al., 2013) and the executive control network (ECN; Beckmann et al., 2005; Seeley et al., 2007; Vincent et al., 2008). However, the literature seems to be not fully consistent regarding this classification. Besides of differences in analysis methods, this is why there might be some overlap between the areas involved in those networks.

Furthermore, somatosensory networks like a sensorimotor network, a visual network, or an auditory network were constantly revealed both in humans (Biswal et al., 1995; Beckmann et al., 2005; Damoiseaux et al., 2006; De Luca et al., 2006) and in rodents (Hutchison et al., 2010; Becerra et al., 2011; Jonckers et al., 2011; Lu et al., 2012; Sierakowiak et al., 2015), even though the extent and overlap between these networks varies between studies and analysis methods.

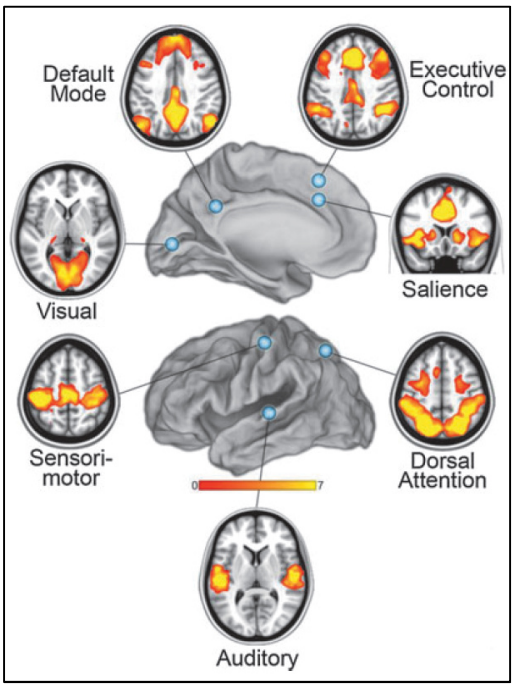

Figure 14: Overview of the Main Resting-State Networks.
All these seven brain networks have been revealed by seed correlation techniques. In addition to the default mode network, other higher order cognitive networks such as the executive control network, the salience network, or the dorsal attention network have been revealed as well. The somatosensory networks include a visual network, an auditory network, and a sensorimotor network. Reproduced with Permission from Raichle, 2011, the publisher for this copyrighted material is MaryAnn Liebert, Inc. publishers.

1.2.7. Resting-State and Schizophrenia

Several studies reported alterations in the resting-state connectivity in patients diagnosed with schizophrenia (for review see e.g. Karbasforoushan and Woodward, 2012; Yu et al., 2015; Sheffield and Barch, 2016; Hu et al., 2017).

Studies investigating the functional connectivity of the DMN in schizophrenic patients found diverging results, reporting both reduced (hypo-) and increased (hyper-) connectivity of the DMN, as well as increased connectivity between the DMN and other non-DMN regions (Greicius, 2008; Broyd et al., 2009; Karbasforoushan and Woodward, 2012). For example, reduced connectivity between the PCC and the lateral parietal mPFC, the precuneus and the cerebellum, modulated by symptom severity, was reported by Bluhm et al., 2007 and further supported by the study of Garrity et al., 2007. The finding of reduced connectivity between the PCC and the mPFC was subsequently replicated, and linked to cognitive impairment of schizophrenic patients (Rotarska-Jagiela et al., 2010; Camchong et al., 2011; Karbasforoushan and Woodward, 2012). However, the majority of studies were reporting an increased connectivity of the DMN. For instance, an increased connectivity between DMN components and the PCC, as well as the mPFC was reported by Whitfield-Gabrieli et al., 2009. Interestingly, the connectivity between the DMN and the mPFC was not only increased in schizophrenic patients, but in first-degree relatives as well (Whitfield-Gabrieli et al., 2009). A number of other studies replicated this finding of hyper-connectivity of the DMN (Mannell et al., 2010; Salvador et al., 2010; Skudlarski et al., 2010; Woodward et al., 2011; Karbasforoushan and Woodward, 2012; Mingoia et al., 2012; Wang et al., 2015). Furthermore, some studies reported reduced deactivations of the DMN (i.e. hyper-connectivity) during the performance of different tasks in task-based fMRI (Pomarol-Clotet et al., 2008; Salgado-Pineda et al., 2011). Additionally, the spatial extend of the DMN appears to be expanded in schizophrenic patients, exhibiting greater connectivity with brain regions normally not included in the DMN (Mannell et al., 2010; Woodward et al., 2011; Karbasforoushan and Woodward, 2012; Mingoia et al., 2012). This evidence of DMN enlargement and reduced segregation between the DMN and other resting-state networks may provide indirect support for the neurodevelopmental hypothesis of schizophrenia, as the etiology of schizophrenia might disrupt the normal processes of network integration and segregation during brain development (Karbasforoushan and Woodward, 2012).

Other findings include reduced resting-state connectivity within the PFC, and between the PFC and other brain regions (PFC dysconnectivity), that might be related to cognitive impairment (Zhou et al., 2007b, 2007a; Rotarska-Jagiela et al., 2010; Cole et al., 2011; Woodward et al., 2011; Karbasforoushan and Woodward,

2012). Additionally, Woodward et al., 2012 found a variable pattern of reduced connectivity between the PFC and the dorsomedial thalamus, as well as increased thalamic connectivity with cortical motor and somatosensory areas (Karbasforoushan and Woodward, 2012; Woodward et al., 2012). Further studies reported reduced connectivity between the ventral mPFC and the amygdala (Hoptman et al., 2010; Tian et al., 2011; Karbasforoushan and Woodward, 2012), as well as widespread reductions in connectivity between cortical regions and the cerebellum (Collin et al., 2011; Liu et al., 2011a; Karbasforoushan and Woodward, 2012). All these findings are in favor of the cognitive dysmetria hypothesis by Andreasen et al., 1998, which posits that schizophrenia is resulting from abnormal functional interactions between the cortex, sub-cortical structures, and the cerebellum (Wolf et al., 1993; Andreasen et al., 1998; Karbasforoushan and Woodward, 2012; Sheffield and Barch, 2016). The disruption of thalamo-cortical networks may actually explain a wide array of clinical and cognitive disturbances observed in schizophrenic patients (Jones, 1997; Karbasforoushan and Woodward, 2012), a view which is supported by findings of reduced prefrontal-thalamic connectivity using both task-based and resting-state fMRI (Mannell et al., 2010; Skudlarski et al., 2010; Karbasforoushan and Woodward, 2012).

Moreover, several studies reported correlations between the functional dysconnectivity and both positive and negative symptoms (Karbasforoushan and Woodward, 2012). For example, hyper-connectivity of the DMN was associated with worse clinical symptoms (Whitfield-Gabrieli et al., 2009; Woodward et al., 2011), or reduced connectivity between the left temporoparietal junction (TPJ) and the bilateral anterior cingulated cortex was associated with more severe auditory-verbal hallucinations (Vercammen et al., 2010; Wolf, 2011).

Finally, there is some evidence for an altered spectral power (i.e. contribution of frequencies to the resting-state signal) in schizophrenic patients. For example, Garrity et al., 2007 reported that most power of the rs-fMRI signal in healthy controls was within the normal range of 0.01-0.1 Hz (0.067 Hz), whereas most power in schizophrenic patients was in the higher frequency range of 0.13 Hz. Subsequently, Mingoia et al., 2013 also reported an altered spectral power of schizophrenic patients, shifted towards higher frequencies compared to controls.

In conclusion, investigations of resting-state connectivity yielded various abnormalities in schizophrenic patients when compared with healthy controls. Even though the findings are often in opposite directions, there is nevertheless a clear evidence for an altered functional connectivity in schizophrenia, which even shows some potential as a possible biomarker for the clinical diagnosis of schizophrenia (Shen et al., 2010; Yu et al., 2013; Wang et al., 2015).

However, little is known about the functional connectivity in rodent animal models of schizophrenia. A thorough search revealed only two studies covering this topic which were published before 2017 (i.e. before formulating hypotheses for this study). The first study of Guevara et al., 2013 investigated the resting-state connectivity of Sprague Dawley rats, which received an injection of LPS into the corpus callosum at postnatal day (PD) 3. This study reported that the seed-based functional connectivity analysis showed no significant effect of LPS exposure, even though there was a consistent trend towards increased connectivity in the LPS group for one of their contrasts (Guevara et al., 2013). Furthermore, the second study of Song et al., 2015 reported an abnormal brain connectivity in a newly developed EGR3 (early growth response) gene transfected rat model.

1.3. Hypotheses and Aim of Thesis

Due to the lack of studies using resting-state fMRI in MIA models, this thesis aimed at further investigating resting-state connectivity in rodent models of schizophrenia by using the LPS model of schizophrenia in rats.

In the following sections, studies on resting-state fMRI and the same behavioral tests applied in this thesis are shortly reviewed, and hypotheses stated based on the current available knowledge. Mouse and rat studies are covered for Poly(I:C) and LPS, with gestational administration times presented in a sequential order within each block.

1.3.1. Elevated Plus Maze

As the EZM is thought to measure a very similar construct as the EPM (see section 1.1.3.1.1), those studies were included in the following as well.

Literature search for the EPM task in rodent models of MIA revealed a total of 24 studies (14 mouse, 10 rats) which were published before 2017 (i.e. before formulating hypotheses for this study; see appendix 6.1.1, tables 25 and 26), reporting mixed results.

Mouse studies using Poly(I:C) during early gestation (~GD 9) as immunogenic agent are consistently reporting no differences between MIA offspring and controls in the EPM task (Meyer et al., 2005; Giovanoli et al., 2013, 2016; Lipina et al., 2013; Li et al., 2014), while only one study using Poly(I:C) on GD 12 reports reduced open arm time and entries in adult MIA offspring suggestive of increased anxiety, however, this effect was only present in males and not in female MIA offspring (Majidi-Zolbanin et al., 2015).

Mouse studies using LPS as immunogenic agent are reporting mixed results regarding its influence on EPM measures. Using LPS during early gestation (GD 9-10) seems to either reduce the time spent in the open arms of the maze in early adult (PD 56-70) offspring (Depino, 2015) or to increase it (Asiaei et al., 2011; Solati et al., 2015). However, one may note that the two latter studies used LPS from *Salmonella enterica*, whereas nearly all other studies investigating MIA in rodents are using LPS from *Escherichia coli*, and the use of LPS from different bacterial strains may result in different immune responses and thus behavioral outcomes (Erridge et al., 2002; Fortier et al., 2007). Using LPS during mid-late gestation (GD 15-17), only one study reports increased time spent in the open arms, and this effect was only present in adult female mice treated with one of the larger doses (Chlodzinska et al., 2011). Enayati et al., 2012 reports dose- and timing-dependent anxiety-like effects in both adolescent (PD 40) and early adult (PD 80) NMRI mice using LPS from *Salmonella enterica*. Babri et al., 2014 reports similar effects in the EPM and EZM in early adult NMRI mice, however in the same study C57BL/6 mice behaved not differently from controls. Hava et al., 2006 reports reduced open arm times in adult (PD 240) C57BL/6 mice, whereas another study from the same lab found no differences from controls during the same age (Golan et al., 2006). However, in the latter study, longer distances moved and more rearing behavior in the closed arms was observed in aged (PD 600) MIA offspring, while the open/closed-arm time ratio still was not different from controls.

From three rat studies using Poly(I:C) during mid-late gestation (GD 14-18) as immunogenic agents, one study reports reduced time spent in the open arms in late adolescent (PD61) offspring (Yee et al., 2011), whereas two studies from another lab report no differences from controls utilizing the EZM (Vorhees et al., 2012, 2015).

From seven rat studies using LPS as immunogenic agent, after early (GD 9-10.5) treatment one study reports no effects in adult (PD90) offspring (Kirsten et al., 2010b) and one study reports reduced time spent in the open arms (Lin et al., 2012). After LPS during mid-late gestation (GD 15-19), three studies report no differences from controls (Foley et al., 2014b; Wischhof et al., 2015b; Yin et al., 2015) and one study reports reduced time in the open arms (Yin et al., 2013). Interestingly, the studies of Yin et al. 2013 and 2015 are from the same department and methodologically quite comparable, apart from the fact that they used Wistar rats in their study from 2013 showing an effect on anxiety related behaviors, while they used Sprague Dawley rats in their study from 2015 where those effects were absent (Yin et al., 2013, 2015). Finally, (Bakos et al., 2004) found increased entries into both open and closed arms (i.e. increased locomotor activity) in adult female MIA offspring. Unfortunately, they do not report the times spent in the open or closed arms, and they also did not look at male behavior in the EPM.

Taken together, prenatal Poly(I:C) treatment seems to mostly have no effects on behavior in the EPM, especially in mice, however the impact of prenatal LPS on anxiety measured by the EPM is still not clear. Because a former study from this department using the same protocol found no differences in adult LPS offspring (Wischhof et al., 2015b), it is hypothesized to replicate the absence of effects on EPM behavior.

Recent studies reporting no differences between MIA and control offspring in mice (Vuillermot et al., 2017; Morais et al., 2018) or rats (Gray et al., 2019) support the notion that prenatal Poly(I:C) has no effect on EPM behavior in the offspring. One may note that (Morais et al., 2018) reported significantly reduced time spent in the open arms by MIA offspring of Swiss mice, however, this statement is based on post-hoc analyses which were done after a non-significant ANOVA result, which is why they here are counted as showing no effect.

Recent studies on the effect of LPS still remain inconclusive. A mouse study using LPS on GD 15-17 reports fewer movements between arms in late adolescent-early adult (PD 63) MIA offspring, indicative of an anxious phenotype, without reporting the time spent in the open or closed arms (Hsueh et al., 2017), whilst others report that MIA offspring (PD 60-120) spent increased time in the open arms (Schaafsma et al., 2017). Another mouse LPS study reports less time spent in the open arms (Wang et al., 2019), but this study used a transvaginal injection paradigm in order to induce a maternal vaginal inflammation, compared to intraperitoneal, intravenous or subcutaneous injection routes used by all other MIA studies. Finally, one rat study using LPS on GD 14 reports no differences in MIA offspring (Mouihate et al., 2019).

1.3.2. Open Field

As the main motivation for using the open field was to assess symptoms of anxiety, i.e. to test for difference in center time, only studies looking at the percentage of center/periphery stay of the animals (i.e. thigmotaxis) were included in the following short review.

Literature search for such open field tasks in rodent models of MIA revealed a total of 23 studies (13 mouse, 10 rats) which were published before 2017 (i.e. before formulating hypotheses for this study; see appendix 6.1.2, tables 27 and 28), reporting mixed results.

From mouse studies using Poly(I:C) during early gestation (GD 9) as immunogenic agent, (Meyer et al., 2005, 2006b, 2008a) are reporting reduced entries into or time spent in the center of the open field by adult Poly(I:C) offspring, without changes in general locomotion. On the other hand, (O'Leary et al., 2014) observed no differences in the open field task, neither in adolescent nor in adult Poly(I:C) offspring. (Smith et al., 2007) used Poly(I:C) on GD 12, and found reduced entries into the center by the Poly(I:C) offspring, accompanied by reductions in overall locomotion. In the study by (Meyer et al., 2006b), in addition to injecting Poly(I:C) on GD 9, they also looked at offspring from dams receiving Poly(I:C) on GD 17, which had no significant effects on the open field behavior of the offspring. Finally, (Ozawa et al., 2006) injected Poly(I:C) from GD 12-17, and are reporting no differences between MIA offspring and controls at the adolescent stage (PD 35). However, they are reporting increased entries into and time spent in the center of the open field by

the MIA offspring at an early adult age (PD ~66), without differences in general locomotion.

Using LPS as immunogenic agent on GD 9 in mice, (Depino, 2015) report early adult MIA offspring have an increased latency to enter the center, and also spent less time in the center compared to controls, accompanied by a hypolocomotion. Injecting LPS from GD 8-15, (Wang et al., 2010) report mixed results in adult LPS offspring. They tested the offspring at four different ages (PD 70, 200, 400 and 600), and while male LPS offspring showed no differences compared to controls on the first three time points, female LPS offspring showed less time spent in the center of the open field accompanied by increased locomotion on PD 200, but not on PD 70 or 400. On PD 600 however, both male and female LPS offspring showed an increased latency to cross the first grid of the open field, without significant changes in other parameters. From five mouse studies using LPS in late gestation (PD 16-17), one report reduced time spent in the center accompanied by a general decrease in locomotion in MIA offspring (Al-Amin et al., 2016). (Babri et al., 2014) and (Golan et al., 2005) found no differences between MIA offspring and controls in open field behavior. In the study by (Chlodzinska et al., 2011), only offspring of the 300µg/kg LPS group showed statistically significant increases of entries into and time spent in the center of the open field, accompanied by an overall increased locomotion. Finally, in the study by (Golan et al., 2006), LPS offspring showed an increased overall locomotion, as well as a tendency towards increased distance moved in the center of the open field at PD 600, but not earlier at PD 240.

Two rat studies using Poly(I:C) on mid-late gestation (GD 14 or 14-18), both report no differences between Poly(I:C) offspring and controls (Vorhees et al., 2012, 2015).

Using LPS as immunogenic agent in rats on GD 10.5, (Lin et al., 2012) found that male offspring spent reduced time in the center and females showed reduced locomotion in a large open field. The two rat studies using LPS during mid gestation (GD 12-13) both report no differences between MIA and control offspring (Poggi et al., 2005; Foley et al., 2014a). Using LPS in mid-late gestation (GD 15-16) in rats, (Harvey and Boksa, 2014a) found no treatment effects in adolescent offspring. However, early adult LPS offspring spent less time in the corners of a large open field than control offspring (Harvey and Boksa, 2014a). In the study by (Wischhof et al., 2015b), LPS offspring showed increased rearings accompanied by an increased

locomotion at both PD 33 and 60. Additionally, LPS offspring spent increased time in the center of the open field at PD 33, while this parameter was only at trend level at PD 60 (Wischhof et al., 2015b). The last three studies using LPS in mid-late gestation found no differences between LPS and control offspring (Foley et al., 2014b; Wischhof et al., 2015a; Santos-Toscano et al., 2016).

Taken together, one cannot yet make clear statements regarding the impact of prenatal Poly(I:C) or LPS on the open field behavior in mice or rats. Previous studies from this department using a similar protocol revealed increased rearings, time in center and overall increased locomotion at PD 33 and 60, but not at PD 100-120 (Wischhof et al., 2015a, 2015b). Therefore it is hypothesized to replicate this hyperactive anxiolytic-like phenotype in juvenile and adolescent but not in adult LPS offspring.

One recent study using a mouse Poly(I:C) model treating dams on either GD 9 or 17 reports decreased time spent in the center of the open field by the Poly(I:C) offspring of both gestational treatment time points, while the general locomotion was increased compared to control offspring (da Silveira et al., 2017). Treating dams with Poly(I:C) on GD 12.5, (Morais et al., 2018) report no differences in open field behavior in adult offspring. (Ronovsky et al., 2017) used a similar paradigm but tested the F2 generation rather than the direct offspring, and found no differences in open field behavior. (Carlezon et al., 2019) also found no treatment effects of prenatal Poly(I:C) alone. They did, however, also apply a two-hit model using a postnatal injection of LPS in addition to the MIA treatment, and two-hit offspring did show reduced time in the center of the open field in male mice, as well as reduced locomotion in female mice (Carlezon et al., 2019). On the other hand, (Dabbah-Assadi et al., 2019) report increased time in the center of the open field in adult female Poly(I:C) offspring, regardless of the gestational treatment time point (either GD 12.5 or 17.5), but not in adult males or adolescent animals of either sex. In contrast to this finding, (Sheu et al., 2019) report no differences in adolescent animals (PD 42), but a reduction in time spent in the center of the open field at PD 63 and 84, after treating dams using Poly(I:C) on GD 17.

A recent study using LPS as immunogenic agent in mice throughout GD 0-16 (four injections in total), found that early adult (PD 60) LPS offspring shows reduced time in the center of the open field (Wang et al., 2019). Using LPS in mice on GD 12.5

(Braun et al., 2019) are reporting that LPS offspring show a lack of decrease in locomotion (habituation) over the 20 minute open field session. In addition, female LPS offspring also showed reduced center time during the second half of the test. Treating mouse dams with LPS on GD 15-17 (Hsueh et al., 2017) found that early adolescent (PD 35) LPS offspring spent less time in the center of the open field compared to controls. (Schaafsma et al., 2017) used the same gestational time points for the LPS injection but investigated the outcome in adult offspring, reporting no differences between the treatment groups.

A recent rat study using LPS on GD 11 reports increased locomotion in juvenile but not in adult LPS offspring (Delattre et al., 2017). (Straley et al., 2017) investigated the effects of prenatal LPS in juvenile, adolescent and early adult rats after injections on two different gestational time points, and report no differences in LPS offspring from dams treated on GD 12 in all age groups. LPS offspring from dams treated on GD 16 however, showed reduced locomotion and a trend towards more time spent in the center on PD 9, increased time spent in the center on PD 30, as well as reduced locomotion on PD 60 (Straley et al., 2017). Lastly, (Mouihate et al., 2019) reports no differences in open field behavior after prenatal LPS treatment on GD 15-19.

Therefore, even looking at more recent results, the effects of MIA on general open field behaviors in mice or rat still remain inconclusive.

1.3.3. Novel Object Recognition

Literature search for (spontaneous) object recognition tests in rodent models of MIA revealed a total of 18 studies (8 mouse, 10 rats) which were published before 2017 (i.e. before formulating hypotheses for this study; see appendix 6.1.3, tables 29 and 30). Although these studies were using different mouse or rat strains, different types and doses of immunogenic agents, as well as different gestational time points, the vast majority report deficits in object recognition tests in MIA offspring.

(Lipina et al., 2013) report only spatial recognition memory deficits but intact object memory in mice after 5 mg Poly(I:C) administered on GD 9. Furthermore, half the dose had no significant effects on either memory forms. In contrast, (Li et al., 2014) report object recognition memory deficits in early adult mice offspring after Poly(I:C) administered on GD 9.5. Mouse studies using Poly(I:C) on either GD 12.5 or throughout GD 12-17 report deficits in object recognition memory in early adult MIA

offspring (Ozawa et al., 2006; Fujita et al., 2016; Han et al., 2016), with the exception of one study by (Ito et al., 2010), which reports enhanced object recognition in late adolescent/early adult MIA offspring compared to controls. However, the latter study differed in several ways from other studies, e.g. they excluded MIA litters from the analysis which did not show PPI deficits compared to controls and they used percent nose pokes to the objects instead of time interacting with the objects as measure for calculating the recognition ratio, in addition to using a very short retention interval of only 5 minutes (Ito et al., 2010). The deficits observed in the described studies often seem to be present already in juvenile or early adolescent MIA offspring (Fujita et al., 2016; Han et al., 2016), even though Ozawa et al., 2006 reports deficits only in early adult and not in adolescent animals.

With regard to mouse studies using LPS as immunogenic agent, (Coyle et al., 2009) found object recognition memory deficits in adult offspring after MIA on GD 8, whereas (Golan et al., 2005) report increased novel object recognition performance compared to controls after MIA on GD 17.

Five rat studies injecting Poly(I:C) on GD 15 all report deficits in object recognition memory in (early) adult MIA offspring (Wolff et al., 2011; Howland et al., 2012; Ballendine et al., 2015; Vernon et al., 2015; Luchicchi et al., 2016), with the exception of (Howland et al., 2012), reporting only deficits in an associative object-in-place test but not in the classical object recognition memory paradigm.

Using LPS as immunogenic agent during mid-late gestation (GD 14-20), (Graciarena et al., 2010) show deficits in early adult offspring using a retention interval of 3h, but not using an retention interval of one minute. (Foley et al., 2014a) found no differences between adolescent MIA and control offspring using a similarly short retention interval of two minutes after LPS on GD 12. Using LPS on GD 15-16, (Harvey and Boksa, 2014a) report no differences as well, in contrast to (Wischhof et al., 2015b) and (Kentner et al., 2016), with both studies reporting deficits in object recognition memory in (early) adult MIA offspring.

Taken together, there are clear hints towards impaired object recognition memory in adult MIA offspring, regardless of the rodent species or type of immunogen used. At least in Poly(I:C) mouse models, these deficits seem to be present already in juvenile

animals, whereas studies using rats and/or LPS as immunogenic agent are reporting mixed results regarding the onset of recognition memory deficits.

Therefore, it was hypothesized that offspring of LPS treated dams in the current study should show deficits (i.e. an reduction) in object recognition memory as adults (PD ~90). Since two of the three studies being methodologically most comparable to this study report no deficits in object memory between PD 43-58 (Foley et al., 2014a; Harvey and Boksa, 2014a), whereas Wischhof et al., 2015 showed deficits in LPS offspring on PD 70, it was further hypothesized that these deficits might manifest earliest at PD ~64, i.e. that juvenile (PD ~30) and adolescent (PD ~42) MIA offspring would not show any differences in object recognition memory compared to controls.

Recent studies using Poly(I:C) mouse models nearly all report deficits in object recognition memory in MIA offspring as adults as well (Han et al., 2017; Richetto et al., 2017; Matsuura et al., 2018; Dabbah-Assadi et al., 2019; Sheu et al., 2019). However, in the study of Dabbah-Assadi et al., 2019, only adult female Poly(I:C) offspring showed these impairments. Richetto et al., 2017 investigated the impact of Poly(I:C) administration on two different gestational time points (GD 9 and 17), and only offspring from dams treated on GD 17 seemed to develop recognition memory deficits. Furthermore, one study failed to show object recognition deficits (Morais et al., 2018). In this study, they report that one-sample t-tests of the discrimination index against the chance level were not significant for all groups. However, in C57BL/6 control mice, this test nearly reached significance ($p=0.066$) compared to C57BL/6 Poly(I:C) mice ($p=0.748$). Considering the quite long retention interval of 24 hours, this suggests almost intact object memory in control mice, but not in Poly(I:C) mice, therefore actually showing a hint towards deficits in object recognition memory in MIA offspring.

Recent studies using rat MIA models also report deficits in object recognition memory using either Poly(I:C) (Osborne et al., 2017; Gray et al., 2019) or LPS (Simões et al., 2018) during mid/late gestation (GD 14-16). (Delattre et al., 2017) are reporting both object- and object-in-place recognition memory deficits in juvenile offspring after LPS on GD 11. In their discussion, they also state that the non-spatial memory impairment persisted until adulthood, however, their results section shows no such deficits in adult MIA offspring. Finally, one further recent study injecting LPS on GD 15-16

reports similar object recognition in late adolescent MIA offspring compared to controls (Swanepoel et al., 2018).

1.3.4. Prepulse Inhibition

Literature search for PPI in rodent models of MIA revealed a total of 54 studies (25 mouse, 29 rats) which were published before 2017 (i.e. before formulating hypotheses for this study; see appendix 6.1.4, tables 31 and 32). Although these studies used different mouse or rat strains, different types and doses of immunogenic agents, as well as different gestational time points, the majority report deficits in PPI in MIA offspring. This is especially true for the mouse studies, whereas there is more variation in the results of rat studies.

1.3.4.1. PPI: Mice – Poly(I:C)

Using Poly(I:C) as immunogenic agent during early gestation on GD 9.5 in mice, (Shi et al., 2003) report deficits in PPI in adolescent (PD~50) MIA offspring, using the highest of the used doses and using the more intense prepulses. (Makinodan et al., 2008) also report PPI deficits in late adolescent MIA offspring after early insult, in line with (Zhu et al., 2014b) and (Gonzalez-Liencres et al., 2016). In the latter study, Poly(I:C) offspring did not only show less PPI than controls using the higher prepulses, but also showed prepulse facilitation when the lowest prepulse was used (Gonzalez-Liencres et al., 2016). Looking at (young) adult offspring, (Meyer et al., 2005) report deficits after early immune activation by Poly(I:C), using the higher doses used. Similar results were found by several others (Meyer et al., 2008b, 2008a, 2010; Li et al., 2009; Vuillermot et al., 2011; O'Leary et al., 2014; Weber-Stadlbauer et al., 2016). One may note that (O'Leary et al., 2014) report PPI deficits in MIA offspring using the two louder prepulses, however, using the lowest prepulse, MIA offspring showed statistically significant increases in PPI compared to controls. (Giovanoli et al., 2016) failed to show PPI deficits in adult Poly(I:C) offspring if MIA was the only factor. However, they used a relatively low dose compared to most other studies, and they did show PPI deficits in MIA offspring exposed to a stress battery during early life (two-hit model).

Some studies investigated the effect of prenatal Poly(I:C) both in adolescent and adult offspring. (Vuillermot et al., 2010) report no differences in PPI between MIA and control offspring after Poly(I:C) on GD 9 at early adolescence (PD 35), however,

these MIA offspring showed deficits in PPI at early adulthood (PD 70). In contrast, (Giovanoli et al., 2013) report no difference in MIA offspring, neither in adolescence (PD ~43) nor as adults (PD ~90). However, similar to their later work mentioned before, they used a relatively low dose compared to others, and they did show PPI deficits in offspring of a two-hit model of combined MIA and stress. (Lipina et al., 2013) used two different doses of Poly(I:C), and observed no differences at both ages using the lower dose. However, using the higher dose, significant PPI impairments were emerging in adult MIA offspring. Finally, (Eßlinger et al., 2016) report no differences in either age group in male animals, but female Poly(I:C) offspring showed PPI impairments as adults that could not be observed as juveniles.

Using Poly(I:C) as immunogenic agent during mid gestation on GD 12 in mice, (Smith et al., 2007) report deficits in PPI in MIA offspring (no age of testing stated). (Deslauriers et al., 2013) are reporting statistically significant PPI deficits in 36 days old Poly(I:C) offspring in the text, their figures however show no such difference. Nevertheless, in the same study, offspring of a two-hit model (Poly(I:C) + restrain stress) showed deficits in PPI, which was later replicated once more (Deslauriers et al., 2013, 2014).

Three studies used Poly(I:C) as immunogenic agent in mice during late gestation on GD 15/16, and all are reporting deficits in adult MIA offspring (Cardon et al., 2010; de Miranda et al., 2010; Zhang and van Praag, 2015). In contrast, the studies of (Meyer et al., 2008b) and (Li et al., 2009) did not observe PPI deficits in adult MIA offspring using Poly(I:C) in mice on GD 17. Two further studies injected Poly(I:C) throughout mid to late gestation (GD 12-17), and both studies report no effects in juveniles (PD 28/35), but in adults (PD ~70) (Ozawa et al., 2006; Han et al., 2016).

1.3.4.2. PPI: Mice – LPS

To the best of my knowledge, no study accessible before 2017 investigated the impact of prenatal LPS on PPI in mice.

1.3.4.3. PPI: Rats – Poly(I:C)

With regard to studies using rats, only one study used Poly(I:C) as immunogenic agent in early gestation on GD 9, reporting PPI impairments in adult MIA offspring (Song et al., 2011). All other rat studies before 2017 injected Poly(I:C) in mid/late

gestation, usually on GD 14 or 15. (Wolff and Bilkey, 2008) report a trend towards statistical significant PPI differences as juveniles (PD 35), which turned into more robust significant PPI differences as adults. (Ballendine et al., 2015) report the opposite, i.e. statistical significant differences as juveniles, which turn into only a trend later as adults, while (Howland et al., 2012) showed statistical significant PPI impairments in MIA offspring as juveniles and during late adolescence (PD 56). In the latter study, prepulse facilitation instead of PPI was observed using the 30 ms ISI. Further, (Wolff and Bilkey, 2010) showed statistical significant PPI impairments in MIA offspring as juveniles and as adults. Most other studies only investigated the MIA effects in young adult offspring, with many studies reporting significantly impaired PPI in Poly(I:C) animals (Cardon et al., 2010; Dickerson et al., 2010; Yee et al., 2011; Maayan et al., 2012; Mattei et al., 2014; Luchicchi et al., 2016). (Vorhees et al., 2012) also state significant PPI impairments in adult female (but not male) Poly(I:C) offspring, although there were no statistically significant effects or interactions revealed by their initial ANOVA analysis. (Missault et al., 2014) report no differences in PPI between Poly(I:C) and control offspring, similar to (Van Den Eynde et al., 2014), who report no differences in PPI neither on PD 56, 90 nor 180. Finally, (Vorhees et al., 2015) report no impairments in PPI in the sub-group of Poly(I:C) offspring from dams which showed high weight gain after Poly(I:C) treatment, but a trend towards increased PPI compared to controls in the sub-group of Poly(I:C) offspring from dams which showed low weight gain after Poly(I:C) treatment.

1.3.4.4. PPI: Rats – LPS

(Fortier et al., 2007) investigated the effects of both prenatal Poly(I:C) and prenatal LPS, using different doses and three gestational timings. Early adult offspring of Poly(I:C) dams did not behave statistically significantly different from control offspring, regardless of the gestational timing of treatment. Injecting LPS during early gestation (GD10-11) also had no significant effects on PPI in the offspring, however, both offspring of LPS dams which received treatment during mid or late gestation (GD 15-16 / 18-19) showed significantly reduced PPI. In contrast, in the study of (Waterhouse et al., 2016) which used the same three gestational timings, only offspring from dams treated during the early gestational window showed significantly decreased PPI, whereas offspring from both later gestational treatment windows behaved not different from control offspring. However, one should note that despite

using the same gestational timings and LPS serotype, several other parameters such as dose and route of injection differed between both studies.

Using LPS during mid gestation on GD 15-16, (Harvey and Boksa, 2014a) report no effects on PPI in late adolescent / young adult (PD ~65) LPS offspring if MIA was the only prenatal insult. However, the study reports additive effects of prenatal LPS and prenatal iron deficiency on PPI in a two-hit model (Harvey and Boksa, 2014a). Using the same gestational timing, (Wischhof et al., 2015b) report no differences in PPI in juvenile and early adolescent LPS offspring, but PPI deficits were observed during puberty (PD 45) and as adults (PD 90). However, one may note that the PPI deficits in adult LPS offspring were only observed after an exploratory second test-session using longer prepulse-pulse intervals which was not planned beforehand, as no significant differences were observed during that age using the prepulse-pulse intervals which were also used on the previous time points (Wischhof et al., 2015b). A second study of this group also reports impaired PPI in adult LPS offspring (Wischhof et al., 2015a), similar to a study by (Santos-Toscano et al., 2016).

Using LPS during late gestation on GD 18-19, (Fortier et al., 2004a) report no differences in PPI in LPS offspring compared to control offspring.

Other working groups used far more severe MIA models. Administering LPS every 2nd day throughout the whole pregnancy, PPI deficits were observed starting at PD 35 (no significant deficits on PD 28), persisting throughout adolescence and adulthood up to an old age (PD 400) (Borrell et al., 2002; Romero et al., 2007, 2010). Another working group also administered LPS every 2nd day throughout pregnancy, however starting only at GD 7. Using this scheme, no differences between LPS and control offspring were observed in juvenile offspring (PD 30), but consistent PPI deficits are reported in adult offspring (Basta-Kaim et al., 2011b, 2011a, 2012, 2015).

Taken together, the majority of studies show that MIA by both Poly(I:C) and LPS often leads to deficits in PPI in the MIA offspring. One may note however, that these differences are not always prominent. For example, some studies investigate PPI using different prepulse-pulse intervals, and in some of them only one or two of the up to five intervals reach the threshold of statistically significant differences, thus the PPI deficits seem to depend on the ISI (Ballendine et al., 2015; Wischhof et al., 2015a; Santos-Toscano et al., 2016). The same can be said regarding studies

investigating PPI using different prepulse intensities, where only some (usually the louder) prepulses reach statistical significance between MIA and control offspring (Shi et al., 2003; Ozawa et al., 2006; Cardon et al., 2010; de Miranda et al., 2010; Vuillermot et al., 2010; Yee et al., 2011; Ballendine et al., 2015; Zhang and van Praag, 2015; Santos-Toscano et al., 2016; Swanepoel et al., 2018). Also, studies using different pulse intensities, reveal that the deficits in MIA offspring also depend on the startle pulse intensity (Li et al., 2009; Vuillermot et al., 2010, 2011; Weber-Stadlbauer et al., 2016). Further, there are a series of studies showing that the deficits are not measurable during the juvenile or early adolescent stage, and only start emerging during or after puberty (Ozawa et al., 2006; Vuillermot et al., 2010; Basta-Kaim et al., 2011a, 2012; Wischhof et al., 2015b; Eßlinger et al., 2016; Han et al., 2016; Ding et al., 2019). The large variability of MIA experiments in general, with dependencies on many different factors, might be further influencing variability in the outcome of MIA on PPI. Finally, apart from very few exceptions, nearly no study is reporting increased PPI in MIA offspring, compared to controls.

Therefore, it was hypothesized that offspring of LPS treated dams in the current study should show deficits in PPI emerging during or after puberty, persisting into adulthood.

Recent studies using Poly(I:C) mouse models add further evidence for PPI deficits in MIA offspring (Richetto et al., 2017; Luan et al., 2018; Nakamura et al., 2019). Interestingly, as written before, there seem to be no studies investigating the impact of prenatal LPS on PPI in mice, even though there are working groups using these models to assess other symptoms of psychiatric diseases (see previous sections on NOR, EPM and OF, for example). The only study in recent years seems to be the one by (Imai et al., 2018), who are reporting no significant differences in PPI between LPS and control offspring in CD-1 mice. Therefore, one might speculate that before either no one felt the desire to investigate the impact of LPS on PPI in mice offspring, or that previous attempts also were “negative” and were therefore never published due to publication bias (for reviews on the problem of publiation bias, see e.g. Mlinarić et al., 2017 or Nair, 2019).

Recent studies using Poly(I:C) rat models are also mostly reporting PPI deficits (Meehan et al., 2017; Li et al., 2018; De Felice et al., 2019; Ding et al., 2019; Gogos et al., 2020), except the studies by (Lins et al., 2018; Gray et al., 2019) which are

reporting no significant effects on PPI. Looking at LPS rat models, only the study of (Swanepoel et al., 2018) reports significant deficits in PPI, whereas two further studies show no differences (Simões et al., 2018; Capellán et al., 2019).

1.3.5. Resting-State fMRI

The only available study published before 2017 (i.e. before formulating hypotheses for this study) using postnatal LPS on resting-state functional connectivity based on rodent models is the study of Guevara et al., 2013, where a trend towards increased connectivity in the LPS group for one of their contrasts was found.

Furthermore, an unpublished Master thesis from this department analyzing resting-state fMRI measurements from LPS offspring based on the works of Wischhof et al., 2015b via ICA and qualitative analysis as well as the dual-regression approach, found hints for increased connectivity of LPS offspring within a DMN-like component as well within an interhemispheric anticorrelations component. However, the former result was attributed at least in part to a vascular origin, while the origin of the latter components later turned out to be the result of scanner artifacts (Coors, 2015, unpublished).

Thus, due to the lack of rodent studies on effects of maternal immune activation on resting-state fMRI, one could only use studies with human schizophrenic patients as further reference, considering that the maternal immune activation models using LPS or Poly(I:C) already have shown good construct validity (Meyer and Feldon, 2010; Reisinger et al., 2015; Haddad et al., 2020b).

Based on the previous findings of human studies, investigating resting-state connectivity in schizophrenic patients and healthy controls, it was hypothesized that LPS rats would display an altered resting-state connectivity compared to control rats. However, due to the bidirectional findings of human studies, it was difficult to further specify the direction of possible changes, i.e. both hypo-connectivity and hyper-connectivity would have been possible. Nevertheless, since the majority of studies reported increased (hyper-) connectivity of the DMN in human patients, and the two available studies investigating resting-state connectivity in rodent models of schizophrenia are pointing towards an increased (hyper-) connectivity as well (see chapter 1.2.7), a potential increased connectivity was considered to be probable in comparison to reduced (hypo-) connectivity.

Although only few studies were published on this topic after 2017, the recent studies investigating resting-state connectivity in the MIA model don't change the general hypothesis, as those results are mixed as well. A study of an MIA model using prenatal IL-6 infusions during whole gestation in Sprague Dawley rats (instead of the indirect induction of inflammation using Poly(I:C) or LPS) found reduced functional connectivity in MIA offspring between PD ~22-50 from the left amygdale to left caudate putamen and ventral pallidum using seed ROI analysis (Mills, 2018). Furthermore, using Poly(I:C) on GD 15, Missault et al., 2019 have found increased functional connectivity in the DMN in a subpopulation of MIA offspring on PD ~84 in Wistar-Han rats using seed ROI analysis. This hyper-connectivity was most pronounced in the posterior parietal and temporal association cortices, and was only shown in Poly(I:C) offspring of those mothers who lost weight after Poly(I:C) injection (Missault et al., 2019). Finally, in a mouse model using Poly(I:C) on GD 12.5, a reduction of functional connectivity in cortical-limbic connectivity circuits and enhanced connectivity in the temporal association cortex in MIA offspring was shown on PD ~84 using seed ROI analysis (Kreitz et al., 2020).

2. Material & Methods

2.1. Animals and LPS Treatment

Male and female Wistar rats were obtained from Charles River (Sulzfeld, Germany) at the age of 8-10 weeks, and housed in groups of four in Standard Makrolon (Type IV) cages until breeding. All breeding animals were kept at 22 °C temperature and 50-55% humidity under a 12 h dark/light cycle (lights on at 7 a.m.) with *ad libitum* access to standard lab chow (Altromin Spezialfutter GmbH & Co. KG, Lage, Germany) and tap water. Starting at PD ~90, the estrous cycle of the female rats was controlled routinely as described by (Howland et al., 2012), i.e. vaginal smear samples were taken by inserting a pipette tip containing 20 µl saline into the vagina and ejecting and immediately reloading the fluid 2-3 times. The samples were loaded onto glass slides and viewed under a light microscope for the determination of the estrous cycle phase using cytological methods (Marcondes et al., 2002; Hubscher et al., 2005). The animals were bred together when the female rats were in the phase of estrus. Pregnancy was verified by the existence of sperm in the vaginal smear the day after breeding, defined as gestational day 0, and pregnant females were housed individually afterwards. Pregnant females were handled and weighed regularly in order to reduce the stress of the following injections. On gestational days 15 and 16, the pregnant rats received intraperitoneal injections of either saline (SAL, 1 ml/kg) or lipopolysaccharides (LPS, 100, 50 or 20 µg/kg, see further explanations below; from *Escherichia coli* 0111:B4, Product Nr. L4391, Batch Nr. 036M4070V, Sigma-Aldrich, Steinheim, Germany). During the following six hours after the injection, an observer not blind to treatment attempted to score sickness behaviors of the dams, i.e. measures of ptosis (droopy eyelids), piloerection (ruffled coat) and lethargy. However, these observations of sickness behavior were discarded after they were declared unsuitable for a clear confirmation of sickness behavior due to the observer not being blind and not using a standardized scale to note the observations. The weight of the dams was controlled the two following days after injections, and the change in weight after the first injection (i.e. from GD 15 to 16) was noted as either weight gain or weight loss (see results, table 2). Finally, dams were left alone without further disturbance until delivery.

The study was started using 100 µg/kg LPS, as this dose was used successfully in previous studies (Wischhof et al., 2015b, 2015a), and the first dam was treated without undesirable effects using that dose. However, in following dams, this dose led to abortions, reflected by bloody vaginal discharge in the days following treatment and finally absence of delivery. In one case it even led to the death of the dam. Therefore, the dose was initially reduced to 50 µg/kg, and after abortions continued, it was further reduced to 20 µg/kg, which finally again led to viable offspring (see results, table 2).

At birth, number and sex of pups of each dam was noted, and the pups were marked by injecting a small amount of black tattoo ink (Deep Colours! GmbH, Neuburg, Germany) into the left or right front paw, according to (Iwaki et al., 1989). Pups were then cross-fostered with surrogate mothers and mixed litters contained both LPS-treated as well as SAL-treated pups. Litters were left undisturbed until weaning at postnatal day (PD) 21. The offspring were housed in same-sex cages in groups of 5-6 under comparable conditions as the breeding animals, but in a separate colony room. Experimental animals had *ad libitum* access to standard lab chow until they reached the age of PD 70, when the feeding regime was switched to a restricted diet of 12 g chow/rat/day, in order to maintain the bodyweights on 85% of those under free feeding conditions.

In total, 25 SAL-treated control (SAL) and 26 LPS-treated experimental (LPS) animals stemming from 5 (SAL) and 5 (LPS) litters were used for this study (see appendix section 6.4.1, table 99), i.e. a number of animals were sampled from the same litter. From the 26 LPS-treated animals, seven stem from one litter of a dam treated with 100 µg/kg LPS, whereas the remaining 19 stem from four litters where dams were each treated with 20 µg/kg LPS.

Additional 10 SAL and 10 LPS animals (see appendix section 6.4.1, table 100) were euthanized and perfused (see section 2.5) on PD 30 for planned histological experiments.

All animal care and experiments were performed in compliance with international guidelines regarding the use of animals in experiments (2010/63/EU) and were approved by the local ethical committee (Az. 522-27-11/02-00 (111)).

2.2. Study Design

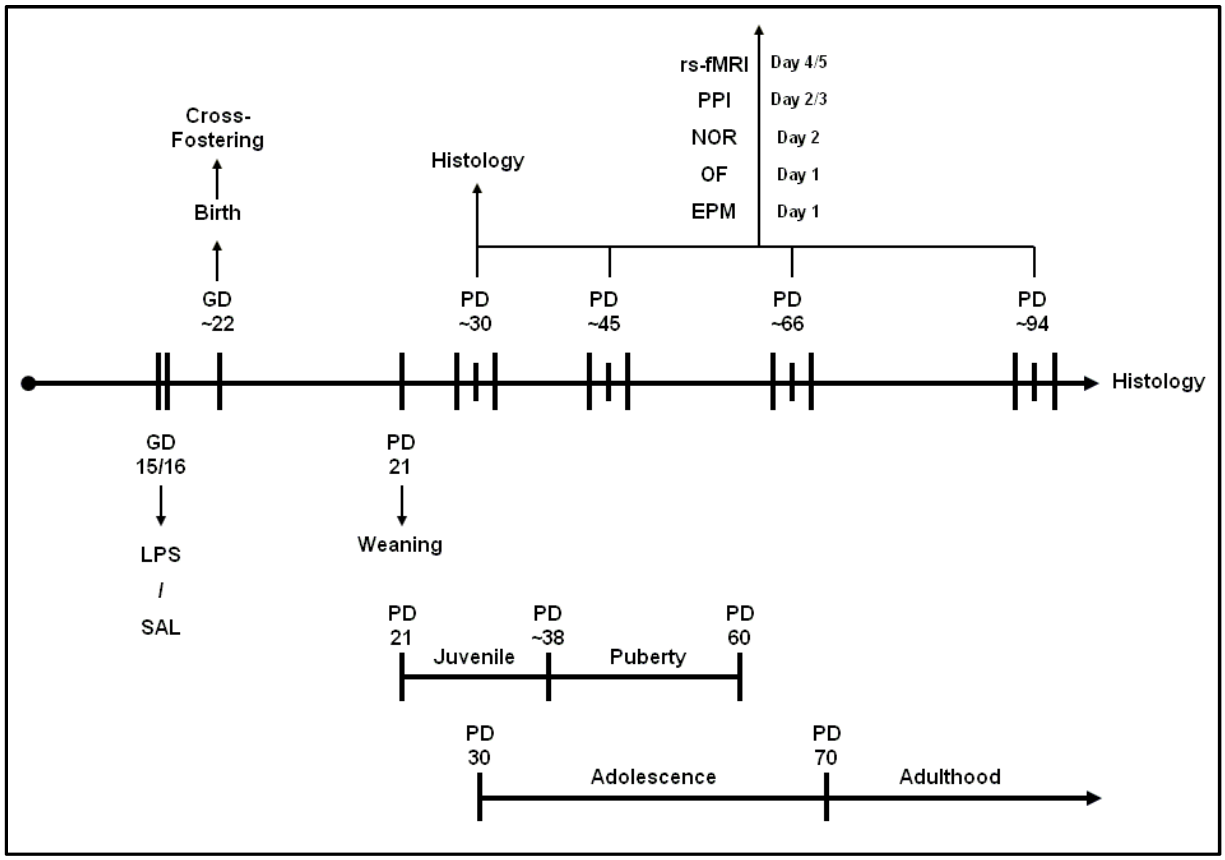

Figure 15: Experimental Design
The pregnancy of dams was verified by existence of sperm in the vaginal smear the day after breeding, defined as gestational day (GD) 0. On GD 15 and 16, dams received injections of either saline (SAL, 1 ml/kg) or lipopolysaccharides (LPS, 100, 50 or 20 µg/kg). After birth on GD~22, animals were cross-fostered with surrogate mothers (mixed litters contained both LPS and SAL offspring). At postnatal day (PD) 21, animals were weaned. A subset of animals was euthanized and perfused for histological experiments on PD~30. The remaining animals underwent a test-battery consisting of the elevated plus maze (EPM), open field (OF), novel object recognition (NOR) and prepulse inhibition (PPI) tests at 4 different developmental stages (juvenile stage on PD~30, puberty on PD~45, late adolescence on PD~66 and adulthood on PD~94). A subset of each experimental group also underwent structural and functional resting-state MRI (rs-fMRI) measurements on the days following the behavioral tests on each of the 4 time blocks. After the last time block, animals were euthanized and perfused for histological experiments.

Starting from PD 21 (weaning), animals were handled regularly and were weighed approximately once a week. Animals were tested in a test battery at four different neurodevelopmental stages, namely PD~30 representing the juvenile stage, PD~45 representing puberty, PD~66 representing late adolescence and PD~94 representing adulthood (see figure 15). The test battery consisted of the elevated plus maze (EPM, section 2.3.1) followed by an open field (OF, section 2.3.2) session on day 1 of each experimental block. On the second day, the animals were first tested in the novel object recognition (NOR, section 2.3.3) test, followed by a first session of prepulse inhibition (PPI, section 2.3.4). A second PPI session was conducted at the

3rd day of each block. All 51 animals underwent the behavioral experiments, but only a subgroup of 10 animals of each experimental group also underwent structural and functional resting-state MRI measurements on either the 4th or 5th day of each experimental block (section 2.4). Approximately a week after the last experimental Block (PD~100), the animals were euthanatized and perfused in order to preserve the brains for histological investigation (section 2.5).

The behavioral test battery was designed in order to supplement the longitudinal resting-state measurements by confirming the presence of core symptoms of schizophrenia-like pathology in the LPS offspring. The EPM and OF tests served as a measure of anxiety-like behaviors, which may be considered a measure of the negative symptoms of schizophrenia (Winship et al., 2019; Ang et al., 2020), the PPI test served as a measure of sensorimotor gating, which has often been seen as a measure of the positive symptoms (Powell et al., 2009; Keil et al., 2016; Ang et al., 2020), while the NOR test served as a measure of recognition memory, corresponding to the cognitive impairments seen in schizophrenia (Young et al., 2009; Rajagopal et al., 2014; Ang et al., 2020).

2.3. Behavioral Experiments

The order in which the animals were tested was pseudo-randomized, but kept constant over all time points (i.e. an animal tested first on PD ~30 was also the first animal to test on PD ~94 etc.).

2.3.1. Elevated Plus Maze

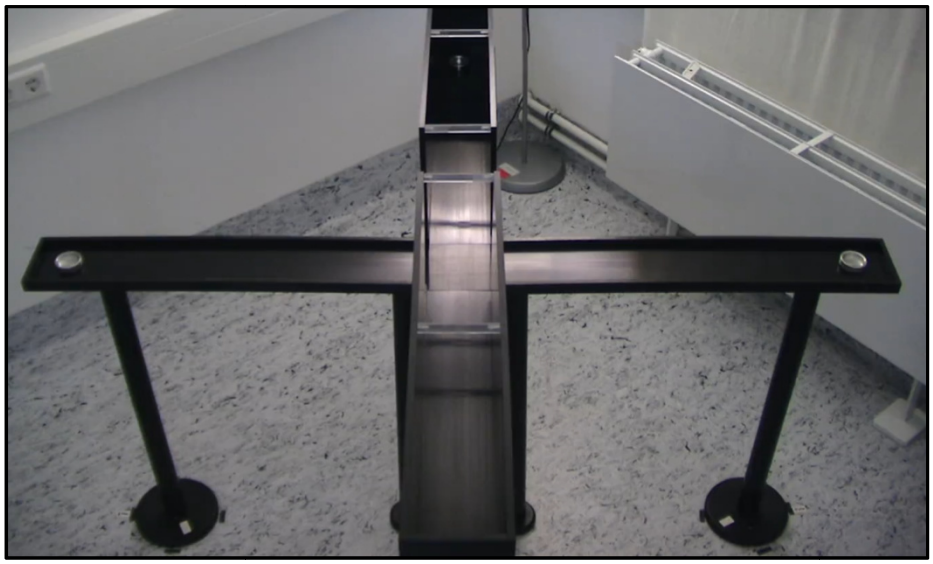

Figure 16: Elevated plus maze

On the first day of each test block, the animals were at first tested for anxiety related behaviors in the elevated plus maze (EPM). The maze was made of black plastic and was elevated 76 cm above the floor (see figure 16). It consisted of two open and two closed arms (76 x 12 cm each, closed arms enclosed with walls of 27 cm height, open arms outlined by 1 cm wide and 1.5 cm high ledges) crosswise connected by a central platform (14 x 14 cm) with each equivalent pair of arms positioned opposite to each other. The maze was indirectly illuminated by a floor lamp resulting in a light intensity of ~55 lx on the open and ~30 lx on the closed arms. The rats were placed on the central platform facing one of the open arms, and their behavior was recorded for 5 minutes by a digital camcorder (Everio GZ-HD3, JVCKENWOOD Deutschland GmbH, Bad Vilbel, Germany) positioned above the maze. The maze was cleaned with 70% ethanol and thoroughly dried before each animal was tested.

The recordings were analyzed by a blind observer using the software BORIS (v.2.993; Friard and Gamba, 2016), and the following behaviors were measured: (1) time spent in the open and closed arms, as well as time spent on the central platform, (2) entries into the open and closed arms, (3) number of rearings (animals are standing upright on two paws with the front paws in the air or leaned against a wall) and (4) number of head dips (risk assessment, defined as peering over the edges of the open arms). Arm entries were counted when all four paws were placed in the respective arm.

Data was prepared as a comma separated file using Excel (2007 v.12, Microsoft Corporation, Redmond, USA) and imported into R (v.4.1.0, R Core Team, 2021), and the open/closed-time ratio was calculated [open arm time / closed arm time] for statistical analysis.

2.3.2. Open Field

Figure 17: Open field box
Shown is one open field box of the Actimot-System produced by TSE

Following the EPM, the animals were placed in the center of infrared-beam operated open field (OF) boxes (see figure 17) made of plastic (44.7 x 44.7 x 44 cm^3, Actimot-System, TSE, Bad Homburg, Germany) and locomotor activity was recorded for 30 minutes. The open field boxes were indirectly illuminated by a floor lamp resulting in a light intensity of ~20 lx in the center of the open field. The open field boxes were cleaned with 70% ethanol and thoroughly dried between each animal.

This session served as habituation to the environment for the novel object recognition test in the same open field boxes 24 h later, as well as test for anxiety and motor related behaviors complementing the EPM experiments.

Parameters analyzed were: (1) Activity (i.e. time spent moving in %), (2) distance traveled in m, (3) time spent in the center of the open field (%, center defined as 50% of the area around the mid-point) and (4) number of rearings in 5 min bins.

Data was prepared as a comma separated file using Excel (2007 v.12, Microsoft Corporation, Redmond, USA) and imported into R (v.4.1.0, R Core Team, 2021) for statistical analysis.

2.3.3. Novel Object Recognition

24 h after habituation in the open field session, animals were subjected to a novel object recognition (NOR) test in order to assess short-term object recognition memory taking place in the same open field boxes and the same lighting condition.

In total, four different kinds of objects were used, but on each time point only two different kinds of objects were used. The objects differed in material (metal, glass or porcelain) and texture (smooth or coarse with ridges, dents or bulges), but were all roughly the same size (4.5-7 cm height, 5-6 cm diameter, measured at the widest point). Test objects for PD ~30 and ~66 were a metal eggcup and a glass salt shaker, whereas objects for PD ~45 and ~94 were a porcelain cup with a lion head bulge and a miniature beer glass (see figure 18). All objects were tested in preliminary investigations in order to ensure comparable interaction times of animals with all 4 objects (data not shown). The objects were placed in the left and right rear corners of the open field, ~4 cm away from the walls (see figure 19), and fixated using repositionable adhesive dots (Pritt Multi Tack, Henkel AG & Co. KGaA, Düsseldorf, Germany). All objects and the open field boxes were cleaned with 70% ethanol and thoroughly dried before and during testing.

Figure 18: Test objects for the novel object recognition test
Test objects for PD ~30 and ~66 were a metal eggcup and a glass salt shaker (left part), whereas objects for PD ~45 and ~94 were a porcelain cup with a lion head bulge and a miniature beer glass (right part).

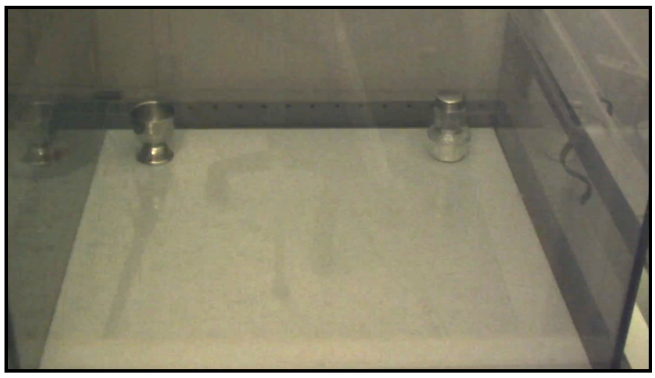

Figure 19: Placement of objects in the open field boxes
The objects were placed in the left and right rear corners of the open field, ~4 cm away from the walls, and fixated using repositionable adhesive dots (Pritt Multi Tack, Henkel AG & Co. KGaA, Düsseldorf, Germany).

At first, the animals were placed in the open field with two identical sample objects (A) for 3 min (sample phase), and afterwards returned to their home cage for an inter-trial interval of 30 min. Then, the animals were placed in the open field with a familiar sample object (A', identical copy of object A presented in the sample phase) on one side and an unfamiliar test object (B) on the other side for 3 min (test phase). Which of the two objects of each time point was used as sample and which as test object, as well as the placement (left or right) of the sample and test object during the test phase was counterbalanced (pseudo randomized). For each test phase, the animals were introduced to the box by placing them at the mid-point of the wall opposite to the objects, with its body parallel to the side walls and its nose pointing away from the objects.

The test was recorded by a digital camcorder (Everio GZ-HD3, JVCKENWOOD Deutschland GmbH, Bad Vilbel, Germany) positioned at a slight angle in front of the open field box. The recordings were analyzed by a blind observer using the software BORIS (v.2.993; Friard and Gamba, 2016), and the time of the animal exploring each object (sniffing, licking, and gnawing) during each phase was measured. Sitting beside or standing on top of the objects with their nose directed away from the object was not scored as object exploration. A recognition index (RI) was calculated, expressing the exploration time of the novel object relative to the total exploration time of both objects during the test phase [recognition index: (B / (A′ + B)) × 100].

Data was prepared as a comma separated file using Excel (2007 v.12, Microsoft Corporation, Redmond, USA) and imported into R (v.4.1.0, R Core Team, 2021) for statistical analysis.

In some cases, the adhesive dots used to fixate the objects to the floor mistakenly protruded from under the object, and the animals gnawed on these adhesive dots. As this could not be scored as exploration of the object itself, but usually accounted for a large amount of the total time of the test phase, these cases (10 samples in total) were excluded from the statistical analysis.

2.3.4. Prepulse Inhibition

On day 2 of each test block and roughly 4 hours after the NOR test, the animals underwent a first session of the prepulse inhibition test. This first session served as a habituation session to provide a more stable PPI response on a 2nd session which followed on day 3, 24 h later. Only the data of this 2nd session on day 3 of each test block was used for statistical analysis.

A startle system with six chambers (35 cm x 35 cm x 35 cm; SR-LAB, San Diego Instruments, San Diego, CA) was used for performing the prepulse inhibition tests. The animals were placed inside a transparent horizontal Plexiglas cylinder (9 cm inner diameter; 16 cm inner length) inside a sound-attenuated, illuminated (~5 lx) and ventilated chamber. Motion-sensitive transducers for detecting the startle response were mounted underneath the cylinders. The output signal of the transducers was digitized (sampling rate: 1 kHz) and stored on a computer using the SRLab software (San Diego Instruments, San Diego, USA). Stored responses were expressed in arbitrary units. White background noise (60 dB SPL), the prepulse (20 ms, 76 dB SPL white noise pulse, 0 ms rise/fall time) and the acoustic startle stimulus (20 ms, 105 dB SPL white noise pulse) were generated by high-frequency loudspeakers mounted in the center of the ceiling of the test chambers.

During an acclimatization period of 5 min, only the white background noise was presented. For taking the effects of short-time habituation into account, the first 10 trials of the test included only the startling stimulus without a preceding prepulse, in order to approach a stable startle response. Afterwards, 50 trials were performed consisting of 10 pulse-alone trials, 20 prepulse-pulse trials (10 with the prepulse preceding the startling pulse by an interstimulus interval (ISI) of 50 ms, 10 with and ISI of 140 ms), 10 prepulse-alone trials and 10 background-noise-alone trials, presented in a pseudo-randomized order (avoiding the presentation of each type of

trial more than twice after another). In the end, 10 pulse-alone trials were presented again. The average inter-trial interval was 25 s.

Data from the SRLab software was exported as a comma separated file using Excel (2007 v.12, Microsoft Corporation, Redmond, USA), and the startle responses during a 100 ms window following the startling stimulus were analyzed using a self-written Excel script. PPI was calculated according to the following formula: (Startle response without prepulse – Startle response with prepulse) / (Startle response without prepulse / 100) = PPI [%]. Afterwards, the data was again saved as comma separated file and imported into R (v.4.1.0, R Core Team, 2021) for statistical analysis.

2.4. Resting-State fMRI

2.4.1. Data Acquisition

Data acquisition was carried out in cooperation with Dr. Ekkehard Küstermann.

This study used a combination of initial anesthesia and following transition to sedation as described in Weber et al., 2006. Animals were initially anesthetized using 4 % isoflurane (CP-Pharma, Burgdorf, Germany) in 0.4 l/min oxygen. Approximately 5 minutes later, the isoflurane was lowered to 1.5% and the animals received a subcutaneous bolus injection of 1 ml/kg (0.05 mg/kg) medetomidine (Cepetor, CP-Pharma, Burgdorf, Germany). Afterwards, the animals were transferred to the scanner and received additional medetomidine boli of 0.34 ml/kg (0.167 mg/kg) every ten minutes for the duration of the MR Image acquisition, with the exception of some of the later scans (~PD66: animals 7.2.3 + 7.2.5 + 8.x.x; ~PD94: animals 7.x.x + 8.x.x)., where the administration of medetomidine was changed to a continuous subcutaneous infusion (0.6 ml/h; 0.01 mg/kg/h) using an infusion pump (AL-1010, World Precision Instruments Inc, Sarasota, FL). The animals were fixed to the animal mount in the scanner using a tooth bar, and foam earplugs were inserted for hearing protection. Respiration was monitored and recorded using a pressure sensitive pad placed beneath the animal’s chest, connected to an animal monitoring system (CED 1401, Cambridge Electronic Design Limited, Milton, England), a data acquisition module (Keithley Instruments, Cleveland, OH) and the Spike 2 software (v.5.0, Cambridge Electronic Design Limited, Milton, England). Rectal body temperature was

monitored and recorded using an optical temperature probe covered with a stainless steel capillary (self-made), which was connected to the same animal monitoring system and software. For comparison and calibration purposes, the rectal temperature was measured once before and after the data acquisition using a simple thermometer (Geratherm plus GT-2020, Geratherm Medical AG, Geschwenda, Germany) as well. In order to keep the body temperature in a physiological range (~37-38 °C, Gordon, 1990), the animal mount was heated by a liquid temperature control system (MS Thermostat, LAUDA, Lauda-Königshofen, Germany), and the temperature of the system was manually adjusted if necessary. After fixation of the animal on the animal mount and before start of the data acquisition, isoflurane was discontinued. Upon completion of the scanning session, the animals were removed from the scanner and received a subcutaneous injection of 1 ml/kg (0.1 mg/kg) atipamezole (Revertor, CP-Pharma, Burgdorf, Germany) in order to reverse the sedation.

All MR scans were carried out on a Bruker 7 Tesla system (BioSpec 70/20 USR, Bruker BioSpin, Ettlingen, Germany) operated using the ParaVision 5.1 software (Bruker BioSpin, Ettlingen, Germany). For excitation, a 72 mm linear-resonator coil (Bruker BioSpin, Ettlingen, Germany), and for reception a 4-channel-phased-array coil (Bruker BioSpin, Ettlingen, Germany) were used. Images were exported as DICOM (Digital Imaging and Communications in Medicine, http://dicom.nema.org/) files from ParaVision.

Prior to the main imaging protocols, initial overview scans using FLASH (Fast Low-Angle Shot) sequences were performed in order to check the positioning of the animals head in the scanner. Following this, shimming (including acquisition of a field map) was carried out in order to correct magnetic field inhomogeneities introduced by the rat.

Next, high-resolution anatomical images were acquired using a TurboRARE (Rapid Acquisition with Relaxation Enhancement) / FLASH 2D sequence (for imaging parameters, see table 1).

In between the anatomical and the functional scans, ^{1}H nuclear magnetic resonance (NMR) spectroscopy scans using a PRESS sequence with the volume of interest located in the prefrontal cortex were carried out as well, in order to indirectly measure

Glutathione (GSH) in this brain area. However, analysis of this NMR spectroscopy data is not part of this Thesis.

Afterwards, the functional scans were carried out using EPI sequences with a TE of 18 ms, as this has proven optimal for IC detection in preliminary tests (data for preliminary tests not shown; for imaging parameters of the final experiments, see table 1), acquiring a total of 12 minutes of resting-state data from each animal.

Finally, a second set of anatomical images were acquired using a TurboRARE / FLASH 2D sequence, which had a lower resolution that was more comparable to the imaging parameters used for the functional scans (for imaging parameters, see table 1), followed by acquisition of a second field map.

Table 1: MR Imaging Parameters

Anatomical Scans (high-resolution)			**Functional Scans**			**Anatomical Scans (low-resolution; comparable to functional scans)**	
Method	TurboRARE		*Method*	EPI		*Method*	TurboRARE
RARE Factor	8		*Slices / Slice Thickness*	17 / 1 mm		*RARE Factor*	8
Slices / Slice Thickness	55 / 0.5 mm		*Matrix / Field of View*	96x48 / 30x15 mm		*Slices / Slice Thickness*	17 / 1 mm
Matrix / Field of View	192x128 / 30x20 mm		*Resolution*	312x312 µm		*Matrix / Field of View*	192x96 / 30x15 mm
Resolution	117x118 µm		*TE / Bandwidth*	18 ms / 200 kHz		*Resolution*	156x156 µm
TR / TE	7 s / 12 ms		*TR / Flip Angle / Number of Images*	1.8 s / 53° / 400		*TR / TE*	7 s / 12 ms
Acquisition time	3 min 46 sec		*Acquisition time*	12 min		*Acquisition time*	1 min 25 sec

2.4.2. Preprocessing

DICOM Images were converted to 4D NIfTI (Neuroimaging Informatics Technology Initiative, http://nifti.nimh.nih.gov/) files using the MRIcron *dcm2nii converter* (Rorden et al., 2007; http://www.mccauslandcenter.sc.edu/mricro/mricron/index.html).

All non-brain tissue was manually deleted from the low-resolution anatomical data by cutting out the brain in Fiji/ImageJ (v.1.52n; Schindelin et al., 2012).

Preprocessing was carried out using a script written by Dr. Ekkehard Küstermann utilizing mainly sub-routines from the FSL 6.0.4 (FMRIB Software Library, FMRIB, Oxford, UK; Jenkinson et al., 2012) and ANTs (Advanced Neuroimaging Tools, v2.3.1; Avants et al., 2011) software packages.

Anatomical and functional volumes were reoriented by using the *–orient* function from Convert3D, a command-line tool based on ITK-SNAP (Yushkevich et al., 2006), so that the voxel coordinate system is represented as "i,j,k = Left, Inferior, Posterior" (i.e. *"-orient LIP"*).

Since some tools of FSL rely on human brain sizes in order to function properly (i.e. they become instable when used with voxel sizes in the µm range), the nominal voxel size of all images was scaled up by a factor of 10.

A mean image of each functional EPI set was calculated using the *fslmaths* function.

A slice-wise motion correction was carried out on the functional EPI volumes using a script which utilizes the *mcflirt* tool of FSL (Kalthoff, 2011; Kalthoff et al., 2011), followed by regression of motion signals (the whole volume was regressed by all slice specific motion parameters and their first derivatives).

Next, the functional EPI volumes were corrected for different slice acquisition times using the *slicetimer* routine from FSL.

The anatomical volumes were interpolated to match the matrix size of the functional EPI volumes using the *flirt* routine from FSL.

All non brain tissue of the functional EPI volumes was masked by applying a mask derived from the manually cut out low-resolution anatomical data using the *fslmaths* routine.

Bias field correction was carried out on the low-resolution anatomical volumes using the *N4BiasFieldCorrection* routine from ANTs (Tustison et al., 2010).

The low-resolution anatomical volumes were normalized to a stereotaxic MRI template by Schwarz et al., 2006, using the *antsRegistration* routine from ANTs. Afterwards, the functional EPI volumes were normalized to the template by applying the transformation data that were gained in the first step by aligning the low-resolution anatomical images to the template.

Spatial smoothing of the functional EPI data was carried out using the *fslmaths* tool of FSL with a Gaussian filter with 8 mm full width at half maximum (FWHM) (corresponding to 0.8 mm for rat brain size).

Afterwards, temporal filtering of the functional EPI was carried out using a high-pass filter with a cut-off of 0.01 Hz using the *fslmaths* tool from FSL.

2.4.3. Data Analysis

Group ICA analyses were carried out using the MELODIC 3.15 (Multivariate Exploratory Linear Optimized Decomposition into Independent Components) tool of FSL (Beckmann and Smith, 2004).

Initially, the data of all SAL rats from all time points were concatenated in the temporal domain, and several 2D ICAs were performed on this whole SAL group data for preliminary investigations, one with automatic dimensionality estimation (resulting in 373 ICs), and the others with fixed numbers of components (15, 20 or 30 ICs).

Due to the large number of components extracted using automatic dimensionality estimation, the results of this ICA was not further analyzed. The ICs of all analyses using a fixed number of components were visually inspected (Kelly et al., 2010; Griffanti et al., 2017), and the areas involved in each component were identified by overlaying them on the template brain and comparing those areas with the rat brain atlas by Paxinos and Watson (Paxinos and Watson, 2006; Schwarz et al., 2006). For this visual inspection, the ICs were thresholded between z-scores from 3-15. The ICs were then either assigned to resting-state networks known from the literature, they were given meaningful names based on the brain areas involved, or they were classified as noise.

The results from the ICA with a fixed number of 20 components were deemed optimal for further analysis, and resulted in 7 ICs of interest (see results section 3.2.1).

ICAs on data from single animals were run on a sub-set of the data in order to perform additional denoising by regression of noise components (using the *fsl_regfilt* function) from the data as described by Kelly et al., 2010. However, a group ICA on the denoised data did not show visual improvements (less ICs classified as noise, or detected known networks showing less noise or appearing more similar to literature

results; data not shown), which is why this additional denoising procedure was not pursued further and was not performed for the final analysis.

The results from the ICA with a fixed number of 20 components using the data of all SAL rats from all time points was then used as a basis for further (statistical) analysis as described in section 2.6.2.

The data of one animal (815, LPS group receiving 20 µg/kg LPS) was excluded from the further analysis, as the resting-state fMRI data from that animal on PD~94 shows a strong signal drop (see appendix 6.3.1 figure 78) after three quarters of the measurement, which led to abnormally high z-scores for this animal in the further analysis steps. As the MRM model used for the statistical comparison (see section 2.6.2) is not able to handle single missing values, the data from all four time points of this animal were excluded.

2.5. Histology

On PD ~100, animals were deeply anesthetized by intraperitoneal injections of 200 mg/kg pentobarbital (Narcoren®, Merial GmbH, Hallbergmoos, Germany) and afterwards perfused with 300 ml phosphate-buffered saline (PBS, pH 7.4) followed by 300 ml of 4 % paraformaldehyde (PFA) in 0.1 M PB (pH 7.4). After perfusion, the brains were extracted and post-fixed in 4 % PFA for 24 h, then transferred into 30% sucrose solution for 72 h at room temperature, and afterwards stored at 4°C until further processing (cutting into 40 µm thick sections with a cryostat and following immunohistochemistry targeting Microglia with an Iba-1 antibody staining; However, analysis of this data is not part of this Thesis).

2.6. Statistics

2.6.1. Behavioral Data

All statistical analyses of the behavioral data were performed within R (v.4.1.0, R Core Team, 2021).

Univariate distributions of all variables were plotted using the Flexplot package (v.0.7.7, Fife, 2019) to visually check for incorrectly and improperly coded as well as missing values (results mostly not shown, except e.g. for open field data in section 3.1.2).

As multiple animals from each litter of treated dams were included in the analysis, representing non-independent samples, and each animal was measured repeatedly on four different times, linear mixed models (LMM) were used for each of the dependent variables with factor ‘Animal’ nested under ‘Litter’ as random intercepts. For the novel object recognition test data, random intercepts for ‘Test Object’ were included additionally. Fixed factors generally included the interaction of the categorical variable ‘Dose’ (3 levels: 0, 20, 100 µg LPS/kg) with the categorical variable ‘Age’ (4 levels: PD ~30, ~45, ~66, ~94), as well as the simple effect of the categorical variable fMRI ‘Scan’ (2 levels: yes, no). For the prepulse inhibition data, a three-way interaction between ‘Dose’, ‘Age’ and the categorical variable ‘ISI’ (Inter-stimulus-interval, 2 levels: 50, 140 ms) was constructed (plus simple effect of ‘Scan’). For the open field test data, a three-way interaction between ‘Dose’, ‘Age’ and the categorical variable ‘Time Interval’ (6 levels: minutes 1-5, 6-10, 11-15, 16-20, 21-25, 26-30) was constructed (plus simple effect of ‘Scan’). In addition, offspring weights were compared by adding a fixed effect variable of feeding type (2 levels: ad-libitum or restrictive diet). All mixed models were constructed using the lmerTest package (v.3.1-3, Kuznetsova et al., 2017), which is based on the lme4 package (v.1.1-26, Bates et al., 2015). Denominator degrees of freedom (*df*) and thus p values were obtained using the Satterthwaite's method. The criterion for statistical significance was set at $\alpha = .05$. Results with p-values < 0.10 were considered as trends for statistical significance. The following significance codes are used in tables and figures throughout this thesis: ≤0.001 ‘***’, ≤0.01 ‘**’, ≤0.05 ‘*’, ≤0.1 ‘.’

The model assumptions were assessed using various visual methods and formal statistical tests of the model residuals. To identify outliers, the conditional (internally) studentized residuals were plotted against the fitted values using the redres package (v.0.0.0.9, Katherine J Goode, 2019, https://goodekat.github.io/redres/). All samples whose residuals exceeded ±3 SD from the mean were defined as outliers, and were thus excluded from the main analysis (Cipra et al., 1990; Lehmann, 2013). If the LMM calculated after excluding these outliers also showed residuals exceeding ±3 SD, they were again excluded in an iterative manner until all residuals of the calculated LMM remained within this limit. However, for these cases a sensitivity analysis (see appendix chapters 6.2.2, 6.2.4, 6.2.6 and 6.2.8) was performed in order to assess the effect of this exclusion on the outcome of the analysis. In order to assess the assumption of normality, histograms of the residuals were plotted using the Flexplot

package (v.0.7.7, Fife, 2019) and visually checked for symmetry. Additionally, Shapiro Wilk tests of the residuals were calculated using the routine from the stats package of R (v.4.1.0, R Core Team, 2021). In cases where non normality was indicated by the Shapiro Wilk test, skewness was calculated using the e1071 package (v.1.7-4, Meyer et al., 2020). Further, to assess the assumption of normality of random intercepts, histograms and Shapiro Wilk tests of the random intercepts were made as well. In order to identify potential heteroscedasticity problems, spread-location plots were generated using the Flexplot package (v.0.7.7, Fife, 2019) and visually checked for deviations from homoscedasticity. Additionally, Levene's test was calculated using the car package (v.3.0-10, Fox and Weisberg, 2019).

Estimated marginal means were extracted from the linear mixed models using the emmeans package (v.1.5.3, Lenth, 2020). Post hoc multiple comparisons were done by calculating simple pair-wise t-test contrasts for 'Dose' and 'Age', also via the emmeans package. P values were adjusted using the Tukey method, but uncorrected p values are reported as well. 95% confidence intervals were calculated only without multiplicity adjustment. In case of the novel object recognition test data, the estimated marginal means of the recognition indices were also compared against chance level (RI of 50%) using one-sided t-tests with and without Sidak correction.

In addition, litter size and male:female ratio of dams were compared using the Welch Two Sample t-test from the stats package of R (v.4.1.0, R Core Team, 2021) between the 20 µg/kg LPS and SAL group.

Plots of the models were generated using the ggplot2 package (v.3.3.3, Wickham, 2016). The estimated marginal means ± their standard error (SEM) were plotted on top of slightly jittered scatter plots of the raw data. Data from all 3 groups of LPS doses were plotted next to each other around each age starting with SAL data (LPS Dose 0) from left to right. The four means of the different ages of each group were connected by lines.

2.6.2. fMRI Data

In order to compare the rsfMRI data from SAL and LPS groups statistically, the dual regression approach was used (Beckmann et al., 2009; Filippini et al., 2009; see section 1.2.4.3). The set of spatial maps from the ICA with 20 ICs using only the SAL group as input was used to generate subject-specific versions of the spatial maps,

and associated time courses of all animals on all time points, using the *dual_regression* function of FSL. Dummy multi-subject design matrix and contrast files were set up using the GLM tool of FSL.

The subject specific spatial maps of the 7 ICs of interest generated by the dual regression approach were compared voxel-wise between the two anesthesia regimes (animals that received boli of medetomidine every ten minutes during scanning and those which received a continuous infusion of medetomidine) within the SAL and LPS groups separately by nonparametric permutation tests with 10000 permutations using the *randomise* function of FSL. Design matrix and contrast files for those comparisons were set up using the GLM tool of FSL. TFCE (Threshold-Free Cluster Enhancement) was used as correction for the multiple comparisons across voxels within each component, but no correction for comparison of multiple ICs was applied. Afterwards, due to the similarity of results of this sub-analysis (see results section 3.2.2), the data from both anesthesia regimes was pooled for the further analysis.

The subject specific spatial maps of the 7 ICs of interest generated by the dual regression approach were then compared voxel-wise between SAL and LPS groups using the “Multivariate and repeated measures” (MRM) toolbox (McFarquhar et al., 2016) run via the SPM12 software package (Statistical Parametric Mapping, Wellcome Trust Centre for Neuroimaging, London, UK; http://www.fil.ion.ucl.ac.uk/spm/) in MatLab R2018a (MathWorks Inc., Natick, MA). Contrasts were setup for the fixed effects as well as the interaction of the categorical variable ‘Dose’ (3 levels: 0, 20, 100 µg LPS/kg) and the categorical variable ‘Age’ (4 levels: PD ~30, ~45, ~66, ~94). Wilks´ lambda was selected as multivariate test statistic, and the p-value calculation was done using the permutation approach (making use of the randomise algorithm by Winkler et al., 2014) with 10,000 permutations and False Discovery Rate (FDR) as a correction method for the multiple comparisons across voxels within each component in its own right (but no correction for comparison of multiple ICs). Comparable to analysis of the behavioral data, the criterion for statistical significance was set at $\alpha = .05$, while results with p-values < 0.10 were considered as trends for statistical significance.

Spatial maps containing each contrasts p-value for every voxel were overlaid onto the component maps, and thresholded for voxels showing statistical significance

(p<0.05; shown in figures as green) or a trend towards statistical significance (p<0.10; shown in figures as bronze).

The FDR approach for correction of multiple comparisons across voxels, and no applied correction for multiple testing of several ICs was done since especially the rs-fMRI part of this thesis is a explorative study where type I errors are preferred over type II errors (Victor et al., 2010).

Mean values for each group were calculated using the subject specific spatial maps of the 7 ICs of interest generated by the dual regression approach via the *fslmaths* function of FSL. A binary mask of the at trend level statistical significant clusters from the MRM (thresholded for p values < 0.10) was applied to the mean value maps for each group via the *fslmaths* function, and mean values and standard deviation (*SD*) within these clusters were calculated via the *fslstats* function of FSL.

Rs-fMRI results were visualized by creating screenshots of the statistical maps overlaid on the structural template brain via *fslview*, and arranging these within GIMP (GNU Image Manipulation Program, v2.10.4, The GIMP Development Team, https://www.gimp.org).

3. Results

In three of four cases, 100 µg/kg LPS resulted in weight loss 24 h after the first injection (i.e. on GD 16; see table 2). For the two dams treated with 50 µg/kg LPS, one gained and one lost weight 24 h after the first injection. In the 20 µg/kg LPS group, weight gain or loss after the first injection was balanced (1:1 ratio). In the SAL group, more dams gained weight than lost weight (2:1 ratio).

The higher LPS doses resulted in abnormal littering. In three of four cases, 100 µg/kg LPS led to abortions, reflected by bloody vaginal discharge in the days following treatment and finally absence of delivery. In one case it even led to the death of the dam. For one of the two dams receiving 50 µg/kg LPS, delivery failure was the same result, while the second dam delivered one female pup. For the 20 µg/kg LPS group, only one dam failed to deliver, while all SAL dams delivered normally.

Comparing the 20 µg/kg LPS group with the SAL group, the Welch Two Sample t-test does not show statistical significance neither for litter size ($t_{8.01} = 1.39$, $p = .202$; 20 µg/kg LPS = 7.33±5.09 pups vs. 0 µg/kg = 10.67±2.94 pups) nor for male:female ratio ($t_{6.47} = -1.63$, $p = .151$; 20 µg/kg = male:female ratio of 2.02±1.36 vs. 0 µg/kg LPS = 1.54±0.65). The statistical model assumptions of the Welch Two Sample t-test were met (data not shown).

Regarding offspring weights, the LMM shows significance for the effect of litter ($X^2_1 = 9.99$, $p = .001$; data not shown). The estimated marginal means of the model are shown in figure 20. The analysis shows a statistical significant interaction effect between LPS dose and age ($F_{6,617.53} = 5.97$, $p = .000$; see table 3) and a statistical significant effect of Feeding type ($F_{1,617.31} = 22.89$, $p = .000$; see table 3). However, as the statistical model assumptions for this LMM were violated (data not shown), no further post-hoc tests were done, and the data was not interpreted any further.

Table 2: Experimental dams
In total 16 dams and 4 sires were used for breeding LPS and SAL offspring, i.e. bucks were reused for multiple pregnancies. Dams 1 and 2 were reused once, i.e. both dams received both treatments in two consecutive pregnancies, but due to described complications with the LPS dose and following time constraints the remaining dams were all used only for one pregnancy each. The change in weight of dams after the first injection (i.e. from GD 15 to 16) was noted either as weight gain or weight loss. [GD] = gestational day

Dam	Buck	LPS dose [µg/kg]	Weight after treatment		Day of Birth [GD]	Pups [n]		Litter size [n]
						Male ♂	Female ♀	
♀ 1	♂ 3	100		Loss	22	5	7	12
♀ 2	♂ 4	100	Gain		-	0	0	0
♀ 3	♂ 2	100		Loss	-	0	0	0
♀ 5	♂ 1	100		Loss	-	0	0	0
♀ 13	♂ 2	50	Gain		22	0	1	1
♀ 14	♂ 1	50		Loss	-	0	0	0
♀ 7	♂ 3	20		Loss	22	4	1	5
♀ 8	♂ 2	20		Loss	22	7	4	11
♀ 11	♂ 3	20	Gain		22	7	4	11
♀ 12	♂ 2	20	Gain		21	8	5	13
♀ 15	♂ 3	20	Gain		21	3	1	4
♀ 16	♂ 4	20		Loss	-	0	0	0
♀ 1	♂ 3	0	Gain		22	5	7	12
♀ 2	♂ 4	0	Gain		22	6	5	11
♀ 4	♂ 3	0		Loss	22	5	5	10
♀ 6	♂ 2	0	Gain		21	7	3	10
♀ 9	♂ 1	0	Gain		21	10	5	15
♀ 10	♂ 1	0		Loss	22	4	2	6

Table 3: ANOVA table of the LMM of the Offspring Weight data
Shown are the sums of squares (SS), mean squares (MS), numerator (df Num) and denominator (df Den) degrees of freedom, F- and p-value for each simple factor as well as for the Dose:Age interaction term. The Dose:Age interaction (p = .000) as well as the simple effect for Feeding (p = .000) show statistical significance.

	SS	*MS*	df_{Num}	df_{Den}	*F*	*p*
Dose	1255.87	627.93	2	6.47	0.82	.481
Age	1779171.56	593057.18	3	617.51	774.56	**.000** ***
Feeding	17532.44	17532.44	1	617.31	22.89	**.000** ***
Scan	405.69	405.69	1	42.73	0.52	.471
Dose:Age	27457.55	4576.25	6	617.53	5.97	**.000** ***

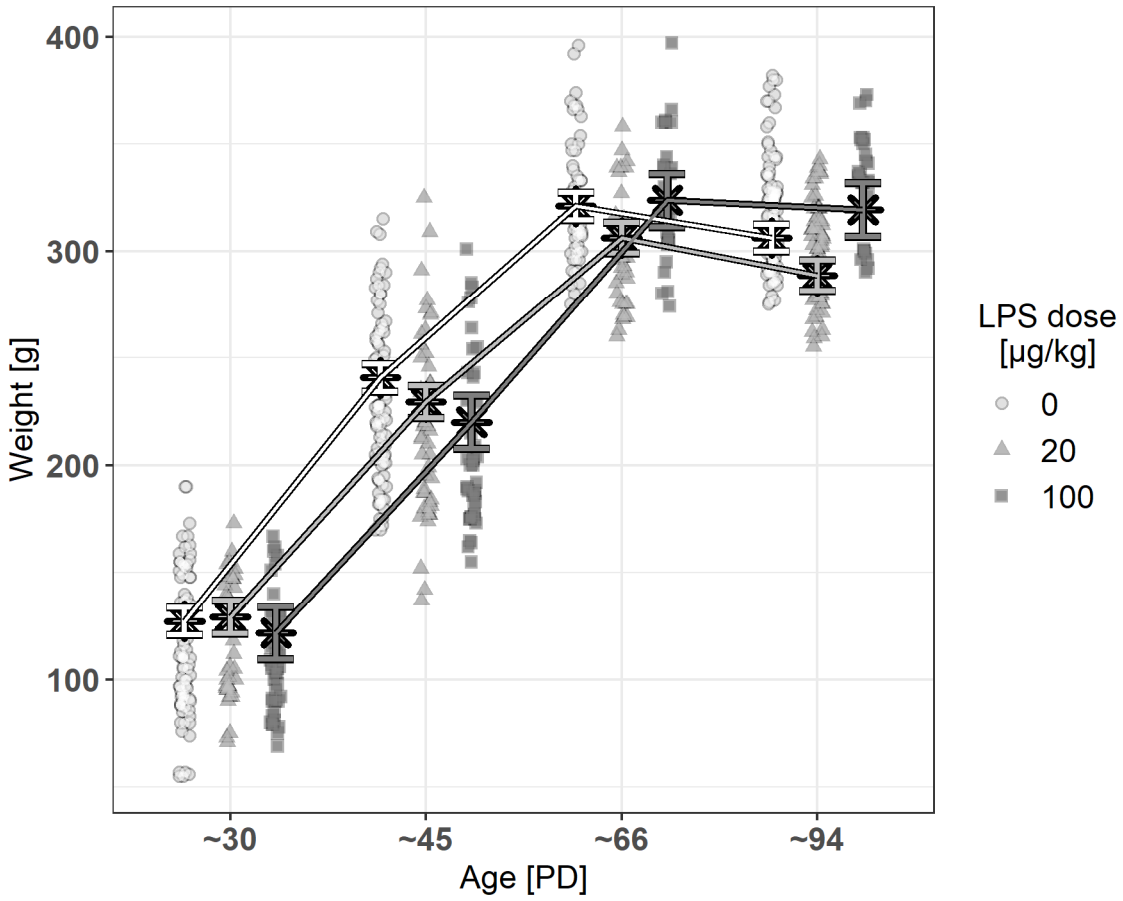

Figure 20: Offspring Weight [g] by Age and LPS dose
Shown are estimated marginal means (⁎) of the offspring weight extracted from the linear mixed model ± SEM on top of the jittered raw data. SAL data (0 µg/kg LPS) shown as white circles, 20 µg/kg LPS as light grey triangles and 100 µg/kg LPS as dark grey squares. Animals were fed ad-libitum until PD 70 (represented by the first 3 time points), and afterwards fed on a diet of 12 g chow/rat/day (represented by the last time point on PD ~94).

3.1. Behavioral Experiments

3.1.1. Elevated Plus Maze

Nine data points from 9 animals were excluded from the EPM analysis for all dependent variables, as the animals were jumping onto and climbing on top of the walls of the closed arm of the maze, which often included doing head dips from that position. When counting the time spent while climbing on the walls as “closed arm time”, interpreting the “closed arm time” as anxiety related behavior does not make sense any more. Another option might have been to count the time spent climbing on the walls as “open arm time”, but instead it was decided to exclude the affected test sessions completely.

3.1.1.1. Time in Open Arms

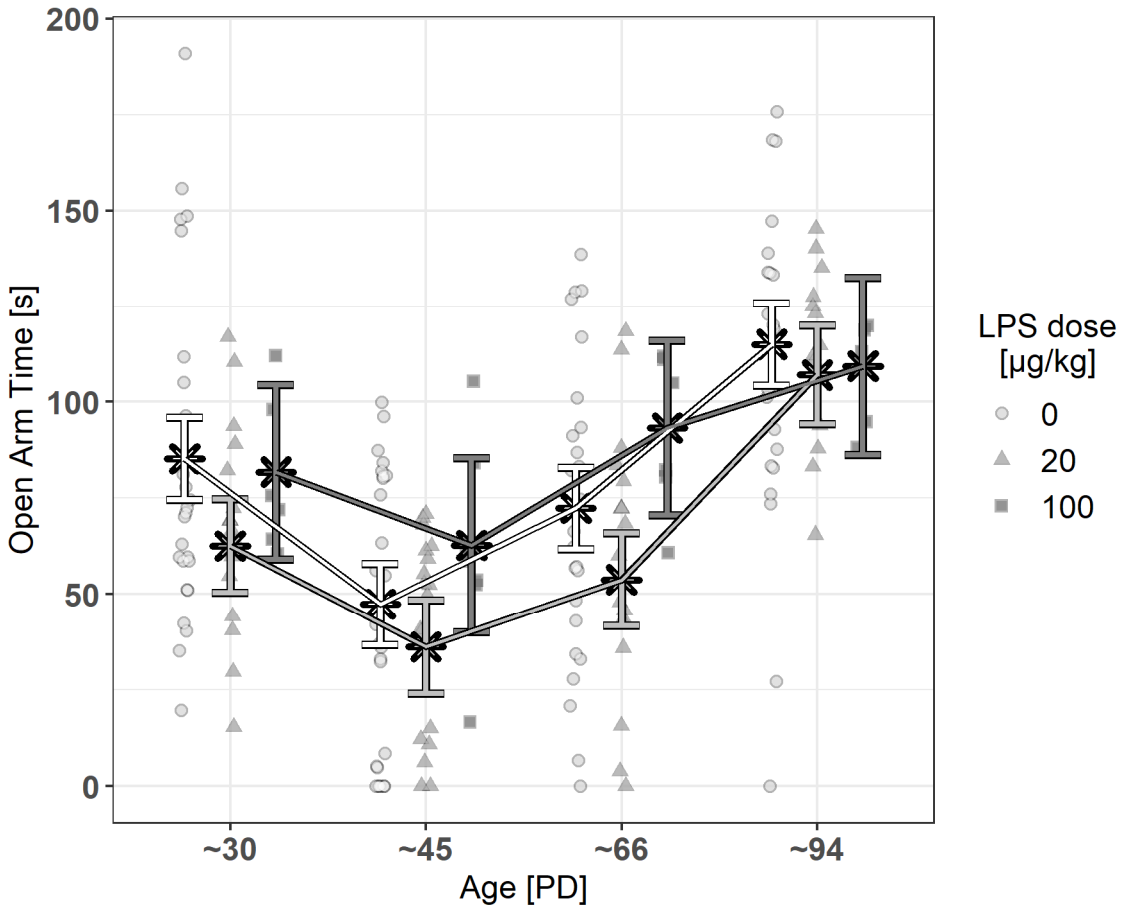

Figure 21: Time in the open arms of the EPM [s] by Age and LPS dose
Shown are estimated marginal means (⁎) of the open arm time extracted from the linear mixed models after outlier removal ± SEM on top of the jittered raw data. SAL data (0 µg/kg LPS) shown as white circles, 20 µg/kg LPS as light grey triangles and 100 µg/kg LPS as dark grey squares.

In addition to the 9 data points that were excluded due to the climbing of animals on the walls of the closed arms, one data point was excluded after outlier analysis.

The statistical model assumptions were met (see appendix 6.2.2.1, figure 59).

The model shows a statistical significance for the effect of litter ($X^2_1 = 19.01$, p = .000; see appendix 6.2.2.1, table 33).

The estimated marginal means of the model are shown in figure 21 and table 5. The analysis shows a statistical significant effect of age ($F_{3,135.32} = 35.97$, p = .000) and scan ($F_{1,40.82} = 8.81$, p = .005; see table 4).

Regarding age differences, the data show a U-shaped pattern, with estimated means for time on the open arms initially decreasing from PD~33 to PD~45, increasing back to a comparable value as on the first time point on PD~66, and increasing even

further on PD~94. This is also shown by the post-hoc multiple comparisons, as in the control group, there is a statistical significant difference for all contrasts except the PD~30-66 contrast (p usually ≤.000; see appendix 6.2.1.1, table 35), and in the 20 µg/kg LPS group, there is a statistical significant difference for all contrasts except the PD~30-66 and the PD~45-~66 contrasts (p usually ≤.000; see appendix 6.2.1.1, table 35). In the 100 µg/kg LPS group, only the PD~45-~66 and PD~45-~94 contrasts are statistically significant ($t_{133.46} = 2.33$, $p = .096$ / $t_{136.49} = 3.40$, $p = .005$; see appendix 6.2.1.1, table 35).

No further post-hoc tests were done for the effect of scan, as this term was only included in the analysis to account for possible variation between animals that were scanned in the fMRI or not.

Table 4: ANOVA table of the LMM of the EPM Open Arm Time data after outlier removal
Shown are the sums of squares (SS), mean squares (MS), numerator (df Num) and denominator (df Den) degrees of freedom, F- and p-value for each simple factor as well as for the Dose:Age interaction term. The simple effects for Age (p = .000) and Scan (p = .005) show statistical significance.

	SS	*MS*	*df Num*	*df Den*	*F*	*p*	
Dose	831.55	415.77	2	7.17	0.70	.529	
Age	64378.25	21459.42	3	135.32	35.97	**.000**	***
Scan	5254.46	5254.46	1	40.82	8.81	**.005**	**
Dose:Age	4457.34	742.89	6	135.35	1.25	.287	

Table 5: Estimated marginal means of the LMM of the EPM Open Arm Time data after outlier removal
Shown are the estimated marginal mean, standard error (SE), degrees of freedom (df) and 95% confidence interval for each LPS dose and Age combination.

LPS dose [µg/kg]	Age [PD]	*Mean*	*SE*	*df*	*95% Confidence Interval*	
					Lower CL	*Upper CL*
0	~30	85.25	10.61	10.34	61.72	108.79
0	~45	47.37	10.61	10.34	23.84	70.90
0	~66	72.39	10.61	10.34	48.85	95.92
0	~94	114.97	10.79	11.04	91.24	138.70
20	~30	62.57	12.10	11.05	35.96	89.18
20	~45	36.25	12.10	11.05	9.64	62.86
20	~66	53.81	12.10	11.05	27.20	80.42
20	~94	107.02	12.81	13.82	79.51	134.54
100	~30	81.80	22.68	8.66	30.20	133.41
100	~45	62.77	22.68	8.66	11.17	114.37
100	~66	93.20	22.68	8.66	41.60	144.81
100	~94	109.33	23.04	9.23	57.40	161.26

Sensitivity analysis (see appendix section 6.2.2.1) including the outlier value doesn't change the interpretation of the results. The greatest changes in estimated marginal means is seen for the 20 µg/kg LPS group on PD~94 (107.02±12.81 excluding versus 100.49±12.76 including outliers; see appendix table 47), while most other means doesn't change much.

3.1.1.2. Time in Center

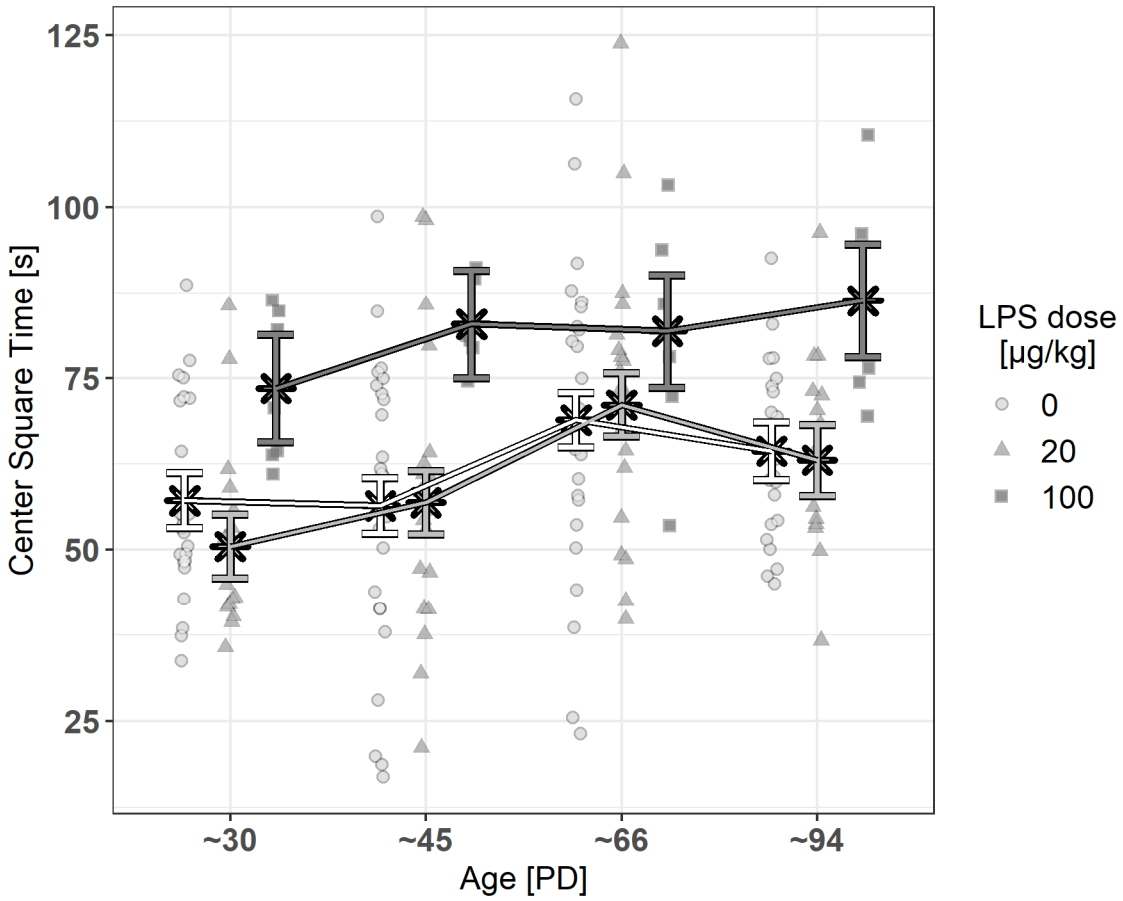

Figure 22: Time in the center of the EPM [s] by Age and LPS dose
Shown are estimated marginal means (⁎) of the central square time extracted from the linear mixed models after outlier removal ± SEM on top of the jittered raw data. SAL data (0 µg/kg LPS) shown as white circles, 20 µg/kg LPS as light grey triangles and 100 µg/kg LPS as dark grey squares.

In addition to the 9 data points that were excluded due to the climbing of animals on the walls of the closed arms, two data points were excluded after outlier analysis.

The statistical model assumptions were met (see appendix 6.2.1.2, figure 60).

The model shows no effect of litter ($X^2_1 = 1.21$, $p = .270$; see appendix 6.2.1.2, table 36).

The estimated marginal means of the model are shown in figure 22 and table 7. The analysis shows a statistical significant effect for age ($F_{3,137.09} = 5.81$, $p = .001$), and a trend towards statistical significance for LPS dose ($F_{2,6.70} = 4.62$, $p = .055$; see table 6).

Post-hoc multiple comparisons show at least a trend towards a statistical significant difference for the 20-100 µg/kg LPS contrast on all time points except on PD ~66 ($p \leq .067$; see appendix 6.2.1.2, table 37), with the 100µg/kg LPS group having a higher estimated mean for the time in the center square than the 20 µg/kg LPS group on all time points. Regarding the difference between the control group and the 100 µg/kg LPS group, only the contrasts on PD~45 and PD~94 show at least a trend towards a statistical significant difference ($p \leq .070$; see appendix 6.2.1.2, table 37). There is no statistical significant difference between the control group and the 20 µg/kg LPS group on any time point.

Regarding age differences, the time spent in the center square of the EPM seems to be higher on PD~66 compared to the other time points, which is shown by the post-hoc multiple comparisons that show a statistical significant difference for the PD~30-~66 and PD~45-~66 contrasts in the control and 20 µg/kg LPS groups ($p \leq .034$; see appendix 6.2.1.2, table 38). In the 100 µg/kg LPS group, all age comparisons are not statistically significant.

Table 6: ANOVA table of the LMM of the EPM Center Square Time data after outlier removal
Shown are the sums of squares (SS), mean squares (MS), numerator (df Num) and denominator (df Den) degrees of freedom, F- and p-value for each simple factor as well as for the Dose:Age interaction term. The simple effect of Age ($p = .001$) shows statistical significance, while the simple effect for Dose shows a trend towards statistical significance ($p = .055$).

	SS	*MS*	df_{Num}	df_{Den}	*F*	*p*	
Dose	2105.35	1052.67	2	6.70	4.62	**.055**	.
Age	3971.40	1323.80	3	137.09	5.81	**.001**	***
Scan	181.07	181.07	1	45.48	0.79	.377	
Dose:Age	1078.74	179.79	6	136.78	0.79	.580	

Table 7: Estimated marginal means of the LMM of the EPM Center Square Time data after outlier removal

Shown are the estimated marginal mean, standard error (SE), degrees of freedom (df) and 95% confidence interval for each LPS dose and Age combination.

LPS dose [µg/kg]	Age [PD]	*Mean*	*SE*	*df*	*95% Confidence Interval*	
					Lower CL	*Upper CL*
0	~30	57.15	3.99	22.70	48.88	65.41
0	~45	56.39	4.05	23.85	48.02	64.75
0	~66	68.89	3.99	22.70	60.63	77.15
0	~94	64.36	4.17	26.39	55.81	72.92
20	~30	50.45	4.63	23.15	40.88	60.01
20	~45	56.85	4.63	23.15	47.28	66.41
20	~66	71.09	4.63	23.15	61.52	80.65
20	~94	63.04	5.18	33.54	52.52	73.56
100	~30	73.52	7.85	14.18	56.70	90.33
100	~45	82.87	7.85	14.18	66.05	99.69
100	~66	81.86	8.24	17.07	64.48	99.24
100	~94	86.33	8.25	17.14	68.94	103.73

Sensitivity analysis (see appendix section 6.2.2.2) including the outlier values doesn't change the interpretation of the results. The greatest changes in estimated marginal means is seen for the 100 µg/kg LPS group on PD~66 (81.86±8.24 excluding versus 92.74±7.81 including outliers; see appendix table 52), while most other means doesn't change much.

3.1.1.3. Head Dips

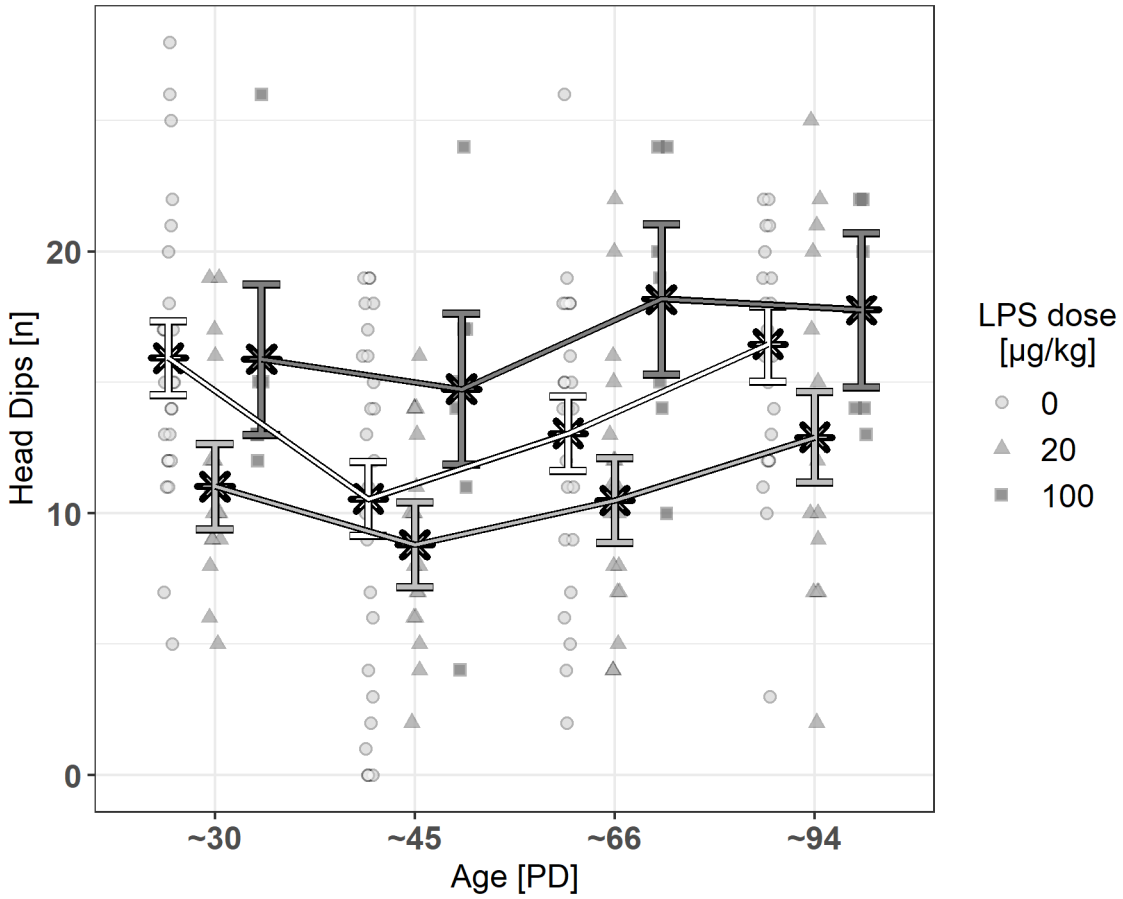

Figure 23: Head Dips in the EPM [n] by Age and LPS dose
Shown are estimated marginal means (⁎) of the head dips extracted from the linear mixed models after outlier removal ± SEM on top of the jittered raw data. SAL data (0 µg/kg LPS) shown as white circles, 20 µg/kg LPS as light grey triangles and 100 µg/kg LPS as dark grey squares.

In addition to the 9 data points that were excluded due to the climbing of animals on the walls of the closed arms, two data points were excluded after outlier analysis.

The statistical model assumptions were met (see appendix 6.2.1.3, figure 61).

The model shows a statistical significance for the effect of litter ($X^2_1 = 4.60$, $p = .032$; see appendix 6.2.1.3, table 39).

The estimated marginal means of the model are shown in figure 23 and table 9. The analysis shows a statistical significant effect for age ($F_{3,134.35} = 8.53$, $p = .000$), and a trend towards statistical significance for scan ($F_{1,43.88} = 3.87$, $p = .056$; see table 8).

Although the analysis shows a general effect of age, post-hoc multiple comparisons only show a statistical significant difference for the different age contrast within the 0µg/kg LPS control group ($p \leq .040$; see appendix 6.2.1.3, table 41), with the

exception of the PD~30-~94 contrast. For the 20 µg/kg LPS group, only the PD~45-~94 contrast shows statistical significance (p = .012; see appendix 6.2.1.3, table 41). Other than that, all other age contrasts for the two LPS groups are not reaching statistical significance.

No further post-hoc tests were done for the effect of scan, as this term was only included in the analysis to account for possible variation between animals that were or were not scanned in the fMRI.

Table 8: ANOVA table of the LMM of the EPM Head Dips data after outlier removal
Shown are the sums of squares (SS), mean squares (MS), numerator (df Num) and denominator (df Den) degrees of freedom, F- and p-value for each simple factor as well as for the Dose:Age interaction term. The simple effect of Age (p = .000) shows statistical significance, while the simple effect for Scan shows a trend towards statistical significance (p = .056).

	SS	*MS*	df_{Num}	df_{Den}	*F*	*p*	
Dose	64.49	32.25	2	7.14	2.40	.160	
Age	344.01	114.67	3	134.35	8.53	**.000**	***
Scan	52.00	52.00	1	43.88	3.87	**.056**	.
Dose:Age	122.55	20.43	6	134.36	1.52	.176	

Table 9: Estimated marginal means of the LMM of the EPM Head Dips data after outlier removal
Shown are the estimated marginal mean, standard error (SE), degrees of freedom (df) and 95% confidence interval for each LPS dose and Age combination.

LPS dose [µg/kg]	Age [PD]	*Mean*	*SE*	*df*	*95% Confidence Interval*	
					Lower CL	*Upper CL*
0	~30	15.91	1.40	12.27	12.86	18.95
0	~45	10.55	1.40	12.27	7.50	13.59
0	~66	13.04	1.42	12.97	9.97	16.12
0	~94	16.44	1.43	13.37	13.35	19.52
20	~30	11.02	1.62	13.19	7.53	14.52
20	~45	8.81	1.62	13.19	5.32	12.31
20	~66	10.50	1.62	13.19	7.00	13.99
20	~94	12.90	1.72	16.57	9.26	16.54
100	~30	15.87	2.88	8.91	9.35	22.40
100	~45	14.73	2.88	8.91	8.20	21.26
100	~66	18.16	2.88	8.91	11.63	24.69
100	~94	17.75	2.95	9.79	11.16	24.34

Sensitivity analysis (see appendix section 6.2.2.3) including the outlier values doesn't change the interpretation of the results. However, the trend towards statistical significance for the effect of scan turns into statistical significance ($F_{1,43.74} = 4.89$, p = .032; see appendix 6.2.2.3, table 55).

All estimated marginal means don’t change much (see appendix 6.2.2.3, table 57).

3.1.1.4. Rearings

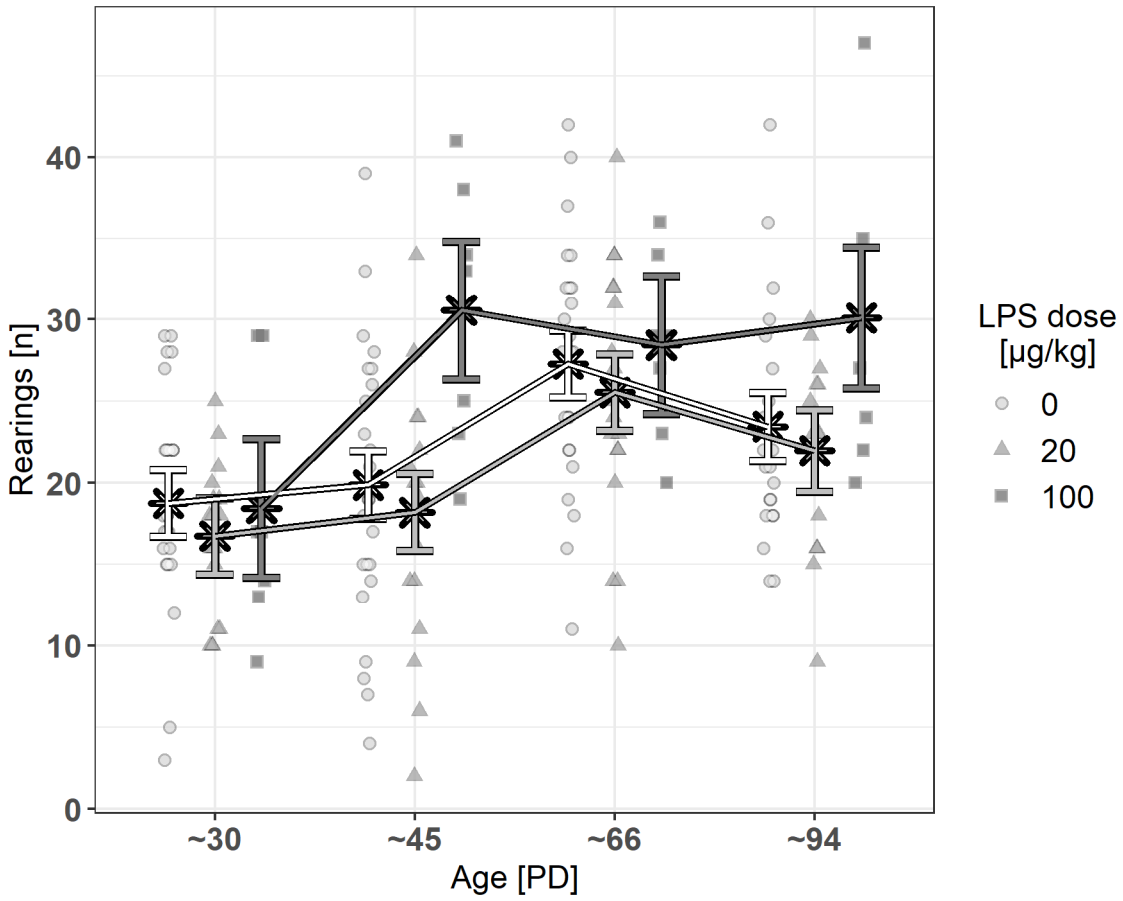

Figure 24: Rearings in the EPM [n] by Age and LPS dose
Shown are estimated marginal means (⁎) of the rearings extracted from the linear mixed models after outlier removal ± SEM on top of the jittered raw data. SAL data (0 µg/kg LPS) shown as white circles, 20 µg/kg LPS as light grey triangles and 100 µg/kg LPS as dark grey squares.

In addition to the 9 data points that were excluded due to the climbing of animals on the walls of the closed arms, two data points were excluded after outlier analysis.

The statistical model assumptions were met (see appendix 6.2.1.4, figure 62).

The model shows a statistical significance for the effect of litter ($X^2_1 = 6.70$, p = .010; see appendix 6.2.1.4, table 42).

The estimated marginal means of the model are shown in figure 24 and table 11. The analysis shows a statistical significant interaction effect between LPS dose and age ($F_{6,134.23} = 2.50$, p = .025; see table 10).

Post-hoc multiple comparisons show a trend towards statistical significant difference for the 20-100 µg/kg LPS contrast on PD ~45 ($t_{9.26} = -2.55$, p = .072; see appendix 6.2.1.4, table 43), with the 100 µg/kg group having a higher estimated mean for the number of rearings than the 20 µg/kg LPS group (LPS-100 = 30.58 vs. LPS-20 = 18.19).

Regarding age differences, the PD~30-~66, PD~30-~94 as well as PD~45-~66 show a statistical significant difference for the SAL and the 20 µg/kg LPS group (p mostly ≤.000, see appendix 6.2.1.4, table 44), with estimated means increasing with age from PD~30 until PD~60, but dropping a bit lower on PD~94. For the SAL group, this drop, i.e. the PD~66-~94 contrast shows statistical significance as well ($t_{134.36} = 2.38$, p = .087, see appendix 6.2.1.4, table 44). However, for the 100 µg/kg LPS group, the contrasts between the PD~30 and all other time points show a statistical significant difference (p ≤.005, see appendix 6.2.1.4, table 44), but not between the other time points, i.e. the estimated means increase from PD~30 to PD~45, but then stay on the same level.

Table 10: ANOVA table of the LMM of the EPM Rearings data after outlier removal
Shown are the sums of squares (SS), mean squares (MS), numerator (df Num) and denominator (df Den) degrees of freedom, F- and p-value for each simple factor as well as for the Dose:Age interaction term. The Dose:Age interaction shows statistical significance (p = .025).

	SS	*MS*	df_{Num}	df_{Den}	*F*	*p*	
Dose	62.56	31.28	2	6.46	1.04	.407	
Age	1740.60	580.20	3	134.20	19.23	**.000**	***
Scan	69.99	69.99	1	41.50	2.32	.135	
Dose:Age	452.28	75.38	6	134.23	2.50	**.025**	*

Table 11: Estimated marginal means of the LMM of the EPM Rearings data after outlier removal
Shown are the estimated marginal mean, standard error (SE), degrees of freedom (df) and 95% confidence interval for each LPS dose and Age combination.

LPS dose [µg/kg]	Age [PD]	*Mean*	*SE*	*df*	*95% Confidence Interval*	
					Lower CL	*Upper CL*
0	~30	18.76	2.03	11.10	14.29	23.22
0	~45	19.87	2.05	11.45	15.39	24.36
0	~66	27.28	2.03	11.10	22.81	31.74
0	~94	23.43	2.08	12.14	18.91	27.96
20	~30	16.73	2.34	12.01	11.64	21.83
20	~45	18.19	2.36	12.49	13.06	23.31
20	~66	25.52	2.34	12.01	20.43	30.62
20	~94	21.96	2.49	15.30	16.66	27.26
100	~30	18.44	4.24	8.45	8.75	28.12
100	~45	30.58	4.24	8.45	20.90	40.26
100	~66	28.44	4.24	8.45	18.75	38.12
100	~94	30.10	4.34	9.28	20.33	39.87

Sensitivity analysis (see appendix section 6.2.2.4) including the outlier values doesn't change the main interpretation of the results. However, the effect of scan is showing a trend towards statistical significance that was not present without the outliers ($F_{1,42.05} = 2.99$, $p = .091$; see appendix 6.2.2.4, table 60).

Furthermore, the trend towards statistical significant difference for the 20-100 µg/kg LPS contrast on PD ~45 is turning into statistical significance, and the 0-100 µg/kg LPS contrast on PD ~45 is showing a trend towards a statistical significant difference as well (see appendix 6.2.2.4, table 63).

All estimated marginal means don't change much (see appendix 6.2.2.4, table 62).

3.1.2. Open Field

3.1.2.1. Distance

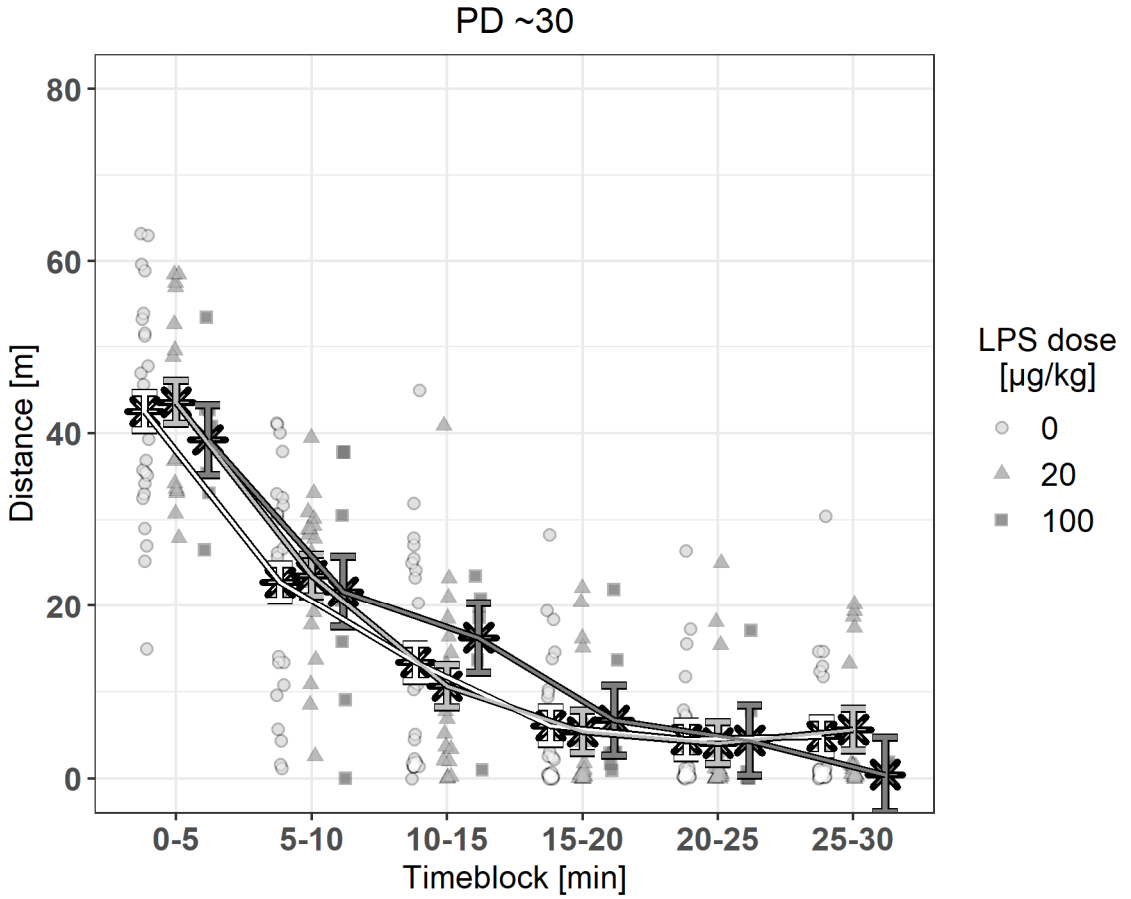

Figure 25: Distance travelled in the OF [m] on PD ~30 by Timeblock and LPS dose
Shown are estimated marginal means (⁎) of the distance travelled extracted from the linear mixed models after outlier removal ± SEM on top of the jittered raw data. SAL data (0 µg/kg LPS) shown as white circles, 20 µg/kg LPS as light grey triangles and 100 µg/kg LPS as dark grey squares.

23 data points were excluded after outlier analysis.

The statistical model assumptions were violated, independently from inclusion or exclusion of outliers (see appendix 6.2.3.1 and 6.2.4.1, figures 67 and 70). The data show non-normality and heteroscedasticity. Therefore, no further post-hoc tests were done, and the data was not interpreted any further.

Looking at the univariate distribution plots for Distance travelled in the OF grouped within LPS dose, age and timeblock, the plots clearly indicate the raw-data is not-normally distributed and showing excessive zeroes / zero-inflation (see figure 29).

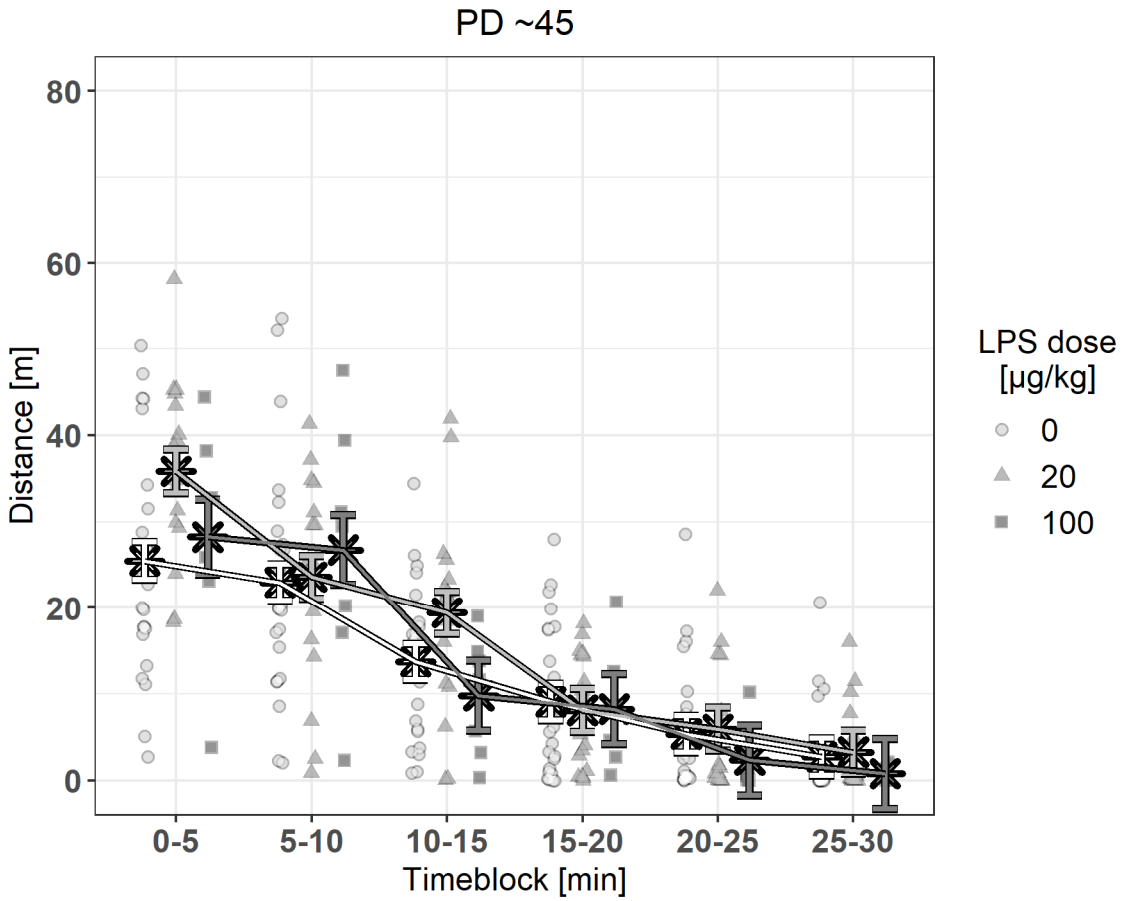

Figure 26: Distance travelled in the OF [m] on PD ~45 by Timeblock and LPS dose
Shown are estimated marginal means (⁎) of the distance travelled extracted from the linear mixed models after outlier removal ± SEM on top of the jittered raw data. SAL data (0 µg/kg LPS) shown as white circles, 20 µg/kg LPS as light grey triangles and 100 µg/kg LPS as dark grey squares.

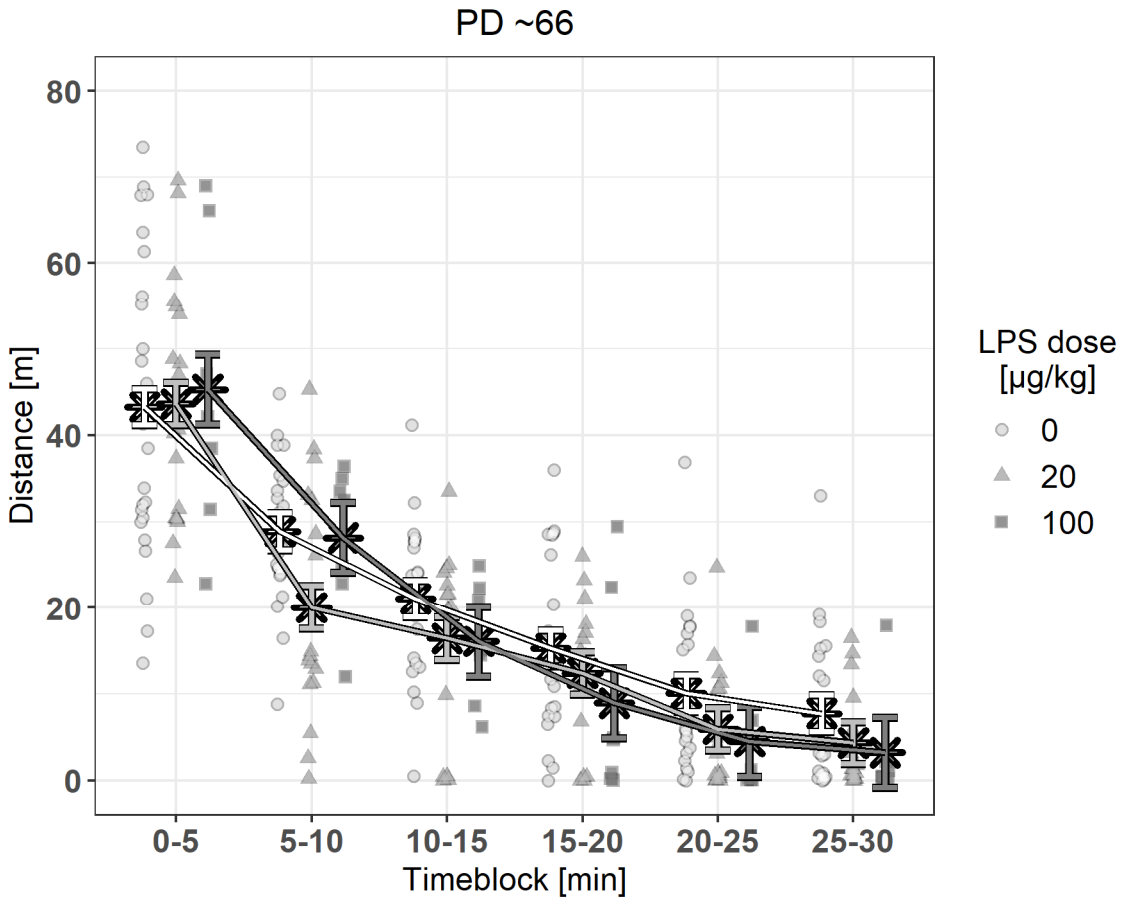

Figure 27: Distance travelled in the OF [m] on PD ~66 by Timeblock and LPS dose
Shown are estimated marginal means (⁎) of the distance travelled extracted from the linear mixed models after outlier removal ± SEM on top of the jittered raw data. SAL data (0 µg/kg LPS) shown as white circles, 20 µg/kg LPS as light grey triangles and 100 µg/kg LPS as dark grey squares.

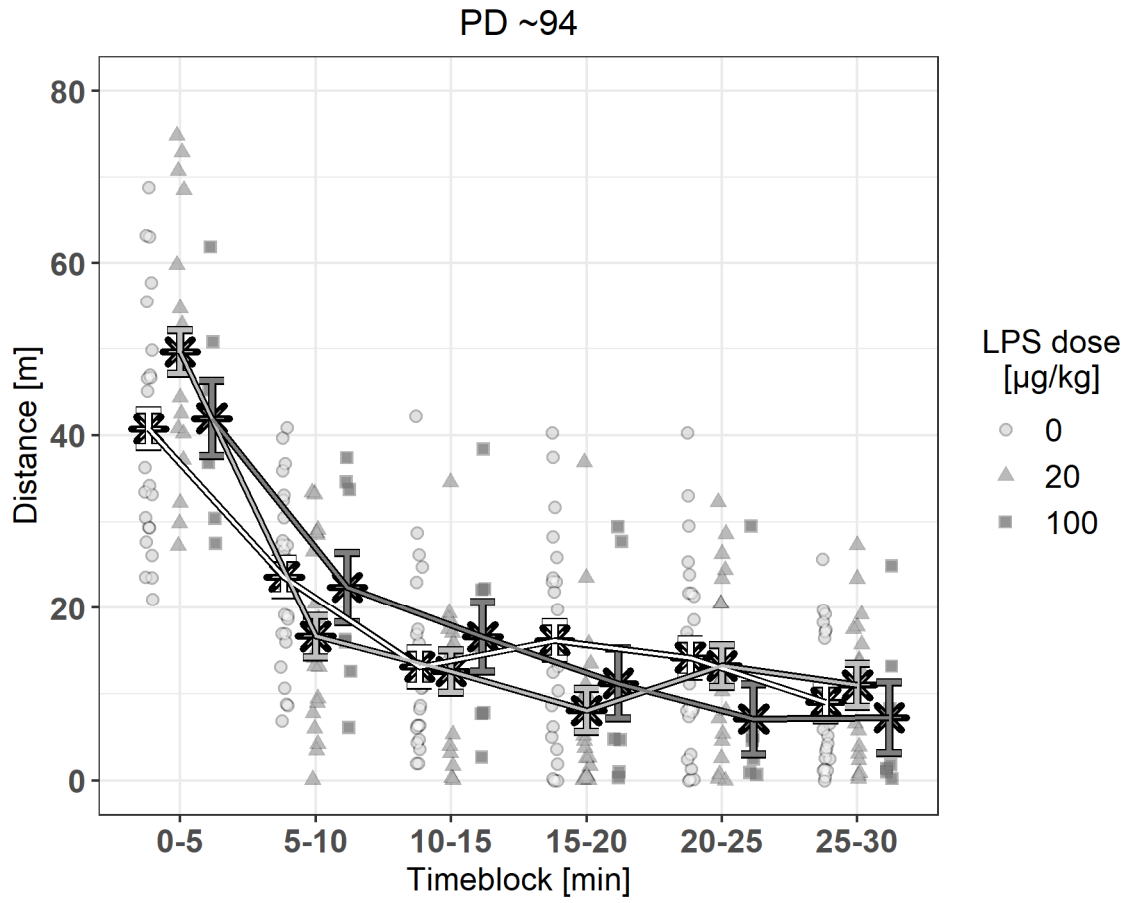

Figure 28: Distance travelled in the OF [m] on PD ~94 by Timeblock and LPS dose
Shown are estimated marginal means (⁎) of the distance travelled extracted from the linear mixed models after outlier removal ± SEM on top of the jittered raw data. SAL data (0 µg/kg LPS) shown as white circles, 20 µg/kg LPS as light grey triangles and 100 µg/kg LPS as dark grey squares.

Table 12: ANOVA table of the LMM of the OF Distance data after outlier removal
Shown are the sums of squares (SS), mean squares (MS), numerator (df Num) and denominator (df Den) degrees of freedom, F- and p-value for each simple factor as well as for the Dose:Age, Dose:Timeblock, Age:Timeblock and Dose:Age:Timeblock interaction terms. The Dose:Age, Dose:Timeblock and Age:Timeblock interactions show statistical significance (p = .013 / .002 / .000).

	SS	*MS*	df_{Num}	df_{Den}	*F*	*p*	
Dose	47.76	23.88	2	5.33	0.27	.775	
Age	3699.34	1233.11	3	1078.87	13.79	**.000**	***
Timeblock	126535.63	25307.13	5	1078.73	283.08	**.000**	***
Scan	0.17	0.17	1	44.26	0.00	.965	
Dose:Age	1454.81	242.47	6	1078.90	2.71	**.013**	*
Dose:Timeblock	2473.72	247.37	10	1078.75	2.77	**.002**	**
Age:Timeblock	5407.56	360.50	15	1078.72	4.03	**.000**	***
Dose:Age:TimeBlock	2436.04	81.20	30	1078.73	0.91	.610	

Table 13: Estimated marginal means of the LMM of the Distance data after outlier removal
Shown are the estimated marginal mean, standard error (SE), degrees of freedom (df) and 95% confidence interval for each LPS dose, Age and Timeblock combination. – Table is continued on the next page.

LPS dose [µg/kg]	Age [PD]	Timeblock [min]	*Mean*	*SE*	*df*	*95% Confidence Interval*	
						Lower CL	*Upper CL*
0	~30	0-5	42.52	2.19	128.16	38.19	46.84
0	~45	0-5	25.48	2.19	127.47	21.15	29.80
0	~66	0-5	43.26	2.11	113.04	39.08	47.44
0	~94	0-5	40.75	2.11	113.04	36.57	44.93
20	~30	0-5	43.58	2.48	122.41	38.66	48.50
20	~45	0-5	35.85	2.55	133.96	30.81	40.88
20	~66	0-5	43.64	2.43	112.20	38.83	48.46
20	~94	0-5	49.63	2.54	134.28	44.60	54.67
100	~30	0-5	39.25	4.05	64.51	31.16	47.34
100	~45	0-5	28.24	4.31	81.96	19.66	36.82
100	~66	0-5	45.29	4.05	64.51	37.20	53.38
100	~94	0-5	41.96	4.31	81.90	33.38	50.54
0	~30	5-10	22.74	2.11	113.04	18.56	26.92
0	~45	5-10	22.96	2.11	113.04	18.78	27.14
0	~66	5-10	28.85	2.15	120.03	24.60	33.10
0	~94	5-10	23.62	2.11	113.04	19.44	27.80
20	~30	5-10	23.55	2.43	112.20	18.74	28.36
20	~45	5-10	23.58	2.48	122.41	18.66	28.50
20	~66	5-10	20.04	2.49	122.24	15.12	24.96
20	~94	5-10	16.66	2.43	112.20	11.84	21.47
100	~30	5-10	21.66	4.05	64.51	13.57	29.75
100	~45	5-10	26.73	4.05	64.51	18.64	34.82
100	~66	5-10	28.15	4.05	64.51	20.06	36.24
100	~94	5-10	22.39	4.05	64.51	14.30	30.48
0	~30	10-15	13.41	2.11	113.04	9.23	17.59
0	~45	10-15	13.72	2.11	113.04	9.54	17.90
0	~66	10-15	21.03	2.15	120.03	16.78	25.28
0	~94	10-15	13.12	2.15	120.62	8.87	17.36
20	~30	10-15	10.67	2.43	112.20	5.86	15.49
20	~45	10-15	19.44	2.43	112.20	14.63	24.26
20	~66	10-15	16.43	2.48	122.34	11.52	21.35
20	~94	10-15	12.61	2.43	112.20	7.80	17.43
100	~30	10-15	16.28	4.05	64.51	8.19	24.36
100	~45	10-15	9.79	4.05	64.51	1.70	17.88
100	~66	10-15	16.08	4.05	64.51	7.99	24.16
100	~94	10-15	16.63	4.05	64.51	8.54	24.72

Continuation of Table 13:

0	~30	15-20	6.08	2.11	113.04	1.90	10.26
0	~45	15-20	9.09	2.11	113.04	4.91	13.27
0	~66	15-20	15.28	2.11	113.04	11.10	19.46
0	~94	15-20	16.20	2.15	119.86	11.96	20.45
20	~30	15-20	5.40	2.43	112.20	0.59	10.22
20	~45	15-20	8.11	2.48	122.41	3.19	13.03
20	~66	15-20	12.39	2.43	112.20	7.57	17.20
20	~94	15-20	8.09	2.49	120.41	3.17	13.01
100	~30	15-20	6.72	4.05	64.51	-1.37	14.81
100	~45	15-20	8.26	4.05	64.51	0.17	16.35
100	~66	15-20	8.93	4.05	64.51	0.84	17.02
100	~94	15-20	11.22	4.05	64.51	3.13	19.31
0	~30	20-25	4.50	2.11	113.04	0.32	8.68
0	~45	20-25	5.37	2.11	113.04	1.19	9.55
0	~66	20-25	10.07	2.11	113.04	5.89	14.25
0	~94	20-25	14.18	2.15	119.87	9.93	18.43
20	~30	20-25	4.10	2.43	112.20	-0.71	8.92
20	~45	20-25	5.93	2.49	120.37	1.01	10.85
20	~66	20-25	5.92	2.43	112.20	1.11	10.74
20	~94	20-25	13.25	2.43	112.20	8.44	18.06
100	~30	20-25	4.39	4.05	64.51	-3.70	12.48
100	~45	20-25	2.35	4.05	64.51	-5.74	10.44
100	~66	20-25	4.50	4.05	64.51	-3.59	12.59
100	~94	20-25	7.10	4.05	64.51	-0.99	15.19
0	~30	25-30	4.87	2.11	113.04	0.69	9.05
0	~45	25-30	2.72	2.15	120.77	-1.52	6.97
0	~66	25-30	7.74	2.11	113.04	3.56	11.92
0	~94	25-30	9.04	2.11	113.04	4.86	13.22
20	~30	25-30	5.65	2.43	112.20	0.84	10.46
20	~45	25-30	3.27	2.49	120.37	-1.65	8.20
20	~66	25-30	4.34	2.43	112.20	-0.47	9.16
20	~94	25-30	11.01	2.48	122.34	6.09	15.93
100	~30	25-30	0.46	4.31	81.96	-8.12	9.04
100	~45	25-30	0.79	4.05	64.51	-7.30	8.88
100	~66	25-30	3.23	4.05	64.51	-4.86	11.32
100	~94	25-30	7.26	4.05	64.51	-0.83	15.35

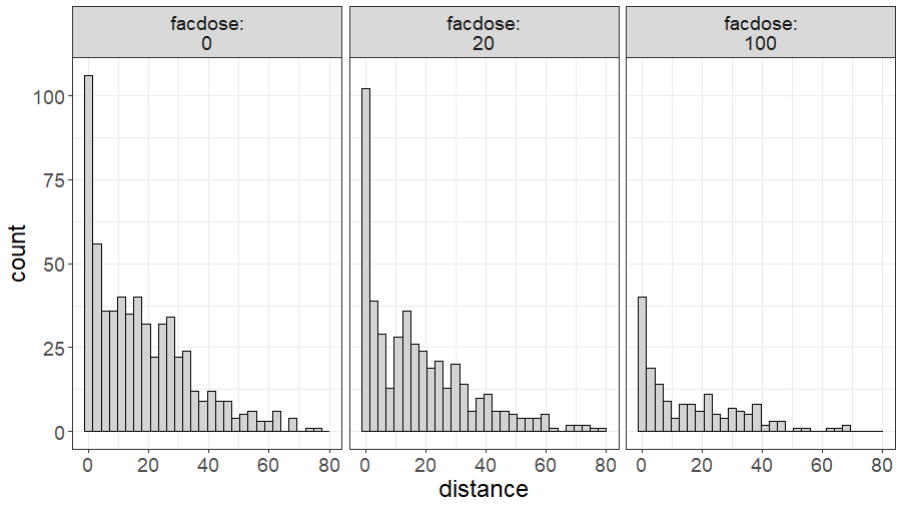

a)

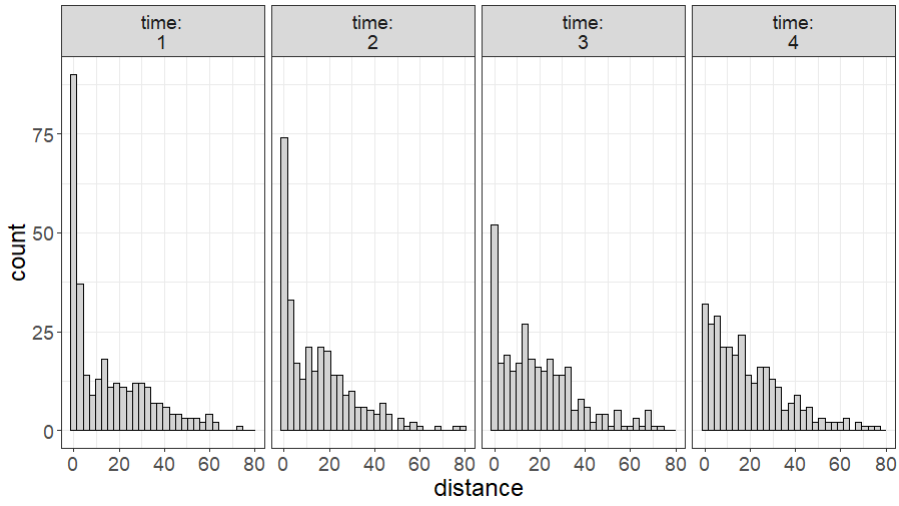

b)

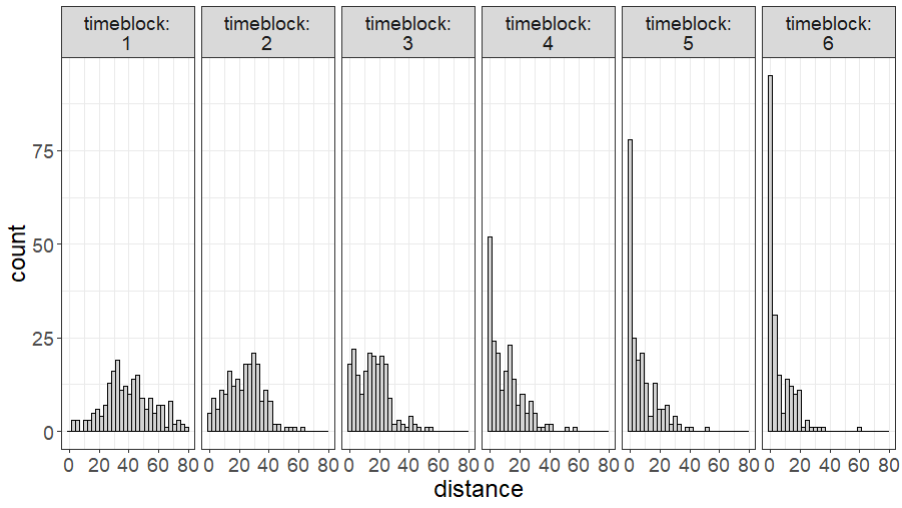

c)

Figure 29: Univariate Plots for Distance travelled in the OF [m]
Shown are univariate plots plots for Distance travelled in the OF [m], **a)** split by LPS dose – here labeled as "facdose 0 – 100" with facdose 0 representing the SAL group and facdose 100 representing the 100 µg/kg LPS group, **b)** split by age – here labeled as "time 1-4" with time 1 representing PD~30 and time 4 representing PD~94 and **c)** split by timeblock – here labeled "1 – 6" with 1 representing the 0-5 min timeblock and 6 representing the 25-30 min timeblock. Most plots indicate non-normal distributed, zero-inflated data.

3.1.2.2. Center Time

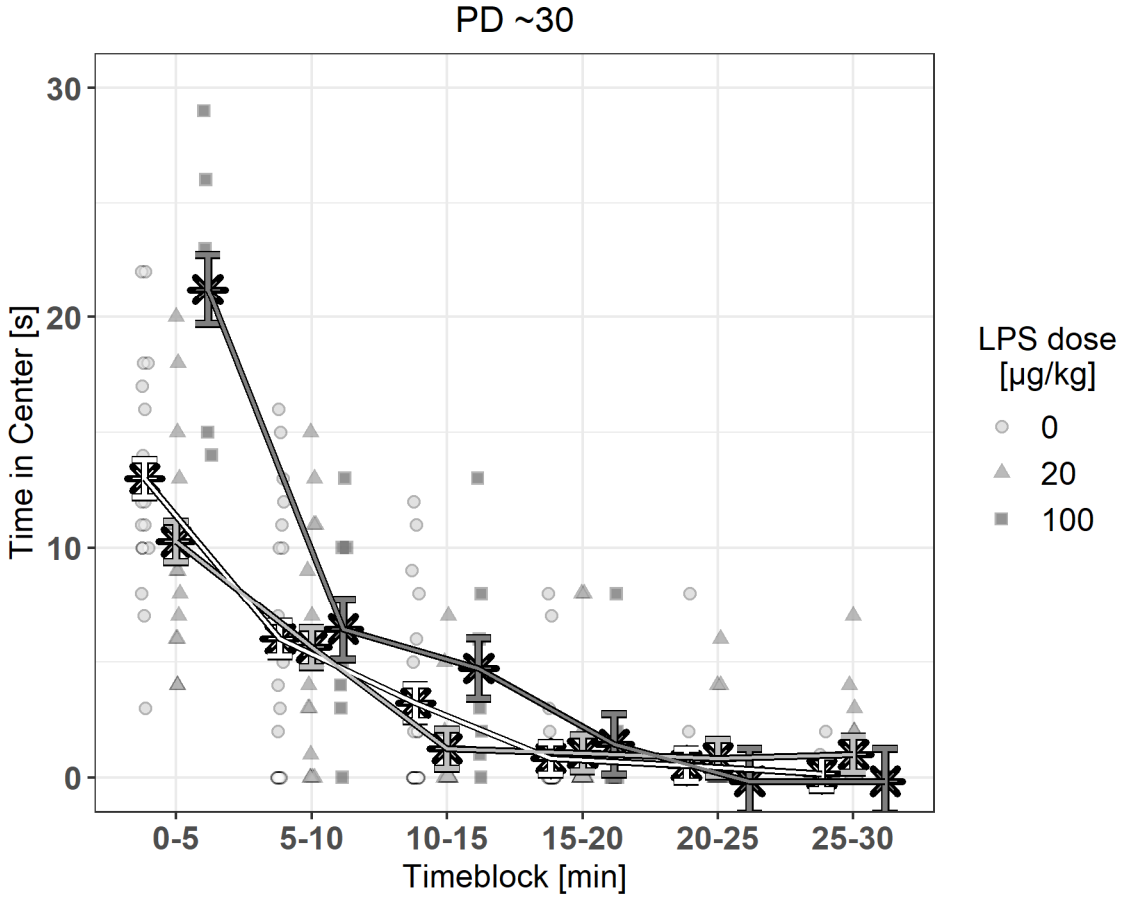

Figure 30: Time in the center of the OF [s] on PD ~30 by Timeblock and LPS dose
Shown are estimated marginal means (⁎) of the central square time extracted from the linear mixed models after outlier removal ± SEM on top of the jittered raw data. SAL data (0 µg/kg LPS) shown as white circles, 20 µg/kg LPS as light grey triangles and 100 µg/kg LPS as dark grey squares.

138 data points were excluded after outlier analysis.

The statistical model assumptions were violated, independently from inclusion or exclusion of outliers (see appendix 6.2.3.2 and 6.2.4.2, figures 68 and 71). The data show non-normality and heteroscedasticity. Therefore, no further post-hoc tests were done, and the data was not interpreted any further.

Looking at the univariate distribution plots for Time in Center of the OF grouped within LPS dose, age and timeblock, the plots clearly indicate the raw-data is not-

normally distributed and showing excessive zeroes / zero-inflation (see figure 34).

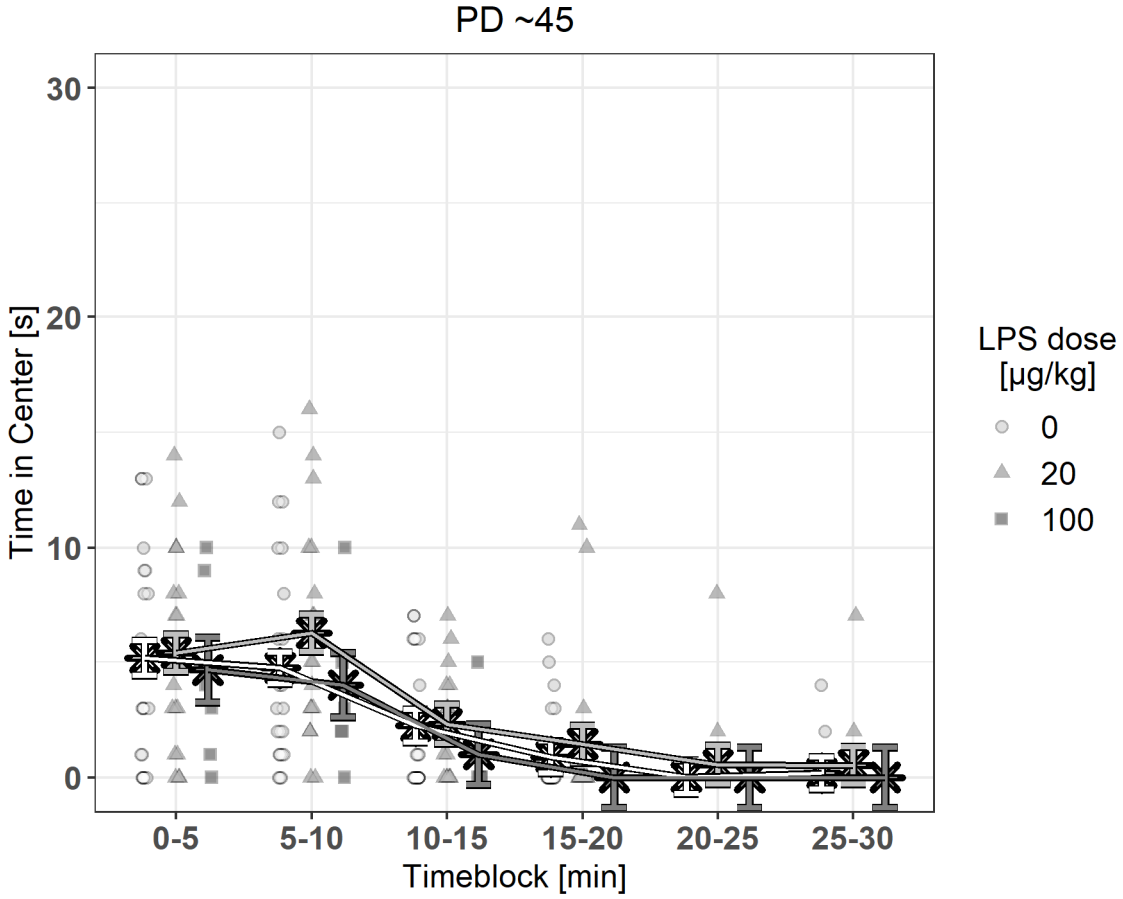

Figure 31: Time in the center of the OF [s] on PD ~45 by Timeblock and LPS dose
Shown are estimated marginal means (⁎) of the central square time extracted from the linear mixed models after outlier removal ± SEM on top of the jittered raw data. SAL data (0 µg/kg LPS) shown as white circles, 20 µg/kg LPS as light grey triangles and 100 µg/kg LPS as dark grey squares.

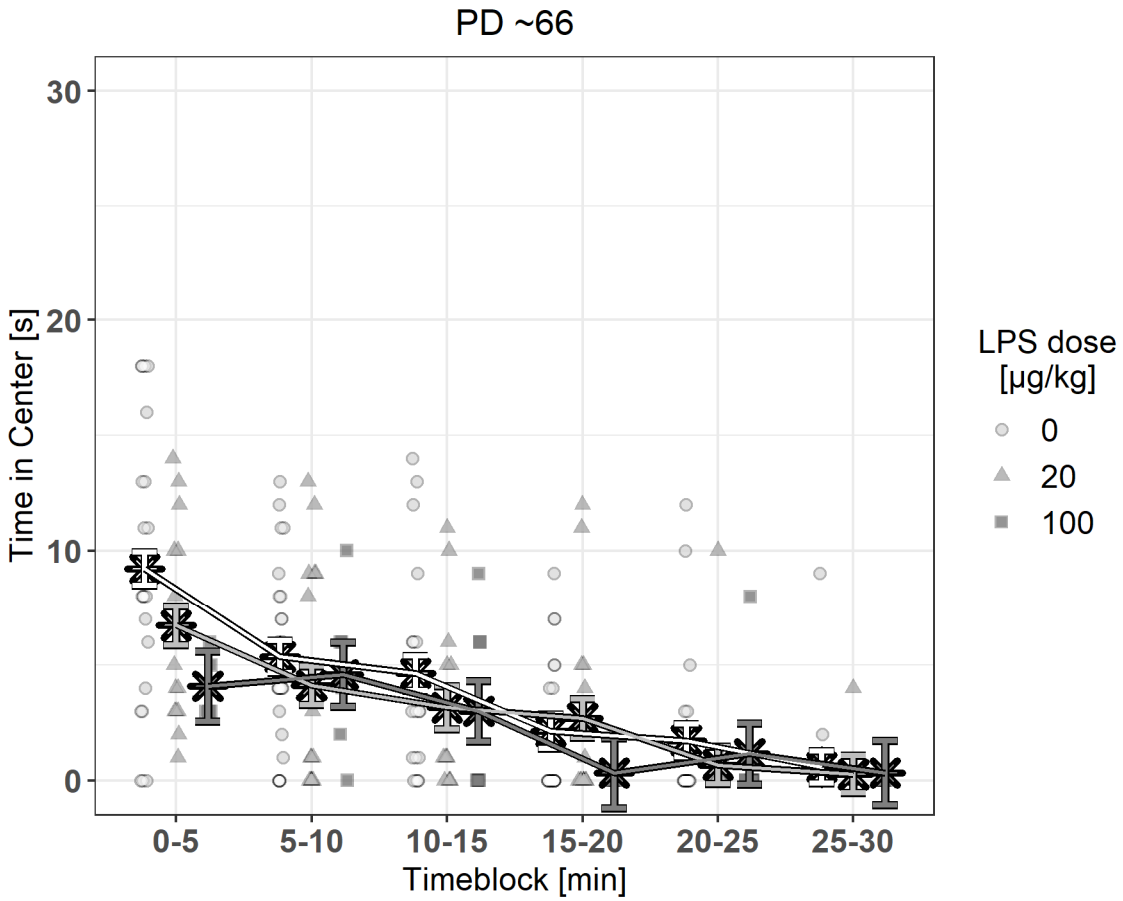

Figure 32: Time in the center of the OF [s] on PD ~66 by Timeblock and LPS dose
Shown are estimated marginal means (⁎) of the central square time extracted from the linear mixed models after outlier removal ± SEM on top of the jittered raw data. SAL data (0 µg/kg LPS) shown as white circles, 20 µg/kg LPS as light grey triangles and 100 µg/kg LPS as dark grey squares.

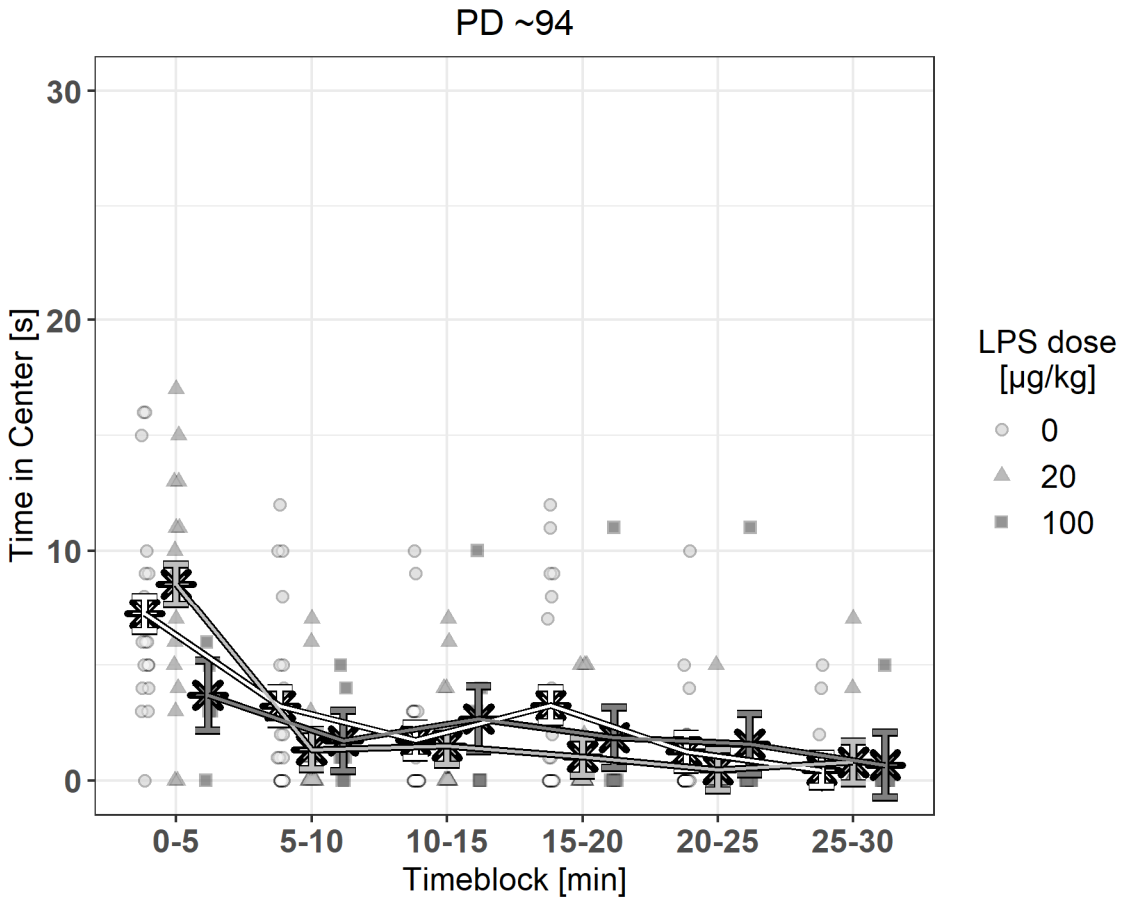

Figure 33: Time in the center of the OF [s] on PD ~94 by Timeblock and LPS dose
Shown are estimated marginal means (⁎) of the central square time extracted from the linear mixed models after outlier removal ± SEM on top of the jittered raw data. SAL data (0 µg/kg LPS) shown as white circles, 20 µg/kg LPS as light grey triangles and 100 µg/kg LPS as dark grey squares.

Table 14: ANOVA table of the LMM of the OF Center Square Time data after outlier removal
Shown are the sums of squares (SS), mean squares (MS), numerator (df Num) and denominator (df Den) degrees of freedom, F- and p-value for each simple factor as well as for the Dose:Age, Dose:Timeblock, Age:Timeblock and Dose:Age:Timeblock interaction terms. The Dose:Age:Timeblock interaction shows statistical significance (p = .000).

	SS	*MS*	df_{Num}	df_{Den}	*F*	*p*	
Dose	9.34	4.67	2	5.02	0.47	.651	
Age	549.47	183.16	3	964.31	18.33	**.000**	***
Timeblock	5526.44	1105.29	5	963.03	110.59	**.000**	***
Scan	0.92	0.92	1	43.33	0.09	.763	
Dose:Age	270.26	45.04	6	964.55	4.51	**.000**	***
Dose:Timeblock	56.57	5.66	10	962.99	0.57	.842	
Age:Timeblock	1667.45	111.16	15	963.19	11.12	**.000**	***
Dose:Age:TimeBlock	661.89	22.06	30	963.17	2.21	**.000**	***

Table 15: Estimated marginal means of the LMM of the OF Center Square Time data after outlier removal

Shown are the estimated marginal mean, standard error (SE), degrees of freedom (df) and 95% confidence interval for each LPS dose, Age and Timeblock combination. – Table is continued on the next page.

LPS dose [µg/kg]	Age [PD]	Timeblock [min]	*Mean*	*SE*	*df*	*95% Confidence Interval*	
						Lower CL	*Upper CL*
0	~30	0-5	12.99	0.82	269.94	11.39	14.60
0	~45	0-5	5.17	0.76	214.50	3.67	6.66
0	~66	0-5	9.20	0.72	186.12	7.77	10.63
0	~94	0-5	7.23	0.76	217.77	5.74	8.72
20	~30	0-5	10.25	0.88	218.15	8.53	11.98
20	~45	0-5	5.41	0.81	165.17	3.81	7.00
20	~66	0-5	6.72	0.85	201.02	5.04	8.40
20	~94	0-5	8.54	0.88	205.26	6.81	10.26
100	~30	0-5	21.21	1.52	150.84	18.22	24.21
100	~45	0-5	4.66	1.40	113.22	1.88	7.43
100	~66	0-5	4.08	1.52	150.93	1.08	7.08
100	~94	0-5	3.69	1.52	150.91	0.69	6.69
0	~30	5-10	6.01	0.74	199.04	4.55	7.47
0	~45	5-10	4.75	0.69	154.41	3.39	6.10
0	~66	5-10	5.36	0.70	164.14	3.98	6.73
0	~94	5-10	3.23	0.77	230.78	1.70	4.76
20	~30	5-10	5.63	0.85	189.37	3.95	7.31
20	~45	5-10	6.26	0.81	165.85	4.67	7.85
20	~66	5-10	4.11	0.83	181.98	2.48	5.74
20	~94	5-10	1.34	0.85	196.00	-0.34	3.02
100	~30	5-10	6.44	1.31	88.52	3.83	9.04
100	~45	5-10	4.00	1.40	113.21	1.22	6.77
100	~66	5-10	4.59	1.40	113.18	1.81	7.36
100	~94	5-10	1.72	1.31	88.52	-0.88	4.32
0	~30	10-15	3.22	0.77	230.13	1.69	4.74
0	~45	10-15	2.24	0.71	174.70	0.84	3.64
0	~66	10-15	4.65	0.76	216.64	3.15	6.14
0	~94	10-15	1.74	0.74	199.99	0.28	3.20
20	~30	10-15	1.24	0.85	184.67	-0.44	2.92
20	~45	10-15	2.31	0.85	200.83	0.64	3.99
20	~66	10-15	3.16	0.93	278.28	1.32	4.99
20	~94	10-15	1.51	0.81	165.66	-0.09	3.10
100	~30	10-15	4.72	1.31	88.52	2.12	7.32
100	~45	10-15	1.01	1.31	88.52	-1.59	3.61
100	~66	10-15	3.01	1.31	88.52	0.41	5.61
100	~94	10-15	2.67	1.40	113.30	-0.10	5.45

Continuation of Table 15:

0	~30	15-20	0.83	0.69	154.41	-0.53	2.18
0	~45	15-20	0.89	0.70	164.41	-0.48	2.27
0	~66	15-20	2.13	0.74	200.71	0.67	3.59
0	~94	15-20	3.26	0.74	202.31	1.80	4.71
20	~30	15-20	1.05	0.79	151.15	-0.51	2.61
20	~45	15-20	1.45	0.81	165.66	-0.14	3.05
20	~66	15-20	2.69	0.83	182.40	1.06	4.33
20	~94	15-20	1.03	0.81	161.30	-0.56	2.63
100	~30	15-20	1.44	1.31	88.52	-1.17	4.04
100	~45	15-20	0.01	1.31	88.52	-2.59	2.61
100	~66	15-20	0.33	1.52	150.86	-2.67	3.32
100	~94	15-20	1.86	1.31	88.52	-0.74	4.47
0	~30	20-25	0.53	0.70	163.62	-0.85	1.91
0	~45	20-25	0.03	0.73	185.66	-1.40	1.46
0	~66	20-25	1.73	0.71	175.19	0.33	3.13
0	~94	20-25	1.24	0.77	234.42	-0.28	2.77
20	~30	20-25	0.84	0.79	151.15	-0.72	2.40
20	~45	20-25	0.56	0.83	177.62	-1.08	2.19
20	~66	20-25	0.67	0.81	161.38	-0.92	2.27
20	~94	20-25	0.46	0.88	222.86	-1.26	2.19
100	~30	20-25	-0.16	1.40	113.30	-2.93	2.61
100	~45	20-25	0.01	1.31	88.52	-2.59	2.61
100	~66	20-25	1.15	1.31	88.52	-1.45	3.75
100	~94	20-25	1.58	1.31	88.52	-1.02	4.18
0	~30	25-30	0.17	0.71	174.64	-1.23	1.58
0	~45	25-30	0.19	0.70	165.24	-1.18	1.57
0	~66	25-30	0.57	0.70	165.19	-0.80	1.95
0	~94	25-30	0.45	0.71	174.13	-0.95	1.85
20	~30	25-30	1.00	0.79	151.15	-0.56	2.56
20	~45	25-30	0.54	0.81	161.40	-1.06	2.13
20	~66	25-30	0.26	0.81	165.85	-1.33	1.85
20	~94	25-30	0.79	0.90	241.94	-0.99	2.57
100	~30	25-30	-0.16	1.40	113.30	-2.93	2.61
100	~45	25-30	0.01	1.31	88.52	-2.59	2.61
100	~66	25-30	0.33	1.40	113.21	-2.44	3.10
100	~94	25-30	0.67	1.40	113.30	-2.10	3.45

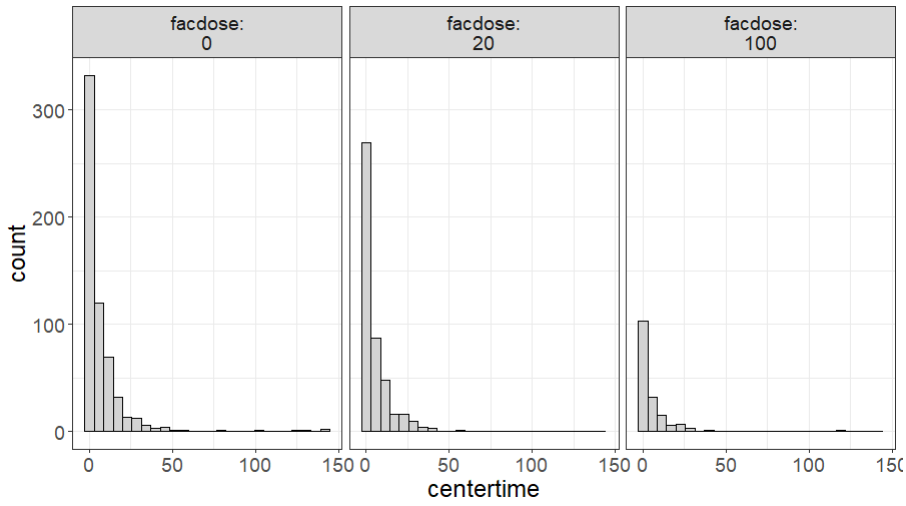

d)

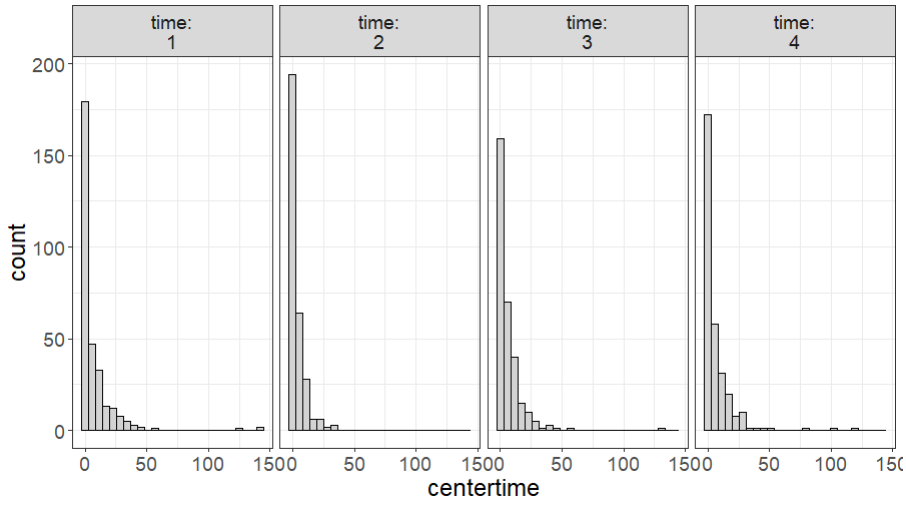

e)

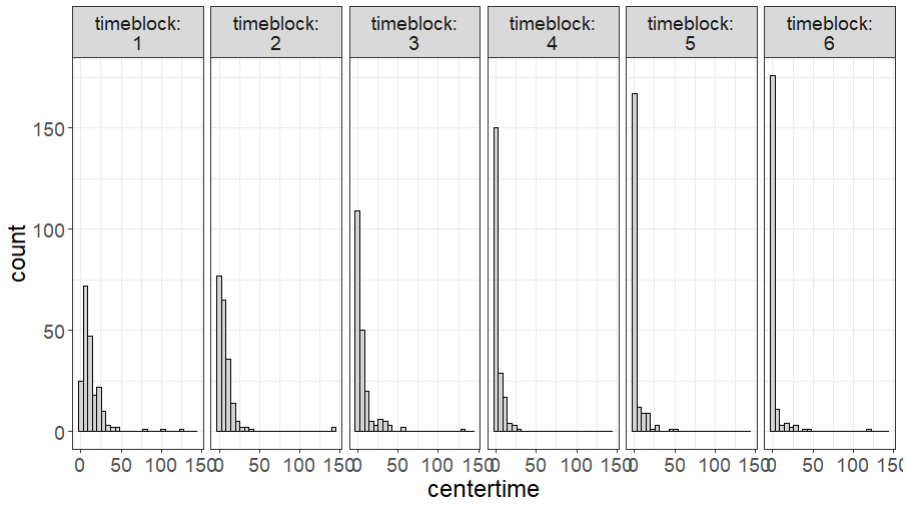

f)

Figure 34: Univariate Plots for Time in the center of the OF [s]
Shown are univariate plots plots for Time in the center of the OF [s], **a)** split by LPS dose – here labeled as "facdose 0 – 100" with facdose 0 representing the SAL group and facdose 100 representing the 100 µg/kg LPS group, **b)** split by age – here labeled as "time 1-4" with time 1 representing PD~30 and time 4 representing PD~94 and **c)** split by timeblock – here labeled "1 – 6" with 1 representing the 0-5 min timeblock and 6 representing the 25-30 min timeblock. All plots indicate non-normal distributed, zero-inflated data.

3.1.2.3. Rearings

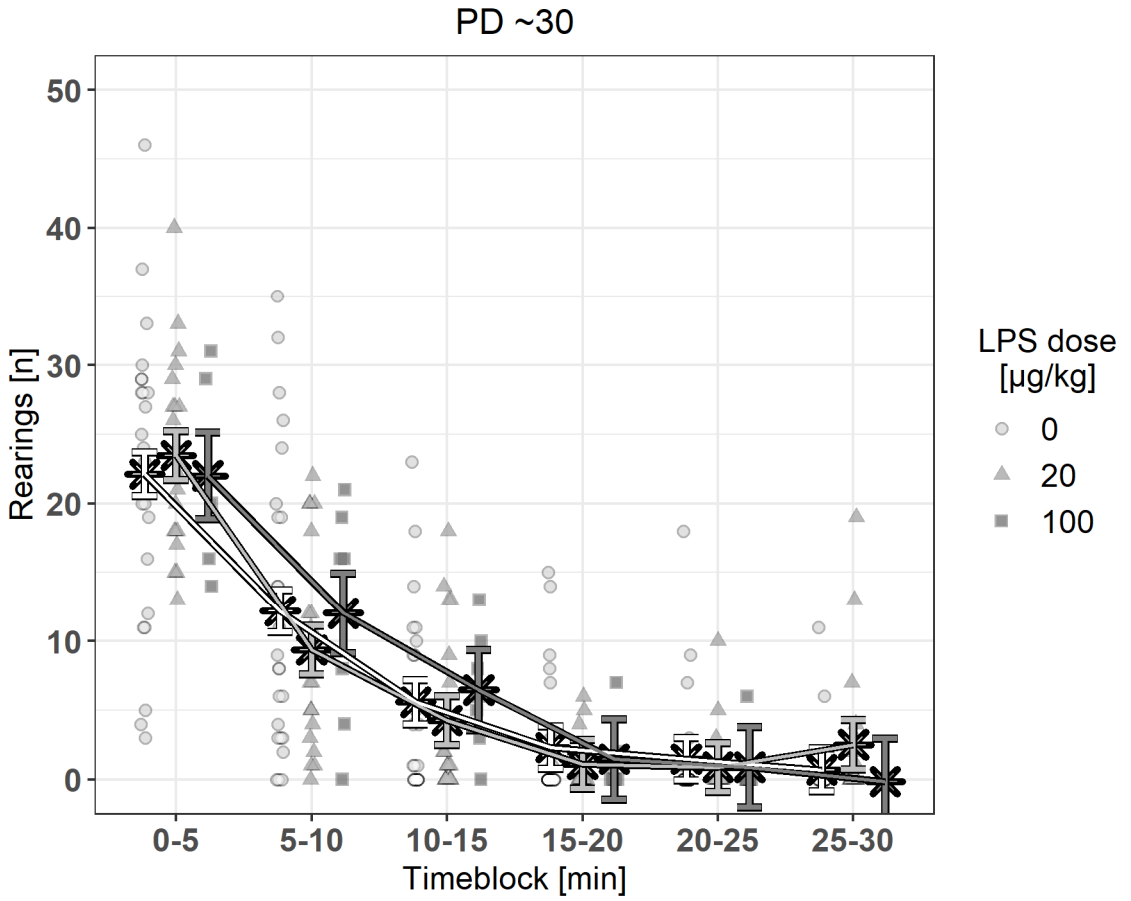

Figure 35: Rearings in the OF [n] on PD ~30 by Timeblock and LPS dose
Shown are estimated marginal means (⁎) of rearings extracted from the linear mixed models after outlier removal ± SEM on top of the jittered raw data. SAL data (0 µg/kg LPS) shown as white circles, 20 µg/kg LPS as light grey triangles and 100 µg/kg LPS as dark grey squares.

43 data points were excluded after outlier analysis.

The statistical model assumptions were violated, independently from inclusion or exclusion of outliers (see appendix 6.2.3.3 and 6.2.4.3, figures 69 and 72). The data show non-normality and heteroscedasticity. Therefore, no further post-hoc tests were done, and the data was not interpreted any further.

Looking at the univariate distribution plots for Rearings in the OF grouped within LPS dose, age and timeblock, the plots clearly indicate the raw-data is not-normally distributed and showing excessive zeroes / zero-inflation (see figure 39).

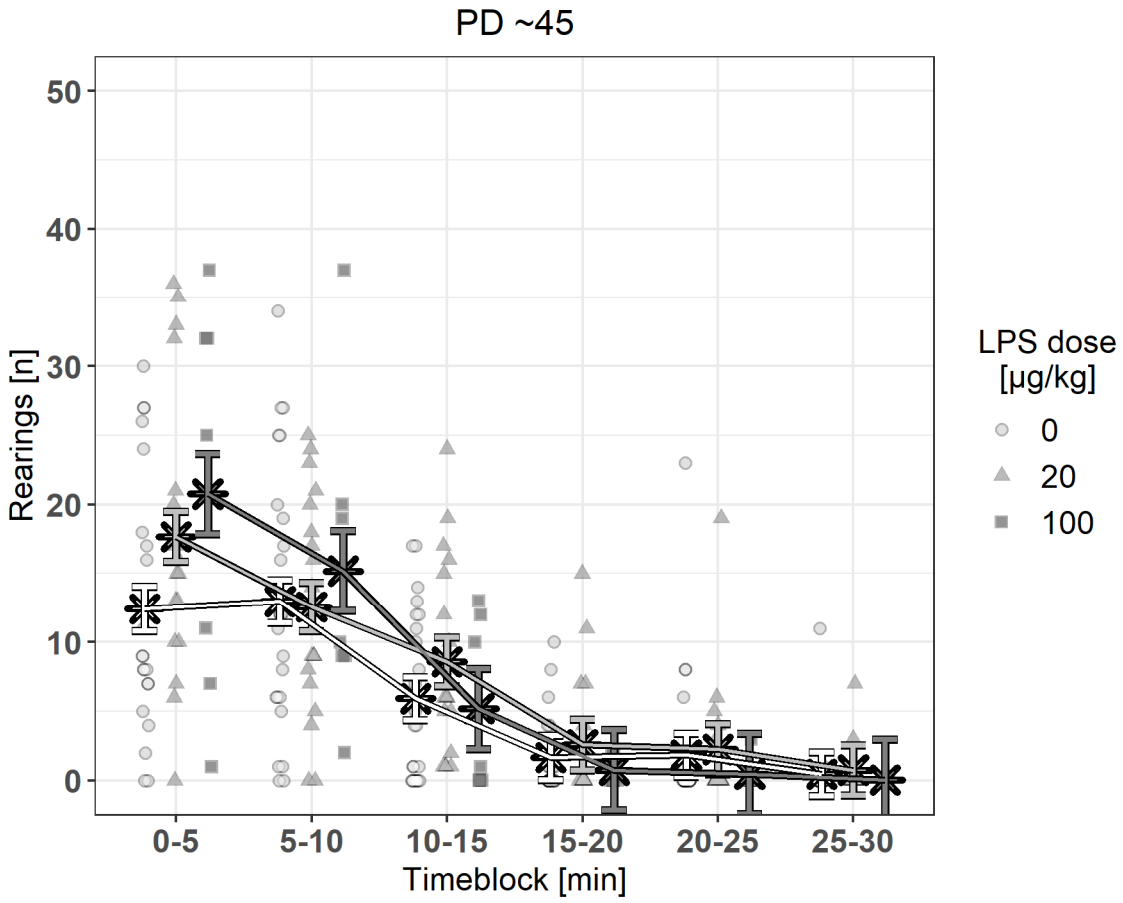

Figure 36: Rearings in the OF [n] on PD ~45 by Timeblock and LPS dose
Shown are estimated marginal means (⁎) of rearings extracted from the linear mixed models after outlier removal ± SEM on top of the jittered raw data. SAL data (0 µg/kg LPS) shown as white circles, 20 µg/kg LPS as light grey triangles and 100 µg/kg LPS as dark grey squares.

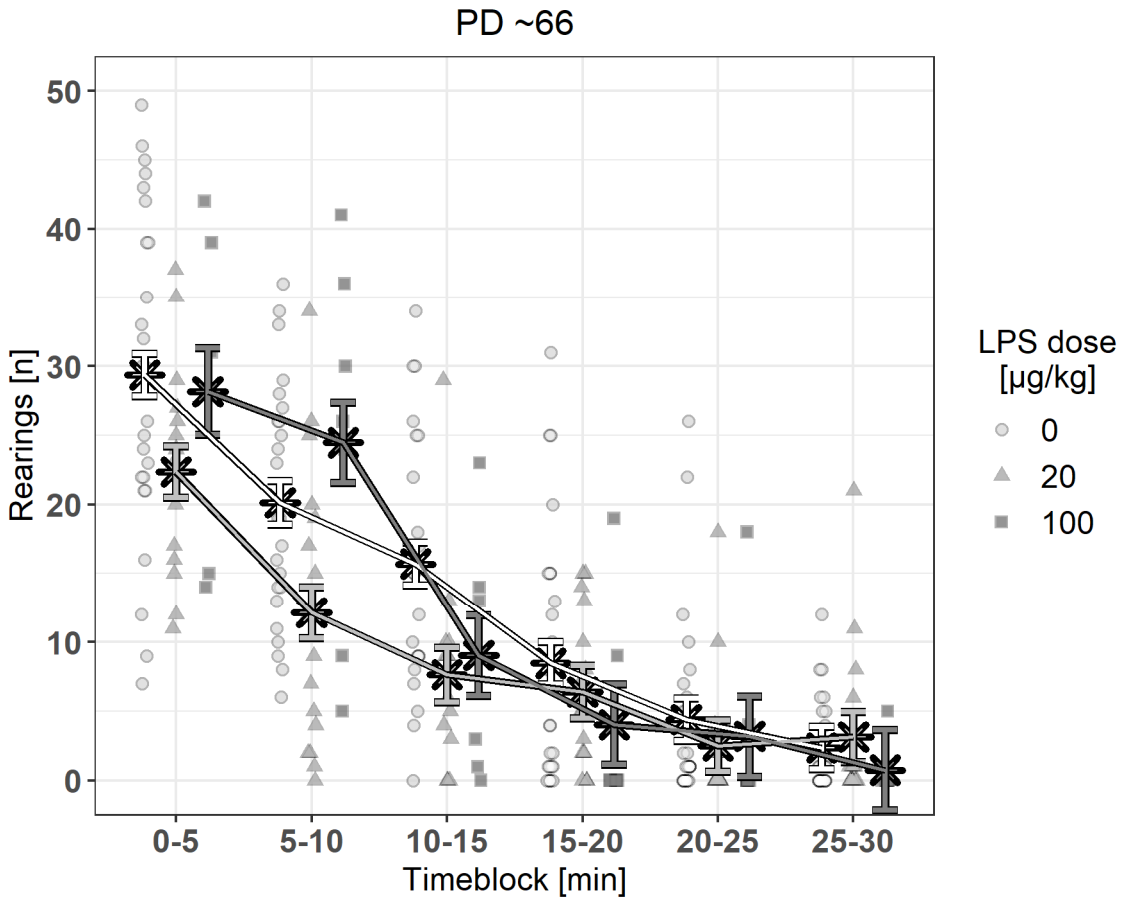

Figure 37: Rearings in the OF [n] on PD ~66 by Timeblock and LPS dose
Shown are estimated marginal means (⁎) of rearings extracted from the linear mixed models after outlier removal ± SEM on top of the jittered raw data. SAL data (0 µg/kg LPS) shown as white circles, 20 µg/kg LPS as light grey triangles and 100 µg/kg LPS as dark grey squares.

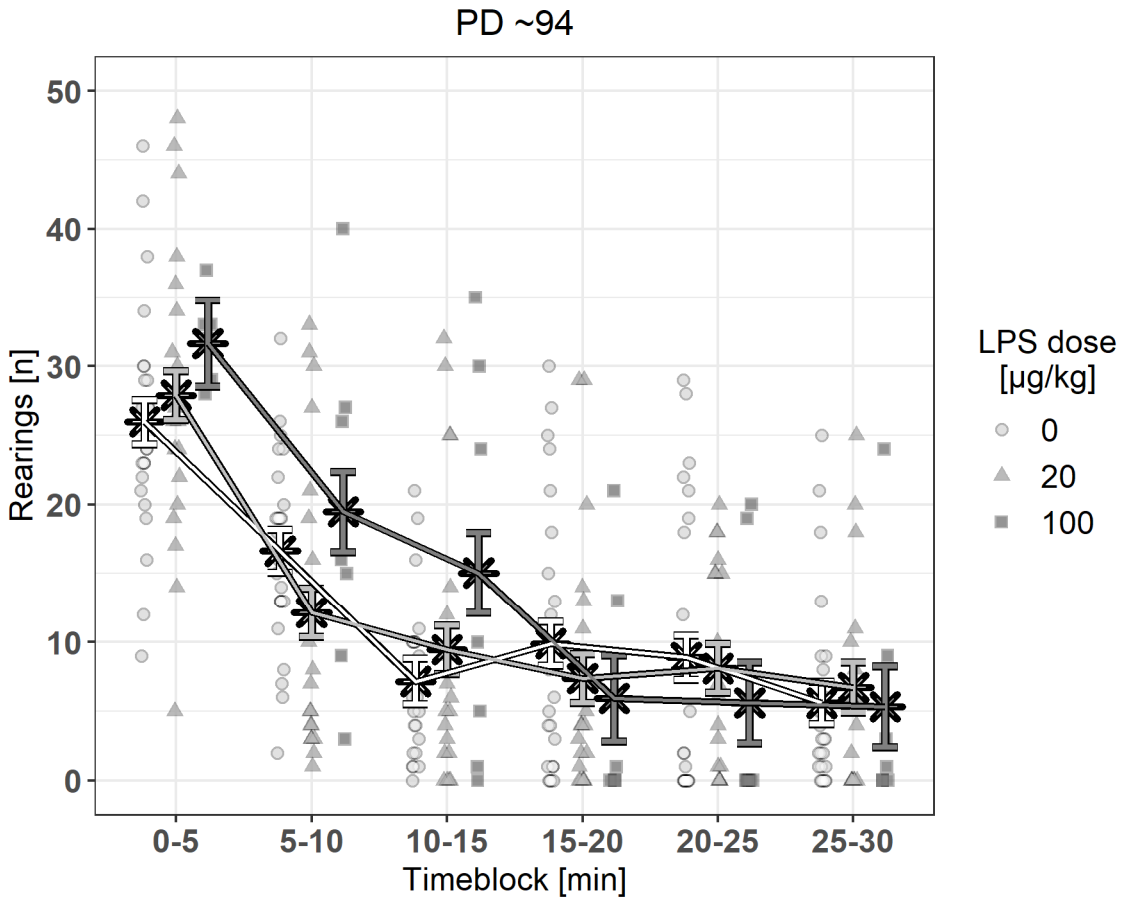

Figure 38: Rearings in the OF [n] on PD ~94 by Timeblock and LPS dose
Shown are estimated marginal means (⁎) of rearings extracted from the linear mixed models after outlier removal ± SEM on top of the jittered raw data. SAL data (0 µg/kg LPS) shown as white circles, 20 µg/kg LPS as light grey triangles and 100 µg/kg LPS as dark grey squares.

Table 16: ANOVA table of the LMM of the OF Rearings data after outlier removal
Shown are the sums of squares (SS), mean squares (MS), numerator (df Num) and denominator (df Den) degrees of freedom, F- and p-value for each simple factor as well as for the Dose:Age, Dose:Timeblock, Age:Timeblock and Dose:Age:Timeblock interaction terms. The Dose:Age, Dose:Timeblock and Age:Timeblock interactions show statistical significance (p = .001 / .006 / .005).

	SS	*MS*	df_{Num}	df_{Den}	*F*	*p*	
Dose	74.97	37.49	2	2.65	0.70	.569	
Age	5885.22	1961.74	3	1059.04	36.73	**.000**	***
Timeblock	49529.92	9905.98	5	1058.69	185.46	**.000**	***
Scan	24.90	24.90	1	44.04	0.47	.498	
Dose:Age	1168.52	194.75	6	1059.30	3.65	**.001**	***
Dose:Timeblock	1330.18	133.02	10	1058.63	2.49	**.006**	**
Age:Timeblock	1771.17	118.08	15	1058.41	2.21	**.005**	**
Dose:Age:TimeBlock	1554.70	51.82	30	1058.43	0.97	.513	

Table 17: Estimated marginal means of the LMM of the OF Rearings data after outlier removal
Shown are the estimated marginal mean, standard error (SE), degrees of freedom (df) and 95% confidence interval for each LPS dose, Age and Timeblock combination. – Table is continued on the next page.

LPS dose [µg/kg]	Age [PD]	Timeblock [min]	*Mean*	*SE*	*df*	*95% Confidence Interval*	
						Lower CL	*Upper CL*
0	~30	0-5	22.13	1.57	192.60	19.04	25.22
0	~45	0-5	12.42	1.63	214.74	9.21	15.64
0	~66	0-5	29.35	1.54	182.24	26.32	32.38
0	~94	0-5	25.97	1.60	210.22	22.82	29.12
20	~30	0-5	23.47	1.77	162.52	19.98	26.95
20	~45	0-5	17.66	1.81	172.20	14.08	21.23
20	~66	0-5	22.35	1.86	198.48	18.68	26.02
20	~94	0-5	27.89	1.77	162.52	24.40	31.38
100	~30	0-5	22.00	3.12	133.24	15.82	28.17
100	~45	0-5	20.75	2.91	102.37	14.99	26.52
100	~66	0-5	28.16	3.12	133.24	21.98	34.34
100	~94	0-5	31.64	3.12	133.14	25.47	37.82
0	~30	5-10	12.19	1.54	182.24	9.16	15.22
0	~45	5-10	12.97	1.57	192.12	9.88	16.06
0	~66	5-10	20.13	1.57	192.60	17.04	23.22
0	~94	5-10	16.63	1.54	182.24	13.60	19.66
20	~30	5-10	9.36	1.77	162.52	5.87	12.85
20	~45	5-10	12.57	1.77	162.52	9.08	16.06
20	~66	5-10	12.15	1.86	200.91	8.49	15.82
20	~94	5-10	12.15	1.77	162.52	8.66	15.64
100	~30	5-10	12.04	2.91	102.37	6.27	17.80
100	~45	5-10	15.18	2.91	102.37	9.42	20.94
100	~66	5-10	24.47	2.91	102.37	18.70	30.23
100	~94	5-10	19.47	2.91	102.37	13.70	25.23
0	~30	10-15	5.59	1.60	202.67	2.44	8.74
0	~45	10-15	5.91	1.54	182.24	2.88	8.94
0	~66	10-15	15.69	1.57	192.69	12.60	18.78
0	~94	10-15	7.15	1.63	223.63	3.94	10.37
20	~30	10-15	4.25	1.77	162.52	0.77	7.74
20	~45	10-15	8.57	1.77	162.52	5.08	12.06
20	~66	10-15	7.64	1.97	239.74	3.76	11.53
20	~94	10-15	9.47	1.77	162.52	5.98	12.95
100	~30	10-15	6.47	2.91	102.37	0.70	12.23
100	~45	10-15	5.18	2.91	102.37	-0.58	10.94
100	~66	10-15	9.04	2.91	102.37	3.27	14.80
100	~94	10-15	15.04	2.91	102.37	9.27	20.80

Continuation of Table 17:

0	~30	15-20	2.31	1.54	182.24	-0.72	5.34
0	~45	15-20	1.65	1.60	210.21	-1.50	4.80
0	~66	15-20	8.47	1.54	182.24	5.44	11.50
0	~94	15-20	9.89	1.60	208.62	6.74	13.04
20	~30	15-20	1.10	1.77	162.52	-2.39	4.59
20	~45	15-20	2.57	1.81	179.09	-1.01	6.14
20	~66	15-20	6.39	1.91	213.61	2.62	10.16
20	~94	15-20	7.36	1.77	162.52	3.87	10.85
100	~30	15-20	1.47	2.91	102.37	-4.30	7.23
100	~45	15-20	0.75	2.91	102.37	-5.01	6.52
100	~66	15-20	4.04	2.91	102.37	-1.73	9.80
100	~94	15-20	5.93	3.12	133.14	-0.25	12.10
0	~30	20-25	1.47	1.54	182.24	-1.56	4.50
0	~45	20-25	1.83	1.54	182.24	-1.20	4.86
0	~66	20-25	4.39	1.54	182.24	1.36	7.42
0	~94	20-25	8.90	1.60	208.84	5.75	12.05
20	~30	20-25	0.89	1.77	162.52	-2.60	4.38
20	~45	20-25	2.25	1.81	171.36	-1.33	5.82
20	~66	20-25	2.49	1.86	189.76	-1.18	6.16
20	~94	20-25	8.10	1.77	162.52	4.61	11.59
100	~30	20-25	0.90	2.91	102.37	-4.87	6.66
100	~45	20-25	0.47	2.91	102.37	-5.30	6.23
100	~66	20-25	3.18	2.91	102.37	-2.58	8.94
100	~94	20-25	5.61	2.91	102.37	-0.15	11.37
0	~30	25-30	0.71	1.57	194.25	-2.38	3.80
0	~45	25-30	0.45	1.57	197.31	-2.64	3.54
0	~66	25-30	2.35	1.54	182.24	-0.68	5.38
0	~94	25-30	5.59	1.54	182.24	2.56	8.62
20	~30	25-30	2.52	1.77	162.52	-0.97	6.01
20	~45	25-30	0.75	1.81	171.36	-2.83	4.32
20	~66	25-30	3.14	1.81	171.36	-0.44	6.71
20	~94	25-30	6.71	1.81	179.09	3.13	10.28
100	~30	25-30	-0.15	3.12	133.20	-6.33	6.03
100	~45	25-30	0.04	2.91	102.37	-5.73	5.80
100	~66	25-30	0.75	2.91	102.37	-5.01	6.52
100	~94	25-30	5.32	2.91	102.37	-0.44	11.09

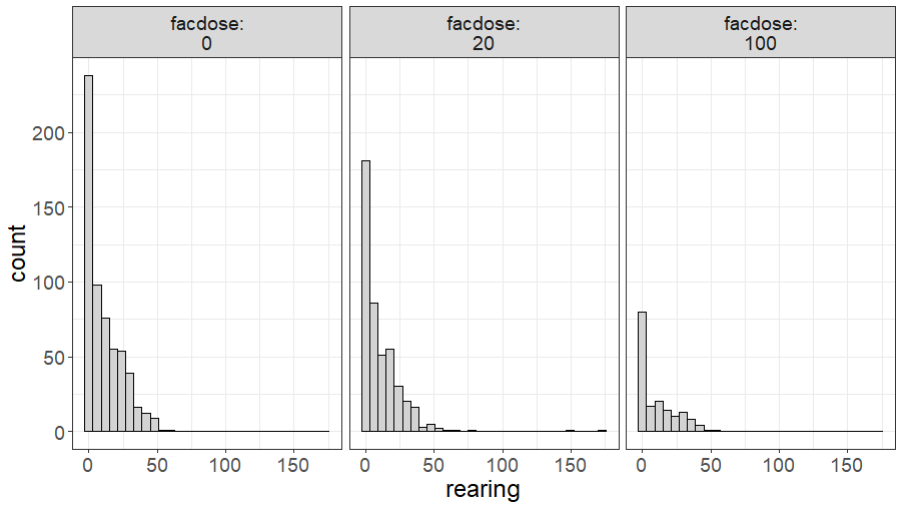

a)

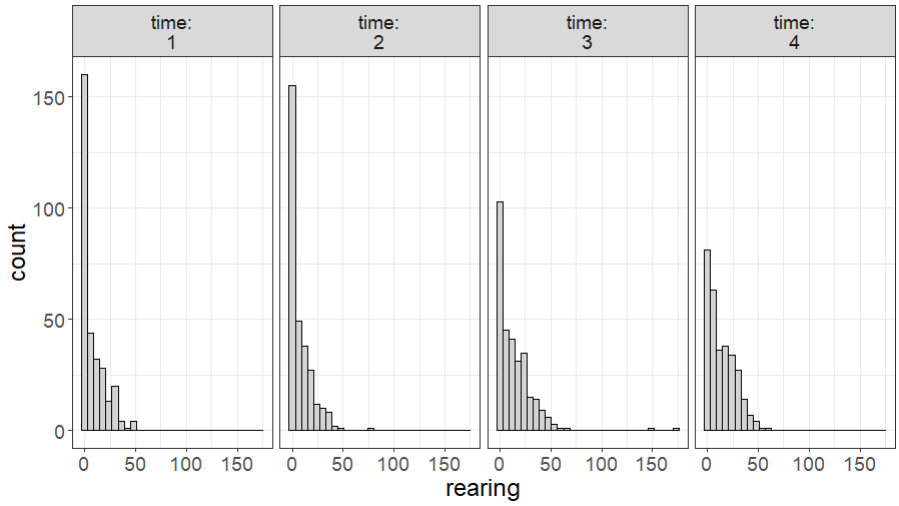

b)

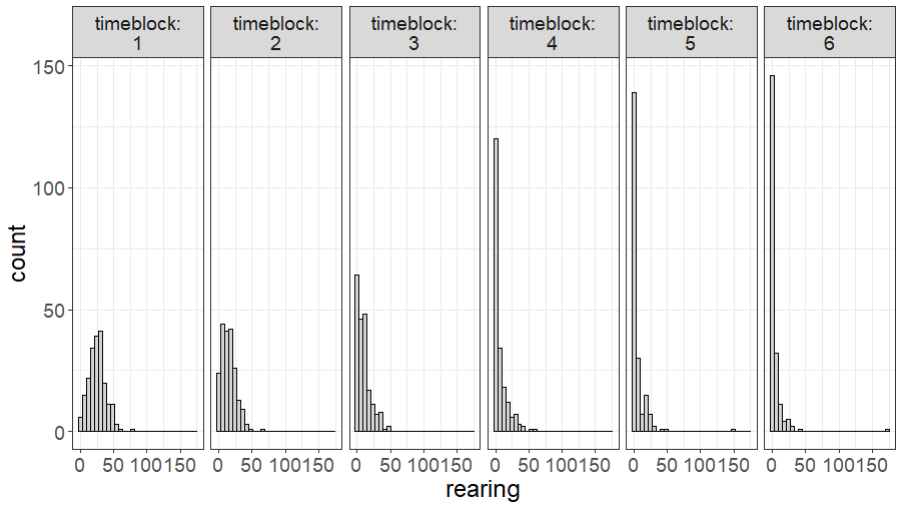

c)

Figure 39: Univariate Plots for Rearings in the OF [n]
Shown are univariate plots plots for Rearings in the OF [s], **a)** split by LPS dose – here labeled as "facdose 0 – 100" with facdose 0 representing the SAL group and facdose 100 representing the 100 µg/kg LPS group, **b)** split by age – here labeled as "time 1-4" with time 1 representing PD~30 and time 4 representing PD~94 and **c)** split by timeblock – here labeled "1 – 6" with 1 representing the 0-5 min timeblock and 6 representing the 25-30 min timeblock. Most plots indicate non-normal distributed, zero-inflated data.

3.1.3. Novel Object Recognition

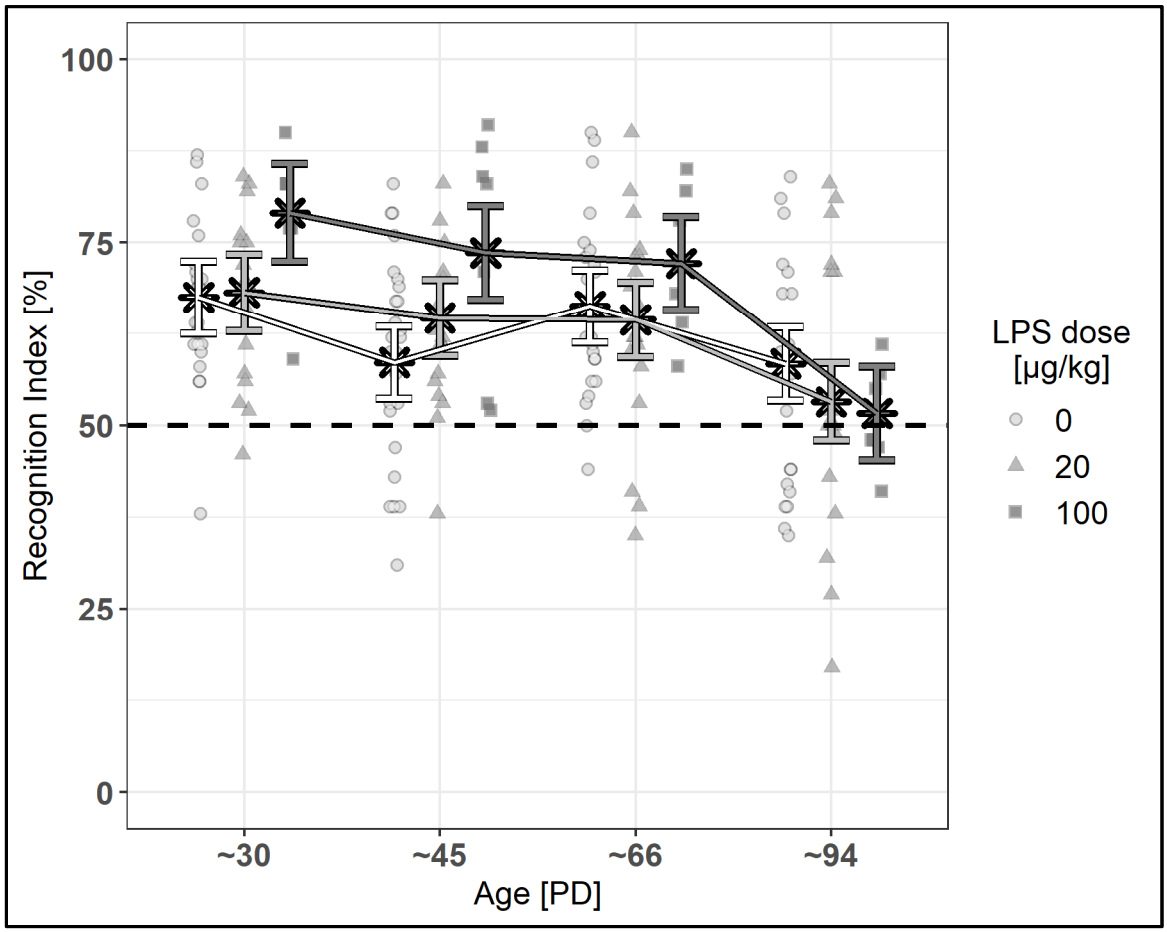

Figure 40: Recognition index [%] by Age and LPS dose
Shown are estimated marginal means (⁎) of the recognition indices extracted from the linear mixed models after outlier removal ± SEM on top of the jittered raw data. SAL data (0 µg/kg LPS) shown as white circles, 20 µg/kg LPS as light grey triangles and 100 µg/kg LPS as dark grey squares. Chance level (RI of 50%) is shown as a dotted line.

10 data points from 9 animals were excluded from the analysis, as in these cases there was either zero interaction with one or both of the objects during the test phase, or in some cases the animals gnawed on the adhesive dots used to fix the items on the ground, rendering the interaction times unusable. Furthermore, one data point was excluded after outlier analysis.

Visually comparing the time spent with both identical objects during the sample phase, this time seems to be similar between all groups and time points, with the exception of a possible higher interaction time of the 100 µg/kg LPS group on PD~30 (see appendix 6.2.5, figure 74).

The statistical model assumptions were met (see appendix 6.2.5, figure 73).

The model shows no effect of litter, but the random effect for test object shows statistical significance (X^2_1 = 15,99, p = <.001; see appendix 6.2.5, table 77), showing the recognition index is not comparable between different items.

The estimated marginal means of the model are shown in figure 40 and table 19. The analysis shows a statistical significant interaction effect between LPS dose and age ($F_{6,133.54}$ = 2.08, p = .060; see table 18).

Post-hoc multiple comparisons show a statistical significant difference for the 0-100 µg/kg LPS contrast on PD ~45 ($t_{164,59}$ = -2.75, p = .018; see appendix 6.2.5, table 78), with the SAL group having a lower estimated mean for the recognition index than the 100 µg/kg LPS group (SAL = 58.54 % vs. LPS-100 = 73.57 %). Furthermore, a statistical significant difference is shown for the PD~45-94 contrast in the 20 µg/kg LPS group ($t_{137,71}$ = 2.79, p = .030; see appendix 6.2.5, table 79) and in the 100 µg/kg LPS group ($t_{130,73}$ = 3.51, p = .003; see appendix 6.2.5, table 79), while the PD~30-94 contrast shows a trend for statistical significance in the 100 µg/kg LPS group ($t_{8.20}$ = 3.10, p = .056; see appendix 6.2.5, table 79). In all these three cases, the mean recognition index on PD~94 is smaller than on the earlier time points (LPS-20 = 64.66 % on PD~45 and 53.21 % on PD~94; LPS-100 = 79.03 % on PD~30, 73.57 % on PD~45 and 51.61 % on PD~94).

In addition, when every mean is compared with the 50 % chance level, only the 100 µg/kg LPS group is showing a statistical significant difference from chance from PD~30 until ~66 (PD~30: $t_{10.69}$ = 4.34, p = .007; PD~45: $t_{9.01}$ = 3.69, p = .030; PD~66: $t_{9.01}$ = 3.46, p = .042; see appendix 6.2.5, table 80), which is no longer seen on PD~94.

Table 18: ANOVA table of the LMM of the NOR data after outlier removal
Shown are the sums of squares (*SS*), mean squares (*MS*), numerator (df_{Num}) and denominator (df_{Den}) degrees of freedom, F- and p-value for each simple factor as well as for the Dose:Age interaction term. The Dose:Age interaction shows a trend for statistical significance (p = .060).

	SS	*MS*	df_{Num}	df_{Den}	*F*	*p*
Dose	541.59	270.79	2	45.66	1.98	.149
Age	2862.01	954.00	3	3.10	6.99	**.069** .
Scan	187.62	187.62	1	45.51	1.37	.247
Dose:Age	1702.14	283.69	6	133.54	2.08	**.060** .

Table 19: Estimated marginal means of the LMM of the NOR data after outlier removal
Shown are the estimated marginal mean, standard error (*SE*), degrees of freedom (*df*) and 95% confidence interval for each LPS dose and Age combination.

LPS dose [µg/kg]	Age [PD]	*Mean*	*SE*	*df*	*95% Confidence Interval*	
					Lower CL	*Upper CL*
0	~30	67.46	4.92	3.20	52.35	82.57
0	~45	58.54	4.92	3.20	43.44	73.65
0	~66	66.26	4.92	3.21	51.17	81.35
0	~94	58.36	5.03	3.51	43.59	73.14
20	~30	68.15	5.23	4.08	53.75	82.54
20	~45	64.66	5.19	3.95	50.19	79.12
20	~66	64.40	5.13	3.80	49.85	78.96
20	~94	53.21	5.28	4.24	38.87	67.54
100	~30	79.03	6.68	10.69	64.27	93.79
100	~45	73.57	6.39	9.01	59.11	88.03
100	~66	72.13	6.39	9.01	57.67	86.59
100	~94	51.61	6.39	9.01	37.15	66.07

Sensitivity analysis (see appendix section 6.2.6) including the outlier value results in disappearance of the statistical significant interaction effect between LPS dose and age ($F_{6,134.13} = 1.71$, $p = .123$; see appendix 6.2.6, table 81), and only the factor age shows a trend to statistical significance ($F_{3,3.05} = 5.86$, $p = .088$; see appendix 6.2.6, table 81). The greatest change in estimated marginal means is seen for the 100 µg/kg LPS group on PD~30 (79.03±6.68 excluding versus 72.44±6.44 including outliers, see appendix table 83), while most other means don't change much (difference<1 %). The results of the post-hoc multiple comparisons change with regards to the disappearance of the trend for statistical significance for the on PD~30-94 contrast in the 100 µg/kg LPS group ($t_{8.24} = 2.37$, $p = .159$; see appendix 6.2.6, table 85), while the main interpretation of the remaining post-hoc tests does not change.

3.1.4. Prepulse Inhibition

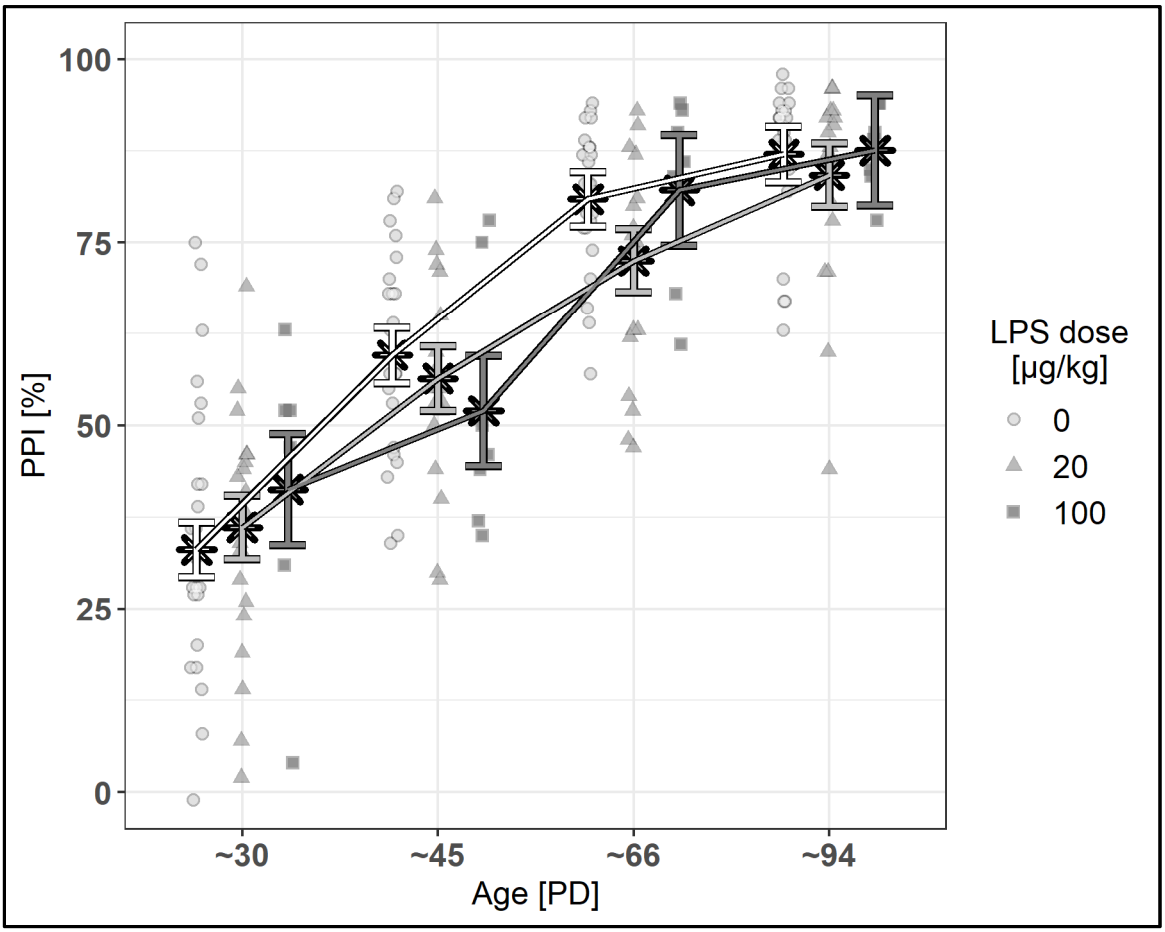

Figure 41: PPI [%] by Age and LPS dose – 50 ms Inter-Stimulus-Interval
Shown are estimated marginal means (⁎) of prepulse inhibition extracted from the linear mixed models after outlier removal ± SEM on top of the jittered raw data. SAL data (0 µg/kg LPS) shown as white circles, 20 µg/kg LPS as light grey triangles and 100 µg/kg LPS as dark grey squares.

12 data points were excluded after outlier analysis.

The statistical model assumptions were met (see appendix 6.2.7, figure 76).

The model shows a trend towards significance for the effect of litter ($X^2_1 = 3{,}48$, $p = .062$; see appendix 6.2.7, table 87).

The estimated marginal means of the model are shown in figures 41 and 42 as well as table 21. The analysis shows a statistical significant interaction effect between LPS dose and age ($F_{6,325.35} = 4.72$, $p = .000$; see table 20) as well as between age and interstimulus interval ($F_{3,325.26} = 2.83$, $p = .039$; see table 20).

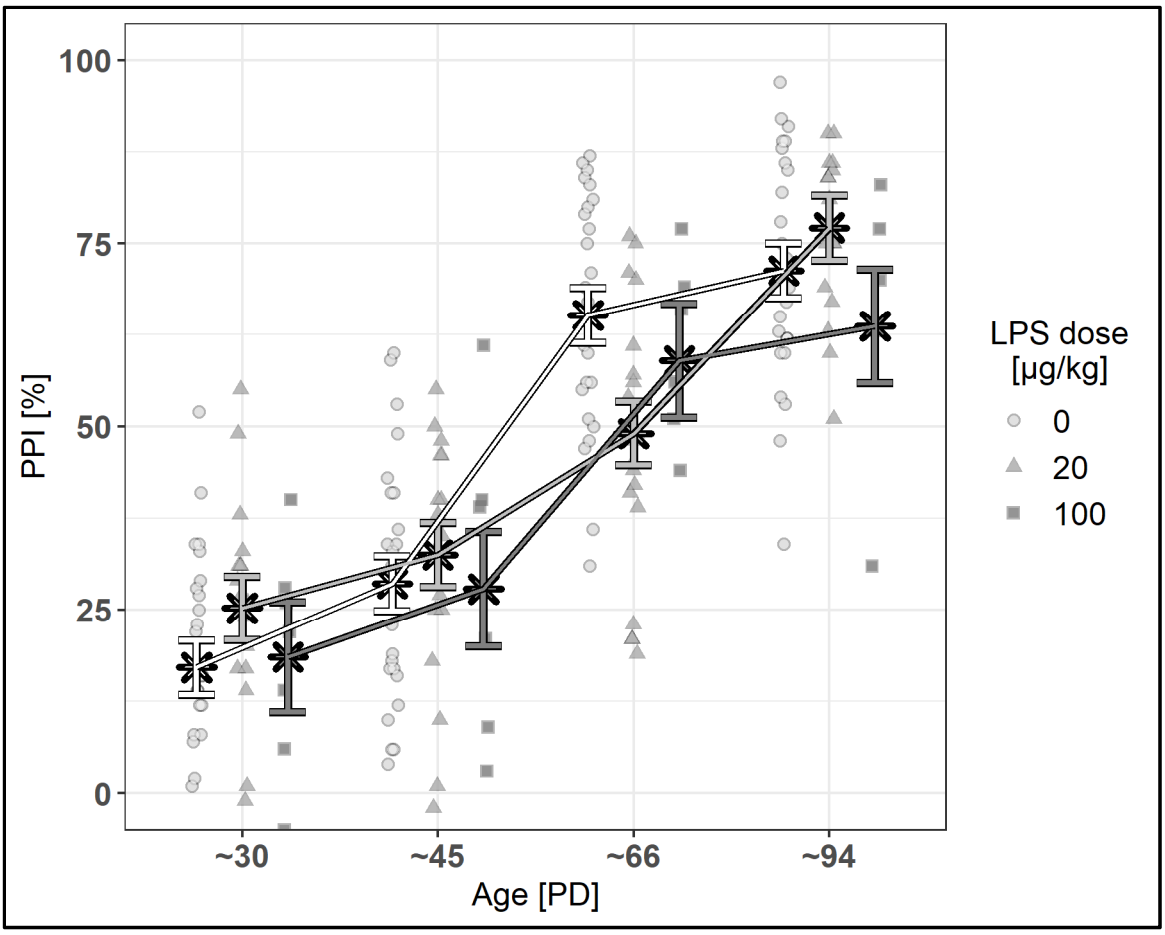

Figure 42: PPI [%] by Age and LPS dose – 140 ms Inter-Stimulus-Interval
Shown are estimated marginal means (⁎) of prepulse inhibition extracted from the linear mixed models after outlier removal ± SEM on top of the jittered raw data. SAL data (0 µg/kg LPS) shown as white circles, 20 µg/kg LPS as light grey triangles and 100 µg/kg LPS as dark grey squares.

Table 20: ANOVA table of the LMM of the PPI data after outlier removal:
Shown are the sums of squares (SS), mean squares (MS), numerator (df Num) and denominator (df Den) degrees of freedom, F- and p-value for each simple factor as well as for the Dose:Age, Dose:ISI, Age:ISI and Dose:Age:ISI interaction terms. The Dose:Age interaction (p = .000) and the Age:ISI interaction (p = .039) show statistical significance.

	SS	*MS*	df_{Num}	df_{Den}	*F*	*p*	
Dose	13.67	6.83	2	6.75	0.04	.957	
Age	115339.43	38446.48	3	325.39	250.33	**.000**	***
ISI	28392.89	28392.89	1	325.84	184.87	**.000**	***
Scan	106.60	106.60	1	43.74	0.69	.409	
Dose:Age	4351.34	725.22	6	325.35	4.72	**.000**	***
Dose:ISI	543.20	271.60	2	325.52	1.77	.172	
Age:ISI	1303.09	434.36	3	325.26	2.83	**.039**	*
Dose:Age:ISI	1283.30	213.88	6	325.11	1.39	.217	

Post-hoc multiple comparisons show a statistical significant difference for the 0-20 µg/kg LPS contrast for the 140 ms ISI on PD ~66 ($t_{20.30}$ = 2.83, p = .027; see appendix 6.2.7, table 88), with the SAL group having a higher estimated mean for the

prepulse inhibition than the 20 µg/kg LPS group (SAL = 65.15 % vs. LPS-100 = 49.01 %).

Regarding age differences, most post hoc contrasts show a statistical significant difference (p usually ≤.000, see appendix 6.2.7, tables 89 and 90), with estimated means increasing with age for all 3 groups and both interstimulus intervals. There are some few exceptions though, e.g. for both interstimulus intervals, the PD~66-~94 contrast is statistically significant for the 20 µg/kg LPS group ($t_{324.36}$ = -2.91, p = .020 for the 50 ms ISI and $t_{325.42}$ = -6.78, p = .000 for the 140 ms ISI, see appendix 6.2.7, tables 89 and 90), while it is not statistically significant for the control and the 100 µg/kg LPS groups, suggesting the latter two groups are reaching their maximum PPI at an earlier age than the 20 µg/kg group. On the other hand, the PD~30-~45 contrast for the 140 ms ISI is statistically significant for the control group ($t_{324.78}$ = -3.24, p = .007, see appendix 6.2.7, table 90), while it is not statistically significant for the two LPS groups, suggesting these start increasing the PPI at a later age. For the 100 µg/kg LPS group, the PD~30-~45 contrast is not statistically significant for the 50 ms ISI as well ($t_{324.36}$ = -0.82, p = .845, see appendix 6.2.7, table 89).

Regarding the interstimulus interval differences, all post hoc contrasts show a statistical significant difference (p usually <.000, see appendix 6.2.7, table 91), except the 50-140 ms contrast for the 20 µg/kg LPS group on PD~94, which only shows a trend to statistical significance ($t_{325.42}$ = 1.70, p = .091, see appendix 6.2.7, table 91).

Sensitivity analysis (see appendix section 6.2.8) including the outlier values shows that the interaction effect between LPS dose and ISI is reaching statistical significance as well ($F_{2,336.00}$ = 3.03, p = .050; see appendix 6.2.8, table 92). Also, the trend towards significance for the effect of litter disappears (X^2_1 = 1,28, p = .257; see appendix 6.2.8, table 93).

Table 21: Estimated marginal means of the LMM of the PPI data after outlier removal
Shown are the estimated marginal mean, standard error (SE), degrees of freedom (df) and 95% confidence interval for each LPS dose, Age and ISI combination.

LPS dose [µg/kg]	Age [PD]	ISI [ms]	*Mean*	*SE*	*df*	*95% Confidence Interval*	
						Lower CL	*Upper CL*
0	~30	50	33.07	3.74	19.59	25.26	40.88
0	~45	50	59.54	3.78	20.35	51.67	67.41
0	~66	50	80.91	3.74	19.59	73.10	88.72
0	~94	50	87.02	3.77	20.35	79.15	94.88
20	~30	50	36.12	4.32	20.80	27.13	45.11
20	~45	50	56.37	4.37	21.91	47.30	65.44
20	~66	50	72.49	4.32	20.80	63.50	81.48
20	~94	50	84.17	4.32	20.80	75.18	93.16
100	~30	50	41.26	7.52	13.07	25.02	57.51
100	~45	50	51.98	7.52	13.07	35.74	68.22
100	~66	50	82.12	7.52	13.07	65.88	98.36
100	~94	50	87.55	7.52	13.07	71.31	103.79
0	~30	140	17.11	3.74	19.59	9.30	24.92
0	~45	140	28.58	3.77	20.35	20.72	36.45
0	~66	140	65.15	3.78	20.39	57.28	73.03
0	~94	140	71.25	3.78	20.36	63.38	79.11
20	~30	140	25.22	4.32	20.80	16.23	34.21
20	~45	140	32.48	4.37	21.91	23.41	41.56
20	~66	140	49.01	4.32	20.80	40.02	58.00
20	~94	140	77.13	4.45	23.00	67.93	86.34
100	~30	140	18.55	7.52	13.07	2.31	34.79
100	~45	140	27.84	7.79	15.02	11.23	44.44
100	~66	140	58.92	7.79	14.97	42.33	75.52
100	~94	140	63.67	7.79	15.02	47.06	80.28

The statistical significant difference for the 0-20 µg/kg LPS contrast for the 140 ms ISI on PD ~66 is giving way to a trend to statistical significance ($t_{27.16} = 2.17$, $p = .094$; see appendix 6.2.8, table 95), just like the PD~66-~94 contrast for the 50 ms ISI in the 20 µg/kg LPS group ($t_{336.00} = -2.34$, $p = .092$, see appendix 6.2.8, table 96). The PD~30-~45 contrast for the 140 ms ISI is no longer statistically significant for the control group ($t_{336.00} = -2.14$, $p = .143$, see appendix6.2.8, table 97). The greatest changes in estimated marginal means are seen for the 100 µg/kg LPS group and the 140 ms ISI (e.g. PD~45: 27.84±7.79 excluding versus 19.00±8.11 including outliers, PD~94: 63.67±7.79 excluding versus 54.29±8.11 including outliers see appendix table 94), while the change in most other means stays within the range of ±3 %.

3.2. Resting-State fMRI

3.2.1. Independent Components / Networks of Interest

The ICA with a dimensionality of 20 components, which was based on the data of the SAL group, yielded 7 IC's which were classified as signal (IC's 1-4, 9-10, 12), and 13 IC's which were classified as noise/unidentifiable (see table 22).

Table 22: Classification of ICs
7 of 20 components from the ICA which was based on the data of the SAL group were classified as signal (IC's 1-4, 9-10, 12), while the rest was classified as noise/unidentifiable.

1	rostral DMN / Default Mode Network	**11**	Unclassified Noise
2	Somatosensory	**12**	Motor
3	Sensorimotor	**13**	Unclassified Noise
4	caudal DMN / Default Mode Network	**14**	Noise (Movement)
5	Noise (Superior Saggital Sinus + Transverse Sinus Meeting Point)	**15**	Unclassified Noise (Brainstem)
6	Superior Saggital Sinus	**16**	Unclassified Noise
7	Noise (Movement)	**17**	Unclassified Noise
8	Noise (Movement)	**18**	Unclassified Noise
9	Striatum / CPu	**19**	Nerves
10	Cerebellum	**20**	Nerves

From the ICs classified as noise, two ICs (5 and 6) represent the large brain vessels, the superior saggital sinus and transverse sinus, with IC 5 also including the lateral and dorsal ventricles (appendix section 6.3.2 figure 79 a-b). Three ICs (7, 8 and 14) were classified as noise stemming from movement (representing for example typical ring-like patterns in the periphery of or even above the brain near the skull, see appendix section 6.3.2 figure 80), and two ICs (19 and 20) were classified as representing (optic) nerves (appendix section 6.3.2 figure 79 d-e). All ICs representing noise which could not be classified more detailed and was thus only labeled as noise/unidentifiable are shown in appendix section 6.3.2 figure 81.

The brain areas covered by the 7 ICs that were classified as signal are listed in table 23, with the areas representing the main focus of the ICs printed in bold and underlined.

Table 23: Brain areas involved in the 7 ICs classified as signal
Shown are the brain areas covered by the 7 ICs that were classified as signal. Within each IC, the involved brain areas are listed from top to bottom starting from the dorsal end of the brain moving into the caudal direction. The brain areas representing the main focus of the ICs are printed in bold and underlined.

IC	1	4	2	3	9	10	12
Network	**DMN (rostral)**	**DMN (caudal)**	**Somatosensory**	**Sensorimotor**	**Striatum / Cpu**	**Cerebellum**	**Motor**
Brain areas covered	**Orbitofrontal Cortex**	**Cingulate Cortex**	**Frontal Association Cortex**	**Motor Cortex**	Orbitofrontal Cortex	**Cerebellum**	**Frontal Association Cortex**
	Medial Prefrontal Cortex	Motor Cortex	**Motor Cortex**	Orbitofrontal Cortex	Insula Cortex		Orbitofrontal Cortex
	Olfactory Nuclei & Tubercle	Septum	Orbitofrontal Cortex	**Somatosensory Cortex**	Piriform Cortex		Olfactory Nuclei
	Motor Cortex	Antero Dorsal Hippocampus	**Somatosensory Cortex**	Cingulate Cortex	Nucleus Accumbens Shell		**Motor Cortex**
	Cingulate Cortex	Somatosensory Cortex	Insular Cortex	Insula Cortex	Nucleus Accumbens Core		
	Piriform Cortex	**Retrosplenial Cortex**		Retrosplenial Cortex	**Caudate Putamen**		
	Entorhinal Cortex	Auditory Cortex		Parietal Association Cortex	Globus Pallidus		
	Septum	Dorsolateral Thalamus		Auditory Cortex			
	Caudate Putamen	Parietal Association Cortex					
	Nucleus Accumbens	**Postero Dorsal Hippocampus**					
	Temporal Association Cortex	**Visual Cortex**					
	Entorhinal Cortex	**Posterior Hippocampus**					
	Auditory Cortex	Subiculum					
	Visual Cortex	Superior Colliculus					

3.2.1.1. Default Mode Network (DMN)

Two IC's are representing the default mode network, with IC 1 representing the more rostral part, and IC 4 representing the more caudal part.

The rostral part of the DMN (see figure 43) primarily consists of three areas in the frontal part of the brain: The *orbitofrontal cortex*, the *medial prefrontal cortex* (i.e. *prelimbic* and *infralimbic cortices*), and the rostral part of the *cingulate cortex*. Other regions included in this part of the network are the *olfactory nuclei and tubercle, motor cortex*, *entorhinal cortex*, *piriform cortex*, *septum*, dorsal part of the *caudate putamen, temporal association cortex, auditory* and *visual cortex*.

The caudal part of the DMN (see figure 44) primarily consists of four areas (six if hippocampus regions are counted separately), in the medial-caudal part of the brain: The caudal part of the *cingulate cortex*, the *retrosplenial cortex*, the *hippocampus* (*postero dorsal and posterior hippocampus*), and the *visual cortex*. Additional areas that are included in this network are the *motor cortex*, *septum*, *antero dorsal hippocampus*, *somatosensory cortex*, *auditory cortex*, *dorsolateral thalamus*, and *parietal association cortex*, *subiculum* and parts of the *superior colliculus*.

3.2.1.2. Somatosensory, Sensorimotor and Motor Networks

There are 3 ICs representing the bilateral somatosensory and motor areas throughout the brain. IC 2 mainly includes some of the rostral motor areas and a lot of the rostral-middle parts of the somatosensory areas, subsequently titled "Somatosensory" network. IC 3 represents the remaining motor areas, and the remaining somatosensory areas from rostral to the caudal end of the cortex, which subsequently is titled as "Sensorimotor" due to its bit larger involvement of motor areas. Furthermore, the most rostral part of the motor cortex and the frontal association cortex are represented in IC 12, subsequently titled "Motor" network.

The somatosensory network (see figure 45) consists of the *frontal association cortex*, the rostral *motor cortex*, and the rostral-medial parts of the *somatosensory cortex* (mainly *primary somatosensory cortex jaw* / *upper lip* / *forelimb region* - *S1J* / *S1ULp* / *S1FL*, as well as *secondary somatosensory cortex* - *S2*). Furthermore, the *orbitofrontal cortex* and the *insular cortex* are parts of this network as well.

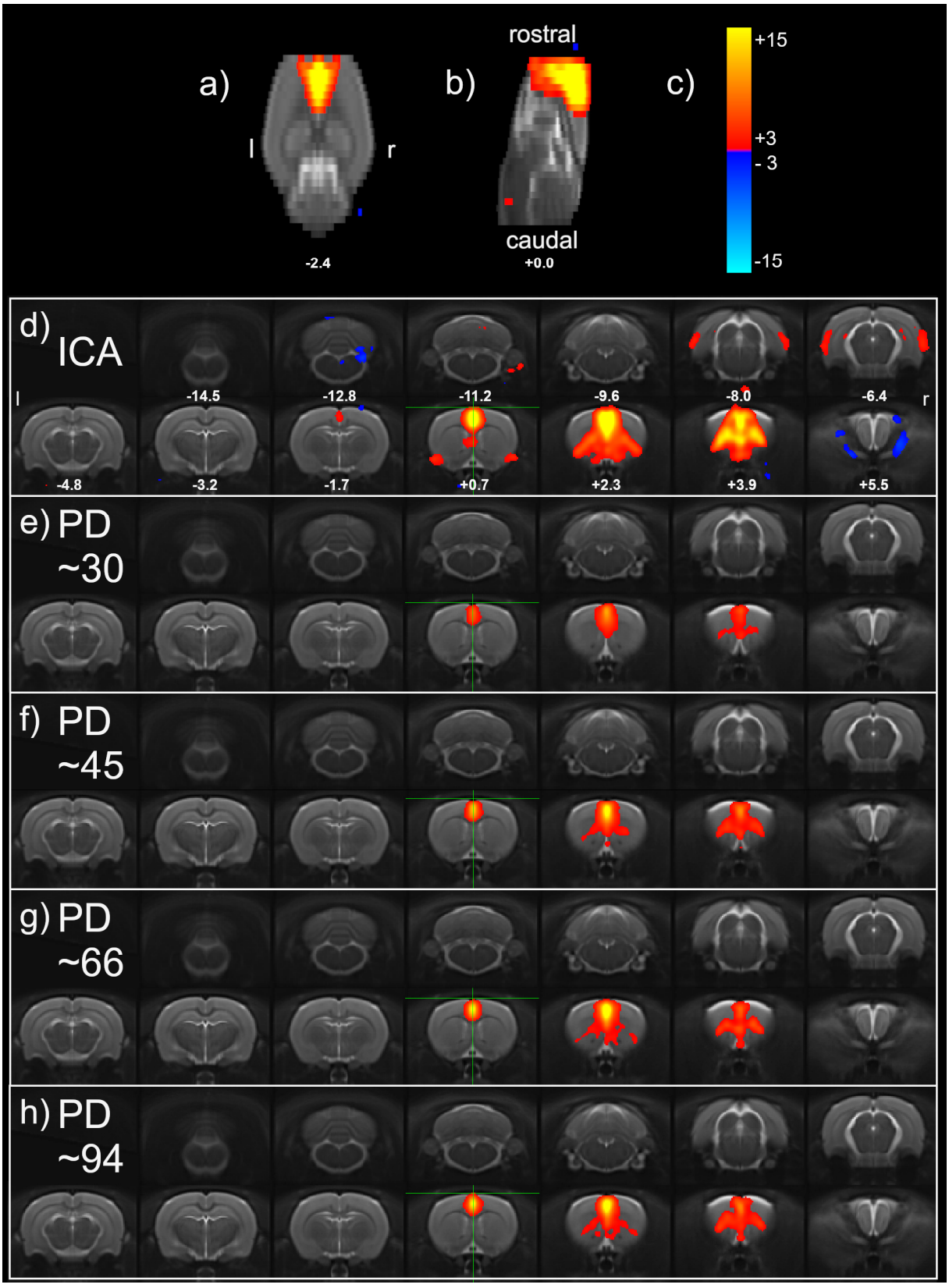

Figure 43: rostral DMN / Default Mode Network
Shown is IC one, representing the rostral Default Mode Network, consisting of e.g. orbitofrontal cortex, medial prefrontal cortex, and cingulate cortex. **a)** horizontal view **b)** saggital view **c)** color-bars referring to Z-scores after Gaussian/Gamma mixture model thresholding **d)** coronal view of the IC extracted directly by the ICA **e) – f)** Mean images of control/saline animals on postnatal days ~30 - ~94. All images are overlaid on the structural template brain. Distances to Bregma (mm) are labeled at the bottom of the images. Images are displayed in neurological convention (l = left, r = right).

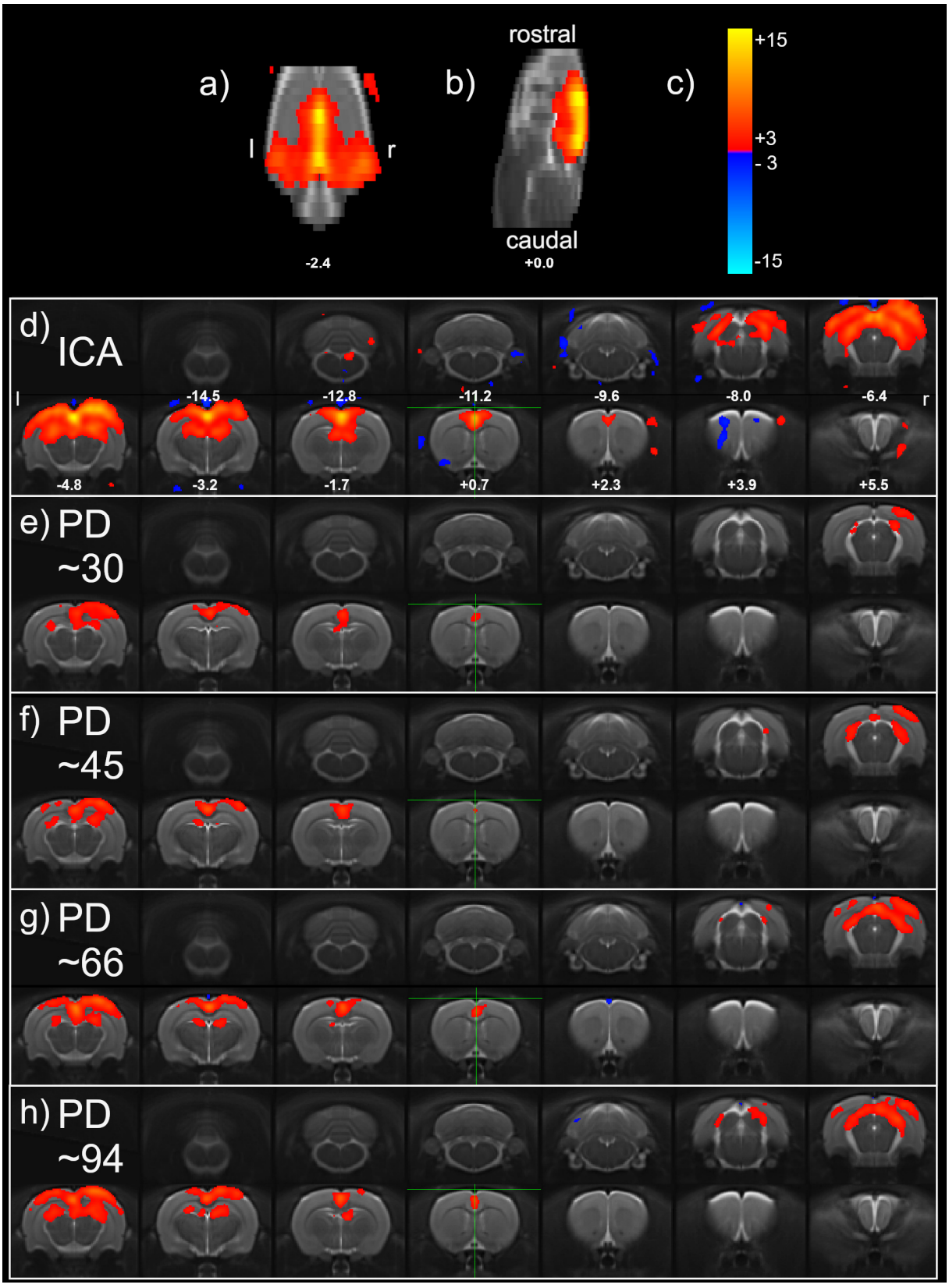

Figure 44: caudal DMN / Default Mode Network
Shown is IC four, representing the caudal Default Mode Network, consisting of e.g. cingulate cortex, retrosplenial cortex, visual cortex and hippocampus. **a)** horizontal view **b)** saggital view **c)** color-bars referring to Z-scores after Gaussian/Gamma mixture model thresholding **d)** coronal view of the IC extracted directly by the ICA **e) – f)** Mean images of control/saline animals on postnatal days ~30 - ~94. All images are overlaid on the structural template brain. Distances to Bregma (mm) are labeled at the bottom of the images. Images are displayed in neurological convention (l = left, r = right).

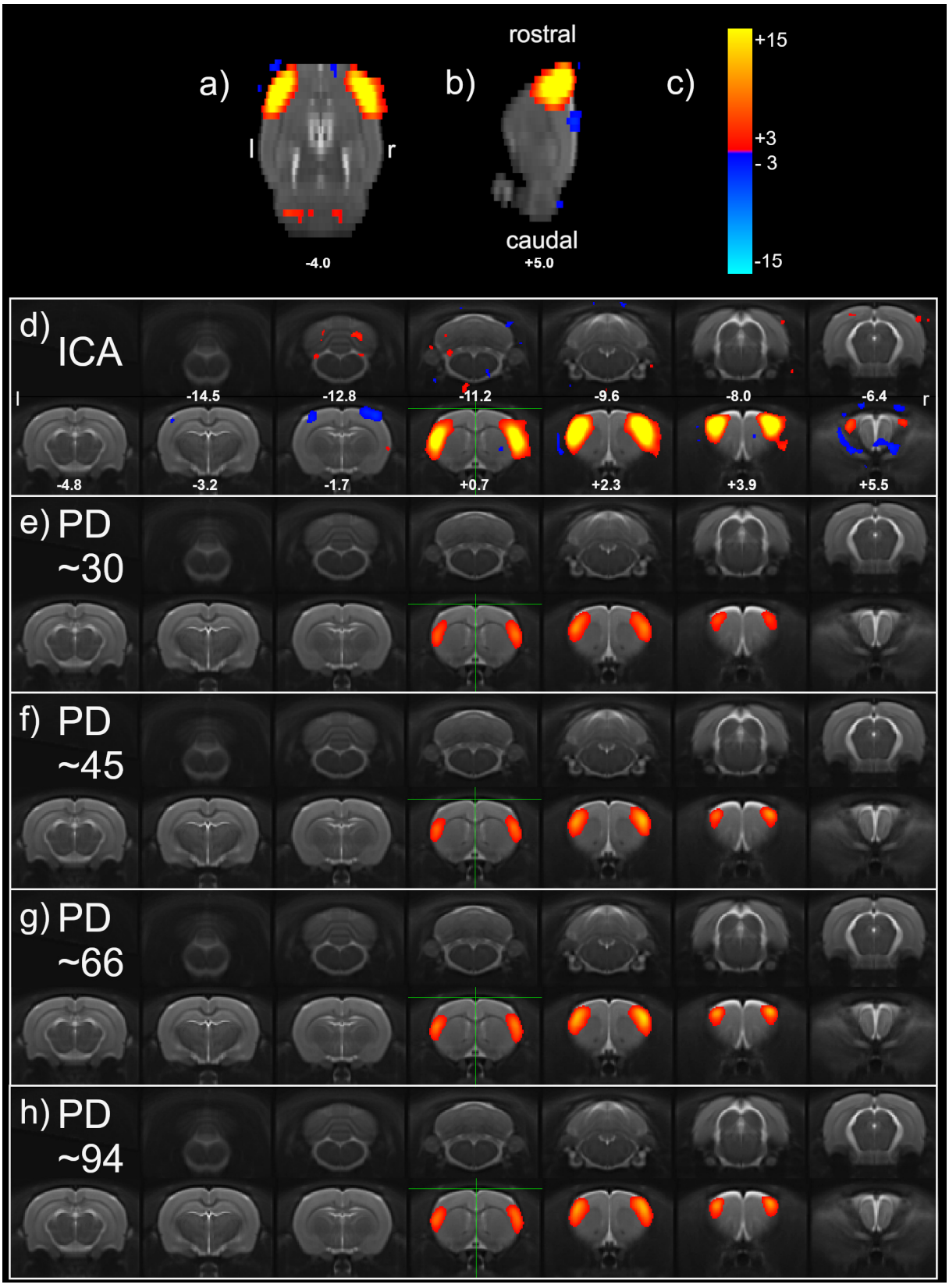

Figure 45: Somatosensory Network
Shown is IC two, representing the Somatosensory Network, consisting of e.g. frontal association cortex, motor cortex and somatosensory cortex. **a)** horizontal view **b)** saggital view **c)** color-bars referring to Z-scores after Gaussian/Gamma mixture model thresholding **d)** coronal view of the IC extracted directly by the ICA **e) – f)** Mean images of control/saline animals on postnatal days ~30 - ~94. All images are overlaid on the structural template brain. Distances to Bregma (mm) are labeled at the bottom of the images. Images are displayed in neurological convention (l = left, r = right).

The sensorimotor network (see figure 46) mainly consists of the rostral-caudal *motor cortex*, as well as the medial-caudal *somatosensory cortex* (*primary somatosensory cortex forelimb / dysgranular / jaw / upper lip / hindlimb / barrel field / trunk region - S1FL* / *S1DZ* / *S1J* / *S1ULp* / *S1HL* / *S1BF* / *S1Tr*, as well as *secondary somatosensory cortex - S2)*. Further areas included are the *auditory cortex*, *parietal association cortex*, parts of the *cingulate* and *retrosplenial cortex,* as well as a bit of *orbitofrontal* and *insular cortex*.

The motor network (see figure 47) consists of the *frontal association cortex* and the most rostral part of the *motor cortex*. Besides these areas, the rostral *orbitofrontal cortex* and the *olfactory nuclei* are part of this component as well.

3.2.1.3. Striatal Network

Another component found, is a striatal network (see figure 48), mostly comprised of the *caudate putamen*, but also involving the *nucleus accumbens*, *globus pallidus*, as well as parts of the *orbitofrontal*, *insular* and *piriform cortex*.

3.2.1.4. Cerebellar Network

Finally, the last component which was classified as signal, represents the *cerebellum* in the caudal part of the brain (see figure 49).

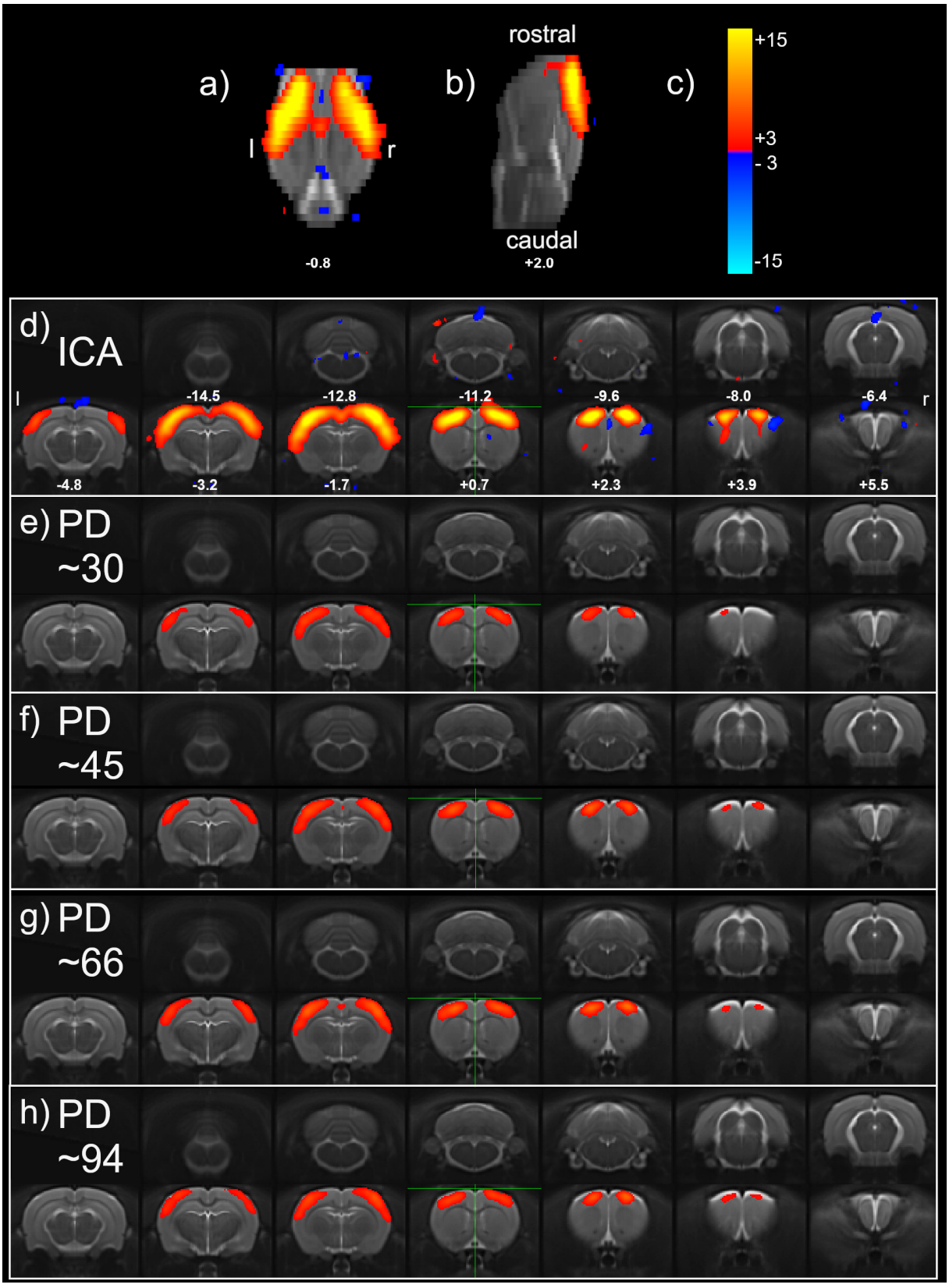

Figure 46: Sensorimotor Network
Shown is IC three, representing the Sensorimotor Network, consisting of e.g. motor cortex, and somatosensory cortex. **a)** horizontal view **b)** saggital view **c)** color-bars referring to Z-scores after Gaussian/Gamma mixture model thresholding **d)** coronal view of the IC extracted directly by the ICA **e) – f)** Mean images of control/saline animals on postnatal days ~30 - ~94. All images are overlaid on the structural template brain. Distances to Bregma (mm) are labeled at the bottom of the images. Images are displayed in neurological convention (l = left, r = right).

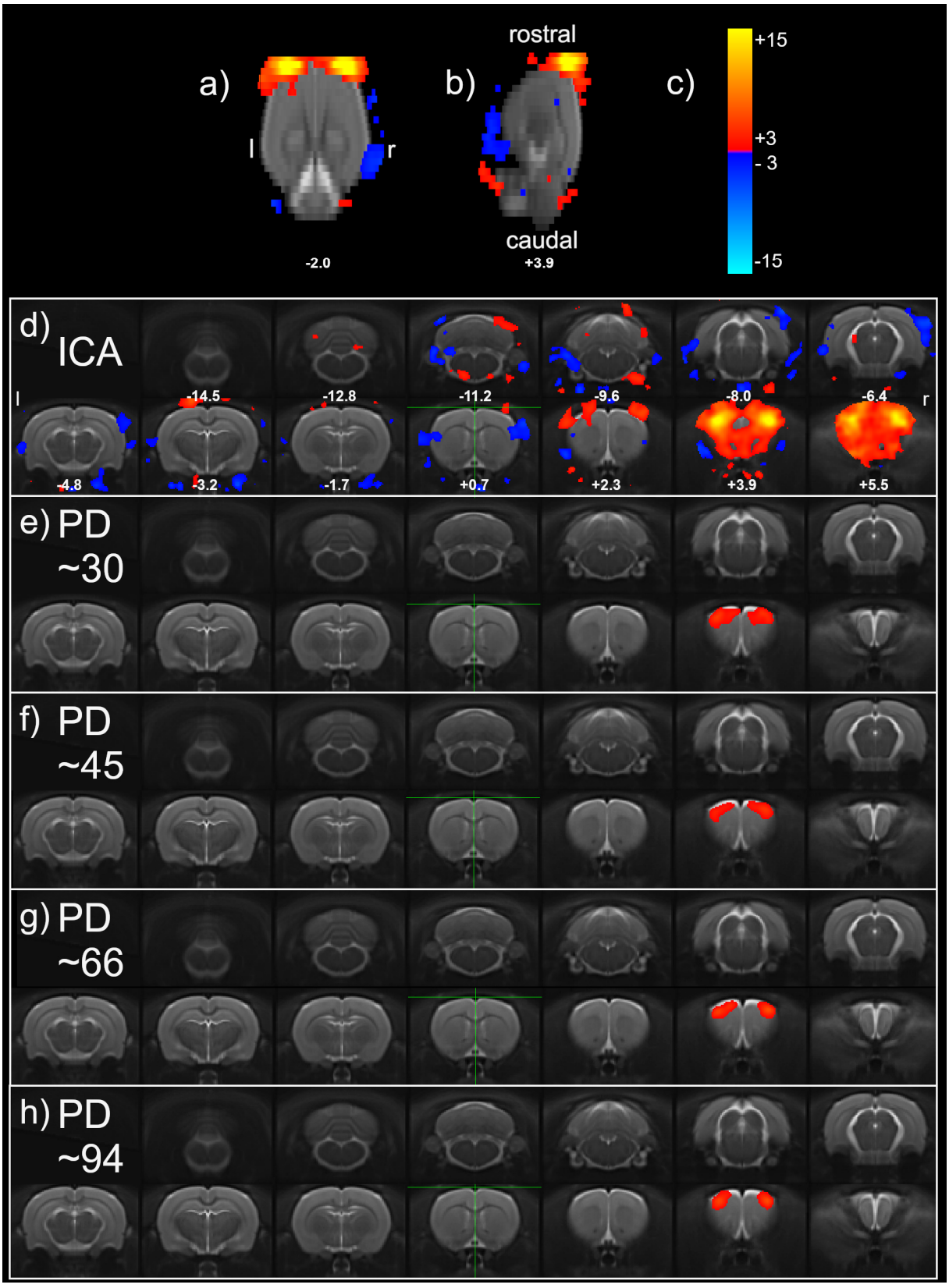

Figure 47: Motor Network
Shown is IC twelve, representing the Motor Network, consisting of e.g. frontal association cortex and motor cortex. **a)** horizontal view **b)** saggital view **c)** color-bars referring to Z-scores after Gaussian/Gamma mixture model thresholding **d)** coronal view of the IC extracted directly by the ICA **e) – f)** Mean images of control/saline animals on postnatal days ~30 - ~94. All images are overlaid on the structural template brain. Distances to Bregma (mm) are labeled at the bottom of the images. Images are displayed in neurological convention (l = left, r = right).

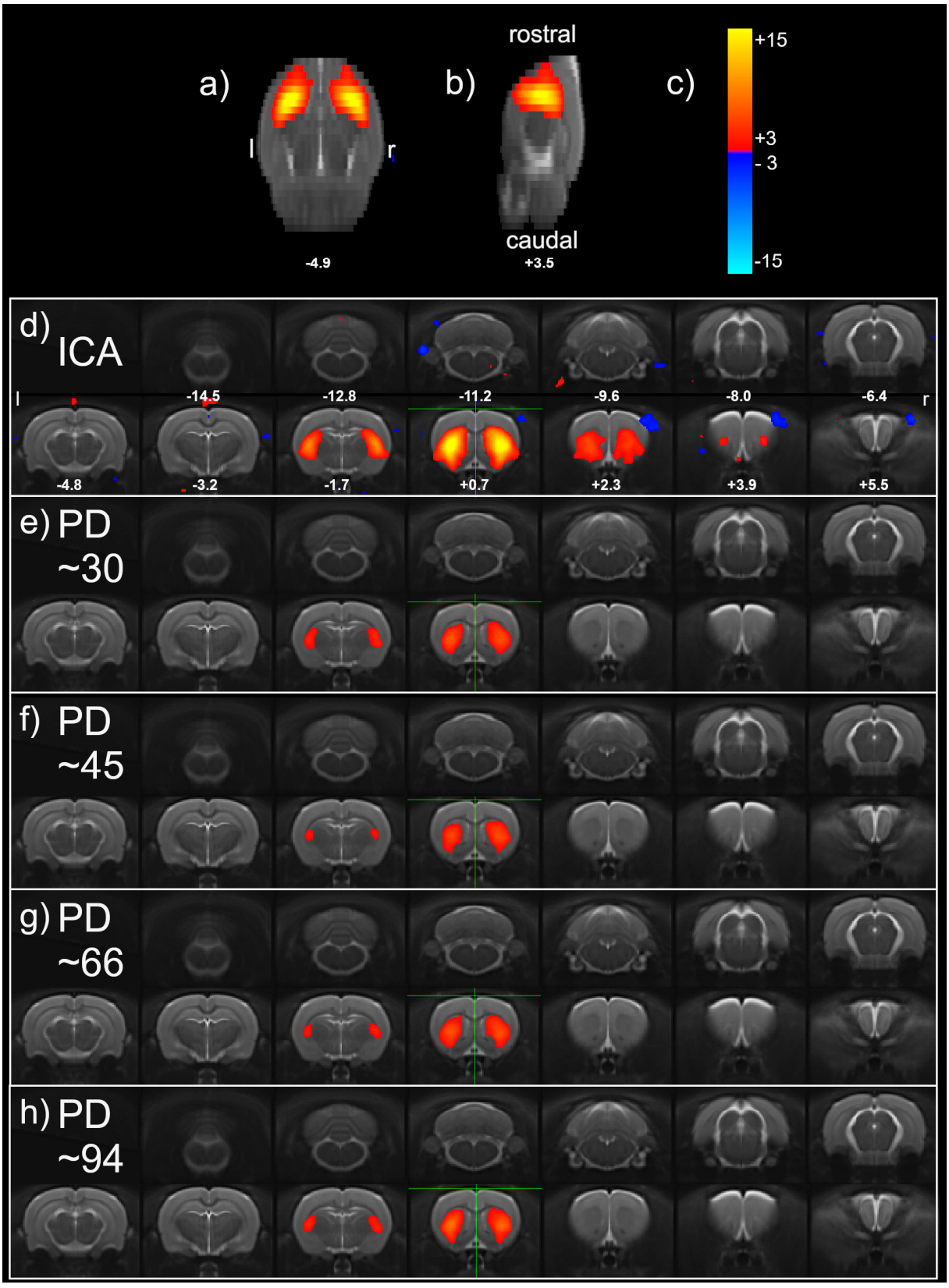

Figure 48: Striatal Network
Shown is IC nine, representing the Striatal Network, consisting of e.g. caudate putamen. **a)** horizontal view **b)** saggital view **c)** color-bars referring to Z-scores after Gaussian/Gamma mixture model thresholding **d)** coronal view of the IC extracted directly by the ICA **e) – f)** Mean images of control/saline animals on postnatal days ~30 - ~94. All images are overlaid on the structural template brain. Distances to Bregma (mm) are labeled at the bottom of the images. Images are displayed in neurological convention (l = left, r = right).

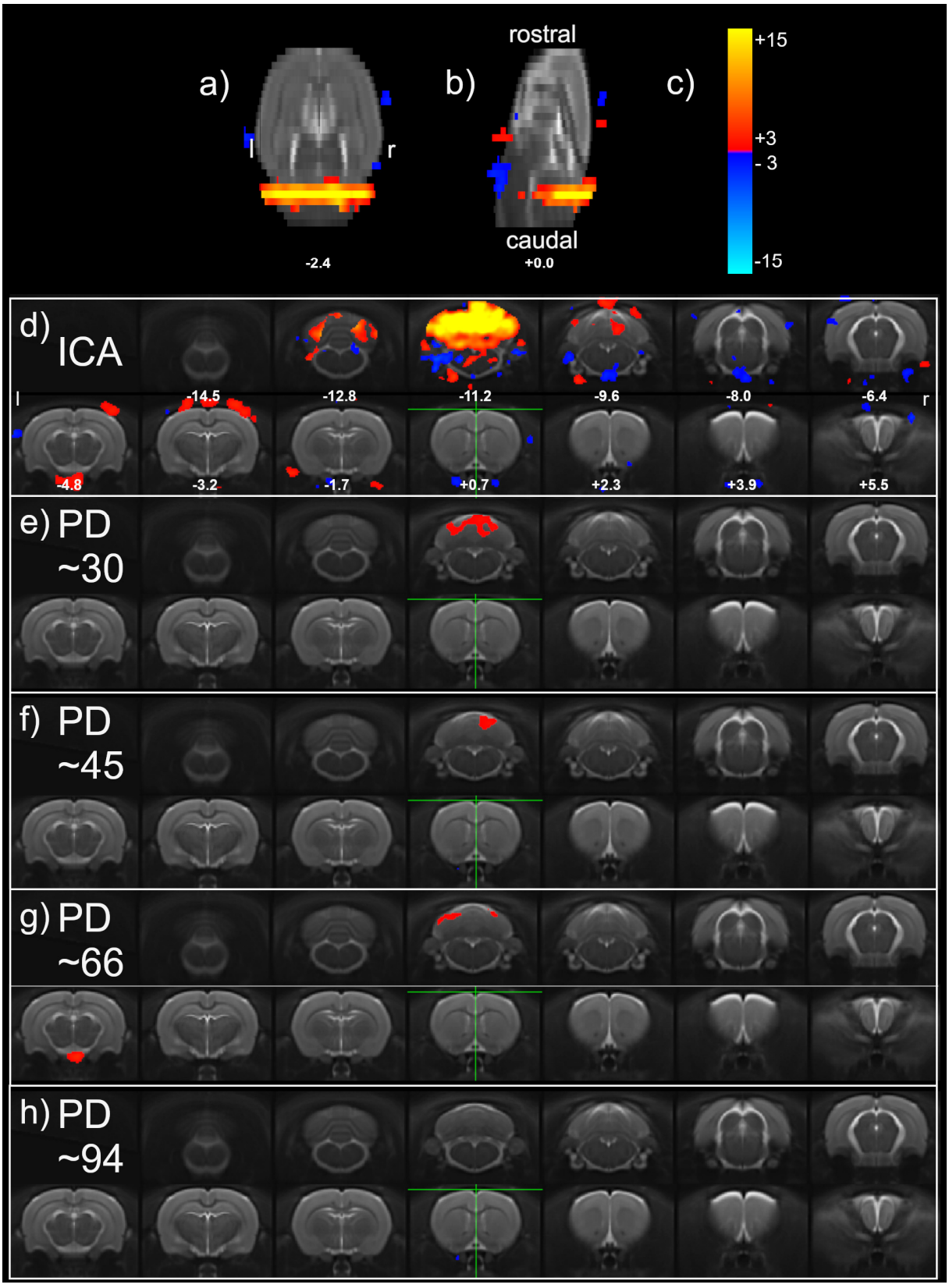

Figure 49: Cerebellum / Cerebellar Network
Shown is IC ten, representing the Cerebellar Network, consisting of the cerebellum. **a)** horizontal view **b)** saggital view **c)** color-bars referring to Z-scores after Gaussian/Gamma mixture model thresholding **d)** coronal view of the IC extracted directly by the ICA **e) – f)** Mean images of control/saline animals on postnatal days ~30 - ~94. All images are overlaid on the structural template brain. Distances to Bregma (mm) are labeled at the bottom of the images. Images are displayed in neurological convention (l = left, r = right).

3.2.2. Anesthesia Comparison

Comparison of the single subject maps (generated via dual_regression) on PD~94 between the two anesthesia regimes (animals that received boli of medetomidine every ten minutes during scanning and those which received a continuous infusion of medetomidine) within the control and LPS groups separately yielded statistically significant voxels in three cases. First, within the control group, a small cluster of two voxels reached statistical significance, with animals receiving boli showing higher z-values, in the cerebellar network (IC 10). The Two voxels were located within the primary somatosensory cortex (barrel field), outside of the main location of the cerebellar IC (see figure 50). The cluster included two more voxels that showed a trend towards statistical significance.

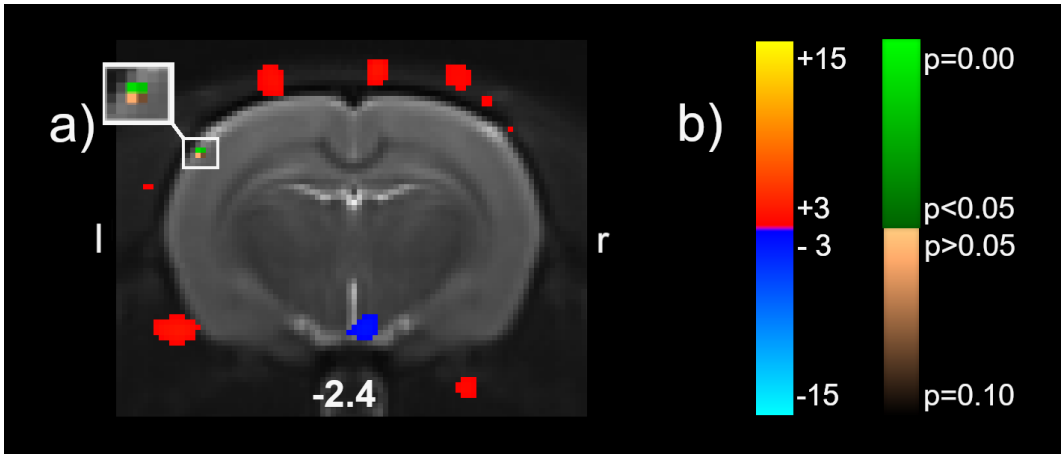

Figure 50: Cerebellar Network – Anesthesia comparison – Statistically significant voxels (SAL) Shown are statistically significant voxels for IC ten, representing the Cerebellar Network, after comparison between the two anesthesia regimes (continous infusion or bolus injection) on PD~94. Within the control group, two voxels located within the primary somatosensory cortex (barrel field), outside of the main location of the main IC, are showing statistical significance (plus 2 more voxels at trend level), with animals receiving boli showing higher z-values. **a)** coronal view **b)** color-bars referring to Z-scores after Gaussian/Gamma mixture model thresholding (blue-red) or p-values after statistical comparison via nonparametric permutation tests (bronze-green). All images are overlaid on the structural template brain. Distances to Bregma (mm) are labeled at the bottom of the images. Images are displayed in neurological convention (l = left, r = right).

Second, within the LPS group, a small cluster of six statistically significant different voxels, with animals receiving boli showing higher z-values, was located in the brainstem outside of the main location of the IC in the somatosensory network (IC 2; see figure 51). Third, also within the LPS group, a single voxel reached statistical significance, with animals receiving boli showing higher z-values, in the striatal network (IC 9). The voxel was located in the cerebellum near the brainstem, outside of the main location of the striatal IC (see figure 52). A second neighboring voxel showed a trend towards statistical significance. Otherwise, no voxels reached the

significance threshold. Therefore, as all clusters reaching the significance threshold were located outside of the main locations of the ICs, the data was deemed comparable and thus data from both anesthesia regimes was pooled for the further analysis.

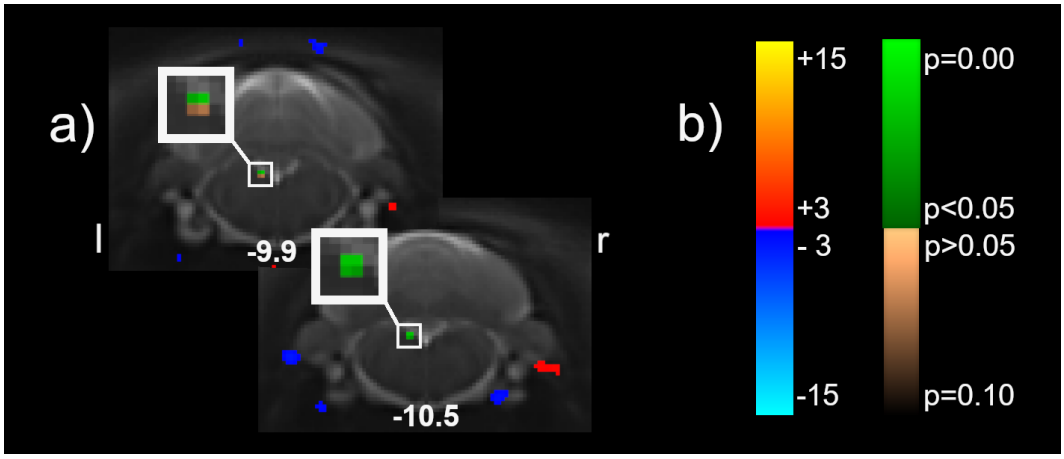

Figure 51: Somatosensory Network – Anesthesia comparison – Statistically significant voxels (LPS)
Shown are statistically significant voxels for IC two, representing the Somatosensory Network, after comparison between the two anesthesia regimes (continous infusion or bolus injection) on PD~94. Within the LPS group, six voxels located in the brainstem outside of the main location of the IC, are showing statistical significance (plus 2 more voxels at trend level), with animals receiving boli showing higher z-values. **a)** coronal view **b)** color-bars referring to Z-scores after Gaussian/Gamma mixture model thresholding (blue-red) or p-values after statistical comparison via nonparametric permutation tests (bronze-green). All images are overlaid on the structural template brain. Distances to Bregma (mm) are labeled at the bottom of the images. Images are displayed in neurological convention (l = left, r = right).

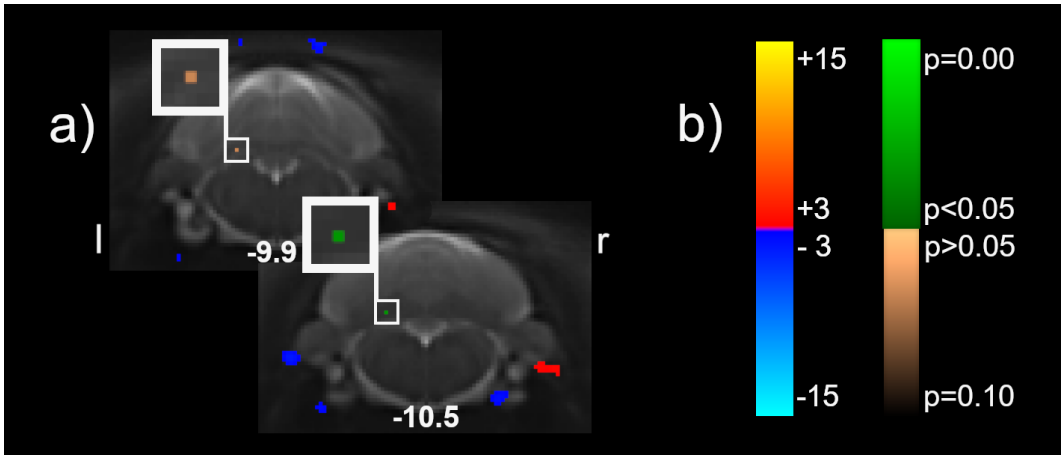

Figure 52: Striatal Network – Anesthesia comparison – Statistically significant voxels (LPS)
Shown are statistically significant voxels for IC nine, representing the Striatal Network, after comparison between the two anesthesia regimes (continous infusion or bolus injection) on PD~94. Within the LPS group, a single voxel located in the cerebellum near the brainstem outside of the main location of the IC, is showing statistical significance (plus another voxel at trend level), with animals receiving boli showing higher z-values. **a)** coronal view **b)** color-bars referring to Z-scores after Gaussian/Gamma mixture model thresholding (blue-red) or p-values after statistical comparison via nonparametric permutation tests (bronze-green). All images are overlaid on the structural template brain. Distances to Bregma (mm) are labeled at the bottom of the images. Images are displayed in neurological convention (l = left, r = right).

3.2.3. Statistically Significant Differences

The statistical model assumptions were not checked in case of the fMRI data. The available post-estimation tools from the “Multivariate and repeated measures” (MRM) toolbox have not proven very suitable for checking model assumptions after the analysis of rat brain data, as the voxels to be checked can only be selected according to the human MNI template coordinate system, whereas no visual selection is possible. Furthermore, due to the voxelwise testing, one must in theory check each voxel for each comparison for itself. Considering the functional MRI data collected consisted of 4608 voxels per volume, and 7 statistical comparisons were run, this would be a very tedious procedure. However, the used MRM model has less strict assumptions than the usually for fMRI data used general linear model (GLM), as the MRM has no assumption of spherical covariance structure, and the used permutation approach does not rely on strong distributional (normality) assumptions.

The effect of litter on the fMRI data was not tested, as the used MRM model is not able to perform multi-level modeling and thus did not allow the addition of such random factors.

No statistical significant effect of LPS dose could be shown. However, the analysis shows a statistical significant effect of age in the cerebellar network. When results at trend level are included, in total three of the seven tested ICs show an effect of age.

3.2.3.1. Age effects

In the somatosensory network (IC two), some small clusters showing a trend towards statistical significance of age are located within the main focus of the IC. These are located bilaterally in the *primary motor cortex*, roughly between Bregma +3.2 mm to +2.4, as well as in the right *primary somatosensory cortex* (*upper lip region)*, and *right granular insular cortex*, located at Bregma +0.7 mm (see figure 56). Additionally, some scattered voxels or smaller clusters outside of the main focus are showing a trend towards statistical significance of age (e.g. in cerebellum located at Bregma -10.3 mm).

In the sensorimotor network (IC three), some small clusters showing a trend towards statistical significance of age are located within the main focus of the IC as well. These are located bilaterally in the *primary* and *secondary motor cortex*, as well as

the *primary* (*forelimb, jaw, dysgranular region; barrel field*) and *secondary somatosensory cortex*, roughly between Bregma +3.2 mm to -2.5 mm (see figure 57). Additionally, some scattered voxels or smaller clusters outside of the main focus focus are showing a trend towards statistical significance of age as well.

Lastly, in the cerebellar network (IC ten), some small clusters showing statistical significance of age, in addition to clusters showing a trend towards statistical significance of age, are located within the main focus of the IC. These are located around the *primary fissure* and *posterior superior fissure* of the cerebelleum, roughly at Bregma -10.5 mm (see figure 58). Additionally, some scattered voxels or smaller clusters outside of the main focus are showing statistical significance of age at least at trend level as well.

Visually comparing the mean component maps of the control group, thresholded between z-values of +3 - +15, there seems to be a slight increase in signal strengths from PD~30 until PD~66 for the somatosensory and sensorimotor networks (see figures 45 and 46 e) to h)). Comparing the mean values of voxels within the (at trend level) statistical significant clusters confirmed that the z-values mostly seem to increase from PD~30 until PD~66, whereas the z-values from PD~94 seem to be smaller than on PD~66 (see table 24 and figures 53-54). In contrast, for the cerebellar network, there seems to be a decrease in signal strengths from PD~30 until PD~94 (see figure 49 e) to h)), also confirmed by comparing the mean values of voxels within the (at trend level) statistical significant clusters (see table 24 and figure 55). The z-values seem to decrease with increasing age, and at PD~94 no voxel of the mean images of the SAL animals has a z-score higher or equal to +3 anymore, i.e. the network seems to be no longer present at all. However, as such age differences without an interaction with the treatment were not the focus of this thesis, additional post-hoc analyses have been omitted due to time constraints.

Table 24: Mean z-values within (at trend level) statistical significant clusters
Shown are mean values and standard deviation (*SD*) within the (at trend level) statistical significant clusters for all three independent components (IC) for each LPS dose and Age combination.

IC	LPS Dose µg/kg]	0		20		100	
	Age [PD]	*Mean*	*SD*	*Mean*	*SD*	*Mean*	*SD*
Somatosensory network	~30	3.75	*2.92*	4.88	*3.89*	4.20	*3.49*
	~45	4.39	*4.07*	4.40	*3.93*	3.88	*3.90*
	~66	5.63	*4.93*	6.09	*4.97*	7.21	*6.11*
	~94	4.62	*4.28*	4.26	*3.88*	4.18	*4.04*
Sensorimotor network	~30	3.27	*2.17*	4.03	*2.66*	3.51	*2.21*
	~45	4.00	*2.54*	4.27	*2.85*	4.15	*3.05*
	~66	4.46	*2.81*	5.00	*3.09*	6.14	*3.80*
	~94	3.66	*2.38*	3.31	*2.17*	3.43	*2.41*
Cerebellum	~30	1.87	*1.52*	1.91	*1.60*	2.01	*1.69*
	~45	1.36	*1.20*	1.10	*0.99*	1.88	*1.70*
	~66	1.36	*1.22*	0.14	*0.49*	2.37	*2.15*
	~94	0.42	*0.58*	0.04	*0.43*	0.58	*0.90*

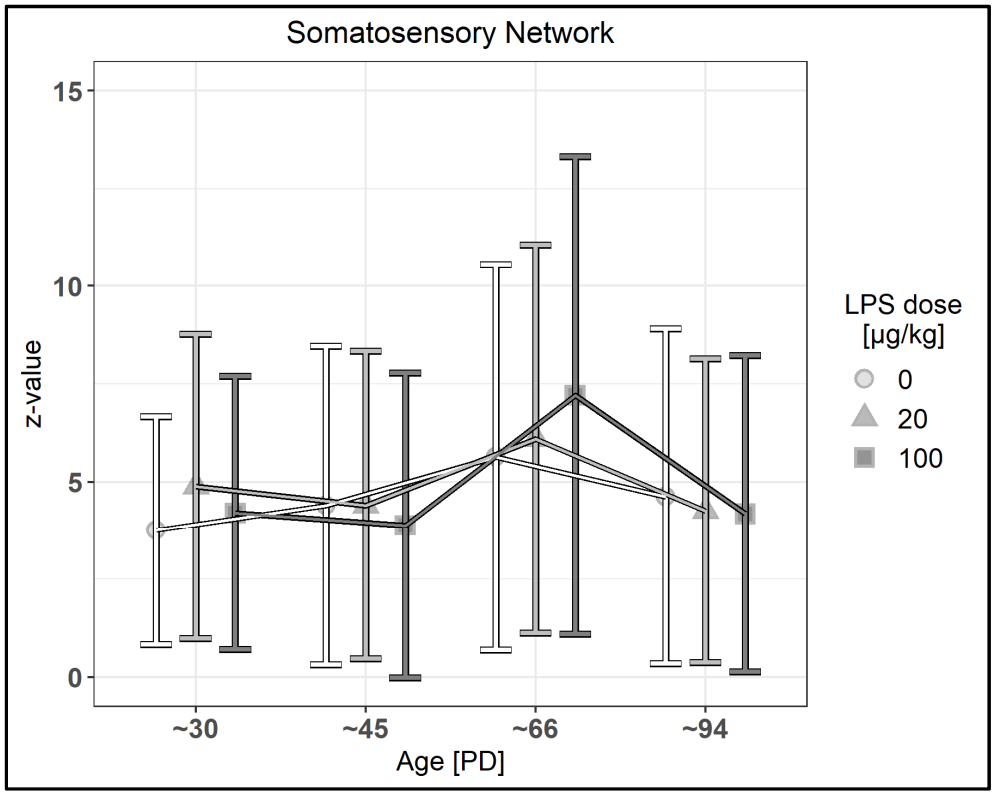

Figure 53: Mean z-values within the at trend level statistical significant Somatosensory Network clusters
Shown are mean values and standard deviation (*SD*) within the at trend level statistical significant clusters for the Somatosensory Network IC for each LPS dose and Age combination.

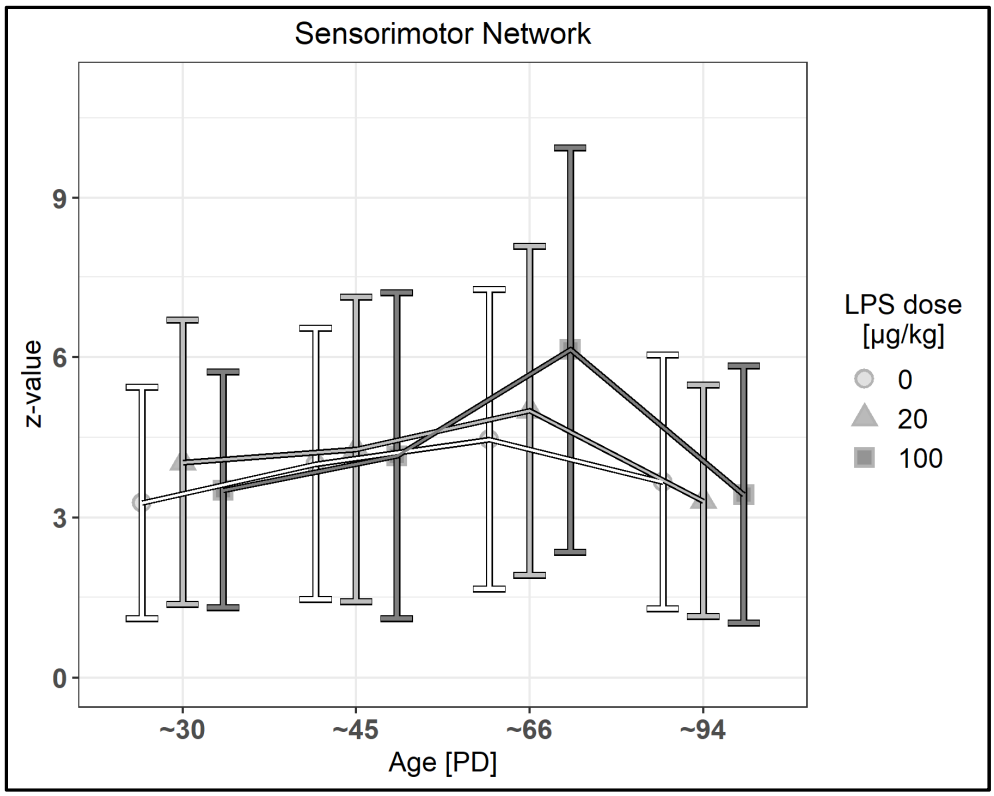

Figure 54: Mean z-values within the at trend level statistical significant Sensorimotor Network clusters
Shown are mean values and standard deviation (*SD*) within the at trend level statistical significant clusters for the Sensorimotor Network IC for each LPS dose and Age combination.

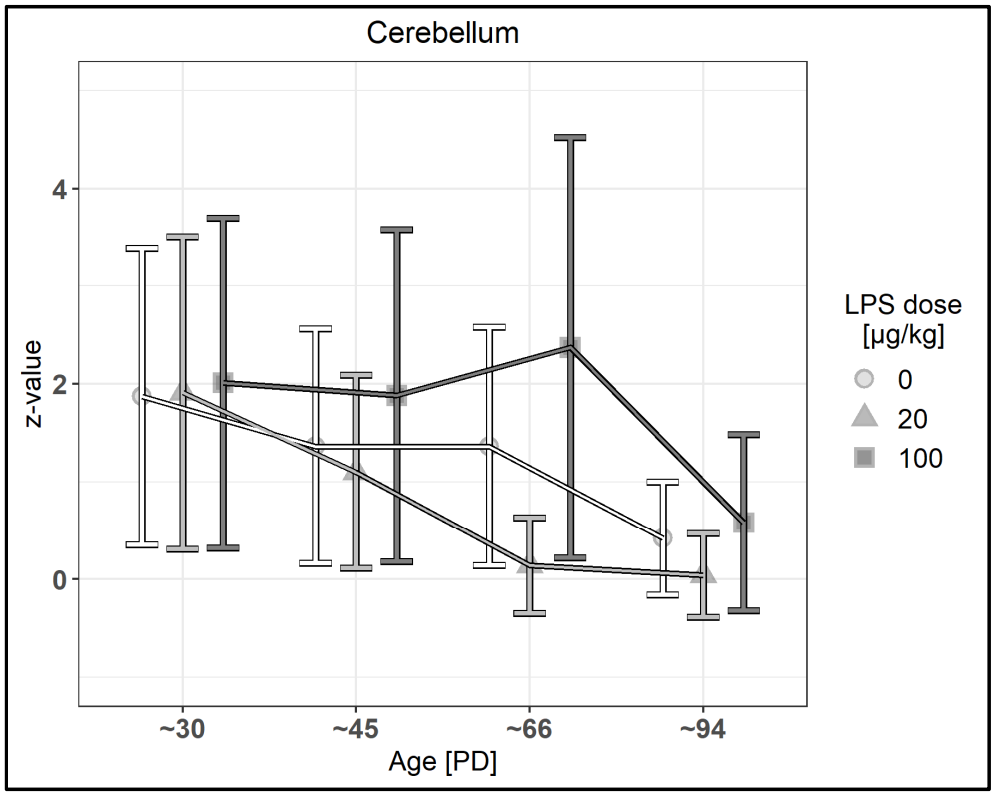

Figure 55: Mean z-values within the statistical significant Cerebellum clusters
Shown are mean values and standard deviation (*SD*) within the at trend level statistical significant clusters for the Cerebellum IC for each LPS dose and Age combination.

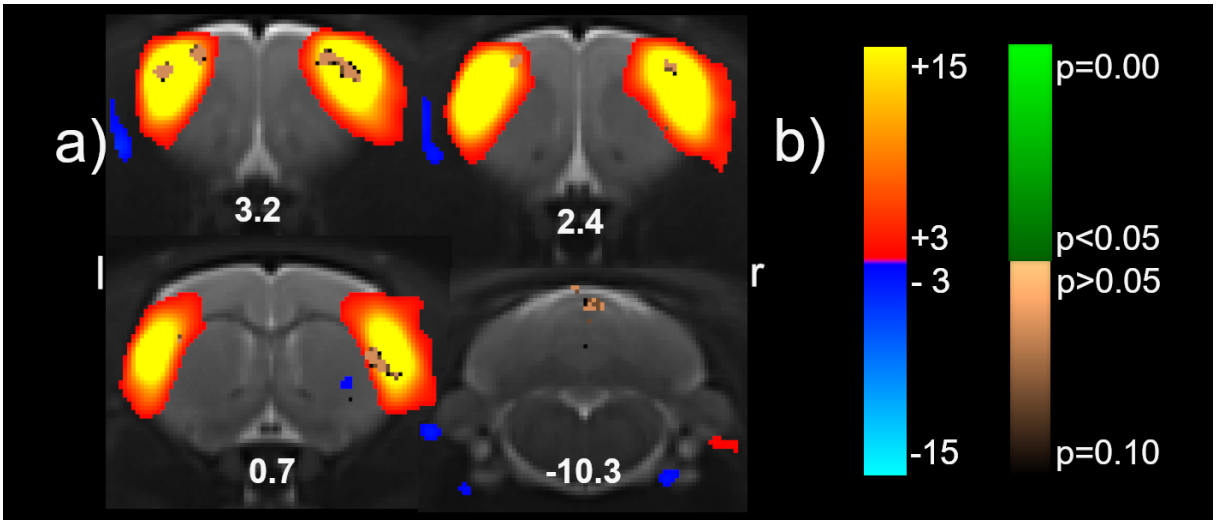

Figure 56: Somatosensory Network – Statistically significant voxels – Age contrast
Shown are statistically significant voxels for IC two, representing the Somatosensory Network. Some small clusters showing a trend towards statistical significance are located within the main focus of the IC (bilaterally in the primary motor cortex, located roughly between Bregma +3.2 mm to +2.4, as well as in the right primary somatosensory cortex, upper lip region, and right granular insular cortex, located at Bregma +0.7 mm), in addition to some scattered voxels or smaller clusters outside of the main focus (e.g. in cerebellum located at Bregma -10.3 mm). **a)** coronal view **b)** color-bars referring to Z-scores after Gaussian/Gamma mixture model thresholding (blue-red) or p-values after statistical comparison via MRM toolbox (bronze-green). All images are overlaid on the structural template brain. Distances to Bregma (mm) are labeled at the bottom of the images. Images are displayed in neurological convention (l = left, r = right).

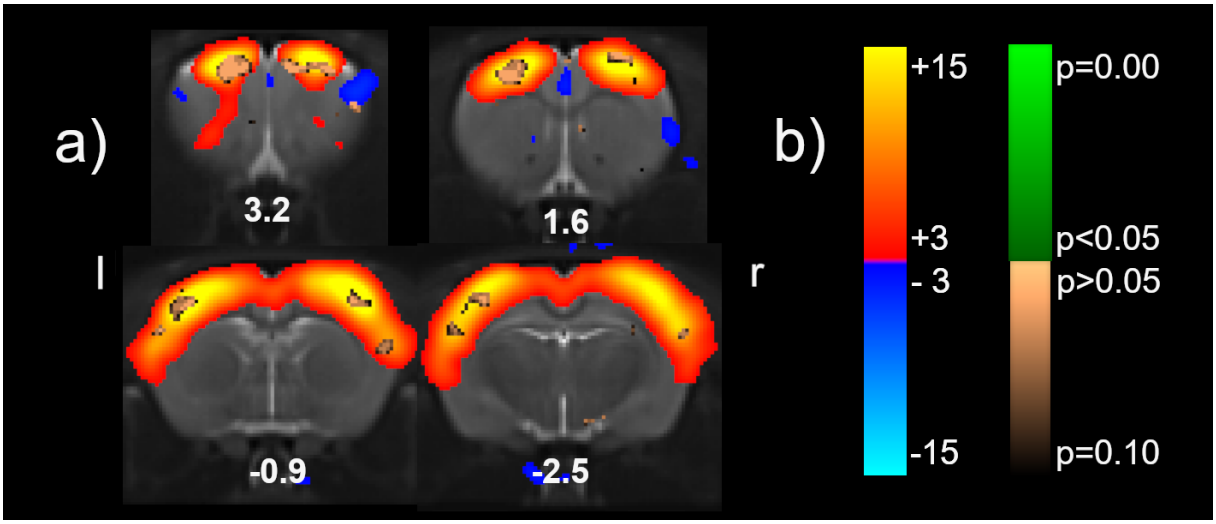

Figure 57: Sensorimotor Network - Statistically significant voxels – Age contrast
Shown are statistically significant voxels for IC three, representing the Sensorimotor Network. Some small clusters showing a trend towards statistical significance are located within the main focus of the IC (bilaterally in the primary and secondary motor cortex, as well as the primary and secondary somatosensory cortex, located roughly between Bregma +3.2 mm to -2.5 mm), in addition to some scattered voxels or smaller clusters outside of the main focus. **a)** coronal view **b)** color-bars referring to Z-scores after Gaussian/Gamma mixture model thresholding (blue-red) or p-values after statistical comparison via MRM toolbox (bronze-green). All images are overlaid on the structural template brain. Distances to Bregma (mm) are labeled at the bottom of the images. Images are displayed in neurological convention (l = left, r = right).

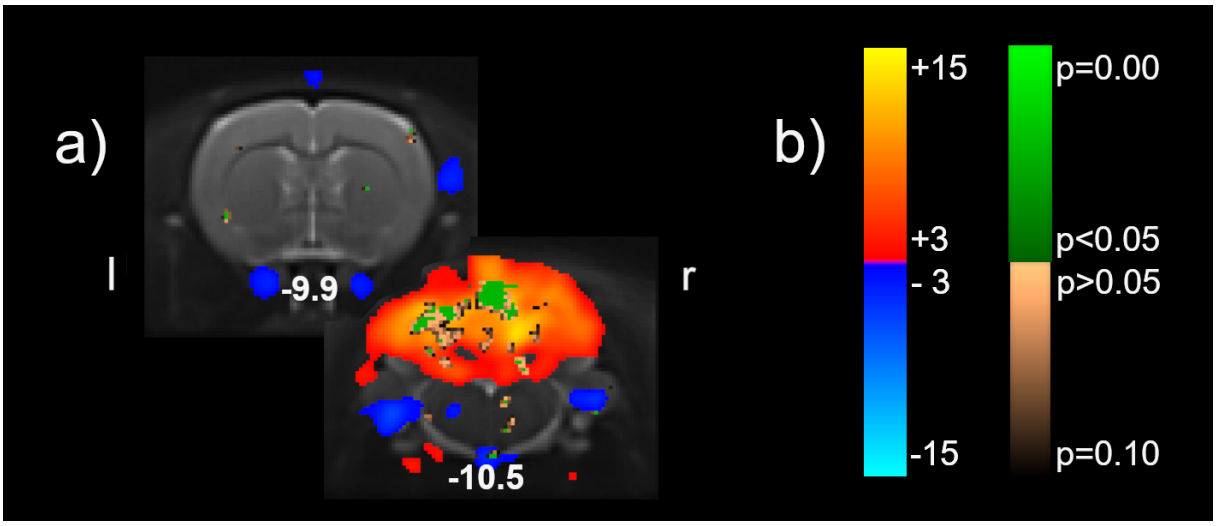

Figure 58: Cerebellar Network - Statistically significant voxels – Age contrast
Shown are statistically significant voxels for IC ten, representing the Cerebellar Network. Some small clusters showing statistical significance, in addition to clusters showing a trend towards statistical significance, are located within the main focus of the IC (around the primary fissure and posterior superior fissure of the cerebelleum, located roughly at Bregma -10.5 mm), in addition to some scattered voxels or smaller clusters outside of the main focus. **a)** coronal view **b)** color-bars referring to Z-scores after Gaussian/Gamma mixture model thresholding (blue-red) or p-values after statistical comparison via MRM toolbox (bronze-green). All images are overlaid on the structural template brain. Distances to Bregma (mm) are labeled at the bottom of the images. Images are displayed in neurological convention (l = left, r = right).

4. Discussion

4.1. Summary of Findings

To summarize, higher LPS doses of 100-50 µg/kg resulted in abnormal littering of dams. For the reduced dose of 20 µg/kg, no statistically significant differences in litter size or male:female ratio compared to SAL were observed. The analysis suggests an interaction effect between LPS dose and age on offspring weights, but due to violation of statistical model assumptions, this observation needs further evaluation using refined statistical methods.

4.1.1. Elevated Plus Maze

In the EPM task, mainly effects of age unrelated to the LPS treatment were observed. Age effects included reduced time spent in the open arm of the EPM and reduced head dips during puberty (PD~45), indicative of increased anxiety during puberty, as well as increased time spent in the center of the EPM during late adolescence/early adulthood (PD~66). A trend for an effect of LPS dose on time spent in the center of the EPM with the 100 µg/kg LPS group showing increased time spent in the center, which may be interpreted as animals being more indecisive, and a statistical significant interaction between LPS dose and age on the number of rearings with the 100 µg/kg LPS group showing increased rearings compared to the 20 µg/kg LPS group on PD ~45 may hint towards effects of the higher LPS dose on EPM measures. However, as only data from one 100 µg/kg LPS litter was included, and the model shows statistically significant litter effects for most of the EPM measures, with the exception of rearings, this finding should only be interpreted carefully without collecting additional supporting data from more litters. Excluding this higher dose litter, the absence of LPS effects on EPM behavior is consistent with the initial hypothesis to replicate the absence of effects found by a former study from this department using the same protocol in adult LPS offspring (Wischhof et al., 2015b).

4.1.2. Open Field

For the open field task, it was initially hypothesized to replicate a hyperactive anxiolytic-like phenotype in juvenile and adolescent but not in adult LPS offspring, which was shown in previous studies from this department using a similar protocol

(Wischhof et al., 2015a, 2015b). However, as the assumptions for the used statistical linear mixed model were violated by non-normality and heteroscedasticity, most probably related to the zero-inflation of the raw data, the data was not interpreted any further. As most of the studies analyzing longitudinal data on e.g. distance travelled in the open field by rats or mice seem to be analyzing the data using the standard repeated measures ANOVA approach without commenting on any violation of statistical model assumptions or zero-inflation of the raw data, it is unclear if this zero-inflation is specific to the data collected within this study, or a general problem of such behavioral measures in the open field test. There are some reports of such right skew of locomotor data in the open field (Welge and Richtand, 2002; Bronson et al., 2011), which use a log-transformation to solve this issue, but such reports are scarce, suggesting this may be a problem specific to few studies and therefore might be related to the way the data are collected. Considering that automated video analysis or the use of automated systems such as the TSE Actimot-System as used in this study is the standard for measuring locomotion in the open field, reducing observer bias and standardizing the test conditions, another explanation would be that such non-normal right skewed data is actually the usual outcome of such experiments, but scientist are simply not aware this is an issue for linear statistical models like the repeated measures ANOVA and related procedures. Actually, many of the MIA papers on open field data cited within this thesis fail to mention the fulfillment or check of statistical model assumptions at all. This lack of reporting on details of assessment of statistical model assumptions is a general problem in the reporting of scientific results in publications known for a long time (Keselman et al., 1998; Osborne, 2008; Ernst and Albers, 2017; Nielsen et al., 2019; Hu and Plonsky, 2021). There is also a study suggesting that this is not simply a reporting issue, i.e. assumptions are checked but not reported when fulfilled, but rather that statistical model assumptions are actually rarely checked at all by scientists (Hoekstra et al., 2012), most probably explained by a lack of knowledge of this topic - a finding which is also supported by my own observations when discussing this topic with fellow research students and professors.

4.1.3. Novel Object recgonition

In the novel object recognition test, a statistical significant interaction between LPS dose and age was found. There does not seem to be a meaningful difference

between the 20 µg/kg LPS group and control animals, but there is a statistical significant difference between control rats and the 100 µg/kg LPS group on PD ~45. In addition, when comparing the RI against chance level, only the 100 µg/kg LPS group is statistically significant different from chance on the first three time points, but not as adults on PD ~94. Therefore, the initial hypothesis that offspring of LPS treated dams in the current study should show deficits in object recognition memory as adults (PD ~90) was partially confirmed.

There are some things to keep in mind when interpreting these results though. First, the deficits were only shown for the highest LPS dose, where only data from one litter was available, which is why this finding should only be interpreted carefully without collecting additional supporting data from more litters. Excluding this higher dose litter, one would have concluded that there are no deficits detectable. Second, the RI of control rats was never statistically significant from chance. Due to this absence of object recognition significantly different from chance in control rats, there might have been methodological problems in the execution of this behavioral test within this thesis. One hint is the statistical significant random effect for test objects, meaning the recognition index is not comparable between the different items used. Identical item pairs were used on time points one and three, as well as a different pair of items on time points two and four. Examining the control group data, one may see a zigzag pattern corresponding to the respective pairs of test items. This is showing that the recognition index is depending on the items and thus not directly comparable when different items were used, although the time spent in the sample phase is comparable between those items. And furthermore, it is also showing that the item pair for time points two and four (porcelain cup with a lion head bulge and a miniature beer glass, see fig. 18 within section 2.3.3) seems to be worse for showing recognition memory within the NOR test than the other two items. Generally, different items leading to a more robust recognition index in control rats could have been used, but in defense, the item pairs used have been selected from a wide range of items which underwent pre-tests with adult Wistar rats in preparation of this thesis, where they have shown RI values comparable to the literature (data not shown). Furthermore, there still is no standard for choosing objects for the NOR test within the literature, and previously used items often have their own disadvantages like item affordances (Chemero and Heyser, 2005; Ennaceur, 2010; Heyser and Chemero,

2012), making the choice of the right objects a non-trivial task when one wants to reduce previously made errors in item selection without introducing new errors.

Finally, another point to discuss in this regards is that the mentioned zigzag pattern is not seen in both LPS groups. Together with the generally increased RI within the higher dose LPS group, even reaching statistical significance compared to controls on PD ~45, this suggesting that LPS animals may not show deficits resulting in reduced recognition memory, but may rather show an increase recognition index in the NOR test instead, a finding which at first may seem counter intuitive, but was also shown by some other researches as well (Golan et al., 2005; Ito et al., 2010). Hovewer, the time course of this memory improvement in this study is opposite compared to that by Ito et al., 2010, as the memory advantages disappear in early adulthood, while in their study this was the time where the memory advantages began to appear.

4.1.4. Prepulse Inhibition

Regarding PPI measured via the acoustic startle response, besides the generally expected interaction between age and interstimulus interval, a statistically significant interaction between dose and age was found. Comparing the groups on individual time points, there was a transient effect of reduced PPI in the 20 µg/kg LPS group compared to the control group on PD ~66. As this deficiency in PPI is no longer detectable on PD ~94, the initial hypothesis of PPI deficits emerging during puberty and persisting into adulthood was only partially confirmed. Nevertheless, although the effect shown is not very pronounced, this work joins the long list of publications that have already shown PPI deficits in the MIA model.

Also, this deficiency was only detected when the longer interstimulus interval of 140 ms was used. This contradicts many previous findings (see introduction section 1.3.4), reporting PPI deficits in MIA offspring using lower interstimulus intervals, but is consistent with results from a former study from this department using the same protocol (Wischhof et al., 2015b) as well as with those from Santos-Toscano et al., 2016.

4.1.5. Resting-State fMRI

Analyzing the resting-state fMRI data with ICA, in total 7 ICs were classified as signal, which could be assigned to known resting-state networks.

Two DMN-like components were detected. One covering the more rostral part, mainly comprised of the *orbitofrontal*, *medial prefrontal* (*prelimbic* and *infralimbic cortices*) and rostral *cingulate cortex*, and one covering the more caudal part of the brain, mainly comprised of the caudal *cingulate* and *retrosplenial cortex*, as well as parts of the *visual cortex* and *hippocampus*. Combined, these two DMN components show strong resemblance to the known rat DMN network from the literature, such as from Lu et al., 2012 (see introduction, section 1.2.6.1.2 figure 13), Sierakowiak et al., 2015, or Dai et al., 2023. The splitting of the DMN into two components is not yet reported in the published literature so far. However, there are only few studies reporting the rat DMN via ICA, and splitting of components into several sub-components is a general observation that can be made depending for example on the used dimensionality of the ICA but also depending on other factors (Abou Elseoud et al., 2009), and thus is not unexpected. In an unpublished Master thesis from this department, a similar split of the DMN like components into a more rostral and a more caudal component was reported previously (Coors, 2015, unpublished). However, the more caudal DMN like component in that thesis was discussed to most likely represent vascular noise, as the main focus of that component was located above the superior and inferior colliculi, i.e. not in gray matter but above the brain, in a position where the superior sagittal sinus and the transverse sinus are meeting (Scremin, 2015). Two ICs appearing similar to that IC were again observed in the analysis of this thesis as well (IC 5 and 6, see table 22 in the results section as well as figure 79 in appendix section 6.3.2), but were directly classified as vascular noise and thus not discussed further.

Three bilateral ICs representing the bilateral somatosensory (*primary* and *secondary somatosensory cortex*) and motor areas (*motor cortex*) were detected (Somatosensory, Sensorimotor and Motor network), which are consistent with the published literature on rs-fMRI in rats analyzed via ICA (Becerra et al., 2011; Jonckers et al., 2011; Liang et al., 2011; Lu et al., 2012) or Seed-ROI analysis (Pawela et al., 2008; Zhao et al., 2008; Liang et al., 2013; Sierakowiak et al., 2015).

Furthermore, a Striatal Network was detected, consisting of the *caudate putamen* with involvement of e.g. *nucleus accumbens* and *globus pallidus*. A similar striatal component/network was previously reported by e.g. Hutchison et al., 2010, Jonckers et al., 2011, or Liang et al., 2011 using ICA as well.

Finally, a Cerebellar Network was found, covering a large part of the cerebellum. A similar IC was observed in Becerra et al., 2011, but there included e.g. the periaqueductal gray and other brainstem regions in addition, which did not show clear participation in this study. However, the rats in the study by Becerra et al. were not sedated but trained to be scanned in an awake state. As anesthesia and sedation are known to alter the strengths of resting-state networks (Massimini et al., 2005; Zhang et al., 2010; Liu et al., 2011b; Kalthoff et al., 2013), such differences of other brain areas involved in some ICs is not unexpected in this case. Furthermore, Hutchison et al., 2010, reported a cerebellar IC in some animals as well, but in most animals the field of view was not large enough to cover the area of the cerebellum.

No effect of LPS treatment on the shape or connectivity strengths of those resting-state networks was shown, thus the initial hypothesis of an altered resting-state connectivity of LPS offspring compared to control rats was not confirmed. However, due a lack of available previous research on resting-state fMRI within MIA models, the initial hypothesis was based on the fact that altered resting-state connectivity can be seen in human schizophrenic patients, and the LPS model as well as other MIA models usually show a great extend of face- and construct-validity (Meyer and Feldon, 2010; Reisinger et al., 2015; Haddad et al., 2020b).

Despite the absence of LPS effects on rsfMRI in this thesis, some recently published studies using other MIA models add further evidence that support the initial hypothesis of altered resting-state connectivity in MIA offspring though. The study by Mills, 2018, investigating an MIA model using prenatal IL-6 infusions during whole gestation in Sprague Dawley rats (instead of the indirect induction of inflammation using Poly(I:C) or LPS) found reduced functional connectivity in MIA offspring between PD ~22-50 from the left amygdale to left caudate putamen and ventral pallidum using seed ROI analysis. Missault et al., 2019, report increased connectivity in the DMN of Poly(I:C) offspring on PD~84 using a seed ROI analysis (maternal injection on GD 15). The alterations in functional connectivity were paralleled by increased anxiety measured by the open field test, but the alteration in functional

connectivity was only observed in the subgroup of offspring from dams that lost weight after the Poly(I:C) injection (Missault et al., 2019) – a topic that is further discussed in section 4.2.4. Finally, in a mouse model using Poly(I:C) on GD 12.5, a reduction of functional connectivity in cortical-limbic connectivity circuits and enhanced connectivity in the temporal association cortex in MIA offspring was shown on PD ~84 using seed ROI analysis by Kreitz et al., 2020. Considering the generally large variability in MIA models (see section 4.2.2), the topic will still need further attention by more studies in the future.

Although no effects of LPS treatment on connectivity of the identified resting-state networks was shown, there were statistically significant effects of age on connectivity in the cerebellar network, with connectivity decreasing with age. One trivial explanation for this finding may be a trend towards fewer coverage of the cerebellum in older rats compared to the earlier time points. Visually comparing the brain slices covering the cerebellum between PD~30 and ~94 can't rule out this may be a reason (data not shown), but a detailed analysis of this aspect was not followed-up due to time-constraints, and thus should be investigated in more detail in the future. Additional experiments specifically tailored at investigating the cerebellum, making sure the coverage is the same over all age groups would of course be the best solution to either confirm or reject the finding of overall functional connectivity decrease within the cerebellar network with increasing age.

When considering results with a trend towards statistical significance, there were age effects on connectivity in the Somatosensory and the Sensorimotor networks as well. However, in contrast to the cerebellar network, the connectivity in the latter two networks was increasing with age until reaching a maximum at PD ~66, after which the connectivity was decreasing until PD ~94.

According to our knowledge, this is the second available study to analyze resting-state fMRI in rats on a longer longitudinal scale, covering four different neurodevelopmental time points from the juvenile stage (PD~30), through puberty (PD~45), late adolescence (PD~66) into adulthood (PD~94). The only other available study covering a comparable age-span with more than two time points measured is the study by Ma et al., 2018. Investigating functional connectivity in the resting-state of awake long evans rats, Ma et al. used a seed ROI analysis to compare five time points from PD~30 over PD~34, PD~41, PD~48 until PD~70-90. Overall, all

subcortical networks showed reduced functional connectivity during development, while sensorimotor and polymodal association cortical systems displayed increased functional connectivity during development (Ma et al., 2018). Also, cortico-cortical connections and cortico-subcortical connections generally showed increases with age. Thus, the results by Ma et al., 2018 are generally in line with the trend towards increased connectivity of the Somatosensory and the Sensorimotor networks in this study. Ma et al., 2018, don't report a drop in functional connectivity in the Sensorimotor networks transitioning into adulthood though. One reason for this divergence may be the difference in definition of the later time points between the two studies. While in this present study the time points showing the drop in functional connectivity were when comparing the animals scanned on ~PD66 (late adolescence) with PD~94 (adulthood), while in the study by Ma et al. the stage of adulthood covered a large time-scale throwing together animals scanned from PD~70 until PD~94, and the authors do not provide more details of the age distribution during this period. The cerebellum was apparently not covered in the study by Ma et al. though, which means that no further conclusions can be drawn from their study with regard to the reduced connectivity found in the cerebellum in this thesis.

4.1.6. Overall summary

Overall, the offspring from dams receiving 20 µg/kg LPS showed transient PPI deficits on PD~66, while no other behavioral deficits were observed. In contrast, the offspring from the single dam receiving the higher dose of 100 µg/kg LPS showed no PPI deficits, but effects on object recognition memory as well as time spent in the center and rearings in the EPM.

No effects of LPS treatment on rs-fMRI connectivity could be observed.

4.2. Methodological Problems in MIA research

4.2.1. Abortive Effect of Pathogenic Agents

This study was started using 100 µg/kg LPS, as this dose was used successfully in previous studies from the same department (Wischhof et al., 2015b, 2015a). The dose used by Wischhof et al. further was based on studies by Cui et al., 2009 and Fortier et al., 2007, as "this dose of LPS induces a reliable cytokine release and

febrile response while having no effect on litter size and dam survival" (Wischhof et al., 2015b). Contrary, during the execution of this study, the LPS dose was stepwise reduced from the initially planned 100 to 20 µg/kg in response to unexpected abortions and one maternal death. After an in-depth literature review, it turned out that abortions and maternal death in response to LPS treatment are not unknown to the literature. Other MIA research articles are describing similar effects of abortions and/or maternal death after the treatment with LPS, often in a dose-dependent manner (Bell and Hallenbeck, 2002; Fortier et al., 2007; Chlodzinska et al., 2011; Oskvig et al., 2012; Hsueh et al., 2017; Schaafsma et al., 2017; Braun et al., 2019). For example, Schaafsma et al., 2017, also injected LPS from the *Escherichia coli* serotype 0111:B4 intraperitoneally on GD 15-17 and only obtained offspring with a dose of 50 µg/kg, while 100 and 250 µg/kg resulted in preterm birth or resorption of fetuses. The same effect of abortions and/or maternal death can be observed after induction of maternal immune activation using Poly(I:C) mimicking a viral infection as well (Meyer et al., 2005; Ozawa et al., 2006; Mueller et al., 2019). In addition, the effect of LPS on dam and fetal survival also seems to be dependent on the gestational timing of the treatment, as in a study by Fortier et al., a dose of LPS that was well tolerated at GD 15–16 was lethal to dams at GD 18–19, whereas at GD 10-11 it induced fetal death but all dams survived (Fortier et al., 2007). One study suggests that this LPS-induced abortion may be partially mediated through the effects of IL-15 on natural killer (NK) cells (Lee et al., 2013). As the effect of LPS generally is also influenced by the route of injection (see section 4.2.2 below), it is reasonable to hypothesize the injection route will influence the outcome on dam and fetal survival on top of the other mentioned factors.

A serious complication in the use of LPS in MIA models playing a part in this regard is that, due to the extraction from bacteria, each batch and lot of LPS can contain different pyrogenic and cytokinogenic activities (Ray et al., 1991; Boksa, 2010). The LPS composition and amount of impurification with nucleic acid and protein contaminants differs depending on the extraction method like trichloroacetic acid or phenol extraction, as well as different additional processing steps (Galanos et al., 1969; Leive and Morrison, 1972; Horan et al., 1989; Nguyen et al., 2019). Furthermore, different serotypes of LPS prepared from *Escherichia coli* also may differ in their pyrogenic activities, and as a consequence in their tendency for producing either a hypothermic or a hyperthermic response due to a differential

release of antipyretic cytokines like TNF-α or IL-10 (Dogan et al., 2000; Ling et al., 2006; Akarsu and Mamuk, 2007; Boksa, 2010). Therefore, Boksa, 2010, suggested that as doses of LPS may not be directly comparable across laboratories on a mg/kg basis, expressing the LPS dosage in terms of international activity units would be preferable, although such practice is not yet routine in the literature. Comparing the certificate of analysis (CoA) available online on the websites from Sigma-Aldrich for the two batches of LPS used in this study and the previous studies by Wischhof et al., 2015b, 2015a with regards to the potency measured in Endotoxin units (EU/ml or EU/mg) gives a hint towards the observed increased fetal mortality in this study. Both the present and the previous studies used the Sigma-Aldrich product L4391 (Escherichia coli O111:B4, γ-irradiated, purified by gel-filtration chromatography), but the studies by Wischhof et al., 2015b, 2015a used a vial from batch number 072M4100V while this study used a vial from batch number 036M4070V. The CoA for the batch used by Wischhof et al. states “Potency (Sample EU/mg) 600000 EU/mg”, whereas the one used in this study states “Potency (Sample EU/mg) > 3000000 EU/mg”. Therefore, the potency of the LPS used within this thesis apparently seems to be five times as high compared to the LPS used by Wischhof et al., 2015b, 2015a. Simply adopting the previous 100 µg/kg dosing scheme may therefore have resulted in injection of a dose five times as high. When the dose was finally reduced to a fifth by only using 20 µg/kg, making it more comparable to the dose used by Wischof et al. in terms of endotoxin units, the fetal and maternal mortality disappeared, confirming the initial dose may have been too high to be tolerated by most dams.

As fetal and maternal mortality is usually an unintended effect in MIA models, some working groups implement preliminary dose-dependence test in order to find a dose tolerated by the dams without inducing fetal abortions or preterm birth (Bell and Hallenbeck, 2002; Oskvig et al., 2012; Hsueh et al., 2017).

4.2.2. High Variability in MIA research

One key issue in MIA research is that there is a lot of variation in the methods applied within the different laboratories in the field, making it hard to compare the available studies.

With Poly(I:C) mimicking viral and LPS mimicking bacterial infections either via TLR3 or via TLR4 and their respective downstream routes (for review see Takeda and

Akira, 2005), there are two major pathogenic agents to choose from when designing an MIA experiment. As can be seen from tables 25 to 32 (appendix section 6.1), while there are some laboratories choosing LPS from *Salmonella enterica*, most studies using LPS are using LPS from *Escherichia coli*. As written before in section 4.2.1, there are different serotypes of *Escherichia coli*, e.g. the often used serotypes 0111:B4, 026:B6 and 055:B5, which may differ in their pyrogenic activities, leading to differences in the triggered immune responses (Dogan et al., 2000; Ling et al., 2006; Akarsu and Mamuk, 2007; Boksa, 2010). Since each batch and lot of LPS can contain different pyrogenic and cytokinogenic activities as well (Ray et al., 1991; Boksa, 2010), one may consider the suggestion from Boksa, 2010, that doses of LPS may not be directly comparable across laboratories on a mg/kg basis, and expressing the LPS dosage in terms of international activity units would be preferable. However, this currently is not adopted from the MIA research community, as from the 46 studies using LPS as pathogenic agent reviewed in sections 1.3.1 - 1.3.4 (overview tables 25 to 32 in appendix section 6.1), the study by Lin et al., 2012, is the only one directly stating the units in their material and methods section. Few like Harvey and Boksa, 2014, are at least stating the lot number by which one may look up the CoA from the manufacturer, but this is the exception. Some studies (e.g. Golan et al., 2005; Hava et al., 2006; Al-Amin et al., 2016; Straley et al., 2017; Swanepoel et al., 2018; Braun et al., 2019; Wang et al., 2019) don't mention the serotype at all, making comparisons even harder.

The variability is not a problem of LPS alone, but is also present in studies using Poly(I:C). Different molecular weights (MW) are shaping the pyrogenic activities and thus elicited immune responses of the Poly(I:C), with high MW Poly(I:C) apparently leading to more pronounced immune reactions than low MW Poly(I:C) (Mian et al., 2013; Zhou et al., 2013; Careaga et al., 2018; Mueller et al., 2019). Some studies are specifically reporting that high MW Poly(I:C) was used in their studies (Howland et al., 2012; Ballendine et al., 2015; Lins et al., 2018), but similar to the lack of reporting of LPS serotype used, this is clearly a minority. Kowash et al., 2019, compared Poly(I:C) from the two most commonly used commercial suppliers, Sigma and InvivoGen, and found they differed substantially in their biomolecular characteristics. The analyzed samples differed in MW and endotoxin (i.e. LPS) contamination, with both factors predicting the maternal IL-6 responses (Kowash et al., 2019). As maternal IL-6, which is discussed as one of the possible links between MIA and the

neurobehavioral outcome in the offspring, is commonly used to assess the effectiveness of the MIA paradigms, with the effects on the offspring being dependent on the magnitude of the elicited maternal IL-6 response (Smith et al., 2007; Deverman and Patterson, 2009; Harvey and Boksa, 2014a; Gumusoglu et al., 2017; Rudolph et al., 2018; Haddad et al., 2020b), this has consequences for the interpretation of the outcome of MIA studies. The variable contamination of Poly(I:C) with endotoxins/LPS has further consequences for the interpretation of Poly(I:C) studies, as responses previously attributed solely to the TLR3 activation by Poly(I:C) might instead be attributable to a combined TLR3 and TLR4 activation with accordingly differing downstream pathways.

In addition to the above, the route of administration (intraperitoneal or subcutaneous) can influence the immune reaction as well (Meyer et al., 2009a; Bao et al., 2022). Another factor that is playing a role in shaping the immune response and also the neurobehavioral outcome of the MIA offspring is the timing of administration (Martin et al., 1995; Fofie and Fewell, 2003; Meyer et al., 2006b, 2006a, 2009b; Fortier et al., 2007; Cui et al., 2009; Li et al., 2009; Meyer and Feldon, 2010; Kentner et al., 2019). Both Poly(I:C) and LPS are injected either during early, mid, or late gestation depending on the working group (see overview tables 25 to 32 in appendix section 6.1). Some working groups are injecting LPS even throughout the whole gestation (Borrell et al., 2002; Romero et al., 2007, 2010). As the 2nd trimester of pregnancy was identified as a critical period for exposure to bacterial or viral infectious agents with relevance for the increase of schizophrenia in the offspring (Mednick et al., 1988; Meyer et al., 2008b; Brown and Derkits, 2010), many studies are using a time-window around GD 14-18 (Golan et al., 2005; Hava et al., 2006; Fortier et al., 2007; Wolff and Bilkey, 2008; Cardon et al., 2010; de Miranda et al., 2010; Dickerson et al., 2010; Wolff et al., 2011; Yee et al., 2011; Chlodzinska et al., 2011; Howland et al., 2012; Maayan et al., 2012; Vorhees et al., 2012, 2015; Enayati et al., 2012; Yin et al., 2013, 2015; Babri et al., 2014; Harvey and Boksa, 2014a; Mattei et al., 2014; Missault et al., 2014; Van Den Eynde et al., 2014; Ballendine et al., 2015; Vernon et al., 2015; Wischhof et al., 2015b, 2015a; Zhang and van Praag, 2015; Al-Amin et al., 2016; Kentner et al., 2016; Luchicchi et al., 2016; Santos-Toscano et al., 2016; Waterhouse et al., 2016; Hsueh et al., 2017; Osborne et al., 2017; Schaafsma et al., 2017; Straley et al., 2017; Imai et al., 2018; Lins et al., 2018; Simões et al., 2018; Swanepoel et al., 2018; Gray et al., 2019; Sheu et al., 2019; Capellán et al., 2019;

De Felice et al., 2019; Gogos et al., 2020). The factor that both rats and mice including different strains are used, is further adding to this variability, as for example Wistar rats have been shown to be more susceptible to the effects of LPS in comparison to Sprague Dawley rats (Fink and Heard, 1990; Lee et al., 2001; Schwartzer et al., 2013; Bao et al., 2022). Even animals from the same strain but bought from different vendors may lead to different outcomes in MIA experiments due to a differing composition of the maternal gut bacteria (Kim et al., 2017). In summary, many factors are influencing the outcome of MIA experiments, leading to a general high variability in the MIA literature. This not only complicates the planning and conduction of further studies, but also complicates the interpretation of the overall MIA publications, as it is quite difficult to find studies from different labs that are really comparable with each other, as every study seems to use a different combination of LPS serotype, dose, injection scheme and gestational timing. Sometimes, relevant factors are not fully reported in the materials and methods section of publications, complicating comparisons and making it difficult to draw conclusions, a step necessary for turning initial hypotheses into theories by accumulation of similar results, ideally also including direct replication of studies.

This topic of variability and need for more standardization (e.g. dosing based on endotoxin units instead of mg/kg basis) was already raised more than ten years ago by Boksa, 2010. Some years ago, Roderick and Kentner, 2019, wrote a short commentary on Murray et al., 2019, which again describes the same problems apparent in the literature on MIA research, and state some solutions to improve this field of research. In the same year, an extensive checklist with reporting guidelines in order to improve the comparability of results from future MIA experiments was published (Kentner et al., 2019). Ideally, future publications will adhere to the proposed guidelines, thus facilitating the comparison of studies while alerting future new researchers in the field to the problem of the multiple influencing factors. This could lead new researchers to look a little more carefully at the individual factors before starting their work, and to plan better thought-out studies in the future. This thesis attempts to lead by example, and provides the list of all relevant factors proposed by Kentner et al., 2019 in table 101 within appendix section 6.4.2. One may note however, that the goal shouldn’t be to fully standardize all MIA experiments in the future, but rather listing all relevant factors needed to draw conclusions between studies (Würbel, 2000; Van der Staay and Steckler, 2002).

4.2.3. Fever or Hypothermia

There is another factor further complicating the research with MIA models not explicitly mentioned in the previous section. The general assumption in MIA models is that when the pregnant dams are injected with pathonegic agents like Poly(I:C) or LPS, this will lead to a fever-inducing immune response with the release of pro-inflammatory cytokines like TNF-α, IL-1 and IL-6 (Luheshi and Rothwell, 1996; Larson and Dunn, 2001; Urakubo et al., 2001; Fortier et al., 2004a, 2004b; Ashdown et al., 2007; Lowe et al., 2008; Meyer et al., 2009b; Arsenault et al., 2014; Kentner et al., 2019). However, it was shown that LPS (100 µg/kg, serotype 0111:B4, injected intraperitoneal on GD 15 and 16, Sprague Dawley rats) seems to result in fever only in ~60 % of cases, whereas in 30 % it results in hypothermia, and in 10 % no temperature change was observed (Lowe et al., 2008). The study of Santos-Toscano et al., 2016, reports that the body temperature of dams receiving LPS (100 µg/kg, serotype 0111:B4, injected intraperitoneal on GD 15 and 16, Sprague Dawley rats) differed significantly from SAL dams, with dams from the LPS group showing a lower core body temperature 2 h after injection. Moreover, the effect of LPS on the body temperature of rats seems to differ between LPS serotypes, and besides induction of fever or hypothermia can include a biphasic response of hypothermia preceeding the fever response as well (van Miert and Frens, 1968; Feldberg and Saxena, 1975; Wan and Grimble, 1986; Romanovsky et al., 1996, 1998; Dogan et al., 2000; Steiner et al., 2005, 2011; Akarsu and Mamuk, 2007). The review by van Miert and Frens, 1968, is showing that such observations of differing responses to LPS in rats is not a new observation, as they reported such different outcomes already over 50 years ago.

Such differences in the body temperature response can also be observed for Poly(I:C), as another study reports that seven out of 43 dams (~16 %) injected with Poly(I:C) (4 mg/kg, high MW on GD 15, Sprague Dawley rats) developed hypothermia, and four additional dams had body temperatures below 36 °C, totaling to ~25 % of dams that did not develop fever after the injection (Lins et al., 2018). Another study is reporting transient hypothermia induction as the main effect of Poly(I:C) treatment (10 mg/kg, on GD 15, Lister hooded rats) on the rats body temperature as well (Goh et al., 2020). With regards to mouse models, it was discussed that hypothermia may even be the predominant response to Poly(I:C) in mice, only preceded by a short phase of fever (Traynor et al., 2004; Cunningham et

al., 2007). The study of Toyama et al., 2015, is showing hypothermia instead of fever as the predominant response to the treatment of Swiss mice with LPS (50, 150 or 300 µg/kg, serotype not stated, injected intraperitoneal on GD 18) as well.

The development of hypothermia after LPS or Poly(I:C) injection is also influenced by the dose, with high doses of those pathogenic agents leading to more severe hypothermia and following symptoms of sepsis and septic shock, and pregnant dams may be more susceptible to the hypothermic effects compared to non-pregnant rats (Martin et al., 1995; Fofie and Fewell, 2003; Opal, 2007; Liu et al., 2012). Additionally, room temperature and stress related to the injection seem to influence the body temperature response of the rats as well (Romanovsky, Andrej, 2005).

As the body temperature change is a consequence of the animals immune response (Romanovsky, Andrej, 2005), it seems logical that fever and hypothermia are the result of the release of different cytokine profiles. While fever is discussed to be the results of the typical pyrogens like TNF-α, IL-1 and IL-6 (Luheshi and Rothwell, 1996; Romanovsky, Andrej, 2005; Ashdown et al., 2006), other cytokines may be responsible for the induction of hypothermia. Interestingly, although TNF-α is discussed to be involved in the fever response, it is also discussed working as a cryogen leading to the induction of hypothermia (Leon, 2004). However, this cryogenic action of TNF-α may be the result of different actions of human and murine TNF-α within rodents (Stefferl et al., 1996). Other anti-inflammatory cytokines that may be involved in the hypothermic response are IL-4, IL-10 and IL-13 (Hart et al., 1989; Fiorentino et al., 1991; Nava et al., 1997; Leon et al., 1999; Ledeboer et al., 2002; Cartmell et al., 2003; Leon, 2004; Woodward et al., 2010; Howes et al., 2014; Miao et al., 2020).

As a result of such different reactions of dams, for example Lowe et al., 2008, specifically excluded all dams that did not show a classical fever reaction from their analysis.

4.2.4. Maternal Weight Loss or Weight Gain

Something else that may be related to the varying immune response of dams to the treatment with LPS and especially Poly(I:C) is the observation that the immune response including change in body temperature and plasma cytokine levels may be associated with a change in maternal body weight within ~24 h after injection of the

pathogenic agents. In the study by Missault et al., 2014, it was shown that regarding to weight change 24 h after Poly(I:C) treatment (4 mg/kg, i.p. GD15, Wistar rats) there were two differing groups of dams. Dams that lost weight after Poly(I:C) treatment showed a significant increase in plasma levels of TNF-α, which was absent in those dams that gained weight after treatment. Additionally, behavioral deficits were shown in the offspring from the weight loss group, which were absent in the weight gain group, suggesting that maternal weight loss after MIA treatment may be an indication both for the maternal sickness behavior and immune response and may also predict the offspring behavioral outcome (Missault et al., 2014). Associations between Poly(I:C) treatment and weight loss of dams has been shown in several cases for Sprague Dawley, Long Evans and Wistar rats (Zuckerman et al., 2003; Zuckerman and Weiner, 2005; Piontkewitz et al., 2011; Richtand et al., 2011; Zhang et al., 2012; Sangha et al., 2014; Ballendine et al., 2015; De Felice et al., 2019). As written in section 4.2.2 above, high MW Poly(I:C) may be leading to a more pronounced immune reaction than low MW Poly(I:C), and in one study using both high MW and low MW Poly(I:C), only dams from the high MW group reacted with weight loss after the injection (Careaga et al., 2018). The association between this weightloss and the fever response including elevated plasma IL-6 and TNF-α levels has been shown by Fortier et al., 2004b, as well. Lins et al., 2018, report a significant effect of high MW Poly(I:C) injected on GD 15 on the weight loss of dams which was correlated with increased serum IL-6 and CXCL1 (chemokine (C-X-C motif) ligand 1) levels, although no effect on body temperature of dams was observed. Serum TNF-α was also not affected, but the offspring from weight loss dams showed various behavioral alterations (Lins et al., 2018). Another study also shows increased plasma IL-6 levels in the absence of effects on dam weight (Meehan et al., 2017). In contrast, Harvey and Boksa, 2012, show an associtation between maternal weight loss and increased plasma IL-6 levels in both Poly(I:C) and LPS. Luchicchi et al., 2016, report PPI and memory deficits in offspring from Poly(I:C) treated dams that lost weight, and in the study by Bronson et al., 2011, only the offspring from dams that lost weight after Poly(I:C) treatment show a decreased amphetamine stimulated locomotion. Two other studies by another working group are showing that both maternal weight loss and also reduced weight gain compared to controls after Poly(I:C) treatment affects the severity of the effects in the offspring (Vorhees et al., 2012, 2015). In contrast, the

study by Wolff and Bilkey, 2010, reports that the PPI deficits in Poly(I:C) offspring are unrelated to maternal weight loss or gain.

Considering LPS, the maternal body weight response after insult during pregnancy seems to be more unclear. On the one hand, in addition to the study by Harvey and Boksa, 2012, one other study reports an association between LPS treatment and weight loss as well (Rousset et al., 2006). On the other hand, two other studies report there seems to be no effect of LPS on maternal weight gain after treatment (Bell and Hallenbeck, 2002; Delattre et al., 2017).

The observed weight loss after MIA treatment may be related to decreased food and water intake, which is of specific importance considering that maternal malnutrition has been implicated as a risk factor for schizophrenia as well (Brown et al., 1996; Susser et al., 1996; Meyer et al., 2009b).

In summary, the maternal weight response to the treatment may be related to the immune response and outcome in the MIA offspring, and thus may explain some of the variability observed in the MIA literature. Within this thesis, the weight gain or loss after LPS treatment was measured (see table 2 in results section 3), but was not analysed further due to the generally low sample size (see next section 4.2.5) and thus expressive power of this study. Generally, in the 20 µg/kg LPS group, weight gain or loss after the first injection was balanced (1:1 ratio), while in the SAL group, more dams gained weight than lost weight (2:1 ratio). However, considering only the subset of litters used for the behavioural experiments, within the 20 µg/kg LPS group, three dams gained weight and only one lost weight after the LPS injection (3:1 ratio). The dam that received 100 µg/kg LPS and still delivered offspring did loose weight after treatment. Again, considering only the subset of litters used for the behavioural experiments, within the control group, four dams gained weight while only one lost weight after treatment (4:1 ratio). In case that maternal weightloss would actually be predicting the effects on LPS offspring and maternal weight gain after treatment may lead to the absence of statistical significant differences between LPS and control offspring, the fact that only one of the four 20 µg/kg LPS dams lost weight may be an explanation for the absence of effects apart from the transient effect on PPI seen within that group within this study.

4.2.5. Inflated Sample Size in MIA Studies

When starting the conduct of the experiments within this thesis, the sample size of animals was planned considering the individual offspring as the experimental unit. Thus, statistical analysis was planned with conventional repeated measures analysis of variance (rmANOVA) in mind. However, although this is practiced similarly by many other working groups within the MIA research community, this approach can actually be considered incorrect, as we only realized later.

One of the basic assumptions that must be met in order to use the statistical ANOVA is the independene of measurements (Keselman et al., 1998; Sullivan et al., 2016). Violating the independence assumption can lead to a serious increase in type I error rate. For example, even considering only a moderate within group correlation, the type I error rate may already increase from the typical 5 % to a 37 % error rate, meaning in more than a third of experiments the null hypothesis is falsely rejected (Lazic, 2010). For those cases where repeated measurements are taken from the same animal, the standard ANOVA is modified and a rmANOVA used instead, which is specifically considering the within-subjects variability separately from the between-subjects variability and thus controls for the dependence of samples keeping the type I error rate constant (Gueorguieva and Krystal, 2004; Lee, 2015).

Rodents including rats are multiparous species, giving birth to several offspring (Rosen et al., 1987; Zorrilla, 1997). Within this thesis, 25 SAL and 26 LPS animals stemming from 5 SAL treated and 5 LPS treated litters were used. But can the animals within one litter really be considered as independent units? Research has shown that actually there are large litter effects apparent, meaning comparing the individuals within one litter they are more similar in several outcome measure than when comparing the individuals between different litters with each other (Holson and Pearce, 1992; Zorrilla, 1997). Ignoring this dependence of multiple nested or hierarchically organized samples is also known as pseudoreplication, and as discussed above, may create serious problems with regards to statistical error rates (Holson and Pearce, 1992; Zorrilla, 1997; Lazic, 2010; Lazic and Essioux, 2013; Sullivan et al., 2016; Smith, 2017; Eisner, 2021).

Considering that in MIA models, the effects observed in the offspring are thought to be a result from the immune response elicited in the dams, and the effect on the

offspring may differ depending on factors such as the production of fever or hypothermia, weight gain or weight loss, probably related to differing cytokine profiles (see sections 4.2.2 - 4.2.4 above), ignoring this dependence of littermates may even be a bigger problem then for other fields of research.

There are different approaches mitigating litter effects in studies of MIA. On the one hand, there are studies which are only using one offspring from each litter for each test in order to avoid the problem of pseudoreplication (Liu et al., 2004; Golan et al., 2006; Romero et al., 2007; Ling et al., 2009; Coyle et al., 2009; Graciarena et al., 2010; Kirsten et al., 2010a; Chlodzinska et al., 2011; Song et al., 2011; Enayati et al., 2012; Lin et al., 2012; Babri et al., 2014; Majidi-Zolbanin et al., 2015; Kentner et al., 2016; Luan et al., 2018; Li et al., 2018; Mouihate et al., 2019). On the other hand, some calculate the statistical analysis using litter means, again reducing the sample size to the number of dams used (Baharnoori et al., 2012; Harvey and Boksa, 2014a, 2014b; Vernon et al., 2015; Zhang and van Praag, 2015; Batinić et al., 2016, 2017; Straley et al., 2017; Lins et al., 2018; Gray et al., 2019), while others are using specific statistical analyses like linear mixed model (LMMs) analysis with litter as random effects factor nested under treatment controlling the type I error rate (Vorhees et al., 2012, 2015; Foley et al., 2014a, 2014b; Missault et al., 2014; Van Den Eynde et al., 2014). However, some working groups seem not to be aware of this problem at all, ignoring the assumption of independence (Wolff and Bilkey, 2008; Howland et al., 2012; Santos-Toscano et al., 2016; Waterhouse et al., 2016; Imai et al., 2018), while many publications are neither stating any information on number of pups analyzed from each litter but nor stating the use of LMMs or similar procedures one would expect in order to control for analysis of multiple offspring from one litter (Borrell et al., 2002; Shi et al., 2003, 2009; Bakos et al., 2004; Poggi et al., 2005; Ozawa et al., 2006; Fortier et al., 2007; Smith et al., 2007; Meyer et al., 2008a; Cardon et al., 2010; Dickerson et al., 2010; Romero et al., 2010; Bitanihirwe et al., 2010; Bronson et al., 2011; Basta-Kaim et al., 2011b; Richtand et al., 2011; Basta-Kaim et al., 2011a, 2012; Yee et al., 2011; Basta-Kaim et al., 2015; Maayan et al., 2012; Deslauriers et al., 2013, 2014; Giovanoli et al., 2013; Lipina et al., 2013; Yin et al., 2013; Khan et al., 2014; Li et al., 2014; Zhu et al., 2014a; Ballendine et al., 2015; Wischhof et al., 2015b, 2015a; Al-Amin et al., 2016; Fujita et al., 2016; Gonzalez-Liencres et al., 2016; Han et al., 2016, 2017; Luchicchi et al., 2016; Reis-Silva et al., 2016; da Silveira et al., 2017; Delattre et al., 2017; Hsueh et al., 2017; Richetto et al.,

2017; Ronovsky et al., 2017; Schaafsma et al., 2017; Matsuura et al., 2018; Morais et al., 2018; Simões et al., 2018; Swanepoel et al., 2018; Capellán et al., 2019; Ding et al., 2019; Wang et al., 2019; Braun et al., 2019), complicating the interpretation of those studies with regards to the possible problem of pseudoreplication. Not considering the dependence of littermates, inflating the sample size and thus type I error rate, may be one additional part of the general high variability within the MIA literature.

Within this thesis, it was finally decided to generally use LMMs with litter as random effects factor nested under LPS dose for all behavioral tests. Actually, the LMM analysis revealed statistical significance for the effect of Litter on time in the open arms, head dips and rearings within the EPM. Regarding PPI, there was a trend towards statistical significance of litter, although one must note this trend disappeared when including all outlier values within the model in the sensitivity analysis. Litter effects on the measure of PPI were described by others as well (Haddad et al., 2020a; Valiquette et al., 2023), while no specific litter effects on EPM measures seem to be described in the literature. Thus, generally the use of LMMs seems to have been the correct decision considering those statisitical significant litter effects. However, in interplay with the dosing problems observed (see section 4.2.1 above), the use of several littermates from few litters leads to a very small sample size considering dams as experimental units. Regarding the 100 µg/kg offspring, the data stems from only one litter of a single dam, meaning the treatment effects for this dose are totally confounded with litter effects. Therefore, it is for example not possible to know whether the observed effects in the NOR test for this group is a real treatment effect. Considering that one of the control litters had results very similar as this one LPS litter (data not shown), it may simply be a random litter effect. Considering dams as experimental unit from the beginning and thus using offspring from 15-25 dams instead of only 5 would have been a statistically better approach.

There are also publications discussing this issue which are suggesting the dependence of littermates or pseudoreplication in general is not such a big problem as sometimes is suggested (Schank and Koehnle, 2009; Giovanoli and Meyer, 2013; Davies and Gray, 2015). Actually, with focus on MIA research, there are also hints that not all animals within one litter are affected in the same way, even though the basic immune response from their mother is shared between littermates. For

example Missault et al., 2014, also observed mRNA levels of inflammatory cytokines in individual foetuses, and observed that littermates had comparable responses in some litters, while within other litters the responses to the treatment was quite different between littermates, suggesting there may be 'responders' and 'non-responders' being affected differently by the maternal immune response. Another study reports that MIA initiated by influenza virus in mice may alter the gene expression differently for each pup within a single litter (Garbett et al., 2012). As there may be effects on the blood flow to individual uterine segments within the uterine horn differing depending on the location (Even et al., 1994), individual fetuses may be affected differently by the maternally released cytokines (Fasolino, 2018).

4.3. Statistical considerations

"*To consult the statistican after an experiment is finished is often merely to ask him to conduct a post mortem examination. He can perhaps say what the experiment died of."* (Fisher, 1938).

This famous quote from one of the driving forces behind several methods of statistics that we encounter everywhere in the scientific literature today is already 85 years old, but is by no means aged. I myself was not very firm with statistical knowledge myself when starting the work for this thesis. Everything going beyond the use of the standard repertoire of statistical tools like the t-tests and ANOVAs (Ali and Bhaskar, 2016) were things I might have read from, but did not know how to exactly utilize. Linear mixed models and the concept of random factors were unknown to me at that time. However, due to backslashes like the abortive effect of the higher LPS dose used (described in section 4.2.1 above) I consulted a large amount of literature about MIA models as well as from the statistical domain, and when I realized that this thesis was about to join a series of publications ignoring the assumption of independence due to the use of inappropriate statistical methods (discussed above in section 4.2.5), I did the only thing that felt right: I threw the initial planned statistics overboard, spent almost a year training myself in the use of statistical methods like LMMs and finally did the statistical analysis as described in this thesis. On this journey, different models were tried which are not reported here as that would have been too extensive. Therefore, although we had initial hypotheses regarding the outcome of the behavioural experiments due to previous experiments to begin with, as different statistical models were tried before it was settled onto the use of LMMs for the

behavioural data, even the behavioural part of this thesis can no longer be considered confirmatory, and this whole thesis should be understood falling into the exploratory domain instead (Fife and Rodgers, 2022). While the analysis of the rs-fMRI data had its own pitfalls, as described in section 4.3.1 below, the use of LMMs for the behavioral data solved the problem of dependence and also had other advantages, such as when in the EPM or NOR test some data points were excluded (described in sections 3.1.1 and 3.1.3) it was no longer required to leave out the whole data from those animals, as LMMs are naturally handling missing values (Gueorguieva and Krystal, 2004; Quené and Van Den Bergh, 2004). Another way to solve the problem of dependence of littermates would have been using only one pup per litter, a practice done by some working groups doing research with MIA (as described in section 4.2.5 above). This would have led to being able to use the simpler analysis of a standard repeated measure ANOVA again, but as the problem of independence in MIA research was only discovered after a bigger part of the data was already collected, this was no longer a viable option. However, for the design of future experiments, researchers should be aware of such flaws, and may design the experiment in a way to be able to use the simpler models as these usually have a greater statistical power (Lazic, 2008).

On the other hand, using more complex models may give additional insight into the data when the sample size allows this. Considering the EPM data, where more than one dependent variable were collected in a single test, fitting a multivariate mixed model instead of several univariate mixed models might have been a better solution, similar as the use of a MANOVA can have benefits such as greater statistical power over the use of several ANOVAs (Spector, 1981). However, fitting such multivariate LMMs is computationally nontrivial (Zhou and Stephens, 2014) and is currently not yet officially implemented in the lme4 package used (Dworkin and Bolker, 2021). Also, in the LMM analysis used, only random intercepts per animal were included. However, the assumption that the slope (i.e. change in the dependent variable over time) is the same for each animal must not be true, especially in the field of MIA considering there are some hints that the individual offspring may be affected differently by the treatment (Garbett et al., 2012; Missault et al., 2014). Plotting the individual animals measurements for NOR, PPI or other observations over time gave a hint that there actually were different slopes for different animals (data not shown). However, it was not possible to model these different slopes in the LMM analysis, as

the sample size was too small to solve all equations. Considering that individual animals may be affected differently by the treatment, one also may consider looking for such individual differences in the data. For example, the study by Golan et al., 2006, investigated several behavioural measures in an MIA model and used hierarchical clustering analysis by which two different clusters where observed in the data, one for most control animals and one for the MIA animals. Even if not all animals in an MIA experiment will show deficits, such a clustering anaylsis may still be able to reveal cluster of those animals which show deficits. Also, by combining multiple domains such as behavioural, rs-fMRI and histological data all in one clustering analysis, this could provide additional insights that can not be revealed using statistical tests within one domain alone.

Today, the choice of statistical methods gets more and more complex, especially since computational power increases. The history of linear mixed model analysis including random effects goes back as far as 1919 when Ronald Fisher introduced random effects models to study the correlations between relatives on the supposition of Mendelian inheritance (Fisher, 1919). However, due to computational complexity of these models, they were not used for a long time. One of the first to use mixed models for the analysis of longitudinal data seems to be Laird and Ware, 1982, but it still took until the 1990s and the increase in computing power of modern computers until more and more researches began to implement these models (Gueorguieva and Krystal, 2004). Besides LMMs, there are other options to choose from as well, such as general equation models (GEEs), making use of the so called ‘sandwich estimator’, which generally should provide similar results as LMMs, but may be beneficial in some situations (Freedman, 2006; Hubbard et al., 2010). This abundance of choices makes it not easy for the unexperienced researcher to select the correct procedures, leading to accumulation of errors in the scientific literature, that are also not corrected via the peer-review procedure (Schroter et al., 2008; Brown et al., 2018), probably due to a lack of statistical knowledge by the researchers performing the peer-review themselves (Goodman et al., 1998; Hoekstra et al., 2012). Changing and improving the statistical education in the future may help (Snee, 1993), but considering not only statistics but nearly all aspects of science get more and more complex today, it is quite optimistic to assume all researchers will learn complex modeling techniques themselves. Thus, where possible, collaborations with statisticians are advisable where possible (Fife, 2020), and the statistical

planning should go hand in hand with the planning of the experiments and not happen afterwards.

4.3.1. Statistical considerations for (rs)-fMRI

Compared to the analysis of the behavioural data, which already may not be trivial for the average scientist with limited statistical knowledge, the statistical analysis of fMRI data poses an even higher challenge. The total amount of complex data that needs to be analyzed within studies measuring fMRI is overwhelming (Lazar et al., 2001; Lindquist, 2008). Within this thesis, one measured fMRI volume consisted of 4608 voxels. For each animal, over the 12 minute resting-state scans, 400 image repetitions were measured, totaling to 1843200 voxels for one animal on one time point. Each of the 20 animals was scanned on four different time points throughout their lifes, adding up to over seven million data points for only one animal. As ICA was used to analyze the resting-state data, which is reducing the raw fMRI data to a lower-dimensional space (Lindquist, 2008), this illustration may exaggerate the problem a bit, but it is still a big difference if one wants to statistically compare 80 data points collected for 20 animals in the NOR test with each other, or if one wants to compare the 368640 data points of only one IC for the same animals with each other.

In order to statistically compare fMRI data, the current practice is still to do a series of multiple comparisons, i.e. calculating one statistical model for each voxel within the brain seperately. Because running multiple tests will on average produce five percent false positive results, which for the example of the 4608 voxels from the rat brain measured in this thesis would mean on average ~230 voxels will falsely return a statistically significant result, afterwards a correction for multiple comparisons (usually family wise error rate, FWER, or false discovery rate, FDR correction) is applied to control the type I error rate (Lindquist, 2008; Lieberman and Cunningham, 2009; Lindquist and Mejia, 2015).

The analysis of longitudinal fMRI data as collected within this thesis further complicates the statistical comparisons by adding another dimension to the data. The general linear model (GLM) which is still the standard method for statistical inference in fMRI does not easily handle longitudinal data (Mcfarquhar, 2018). Nevertheless, there are different methods available, including the mixed model approach (Skup,

2010). However, with more complex experimental designs, the realization of such mixed effects analyses in the typical software packages such as SPM12 or FSL is either not possible or very complex to implement (McFarquhar et al., 2016). The widely used FSL package, which was also used for running the ICA within this thesis, relies on specification of a design matrix in order to run a statistical analysis. Specification of the correct design matrix for the experimental design of this thesis, consisting of three dose groups with a differing amount of animals each, and four measurements in each animal, turned out to be a non-trivial task. In addition, FSLs algorithm assumes compound symmetry (sphericity) due to the underlying ordinary least squares (OLS) estimation, which is not necessarily true especially with unequal spacings between the longitudinal measurements (Huynh and Feldt, 1970; Guillaume et al., 2014; McFarquhar et al., 2016). Thus, in the end, the MRM toolbox (McFarquhar et al., 2016) was chosen to analyze the rs-fMRI data as this package allowed simpler analysis without manual specification of such a design matrix.

In line with the lack of model assessment in the general scientific literature (Hoekstra et al., 2012), the statistical model assumptions in fMRI studies are rarely assessed and less often reported (Razavi et al., 2003). That is not surprising, considering the high amount of data points are making it unpractical to check assumptions for every voxel. However, it should at least be checked whether the model assumptions seem appropriate for the peak voxels of interest (Poline and Brett, 2012; McFarquhar et al., 2016). The MRM toolbox used within this thesis theoretically allows the examination of the model assumptions through a number of standard residual plots and inferential tests (McFarquhar et al., 2016), however, the toolbox is programmed in a way which makes this assessment unsuitable for rat brain data, as the voxels to be checked can only be selected according to the human MNI template coordinate system, whereas no visual selection is possible.

Despite analysis with the MRM toolbox, analyzing the data using a GEE model such as the sandwich estimator (SwE) would theoretically have been another option (Guillaume et al., 2014, 2015; Guillaume, 2015). However, the SwE tool for FSL was implemented only recently by the end of 2019, and the first years after the release nearly no user guidance was available. However, a user guide was added to the FSL website recently, making this a more accessible option for future longitudinal studies collecting fMRI data.

4.4. Inflammation and neuropsychiatric disorders

Because LPS itself does not appear to cross the placental barrier in pregnant rats (Goto et al., 1994; Ashdown et al., 2006), the involvement of proinflammatory cytokines of maternal origin has often been considered as an intermediate link (Lanté et al., 2007). In addition to MIA, being a stressor itself, other forms of stress during pregnancy, for example maternal malnutrition (Susser et al., 1996; St Clair et al., 2005; Penner and Brown, 2007), the experience of severe adverse life events (Khashan et al., 2008), or obstetric complications (Geddes and Lawrie, 1995; Cannon et al., 2002; Byrne et al., 2007) have been implicated as risk factors for neuropsychiatric disorders as well. And in the recent years, evidence is growing suggesting that stress itself is able to induce inflammatory responses in the brain and periphery, also leading to elevated circulating cytokines (Rohleder, 2014; Calcia et al., 2016; Liu et al., 2017), further strengthening the hypothesis that inflammation may be the intermediaty link between MIA or other prenatal stressors and the development of neuropsychiatric disorders like schizophrenia (Hantsoo et al., 2019). However, although proinflammatory cytokines participate in the neurodevelopmental damage, they probably do so in response to another signals, and one of the possible candidates in this respect is oxidative stress (Lanté et al., 2007). There is increasing evidence for elevated oxidative stress, as well as a reduced antioxidant defense in schizophrenia (Mahadik and Mukherjee, 1996; Do et al., 2000; Lanté et al., 2007; Young et al., 2007; Bošković et al., 2011; Anderson et al., 2013; Monji et al., 2013; Emiliani et al., 2014; Leza et al., 2015). Oxidative stress is also known to participate in the host response to LPS (Salvemini and Cuzzocrea, 2002), and thus may be an explanation for the effects of prenatal immune challenge in the LPS and Poly(I:C) model (Lanté et al., 2007). Oxidative stress is a result of an imbalance between increased production of reactive oxygen species (ROS) and a deficient antioxidant defense (Emiliani et al., 2014). As it is not easy to directly measure an increase in ROS, oxidative stress is usally measured indirectly e.g. via protein carbonylation, lipid-peroxidation (for example thiobarbituric acid related substances (TBARS)) or DNA damage (for review, see Katerji et al., 2019). Another way to measure oxidative stress is to measure the antioxidant defense, such as the nonenzymatic antioxidant glutathione (GSH) (Katerji et al., 2019). Reduced GSH levels have been observed both in human schizophrenic patients (Do et al., 2000, 2004; Gysin et al., 2007; Lavoie et al., 2008; Matsuzawa et al., 2008; Wood et al., 2009) and in animal models

such as the Poly(I:C) (Ribeiro et al., 2013) or LPS model (Kheir-Eldin et al., 2001; Ling et al., 2002, 2004b, 2004a, 2006; Lanté et al., 2007; Zhu et al., 2007; Paintlia et al., 2008). In addition, GSH deficient mouse models show behavioural and cellular deficits that overlap with other animal models for schizophrenia (Steullet et al., 2006, 2010; Kulak et al., 2012). One way of measuring GSH is via ^{1}H-NMR spectroscopy (Trabesinger et al., 1999; Do et al., 2000). Thus, it was decided to indirectly measure Glutathione (GSH) via ^{1}H-NMR spectroscopy using a PRESS sequence in the prefrontal cortex, a brain area often implicated in the deficits seen in schizophrenic patients (Weinberger et al., 2001; Barch, 2005; Salgado-Pineda et al., 2007), within the MRI sessions that the animals underwent within this thesis in addition to the rs-fMRI measurements. The analysis of this NMR spectroscopy data was not part of this thesis, but this data will still allow further links between LPS and oxidative stress to be investigated in the future. Generally, combining such measurements is adviced for future studies measuring rs-fMRI in MIA models, as this additional NMR spectroscopy measurement does only take a short amount of additional time when the animals are positioned in the MRI scanner anyway.

One source of ROS which play a role in oxidative stress are activated microglia (Simpson and Oliver, 2020), and schizophrenia is also linked with chronic activation of microglia (Monji et al., 2009, 2013). In activated microglia, a protein called ionized calcium binding adaptor molecule 1 (Iba-1) is upregulated (Sasaki et al., 2001; Wittekindt et al., 2022), and thus can be used for the visualization of microglial cells by targeting them via immunohistological staining techniques. After finishing all experiments on GD~100, the animals used within this thesis were perfused and their brains used for immunohistochemistry staining targeting microglia with an Iba-1 antibody staining. Similar as with the GSH measurements mentioned above, analysis of this data was not part of this thesis, but will allow the investigation of the connection between LPS, oxidative stress and the involvement of activated microglia in the future. Also, a smaller cohort of ten LPS and ten SAL animals perfused on PD 30 in addition, allowing for detection of microglial changes over time by comparing the juvenile brains with those of the adult animals.

4.5. Conclusion and Outlook

To conclude, no effects of LPS treatment on rs-fMRI connectivity could be observed within this thesis. However, whether the implementation of the LPS model really worked as intended remains questionable.

The initially planned dose of 100 µg/kg LPS, which was also used by others in the past, led to viable offspring only in one dam. This litter showed effects on object recognition memory as well as time spent in the center and rearings in the EPM. However, deficits in PPI, which often are used as a benchmark test for the validity of animal models for schizophrenia, were absent. Considering there may be litter effects in the LPS model, and thus considering the dam as the experimental unit, this leads to a sample size of one for this dose anyway, which makes drawing any conclusions impossible.

Reducing the dose to 20 µg/kg LPS, which was supported by the potency of the lot of LPS used (measured in endotoxin units), led to viable offspring which actually showed a transient PPI deficit on PD~66. However, no other behavioral deficits could be observed. Again, considering the litter effects and dams as the experimental units, the sample size for this group is still very low (n = 5). With regards to the rs-fMRI measurements, the sample size is even lower, as only six animals from two dams were scanned in the MRI from the 20 µg/kg LPS group.

Unfortunately, no direct confirmation of the maternal immune response was carried out, e.g. via measurement of maternal serum/plasma levels of inflammatory cytokines. Sickness behavior of the dams was tried to be monitored but the observations were deemed unsuitable (observer not being blind and not using a standardized scale to note the observations). As the development of the maternal weight on the days after the LPS injection was measured, which is sometimes linked to the maternal immune response within the literature, at least an indirect measure for confirming the immune response was available. The dam that received 100 µg/kg LPS and still delivered offspring did loose weight after treatment. The distribution of weight loss and weight gain in the control group was comparable to that in the 20 µg/kg LPS group. Three dams treated with 20 µg/kg LPS gained weight and only one lost weight after the LPS injection, which could be an indicator of the lack of an inflammatory immune response in most of the dams from this group. However, as the

link between weight loss and the maternal immunge response is not fully confirmed yet, especially not yet in the LPS model (most of the hints are coming from the Poly(I:C) model), this remains pure speculation.

The bottom line that can be drawn from this thesis therefore remains that experiments using the MIA model are a complex matter with many influencing factors that must be considered in order to generate meaningful results. In order to improve the MIA research in the future, the pathogenic agent used should be carefully considered. Once decided, one should consider running dose-response studies beforehand with the batches/lots of LPS or Poly(I:C) to be used in order to find the optimal dose, which is producing viable offspring and also eliciting the maternal immune response expected, as already practiced by some working groups (Fortier et al., 2004a; Meyer et al., 2005; Missault et al., 2014). The immune response should be confirmed by measurement of serum or plasma cytokine measurements such as IL-6 or TNF-α. Additionally, measuring the body temperature in order to confirm fever or hypothermia is advised. As rectal temperature measurements in rats can lead to a rise in body temperatue due to the measurement itself (Dangarembizi et al., 2017), the use of an implanted telemetry system allowing wireless readout of the body temperature is adviced instead. Considering the planning of the sample size, researchers should be aware of potential litter effects and thus include the possible mitigation strategies such as only using one pup per litter, litter-mean statistics or statistical models such as LMMs in their considerations in order to being able to obtain meaningful results in the end. The exact methodology should be reported in publications for example using the proposed reporting guidelines published by Kentner et al., 2019. The publication and attached reporting guideline by Kentner et al., 2019, generally provides a good overview of what to consider when planning future MIA experiments.

5. References

Abi-Dargham A (2007) Alterations of serotonin transmission in schizophrenia. *Int Rev Neurobiol* 78:133–164 10.1016/S0074-7742(06)78005-9

Abi-Dargham A, Mawlawi O, Lombardo I, Gil R, Martinez D, Huang Y, Hwang D-R, Keilp J, Kochan L, Van Heertum R, Gorman JM, Laruelle M (2002) Prefrontal dopamine D1 receptors and working memory in schizophrenia. *J Neurosci* 22(9):3708–3719 20026302

Abou Elseoud A, Starck T, Remes J, Veijola J, Nikkinen J, Tervonen O, Kiviniemi V (2009) Model order of group PICA and resting state signal sources. *Neuroimage* 47:S101 10.1016/S1053-8119(09)70859-6

Achard S (2006) A Resilient, Low-Frequency, Small-World Human Brain Functional Network with Highly Connected Association Cortical Hubs. *J Neurosci* 26(1):63–72 10.1523/JNEUROSCI.3874-05.2006

Achard S, Bullmore E (2007) Efficiency and cost of economical brain functional networks. *PLoS Comput Biol* 3(2):e17 10.1371/journal.pcbi.0030017

Aertsen AM, Gerstein GL, Habib MK, Palm G (1989) Dynamics of neuronal firing correlation: modulation of “effective connectivity”. *J Neurophysiol* 61(5):900–917

Akarsu ES, Mamuk S (2007) Escherichia coli lipopolysaccharides produce serotype-specific hypothermic response in biotelemetered rats. *Am J Physiol Regul Integr Comp Physiol* 292(5):R1846–R1850 10.1152/ajpregu.00786.2006

Akkerman S, Blokland A, Reneerkens O, van Goethem NP, Bollen E, Gijselaers HJM, Lieben CKJ, Steinbusch HWM, Prickaerts J (2012) Object recognition testing: Methodological considerations on exploration and discrimination measures. *Behav Brain Res* 232(2):335–347 10.1016/j.bbr.2012.03.022

Al-Amin MM, Sultana R, Sultana S, Rahman MM, Reza HM (2016) Astaxanthin ameliorates prenatal LPS-exposed behavioral deficits and oxidative stress in adult offspring. *BMC Neurosci* 17(1):11 10.1186/s12868-016-0245-z

Alexopoulou L, Holt AC, Medzhitov R, Flavell RA (2001) Recognition of double-stranded RNA and activation of NF-κB by Toll-like receptor 3. *Nature* 413(6857):732–738 10.1038/35099560

Ali Z, Bhaskar Sb (2016) Basic statistical tools in research and data analysis. *Indian J Anaesth* 60(9):662 10.4103/0019-5049.190623

Anderson G, Berk M, Dodd S, Bechter K, Altamura AC, Dell’Osso B, Kanba S, Monji A, Fatemi SH, Buckley P, Debnath M, Das UN, Meyer U, Müller N, Kanchanatawan B, Maes M (2013) Immuno-inflammatory, oxidative and nitrosative stress, and neuroprogressive pathways in the etiology, course and treatment of schizophrenia. *Prog Neuro-Psychopharmacology Biol Psychiatry* 42:1–4 10.1016/j.pnpbp.2012.10.008

Andrade MMM, Tomé MF, Santiago ES, Lúcia-Santos A, De Andrade TGCS (2003) Longitudinal study of daily variation of rats’ behavior in the elevated plus-maze. *Physiol Behav* 78(1):125–133 10.1016/S0031-9384(02)00941-1

Andreasen NC, Paradiso S, O'Leary DS (1998) "Cognitive dysmetria" as an integrative theory of schizophrenia: a dysfunction in cortical-subcortical-cerebellar circuitry? *Schizophr Bull* 24(2):203–218

Andrews-Hanna JR, Reidler JS, Sepulcre J, Poulin R, Buckner RL (2010) Functional-Anatomic Fractionation of the Brain's Default Network. *Neuron* 65(4):550–562 10.1016/j.neuron.2010.02.005

Ang MJ, Lee S, Kim J-C, Kim S-H, Moon C (2020) Behavioral Tasks Evaluating Schizophrenia-like Symptoms in Animal Models: A Recent Update. *Curr Neuropharmacol* 19(5):641–664 10.2174/1570159x18666200814175114

Antunes M, Biala G (2012) The novel object recognition memory: Neurobiology, test procedure, and its modifications. *Cogn Process* 13(2):93–110 10.1007/s10339-011-0430-z

Arnold SE, Talbot K, Hahn C-G (2005) Neurodevelopment, neuroplasticity, and new genes for schizophrenia. *Prog Brain Res* 147:319–345 10.1016/S0079-6123(04)47023-X

Arsenault D, St-Amour I, Cisbani G, Rousseau LS, Cicchetti F (2014) The different effects of LPS and poly I: C prenatal immune challenges on the behavior, development and inflammatory responses in pregnant mice and their offspring. *Brain Behav Immun* 38:77–90 10.1016/j.bbi.2013.12.016

Ashburner J, Friston K (1997) Multimodal image coregistration and partitioning--a unified framework. *Neuroimage* 6(3):209–217 10.1006/nimg.1997.0290

Ashburner J, Friston KJ (1999) Nonlinear spatial normalization using basis functions. *Hum Brain Mapp* 7(4):254–266 10.1002/(SICI)1097-0193(1999)7:4<254::AID-HBM4>3.0.CO;2-G

Ashburner J, Friston KJ (2005) Unified segmentation. *Neuroimage* 26(3):839–851 10.1016/j.neuroimage.2005.02.018

Ashdown H, Dumont Y, Ng M, Poole S, Boksa P, Luheshi GN (2006) The role of cytokines in mediating effects of prenatal infection on the fetus: implications for schizophrenia. *Mol Psychiatry* 11(1):47–55 10.1038/sj.mp.4001748

Ashdown H, Poole S, Boksa P, Luheshi GN (2007) Interleukin-1 receptor antagonist as a modulator of gender differences in the febrile response to lipopolysaccharide in rats. *Am J Physiol Regul Integr Comp Physiol* 292(4):R1667-74 10.1152/ajpregu.00274.2006

Asiaei M, Solati J, Salari AA (2011) Prenatal exposure to lps leads to long-lasting physiological consequences in male offspring. *Dev Psychobiol* 53(8):828–838 10.1002/dev.20568

Avants BB, Tustison NJ, Song G, Cook PA, Klein A, Gee JC (2011) A reproducible evaluation of ANTs similarity metric performance in brain image registration. *Neuroimage* 54(3):2033–2044 10.1016/j.neuroimage.2010.09.025

Babri S, Doosti MH, Salari AA (2014) Strain-dependent effects of prenatal maternal immune activation on anxiety- and depression-like behaviors in offspring. *Brain Behav Immun* 37:164–176 10.1016/j.bbi.2013.12.003

Baharnoori M, Bhardwaj SK, Srivastava LK (2012) Neonatal behavioral changes in rats with gestational exposure to lipopolysaccharide: A prenatal infection model for developmental neuropsychiatric disorders. *Schizophr Bull* 38(3):444–456 10.1093/schbul/sbq098

Bakhshi K, Chance S a. (2015) The neuropathology of schizophrenia: A selective review of past studies and emerging themes in brain structure and cytoarchitecture. *Neuroscience* 303:82–102 10.1016/j.neuroscience.2015.06.028

Bakos J, Duncko R, Makatsori A, Pirnik Z, Kiss A, Jezova D (2004) Prenatal immune challenge affects growth, behavior, and brain dopamine in offspring. *Ann N Y Acad Sci* 1018:281–287 10.1196/annals.1296.033

Ballendine SA, Greba Q, Dawicki W, Zhang X, Gordon JR, Howland JG (2015) Behavioral alterations in rat offspring following maternal immune activation and ELR-CXC chemokine receptor antagonism during pregnancy: Implications for neurodevelopmental psychiatric disorders. *Prog Neuro-Psychopharmacology Biol Psychiatry* 57:155–165 10.1016/j.pnpbp.2014.11.002

Bannister PR, Brady JM, Jenkinson M (2007) Integrating temporal information with a non-rigid method of motion correction for functional magnetic resonance images. *Image Vis Comput* 25(3):311–320 10.1016/j.imavis.2005.10.002

Bao M, Hofsink N, Plösch T (2022) LPS vs. Poly I:C Model: Comparison of Long-Term Effects of Bacterial and Viral Maternal Immune Activation (MIA) on the Offspring. *Am J Physiol - Regul Integr Comp Physiol* 322(2) 10.1152/AJPREGU.00087.2021

Barbas H (2007) Specialized elements of orbitofrontal cortex in primates. *Ann N Y Acad Sci* 1121:10–32 10.1196/annals.1401.015

Barch DM (2005) The Cognitive Neuroscience of Schizophrenia. *Annu Rev Clin Psychol* 1(1):321–353 10.1146/annurev.clinpsy.1.102803.143959

Barkhof F, Haller S, Rombouts S a RB (2014) Resting-State Functional MR Imaging: A New Window to the Brain. *Radiology* 272(1):29–49 10.1148/radiol.14132388

Barnett SA (1975) The Rat: A Study in Behaviour, 2nd ed. Chicago: University Of Chicago Press.

Basta-Kaim A, Budziszewska B, Leśkiewicz M, Fijał K, Regulska M, Kubera M, Wędzony K, Lasoń W (2011a) Hyperactivity of the hypothalamus-pituitary-adrenal axis in lipopolysaccharide-induced neurodevelopmental model of schizophrenia in rats: Effects of antipsychotic drugs. *Eur J Pharmacol* 650(2–3):586–595 10.1016/j.ejphar.2010.09.083

Basta-Kaim A, Fijał K, Budziszewska B, Regulska M, Leśkiewicz M, Kubera M, Gołembiowska K, Lasoń W, Wędzony K (2011b) Prenatal lipopolysaccharide treatment enhances MK-801-induced psychotomimetic effects in rats. *Pharmacol Biochem Behav* 98(2):241–249 10.1016/j.pbb.2010.12.026

Basta-Kaim A, Fijał K, Ślusarczyk J, Trojan E, Głombik K, Budziszewska B, Leśkiewicz M, Regulska M, Kubera M, Lasoń W, We'dzony K (2015) Prenatal administration of lipopolysaccharide induces sex-dependent changes in glutamic acid decarboxylase and parvalbumin in the adult rat brain. *Neuroscience*

287:78–92 10.1016/j.neuroscience.2014.12.013

Basta-Kaim A, Szczęeny E, Leśkiewicz M, Głombik K, Ślusarczyk J, Budziszewska B, Regulska M, Kubera M, Nowak W, Wędzony K, Lasoń W (2012) Maternal immune activation leads to age-related behavioral and immunological changes in male rat offspring - The effect of antipsychotic drugs. *Pharmacol Reports* 64(6):1400–1410 10.1016/S1734-1140(12)70937-4

Bates D, Mächler M, Bolker B, Walker S (2015) Fitting Linear Mixed-Effects Models Using lme4. *J Stat Softw* 67(1):201–210 10.18637/jss.v067.i01

Batinić B, Santrač A, Divović B, Timić T, Stanković T, Obradović AL, Joksimović S, Savić MM (2016) Lipopolysaccharide exposure during late embryogenesis results in diminished locomotor activity and amphetamine response in females and spatial cognition impairment in males in adult, but not adolescent rat offspring. *Behav Brain Res* 299:72–80 10.1016/j.bbr.2015.11.025

Batinić B, Santrač A, Jančić I, Li G, Vidojević A, Marković B, Cook JM, Savić MM (2017) Positive modulation of α5 GABAA receptors in preadolescence prevents reduced locomotor response to amphetamine in adult female but not male rats prenatally exposed to lipopolysaccharide. *Int J Dev Neurosci* 61(April):31–39 10.1016/j.ijdevneu.2017.06.001

Bauer S, Kerr BJ, Patterson PH (2007) The neuropoietic cytokine family in development, plasticity, disease and injury. *Nat Rev Neurosci* 8(3):221–232 10.1038/nrn2054

Bäuml J, Brönner M, Leucht S (2012) Schizophrenie, schizotype und wahnhafte Störungen (F20-F25). In: Kurzlehrbuch Psychatrie und Psychotherapie (Leucht S, Förstl H, eds), pp 75–100. Stuttgart, DE: Georg Thieme Verlag.

Bayer SA, Altman J, Russo RJ, Zhang X (1993) Timetables of neurogenesis in the human brain based on experimentally determined patterns in the rat. *Neurotoxicology* 14(1):83–144

Bayer TA, Falkai P, Maier W (1999) Genetic and non-genetic vulnerability factors in schizophrenia: the basis of the “Two hit hypothesis.” *J Psychiatr Res* 33(6):543–548 10.1016/S0022-3956(99)00039-4

Becerra L, Pendse G, Chang PC, Bishop J, Borsook D (2011) Robust reproducible resting state networks in the awake rodent brain. *PLoS One* 6(10) 10.1371/journal.pone.0025701

Beckmann CF, DeLuca M, Devlin JT, Smith SM (2005) Investigations into resting-state connectivity using independent component analysis. *Philos Trans R Soc Lond B Biol Sci* 360(1457):1001–1013 10.1098/rstb.2005.1634

Beckmann CF, Smith SM (2004) Probabilistic Independent Component Analysis for Functional Magnetic Resonance Imaging. *IEEE Trans Med Imaging* 23(2):137–152 10.1109/TMI.2003.822821

Beckmann CF, Smith SM (2005) Tensorial extensions of independent component analysis for multisubject FMRI analysis. *Neuroimage* 25(1):294–311 10.1016/j.neuroimage.2004.10.043

Beckmann H (1999) Developmental malformations in cerebral structures of schizophrenic patients. *Eur Arch Psychiatry Clin Neurosci* 249 Suppl:44–47

Beckmann, Mackay, Filippini, Smith (2009) Group comparison of resting-state FMRI data using multi-subject ICA and dual regression. *Neuroimage* 47(Suppl 1):S148 10.1073/pnas.0811879106

Bell AJ, Sejnowski TJ (1995) An information-maximization approach to blind separation and blind deconvolution. *Neural Comput* 7(6):1129–1159

Bell MJ, Hallenbeck JM (2002) Effects of intrauterine inflammation on developing rat brain. *J Neurosci Res* 70(4):570–579 10.1002/jnr.10423

Bevins RA, Besheer J (2006) Object recognition in rats and mice: a one-trial non-matching-to-sample learning task to study “recognition memory”. *Nat Protoc* 1(3):1306–1311 10.1038/nprot.2006.205

Biedermann S V., Biedermann DG, Wenzlaff F, Kurjak T, Nouri S, Auer MK, Wiedemann K, Briken P, Haaker J, Lonsdorf TB, Fuss J (2017) An elevated plus-maze in mixed reality for studying human anxiety-related behavior. *BMC Biol* 15(1):1–13 10.1186/s12915-017-0463-6

Bilbo SD, Schwarz JM (2012) The immune system and developmental programming of brain and behavior. *Front Neuroendocrinol* 33(3):267–286 10.1016/j.yfrne.2012.08.006

Binder JR, Frost JA, Hammeke TA, Bellgowan PS, Rao SM, Cox RW (1999) Conceptual processing during the conscious resting state. A functional MRI study. *J Cogn Neurosci* 11(1):80–95

Birn RM, Diamond JB, Smith M a., Bandettini P a. (2006) Separating respiratory-variation-related fluctuations from neuronal-activity-related fluctuations in fMRI. *Neuroimage* 31(4):1536–1548 10.1016/j.neuroimage.2006.02.048

Birn RM, Molloy EK, Patriat R, Parker T, Meier TB, Kirk GR, Nair VA, Meyerand ME, Prabhakaran V (2013) The effect of scan length on the reliability of resting-state fMRI connectivity estimates. *Neuroimage* 83:550–558 10.1016/j.neuroimage.2013.05.099

Birn RM, Murphy K, Bandettini P a. (2008) The effect of respiration variations on independent component analysis results of resting state functional connectivity. *Hum Brain Mapp* 29(7):740–750 10.1002/hbm.20577

Biswal B, Yetkin FZ, Haughton VM, Hyde JS (1995) Functional connectivity in the motor cortex of resting human brain using echo-planar MRI. *Magn Reson Med* 34(4):537–541 10.1002/mrm.1910340409

Biswal BB et al. (2010) Toward discovery science of human brain function. *Proc Natl Acad Sci* 107(10):4734–4739 10.1073/pnas.0911855107

Biswal BB, Van Kylen J, Hyde JS (1997) Simultaneous assessment of flow and BOLD signals in resting-state functional connectivity maps. *NMR Biomed* 10(4–5):165–170

Bitanihirwe BK, Peleg-Raibstein D, Mouttet F, Feldon J, Meyer U (2010) Late

prenatal immune activation in mice leads to behavioral and neurochemical abnormalities relevant to the negative symptoms of schizophrenia. *Neuropsychopharmacology* 35(12):2462–2478 10.1038/npp.2010.129

Bluhm RL, Miller J, Lanius R a., Osuch E a., Boksman K, Neufeld RWJ, Théberge J, Schaefer B, Williamson P (2007) Spontaneous low-frequency fluctuations in the BOLD signal in schizophrenic patients: Anomalies in the default network. *Schizophr Bull* 33(4):1004–1012 10.1093/schbul/sbm052

Boksa P (2010) Effects of prenatal infection on brain development and behavior: A review of findings from animal models. *Brain Behav Immun* 24(6):881–897 10.1016/j.bbi.2010.03.005

Borrell J, Vela JM, Arévalo-Martin A, Molina-Holgado E, Guaza C (2002) Prenatal immune challenge disrupts sensorimotor gating in adult rats: Implications for the etiopathogenesis of schizophrenia. *Neuropsychopharmacology* 26(2):204–215 10.1016/S0893-133X(01)00360-8

Bošković M, Vovk T, Kores Plesničar B, Grabnar I (2011) Oxidative stress in schizophrenia. *Curr Neuropharmacol* 9(2):301–312 10.2174/157015911795596595

Boveroux P, Vanhaudenhuyse A, Bruno M-A, Noirhomme Q, Lauwick S, Luxen A, Degueldre C, Plenevaux A, Schnakers C, Phillips C, Brichant J-F, Bonhomme V, Maquet P, Greicius MD, Laureys S, Boly M (2010) Breakdown of within- and between-network resting state functional magnetic resonance imaging connectivity during propofol-induced loss of consciousness. *Anesthesiology* 113(5):1038–1053 10.1097/ALN.0b013e3181f697f5

Bowers M, Boutros N, D'Souza DC, Madonick S (2001) Substance Abuse as a Risk Factor for Schizophrenia and Related Disorders. *Int J Ment Health* 30(1):33–57

Braff DL, Swerdlow NR, Geyer MA (1999) Symptom correlates of prepulse inhibition deficits in male schizophrenic patients. *Am J Psychiatry* 156(4):596–602 10.1176/ajp.156.4.596

Braun AE, Carpentier PA, Babineau BA, Narayan AR, Kielhold ML, Moon HM, Shankar A, Su J, Saravanapandian V, Haditsch U, Palmer TD (2019) "Females are not just 'Protected' Males": Sex-specific vulnerabilities in placenta and brain after prenatal immune disruption. *eNeuro* 6(6) 10.1523/ENEURO.0358-19.2019

Bronson SL, Ahlbrand R, Horn PS, Kern JR, Richtand NM (2011) Individual differences in maternal response to immune challenge predict offspring behavior: Contribution of environmental factors. *Behav Brain Res* 220(1):55–64 10.1016/j.bbr.2010.12.040

Brown AS, Cohen P, Harkavy-Friedman J, Babulas V, Malaspina D, Gorman JM, Susser ES (2001a) Prenatal rubella, premorbid abnormalities, and adult schizophrenia. *Biol Psychiatry* 49(6):473–486 10.1016/S0006-3223(01)01068-X

Brown AS, Derkits EJ (2010) Prenatal infection and schizophrenia: A review of epidemiologic and translational studies. *Am J Psychiatry* 167(3):261–280 10.1176/appi.ajp.2009.09030361

Brown AS, Schaefer CA, Quesenberry CP, Liu L, Babulas VP, Susser ES (2005)

Maternal exposure to toxoplasmosis and risk of schizophrenia in adult offspring. *Am J Psychiatry* 162(4):767–773 10.1176/appi.ajp.162.4.767

Brown AS, Susser ES, Butler PD, Richardson Andrews R, Kaufmann CA, Gorman JM (1996) Neurobiological plausibility of prenatal nutritional deprivation as a risk factor for schizophrenia. *J Nerv Ment Dis* 184(2):71–85 10.1097/00005053-199602000-00003

Brown AW, Kaiser KA, Allison DB (2018) Issues with data and analyses: Errors, underlying themes, and potential solutions. *Proc Natl Acad Sci* 115(11):2563–2570 10.1073/pnas.1708279115

Brown GD, Yamada S, Sejnowski TJ (2001b) Independent component analysis at the neural cocktail party. *Trends Neurosci* 24(1):54–63

Brown RW, Cheng Y-CN, Haacke EM, Thompson MR, Venkatesan R (2014) Magnetic Resonance Imaging: Physical Principles and Sequence Design, 2nd ed. Hoboken, NJ: John Wiley & Sons.

Broyd SJ, Demanuele C, Debener S, Helps SK, James CJ, Sonuga-Barke EJS (2009) Default-mode brain dysfunction in mental disorders: A systematic review. *Neurosci Biobehav Rev* 33(3):279–296 10.1016/j.neubiorev.2008.09.002

Buckner RL, Andrews-Hanna JR, Schacter DL (2008) The Brain's Default Network: Anatomy, Function, and Relevance to Disease. *Ann N Y Acad Sci* 1124(1):1–38 10.1196/annals.1440.011

Buckner RL, Vincent JL (2007) Unrest at rest: default activity and spontaneous network correlations. *Neuroimage* 37(4):1091–1096; discussion 1097-9 10.1016/j.neuroimage.2007.01.010

Bulmer MG (1979) Descriptive Properties of Distributions. In: Principles of Statistics. New York: Dover Publications, Inc.

Byrne M, Agerbo E, Bennedsen B, Eaton WW, Mortensen PB (2007) Obstetric conditions and risk of first admission with schizophrenia: a Danish national register based study. *Schizophr Res* 97(1–3):51–59 10.1016/j.schres.2007.07.018

Calcia MA, Bonsall DR, Bloomfield PS, Selvaraj S, Barichello T, Howes OD (2016) Stress and neuroinflammation: a systematic review of the effects of stress on microglia and the implications for mental illness. *Psychopharmacology (Berl)* 233(9):1637–1650 10.1007/s00213-016-4218-9

Calhoun V, Golay X, Pearlson G (2000) Improved fMRI slice timing correction: interpolation errors and wrap around effects. *Proceedings, ISMRM, 9th Annu Meet Denver*:810

Calhoun VD, Adali T, Pearlson GD, Pekar JJ (2001) A method for making group inferences from functional MRI data using independent component analysis. *Hum Brain Mapp* 14(3):140–151 10.1002/hbm.1048

Camchong J, MacDonald AW, Bell C, Mueller BA, Lim KO (2011) Altered functional and anatomical connectivity in schizophrenia. *Schizophr Bull* 37(3):640–650 10.1093/schbul/sbp131

Cannon M, Jones PB, Murray RM (2002) Obstetric complications and schizophrenia: historical and meta-analytic review. *Am J Psychiatry* 159(7):1080–1092

Capellán R, Moreno-Fernández M, Orihuel J, Roura-Martínez D, Ucha M, Ambrosio E, Higuera-Matas A (2019) Ex vivo 1H-MRS brain metabolic profiling in a two-hit model of neurodevelopmental disorders: Prenatal immune activation and peripubertal stress. *Schizophr Res*(xxxx):1–9 10.1016/j.schres.2019.11.007

Caprihan A, Jones T, Chen H, Lemke N, Abbott C, Qualls C, Canive J, Gasparovic C, Bustillo JR (2015) The Paradoxical Relationship between White Matter, Psychopathology and Cognition in Schizophrenia: A Diffusion Tensor and Proton Spectroscopic Imaging Study. *Neuropsychopharmacology* 40(9):2248–2257 10.1038/npp.2015.72

Cardon M, Ron-Harel N, Cohen H, Lewitus GM, Schwartz M (2010) Dysregulation of kisspeptin and neurogenesis at adolescence link inborn immune deficits to the late onset of abnormal sensorimotor gating in congenital psychological disorders. *Mol Psychiatry* 15(4):415–425 10.1038/mp.2009.66

Careaga M, Taylor SL, Chang C, Chiang A, Ku KM, Berman RF, Van de Water JA, Bauman MD (2018) Variability in PolyIC induced immune response: Implications for preclinical maternal immune activation models. *J Neuroimmunol* 323:87–93 10.1016/j.jneuroim.2018.06.014

Carlezon WA, Kim W, Missig G, Finger BC, Landino SM, Alexander AJ, Mokler EL, Robbins JO, Li Y, Bolshakov VY, McDougle CJ, Kim KS (2019) Maternal and early postnatal immune activation produce sex-specific effects on autism-like behaviors and neuroimmune function in mice. *Sci Rep* 9(1):1–18 10.1038/s41598-019-53294-z

Carlsson A (1977) Does dopamine play a role in schizophrenia? *Psychol Med* 7(04):583 10.1017/S003329170000622X

Carlsson A, Carlsson ML (2006) A dopaminergic deficit hypothesis of schizophrenia: the path to discovery. *Dialogues Clin Neurosci* 8(1):137–142

Carmichael ST, Price JL (1995) Limbic connections of the orbital and medial prefrontal cortex in macaque monkeys. *J Comp Neurol* 363(4):615–641 10.1002/cne.903630408

Carobrez AP, Bertoglio LJ (2005) Ethological and temporal analyses of anxiety-like behavior: the elevated plus-maze model 20 years on. *Neurosci Biobehav Rev* 29(8):1193–1205 10.1016/j.neubiorev.2005.04.017

Carola V, D'Olimpio F, Brunamonti E, Mangia F, Renzi P (2002) Evaluation of the elevated plus-maze and open-field tests for the assessment of anxiety-related behaviour in inbred mice. *Behav Brain Res* 134(1–2):49–57 10.1016/S0166-4328(01)00452-1

Cartmell T, Ball C, Bristow AF, Mitchell D, Poole S (2003) Endogenous Interleukin-10 is Required for the Defervescence of Fever Evoked by Local Lipopolysaccharide-Induced and Staphylococcus Aureus -Induced Inflammation in Rats. *J Physiol* 549(2):653–664 10.1113/jphysiol.2002.037291

Caruncho HJ, Dopeso-Reyes IG, Loza MI, Rodríguez MA (2004) A GABA, reelin, and

the neurodevelopmental hypothesis of schizophrenia. *Crit Rev Neurobiol* 16(1–2):25–32

Castanheira L, Ferreira MF, Sebastião AM, Telles-Correia D (2018) Anxiety Assessment in Pre-clinical Tests and in Clinical Trials: A Critical Review. *Curr Top Med Chem* 18(19):1656–1676 10.2174/1568026618666181115102518

Chakravarti A (1999) Population genetics--making sense out of sequence. *Nat Genet* 21(1 Suppl):56–60 10.1038/4482

Chang C, Cunningham JP, Glover GH (2009) Influence of heart rate on the BOLD signal: the cardiac response function. *Neuroimage* 44(3):857–869 10.1016/j.neuroimage.2008.09.029

Chemero A, Heyser C (2005) Object exploration and a problem with reductionism. *Synthese* 147(3):403–423 10.1007/s11229-005-8363-7

Chen JE, Glover GH (2015) Functional Magnetic Resonance Imaging Methods. *Neuropsychol Rev* 2:289–313 10.1007/s11065-015-9294-9

Chen YR, Swann AC, Burt DB (1996) Stability of diagnosis in schizophrenia. *Am J Psychiatry* 153(5):682–686

Chlodzinska N, Gajerska M, Bartkowska K, Turlejski K, Djavadian RL (2011) Lipopolysaccharide injected to pregnant mice affects behavior of their offspring in adulthood. *Acta Neurobiol Exp (Wars)* 71(4):519–527

Chou Y, Panych LP, Dickey CC, Petrella JR, Chen N (2012) Investigation of long-term reproducibility of intrinsic connectivity network mapping: a resting-state fMRI study. *AJNR Am J Neuroradiol* 33(5):833–838 10.3174/ajnr.A2894

Chu JSG, Evans JA (2021) Slowed canonical progress in large fields of science. *Proc Natl Acad Sci U S A* 118(41):1–5 10.1073/pnas.2021636118

Chubb JE, Bradshaw NJ, Soares DC, Porteous DJ, Millar JK (2008) The DISC locus in psychiatric illness. *Mol Psychiatry* 13(1):36–64 10.1038/sj.mp.4002106

Church SM, Cotter D, Bramon E, Murray RM (2002) Does schizophrenia result from developmental or degenerative processes? *J Neural Transm Suppl*(63):129–147

Cipra T, Fuchs A, Formánek J, Kubát J, Mikisková H, Zajícek P, Dvorák J (1990) Detection and interpolation of outliers in biosignals. *Act Nerv Super (Praha)* 32(4):283–291

Clancy B, Darlington RB, Finlay BL (2001) Translating developmental time across mammalian species. *Neuroscience* 105(1):7–17 10.1016/S0306-4522(01)00171-3

Clarke DD, Sokoloff L (1999) Circulation and energy metabolism of the brain. In: Basic Neurochemistry. Molecular, Cellular and Medical Aspects, 6th ed. (Agranoff BW, Siegel GJ, eds), pp 637–670. Philadelphia, PA: Lippincott-Raven.

Cohen SJ, Stackman RW (2015) Assessing rodent hippocampal involvement in the novel object recognition task. A review. *Behav Brain Res* 285:105–117 10.1016/j.bbr.2014.08.002

Cole DM, Smith SM, Beckmann CF (2010) Advances and pitfalls in the analysis and interpretation of resting-state FMRI data. *Front Syst Neurosci* 4(April):8 10.3389/fnsys.2010.00008

Cole MW, Anticevic A, Repovs G, Barch D (2011) Variable Global Dysconnectivity and Individual Differences in Schizophrenia. *Biol Psychiatry* 70(1):43–50 10.1016/j.biopsych.2011.02.010

Collin G, Hulshoff Pol HE, Haijma S V, Cahn W, Kahn RS, van den Heuvel MP (2011) Impaired cerebellar functional connectivity in schizophrenia patients and their healthy siblings. *Front psychiatry* 2:73 10.3389/fpsyt.2011.00073

Coors A (2015) Does prenatal LPS exposure alter brain connectivity? A resting-state fMRI study in adult rats. Department for Biology/Chemistry (FB2), University of Bremen, Bremen, Germany [Unpublished master's thesis]

Corbetta M, Shulman GL (2002) Control of goal-directed and stimulus-driven attention in the brain. *Nat Rev Neurosci* 3(3):215–229 10.1038/nrn755

Cordes D, Haughton V, Carew JD, Arfanakis K, Maravilla K (2002) Hierarchical clustering to measure connectivity in fMRI resting-state data. *Magn Reson Imaging* 20(4):305–317

Cordes D, Haughton VM, Arfanakis K, Carew JD, Turski P a, Moritz CH, Quigley M a, Meyerand ME (2001) Frequencies contributing to functional connectivity in the cerebral cortex in “resting-state” data. *AJNR Am J Neuroradiol* 22(7):1326–1333

Cordes D, Haughton VM, Arfanakis K, Wendt GJ, Turski PA, Moritz CH, Quigley MA, Meyerand ME (2000) Mapping functionally related regions of brain with functional connectivity MR imaging. *AJNR Am J Neuroradiol* 21(9):1636–1644

Costa E, Dong E, Grayson DR, Ruzicka WB, Simonini M V, Veldic M, Guidotti A (2006) Epigenetic targets in GABAergic neurons to treat schizophrenia. *Adv Pharmacol* 54:95–117

Coyle P, Tran N, Fung JNT, Summers BL, Rofe AM (2009) Maternal dietary zinc supplementation prevents aberrant behaviour in an object recognition task in mice offspring exposed to LPS in early pregnancy. *Behav Brain Res* 197(1):210–218 10.1016/j.bbr.2008.08.022

Crow TJ (2007) How and why genetic linkage has not solved the problem of psychosis: review and hypothesis. *Am J Psychiatry* 164(1):13–21 10.1176/appi.ajp.164.1.13

Cui K, Ashdown H, Luheshi GN, Boksa P (2009) Effects of prenatal immune activation on hippocampal neurogenesis in the rat. *Schizophr Res* 113(2–3):288–297 10.1016/j.schres.2009.05.003

Cunningham C, Campion S, Teeling J, Felton L, Perry VH (2007) The sickness behaviour and CNS inflammatory mediator profile induced by systemic challenge of mice with synthetic double-stranded RNA (poly I:C). *Brain Behav Immun* 21(4):490–502 10.1016/j.bbi.2006.12.007

da Silveira VT, Medeiros D de C, Ropke J, Guidine PA, Rezende GH, Moraes MFD, Mendes EMAM, Macedo D, Moreira FA, de Oliveira ACP (2017) Effects of early

or late prenatal immune activation in mice on behavioral and neuroanatomical abnormalities relevant to schizophrenia in the adulthood. *Int J Dev Neurosci* 58:1–8 10.1016/j.ijdevneu.2017.01.009

Dabbah-Assadi F, Alon D, Golani I, Doron R, Kremer I, Beloosesky R, Shamir A (2019) The influence of immune activation at early vs late gestation on fetal NRG1-ErbB4 expression and behavior in juvenile and adult mice offspring. *Brain Behav Immun* 79(August 2018):207–215 10.1016/j.bbi.2019.02.002

Dai T, Seewoo BJ, Hennessy LA, Bolland SJ, Rosenow T, Rodger J (2023) Identifying reproducible resting state networks and functional connectivity alterations following chronic restraint stress in anaesthetized rats. *Front Neurosci* 17(May):1–16 10.3389/fnins.2023.1151525

Dalton VS, Verdurand M, Walker A, Hodgson DM, Zavitsanou K (2012) Synergistic Effect between Maternal Infection and Adolescent Cannabinoid Exposure on Serotonin 5HT1A Receptor Binding in the Hippocampus: Testing the “Two Hit” Hypothesis for the Development of Schizophrenia. *ISRN Psychiatry* 2012:451865 10.5402/2012/451865

Damoiseaux JS, Rombouts SARB, Barkhof F, Scheltens P, Stam CJ, Smith SM, Beckmann CF (2006) Consistent resting-state networks across healthy subjects. *Proc Natl Acad Sci U S A* 103(37):13848–13853 10.1073/pnas.0601417103

Dangarembizi R, Erlwanger KH, Mitchell D, Hetem RS, Madziva MT, Harden LM (2017) Measurement of body temperature in normothermic and febrile rats: Limitations of using rectal thermometry. *Physiol Behav* 179:162–167 10.1016/j.physbeh.2017.06.002

Dantzer R, O’Connor JC, Freund GG, Johnson RW, Kelley KW (2008) From inflammation to sickness and depression: when the immune system subjugates the brain. *Nat Rev Neurosci* 9(1):46–56 10.1038/nrn2297

Dashraath P, Wong JLJ, Lim MXK, Lim LM, Li S, Biswas A, Choolani M, Mattar C, Su LL (2020) Coronavirus disease 2019 (COVID-19) pandemic and pregnancy. *Am J Obstet Gynecol* 222(6):521–531 10.1016/j.ajog.2020.03.021

Davies G, Welham J, Chant D, Torrey EF, McGrath J (2003) A systematic review and meta-analysis of Northern Hemisphere season of birth studies in schizophrenia. *Schizophr Bull* 29(3):587–593

Davies GM, Gray A (2015) Don’t let spurious accusations of pseudoreplication limit our ability to learn from natural experiments (and other messy kinds of ecological monitoring). *Ecol Evol* 5(22):5295–5304 10.1002/ece3.1782

Davis KL, Kahn RS, Ko G, Davidson M (1991) Dopamine in schizophrenia: a review and reconceptualization. *Am J Psychiatry* 148(11):1474–1486

Davis M, File SE (1984) Intrinsic and extrinsic mechanisms of habituation and sensitization: Implications for the design and analysis of experiments. In: Habituation, Sensitization, and Behavior, 1st ed. (Peeke HVS, Petrinovich L, eds), pp 287–323. New York: Academic Press.

Davis M, Gendelman DS, Tischler MD, Gendelman PM (1982) A primary acoustic startle circuit: lesion and stimulation studies. *J Neurosci* 2:791–805

Day GS, Farb NAS, Tang-Wai DF, Masellis M, Black SE, Freedman M, Pollock BG, Chow TW (2013) Salience Network Resting-State Activity. *JAMA Neurol* 10.1001/jamaneurol.2013.3258

De Felice M, Melis M, Aroni S, Muntoni AL, Fanni S, Frau R, Devoto P, Pistis M (2019) The PPARα agonist fenofibrate attenuates disruption of dopamine function in a maternal immune activation rat model of schizophrenia. *CNS Neurosci Ther* 25(5):549–561 10.1111/cns.13087

De Luca M, Beckmann CF, De Stefano N, Matthews PM, Smith SM (2006) fMRI resting state networks define distinct modes of long-distance interactions in the human brain. *Neuroimage* 29(4):1359–1367 10.1016/j.neuroimage.2005.08.035

De Luca M, Smith S, De Stefano N, Federico A, Matthews PM (2005) Blood oxygenation level dependent contrast resting state networks are relevant to functional activity in the neocortical sensorimotor system. *Exp brain Res* 167(4):587–594 10.1007/s00221-005-0059-1

de Miranda J, Yaddanapudi K, Hornig M, Villar G, Serge R, Ian Lipkin W (2010) Induction of toll-like receptor 3-mediated immunity during gestation inhibits cortical neurogenesis and causes behavioral disturbances. *MBio* 1(4):1–10 10.1128/mBio.00176-10

Delattre AM, Carabelli B, Mori MA, Kempe PG, Rizzo de Souza LE, Zanata SM, Machado RB, Suchecki D, Andrade da Costa BLS, Lima MMS, Ferraz AC (2017) Maternal Omega-3 Supplement Improves Dopaminergic System in Pre- and Postnatal Inflammation-Induced Neurotoxicity in Parkinson's Disease Model. *Mol Neurobiol* 54(3):2090–2106 10.1007/s12035-016-9803-8

DeLisi LE, Shaw SH, Crow TJ, Shields G, Smith AB, Larach VW, Wellman N, Loftus J, Nanthakumar B, Razi K, Stewart J, Comazzi M, Vita A, Heffner T, Sherrington R (2002) A genome-wide scan for linkage to chromosomal regions in 382 sibling pairs with schizophrenia or schizoaffective disorder. *Am J Psychiatry* 159(5):803–812

Depino AM (2015) Early prenatal exposure to LPS results in anxiety- and depression-related behaviors in adulthood. *Neuroscience* 299:56–65 10.1016/j.neuroscience.2015.04.065

Dere E, Huston JP, De Souza Silva MA (2007) The pharmacology, neuroanatomy and neurogenetics of one-trial object recognition in rodents. *Neurosci Biobehav Rev* 31(5):673–704 10.1016/j.neubiorev.2007.01.005

Deslauriers J, Larouche A, Sarret P, Grignon S (2013) Combination of prenatal immune challenge and restraint stress affects prepulse inhibition and dopaminergic/GABAergic markers. *Prog Neuro-Psychopharmacology Biol Psychiatry* 45:156–164 10.1016/j.pnpbp.2013.05.006

Deslauriers J, Racine W, Sarret P, Grignon S (2014) Preventive effect of alpha-lipoic acid on prepulse inhibition deficits in a juvenile two-hit model of schizophrenia. *Neuroscience* 272:261–270 10.1016/j.neuroscience.2014.04.061

Deverman BE, Patterson PH (2009) Cytokines and CNS Development. *Neuron* 64(1):61–78 10.1016/j.neuron.2009.09.002

Dickerson DD, Wolff AR, Bilkey DK (2010) Abnormal long-range neural synchrony in a maternal immune activation animal model of schizophrenia. *J Neurosci* 30(37):12424–12431 10.1523/JNEUROSCI.3046-10.2010

Ding S, Hu Y, Luo B, Cai Y, Hao K, Yang Y, Zhang Y, Wang X, Ding M, Zhang H, Li W, Lv L (2019) Age-related changes in neuroinflammation and prepulse inhibition in offspring of rats treated with Poly I:C in early gestation. *Behav Brain Funct* 15(1):1–10 10.1186/s12993-019-0154-2

Dix SL, Aggleton JP (1999) Extending the spontaneous preference test of recognition: Evidence of object-location and object-context recognition. *Behav Brain Res* 99(2):191–200 10.1016/S0166-4328(98)00079-5

Do KQ, Bovet P, Cuenod M (2004) Schizophrenia: Glutathione deficit as a new vulnerability factor for disconnectivity syndrome. *Schweizer Arch fur Neurol und Psychiatr* 155(8):375–385

Do KQ, Trabesinger a H, Kirsten-Krüger M, Lauer CJ, Dydak U, Hell D, Holsboer F, Boesiger P, Cuénod M (2000) Schizophrenia: glutathione deficit in cerebrospinal fluid and prefrontal cortex in vivo. *Eur J Neurosci* 12(10):3721–3728

Dogan MD, Ataoglu H, Akarsu ES (2000) Effects of different serotypes of Escherichia coli lipopolysaccharides on body temperature in rats. *Life Sci* 67(19):2319–2329 10.1016/S0024-3205(00)00821-3

Doniger GM, Foxe JJ, Murray MM, Higgins BA, Javitt DC (2002) Impaired Visual Object Recognition and Dorsal/Ventral Stream Interaction in Schizophrenia. *Arch Gen Psychiatry* 59(11):1011 10.1001/archpsyc.59.11.1011

Duan J, Martinez M, Sanders AR, Hou C, Burrell GJ, Krasner AJ, Schwartz DB, Gejman P V (2007) DTNBP1 (Dystrobrevin binding protein 1) and schizophrenia: association evidence in the 3' end of the gene. *Hum Hered* 64(2):97–106 10.1159/000101961

Dworkin I, Bolker B (2021) Multivariate modeling via mixed models. [Accessed October 31, 2023]https://mac-theobio.github.io/QMEE/lectures/MultivariateMixed.notes.html

Eisner DA (2021) Pseudoreplication in physiology: More means less. *J Gen Physiol* 153(2) 10.1085/jgp.202012826

Emiliani FE, Sedlak TW, Sawa A (2014) Oxidative stress and schizophrenia: recent breakthroughs from an old story. *Curr Opin Psychiatry* 27(3):185–190 10.1097/YCO.0000000000000054

Enayati M, Solati J, Hosseini MH, Shahi HR, Saki G, Salari AA (2012) Maternal infection during late pregnancy increases anxiety- and depression-like behaviors with increasing age in male offspring. *Brain Res Bull* 87(2–3):295–302 10.1016/j.brainresbull.2011.08.015

Engel AL, Holt GE, Lu H (2011) The pharmacokinetics of Toll-like receptor agonists and the impact on the immune system. *Expert Rev Clin Pharmacol* 4(2):275–289 10.1586/ecp.11.5

Ennaceur A (2010) One-trial object recognition in rats and mice: Methodological and

theoretical issues. *Behav Brain Res* 215(2):244–254 10.1016/j.bbr.2009.12.036

Ennaceur A (2014) Tests of unconditioned anxiety - Pitfalls and disappointments. *Physiol Behav* 135:55–71 10.1016/j.physbeh.2014.05.032

Ennaceur A, Chazot PL (2016) Preclinical animal anxiety research – flaws and prejudices. *Pharmacol Res Perspect* 4(2):1–37 10.1002/prp2.223

Ennaceur A, Delacour J (1988) A new one-trial test for neurobiological studies of memory in rats. I. Behavioural Data. *Behav Brain Res* 31(1):47–59 10.1016/S0166-4328(05)80315-8

Ernst AF, Albers CJ (2017) Regression assumptions in clinical psychology research practice-a systematic review of common misconceptions. *PeerJ* 2017(5):1–16 10.7717/peerj.3323

Erridge C, Bennett-Guerrero E, Poxton IR (2002) Structure and function of lipopolysaccharides. *Microbes Infect* 4(8):837–851 10.1016/S1286-4579(02)01604-0

Eßlinger M, Wachholz S, Manitz MP, Plümper J, Sommer R, Juckel G, Friebe A (2016) Schizophrenia associated sensory gating deficits develop after adolescent microglia activation. *Brain Behav Immun* 58:99–106 10.1016/j.bbi.2016.05.018

Even MD, Laughlin MH, Krause GF, vom Saal FS (1994) Differences in blood flow to uterine segments and placentae in relation to sex, intrauterine location and side in pregnant rats. *Reproduction* 102(1):245–252 10.1530/jrf.0.1020245

Fasolino V (2018) Development and behavioural validation of a neurodevelopmental model for schizophrenia. Division of Pharmacy & Optometry, The University of Manchester, Manchester, England [Master's thesis]

Fatemi SH, Folsom TD (2009) The Neurodevelopmental Hypothesis of Schizophrenia, Revisited. *Schizophr Bull* 35(3):528–548 10.1093/schbul/sbn187

Fatemi SH, Pearce DA, Brooks AI, Sidwell RW (2005) Prenatal viral infection in mouse causes differential expression of genes in brains of mouse progeny: A potential animal model for schizophrenia and autism. *Synapse* 57(2):91–99 10.1002/syn.20162

Feigenson KA, Kusnecov AW, Silverstein SM (2014) Inflammation and the two-hit hypothesis of schizophrenia. *Neurosci Biobehav Rev* 38:72–93 10.1016/j.neubiorev.2013.11.006

Feldberg W, Saxena PN (1975) Prostaglandins, endotoxin and lipid A on body temperature in rats. *J Physiol* 249(3):601–615 10.1113/jphysiol.1975.sp011033

Fendt M, Koch M (2013) Translational value of startle modulations. *Cell Tissue Res* 354(1):287–295 10.1007/s00441-013-1599-5

Fendt M, Li L, Yeomans JS (2001) Brain stem circuits mediating prepulse inhibition of the startle reflex. *Psychopharmacology (Berl)* 156(2–3):216–224 10.1007/s002130100794

Fernandes C, File SE (1996) The influence of open arm ledges and maze experience in the elevated plus-maze. *Pharmacol Biochem Behav* 54(1):31–40 10.1016/0091-3057(95)02171-X

Fife D (2019) Flexplot: graphically-based data analysis. :1–35 10.31234/osf.io/kh9c3

Fife D (2020) The Eight Steps of Data Analysis: A Graphical Framework to Promote Sound Statistical Analysis. *Perspect Psychol Sci* 15(4):1054–1075 10.1177/1745691620917333

Fife DA, Rodgers JL (2022) Understanding the exploratory/confirmatory data analysis continuum: Moving beyond the “replication crisis”. *Am Psychol* 77(3):453–466 10.1037/amp0000886

Filippini N, MacIntosh BJ, Hough MG, Goodwin GM, Frisoni GB, Smith SM, Matthews PM, Beckmann CF, Mackay CE (2009) Distinct patterns of brain activity in young carriers of the APOE-epsilon4 allele. *Proc Natl Acad Sci U S A* 106(17):7209–7214 10.1073/pnas.0811879106

Fink MP, Heard SO (1990) Laboratory models of sepsis and septic shock. *J Surg Res* 49(2):186–196

Fiorentino DF, Zlotnik A, Mosmann TR, Howard M, O’Garra A (1991) IL-10 inhibits cytokine production by activated macrophages. *J Immunol* 147(11):3815–3822

Fisher RA (1919) XV.—The Correlation between Relatives on the Supposition of Mendelian Inheritance. *Trans R Soc Edinburgh* 52(2):399–433 10.1017/S0080456800012163

Fisher RA (1938) Presidential Address. *Sankhyā Indian J Stat* 4(1):14–17

Floyd NS, Price JL, Ferry AT, Keay KA, Bandler R (2000) Orbitomedial prefrontal cortical projections to distinct longitudinal columns of the periaqueductal gray in the rat. *J Comp Neurol* 422(4):556–578

Floyd NS, Price JL, Ferry AT, Keay KA, Bandler R (2001) Orbitomedial prefrontal cortical projections to hypothalamus in the rat. *J Comp Neurol* 432(3):307–328

Fofie AE, Fewell JE (2003) Influence of pregnancy on plasma cytokines and the febrile response to intraperitoneal administration of bacterial endotoxin in rats. *Exp Physiol* 88(6):747–754 10.1113/eph8802594

Foley KA, MacFabe DF, Vaz A, Ossenkopp KP, Kavaliers M (2014a) Sexually dimorphic effects of prenatal exposure to propionic acid and lipopolysaccharide on social behavior in neonatal, adolescent, and adult rats: Implications for autism spectrum disorders. *Int J Dev Neurosci* 39(C):68–78 10.1016/j.ijdevneu.2014.04.001

Foley KA, Ossenkopp KP, Kavaliers M, MacFabe DF (2014b) Pre- and neonatal exposure to lipopolysaccharide or the enteric metabolite, propionic acid, alters development and behavior in adolescent rats in a sexually dimorphic manner. *PLoS One* 9(1):1–13 10.1371/journal.pone.0087072

Fonov V, Evans A, McKinstry R, Almli C, Collins D (2009) Unbiased nonlinear average age-appropriate brain templates from birth to adulthood. *Neuroimage*

47:S102 [Accessed August 13, 2015]10.1016/S1053-8119(09)70884-5

Fonov V, Evans AC, Botteron K, Almli CR, McKinstry RC, Collins DL (2011) Unbiased average age-appropriate atlases for pediatric studies. *Neuroimage* 54(1):313–327 [Accessed August 13, 2015]10.1016/j.neuroimage.2010.07.033

Fortier M-È, Joober R, Luheshi GN, Boksa P (2004a) Maternal exposure to bacterial endotoxin during pregnancy enhances amphetamine-induced locomotion and startle responses in adult rat offspring. *J Psychiatr Res* 38(3):335–345 10.1016/j.jpsychires.2003.10.001

Fortier M-E, Kent S, Ashdown H, Poole S, Boksa P, Luheshi GN (2004b) The viral mimic, polyinosinic:polycytidylic acid, induces fever in rats via an interleukin-1-dependent mechanism. *Am J Physiol Regul Integr Comp Physiol* 287(4):R759-66 10.1152/ajpregu.00293.2004

Fortier M-E, Luheshi GN, Boksa P (2007) Effects of prenatal infection on prepulse inhibition in the rat depend on the nature of the infectious agent and the stage of pregnancy. *Behav Brain Res* 181(2):270–277 10.1016/j.bbr.2007.04.016

Fox J, Weisberg S (2019) An R companion to applied regression. Thousand Oaks, CA: SAGE Publications, Inc. [Accessed July 3, 2021]

Fox MD, Corbetta M, Snyder AZ, Vincent JL, Raichle ME (2006) Spontaneous neuronal activity distinguishes human dorsal and ventral attention systems. *Proc Natl Acad Sci U S A* 103(26):10046–10051 10.1073/pnas.0604187103

Fox MD, Raichle ME (2007) Spontaneous fluctuations in brain activity observed with functional magnetic resonance imaging. *Nat Rev Neurosci* 8(9):700–711 10.1038/nrn2201

Fox MD, Snyder AZ, Vincent JL, Corbetta M, Van Essen DC, Raichle ME (2005) From The Cover: The human brain is intrinsically organized into dynamic, anticorrelated functional networks. *Proc Natl Acad Sci* 102(27):9673–9678 10.1073/pnas.0504136102

Freedman DA (2006) On The So-Called “Huber Sandwich Estimator” and “Robust Standard Errors.” *Am Stat* 60(4):299–302 10.1198/000313006X152207

Friard O, Gamba M (2016) BORIS: a free, versatile open-source event-logging software for video/audio coding and live observations. *Methods Ecol Evol*:n/a-n/a 10.1111/2041-210X.12584

Friston KJ, Frith CD, Liddle PF, Frackowiak RS (1993) Functional connectivity: the principal-component analysis of large (PET) data sets. *J Cereb Blood Flow Metab* 13:5–14 10.1038/jcbfm.1993.4

Friston KJ, Josephs O, Zarahn E, Holmes a. P, Rouquette S, Poline J-B (2000) To Smooth or Not to Smooth? *Neuroimage* 12(2):196–208 10.1006/nimg.2000.0609

Fujita Y, Ishima T, Hashimoto K (2016) Supplementation with D-serine prevents the onset of cognitive deficits in adult offspring after maternal immune activation. *Sci Rep* 6(September):1–10 10.1038/srep37261

Galanos C, Lüderitz O, Westphal O (1969) A New Method for the Extraction of R

Lipopolysaccharides. *Eur J Biochem* 9(2):245–249 10.1111/j.1432-1033.1969.tb00601.x

Gandhi R, Hayley S, Gibb J, Merali Z, Anisman H (2007) Influence of poly I:C on sickness behaviors, plasma cytokines, corticosterone and central monoamine activity: Moderation by social stressors. *Brain Behav Immun* 21(4):477–489 10.1016/j.bbi.2006.12.005

Garbett KA, Hsiao EY, Kálmán S, Patterson PH, Mirnics K (2012) Effects of maternal immune activation on gene expression patterns in the fetal brain. *Transl Psychiatry* 2(November 2011) 10.1038/tp.2012.24

García Bueno B, Caso JR, Madrigal JLM, Leza JC (2016) Innate immune receptor Toll-like receptor 4 signalling in neuropsychiatric diseases. *Neurosci Biobehav Rev* 64:134–147 10.1016/j.neubiorev.2016.02.013

Garrity AG, Pearlson GD, McKiernan K, Lloyd D, Kiehl K a., Calhoun VD (2007) Aberrant "default mode" functional connectivity in schizophrenia. *Am J Psychiatry* 164(3):450–457 10.1176/appi.ajp.164.3.450

Gaskin S, Tardif M, Cole E, Piterkin P, Kayello L, Mumby DG (2010) Object familiarization and novel-object preference in rats. *Behav Processes* 83(1):61–71 10.1016/j.beproc.2009.10.003

Geddes JR, Lawrie SM (1995) Obstetric complications and schizophrenia: a meta-analysis. *Br J Psychiatry* 167(6):786–793

Gilmore JH, Jarskog LF (1997) Exposure to infection and brain development: cytokines in the pathogenesis of schizophrenia. *Schizophr Res* 24(3):365–367 10.1016/S0920-9964(96)00123-5

Giovanoli S, Engler H, Engler A, Richetto J, Feldon J, Riva MA, Schedlowski M, Meyer U (2016) Preventive effects of minocycline in a neurodevelopmental two-hit model with relevance to schizophrenia. *Transl Psychiatry* 6(September 2015) 10.1038/tp.2016.38

Giovanoli S, Engler H, Engler A, Richetto J, Voget M, Willi R, Winter C, Riva MA, Mortensen PB, Feldon J, Schedlowski M, Meyer U (2013) Stress in Puberty Unmasks Latent Neuropathological Consequences of Prenatal Immune Activation in Mice. *Science (80-)* 339(6123):1095–1099 10.1126/science.1228261

Giovanoli S, Meyer U (2013) Response to comment on "Stress in puberty unmasks latent neuropathological consequences of prenatal immune activation in mice." *Science (80-)* 340(6134) 10.1126/science.1238060

Gogos A, Sbisa A, Witkamp D, van den Buuse M (2020) Sex differences in the effect of maternal immune activation on cognitive and psychosis-like behaviour in Long Evans rats. *Eur J Neurosci*:ejn.14671 10.1111/ejn.14671

Goh J-Y, O'Sullivan SE, Shortall SE, Zordan N, Piccinini AM, Potter HG, Fone KCF, King M V. (2020) Gestational poly(I:C) attenuates, not exacerbates, the behavioral, cytokine and mTOR changes caused by isolation rearing in a rat 'dual-hit' model for neurodevelopmental disorders. *Brain Behav Immun* 89(1–3):100–117 10.1016/j.bbi.2020.05.076

Golan H, Stilman M, Lev V, Huleihel M (2006) Normal aging of offspring mice of mothers with induced inflammation during pregnancy. *Neuroscience* 141(4):1909–1918 10.1016/j.neuroscience.2006.05.045

Golan HM, Lev V, Hallak M, Sorokin Y, Huleihel M (2005) Specific neurodevelopmental damage in mice offspring following maternal inflammation during pregnancy. *Neuropharmacology* 48(6):903–917 10.1016/j.neuropharm.2004.12.023

Gonzalez-Liencres C, Juckel G, Esslinger M, Wachholz S, Manitz MP, Brüne M, Friebe A (2016) Emotional contagion is not altered in mice prenatally exposed to poly (I:C) on gestational day 9. *Front Behav Neurosci* 10(Jun):1–7 10.3389/fnbeh.2016.00134

Goodman SN, Altman DG, George SL (1998) Statistical reviewing policies of medical journals. *J Gen Intern Med* 13(11):753–756 10.1046/j.1525-1497.1998.00227.x

Gordon CJ (1990) Thermal biology of the laboratory rat. *Physiol Behav* 47(5):963–991 10.1016/0031-9384(90)90025-Y

Gorges M, Roselli F, Müller HP, Ludolph AC, Rasche V, Kassubek J (2017) Functional connectivity mapping in the animal model: Principles and applications of resting-state fMRI. *Front Neurol* 8(MAY):1–14 10.3389/fneur.2017.00200

Goto M, Yoshioka T, Ravindranath T, Battelino T, Young RI, Zeller WP (1994) LPS injected into the pregnant rat late in gestation does not induce fetal endotoxemia. *Res Commun Mol Pathol Pharmacol* 85(1):109–112

Gottesman II, McGuffin P, Farmer AE (1987) Clinical genetics as clues to the “real” genetics of schizophrenia (a decade of modest gains while playing for time). *Schizophr Bull* 13(1):23–47

Graciarena M, Depino AM, Pitossi FJ (2010) Prenatal inflammation impairs adult neurogenesis and memory related behavior through persistent hippocampal TGFβ1 downregulation. *Brain Behav Immun* 24(8):1301–1309 10.1016/j.bbi.2010.06.005

Gray A, Tattoli R, Dunn A, Hodgson DM, Michie PT, Harms L (2019) Maternal immune activation in mid-late gestation alters amphetamine sensitivity and object recognition, but not other schizophrenia-related behaviours in adult rats. *Behav Brain Res* 356:358–364 10.1016/j.bbr.2018.08.016

Greicius M (2008) Resting-state functional connectivity in neuropsychiatric disorders. *Curr Opin Neurol* 21(4):424–430 10.1097/wco.0b013e328306f2c5

Greicius MD, Flores BH, Menon V, Glover GH, Solvason HB, Kenna H, Reiss AL, Schatzberg AF (2007) Resting-state functional connectivity in major depression: abnormally increased contributions from subgenual cingulate cortex and thalamus. *Biol Psychiatry* 62(5):429–437 10.1016/j.biopsych.2006.09.020

Greicius MD, Kiviniemi V, Tervonen O, Vainionpää V, Alahuhta S, Reiss AL, Menon V (2008) Persistent default-mode network connectivity during light sedation. *Hum Brain Mapp* 29(7):839–847 10.1002/hbm.20537

Greicius MD, Krasnow B, Reiss AL, Menon V (2003) Functional connectivity in the

resting brain: a network analysis of the default mode hypothesis. *Proc Natl Acad Sci U S A* 100(1):253–258 10.1073/pnas.0135058100

Greicius MD, Srivastava G, Reiss AL, Menon V (2004) Default-mode network activity distinguishes Alzheimer's disease from healthy aging: evidence from functional MRI. *Proc Natl Acad Sci U S A* 101(13):4637–4642 10.1073/pnas.0308627101

Griebel G, Moreau J, Jenck F, Martin JR, Misslin R (1993) Some critical determinants of the behaviour of rats in the elevated plus-maze. *Behav Processes* 29(1–2):37–47 10.1016/0376-6357(93)90026-N

Griffanti L, Douaud G, Bijsterbosch J, Evangelisti S, Alfaro-Almagro F, Glasser MF, Duff EP, Fitzgibbon S, Westphal R, Carone D, Beckmann CF, Smith SM (2017) Hand classification of fMRI ICA noise components. *Neuroimage* 154:188–205 10.1016/j.neuroimage.2016.12.036

Gueorguieva R, Krystal JH (2004) Move over ANOVA: Progress in Analyzing Repeated-Measures Data and Its Reflection in Papers Published in the Archives of General Psychiatry. *Arch Gen Psychiatry* 61(3):310–317 10.1001/archpsyc.61.3.310

Guevara E, Berti R, Londono N, Xie N, Bellec P, Lesage R, Lodygensky G a. (2013) Imaging of an inflammatory injury in the newborn rat brain with Photoacoustic tomography. *PLoS One* 8(12):1–8 10.1371/journal.pone.0083045

Guillaume B (2015) Accurate Non-Iterative Modelling and Inference of Longitudinal Neuroimaging Data.

Guillaume B, Hua X, Thompson PM, Waldorp L, Nichols TE (2014) Fast and accurate modelling of longitudinal and repeated measures neuroimaging data. *Neuroimage* 94:287–302 10.1016/j.neuroimage.2014.03.029

Guillaume B, Nichols TE, Adni the (2015) Non-parametric Inference for Longitudinal and Repeated-Measures Neuroimaging Data with the Wild Bootstrap. *Organ Hum Brain Mapp*:2

Guillin O, Abi-Dargham A, Laruelle M (2007) Neurobiology of dopamine in schizophrenia. *Int Rev Neurobiol* 78:1–39 10.1016/S0074-7742(06)78001-1

Gumusoglu SB, Fine RS, Murray SJ, Bittle JL, Stevens HE (2017) The role of IL-6 in neurodevelopment after prenatal stress. *Brain Behav Immun* 65:274–283 10.1016/j.bbi.2017.05.015

Guo CC, Kurth F, Zhou J, Mayer EA, Eickhoff SB, Kramer JH, Seeley WW (2012) One-year test-retest reliability of intrinsic connectivity network fMRI in older adults. *Neuroimage* 61(4):1471–1483 10.1016/j.neuroimage.2012.03.027

Gusnard D a, Akbudak E, Shulman GL, Raichle ME (2001) Medial prefrontal cortex and self-referential mental activity: Relation to a default mode of brain function. Proceedings of the National Academy of. *Sciences (New York)* 98(15):4259–4264

Gusnard DA, Raichle ME (2001) Searching for a baseline: functional imaging and the resting human brain. *Nat Rev Neurosci* 2(10):685–694 10.1038/35094500

Gysin R, Kraftsik R, Sandell J, Bovet P, Chappuis C, Conus P, Deppen P, Preisig M, Ruiz V, Steullet P, Tosic M, Werge T, Cuénod M, Do KQ (2007) Impaired glutathione synthesis in schizophrenia: convergent genetic and functional evidence. *Proc Natl Acad Sci U S A* 104(42):16621–16626 10.1073/pnas.0706778104

Haddad FL, Lu L, Baines KJ, Schmid S (2020a) Sensory filtering disruption caused by poly I:C - Timing of exposure and other experimental considerations. *Brain, Behav Immun - Heal* 9(October) 10.1016/j.bbih.2020.100156

Haddad FL, Patel S V., Schmid S (2020b) Maternal Immune Activation by Poly I:C as a preclinical Model for Neurodevelopmental Disorders: A focus on Autism and Schizophrenia. *Neurosci Biobehav Rev* 113(February 2019):546–567 10.1016/j.neubiorev.2020.04.012

Hafner H (1998) Onset and course of the first schizophrenic episode. *Kaohsiung J Med Sci* 14(7):413–431

Häfner H, Heiden W an der, Behrens S (1998) Causes and consequences of the gender difference in age at onset of schizophrenia. *Schizophr …*(table 1)

Hall CS (1934) Emotional behavior in the rat. I. Defecation and urination as measures of individual differences in emotionality. *J Comp Psychol* 18(3):385–403 10.1037/h0071444

Hall J (2017) Schizophrenia - An anxiety disorder? *Br J Psychiatry* 211(5):262–263 10.1192/bjp.bp.116.195370

Han M, Zhang J chun, Huang XF, Hashimoto K (2017) Intake of 7,8-dihydroxyflavone from pregnancy to weaning prevents cognitive deficits in adult offspring after maternal immune activation. *Eur Arch Psychiatry Clin Neurosci* 267(5):479–483 10.1007/s00406-017-0802-1

Han M, Zhang JC, Yao W, Yang C, Ishima T, Ren Q, Ma M, Dong C, Huang XF, Hashimoto K (2016) Intake of 7,8-Dihydroxyflavone During Juvenile and Adolescent Stages Prevents Onset of Psychosis in Adult Offspring After Maternal Immune Activation. *Sci Rep* 6(November):1–10 10.1038/srep36087

Handley SL, Mithani S (1984) Effects of alpha-adrenoceptor agonists and antagonists in a maze-exploration model of 'fear'-motivated behaviour. *Naunyn Schmiedebergs Arch Pharmacol* 327(1):1–5 10.1007/BF00504983

Hänninen K, Katila H, Saarela M, Rontu R, Mattila KM, Fan M, Hurme M, Lehtimäki T (2008) Interleukin-1 beta gene polymorphism and its interactions with neuregulin-1 gene polymorphism are associated with schizophrenia. *Eur Arch Psychiatry Clin Neurosci* 258(1):10–15 10.1007/s00406-007-0756-9

Hantsoo L, Kornfield S, Anguera MC, Epperson CN (2019) Inflammation: A Proposed Intermediary Between Maternal Stress and Offspring Neuropsychiatric Risk. *Biol Psychiatry* 85(2):97–106 10.1016/j.biopsych.2018.08.018

Harrison PJ, Freemantle N, Geddes JR (2003) Meta-analysis of brain weight in schizophrenia. *Schizophr Res* 64(1):25–34 10.1016/S0920-9964(02)00502-9

Hart PH, Vitti GF, Burgess DR, Whitty GA, Piccoli DS, Hamilton JA (1989) Potential

antiinflammatory effects of interleukin 4: suppression of human monocyte tumor necrosis factor alpha, interleukin 1, and prostaglandin E2. *Proc Natl Acad Sci* 86(10):3803–3807 10.1073/pnas.86.10.3803

Hartvig N V, Jensen JL (2000) Spatial mixture modeling of fMRI data. *Hum Brain Mapp* 11(4):233–248

Harvey L, Boksa P (2012) A stereological comparison of GAD67 and reelin expression in the hippocampal stratum oriens of offspring from two mouse models of maternal inflammation during pregnancy. *Neuropharmacology* 62(4):1767–1776 10.1016/j.neuropharm.2011.11.022

Harvey L, Boksa P (2014a) Additive effects of maternal iron deficiency and prenatal immune activation on adult behaviors in rat offspring. *Brain Behav Immun* 40:27–37 10.1016/j.bbi.2014.06.005

Harvey L, Boksa P (2014b) Do prenatal immune activation and maternal iron deficiency interact to affect neurodevelopment and early behavior in rat offspring? *Brain Behav Immun* 35:144–154 10.1016/j.bbi.2013.09.009

Hava G, Vered L, Yael M, Mordechai H, Mahoud H (2006) Alterations in behavior in adult offspring mice following maternal inflammation during pregnancy. *Dev Psychobiol* 48(2):162–168 10.1002/dev.20116

Hayden MS, Ghosh S (2012) NF-κB, the first quarter-century: remarkable progress and outstanding questions. *Genes Dev* 26(3):203–234 10.1101/gad.183434.111

Heckers S, Curran T, Goff D, Rauch SL, Fischman AJ, Alpert NM, Schacter DL (2000) Abnormalities in the thalamus and prefrontal cortex during episodic object recognition in schizophrenia. *Biol Psychiatry* 48(7):651–657 10.1016/S0006-3223(00)00919-7

Hendrix A (2003) Magnets, Spins, and Resonances: An introduction to the basics of Magnetic Resonance. Erlangen: Siemens AG.

Hendrix A (2004) Magnets, Flows, and Artifacts: Basics, Techniques, and Applications of Magnetic Resonance Tomography. Erlangen: Siemens AG.

Heston LL (1966) Psychiatric disorders in foster home reared children of schizophrenic mothers. *Br J Psychiatry* 112(489):819–825

Heyser CJ, Chemero A (2012) Novel object exploration in mice: Not all objects are created equal. *Behav Processes* 89(3):232–238 10.1016/j.beproc.2011.12.004

Himberg J, Hyvärinen A, Esposito F (2004) Validating the independent components of neuroimaging time series via clustering and visualization. *Neuroimage* 22(3):1214–1222 10.1016/j.neuroimage.2004.03.027

Hoekstra R, Kiers HAL, Johnson A (2012) Are assumptions of well-known statistical techniques checked, and why (not)? *Front Psychol* 3(MAY):1–9 10.3389/fpsyg.2012.00137

Hoffman HS, Ison JR (1980) Reflex modification in the domain of startle: I. Some empirical findings and their implications for how the nervous system processes sensory input. *Psychol Rev* 87(2):175–189 10.1037/0033-295x.87.2.175

Höistad M, Segal D, Takahashi N, Sakurai T, Buxbaum JD, Hof PR (2009) Linking white and grey matter in schizophrenia: oligodendrocyte and neuron pathology in the prefrontal cortex. *Front Neuroanat* 3(July):9 10.3389/neuro.05.009.2009

Holmes AP, Josephs O, Büchel C, Friston KJ (1997) Statistical modelling of low-frequency confounds in fMRI. *Neuroimage* 5:S480

Holson RR, Pearce B (1992) Principles and pitfalls in the analysis of prenatal treatment effects in multiparous species. *Neurotoxicol Teratol* 14(3):221–228 10.1016/0892-0362(92)90020-B

Hoptman MJ, D'Angelo D, Catalano D, Mauro CJ, Shehzad ZE, Kelly AMC, Castellanos FX, Javitt DC, Milham MP (2010) Amygdalofrontal functional disconnectivity and aggression in schizophrenia. *Schizophr Bull* 36(5):1020–1028 10.1093/schbul/sbp012

Horan MA, Little RA, Rothwell NJ, Strijbos PJLM (1989) Comparison of the effects of several endotoxin preparations on body temperature and metabolic rate in the rat. *Can J Physiol Pharmacol* 67(9):1011–1014 10.1139/y89-159

Howes A, Gabryšová L, O'Garra A (2014) Role of IL-10 and the IL-10 Receptor in Immune Responses. *Ref Modul Biomed Sci* 1:1–11 10.1016/b978-0-12-801238-3.00014-3

Howes OD, Kapur S (2009) The dopamine hypothesis of schizophrenia: version III--the final common pathway. *Schizophr Bull* 35(3):549–562 10.1093/schbul/sbp006

Howland JG, Cazakoff BN, Zhang Y (2012) Altered object-in-place recognition memory, prepulse inhibition, and locomotor activity in the offspring of rats exposed to a viral mimetic during pregnancy. *Neuroscience* 201:184–198 10.1016/j.neuroscience.2011.11.011

Hsueh PT, Wang HH, Liu CL, Ni WF, Chen YL, Liu JK (2017) Expression of cerebral serotonin related to anxiety-like behaviors in C57BL/6 offspring induced by repeated subcutaneous prenatal exposure to low-dose lipopolysaccharide. *PLoS One* 12(6):1–26 10.1371/journal.pone.0179970

Hu ML, Zong XF, Mann JJ, Zheng JJ, Liao YH, Li ZC, He Y, Chen XG, Tang JS (2017) A Review of the Functional and Anatomical Default Mode Network in Schizophrenia. *Neurosci Bull* 33(1):73–84 10.1007/s12264-016-0090-1

Hu Y, Plonsky L (2021) Statistical assumptions in L2 research: A systematic review. *Second Lang Res* 37(1):171–184 10.1177/0267658319877433

Hubbard AE, Ahern J, Fleischer NL, Laan M Van Der, Lippman SA, Jewell N, Bruckner T, Satariano WA (2010) To GEE or not to GEE: Comparing population average and mixed models for estimating the associations between neighborhood risk factors and health. *Epidemiology* 21(4):467–474 10.1097/EDE.0b013e3181caeb90

Hubscher CH, Brooks DL, Johnson JR (2005) A quantitative method for assessing stages of the rat estrous cycle. *Biotech Histochem* 80(2):79–87 10.1080/10520290500138422

Huettel SA, Song AW, McCarthy G (2004) Functional magnetic resonance imaging, 1st ed. Sunderland, MA: Sinauer Associates.

Huettel SA, Song AW, McCarthy G (2009) Functional Magnetic Resonance Imaging, 2nd ed. Sunderland, MA: Sinauer Associates.

Hutchison RM, Mirsattari SM, Jones CK, Gati JS, Leung LS (2010) Functional networks in the anesthetized rat brain revealed by independent component analysis of resting-state FMRI. *J Neurophysiol* 103(6):3398–3406 10.1152/jn.00141.2010

Huynh H, Feldt LS (1970) Conditions Under Which Mean Square Ratios in Repeated Measurements Designs Have Exact F-Distributions. *J Am Stat Assoc* 65(332):1582 10.2307/2284340

Hyman SE, Cohen JD (2013) Disorders of Thought and Volition: Schizophrenia. In: Principles of Neural Science, 5th ed. (Kandel ER, Schwartz JH, Jessel TM, Siegelbaum SA, Hudspeth AJ, eds), pp 1389–1399. New York, NY: McGraw-Hill.

Hyvärinen A, Oja E (2000) Independent component analysis: Algorithms and applications. *Neural Networks* 13(4–5):411–430 10.1016/S0893-6080(00)00026-5

Imai K, Kotani T, Tsuda H, Nakano T, Ushida T, Iwase A, Nagai T, Toyokuni S, Suzumura A, Kikkawa F (2018) Administration of molecular hydrogen during pregnancy improves behavioral abnormalities of offspring in a maternal immune activation model. *Sci Rep* 8(1):1–12 10.1038/s41598-018-27626-4

Imhof JT, Coelho ZMI, Schmitt ML, Morato GS, Carobrez AP (1993) Influence of gender and age on performance of rats in the elevated plus maze apparatus. *Behav Brain Res* 56(2):177–180 10.1016/0166-4328(93)90036-P

Ison JR, Bowen GP, Pak J, Gutierrez E (1997) Changes in the strength of prepulse inhibition with variation in the startle baseline associated with individual differences and with old age in rats and mice. *Psychobiology* 25(3):266–274 10.3758/BF03331936

Ito HT, Smith SEP, Hsiao E, Patterson PH (2010) Maternal immune activation alters nonspatial information processing in the hippocampus of the adult offspring. *Brain Behav Immun* 24(6):930–941 10.1016/j.bbi.2010.03.004

Iwaki S, Matsuo a, Kast a (1989) Identification of newborn rats by tattooing. *Lab Anim* 23(4):361–364 10.1258/002367789780746024

Jakob H, Beckmann H (1986) Prenatal developmental disturbances in the limbic allocortex in schizophrenics. *J Neural Transm* 65(3–4):303–326 10.1007/BF01249090

Jakob H, Beckmann H (1994) Circumscribed malformation and nerve cell alterations in the entorhinal cortex of schizophrenics. Pathogenetic and clinical aspects. *J Neural Transm Gen Sect* 98(2):83–106

Jarskog LF, Miyamoto S, Lieberman JA (2007) Schizophrenia: new pathological insights and therapies. *Annu Rev Med* 58:49–61 10.1146/annurev.med.58.060904.084114

Javitt DC, Zukin SR (1991) Recent advances in the phencyclidine model of schizophrenia. *Am J Psychiatry* 148(10):1301–1308

Jenkinson M, Beckmann CF, Behrens TEJ, Woolrich MW, Smith SM (2012) FSL. *Neuroimage* 62(2):782–790 10.1016/j.neuroimage.2011.09.015

Jezzard P (2012) Correction of geometric distortion in fMRI data. *Neuroimage* 62(2):648–651 10.1016/j.neuroimage.2011.09.010

Johnston JM, Vaishnavi SN, Smyth MD, Zhang D, He BJ, Zempel JM, Shimony JS, Snyder AZ, Raichle ME (2008) Loss of resting interhemispheric functional connectivity after complete section of the corpus callosum. *J Neurosci* 28(25):6453–6458 10.1523/JNEUROSCI.0573-08.2008

Jonckers E, van Audekerke J, de Visscher G, van der Linden A, Verhoye M (2011) Functional connectivity fMRI of the rodent brain: Comparison of functional connectivity networks in rat and mouse. *PLoS One* 6(4) 10.1371/journal.pone.0018876

Jones C, Watson D, Fone K (2011) Animal models of schizophrenia. *Br J Pharmacol* 164(4):1162–1194 10.1111/j.1476-5381.2011.01386.x

Jones EG (1997) Cortical development and thalamic pathology in schizophrenia. *Schizophr Bull* 23(3):483–501

Jung BA, Weigel M (2013) Spin echo magnetic resonance imaging. *J Magn Reson Imaging* 37(4):805–817 10.1002/jmri.24068

Kalthoff D (2011) Functional connectivity of the rat brain in magnetic resonance imaging.

Kalthoff D, Po C, Wiedermann D, Hoehn M (2013) Reliability and spatial specificity of rat brain sensorimotor functional connectivity networks are superior under sedation compared with general anesthesia. *NMR Biomed* 26(6):638–650 10.1002/nbm.2908

Kalthoff D, Seehafer JU, Po C, Wiedermann D, Hoehn M (2011) Functional connectivity in the rat at 11.7T: Impact of physiological noise in resting state fMRI. *Neuroimage* 54(4):2828–2839 10.1016/j.neuroimage.2010.10.053

Kalus P, Senitz D, Beckmann H (1999) Disturbances of corticogenesis in schizophrenia: morphological findings provide new evidence for the maldevelopmental hypothesis. *Neuropsychobiology* 40(1):1–13 26591

Kapur S, Remington G (1996) Serotonin-dopamine interaction and its relevance to schizophrenia. *Am J Psychiatry* 153(4):466–476

Karbasforoushan H, Woodward ND (2012) Resting-state networks in schizophrenia. *Curr Top Med Chem* 12(21):2404–2414 10.2174/1568026611212210011

Katerji M, Filippova M, Duerksen-Hughes P (2019) Approaches and Methods to Measure Oxidative Stress in Clinical Samples: Research Applications in the Cancer Field. *Oxid Med Cell Longev* 2019:1–29 10.1155/2019/1279250

Keil J, Romero YR, Balz J, Henjes M, Senkowski D (2016) Positive and negative

symptoms in schizophrenia relate to distinct oscillatory signatures of sensory gating. *Front Hum Neurosci* 10(MAR2016):1–11 10.3389/fnhum.2016.00104

Kelly RE, Alexopoulos GS, Wang Z, Gunning FM, Murphy CF, Morimoto SS, Kanellopoulos D, Jia Z, Lim KO, Hoptman MJ (2010) Visual inspection of independent components: Defining a procedure for artifact removal from fMRI data. *J Neurosci Methods* 189(2):233–245 10.1016/j.jneumeth.2010.03.028

Kentner AC, Bilbo SD, Brown AS, Hsiao EY, McAllister AK, Meyer U, Pearce BD, Pletnikov M V., Yolken RH, Bauman MD (2019) Maternal immune activation: reporting guidelines to improve the rigor, reproducibility, and transparency of the model. *Neuropsychopharmacology* 44(2):245–258 10.1038/s41386-018-0185-7

Kentner AC, Khoury A, Lima Queiroz E, MacRae M (2016) Environmental enrichment rescues the effects of early life inflammation on markers of synaptic transmission and plasticity. *Brain Behav Immun* 57:151–160 10.1016/j.bbi.2016.03.013

Keselman HJ, Huberty CJ, Cribbie RA, Lowman LL, Lix LM, Donahue B, Petoskey MD, Olejnik S, Kowalchuk RK, Keselman JC, Levin JR (1998) Statistical practices of educational researchers: An analysis of their ANOVA, MANOVA, and ANCOVA analyses. *Rev Educ Res* 68(3):350–386 10.3102/00346543068003350

Keshavan MS, Tandon R, Boutros NN, Nasrallah HA (2008) Schizophrenia, "just the facts": What we know in 2008. Part 3: Neurobiology. *Schizophr Res* 106(2–3):89–107 10.1016/j.schres.2008.07.020

Kety SS, Rosenthal D, Wender PH, Schulsinger F (1968) The types and prevalence of mental illness in the biological and adoptive families of adopted schizophrenics. *J Psychiatr Res* 6:345–362 10.1016/0022-3956(68)90026-5

Khan D, Fernando P, Cicvaric A, Berger A, Pollak A, Monje FJ, Pollak DD (2014) Long-term effects of maternal immune activation on depression-like behavior in the mouse. *Transl Psychiatry* 4(2):e363–e363 10.1038/tp.2013.132

Khanmohammadi S, Rezaei N (2021) Role of Toll-like receptors in the pathogenesis of COVID-19. *J Med Virol* 93(5):2735–2739 10.1002/jmv.26826

Khashan AS, Abel KM, McNamee R, Pedersen MG, Webb RT, Baker PN, Kenny LC, Mortensen PB (2008) Higher risk of offspring schizophrenia following antenatal maternal exposure to severe adverse life events. *Arch Gen Psychiatry* 65(2):146–152 10.1001/archgenpsychiatry.2007.20

Kheir-Eldin a a, Motawi TK, Gad MZ, Abd-ElGawad HM (2001) Protective effect of vitamin E, beta-carotene and N-acetylcysteine from the brain oxidative stress induced in rats by lipopolysaccharide. *Int J Biochem Cell Biol* 33(5):475–482 Doi: 10.1016/s1357-2725(01)00032-2

Kim JS, Kornhuber HH, Schmid-Burgk W, Holzmüller B (1980) Low cerebrospinal fluid glutamate in schizophrenic patients and a new hypothesis on schizophrenia. *Neurosci Lett* 20(3):379–382 10.1016/0304-3940(80)90178-0

Kim S, Kim H, Yim YS, Ha S, Atarashi K, Tan TG, Longman RS, Honda K, Littman DR, Choi GB, Huh JR (2017) Maternal gut bacteria promote neurodevelopmental abnormalities in mouse offspring. *Nature* 549(7673):528–532

10.1038/nature23910

Kirsten TB, Taricano M, Flório JC, Palermo-Neto J, Bernardi MM (2010a) Prenatal lipopolysaccharide reduces motor activity after an immune challenge in adult male offspring. *Behav Brain Res* 211(1):77–82 10.1016/j.bbr.2010.03.009

Kirsten TB, Taricano M, Maiorka PC, Palermo-Neto J, Bernardi MM (2010b) Prenatal lipopolysaccharide reduces social behavior in male offspring. *Neuroimmunomodulation* 17(4):240–251 10.1159/000290040

Koch M (1999) The neurobiology of startle. *Prog Neurobiol* 59(2):107–128 10.1016/S0301-0082(98)00098-7

Koch M (2006) Animal Models of Schizophrenia. In: Animal Models of Neuropsychiatric Diseases (Koch M, ed), pp 337–402. London, UK: Imperial College Press. 10.1142/9781860948022_0008

Koch M, Lingenhöhl K, Pilz PKD (1992) Loss of the acoustic startle response following neurotoxic lesions of the caudal pontine reticular formation: Possible role of giant neurons. *Neuroscience* 49(3):617–625 10.1016/0306-4522(92)90231-P

Koike T, Kan S, Misaki M, Miyauchi S (2011) Connectivity pattern changes in default-mode network with deep non-REM and REM sleep. *Neurosci Res* 69(4):322–330 10.1016/j.neures.2010.12.018

Kolb B (1990) Association cortex in the rat. In: The Cerebral Cortex of the Rat (Kolb B, ed), pp 433–435. Cambridge, MA: MIT Press.

Kowash HM, Potter HG, Edye ME, Prinssen EP, Bandinelli S, Neill JC, Hager R, Glazier JD (2019) Poly(I:C) source, molecular weight and endotoxin contamination affect dam and prenatal outcomes, implications for models of maternal immune activation. *Brain Behav Immun* 82(July):160–166 10.1016/j.bbi.2019.08.006

Kreitz S, Zambon A, Ronovsky M, Budinsky L, Helbich TH, Sideromenos S, Ivan C, Konerth L, Wank I, Berger A, Pollak A, Hess A, Pollak DD (2020) Maternal immune activation during pregnancy impacts on brain structure and function in the adult offspring. *Brain Behav Immun* 83(September 2019):56–67 10.1016/j.bbi.2019.09.011

Kulak A, Cuenod M, Do KQ (2012) Behavioral phenotyping of glutathione-deficient mice: Relevance to schizophrenia and bipolar disorder. *Behav Brain Res* 226(2):563–570 10.1016/j.bbr.2011.10.020

Kuznetsova A, Brockhoff PB, Christensen RHB (2017) lmerTest Package: Tests in Linear Mixed Effects Models . *J Stat Softw* 82(13) 10.18637/jss.v082.i13

La-Vu M, Tobias BC, Schuette PJ, Adhikari A (2020) To Approach or Avoid: An Introductory Overview of the Study of Anxiety Using Rodent Assays. *Front Behav Neurosci* 14(August):1–7 10.3389/fnbeh.2020.00145

Laird NM, Ware JH (1982) Random-Effects Models for Longitudinal Data. *Biometrics* 38(4):963 10.2307/2529876

Lancelot S, Roche R, Slimen A, Bouillot C, Levigoureux E, Langlois J-B, Zimmer L, Costes N (2014) A Multi-Atlas Based Method for Automated Anatomical Rat Brain MRI Segmentation and Extraction of PET Activity. *PLoS One* 9(10):e109113 10.1371/journal.pone.0109113

Lanté F, Meunier J, Guiramand J, Maurice T, Cavalier M, de Jesus Ferreira MC, Aimar R, Cohen-Solal C, Vignes M, Barbanel G (2007) Neurodevelopmental damage after prenatal infection: Role of oxidative stress in the fetal brain. *Free Radic Biol Med* 42(8):1231–1245 10.1016/j.freeradbiomed.2007.01.027

Larson-Prior LJ, Power JD, Vincent JL, Nolan TS, Coalson RS, Zempel J, Snyder AZ, Schlaggar BL, Raichle ME, Petersen SE (2011) Modulation of the brain's functional network architecture in the transition from wake to sleep. *Prog Brain Res* 193:277–294 10.1016/B978-0-444-53839-0.00018-1

Larson-Prior LJ, Zempel JM, Nolan TS, Prior FW, Snyder AZ, Raichle ME (2009) Cortical network functional connectivity in the descent to sleep. *Proc Natl Acad Sci U S A* 106(11):4489–4494 10.1073/pnas.0900924106

Larson SJ, Dunn AJ (2001) Behavioral Effects of Cytokines. *Brain Behav Immun* 15(4):371–387 10.1006/brbi.2001.0643

Lavoie S, Murray MM, Deppen P, Knyazeva MG, Berk M, Boulat O, Bovet P, Bush AI, Conus P, Copolov D, Fornari E, Meuli R, Solida A, Vianin P, Cuénod M, Buclin T, Do KQ (2008) Glutathione precursor, N-acetyl-cysteine, improves mismatch negativity in schizophrenia patients. *Neuropsychopharmacology* 33(9):2187–2199 10.1038/sj.npp.1301624

Lazar NA, Eddy WF, Genovese CR, Welling J (2001) Statistical issues in fMRI for brain imaging. *Int Stat Rev* 69(1):105–127 10.1111/j.1751-5823.2001.tb00482.x

Lazic SE (2008) Why we should use simpler models if the data allow this: Relevance for ANOVA designs in experimental biology. *BMC Physiol* 8(1):1–7 10.1186/1472-6793-8-16

Lazic SE (2010) The problem of pseudoreplication in neuroscientific studies: Is it affecting your analysis? *BMC Neurosci* 11:1–17 10.1186/1471-2202-11-5

Lazic SE, Essioux L (2013) Improving basic and translational science by accounting for litter-to-litter variation in animal models. *BMC Neurosci* 14 10.1186/1471-2202-14-37

Ledeboer A, Binnekade R, Brevé JJP, Bol JGJM, Tilders FJH, Van Dam A-M (2002) Site-specific modulation of LPS-induced fever and interleukin-1β expression in rats by interleukin-10. *Am J Physiol Integr Comp Physiol* 282(6):R1762–R1772 10.1152/ajpregu.00766.2001

Lee AJ, Kandiah N, Karimi K, Clark DA, Ashkar AA (2013) Interleukin-15 is required for maximal lipopolysaccharide-induced abortion. *J Leukoc Biol* 93(6):905–912 10.1189/jlb.0912442

Lee KY, Perretta SG, Zar H, Mueller RA, Boysen PG (2001) Increase in rat plasma antioxidant activity after E. coli lipopolysaccharide administration. *Yonsei Med J* 42(1):114–119 10.3349/ymj.2001.42.1.114

Lee Y (2015) What repeated measures analysis of variances really tells us. *Korean J Anesthesiol* 68(4):340–345 10.4097/kjae.2015.68.4.340

Lehmann R (2013) 3σ-Rule for Outlier Detection from the Viewpoint of Geodetic Adjustment. *J Surv Eng* 139(4):157–165 10.1061/(ASCE)SU.1943-5428.0000112

Leive L, Morrison DC (1972) [23] Isolation of lipopolysaccharides from bacteria. In: Methods in Enzymology, pp 254–262 10.1016/0076-6879(72)28025-9

Lenth RV (2020) emmeans: Estimated Marginal Means, aka Least-Squares Means. https://cran.r-project.org/package=emmeans

Leon LR (2004) Hypothermia in systemic inflammation: Role of cytokines. *Front Biosci* 9(12):1877–1888

Leon LR, Kozak W, Rudolph K, Kluger MJ (1999) An antipyretic role for interleukin-10 in LPS fever in mice. *Am J Physiol Integr Comp Physiol* 276(1):R81–R89 10.1152/ajpregu.1999.276.1.R81

Lewandowski KE (2007) Relationship of catechol-O-methyltransferase to schizophrenia and its correlates: evidence for associations and complex interactions. *Harv Rev Psychiatry* 15(5):233–244 10.1080/10673220701650409

Lewis DA, Hashimoto T, Volk DW (2005) Cortical inhibitory neurons and schizophrenia. *Nat Rev Neurosci* 6(4):312–324 10.1038/nrn1648

Lewis DA, Levitt P (2002) Schizophrenia as a Disorder of Neurodevelopment. *Annu Rev Neurosci* 25(1):409–432 10.1146/annurev.neuro.25.112701.142754

Leza JC, Bueno BG, Bioque M, Arango C, Parellada M, Do K, O'Donnell P, Bernardo M (2015) Inflammation in schizophrenia: a question of balance. *Neurosci Biobehav Rev* 55:612–626 10.1016/j.neubiorev.2015.05.014

Li D, He L (2007) Association study between the dystrobrevin binding protein 1 gene (DTNBP1) and schizophrenia: a meta-analysis. *Schizophr Res* 96(1–3):112–118 10.1016/j.schres.2007.05.017

Li Q, Cheung C, Wei R, Hui ES, Feldon J, Meyer U, Chung S, Chua SE, Sham PC, Wu EX, McAlonan GM (2009) Prenatal immune challenge is an environmental risk factor for brain and behavior change relevant to schizophrenia: Evidence from MRI in a mouse model. *PLoS One* 4(7) 10.1371/journal.pone.0006354

Li WY, Chang YC, Lee LJH, Lee LJ (2014) Prenatal infection affects the neuronal architecture and cognitive function in adult mice. *Dev Neurosci* 36(5):359–370 10.1159/000362383

Li X, Tian X, Lv L, Hei G, Huang X, Fan X, Zhang J, Zhang J, Pang L, Song X (2018) Microglia activation in the offspring of prenatal Poly I: C exposed rats: A PET imaging and immunohistochemistry study. *Gen Psychiatry* 31(1):29–36 10.1136/gpsych-2018-000006

Liang Z, King J, Zhang N (2011) Uncovering intrinsic connectional architecture of functional networks in awake rat brain. *J Neurosci* 31(10):3776–3783 10.1523/JNEUROSCI.4557-10.2011

Liang Z, Li T, King J, Zhang N (2013) Mapping thalamocortical networks in rat brain using resting-state functional connectivity. *Neuroimage* 83:237–244 10.1016/j.neuroimage.2013.06.029

Lichtermann D, Karbe E, Maier W (2000) The genetic epidemiology of schizophrenia and of schizophrenia spectrum disorders. *Eur Arch Psychiatry Clin Neurosci* 250(6):304–310

Lieberman MD, Cunningham WA (2009) Type I and Type II error concerns in fMRI research: Re-balancing the scale. *Soc Cogn Affect Neurosci* 4(4):423–428 10.1093/scan/nsp052

Lin YL, Lin SY, Wang S (2012) Prenatal lipopolysaccharide exposure increases anxiety-like behaviors and enhances stress-induced corticosterone responses in adult rats. *Brain Behav Immun* 26(3):459–468 10.1016/j.bbi.2011.12.003

Lindquist MA (2008) The Statistical Analysis of fMRI Data. *Stat Sci* 23(4):439–464 10.1214/09-STS282

Lindquist MA, Mejia A (2015) Zen and the Art of Multiple Comparisons. *Psychosom Med* 77(2):114–125 10.1097/PSY.0000000000000148

Ling Z, Chang QA, Tong CW, Leurgans SE, Lipton JW, Carvey PM (2004a) Rotenone potentiates dopamine neuron loss in animals exposed to lipopolysaccharide prenatally. *Exp Neurol* 190(2):373–383 10.1016/j.expneurol.2004.08.006

Ling Z, Zhu Y, Tong C wai, Snyder JA, Lipton JW, Carvey PM (2006) Progressive dopamine neuron loss following supra-nigral lipopolysaccharide (LPS) infusion into rats exposed to LPS prenatally. *Exp Neurol* 199(2):499–512 10.1016/j.expneurol.2006.01.010

Ling Z, Zhu Y, Tong CW, Snyder JA, Lipton JW, Carvey PM (2009) Prenatal lipopolysaccharide does not accelerate progressive dopamine neuron loss in the rat as a result of normal aging. *Exp Neurol* 216(2):312–320 10.1016/j.expneurol.2008.12.004

Ling ZD, Chang Q, Lipton JW, Tong CW, Landers TM, Carvey PM (2004b) Combined toxicity of prenatal bacterial endotoxin exposure and postnatal 6-hydroxydopamine in the adult rat midbrain. *Neuroscience* 124(3):619–628 10.1016/j.neuroscience.2003.12.017

Ling ZD, Gayle DA, Ma SY, Lipton JW, Tong CW, Hong JS, Carvey PM (2002) In utero bacterial endotoxin exposure causes loss of tyrosine hydroxylase neurons in the postnatal rat midbrain. *Mov Disord* 17(1):116–124 10.1002/mds.10078

Lins BR, Hurtubise JL, Roebuck AJ, Marks WN, Zabder NK, Scott GA, Greba Q, Dawicki W, Zhang X, Rudulier CD, Gordon JR, Howland JG (2018) Prospective analysis of the effects of maternal immune activation on rat cytokines during pregnancy and behavior of the male offspring relevant to Schizophrenia. *eNeuro* 5(4) 10.1523/ENEURO.0249-18.2018

Lipina T V., Zai C, Hlousek D, Roder JC, Wong AHC (2013) Maternal immune activation during gestation interacts with Disc1 point mutation to exacerbate schizophrenia-related behaviors in mice. *J Neurosci* 33(18):7654–7666

10.1523/JNEUROSCI.0091-13.2013

Lister RG (1987) The use of a plus-maze to measure anxiety in the mouse. *Psychopharmacology (Berl)* 92(t 987):180–185

Liu E, Lewis K, Al-Saffar H, Krall CM, Singh a., Kulchitsky V a., Corrigan JJ, Simons CT, Petersen SR, Musteata FM, Bakshi CS, Romanovsky a. a., Sellati TJ, Steiner a. a. (2012) Naturally occurring hypothermia is more advantageous than fever in severe forms of lipopolysaccharide- and Escherichia coli-induced systemic inflammation. *AJP Regul Integr Comp Physiol* 302(12):R1372–R1383 10.1152/ajpregu.00023.2012

Liu H, Fan G, Xu K, Wang F (2011a) Changes in cerebellar functional connectivity and anatomical connectivity in schizophrenia: a combined resting-state functional MRI and diffusion tensor imaging study. *J Magn Reson Imaging* 34(6):1430–1438 10.1002/jmri.22784

Liu X, Lee JG, Yee SK, Bresee CJ, Poland RE, Pechnick RN (2004) Endotoxin exposure in utero increases ethanol consumption in adult male offspring. *Neuroreport* 15(1):203–206 10.1097/01.wnr.0000103454.27946.88

Liu X, Zhu XH, Zhang Y, Chen W (2011b) Neural origin of spontaneous hemodynamic fluctuations in rats under burst-suppression anesthesia condition. *Cereb Cortex* 21(2):374–384 10.1093/cercor/bhq105

Liu Y-Z, Wang Y-X, Jiang C-L (2017) Inflammation: The Common Pathway of Stress-Related Diseases. *Front Hum Neurosci* 11 10.3389/fnhum.2017.00316

Liu Y, Liang M, Zhou Y, He Y, Hao Y, Song M, Yu C, Liu H, Liu Z, Jiang T (2008) Disrupted small-world networks in schizophrenia. *Brain* 131(Pt 4):945–961 10.1093/brain/awn018

Logothetis NK (2002) The neural basis of the blood-oxygen-level-dependent functional magnetic resonance imaging signal. *Philos Trans R Soc B Biol Sci* 357(1424):1003–1037 10.1098/rstb.2002.1114

Logothetis NK, Pauls J, Augath M, Trinath T, Oeltermann A (2001) Neurophysiological investigation of the basis of the fMRI signal. *Nature* 412(6843):150–157 10.1038/35084005

Lowe GC, Luheshi GN, Williams S (2008) Maternal infection and fever during late gestation are associated with altered synaptic transmission in the hippocampus of juvenile offspring rats. *Am J Physiol Regul Integr Comp Physiol* 295(5):R1563-71 10.1152/ajpregu.90350.2008

Lowe MJ, Dzemidzic M, Lurito JT, Mathews VP, Phillips MD (2000) Correlations in low-frequency BOLD fluctuations reflect cortico-cortical connections. *Neuroimage* 12(5):582–587 10.1006/nimg.2000.0654

Lowe MJ, Mock BJ, Sorenson J a (1998) Functional connectivity in single and multislice echoplanar imaging using resting-state fluctuations. *Neuroimage* 7(2):119–132 10.1006/nimg.1997.0315

Lowe MJ, Sorenson JA (1997) Spatially filtering functional magnetic resonance imaging data. *Magn Reson Med* 37(5):723–729 10.1002/mrm.1910370514

Lu H, Zou Q, Gu H, Raichle ME, Stein E a., Yang Y (2012) Rat brains also have a default mode network. *Proc Natl Acad Sci* 109(10):3979–3984 10.1073/pnas.1200506109

Luan W, Hammond LA, Vuillermot S, Meyer U, Eyles DW (2018) Maternal Vitamin D Prevents Abnormal Dopaminergic Development and Function in a Mouse Model of Prenatal Immune Activation. *Sci Rep* 8(1):1–12 10.1038/s41598-018-28090-w

Luchicchi A, Lecca S, Melis M, De Felice M, Cadeddu F, Frau R, Muntoni AL, Fadda P, Devoto P, Pistis M (2016) Maternal immune activation disrupts dopamine system in the offspring. *Int J Neuropsychopharmacol* 19(7):1–10 10.1093/ijnp/pyw007

Luheshi G, Rothwell N (1996) Cytokines and Fever. *Int Arch Allergy Immunol* 109(4):301–307 10.1159/000237256

Lyon L, Saksida LM, Bussey TJ (2012) Spontaneous object recognition and its relevance to schizophrenia: A review of findings from pharmacological, genetic, lesion and developmental rodent models. *Psychopharmacology (Berl)* 220(4):647–672 10.1007/s00213-011-2536-5

Ma Z, Ma Y, Zhang N (2018) Development of brain-wide connectivity architecture in awake rats. *Neuroimage* 176(3):380–389 10.1016/j.neuroimage.2018.05.009

Maayan R, Ram E, Biton D, Cohen H, Baharav E, Strous RD, Weizman A (2012) The influence of DHEA pretreatment on prepulse inhibition and the HPA-axis stress response in rat offspring exposed prenatally to polyriboinosinic-polyribocytidylic-acid (PIC). *Neurosci Lett* 521(1):6–10 10.1016/j.neulet.2012.05.034

Magnuson ME, Thompson GJ, Pan WJ, Keilholz SD (2014) Time-dependent effects of isoflurane and dexmedetomidine on functional connectivity, spectral characteristics, and spatial distribution of spontaneous BOLD fluctuations. *NMR Biomed* 27(3):291–303 10.1002/nbm.3062

Mahadik SP, Mukherjee S (1996) Free radical pathology and antioxidant defense in schizophrenia: A review. *Schizophr Res* 19(1):1–17 10.1016/0920-9964(95)00049-6

Majidi-Zolbanin J, Doosti MH, Kosari-Nasab M, Salari AA (2015) Prenatal maternal immune activation increases anxiety- and depressive-like behaviors in offspring with experimental autoimmune encephalomyelitis. *Neuroscience* 294:69–81 10.1016/j.neuroscience.2015.03.016

Mäki P, Veijola J, Jones PB, Murray GK, Koponen H, Tienari P, Miettunen J, Tanskanen P, Wahlberg K-E, Koskinen J, Lauronen E, Isohanni M (2005) Predictors of schizophrenia--a review. *Br Med Bull* 73–74:1–15 10.1093/bmb/ldh046

Makinodan M, Tatsumi K, Manabe T, Yamauchi T, Makinodan E, Matsuyoshi H, Shimoda S, Noriyama Y, Kishinioto T, Wanaka A (2008) Maternal immune activation in mice delays myelination and axonal development in the hippocampus of the offspring. *J Neurosci Res* 86(10):2190–2200 10.1002/jnr.21673

Mannell M V, Franco AR, Calhoun VD, Cañive JM, Thoma RJ, Mayer AR (2010)

Resting state and task-induced deactivation: A methodological comparison in patients with schizophrenia and healthy controls. *Hum Brain Mapp* 31(3):424–437 10.1002/hbm.20876

Marcondes FK, Bianchi F., Tanno A. (2002) Determination of The Estrous Cycle Phases of Rats: Some Helpful Considerations. *Brazilian J Biol* 62(4):609–614 10.1590/S1519-69842002000400008

Martin SM, Malkinson TJ, Veale WL, Pittman QJ (1995) Fever in pregnant, parturient, and lactating rats. *Am Physiol Soc* 268:R919–R923

Massimini M, Ferrarelli F, Huber R, Esser SK, Singh H, Tononi G (2005) Breakdown of Cortical Effective Connectivity During Sleep. *Science (80-)* 309(5744):2228–2232 10.1126/science.1117256

Matsuura A, Ishima T, Fujita Y, Iwayama Y, Hasegawa S, Kawahara-Miki R, Maekawa M, Toyoshima M, Ushida Y, Suganuma H, Kida S, Yoshikawa T, Iyo M, Hashimoto K (2018) Dietary glucoraphanin prevents the onset of psychosis in the adult offspring after maternal immune activation. *Sci Rep* 8(1):1–12 10.1038/s41598-018-20538-3

Matsuzawa D, Obata T, Shirayama Y, Nonaka H, Konazawa Y, Yoshitome E, Takanashi J, Matsuda T, Shimizu E, Ikehira H, Iyo M, Hashimoto K (2008) Negative correlation between brain glutathione level and negative symptoms in schizophrenia: A 3T 1H-MRS study. *PLoS One* 3(4) 10.1371/journal.pone.0001944

Mattei D, Djodari-Irani A, Hadar R, Pelz A, de Cossío LF, Goetz T, Matyash M, Kettenmann H, Winter C, Wolf SA (2014) Minocycline rescues decrease in neurogenesis, increase in microglia cytokines and deficits in sensorimotor gating in an animal model of schizophrenia. *Brain Behav Immun* 38:175–184 10.1016/j.bbi.2014.01.019

McClellan JM, Susser E, King M-C (2007) Schizophrenia: a common disease caused by multiple rare alleles. *Br J Psychiatry* 190:194–199 10.1192/bjp.bp.106.025585

Mcfarquhar M (2018) Modelling group-level repeated measures of neuroimaging data using the univariate general linear model. :1–24 10.17605/OSF.IO/A5469

McFarquhar M, McKie S, Emsley R, Suckling J, Elliott R, Williams S (2016) Multivariate and repeated measures (MRM): A new toolbox for dependent and multimodal group-level neuroimaging data. *Neuroimage* 132:373–389 10.1016/j.neuroimage.2016.02.053

McGrath J, Saha S, Chant D, Welham J (2008) Schizophrenia: A Concise Overview of Incidence, Prevalence, and Mortality. *Epidemiol Rev* 30(1):67–76 10.1093/epirev/mxn001

McGrath JJ, Welham JL (1999) Season of birth and schizophrenia: a systematic review and meta-analysis of data from the Southern Hemisphere. *Schizophr Res* 35(3):237–242

McKeown MJ, Makeig S, Brown GG, Jung T, Kindermann SS, Bell AJ, Sejnowski TJ (1998) Analysis of fMRI data by blind separation into independant spatial components. *Hum Brain Mapp* 6(June 1997):160–188

Mednick SA, Machon RA, Huttunen MO, Bonett D (1988) Adult schizophrenia following prenatal exposure to an influenza epidemic. *Arch Gen Psychiatry* 45(2):189–192

Medzhitov R, Preston-Hurlburt P, Janeway CA (1997) A human homologue of the Drosophila toll protein signals activation of adaptive immunity. *Nature* 388(6640):394–397 10.1038/41131

Meehan C, Harms L, Frost JD, Barreto R, Todd J, Schall U, Shannon Weickert C, Zavitsanou K, Michie PT, Hodgson DM (2017) Effects of immune activation during early or late gestation on schizophrenia-related behaviour in adult rat offspring. *Brain Behav Immun* 63:8–20 10.1016/j.bbi.2016.07.144

Meyer D, Dimitriadou E, Hornik K, Weingessel A, Leisch F (2020) e1071: Misc Functions of the Department of Statistics, Probability Theory Group (Formerly: E1071), TU Wien.

Meyer U, Feldon J (2010) Epidemiology-driven neurodevelopmental animal models of schizophrenia. *Prog Neurobiol* 90(3):285–326 10.1016/j.pneurobio.2009.10.018

Meyer U, Feldon J, Fatemi SH (2009a) In-vivo rodent models for the experimental investigation of prenatal immune activation effects in neurodevelopmental brain disorders. *Neurosci Biobehav Rev* 33(7):1061–1079 10.1016/j.neubiorev.2009.05.001

Meyer U, Feldon J, Schedlowski M, Yee BK (2005) Towards an immuno-precipitated neurodevelopmental animal model of schizophrenia. *Neurosci Biobehav Rev* 29(6):913–947 10.1016/j.neubiorev.2004.10.012

Meyer U, Feldon J, Schedlowski M, Yee BK (2006a) Immunological stress at the maternal-foetal interface: A link between neurodevelopment and adult psychopathology. *Brain Behav Immun* 20(4):378–388 10.1016/j.bbi.2005.11.003

Meyer U, Feldon J, Yee BK (2009b) A review of the fetal brain cytokine imbalance hypothesis of schizophrenia. *Schizophr Bull* 35(5):959–972 10.1093/schbul/sbn022

Meyer U, Murray PJ, Urwyler A, Yee BK, Schedlowski M, Feldon J (2008a) Adult behavioral and pharmacological dysfunctions following disruption of the fetal brain balance between pro-inflammatory and IL-10-mediated anti-inflammatory signaling. *Mol Psychiatry* 13(2):208–221 10.1038/sj.mp.4002042

Meyer U, Nyffeler M, Engler A, Urwyler A, Schedlowski M, Knuesel I, Yee BK, Feldon J (2006b) The time of prenatal immune challenge determines the specificity of inflammation-mediated brain and behavioral pathology. *J Neurosci* 26(18):4752–4762 10.1523/JNEUROSCI.0099-06.2006

Meyer U, Nyffeler M, Yee BK, Knuesel I, Feldon J (2008b) Adult brain and behavioral pathological markers of prenatal immune challenge during early/middle and late fetal development in mice. *Brain Behav Immun* 22(4):469–486 10.1016/j.bbi.2007.09.012

Meyer U, Spoerri E, Yee BK, Schwarz MJ, Feldon J (2010) Evaluating early preventive antipsychotic and antidepressant drug treatment in an infection-based

neurodevelopmental mouse model of schizophrenia. *Schizophr Bull* 36(3):607–623 10.1093/schbul/sbn131

Meyer U, Yee BK, Feldon J (2007) The neurodevelopmental impact of prenatal infections at different times of pregnancy: the earlier the worse? *Neuroscientist* 13(3):241–256 10.1177/1073858406296401

Mian MF, Ahmed AN, Rad M, Babaian A, Bowdish D, Ashkar AA (2013) Length of dsRNA (poly I:C) drives distinct innate immune responses, depending on the cell type. *J Leukoc Biol* 94(5):1025–1036 10.1189/jlb.0312125

Miao W, Zhao Y, Huang Y, Chen D, Luo C, Su W, Gao Y (2020) IL-13 Ameliorates Neuroinflammation and Promotes Functional Recovery after Traumatic Brain Injury. *J Immunol* 204(6):1486–1498 10.4049/jimmunol.1900909

Mills B (2018) Resting State Functional Connectivity MRI in the Rodent Brain: Applications to Human Disease.

Mingoia G, Langbein K, Dietzek M, Wagner G, Smesny S, Scherpiet S, Maitra R, Reichenbach JR, Schlösser RGM, Gaser C, Sauer H, Nenadic I (2013) Frequency domains of resting state default mode network activity in schizophrenia. *Psychiatry Res Neuroimaging* 214(1):80–82 10.1016/j.pscychresns.2013.05.013

Mingoia G, Wagner G, Langbein K, Maitra R, Smesny S, Dietzek M, Burmeister HP, Reichenbach JR, Schlösser RGM, Gaser C, Sauer H, Nenadic I (2012) Default mode network activity in schizophrenia studied at resting state using probabilistic ICA. *Schizophr Res* 138(2–3):143–149 10.1016/j.schres.2012.01.036

Missault S, Anckaerts C, Ahmadoun S, Blockx I, Barbier M, Bielen K, Shah D, Kumar-Singh S, De Vos WH, Van der Linden A, Dedeurwaerdere S, Verhoye M (2019) Hypersynchronicity in the default mode-like network in a neurodevelopmental animal model with relevance for schizophrenia. *Behav Brain Res* 364(December 2018):303–316 10.1016/j.bbr.2019.02.040

Missault S, Van den Eynde K, Vanden Berghe W, Fransen E, Weeren A, Timmermans JP, Kumar-Singh S, Dedeurwaerdere S (2014) The risk for behavioural deficits is determined by the maternal immune response to prenatal immune challenge in a neurodevelopmental model. *Brain Behav Immun* 42:138–146 10.1016/j.bbi.2014.06.013

Missig G, Robbins JO, Mokler EL, McCullough KM, Bilbo SD, McDougle CJ, Carlezon WA (2019) Sex-dependent neurobiological features of prenatal immune activation via TLR7. *Mol Psychiatry* 10.1038/s41380-018-0346-4

Mlinarić A, Horvat M, Šupak Smolčić V (2017) Dealing with the positive publication bias: Why you should really publish your negative results. *Biochem Medica* 27(3):030201 10.11613/BM.2017.030201

Moghaddam B (2003) Bringing order to the glutamate chaos in schizophrenia. *Neuron* 40(5):881–884

Mohammad F, Ho J, Woo JH, Lim CL, Poon DJJ, Lamba B, Claridge-Chang A (2016) Concordance and incongruence in preclinical anxiety models: Systematic review and meta-analyses. *Neurosci Biobehav Rev* 68:504–529

10.1016/j.neubiorev.2016.04.011

Monji A, Kato T, Kanba S (2009) Cytokines and schizophrenia: Microglia hypothesis of schizophrenia. *Psychiatry Clin Neurosci* 63(3):257–265 10.1111/j.1440-1819.2009.01945.x

Monji A, Kato TA, Mizoguchi Y, Horikawa H, Seki Y, Kasai M, Yamauchi Y, Yamada S, Kanba S (2013) Neuroinflammation in schizophrenia especially focused on the role of microglia. *Prog Neuro-Psychopharmacology Biol Psychiatry* 42:115–121 10.1016/j.pnpbp.2011.12.002

Montgomery KC (1955) The relation between fear induced by novel stimulation and exploratory drive. *J Comp Physiol Psychol* 48(4):254–260 10.1037/h0043788

Moore THM, Zammit S, Lingford-Hughes A, Barnes TRE, Jones PB, Burke M, Lewis G (2007) Cannabis use and risk of psychotic or affective mental health outcomes: a systematic review. *Lancet (London, England)* 370(9584):319–328 10.1016/S0140-6736(07)61162-3

Morais LH, Felice D, Golubeva A V., Moloney G, Dinan TG, Cryan JF (2018) Strain differences in the susceptibility to the gut-brain axis and neurobehavioural alterations induced by maternal immune activation in mice. *Behav Pharmacol* 29:181–198 10.1097/FBP.0000000000000374

Mouihate A, Kalakh S, Almutairi R, Alashqar A (2019) Prenatal Inflammation Dampens Neurogenesis and Enhances Serotonin Transporter Expression in the Hippocampus of Adult Female Rats. *Med Princ Pract* 28(4):352–360 10.1159/000499658

Mueller FS, Richetto J, Hayes LN, Zambon A, Pollak DD, Sawa A, Meyer U, Weber-Stadlbauer U (2019) Influence of poly(I:C) variability on thermoregulation, immune responses and pregnancy outcomes in mouse models of maternal immune activation. *Brain Behav Immun* 80(January):406–418 10.1016/j.bbi.2019.04.019

Munafo MR, Attwood AS, Flint J (2007) Neuregulin 1 Genotype and Schizophrenia. *Schizophr Bull* 34(1):9–12 10.1093/schbul/sbm129

Murray KN, Edye ME, Manca M, Vernon AC, Oladipo JM, Fasolino V, Harte MK, Mason V, Grayson B, McHugh PC, Knuesel I, Prinssen EP, Hager R, Neill JC (2019) Evolution of a maternal immune activation (mIA) model in rats: Early developmental effects. *Brain Behav Immun* 75:48–59 10.1016/j.bbi.2018.09.005

Nair A (2019) Publication bias - Importance of studies with negative results! *Indian J Anaesth* 63(6):505 10.4103/ija.IJA_142_19

Nakamura JP, Schroeder A, Hudson M, Jones N, Gillespie B, Du X, Notaras M, Swaminathan V, Reay WR, Atkins JR, Green MJ, Carr VJ, Cairns MJ, Sundram S, Hill RA (2019) The maternal immune activation model uncovers a role for the Arx gene in GABAergic dysfunction in schizophrenia. *Brain Behav Immun* 81(May):161–171 10.1016/j.bbi.2019.06.009

Narang K, Enninga EAL, Gunaratne MDSK, Ibirogba ER, Trad ATA, Elrefaei A, Theiler RN, Ruano R, Szymanski LM, Chakraborty R, Garovic VD (2020) SARS-CoV-2 Infection and COVID-19 During Pregnancy: A Multidisciplinary Review.

Mayo Clin Proc 95(8):1750–1765 10.1016/j.mayocp.2020.05.011

Nava F, Calapai G, Facciolá G, Cuzzocrea S, Marciano MC, De Sarro A, Caputi AP (1997) Effects of interleukin-10 on water intake, locomotory activity, and rectal temperature in rat treated with endotoxin. *Int J Immunopharmacol* 19(1):31–38 10.1016/S0192-0561(97)00006-4

Nguyen MP, Tran LVH, Namgoong H, Kim YH (2019) Applications of different solvents and conditions for differential extraction of lipopolysaccharide in Gram-negative bacteria. *J Microbiol* 57(8):644–654 10.1007/s12275-019-9116-5

Nichols T, Holmes A (2003) Nonparametric Permutation Tests for Functional Neuroimaging. *Hum Brain Funct Second Ed* 15(1):887–910 10.1016/B978-012264841-0/50048-2

Nicodemus KK, Kolachana BS, Vakkalanka R, Straub RE, Giegling I, Egan MF, Rujescu D, Weinberger DR (2007) Evidence for statistical epistasis between catechol-O-methyltransferase (COMT) and polymorphisms in RGS4, G72 (DAOA), GRM3, and DISC1: influence on risk of schizophrenia. *Hum Genet* 120(6):889–906 10.1007/s00439-006-0257-3

Nie B, Chen K, Zhao S, Liu J, Gu X, Yao Q, Hui J, Zhang Z, Teng G, Zhao C, Shan B (2013) A rat brain MRI template with digital stereotaxic atlas of fine anatomical delineations in paxinos space and its automated application in voxel-wise analysis. *Hum Brain Mapp* 34(6):1306–1318 10.1002/hbm.21511

Nielsen EE, Nørskov AK, Lange T, Thabane L, Wetterslev J, Beyersmann J, De Unã-Álvarez J, Torri V, Billot L, Putter H, Winkel P, Gluud C, Jakobsen JC (2019) Assessing assumptions for statistical analyses in randomised clinical trials. *BMJ Evidence-Based Med* 24(5):185–189 10.1136/bmjebm-2019-111174

Noirhomme Q, Soddu A, Lehembre R, Vanhaudenhuyse A, Boveroux P, Boly M, Laureys S (2010) Brain connectivity in pathological and pharmacological coma. *Front Syst Neurosci* 4:160 10.3389/fnsys.2010.00160

O'Leary C, Desbonnet L, Clarke N, Petit E, Tighe O, Lai D, Harvey R, Waddington JL, O'Tuathaigh C (2014) Phenotypic effects of maternal immune activation and early postnatal milieu in mice mutant for the schizophrenia risk gene neuregulin-1. *Neuroscience* 277:294–305 10.1016/j.neuroscience.2014.06.028

Ogawa S, Lee T, Kay A, Tank D (1990) Brain magnetic resonance imaging with contrast dependent on blood oxygenation. *Proc …* 87(24):9868–9872 10.1073/pnas.87.24.9868

Olabi B, Ellison-Wright I, McIntosh a M, Wood SJ, Bullmore E, Lawrie SM (2011) Are there progressive brain changes in schizophrenia? A meta-analysis of structural magnetic resonance imaging studies. *Biol Psychiatry* 70(1):88–96 10.1016/j.biopsych.2011.01.032

Olney JW, Farber NB (1995) Glutamate receptor dysfunction and schizophrenia. *Arch Gen Psychiatry* 52(12):998–1007

Ongür D, Price JL (2000) The organization of networks within the orbital and medial prefrontal cortex of rats, monkeys and humans. *Cereb Cortex* 10(3):206–219

Opal S (2007) The host response to endotoxin, antilipopolysaccharide strategies, and the management of severe sepsis. *Int J Med Microbiol* 297(5):365–377 10.1016/j.ijmm.2007.03.006

Osborne AL, Solowij N, Babic I, Huang XF, Weston-Green K (2017) Improved Social Interaction, Recognition and Working Memory with Cannabidiol Treatment in a Prenatal Infection (poly I:C) Rat Model. *Neuropsychopharmacology* 42(7):1447–1457 10.1038/npp.2017.40

Osborne JW (2008) Sweating the small stuff in educational psychology: How effect size and power reporting failed to change from 1969 to 1999, and what that means for the future of changing practices. *Educ Psychol* 28(2):151–160 10.1080/01443410701491718

Oskvig DB, Elkahloun AG, Johnson KR, Phillips TM, Herkenham M (2012) Maternal immune activation by LPS selectively alters specific gene expression profiles of interneuron migration and oxidative stress in the fetus without triggering a fetal immune response. *Brain Behav Immun* 26(4):623–634 10.1016/j.bbi.2012.01.015

Ozawa K, Hashimoto K, Kishimoto T, Shimizu E, Ishikura H, Iyo M (2006) Immune activation during pregnancy in mice leads to dopaminergic hyperfunction and cognitive impairment in the offspring: A neurodevelopmental animal model of schizophrenia. *Biol Psychiatry* 59(6):546–554 10.1016/j.biopsych.2005.07.031

Paintlia MK, Paintlia AS, Contreras MA, Singh I, Singh AK (2008) Lipopolysaccharide-induced peroxisomal dysfunction exacerbates cerebral white matter injury: Attenuation by N-acetyl cysteine. *Exp Neurol* 210(2):560–576 10.1016/j.expneurol.2007.12.011

Pan W-J, Billings JCW, Grooms JK, Shakil S, Keilholz SD (2015) Considerations for resting state functional MRI and functional connectivity studies in rodents. *Front Neurosci* 9(August):1–17 10.3389/fnins.2015.00269

Patriat R, Molloy EK, Meier TB, Kirk GR, Nair VA, Meyerand ME, Prabhakaran V, Birn RM (2013) The effect of resting condition on resting-state fMRI reliability and consistency: a comparison between resting with eyes open, closed, and fixated. *Neuroimage* 78:463–473 10.1016/j.neuroimage.2013.04.013

Patterson PH (2009) Immune involvement in schizophrenia and autism: Etiology, pathology and animal models. *Behav Brain Res* 204(2):313–321 10.1016/j.bbr.2008.12.016

Pawela CP, Biswal BB, Cho YR, Kao DS, Li R, Jones SR, Schulte ML, Matloub HS, Hudetz AG, Hyde JS (2008) Resting-state functional connectivity of the rat brain. *Magn Reson Med* 59(5):1021–1029 10.1002/mrm.21524

Paxinos G, Watson C (2006) The Rat Brain in Stereotaxic Coordinates, 6th ed. London, UK: Academic Press, Elsevier Inc.

Pelletier M, Achim AM, Montoya A, Lal S, Lepage M (2005) Cognitive and clinical moderators of recognition memory in schizophrenia: A meta-analysis. *Schizophr Res* 74(2–3):233–252 10.1016/j.schres.2004.08.017

Pellow S, Chopin P, File SE, Briley M (1985) Validation of open : closed arm entries

in an elevated plus-maze as a measure of anxiety in the rat. *J Neurosci Methods* 14(3):149–167 10.1016/0165-0270(85)90031-7

Penner JD, Brown AS (2007) Prenatal infectious and nutritional factors and risk of adult schizophrenia. *Expert Rev Neurother* 7(7):797–805 10.1586/14737175.7.7.797

Penny WD, Trujillo-Barreto NJ, Friston KJ (2005) Bayesian fMRI time series analysis with spatial priors. *Neuroimage* 24(2):350–362 10.1016/j.neuroimage.2004.08.034

Perry TL (1982) Normal cerebrospinal fluid and brain glutamate levels in schizophrenia do not support the hypothesis of glutamatergic neuronal dysfunction. *Neurosci Lett* 28(1):81–85

Pilz PK, Schnitzler HU, Menne D (1987) Acoustic startle threshold of the albino rat (Rattus norvegicus). *J Comp Psychol* 101(1):67–72

Piontkewitz Y, Arad M, Weiner I (2011) Risperidone administered during asymptomatic period of adolescence prevents the emergence of brain structural pathology and behavioral abnormalities in an animal model of schizophrenia. *Schizophr Bull* 37(6):1257–1269 10.1093/schbul/sbq040

Poggi SH, Park J, Toso L, Abebe D, Roberson R, Woodard JE, Spong CY (2005) No phenotype associated with established lipopolysaccharide model for cerebral palsy. *Am J Obstet Gynecol* 192(3):727–733 10.1016/j.ajog.2004.12.053

Poline JB, Brett M (2012) The general linear model and fMRI: Does love last forever? *Neuroimage* 62(2):871–880 10.1016/j.neuroimage.2012.01.133

Pomarol-Clotet E, Salvador R, Sarró S, Gomar J, Vila F, Martínez A, Guerrero A, Ortiz-Gil J, Sans-Sansa B, Capdevila A, Cebamanos JM, McKenna PJ (2008) Failure to deactivate in the prefrontal cortex in schizophrenia: dysfunction of the default mode network? *Psychol Med* 38(8):1185–1193 10.1017/S0033291708003565

Powell CM, Miyakawa T (2006) Schizophrenia-relevant behavioral testing in rodent models: a uniquely human disorder? *Biol Psychiatry* 59(12):1198–1207 10.1016/j.biopsych.2006.05.008

Powell SB, Zhou X, Geyer MA (2009) Prepulse inhibition and genetic mouse models of schizophrenia. *Behav Brain Res* 204(2):282–294 10.1016/j.bbr.2009.04.021

Price JL (2007) Definition of the orbital cortex in relation to specific connections with limbic and visceral structures and other cortical regions. *Ann N Y Acad Sci* 1121:54–71 10.1196/annals.1401.008

Prut L, Belzung C (2003) The open field as a paradigm to measure the effects of drugs on anxiety-like behaviors: A review. *Eur J Pharmacol* 463(1–3):3–33 10.1016/S0014-2999(03)01272-X

Quené H, Van Den Bergh H (2004) On multi-level modeling of data from repeated measures designs: A tutorial. *Speech Commun* 43(1–2):103–121 10.1016/j.specom.2004.02.004

R Core Team (2021) R: A language and environment for statistical computing. *R Found Stat Comput Vienna, Austria*

Raichle ME (2010) Two views of brain function. *Trends Cogn Sci* 14(4):180–190 10.1016/j.tics.2010.01.008

Raichle ME (2011) The restless brain. *Brain Connect* 1(1):3–12 10.1089/brain.2011.0019

Raichle ME (2015) The Brain ' s Default Mode Network. *Annu Rev Neurosci* 38:433–447 10.1146/annurev-neuro-071013-014030

Raichle ME, MacLeod a M, Snyder a Z, Powers WJ, Gusnard D a, Shulman GL (2001) A default mode of brain function. *Proc Natl Acad Sci U S A* 98(2):676–682 10.1073/pnas.98.2.676

Raichle ME, Mintun MA (2006) Brain Work and Brain Imaging. *Annu Rev Neurosci* 29(1):449–476 10.1146/annurev.neuro.29.051605.112819

Rajagopal L, Massey B, Huang M, Oyamada Y, Meltzer H (2014) The Novel Object Recognition Test in Rodents in Relation to Cognitive Impairment in Schizophrenia. *Curr Pharm Des* 20(31):5104–5114 10.2174/1381612819666131216114240

Ramos A (2008) Animal models of anxiety: do I need multiple tests? *Trends Pharmacol Sci* 29(10):493–498 10.1016/j.tips.2008.07.005

Ray A, Redhead K, Selkirk S, Poole S (1991) Variability in LPS composition, antigenicity and reactogenicity of phase variants of Bordetella pertussis. *FEMS Microbiol Lett* 79(2–3):211–217

Razavi M, Grabowski TJ, Vispoel WP, Monahan P, Mehta S, Eaton B, Bolinger L (2003) Model Assessment and Model Building in fMRI. *Hum Brain Mapp* 20(4):227–238 10.1002/hbm.10141

Reijmers LG, Peeters BW (1994) Effects of acoustic prepulses on the startle reflex in rats: a parametric analysis. *Brain Res* 661(1–2):174–180 10.1016/0006-8993(94)91204-1

Reis-Silva TM, Cohn DWH, Sandini TM, Udo MSB, Teodorov E, Bernardi MM (2016) Prenatal lipopolysaccharide exposure affects sexual dimorphism in different germlines of mice with a depressive phenotype. *Life Sci* 149:129–137 10.1016/j.lfs.2016.02.068

Reisinger S, Khan D, Kong E, Berger A, Pollak A, Pollak DD (2015) The Poly(I:C)-induced maternal immune activation model in preclinical neuropsychiatric drug discovery. *Pharmacol Ther* 149:213–226 10.1016/j.pharmthera.2015.01.001

Ribeiro BMM, do Carmo MRS, Freire RS, Rocha NFM, Borella VCM, de Menezes AT, Monte AS, Gomes PXL, de Sousa FCF, Vale ML, de Lucena DF, Gama CS, Mac??do D (2013) Evidences for a progressive microglial activation and increase in iNOS expression in rats submitted to a neurodevelopmental model of schizophrenia: Reversal by clozapine. *Schizophr Res* 151(1–3):12–19 10.1016/j.schres.2013.10.040

Richetto J, Massart R, Weber-Stadlbauer U, Szyf M, Riva MA, Meyer U (2017) Genome-wide DNA Methylation Changes in a Mouse Model of Infection-Mediated Neurodevelopmental Disorders. *Biol Psychiatry* 81(3):265–276 10.1016/j.biopsych.2016.08.010

Richtand NM, Ahlbrand R, Horn P, Stanford K, Bronson SL, McNamara RK (2011) Effects of risperidone and paliperidone pre-treatment on locomotor response following prenatal immune activation. *J Psychiatr Res* 45(9):1194–1201 10.1016/j.jpsychires.2011.02.007

Risch N (1990) Linkage strategies for genetically complex traits. I. Multilocus models. *Am J Hum Genet* 46(2):222–228

Roche A (2011) A four-dimensional registration algorithm with application to joint correction of motion and slice timing in fMRI. *IEEE Trans Med Imaging* 30(8):1546–1554 10.1109/TMI.2011.2131152

Roderick RC, Kentner AC (2019) Building a framework to optimize animal models of maternal immune activation: Like your ongoing home improvements, it's a work in progress. *Brain Behav Immun* 75(October):6–7 10.1016/j.bbi.2018.10.011

Rodgers RJ, Dalvi A (1997) Anxiety, defence and the elevated plus-maze. *Neurosci Biobehav Rev* 21(6):801–810 10.1016/S0149-7634(96)00058-9

Rohleder N (2014) Stimulation of Systemic Low-Grade Inflammation by Psychosocial Stress. *Psychosom Med* 76(3):181–189 10.1097/PSY.0000000000000049

Rolls ET, Baylis LL (1994) Gustatory, olfactory, and visual convergence within the primate orbitofrontal cortex. *J Neurosci* 14(9):5437–5452

Romanovsky, Andrej A (2005) Fever and hypothermia in systemic inflammation: recent discoveries and revisions. *Front Biosci* 10(1–3):2193 10.2741/1690

Romanovsky AA, Kulchitsky VA, Akulich N V., Koulchitsky S V., Simons CT, Sessler DI, Gourine VN (1996) First and second phases of biphasic fever: Two sequential stages of the sickness syndrome? *Am J Physiol - Regul Integr Comp Physiol* 271(1 40-1) 10.1152/ajpregu.1996.271.1.r244

Romanovsky AA, Kulchitsky VA, Simons CT, Sugimoto N (1998) Methodology of fever research: why are polyphasic fevers often thought to be biphasic? *Am J Physiol Integr Comp Physiol* 275(1):R332–R338 10.1152/ajpregu.1998.275.1.R332

Rombouts SARB, Barkhof F, Goekoop R, Stam CJ, Scheltens P (2005) Altered resting state networks in mild cognitive impairment and mild Alzheimer's disease: an fMRI study. *Hum Brain Mapp* 26(4):231–239 10.1002/hbm.20160

Rombouts SARB, Damoiseaux JS, Goekoop R, Barkhof F, Scheltens P, Smith SM, Beckmann CF (2009) Model-free group analysis shows altered BOLD FMRI networks in dementia. *Hum Brain Mapp* 30(1):256–266 10.1002/hbm.20505

Romero E, Ali C, Molina-Holgado E, Castellano B, Guaza C, Borrell J (2007) Neurobehavioral and immunological consequences of prenatal immune activation in rats. Influence of antipsychotics. *Neuropsychopharmacology* 32(8):1791–1804 10.1038/sj.npp.1301292

Romero E, Guaza C, Castellano B, Borrell J (2010) Ontogeny of sensorimotor gating and immune impairment induced by prenatal immune challenge in rats: implications for the etiopathology of schizophrenia. *Mol Psychiatry* 15(4):372–383 10.1038/mp.2008.44

Ronovsky M, Berger S, Zambon A, Reisinger SN, Horvath O, Pollak A, Lindtner C, Berger A, Pollak DD (2017) Maternal immune activation transgenerationally modulates maternal care and offspring depression-like behavior. *Brain Behav Immun* 63:127–136 10.1016/j.bbi.2016.10.016

Rorden C, Karnath H-O, Bonilha L (2007) Improving lesion-symptom mapping. *J Cogn Neurosci* 19(7):1081–1088 10.1162/jocn.2007.19.7.1081

Rosazza C, Minati L (2011) Resting-state brain networks: literature review and clinical applications. *Neurol Sci* 32(5):773–785 10.1007/s10072-011-0636-y

Rosen M, Kahan E, Derazne E (1987) The influence of the first-mating age of rats on the number of pups born, their weights and their mortality. *Lab Anim* 21(4):348–352 10.1258/002367787781363282

Rotarska-Jagiela A, van de Ven V, Oertel-Knöchel V, Uhlhaas PJ, Vogeley K, Linden DEJ (2010) Resting-state functional network correlates of psychotic symptoms in schizophrenia. *Schizophr Res* 117(1):21–30 10.1016/j.schres.2010.01.001

Rousset CI, Chalon S, Cantagrel S, Bodard S, Andres C, Gressens P, Saliba E (2006) Maternal exposure to LPS induces hypomyelination in the internal capsule and programmed cell death in the deep gray matter in newborn rats. *Pediatr Res* 59(3):428–433 10.1203/01.pdr.0000199905.08848.55

Rudolph MD, Graham AM, Feczko E, Miranda-Dominguez O, Rasmussen JM, Nardos R, Entringer S, Wadhwa PD, Buss C, Fair DA (2018) Maternal IL-6 during pregnancy can be estimated from newborn brain connectivity and predicts future working memory in offspring. *Nat Neurosci* 21(5):765–772 10.1038/s41593-018-0128-y

Salgado-Pineda P, Caclin A, Baeza I, Junqué C, Bernardo M, Blin O, Fonlupt P (2007) Schizophrenia and frontal cortex: Where does it fail? *Schizophr Res* 91(1–3):73–81 10.1016/j.schres.2006.12.028

Salgado-Pineda P, Fakra E, Delaveau P, McKenna PJ, Pomarol-Clotet E, Blin O (2011) Correlated structural and functional brain abnormalities in the default mode network in schizophrenia patients. *Schizophr Res* 125(2–3):101–109 10.1016/j.schres.2010.10.027

Salvador R, Sarró S, Gomar JJ, Ortiz-Gil J, Vila F, Capdevila A, Bullmore E, McKenna PJ, Pomarol-Clotet E (2010) Overall brain connectivity maps show cortico-subcortical abnormalities in schizophrenia. *Hum Brain Mapp* 31(12):2003–2014 10.1002/hbm.20993

Salvador R, Suckling J, Coleman MR, Pickard JD, Menon D, Bullmore E (2005a) Neurophysiological architecture of functional magnetic resonance images of human brain. *Cereb Cortex* 15(9):1332–1342 10.1093/cercor/bhi016

Salvador R, Suckling J, Schwarzbauer C, Bullmore E (2005b) Undirected graphs of frequency-dependent functional connectivity in whole brain networks. *Philos*

Trans R Soc B Biol Sci 360(1457):937–946 10.1098/rstb.2005.1645

Salvemini D, Cuzzocrea S (2002) Oxidative stress in septic shock and disseminated intravascular coagulation. *Free Radic Biol Med* 33(9):1173–1185

Sämann PG, Wehrle R, Hoehn D, Spoormaker VI, Peters H, Tully C, Holsboer F, Czisch M (2011) Development of the brain's default mode network from wakefulness to slow wave sleep. *Cereb Cortex* 21(9):2082–2093 10.1093/cercor/bhq295

Sangha S, Greba Q, Robinson PD, Ballendine SA, Howland JG (2014) Heightened fear in response to a safety cue and extinguished fear cue in a rat model of maternal immune activation. *Front Behav Neurosci* 8(MAY):1–11 10.3389/fnbeh.2014.00168

Santos-Toscano R, Borcel É, Ucha M, Orihuel J, Capellán R, Roura-Martínez D, Ambrosio E, Higuera-Matas A (2016) Unaltered cocaine self-administration in the prenatal LPS rat model of schizophrenia. *Prog Neuro-Psychopharmacology Biol Psychiatry* 69:38–48 10.1016/j.pnpbp.2016.04.008

Sasaki Y, Ohsawa K, Kanazawa H, Kohsaka S, Imai Y (2001) Iba1 is an actin-cross-linking protein in macrophages/microglia. *Biochem Biophys Res Commun* 286(2):292–297 10.1006/bbrc.2001.5388

Schaafsma W, Basterra LB, Jacobs S, Brouwer N, Meerlo P, Schaafsma A, Boddeke EWGM, Eggen BJL (2017) Maternal inflammation induces immune activation of fetal microglia and leads to disrupted microglia immune responses, behavior, and learning performance in adulthood. *Neurobiol Dis* 106:291–300 10.1016/j.nbd.2017.07.017

Schank JC, Koehnle TJ (2009) Pseudoreplication is a pseudoproblem. *J Comp Psychol* 123(4):421–433 10.1037/a0013579

Schindelin J, Arganda-Carreras I, Frise E, Kaynig V, Longair M, Pietzsch T, Preibisch S, Rueden C, Saalfeld S, Schmid B, Tinevez J-Y, White DJ, Hartenstein V, Eliceiri K, Tomancak P, Cardona A (2012) Fiji: an open-source platform for biological-image analysis. *Nat Methods* 9(7):676–682 10.1038/nmeth.2019

Schneider P, Ho YJ, Spanagel R, Pawlak CR (2011) A novel elevated plus-maze procedure to avoid the one-trial tolerance problem. *Front Behav Neurosci* 5(JULY):1–8 10.3389/fnbeh.2011.00043

Schöpf V, Windischberger C, Kasess CH, Lanzenberger R, Moser E (2010) Group ICA of resting-state data: A comparison. *Magn Reson Mater Physics, Biol Med* 23(5–6):317–325 10.1007/s10334-010-0212-0

Schrader AJ, Taylor RM, Lowery-Gionta EG, Moore NLT (2018) Repeated elevated plus maze trials as a measure for tracking within-subjects behavioral performance in rats (Rattus norvegicus). *PLoS One* 13(11):1–15 10.1371/journal.pone.0207804

Schroter S, Black N, Evans S, Godlee F, Osorio L, Smith R (2008) What errors do peer reviewers detect, and does training improve their ability to detect them? *J R Soc Med* 101(10):507–514 10.1258/jrsm.2008.080062

Schultz SH, North SW, Shields CG (2007) Schizophrenia: A review. *Am Fam Physician* 75(12):1821–1829

Schwab SG, Plummer C, Albus M, Borrmann-Hassenbach M, Lerer B, Trixler M, Maier W, Wildenauer DB (2008) DNA sequence variants in the metabotropic glutamate receptor 3 and risk to schizophrenia: an association study. *Psychiatr Genet* 18(1):25–30 10.1097/YPG.0b013e3282ef48d9

Schwartzer JJ, Careaga M, Onore CE, Rushakoff JA, Berman RF, Ashwood P (2013) Maternal immune activation and strain specific interactions in the development of autism-like behaviors in mice. *Transl Psychiatry* 3(November 2012) 10.1038/tp.2013.16

Schwarz AJ, Danckaert A, Reese T, Gozzi A, Paxinos G, Watson C, Merlo-Pich E V., Bifone A (2006) A stereotaxic MRI template set for the rat brain with tissue class distribution maps and co-registered anatomical atlas: Application to pharmacological MRI. *Neuroimage* 32(2):538–550 [Accessed October 21, 2015]10.1016/j.neuroimage.2006.04.214

Scouten A, Papademetris X, Constable RT (2006) Spatial resolution, signal-to-noise ratio, and smoothing in multi-subject functional MRI studies. *Neuroimage* 30(3):787–793 [Accessed October 22, 2015]10.1016/j.neuroimage.2005.10.022

Scremin OU (2015) Cerebral Vascular System. In: The Rat Nervous System, 4th ed. (Paxinos G, ed), pp 985–1011. London, UK: Elsevier. 10.1016/B978-0-12-374245-2.00031-0

Seeley WW, Menon V, Schatzberg AF, Keller J, Glover GH, Kenna H, Reiss AL, Greicius MD (2007) Dissociable Intrinsic Connectivity Networks for Salience Processing and Executive Control. *J Neurosci* 27(9):2349–2356 10.1523/JNEUROSCI.5587-06.2007

Seibenhener ML, Wooten MC (2015) Use of the open field maze to measure locomotor and anxiety-like behavior in mice. *J Vis Exp*(96):1–6 10.3791/52434

Seibert TM, Majid DSA, Aron AR, Corey-Bloom J, Brewer JB (2012) Stability of resting fMRI interregional correlations analyzed in subject-native space: a one-year longitudinal study in healthy adults and premanifest Huntington's disease. *Neuroimage* 59(3):2452–2463 10.1016/j.neuroimage.2011.08.105

Semple DM, McIntosh AM, Lawrie SM (2005) Cannabis as a risk factor for psychosis: systematic review. *J Psychopharmacol* 19(2):187–194

Sheffield JM, Barch DM (2016) Cognition and resting-state functional connectivity in schizophrenia. *Neurosci Biobehav Rev* 61:108–120 10.1016/j.neubiorev.2015.12.007

Sheldon AB (1969) Preference for familiar versus novel stimuli as a function of the familiarity of the environment. *J Comp Physiol Psychol* 67(4):516–521 10.1037/h0027305

Shen H, Wang L, Liu Y, Hu D (2010) Discriminative analysis of resting-state functional connectivity patterns of schizophrenia using low dimensional embedding of fMRI. *Neuroimage* 49(4):3110–3121 10.1016/j.neuroimage.2009.11.011

Shenton ME, Dickey CC, Frumin M, McCarley RW (2001) A review of MRI findings in schizophrenia. *Schizophr Res* 49:1–52 10.1016/S0920-9964(01)00163-3

Shepherd JK, Grewal SS, Fletcher A, Bill DJ, Dourish CT (1994) Behavioural and pharmacological characterisation of the elevated "zero-maze" as an animal model of anxiety. *Psychopharmacology (Berl)* 116(1):56–64 10.1007/BF02244871

Sheu JR, Hsieh CY, Jayakumar T, Tseng MF, Lee HN, Huang SW, Manubolu M, Yang CH (2019) A critical period for the development of schizophrenia-like pathology by aberrant postnatal neurogenesis. *Front Neurosci* 13(JUN):1–18 10.3389/fnins.2019.00635

Shi L, Fatemi SH, Sidwell RW, Patterson PH (2003) Maternal influenza infection causes marked behavioral and pharmacological changes in the offspring. *J Neurosci* 23(1):297–302

Shi L, Smith SEP, Malkova N, Tse D, Su Y, Patterson PH (2009) Activation of the maternal immune system alters cerebellar development in the offspring. *Brain Behav Immun* 23(1):116–123 10.1016/j.bbi.2008.07.012

Shmuel A, Leopold DA (2008) Neuronal correlates of spontaneous fluctuations in fMRI signals in monkey visual cortex: Implications for functional connectivity at rest. *Hum Brain Mapp* 29(7):751–761 10.1002/hbm.20580

Shmuel A, Yacoub E, Pfeuffer J, Van de Moortele PF, Adriany G, Hu X, Ugurbil K (2002) Sustained negative BOLD, blood flow and oxygen consumption response and its coupling to the positive response in the human brain. *Neuron* 36(6):1195–1210

Shmueli K, van Gelderen P, de Zwart JA, Horovitz SG, Fukunaga M, Jansma JM, Duyn JH (2007) Low-frequency fluctuations in the cardiac rate as a source of variance in the resting-state fMRI BOLD signal. *Neuroimage* 38(2):306–320 10.1016/j.neuroimage.2007.07.037

Shulman GL, Fiez JA, Corbetta M, Buckner RL, Miezin FM, Raichle ME, Petersen SE (1997) Common Blood Flow Changes across Visual Tasks: II. Decreases in Cerebral Cortex. *J Cogn Neurosci* 9(5):648–663 10.1162/jocn.1997.9.5.648

Sierakowiak A, Monnot C, Aski SN, Uppman M, Li T-Q, Damberg P, Brené S (2015) Default Mode Network, Motor Network, Dorsal and Ventral Basal Ganglia Networks in the Rat Brain: Comparison to Human Networks Using Resting State-fMRI. *PLoS One* 10(3):e0120345 10.1371/journal.pone.0120345

Silverstein SM, Spaulding WD, Menditto AA (2006) Schizophrenia. Cambridge, MA: Hogrefe & Huber Publishers.

Simões LR, Sangiogo G, Tashiro MH, Generoso JS, Faller CJ, Dominguini D, Mastella GA, Scaini G, Giridharan VV, Michels M, Florentino D, Petronilho F, Réus GZ, Dal-Pizzol F, Zugno AI, Barichello T (2018) Maternal immune activation induced by lipopolysaccharide triggers immune response in pregnant mother and fetus, and induces behavioral impairment in adult rats. *J Psychiatr Res* 100:71–83 10.1016/j.jpsychires.2018.02.007

Simpson DSA, Oliver PL (2020) ROS Generation in Microglia: Understanding

Oxidative Stress and Inflammation in Neurodegenerative Disease. *Antioxidants* 9(8):743 10.3390/antiox9080743

Simpson JR, Drevets WC, Snyder AZ, Gusnard DA, Raichle ME (2001a) Emotion-induced changes in human medial prefrontal cortex: II. During anticipatory anxiety. *Proc Natl Acad Sci* 98(2):688–693 10.1073/pnas.98.2.688

Simpson JR, Snyder AZ, Gusnard DA, Raichle ME (2001b) Emotion-induced changes in human medial prefrontal cortex: I. During cognitive task performance. *Proc Natl Acad Sci* 98(2):683–687 10.1073/pnas.98.2.683

Skudlarski P, Jagannathan K, Anderson K, Stevens MC, Calhoun VD, Skudlarska B a., Pearlson G (2010) Brain Connectivity Is Not Only Lower but Different in Schizophrenia: A Combined Anatomical and Functional Approach. *Biol Psychiatry* 68(1):61–69 10.1016/j.biopsych.2010.03.035

Skudlarski P, Schretlen DJ, Thaker GK, Stevens MC, Keshavan MS, Sweeney J a., Tamminga C a., Clementz B a., O'Neil K, Pearlson GD (2013) Diffusion tensor imaging white matter endophenotypes in patients with schizophrenia or psychotic bipolar disorder and their relatives. *Am J Psychiatry* 170(8):886–898 10.1176/appi.ajp.2013.12111448

Skup M (2010) Longitudinal fMRI analysis: A review of methods. *Stat Interface* 3(2):235–252 10.1016/j.bbi.2008.05.010

Sladky R, Friston KJ, Tröstl J, Cunnington R, Moser E, Windischberger C (2011) Slice-timing effects and their correction in functional MRI. *Neuroimage* 58(2):588–594 10.1016/j.neuroimage.2011.06.078

Smith PF (2017) A Guerilla Guide to Common Problems in "Neurostatistics": Essential Statistical Topics in Neuroscience. *J Undergrad Neurosci Educ* 16(1):R1–R12

Smith SEP, Li J, Garbett K, Mirnics K, Patterson PH (2007) Maternal immune activation alters fetal brain development through interleukin-6. *J Neurosci* 27(40):10695–10702 10.1523/JNEUROSCI.2178-07.2007

Snee RD (1993) What's Missing in Statistical Education? *Am Stat* 47(2):149 10.2307/2685201

Sokoloff L, Mangold R, Wechsler RL, Kennedy C, Kety SS (1955) The effect of mental arithmetic on cerebral circulation and metabolism. *J Clin Invest* 34(7 Pt 1):1101–1108 10.1172/JCI103159

Solati J, Kleehaupt E, Kratz O, Moll GH, Golub Y (2015) Inverse effects of lipopolysaccharides on anxiety in pregnant mice and their offspring. *Physiol Behav* 139:369–374 10.1016/j.physbeh.2014.10.016

Song T, Nie B, Ma E, Che J, Sun S, Wang Y, Shan B, Liu Y, Luo S, Ma G, Li K (2015) Functional magnetic resonance imaging reveals abnormal brain connectivity in EGR3 gene transfected rat model of schizophrenia. *Biochem Biophys Res Commun* 460(3):678–683 10.1016/j.bbrc.2015.03.089

Song X, Li W, Yang Y, Zhao J, Jiang C, Li W, Lv L (2011) The nuclear factor-κB inhibitor pyrrolidine dithiocarbamate reduces polyinosinic-polycytidilic acid-

induced immune response in pregnant rats and the behavioral defects of their adult offspring. *Behav Brain Funct* 7:1–9 10.1186/1744-9081-7-50

Spector PE (1981) Multivariate data analysis for outcome studies. *Am J Community Psychol* 9(1):45–53 10.1007/BF00896359

St Clair D, Xu M, Wang P, Yu Y, Fang Y, Zhang F, Zheng X, Gu N, Feng G, Sham P, He L (2005) Rates of adult schizophrenia following prenatal exposure to the Chinese famine of 1959-1961. *JAMA* 294(5):557–562 10.1001/jama.294.5.557

Steckler T, Drinkenburg WH, Sahgal a, Aggleton JP (1998) Recognition memory in rats--I. Concepts and classification. *Prog Neurobiol* 54(3):289–311 10.1016/S0301-0082(97)00061-0

Stefferl A, Hopkins SJ, Rothwell NJ, Luheshi GN (1996) The role of TNF-α in fever: opposing actions of human and murine TNF-α and interactions with IL-β in the rat. *Br J Pharmacol* 118(8):1919–1924 10.1111/j.1476-5381.1996.tb15625.x

Steiner AA, Chakravarty S, Robbins JR, Dragic AS, Pan J, Herkenham M, Romanovsky AA (2005) Thermoregulatory responses of rats to conventional preparations of lipopolysaccharide are caused by lipopolysaccharide per se—not by lipoprotein contaminants. *Am J Physiol Integr Comp Physiol* 289(2):R348–R352 10.1152/ajpregu.00223.2005

Steiner AA, Molchanova AY, Dogan MD, Patel S, Pétervári E, Balaskó M, Wanner SP, Eales J, Oliveira DL, Gavva NR, Almeida MC, Székely M, Romanovsky AA (2011) The hypothermic response to bacterial lipopolysaccharide critically depends on brain CB1, but not CB2 or TRPV1, receptors. *J Physiol* 589(Pt 9):2415–2431 10.1113/jphysiol.2010.202465

Steullet P, Cabungcal J-H, Kulak A, Kraftsik R, Chen Y, Dalton TP, Cuenod M, Do KQ (2010) Redox Dysregulation Affects the Ventral But Not Dorsal Hippocampus: Impairment of Parvalbumin Neurons, Gamma Oscillations, and Related Behaviors. *J Neurosci* 30(7):2547–2558 10.1523/JNEUROSCI.3857-09.2010

Steullet P, Neijt HC, Cuénod M, Do KQ (2006) Synaptic plasticity impairment and hypofunction of NMDA receptors induced by glutathione deficit: Relevance to schizophrenia. *Neuroscience* 137(3):807–819 10.1016/j.neuroscience.2005.10.014

Stitt CL, Hoffmann HS, Marsh RR (1976) Interaction versus independence of startle-modification processes in the rat. *J Exp Psychol Anim Behav Process* 2(3):260–265 10.1037//0097-7403.2.3.260

Stone J V. (2004) Independent Component Analysis - A Tutorial Introduction. Cambridge, MA: MIT Press.

Stone J V (2002) Independent component analysis: an introduction. *Trends Cogn Sci* 6(2):59–64 10.1016/S1364-6613(00)01813-1

Straley ME, Van Oeffelen W, Theze S, Sullivan AM, O'Mahony SM, Cryan JF, O'Keeffe GW (2017) Distinct alterations in motor & reward seeking behavior are dependent on the gestational age of exposure to LPS-induced maternal immune activation. *Brain Behav Immun* 63:21–34 10.1016/j.bbi.2016.06.002

Strother BYSC (2006) Evaluating fMRI Preprocessing Pipelines. *IEEE Eng Med Biol Soc* 25(2):27–41

Sullivan LM, Weinberg J, Keaney JF (2016) Common statistical pitfalls in basic science research. *J Am Heart Assoc* 5(10):1–9 10.1161/JAHA.116.004142

Sullivan PF, Kendler KS, Neale MC (2003) Schizophrenia as a complex trait: evidence from a meta-analysis of twin studies. *Arch Gen Psychiatry* 60(12):1187–1192 10.1001/archpsyc.60.12.1187

Susser E, Neugebauer R, Hoek HW, Brown AS, Lin S, Labovitz D, Gorman JM (1996) Schizophrenia after prenatal famine. Further evidence. *Arch Gen Psychiatry* 53(1):25–31 10.1001/archpsyc.1996.01830010027005

Swanepoel T, Möller M, Harvey BH (2018) N-acetyl cysteine reverses bio-behavioural changes induced by prenatal inflammation, adolescent methamphetamine exposure and combined challenges. *Psychopharmacology (Berl)* 235(1):351–368 10.1007/s00213-017-4776-5

Swerdlow NR, Braff DL, Geyer MA (2016) Sensorimotor gating of the startle reflex: What we said 25 years ago, what has happened since then, and what comes next. *J Psychopharmacol* 30(11):1072–1081 10.1177/0269881116661075

Swerdlow NR, Braff DL, Taaid N, Geyer MA (1994) Assessing the validity of an animal model of deficient sensorimotor gating in schizophrenic patients. *Arch Gen Psychiatry* 51(2):139–154 10.1001/archpsyc.1994.03950020063007

Swerdlow NR, Geyer MA (1998) Using an animal model of deficient sensorimotor gating to study the pathophysiology and new treatments of schizophrenia. *Schizophr Bull* 24(2):285–301 10.1093/oxfordjournals.schbul.a033326

Swerdlow NR, Light GA (2015) Animal Models of Deficient Sensorimotor Gating in Schizophrenia: Are They Still Relevant? In: Brain Imaging in Behavioral Neuroscience, pp 305–325 10.1007/7854_2015_5012

Takeda K, Akira S (2005) Toll-like receptors in innate immunity. *Int Immunol* 17(1):1–14 10.1093/intimm/dxh186

Takeuchi O, Akira S (2007) Recognition of viruses by innate immunity. *Immunol Rev* 220(1):214–224 10.1111/j.1600-065X.2007.00562.x

Talairach J, Tournoux P (1988) Co-Planar Stereotaxic Atlas of the Human Brain. Stuttgart: Georg Theme Verlag.

Talkowski ME, Kirov G, Bamne M, Georgieva L, Torres G, Mansour H, Chowdari K V, Milanova V, Wood J, McClain L, Prasad K, Shirts B, Zhang J, O'Donovan MC, Owen MJ, Devlin B, Nimgaonkar VL (2008) A network of dopaminergic gene variations implicated as risk factors for schizophrenia. *Hum Mol Genet* 17(5):747–758 10.1093/hmg/ddm347

Tamminga C a, Holcomb HH (2005) Phenotype of schizophrenia: a review and formulation. *Mol Psychiatry* 10(1):27–39 10.1038/sj.mp.4001563

Tan W, Wang Y, Gold B, Chen J, Dean M, Harrison PJ, Weinberger DR, Law AJ (2007) Molecular cloning of a brain-specific, developmentally regulated

neuregulin 1 (NRG1) isoform and identification of a functional promoter variant associated with schizophrenia. *J Biol Chem* 282(33):24343–24351 10.1074/jbc.M702953200

Tandon R, Keshavan M, Nasrallah H (2008a) Schizophrenia, “Just the Facts” What we know in 2008. 2. Epidemiology and etiology. *Schizophr Res* 102(1–3):1–18 10.1016/j.schres.2008.04.011

Tandon R, Keshavan MS, Nasrallah HA (2008b) Schizophrenia,“just the facts”: What we know in 2008: Part 1: Overview. *Schizophr Res* 100:4–19 10.1016/j.schres.2008.01.022

Temmingh H, Stein DJ (2015) Anxiety in Patients with Schizophrenia: Epidemiology and Management. *CNS Drugs* 29(10):819–832 10.1007/s40263-015-0282-7

Thirion B, Dodel S, Poline J-B (2006) Detection of signal synchronizations in resting-state fMRI datasets. *Neuroimage* 29(1):321–327 10.1016/j.neuroimage.2005.06.054

Tian L, Meng C, Yan H, Zhao Q, Liu Q, Yan J, Han Y, Yuan H, Wang L, Yue W, Zhang Y, Li X, Zhu C, He Y, Zhang D (2011) Convergent evidence from multimodal imaging reveals amygdala abnormalities in schizophrenic patients and their first-degree relatives. *PLoS One* 6(12):e28794 10.1371/journal.pone.0028794

Torrealba F, Valdés JL (2008) The parietal association cortex of the rat. *Biol Res* 41(4):369–377 /S0716-97602008000400002

Torrey EF, Miller J, Rawlings R, Yolken RH (1997) Seasonality of births in schizophrenia and bipolar disorder: a review of the literature. *Schizophr Res* 28(1):1–38

Toyama RP, Xikota JC, Schwarzbold ML, Frode TS, Buss ZDS, Nunes JC, Funchal GDG, Nunes FC, Walz R, Pires MMDS (2015) Dose-dependent sickness behavior, abortion and inflammation induced by systemic LPS injection in pregnant mice. *J Matern Neonatal Med* 28(4):426–430 10.3109/14767058.2014.918600

Trabesinger AH, Weber OM, Duc CO, Boesiger P (1999) Detection of glutathione in the human brain in vivo by means of double quantum coherence filtering. *Magn Reson Med* 42(2):283–289 10.1002/(SICI)1522-2594(199908)42:2<283::AID-MRM10>3.0.CO;2-Q

Traynor TR, Majde JA, Bohnet SG, Krueger JM (2004) Intratracheal double-stranded RNA plus interferon-γ: A model for analysis of the acute phase response to respiratory viral infections. *Life Sci* 74(20):2563–2576 10.1016/j.lfs.2003.10.010

Tustison NJ, Avants BB, Cook PA, Yuanjie Zheng, Egan A, Yushkevich PA, Gee JC (2010) N4ITK: Improved N3 Bias Correction. *IEEE Trans Med Imaging* 29(6):1310–1320 10.1109/TMI.2010.2046908

Upadhyay J, Baker SJ, Chandran P, Miller L, Lee Y, Marek GJ, Sakoglu U, Chin CL, Luo F, Fox GB, Day M (2011) Default-Mode-Like Network Activation in Awake Rodents. *PLoS One* 6(11) 10.1371/journal.pone.0027839

Urakubo A, Jarskog LF, Lieberman JA, Gilmore JH (2001) Prenatal exposure to maternal infection alters cytokine expression in the placenta, amniotic fluid, and fetal brain. *Schizophr Res* 47(1):27–36 10.1016/S0920-9964(00)00032-3

Valdés-Hernández PA, Sumiyoshi A, Nonaka H, Haga R, Aubert-Vásquez E, Ogawa T, Iturria-Medina Y, Riera JJ, Kawashima R (2011) An in vivo MRI Template Set for Morphometry, Tissue Segmentation, and fMRI Localization in Rats. *Front Neuroinform* 5:26 10.3389/fninf.2011.00026

Valiquette V, Guma E, Cupo L, Gallino D, Anastassiadis C, Snook E, Devenyi GA, Chakravarty MM (2023) Examining litter specific variability in mice and its impact on neurodevelopmental studies. *Neuroimage* 269(September 2022):119888 10.1016/j.neuroimage.2023.119888

van Buuren M, Gladwin TE, Zandbelt BB, van den Heuvel M, Ramsey NF, Kahn RS, Vink M (2009) Cardiorespiratory effects on default-mode network activity as measured with fMRI. *Hum Brain Mapp* 30(9):3031–3042 10.1002/hbm.20729

Van den Buuse M, Garner B, Koch M (2003) Neurodevelopmental animal models of schizophrenia: effects on prepulse inhibition. *Curr Mol Med* 3(5):459–471 10.2174/1566524033479627

Van Den Eynde K, Missault S, Fransen E, Raeymaekers L, Willems R, Drinkenburg W, Timmermans JP, Kumar-Singh S, Dedeurwaerdere S (2014) Hypolocomotive behaviour associated with increased microglia in a prenatal immune activation model with relevance to schizophrenia. *Behav Brain Res* 258:179–186 10.1016/j.bbr.2013.10.005

van den Heuvel M, Mandl R, Hulshoff Pol H (2008a) Normalized cut group clustering of resting-state FMRI data. *PLoS One* 3(4):e2001 10.1371/journal.pone.0002001

van den Heuvel MP, Hulshoff Pol HE (2010) Exploring the brain network: A review on resting-state fMRI functional connectivity. *Eur Neuropsychopharmacol* 20(8):519–534 10.1016/j.euroneuro.2010.03.008

van den Heuvel MP, Stam CJ, Boersma M, Hulshoff Pol HE (2008b) Small-world and scale-free organization of voxel-based resting-state functional connectivity in the human brain. *Neuroimage* 43(3):528–539 10.1016/j.neuroimage.2008.08.010

Van der Staay FJ, Steckler T (2002) The fallacy of behavioral phenotyping without standardisation. *Genes, Brain Behav* 1(1):9–13 10.1046/j.1601-1848.2001.00007.x

Van Dijk KRA, Hedden T, Venkataraman A, Evans KC, Lazar SW, Buckner RL (2010) Intrinsic functional connectivity as a tool for human connectomics: theory, properties, and optimization. *J Neurophysiol* 103(1):297–321 10.1152/jn.00783.2009

van Miert AS, Frens J (1968) The reaction of different animal species to bacterial pyrogens. *Zentralbl Veterinarmed A* 15(6):532–543 10.1111/j.1439-0442.1968.tb00456.x

van Rossum JM (1966) The significance of dopamine-receptor blockade for the mechanism of action of neuroleptic drugs. *Arch Int Pharmacodyn thérapie* 160(2):492–494

Vercammen A, Knegtering H, den Boer JA, Liemburg EJ, Aleman A (2010) Auditory hallucinations in schizophrenia are associated with reduced functional connectivity of the temporo-parietal area. *Biol Psychiatry* 67(10):912–918 10.1016/j.biopsych.2009.11.017

Vernon AC, So PW, Lythgoe DJ, Chege W, Cooper JD, Williams SCR, Kapur S (2015) Longitudinal in vivo maturational changes of metabolites in the prefrontal cortex of rats exposed to polyinosinic-polycytidylic acid in utero. *Eur Neuropsychopharmacol* 25(12):2210–2220 10.1016/j.euroneuro.2015.09.022

Victor A, Elsässer A, Hommel G, Blettner M (2010) Judging a plethora of p-values: how to contend with the problem of multiple testing: part 10 of a series on evaluation of scientific publications. *Dtsch Arztebl Int* 107(4):50–56 10.3238/arztebl.2009.0050

Vincent JL, Kahn I, Snyder AZ, Raichle ME, Buckner RL (2008) Evidence for a Frontoparietal Control System Revealed by Intrinsic Functional Connectivity. *J Neurophysiol* 100(6):3328–3342 10.1152/jn.90355.2008

Vincent JL, Patel GH, Fox MD, Snyder AZ, Baker JT, Van Essen DC, Zempel JM, Snyder LH, Corbetta M, Raichle ME (2007) Intrinsic functional architecture in the anaesthetized monkey brain. *Nature* 447(7140):83–86 10.1038/nature05758

Vincent JL, Snyder AZ, Fox MD, Shannon BJ, Andrews JR, Raichle ME, Buckner RL (2006) Coherent spontaneous activity identifies a hippocampal-parietal memory network. *J Neurophysiol* 96(6):3517–3531 [Accessed August 18, 2015]10.1152/jn.00048.2006

Vorhees C V., Graham DL, Braun AA, Schaefer TL, Skelton MR, Richtand NM, Williams MT (2012) Prenatal immune challenge in rats: Altered responses to dopaminergic and glutamatergic agents, prepulse inhibition of acoustic startle, and reduced route-based learning as a function of maternal body weight gain after prenatal exposure to poly IC. *Synapse* 66(8):725–737 10.1002/syn.21561

Vorhees C V., Graham DL, Braun AA, Schaefer TL, Skelton MR, Richtand NM, Williams MT (2015) Prenatal immune challenge in rats: Effects of polyinosinic-polycytidylic acid on spatial learning, prepulse inhibition, conditioned fear, and responses to MK-801 and amphetamine. *Neurotoxicol Teratol* 47:54–65 10.1016/j.ntt.2014.10.007

Vuillermot S, Feldon J, Meyer U (2011) Nurr1 is not essential for the development of prepulse inhibition deficits induced by prenatal immune activation. *Brain Behav Immun* 25(7):1316–1321 10.1016/j.bbi.2011.06.012

Vuillermot S, Luan W, Meyer U, Eyles D (2017) Vitamin D treatment during pregnancy prevents autism-related phenotypes in a mouse model of maternal immune activation. *Mol Autism* 8(1):1–13 10.1186/s13229-017-0125-0

Vuillermot S, Weber L, Feldon J, Meyer U (2010) A longitudinal examination of the neurodevelopmental impact of prenatal immune activation in mice reveals primary defects in dopaminergic development relevant to schizophrenia. *J Neurosci* 30(4):1270–1287 10.1523/JNEUROSCI.5408-09.2010

Walf AA, Frye CA (2007) The use of the elevated plus maze as an assay of anxiety-

related behavior in rodents. *Nat Protoc* 2(2):322–328 10.1038/nprot.2007.44

Wan J, Grimble RF (1986) Diurnal influences on the metabolic effects of two types of Escherichia coli endotoxin in rats. *Proc Nutr Soc* 45(1):83A 10.1079/PNS19860042

Wang H, Meng XH, Ning H, Zhao XF, Wang Q, Liu P, Zhang H, Zhang C, Chen GH, Xu DX (2010) Age- and gender-dependent impairments of neurobehaviors in mice whose mothers were exposed to lipopolysaccharide during pregnancy. *Toxicol Lett* 192(2):245–251 10.1016/j.toxlet.2009.10.030

Wang H, Zeng L-L, Chen Y, Yin H, Tan Q, Hu D (2015) Evidence of a dissociation pattern in default mode subnetwork functional connectivity in schizophrenia. *Sci Rep* 5(May):14655 10.1038/srep14655

Wang HL, Pei DE, Yang RD, Wan CL, Ye YM, Peng SS, Zeng QQ, Yu Y (2019) Prenatal maternal vaginal inflammation increases anxiety and alters HPA axis signalling in adult male mice. *Int J Dev Neurosci* 75(April):27–35 10.1016/j.ijdevneu.2019.04.001

Wang J-H, Zuo X-N, Gohel S, Milham MP, Biswal BB, He Y (2011) Graph theoretical analysis of functional brain networks: test-retest evaluation on short- and long-term resting-state functional MRI data. *PLoS One* 6(7):e21976 10.1371/journal.pone.0021976

Wastnedge EAN, Reynolds RM, van Boeckel SR, Stock SJ, Denison FC, Maybin JA, Critchley HOD (2021) Pregnancy and COVID-19. *Physiol Rev* 101(1):303–318 10.1152/physrev.00024.2020

Waterhouse U, Roper VE, Brennan KA, Ellenbroek BA (2016) Nicotine ameliorates cognitive deficits induced by maternal LPS exposure: A study in rats. *Dis Model Mech*(May):dmm.025072 10.1242/dmm.025072

Weber-Stadlbauer U, Richetto J, Labouesse MA, Bohacek J, Mansuy IM, Meyer U (2016) Transgenerational transmission and modification of pathological traits induced by prenatal immune activation. *Mol Psychiatry*(February):1–11 10.1038/mp.2016.41

Weber R, Ramos-Cabrer P, Wiedermann D, van Camp N, Hoehn M (2006) A fully noninvasive and robust experimental protocol for longitudinal fMRI studies in the rat. *Neuroimage* 29(4):1303–1310 10.1016/j.neuroimage.2005.08.028

Weinberger DR (1987) Implications of Normal Brain Development for the Pathogenesis of Schizophrenia. *Arch Gen Psychiatry* 44(7):660 10.1001/archpsyc.1987.01800190080012

Weinberger DR, Egan MF, Bertolino A, Callicott JH, Mattay VS, Lipska BK, Berman KF, Goldberg TE (2001) Prefrontal neurons and the genetics of schizophrenia. *Biol Psychiatry* 50(11):825–844 10.1016/S0006-3223(01)01252-5

Weissenbacher A, Kasess C, Gerstl F, Lanzenberger R, Moser E, Windischberger C (2009) Correlations and anticorrelations in resting-state functional connectivity MRI: a quantitative comparison of preprocessing strategies. *Neuroimage* 47(4):1408–1416 10.1016/j.neuroimage.2009.05.005

Welge JA, Richtand NM (2002) Regression modeling of rodent locomotion data. *Behav Brain Res* 128(1):61–69 10.1016/S0166-4328(01)00311-4

Wenling Y, Junchao Q, Zhirong X, Shi O (2020) Pregnancy and COVID-19: Management and challenges. *Rev Inst Med Trop Sao Paulo* 62(August):1–9 10.1590/S1678-9946202062062

Whitfield-Gabrieli S, Thermenos HW, Milanovic S, Tsuang MT, Faraone S V, McCarley RW, Shenton ME, Green AI, Nieto-Castanon A, LaViolette P, Wojcik J, Gabrieli JDE, Seidman LJ (2009) Hyperactivity and hyperconnectivity of the default network in schizophrenia and in first-degree relatives of persons with schizophrenia. *Proc Natl Acad Sci U S A* 106(4):1279–1284 10.1073/pnas.0809141106

Whitlow CT, Casanova R, Maldjian JA (2011) Effect of resting-state functional MR imaging duration on stability of graph theory metrics of brain network connectivity. *Radiology* 259(2):516–524 10.1148/radiol.11101708

Wickham H (2016) ggplot2 - Elegant Graphics for Data Analysis, 2nd ed. Houston, Texas, USA: Springer International Publishing. 10.1007/978-3-319-24277-4

Williams K a., Magnuson M, Majeed W, LaConte SM, Peltier SJ, Hu X, Keilholz SD (2010) Comparison of α-chloralose, medetomidine and isoflurane anesthesia for functional connectivity mapping in the rat. *Magn Reson Imaging* 28(7):995–1003 10.1016/j.mri.2010.03.007

Williamson LL, Sholar PW, Mistry RS, Smith SH, Bilbo SD (2011) Microglia and Memory: Modulation by Early-Life Infection. *J Neurosci* 31(43):15511–15521 10.1523/JNEUROSCI.3688-11.2011

Winkler AM, Ridgway GR, Webster M a., Smith SM, Nichols TE (2014) Permutation inference for the general linear model. *Neuroimage* 92:381–397 10.1016/j.neuroimage.2014.01.060

Winship IR, Dursun SM, Baker GB, Balista PA, Kandratavicius L, Maia-de-Oliveira JP, Hallak J, Howland JG (2019) An Overview of Animal Models Related to Schizophrenia. *Can J Psychiatry* 64(1):5–17 10.1177/0706743718773728

Winters BD, Saksida LM, Bussey TJ (2008) Object recognition memory: Neurobiological mechanisms of encoding, consolidation and retrieval. *Neurosci Biobehav Rev* 32(5):1055–1070 10.1016/j.neubiorev.2008.04.004

Wischhof L, Irrsack E, Dietz F, Koch M (2015a) Maternal lipopolysaccharide treatment differentially affects 5-HT2A and mGlu2/3 receptor function in the adult male and female rat offspring. *Neuropharmacology* 97:275–288 10.1016/j.neuropharm.2015.05.029

Wischhof L, Irrsack E, Osorio C, Koch M (2015b) Prenatal LPS-exposure - a neurodevelopmental rat model of schizophrenia - differentially affects cognitive functions, myelination and parvalbumin expression in male and female offspring. *Prog Neuropsychopharmacol Biol Psychiatry* 57:17–30 10.1016/j.pnpbp.2014.10.004

Wise RG, Ide K, Poulin MJ, Tracey I (2004) Resting fluctuations in arterial carbon dioxide induce significant low frequency variations in BOLD signal. *Neuroimage*

21(4):1652–1664 10.1016/j.neuroimage.2003.11.025

Wittekindt M, Kaddatz H, Joost S, Staffeld A, Bitar Y, Kipp M, Frintrop L (2022) Different Methods for Evaluating Microglial Activation Using Anti-Ionized Calcium-Binding Adaptor Protein-1 Immunohistochemistry in the Cuprizone Model. *Cells* 11(11):1723 10.3390/cells11111723

Wolf N (2011) Dysconnectivity of multiple resting-state networks in patients with schizophrenia who have persistent auditory verbal hallucinations. *J Psychiatry Neurosci* 36(6):366–374 10.1503/jpn.110008

Wolf SS, Hyde TM, Weinberger DR (1993) Neurobiology of schizophrenia. *Curr Opin Neurol Neurosurg* 6(1):86–92

Wolff AR, Bilkey DK (2008) Immune activation during mid-gestation disrupts sensorimotor gating in rat offspring. *Behav Brain Res* 190(1):156–159 10.1016/j.bbr.2008.02.021

Wolff AR, Bilkey DK (2010) The maternal immune activation (MIA) model of schizophrenia produces pre-pulse inhibition (PPI) deficits in both juvenile and adult rats but these effects are not associated with maternal weight loss. *Behav Brain Res* 213(2):323–327 10.1016/j.bbr.2010.05.008

Wolff AR, Cheyne KR, Bilkey DK (2011) Behavioural deficits associated with maternal immune activation in the rat model of schizophrenia. *Behav Brain Res* 225(1):382–387 10.1016/j.bbr.2011.07.033

Wood SJ, Berger GE, Wellard RM, Proffitt TM, McConchie M, Berk M, McGorry PD, Pantelis C (2009) Medial temporal lobe glutathione concentration in first episode psychosis: A 1H-MRS investigation. *Neurobiol Dis* 33(3):354–357 10.1016/j.nbd.2008.11.018

Woodward EA, Prêle CM, Nicholson SE, Kolesnik TB, Hart PH (2010) The anti-inflammatory effects of interleukin-4 are not mediated by suppressor of cytokine signalling-1 (SOCS1). *Immunology* 10.1111/j.1365-2567.2010.03281.x

Woodward ND, Karbasforoushan H, Heckers S (2012) Thalamocortical dysconnectivity in schizophrenia. *Am J Psychiatry* 169(10):1092–1099 10.1176/appi.ajp.2012.12010056

Woodward ND, Rogers B, Heckers S (2011) Functional resting-state networks are differentially affected in schizophrenia. *Schizophr Res* 130(1–3):86–93 10.1016/j.schres.2011.03.010

Wright IC, Rabe-Hesketh S, Woodruff PWR, David AS, Murray RM, Bullmore ET (2000) Meta-analysis of regional brain volumes in schizophrenia. *Am J Psychiatry* 157(1):16–25 10.1176/appi.ajp.157.1.16

Würbel H (2000) Behaviour and the standardization fallacy. *Nat Genet* 26(3):263–263 10.1038/81541

Xiong J, Parsons LM, Gao JH, Fox PT (1999) Interregional connectivity to primary motor cortex revealed using MRI resting state images. *Hum Brain Mapp* 8(2–3):151–156

Yee N, Ribic A, de Roo CC, Fuchs E (2011) Differential effects of maternal immune activation and juvenile stress on anxiety-like behaviour and physiology in adult rats: No evidence for the “double-hit hypothesis.” *Behav Brain Res* 224(1):180–188 10.1016/j.bbr.2011.05.040

Yin P, Liu J, Li Z, Wang YY, Qiao NN, Huang SY, Li BM, Sun RP (2013) Prenatal immune challenge in rats increases susceptibility to seizure-induced brain injury in adulthood. *Brain Res* 1519:78–86 10.1016/j.brainres.2013.04.047

Yin P, Zhang X-T, Li J, Yu L, Wang J-W, Lei G-F, Sun R-P, Li B-M (2015) Maternal immune activation increases seizure susceptibility in juvenile rat offspring. *Epilepsy Behav* 47:93–97 10.1016/j.yebeh.2015.04.018

Yirmiya R, Goshen I (2011) Immune modulation of learning, memory, neural plasticity and neurogenesis. *Brain Behav Immun* 25(2):181–213 10.1016/j.bbi.2010.10.015

Young J, McKinney SB, Ross BM, Wahle KWJ, Boyle SP (2007) Biomarkers of oxidative stress in schizophrenic and control subjects. *Prostaglandins Leukot Essent Fat Acids* 76(2):73–85 10.1016/j.plefa.2006.11.003

Young JW, Powell SB, Risbrough V, Marston HM, Geyer MA (2009) Using the MATRICS to guide development of a preclinical cognitive test battery for research in schizophrenia. *Pharmacol Ther* 122(2):150–202 10.1016/j.pharmthera.2009.02.004

Yu Q, Allen EA, Sui J, Arbabshirani MR, Calhoun VD (2015) Brain connectivity networks in schizophrenia underlying resting state functional magnetic resonance imaging. *Curr Top Med Chem* 12(21):2415–2425

Yu Y, Shen H, Zhang H, Zeng L-L, Xue Z, Hu D (2013) Functional connectivity-based signatures of schizophrenia revealed by multiclass pattern analysis of resting-state fMRI from schizophrenic patients and their healthy siblings. *Biomed Eng Online* 12(1):10 10.1186/1475-925X-12-10

Yue YR, Loh JM, Lindquist M a (2010) Adaptive spatial smoothing of fMRI images. *Stat Interface* 3:3–13 10.4310/SII.2010.v3.n1.a1

Yushkevich PA, Piven J, Hazlett HC, Smith RG, Ho S, Gee JC, Gerig G (2006) User-guided 3D active contour segmentation of anatomical structures: Significantly improved efficiency and reliability. *Neuroimage* 31(3):1116–1128 10.1016/j.neuroimage.2006.01.015

Zhang N, Rane P, Huang W, Liang Z, Kennedy D, Frazier J a., King J (2010) Mapping resting-state brain networks in conscious animals. *J Neurosci Methods* 189(2):186–196 10.1016/j.jneumeth.2010.04.001

Zhang Y, Cazakoff BN, Thai CA, Howland JG (2012) Prenatal exposure to a viral mimetic alters behavioural flexibility in male, but not female, rats. *Neuropharmacology* 62(3):1299–1307 10.1016/j.neuropharm.2011.02.022

Zhang Z, van Praag H (2015) Maternal immune activation differentially impacts mature and adult-born hippocampal neurons in male mice. *Brain Behav Immun* 45:60–70 10.1016/j.bbi.2014.10.010

Zhao F, Zhao T, Zhou L, Wu Q, Hu X (2008) BOLD study of stimulation-induced neural activity and resting-state connectivity in medetomidine-sedated rat. *Neuroimage* 39(1):248–260 10.1016/j.neuroimage.2007.07.063

Zhou X, Stephens M (2014) Efficient multivariate linear mixed model algorithms for genome-wide association studies. *Nat Methods* 11(4):407–409 10.1038/nmeth.2848

Zhou Y, Guo M, Wang X, Li J, Wang Y, Ye L, Dai M, Zhou L, Persidsky Y, Ho W (2013) TLR3 activation efficiency by high or low molecular mass poly I:C. *Innate Immun* 19(2):184–192 10.1177/1753425912459975

Zhou Y, Liang M, Jiang T, Tian L, Liu Y, Liu Z, Liu H, Kuang F (2007a) Functional dysconnectivity of the dorsolateral prefrontal cortex in first-episode schizophrenia using resting-state fMRI. *Neurosci Lett* 417(3):297–302 10.1016/j.neulet.2007.02.081

Zhou Y, Liang M, Tian L, Wang K, Hao Y, Liu H, Liu Z, Jiang T (2007b) Functional disintegration in paranoid schizophrenia using resting-state fMRI. *Schizophr Res* 97(1–3):194–205 10.1016/j.schres.2007.05.029

Zhu F, Zheng Y, Ding YQ, Liu Y, Zhang X, Wu R, Guo X, Zhao J (2014a) Minocycline and risperidone prevent microglia activation and rescue behavioral deficits induced by neonatal intrahippocampal injection of lipopolysaccharide in rats. *PLoS One* 9(4) 10.1371/journal.pone.0093966

Zhu F, Zheng Y, Liu Y, Zhang X, Zhao J (2014b) Minocycline alleviates behavioral deficits and inhibits microglial activation in the offspring of pregnant mice after administration of polyriboinosinic-polyribocytidilic acid. *Psychiatry Res* 219(3):680–686 10.1016/j.psychres.2014.06.046

Zhu Y, Carvey PM, Ling Z (2007) Altered glutathione homeostasis in animals prenatally exposed to lipopolysaccharide. *Neurochem Int* 50(4):671–680 10.1016/j.neuint.2006.12.013

Zimmer A, Youngblood A, Adnane A, Miller BJ, Goldsmith DR (2021) Prenatal exposure to viral infection and neuropsychiatric disorders in offspring: A review of the literature and recommendations for the COVID-19 pandemic. *Brain Behav Immun* 91(October 2020):756–770 10.1016/j.bbi.2020.10.024

Zorrilla EP (1997) Multiparous species present problems (and possibilities) to developmentalists. *Dev Psychobiol* 30(2):141–150 10.1002/(SICI)1098-2302(199703)30:2<141::AID-DEV5>3.0.CO;2-Q

Zuckerman L, Rehavi M, Nachman R, Weiner I (2003) Immune activation during pregnancy in rats leads to a postpubertal emergence of disrupted latent inhibition, dopaminergic hyperfunction, and altered limbic morphology in the offspring: a novel neurodevelopmental model of schizophrenia. *Neuropsychopharmacology* 28(10):1778–1789 10.1038/sj.npp.1300248

Zuckerman L, Weiner I (2005) Maternal immune activation leads to behavioral and pharmacological changes in the adult offspring. *J Psychiatr Res* 39(3):311–323 10.1016/j.jpsychires.2004.08.008

Zuo XN, Kelly C, Adelstein JS, Klein DF, Castellanos FX, Milham MP (2010) Reliable

intrinsic connectivity networks: Test-retest evaluation using ICA and dual regression approach. *Neuroimage* 49(3):2163–2177 10.1016/j.neuroimage.2009.10.080

Acknowledgments

I would like to express my deepest gratitude to Michael Koch and Ekkehard Küstermann for the opportunity to carry out my thesis on this topic, as well as for being reviewers of my dissertation. Big thanks to Ekkehard for all the help with and wonderful time during MRI data collection and preprocessing. Furthermore, I would like to thank both of them for all the support they offered me over the last years, and for being patient until the end.

Many thanks to all the (former) members of the Department of Neuropharmacology of the University of Bremen, especially to Julia, Nadine, Imandra, Kim, Jannis, Ellen and Marilena, for all the help in and out the lab, but especially for the wonderful time we had together. Many thanks for the wonderful time and the interesting lunch table discussions also to the "In-vivo-MR" AG - Ekkehard, Wolfgang and Peter.

In Addition, I would like to thank Dirk Wiedermann for providing the slice-wise motion correction script of Daniel Kalthoff, as well as Adam James Schwarz for providing the stereotaxic MRI rat brain template.

Many thanks to GCP-Service International, especially to Andreas Grund for giving me the opportunity of finalizing this thesis while already still being a part of such a wonderful team, and to all (former) members of the Regulatory Affairs team, especially to Martin, Violetta and Alexandra, once again for all the for the wonderful time in the past three years and the emotional support when talking about my thesis.

Moreover, I would like to thank my whole family for all their support during the time of my studies.

Last but not least, I want do deeply thank Jana Müller: For all the support during the past twelve years, no matter what issue I needed help with, for listening when I needed someone to listen, for taking the plunge with me by moving out from our protected homes into the unknown depths of the cozy cave - for the best time of my life. I love you.

6. Appendix

6.1. Overview of Published Studies Investigating EPM, OF, NOR and PPI Behaviour in LPS or Poly(I:C) Models

6.1.1. EPM

Table 25: Overview of published studies utilizing the elevated plus maze (EPM) or elevated zero maze (EZM) in Poly(I:C) and LPS mouse models
Shown are studies published before the year 2021 investigating elevated plus maze (EPM) or elevated zero maze (EZM) behavior in Poly(I:C) and LPS mouse models. The findings are categorized as no difference in behavior (≈), behavioural deficits (↓) meaning an increase in anxiety related behavior or behavioural improvements (↑) meaning a reduction of anxiety related behavior compared to controls.

Species	Substance	Authors	Year	Strain	LPS Serotype / Poly(I:C) MW	Dose	Route	Timing [GD]	Age [PD]	Findings	Session Time [min]	Comments
Mouse	Poly(I:C)	Meyer *et al.*	2005	C57BL6/J	-	2.5 mg/kg 5.0 mg/kg 10.0 mg/kg	i.v.	9	~100	≈	-	Authors mention using EPM in discussion (no stat. sign. effects observed), but did not show any data
		Giovanoli *et al.*	2013	C57BL/6	-	1 mg/kg	i.v.	9	41-45 70-110	≈ ≈	-	
		Lipina *et al.*	2013	C57BL/6	-	5 mg/kg	i.v.	9	-	≈	5	
		Li *et al.*	2014	C57BL/6J	-	20 mg/kg	i.p.	9.5	>60	≈	10	
		Majidi-Zolbanin *et al.*	2015	C57BL/6	-	20 mg/kg	i.p.	12	87	↓	5	Decreased open arm time in male Poly(I:C) offspring
		Giovanoli *et al.*	2016	C57BL/6J	-	1 mg/kg	i.v.	9	70-90	≈	5	
		Vuillermot *et al.*	2017	C57BL6/N	-	5 mg/kg	i.v.	9	30-40	≈	5	
		Morais *et al.*	2018	C57BL/6J Swiss	-	20 mg/kg	i.p.	12.5	77	≈ ≈	6	No significant treatment effect in ANOVA; Authors nonetheless state sig. effects of Poly(I:C) in Swiss mice
	LPS	Golan *et al.*	2006	C57BL/6	-	120 µg/kg	i.p.	17	240 600	≈ (↓)	5	Longer distances and more rearings in closed arms in LPS offspring at PD600, but no differences in open/closed ratio
		Hava *et al.*	2006	C57BL/6	-	120 µg/kg	i.p.	17	240	↓	5	Increased closed/open arm ratio in LPS offspring

		Asiaei, Solati & Salari	2011	C57BL/6	Salmonella enterica, entridis	50 µg/kg 100 µg/kg 150 µg/kg	i.p.	10	61	↑ ↑ ↑	5	Increased open arm time and entries in LPS offspring
		Chlodzinska *et al.*	2011	Swiss	0111:B4	100 µg/kg 300 µg/kg 1000 µg/kg 2000 µg/kg	i.p.	16-17	>90	≈ (↑) - -	5	Increased time in open arms in female 300µg/kg offspring; 1000 & 2000 µg/kg groups no offspring
		Enayati *et al.*	2012	NMRI	Salmonella enterica, entridis	50 µg/kg 300 µg/kg 500 µg/kg	i.p.	15 / 16 / 17	40 / 80	≈/≈ / ≈/≈ / ≈/↓ ≈/↓ / ↓/↓ / ≈/↓ ≈/↓ / ↓/↓ / ↓/↓	5	Decreased open arm time and/or entries in LPS offspring, depending on the dose/timing/age
		Babri *et al.*	2014	NMRI C57BL/6	055:B5	500 µg/kg	i.p.	17	80 / 90	↓/↓ ≈/≈	5	EZM (PD80) + EPM (PD90); Decreased open time, entries (and head-dips) in NMRI LPS offspring
		Depino	2015	C57BL/6J	0111:B4	25 µg/kg	s.c.	9	56-70	↓	5	Decreased open arm time and distance in LPS offspring
		Solati *et al.*	2015	NMRI	Salmonella enterica, abortus equi	30 µg/kg 60 µg/kg 120 µg/kg 240 µg/kg 480 µg/kg	s.c.	10	60-70	≈ ↑ ↑ ↑ ↑	5	Increased open arm time and entries in LPS offspring
		Hsueh *et al.*	2017	C57BL/6	055:B5	25, 25, 50 µg/kg	s.c.	15-17	63	(↓)	10	Fewer movements (entries) between arms in female LPS offspring
		Schaafsma *et al.*	2017	C57BL/6JOlaHsd	0111:B4	250 µg/kg 100 µg/kg 50 µg/kg	-	15-17	60-120	- - ↑	5	Increased open arm time in 50µg/kg LPS offspring; 100 & 250µg/kg groups no viable offspring
		Wang *et al.*	2019	C57BL/6J	-	2 µg (20µl of 0.1 mg/mL)	transvaginal	0-16 4 x	60	↓	5	Decreased open arm time and entries in male LPS offspring

Table 26: Overview of published studies utilizing the elevated plus maze (EPM) or elevated zero maze (EZM) in Poly(I:C) and LPS rat models
Shown are studies published before the year 2021 investigating elevated plus maze (EPM) or elevated zero maze (EZM) behavior in Poly(I:C) and LPS rat models. The findings are categorized as no difference in behavior (≈), behavioural deficits (↓) meaning an increase in anxiety related behavior or behavioural improvements (↑) meaning a reduction of anxiety related behavior compared to controls.

Species	Substance	Authors	Year	Strain	LPS Serotype / Poly(I:C) MW	Dose	Route	Timing [GD]	Age [PD]	Findings	Session Time [min]	Comments
Rat	Poly(I:C)	Yee *et al.*	2011	Sprague-Dawley	-	4 mg/kg	i.v.	15	61	↓	5	Decreased open time and entries in Poly(I:C) offspring
		Vorhees *et al.*	2012	Sprague-Dawley	-	8 mg/kg	i.p.	14	65	≈	5	EZM
		Vorhees *et al.*	2015	Sprague-Dawley	-	8 mg/kg	i.p.	14-18	65	≈	-	EZM
		Gray *et al.*	2019	Wistar	-	5 mg/kg	i.v.	14	>70	≈	10	
	LPS	Bakos *et al.*	2004	Wistar	0111:B4	20-80 µg/kg	s.c.	15-19	~90	(↑)	5	Increased open and closed arm entries in female LPS offspring
		Kirsten *et al.*	2010	Wistar	0127:B8	100 µg/kg	i.p.	9.5	90-95	≈	5	All litters with <8 pups/litter were culled (i.e. excluded), despite stat. sign. effects on pups/litter in the LPS group (with LPS producing on average <~8 pups/litter)
		Lin, Lin & Wang	2012	Sprague-Dawley	026:B6	66µg/kg (20000 U/kg)	i.p.	10.5	93	↓	5	Decreased open arm time in LPS offspring
		Yin *et al.*	2013	Wistar	055:B5	200 µg/kg	i.p.	15-16	68	↓	5	Decreased open arm time in LPS offspring
		Foley *et al.*	2014	Long-Evans	0111:B4	50 µg/kg	s.c.	15-16	40	≈	5	No stat. sign. differences; In general very low open arm times, with LPS offspring spending nearly no time on open arms
		Wischhof *et al.*	2015	Wistar	0111:B4	100 µg/kg	i.p.	15-16	120	≈	5	
		Yin *et al.*	2015	Sprague-Dawley	055:B5	200 µg/kg	i.p.	15-16	30	≈	5	
		Mouihate *et al.*	2019	Sprague-Dawley	026:B6	100 µg/kg	-	15, 17, 19	30 70	≈ ≈	5	

6.1.2. OF

Table 27: Overview of published studies utilizing the open field test to assess anxiety related behaviour in Poly(I:C) and LPS mouse models
Shown are studies published before the year 2021 investigating anxiety related behaviours in the open field (OF) in Poly(I:C) and LPS mouse models. The findings are categorized as no difference in behavior (≈), behavioural deficits (↓) meaning an increase in anxiety related behavior or behavioural improvements (↑) meaning a reduction of anxiety related behavior compared to controls.

Species	Substance	Authors	Year	Strain	LPS Serotype / Poly(I:C) MW	Dose	Route	Timing [GD]	Age [PD]	Findings	Session Time [min]	Comments
Mouse	Poly(I:C)	Meyer et al.	2005	C57BL6/J	-	2.5 mg/kg 5.0 mg/kg 10.0 mg/kg	i.v.	9	~100	↓ ↓ ↓	30	Poly(I:C) offspring reduced entries into center, but no differences in locomotion
		Meyer et al.	2006	C57BL6/J	-	5 mg/kg	i.v.	9 17	~105	↓ ≈	60	GD9 Poly(I:C) offspring reduced entries into center, but no differences in locomotion
		Ozawa et al.	2006	BALB/c	-	5.0 mg/kg	i.p.	12-17	35 63-70	≈ ↑	10 / 120	Adult Poly(I:C) offspring increased entries into and increased time spent in center, but no differences in locomotion
		Smith et al.	2007	C57BL/6J	-	20 mg/kg	i.p.	12	-	↓	10	Poly(I:C) offspring reduced entries into center, and reduced locomotion
		Meyer et al.	2008	FVB	-	2 mg/kg	i.v.	9	~105	↓	30	Poly(I:C) offspring reduced time in center, but no differences in locomotion
		O'Leary et al.	2014	C57BL/6	-	5 mg/kg	i.p.	9	35-40 90-135	≈ ≈	10	
		da Silveira et al.	2017	C57BL/6	-	5 mg/kg	i.v.	9 17	70	↓↑ ↓↑	20	Poly(I:C) offspring reduced time in center, but increased locomotion
		Ronovsky et al.	2017	C57BL6/N	-	20 mg/kg	i.p.	12.5	>56	≈	60	No differences in locomotion or time in center in F2 generation (F1 offspring not tested)
		Morais et al.	2018	C57BL/6J Swiss	-	20 mg/kg	i.p.	12.5	70	≈ ≈	10	
		Dabbah-Assadi et al.	2019	CD-1	-	5 mg/kg	i.p.	12.5 17.5	Adolescence / Adulthood	≈ / (↑) ≈ / (↑)	30	Adult female Poly(I:C) offspring increased time in center, but no differences in locomotion
		Sheu et al.	2019	C57BL/6	-	5 mg/kg	i.v.	17	42 63 84	≈ ↓ ↓	10 / 60	Poly(I:C) offspring reduced time in center at PD 63 and 84, but no differences in locomotion

		Carlezon et al.	2019	C57BL/6J	- / 0111:B4	20 mg/kg +10 mg/kg	i.p. +s.c.	12.5 +PD9	42-49	≈(↓)	10	Offspring of a 2-hit model (prenatal Poly(I:C) + postnatal LPS) show reduced time in center in male 2-hit offspring reduced locomotion in female 2-hit offspring
	LPS	Golan et al.	2005	C57BL/6	-	120 µg/kg	i.p.	17	270	≈	5	
		Golan et al.	2006	C57BL/6	-	120 µg/kg	i.p.	17	240 600	≈ ↑	5	LPS offspring increased locomotion, and tendency to increased distance moved in center at PD600
		Wang et al.	2010	CD-1	0127:B8	8 µg/kg	i.p.	8-15	70 200 400 600	≈ ≈ (↑↓) ≈ ↓	5	Female PD200 LPS offspring less time spent in center, but increased locomotion. PD600 LPS offspring increased latency to the first grid crossing
		Chlodzinska et al.	2011	Swiss	0111:B4	100 µg/kg 300 µg/kg 1000 µg/kg 2000 µg/kg	i.p.	16-17	>90	≈ ↑ - -	5	300µg LPS offspring increased entries into and increased time in center, as well as increased locomotion
		Babri et al.	2014	NMRI C57BL/6	055:B5	500 µg/kg	i.p.	17	80	≈ ≈	5	
		Depino	2015	C57BL/6J	0111:B4	25 µg/kg	s.c.	9	56-70	↓	5	LPS offspring reduced time in center, increased latency to enter center, and decreased locomotion
		Al-Amin et al.	2016	Swiss	-	300 µg/kg	i.p.	16-17	133	↓	20	LPS offspring reduced time in center, and decreased locomotion
		Hsueh et al.	2017	C57BL/6	055:B5	25, 25, 50 µg/kg	s.c.	15-17	35	↓	10	LPS offspring less time in center, but no differences in locomotion
		Schaafsma et al.	2017	C57BL/6J OlaHsd	0111:B4	250, 100, 50 µg/kg	-	15-17	60-120	≈	5	
		Braun et al.	2019	C57BL/6J	-	60 µg/kg	i.p.	12.5	Adulthood	↓	20	LPS offspring show lack of decrease in locomotion (no habituation, min 1-10 vs 11-20) Female LPS offspring show lack of habituation to OF (reduced center time during min 10-20)
		Wang et al.	2019	C57BL/6J	-	2 µg (20µl of 0.1 mg/mL)	transvaginal	0-16 4 x	60	↓	30	LPS offspring reduced time in center, but no difference in locomotion

Table 28: Overview of published studies utilizing the open field test to assess anxiety related behaviour in Poly(I:C) and LPS rat models
Shown are studies published before the year 2021 investigating anxiety related behaviours in the open field (OF) in Poly(I:C) and LPS rat models. The findings are categorized as no difference in behavior (≈), behavioural deficits (↓) meaning an increase in anxiety related behavior or behavioural improvements (↑) meaning a reduction of anxiety related behavior compared to controls.

Species	Substance	Authors	Year	Strain	LPS Serotype / Poly(I:C) MW	Dose	Route	Timing [GD]	Age [PD]	Findings	Session Time [min]	Comments
Rat	Poly(I:C)	Vorhees et al.	2012	Sprague-Dawley	-	8 mg/kg	i.p.	14	66	≈	60	
		Vorhees et al.	2015	Sprague-Dawley	-	8 mg/kg	i.p.	14-18	66	≈	60	
	LPS	Poggi et al.	2005	Fisher 344	0111:B4	100 µg/kg	intra-cervically	13	75	≈	45	
		Lin, Lin, Wang	2012	Sprague-Dawley	026:B6	66µg/kg 20000 U/kg	i.p.	10.5	90	↓	15	Male LPS offspring reduced time in center of large OF, Female LPS offspring reduced locomotion in large OF, but no difference in locomotion in small OF
		Foley et al.	2014	Long-Evans	0111:B4	50 µg/kg	s.c.	12	33	≈	15	
		Foley et al.	2014	Long-Evans	0111:B4	50 µg/kg	s.c.	15-16	42	≈	60	
		Harvey & Boksa	2014	Sprague-Dawley	0111:B4	50 µg/kg	i.p.	15-16	35-38 70	≈ ↑	30	Adult LPS offspring reduced time in corners of large OF
		Wischhof et al.	2015	Wistar	0111:B4	100 µg/kg	i.p.	15-16	33 60	↑ ↑	60	LPS offspring increased rearings, and increased locomotion; Increased time in center at PD33 (trend at PD60)
		Wischhof et al.	2015	Wistar	0111:B4	100 µg/kg	i.p.	15-16	100-120	≈	30	
		Santos-Toscano et al.	2016	Sprague-Dawley	0111:B4	100 µg/kg	i.p.	15-16	60-72	≈	10	
		Delattre et al.	2017	Wistar	026:B6	1 mg/kg	i.p.	11	22 99	↑ ≈	5	Juvenile LPS offspring increased locomotion
		Straley et al.	2017	Sprague-Dawley	-	50 µg/kg	i.p.	12 16	9 / 30 / 60	≈ / ≈ / ≈ ↓(↑) / ↑ / ↓	5 (PD9) 10 (PD>30)	GD16 LPS offspring reduced locomotion and trend to more time in center on PD9, GD16 LPS offspring no differences in locotion but more time in center on PD30, and GD16 LPS offspring reduced locomotion but no differemces in center time on PD60
		Mouihate et al.	2019	Sprague-Dawley	026:B6	100 µg/kg	-	15, 17, 19	30 70	≈ ≈		

6.1.3. NOR

Table 29: Overview of published studies utilizing the novel object recognition (NOR) test in Poly(I:C) and LPS mouse models
Shown are studies published before the year 2021 investigating Novel Object Recognition (NOR) in Poly(I:C) and LPS mouse models. The findings are categorized as no difference in behavior (≈), behavioural deficits (↓) meaning a reduction in novel object recognition memory or behavioural improvements (↑) meaning an increase in novel object recognition memory compared to controls.

Species	Substance	Authors	Year	Strain	LPS Serotype / Poly(I:C) MW	Dose	Route	Timing [GD]	Age [PD]	Findings	Session Time [min]	Retention Interval	Comments
Mouse	Poly(I:C)	Ozawa *et al.*	2006	BALB/c	-	5.0 mg/kg	i.p.	12-17	35 63-70	≈ / ≈ ↓ / ≈	5	1 h / 24 h	
		Ito *et al.*	2010	C57BL/6J	-	20 mg/kg	i.p.	12.5	42-77	↑	5	5 min	Exluded PolyIC litters which PPI did not differ from controls; Used 'percent nose pokes per novel object' as dependent variable
		Lipina *et al.*	2013	C57BL/6J	-	2.5 mg/kg 5 mg/kg	i.v.	9	-	≈ / ≈ ↓ / ≈	5	2 min	Spatial- / Object-recognition
		Li *et al.*	2014	C57BL/6J	-	20 mg/kg	i.p.	9.5	>60	↓	8	10 min	
		Fujita, Ishima & Hashimoto	2016	ddY	-	5 mg/kg	i.p.	12-17	30 70-84	↓ ↓	5	24 h	
		Han *et al.*	2016	ddY	-	5 mg/kg	i.p.	12-17	28 70-84	↓ ↓	5	24 h	
		Han *et al.*	2017	ddY	-	5 mg/kg	i.p.	12-17	70-84	↓	5	24 h	
		Richetto *et al.*	2017	C57BL6/N	-	5 mg/kg	i.v.	9 17	100	≈ ↓	2	1 min	Y-maze Spatial recognition
		Matsuura *et al.*	2018	ddY	-	5 mg/kg	i.p.	12-15	34-45 76-77	↓ ↓	5	24 h	
		Morais *et al.*	2018	C57BL/6J Swiss	-	20 mg/kg	i.p.	12.5	70	≈ ≈	10	24 h	
		Dabbah-Assadi *et al.*	2019	CD-1	-	5 mg/kg	i.p.	12.5 17.5	Adolescence / Adulthood	≈ / ≈ ≈ / (↓)	5	5 min	Adult female GD 17.5 offspring deficits
		Sheu *et al.*	2019	C57BL/6	-	5 mg/kg	i.v.	17	42 63 84	≈ ↓ ↓	5	30 min	Spatial recognition
	LPS	Golan *et al.*	2005	C57BL/6	-	120 µg/kg	i.p.	17	Adulthood	↑	15	24 h	
		Coyle *et al.*	2009	C57BL/6J	0111:B4	300 µg/kg	s.c.	8	86	↓	3	15 min	

Table 30: Overview of published studies utilizing the novel object recognition (NOR) test in Poly(I:C) and LPS rat models
Shown are studies published before the year 2021 investigating Novel Object Recognition (NOR) in Poly(I:C) and LPS rat models. The findings are categorized as no difference in behavior (≈), behavioural deficits (↓) meaning a reduction in novel object recognition memory or behavioural improvements (↑) meaning an increase in novel object recognition memory compared to controls.

Species	Substance	Authors	Year	Strain	LPS Serotype / Poly(I:C) MW	Dose	Route	Injection [GD]	Age [PD]	Findings	Session Time [min]	Retention Interval	Comments
Rat	Poly(I:C)	Wolff, Cheyne & Bilkey	2011	Sprague-Dawley	-	4 mg/kg	i.v.	15	>90	↓	5	30 min	2 Trial-phases per day for 3 days; Test phase on final trial of 3rd day
		Howland, Cazakoff, Zhang	2012	Long-Evans	high MW	4 mg/kg	i.v.	15	60-90	≈ / ≈ / ↓	4	24 h	Object - / Spatial- / Object-in-Place recognition
		Ballendine *et al.*	2015	Long-Evans	high MW	4 mg/kg	i.v.	15	60-80	↓	5	1 h	Object-in-Place recognition
		Vernon *et al.*	2015	Sprague-Dawley	-	4 mg/kg	i.v.	15	170	↓	5	24 h	
		Luchicchi *et al.*	2016	Sprague-Dawley	-	4 mg/kg	i.v.	15	60-90	↓	3	1 h	
		Osborne *et al.*	2017	Sprague-Dawley	-	4 mg/kg	i.v.	15	72	↓	3	1 h	
		Gray *et al.*	2019	Wistar	-	5 mg/kg	i.v.	14	>70	≈ ↓	5	15 min 4 h	PolyIC offspring deficits in pooled data (m+f & 15m+4h)
	LPS	Graciarena *et al.*	2010	Wistar	0111:B4	500 µg/kg	s.c.	14, 16, 18, 20	60?	≈ ↓	5	1 min 3 h	
		Foley *et al.*	2014	Long-Evans	0111:B4	50 µg/kg	s.c.	12	43	≈	5	2 min	
		Harvey & Boksa	2014	Sprague-Dawley	0111:B4	50 µg/kg	i.p.	15-16	54-58	≈	3	1 h	
		Wischhof *et al.*	2015	Wistar	0111:B4	100 µg/kg	i.p.	15-16	70	↓	3	30 min	
		Kentner *et al.*	2016	Sprague-Dawley	026:B6	100 µg/kg	i.p.	15	~92	↓	5	1 h	Object-in-Place recognition
		Delattre *et al.*	2017	Wistar	026:B6	1 mg/kg	i.p.	11	23-24 101-102	↓ / ↓ - / ≈	5	24 h	4 sample phases (3min each) separated by 15 min Object - / Object-in-Place recognition
		Simões *et al.*	2018	Wistar	055:B5	250 µg/kg	i.p.	15	62	↓	5	24 h	
		Swanepoel *et al.*	2018	Sprague-Dawley	-	100 µg/kg	s.c.	15-16	63	≈	5	1.5 h	

6.1.4. PPI

Table 31: Overview of published studies utilizing the prepulse inhibition (PPI) test in Poly(I:C) and LPS mouse models
Shown are studies published before the year 2021 investigating prepulse inhibition (PPI) in Poly(I:C) and LPS mouse models. The findings are categorized as no difference in behavior (≈), a reduction in PPI (↓) or an increase in PPI (↑) compared to controls. For those studies where more than one prepulse-pulse interval (PP-P ISI) or prepulse volume (PP above background (BG) noise) was used, but only some of those showed statistically significant differences, the statistically significant parameters were marked in red.

Species	Substance	Authors	Year	Strain	LPS Serotype / Poly(I:C) MW	Dose	Route	Timing [GD]	Age [PD]	Findings	PP-P ISI [ms]	PP [dB] above BG (PP [dB])	Comments
Mouse	Poly(I:C)	Shi *et al.*	2003	BALB/c	-	2.5 mg/kg 5 mg/kg 10 mg/kg 20 mg/kg	i.p.	9.5	46-56	- - ≈ ↓	100	+3dB(68) +5dB(70) +10dB(75) +15dB(80)	
		Meyer *et al.*	2005	C57BL6/J	-	2.5 mg/kg 5.0 mg/kg 10.0 mg/kg	i.v.	9	~100	≈ ↓ ↓	100	+4dB(69) +8dB(73) +12dB(77) +16dB(81) +20dB(85)	
		Ozawa *et al.*	2006	BALB/c	-	5 mg/kg	i.p.	12-17	35 63-70	≈ ↓	100	+3dB(68) +6dB(71) +10dB(75) +15dB(80)	
		Smith *et al.*	2007	C57BL/6J	-	20 mg/kg	i.p.	12	-	↓	-	+5dB(74) +15dB(84)	
		Makinodan *et al.*	2008	C57BL/6	-	60 mg/kg	i.p.	9.5	63	↓	50	+15dB(85)	
		Meyer *et al.*	2008a	C57BL6/J	-	5 mg/kg	i.v.	9 17	~100	↓ ≈	100	+4dB(69) +8dB(73) +12dB(77) +16dB(81) +20dB(85)	
		Meyer *et al.*	2008b	FVB	-	2 mg/kg	i.v.	9	105	↓	-	+4dB(69) +8dB(73) +12dB(77) +16dB(81) +20dB(85)	

		Li *et al.*	2009	C57BL6/N	-	5 mg/kg	i.v.	9 17	91	↓ ≈	100	+6dB(71) +12dB(77) +18dB(83)	Effect depends on startle pulse intensitiy
		Cardon *et al.*	2010	C57BL/6	-	4 mg/kg	i.v.	15	- (adult)	↓	100	+4dB(69) +8dB(73) +12dB(78) +16dB(81)	
		de Miranda *et al.*	2010	C57BL/6	-	5 mg/kg	i.p.	16	~110	↓	100	+2dB(62) +4dB(64) +8dB(68) +16dB(76)	
		Meyer *et al.*	2010	C57BL/6	-	2 mg/kg	i.v.	9	>90	↓	100	+6dB(71) +12dB(77) +18dB(83)	
		Vuillermot *et al.*	2010	C57BL/6J	-	5 mg/kg	i.v.	9	35 70	≈ ↓	100	+6dB(71) +12dB(77) +18dB(83)	Effect depends on startle pulse intensitiy
		Vuillermot, Feldon & Meyer	2011	C57BL/6	-	5 mg/kg	i.v.	9	>70	↓	100	+6dB(71) +12dB(77) +18dB(83)	Effect depends on startle pulse intensitiy
		Deslauriers *et al.*	2013	C57BL/6	-	20 mg/kg	i.p.	12	36	≈/(↓)	100	+4dB(75) +8dB(79) +12dB(83) +16dB(87)	Text states PPI deficits in Poly(I:C) offspring, which is not reflected in the figures; Offspring of a 2-hit model (Poly(I:C) + restraint stress) show deficits in PPI
		Giovanoli *et al.*	2013	C57BL/6	-	1 mg/kg	i.v.	9	41-45 70-110	≈ ≈	-	+4dB(69) +8dB(73) +12dB(77) +16dB(81) +20dB(85)	Offspring of a 2-hit model (Poly(I:C) + stress battery) show deficits in PPI
		Lipina *et al.*	2013	C57BL/6	-	2.5 mg/kg 5 mg/kg	i.v.	9	56 / 112	≈ / ≈ ≈ / ↓	100	-(69) -(73) -(81)	5mg/kg Poly(I:C) offspring PPI deficits as adults
		Deslauriers *et al.*	2014	C57BL/6	-	20 mg/kg	i.p.	12	36	- / (↓)	100	+4dB(75) +8dB(79) +12dB(83) +16dB(87)	Offspring of a 2-hit model (Poly(I:C) + restraint stress) show deficits in PPI; Poly(I:C) without restraint stress not tested
		O'Leary *et al.*	2014	C57BL/6	-	5 mg/kg	i.p.	9	90-135	↓	100	+4dB(69) +8dB(73) +16dB(81)	Effect depends on startle pulse intensitiy; Poly(I:C) offspring shows increased PPI compared to controls using lowest prepulse

		Zhu *et al.*	2014	C57BL/6	-	20 mg/kg	i.p.	9	60	↓	100	+6dB(74) +10dB(78) +14dB(82)	
		Zhang & van Praag	2015	C57BL/6J	-	5 mg/kg	i.p.	15	90	↓	120	+4dB(72) +8dB(76) +16dB(84)	
		Eßlinger *et al.*	2016	BALB/c	-	20 mg/kg	i.p.	9	30 100	≈ (↓)	100	+25dB(90)	Only female Poly(I:C) offspring shows PPI deficits as adults
		Giovanoli *et al.*	2016	C57BL/6J	-	1 mg/kg	i.v.	9	70-90	≈	100	+4dB(69) +8dB(73) +12dB(77) +16dB(81) +20dB(85)	Offspring of a 2-hit model (Poly(I:C) + stress battery) show deficits in PPI
		Gonzalez-Liencres *et al.*	2016	C57BL/6J	-	20 mg/kg	i.p.	9	50-55	↓	100	+5dB(70) +12dB(77) +18dB(83)	Poly(I:C) offspring shows prepulse facilitation using lowest prepulse
		Han *et al.*	2016	ddY	-	5 mg/kg	i.p.	12-17	28 70-84	≈ ↓	100	+4dB(69) +8dB(73) +12dB(77) +16dB(81)	
		Weber-Stadlbauer *et al.*	2016	C57BL6/N	-	5 mg/kg	i.v.	9	>70	↓	100	+6dB(71) +12dB(77) +18dB(83)	Effect depends on startle pulse intensitiy; Poly(I:C) F1 generation offspring shows PPI deficits, whereas F2 generation offspring does not
		Richetto *et al.*	2017	C57BL6/N	-	5 mg/kg	i.v.	9 17	100	↓ ≈	100	+4dB(69) +8dB(73) +12dB(77) +16dB(81) +20dB(85)	
		Luan *et al.*	2018	C57BL6/N	-	5.0 mg/kg	i.v.	9	>70	↓	-	+6dB(-) +12dB(-) +18dB(-)	Effect depends on startle pulse intensitiy
		Nakamura *et al.*	2019	C57BL/6	-	20 mg/kg	i.p.	17.5	84	↓	100	+8dB(78)	
	LPS	Imai *et al.*	2018	CD-1	055:B5	75 µg/kg	i.p.	17	~30	≈	100	+4dB(69) +8dB(73) +12dB(77) +16dB(81)	

Table 32: Overview of publishe studies utilizing the prepulse inhibition (PPI) test in Poly(I:C) and LPS rat models
Shown are studies published before the year 2021 investigating prepulse inhibition (PPI) in Poly(I:C) and LPS rat models. The findings are categorized as no difference in behavior (≈), a reduction in PPI (↓) or an increase in PPI (↑) compared to controls. For those studies where more than one prepulse-pulse interval (PP-P ISI) or prepulse volume (PP above background (BG) noise) was used, but only some of those showed statistically significant differences, the statistically significant parameters were marked in red.

Species	Substance	Authors	Year	Strain	LPS Serotype / Poly(I:C) MW	Dose	Route	Timing [GD]	Age [PD]		PP ISI [ms]	PPI	Commentary
Rat	Poly(I:C)	Wolff & Bilkey	2008	Sprague-Dawley	-	4 mg/kg	i.v.	15	34-35 >56	(↓) ↓	100	+4dB(72) +8dB(76) +12dB(80) +16dB(84)	Trend towards stat. sign. differences in between juvenile animals (with Poly(I:C) offspring showing prepulse facilitation at the lowest prepulse); Adult Poly(I:C) offspring shows PPI deficits
		Cardon *et al.*	2010	Lewis	-	4 mg/kg	i.v.	15	- (adult)	↓	100	+4dB(69) +8dB(73) +12dB(78) +16dB(81)	adult female Poly(I:C) offspring deficits
		Dickerson, Wolff, Bilkey	2010	Sprague-Dawley	-	4 mg/kg	i.v.	15	>90	↓	100	+12dB(80)	Authors measured PPI using +4/8/12/16dB prepulses, but only analyzed the +12dB data due to "best seperation between MIA and CTL animals"
		Wolff & Bilkey	2010	Sprague-Dawley	-	4 mg/kg	i.v.	15	35 90	↓ ↓	100	+4dB(72) +8dB(76) +12dB(80) +16dB(84)	
		Song *et al.*	2011	Sprague-Dawley	-	5 mg/kg	i.v.	9	90	↓	100	+2dB(72) +4dB(74) +8dB(78)	
		Yee *et al.*	2011	Sprague-Dawley	-	4 mg/kg	i.v.	15	68	↓	100	+4dB(72) +8dB(76) +12dB(80) +16dB(84)	
		Howland, Cazakoff, Zhang	2012	Long-Evans	high MW	4 mg/kg	i.v.	15	35 56	↓ ↓	30 50 80 140	+3dB(73) +6dB(76) +12dB(82)	Prepulse facilitation was observed using 30ms ISI

		Maayan *et al.*	2012	Wistar	-	4 mg/kg	i.v.	15	90	↓	100	+4dB(72) +8dB(76) +12dB(80) +16dB(84)	
		Vorhees *et al.*	2012	Sprague-Dawley	-	8 mg/kg	i.p.	14	67	≈ (↓)	100	+3dB(73) +5dB(75) +10dB(80)	No significant treatment effects or interactions in ANOVA; Authors nonetheless state sig. effects in adult female Poly(I:C) offspring
		Mattei *et al.*	2014	Wistar	-	4 mg/kg	i.v.	15	90-98	↓	100	+4dB(64) +8dB(68) +12dB(72)	
		Missault *et al.*	2014	Wistar	-	4 mg/kg	s.c.	15	76-79	≈	100	+5dB(70) +10dB(75) +15dB(80)	
		Van den Eynde *et al.*	2014	Sprague-Dawley	-	4 mg/kg	i.v.	15	56 90 180	≈ ≈ ≈	100	+4dB(69) +10dB(75) +16dB(81)	
		Ballendine *et al.*	2015	Long-Evans	high MW	4 mg/kg	i.v.	15	35-36 56-57	↓ (↓)	30 50 80 140	+3dB(73) +6dB(76) +12dB(82)	Poly(I:C) offspring show stat. sig. differences in PPI as juveniles (PD36); Only a trend towards stat. sign. differences was observed in late adolescence (PD57)
		Vorhees *et al.*	2015	Sprague-Dawley	-	8 mg/kg	i.p.	14-18	67	(↑) / ≈	100	+3dB(73) +5dB(75) +10dB(80)	Offspring from low weight gain Poly(I:C) dams show a trend towards increased PPI compared to controls; Offspring from high weight gain Poly(I:C) dams show no differences to controls
		Luchicchi *et al.*	2016	Sprague-Dawley	-	4 mg/kg	i.v.	15	60-90	↓	100	+4dB(74) +8dB(78) +16dB(86)	
		Meehan *et al.*	2017	Wistar	-	4 mg/kg	i.v.	10 19	70-84	↓ ↓	8 16 32 64 128 256	+4dB(74) +8dB(78) +16dB(86)	
		Li *et al.*	2018	Sprague-Dawley	-	10 mg/kg	i.v.	9	>56	↓	100	+2dB(72) +4dB(74) +8dB(78)	
		Lins *et al.*	2018	Sprague-Dawley	high MW	4 mg/kg	i.v.	15	56-105	≈	30 80	+3dB(73) +6dB(76) +12dB(82)	Offspring of both treatment groups show prepulse facilitation using 30ms ISI and the two lower prepulses

		De Felice *et al.*	2019	Sprague-Dawley	-	4 mg/kg	i.v.	15	60-70	↓	100	+4dB(74) +8dB(78) +16dB(86)	
		Ding *et al.*	2019	Sprague-Dawley	-	10 mg/kg	i.v.	9 40 60	40 60	≈ ↓	100	+5dB(75) +10dB(80) +15dB(85)	
		Gray *et al.*	2019	Wistar	-	5 mg/kg	i.v.	14	>70	≈	50 100	+4dB(74) +8dB(78) +16dB(86)	
		Gogos *et al.*	2020	Long-Evans	-	4 mg/kg	i.v.	15	-	↓	100	+2dB(72) +4dB(74) +8dB(78) +12dB(82) +16dB(86)	
		Fortier, Luheshi & Boksa	2007	Sprague-Dawley	0111:B4	PolyIC: 750 µg/kg 1 mg/kg / LPS: 25 µg/kg 50 µg/kg 100 µg/kg	i.p.	10-11 15-16 18-19	70	≈ / ≈ ↓ / ≈ ↓ / ≈	100	+4dB(69) +8dB(73) +12dB(77)	
	LPS	Borrell *et al.*	2002	Wistar	026:B6	1 mg/kg	s.c.	1-21 every 2nd day	60 100 300	↓ ↓ ↓	100	+10dB(55)	
		Fortier *et al.*	2004	Sprague-Dawley	0128:B12	50 µg/kg	i.p.	18-19	70	≈	100	+3dB(73) +6dB(76) +9dB(79) +12dB(82) +15dB(85)	
		Romero *et al.*	2007	Wistar	026:B6	2 mg/kg	s.c.	1-21	~180	↓	100	+10dB(56)	
		Romero *et al.*	2010	Wistar	026:B6	2 mg/kg	s.c.	1-21	28 35 70 170 400	≈ ↓ ↓ ↓ ↓	100	+6dB(52) +12dB(58)	

		Basta-Kaim *et al.*	2011b	Wistar	026:B6	1 mg/kg	s.c.	7-21 every 2nd day	90	↓	100	+6dB(71) +9dB(74) +12dB(77)	
		Basta-Kaim *et al.*	2011a	Wistar	026:B6	1 mg/kg	s.c.	7-21 every 2nd day	30 90	≈ ↓	100	+6dB(71) +9dB(74) +12dB(77)	
		Basta-Kaim *et al.*	2012	Wistar	026:B6	1 mg/kg	s.c.	7-21 every 2nd day	30 90	≈ ↓	100	+6dB(71) +9dB(74) +12dB(77)	
		Harvey & Boksa	2014	Sprague-Dawley	0111:B4	50 µg/kg	i.p.	15-16	64-67	≈	100	+4dB(69) +8dB(73) +12dB(77)	
		Basta-Kaim *et al.*	2015	Wistar	026:B6	1 mg/kg	s.c.	7-21 every 2nd day	90	↓	100	+6dB(71) +9dB(74) +12dB(77)	
		Wischhof et al.	2015b	Wistar	0111:B4	100 µg/kg	i.p.	15-16	28 35 45 90	≈ ≈ ↓ ↓	30 50 100 120	+16dB(76)	
		Wischhof et al.	2015a	Wistar	0111:B4	100 µg/kg	i.p.	15-16	90-120	↓	30 100 240	+16dB(76)	
		Santos-Toscano *et al.*	2016	Sprague-Dawley	0111:B4	100 µg/kg	i.p.	15-16	72-77	↓	100 120	+4dB(69) +8dB(73) +12dB(77)	
		Waterhouse *et al.*	2016	Sprague-Dawley	0111:B4	0.5 mg/kg	s.c.	10-11 15-16 18-19	>110	↓ ≈ ≈	100	-(72) -(74) -(78) -(86)	
		Simões *et al.*	2018	Wistar	055:B5	250 µg/kg	i.p.	15	~60	≈	80	-(65) -(70) -(75)	
		Swanepoel *et al.*	2018	Sprague-Dawley	-	100 µg/kg	s.c.	15-16	64	↓	-	+4dB(72) +6/8dB(74/76) +12dB(80) +16dB(84)	
		Capellán *et al.*	2019	Sprague-Dawley	0111:B4	100 µg/kg	i.p.	15-16	70-73	≈	30 120	+4dB(69) +12dB(77)	Trials resulting in prepulse facilitation were excluded from analysis

6.2. Statistics

6.2.1. EPM

6.2.1.1. Time in Open Arms

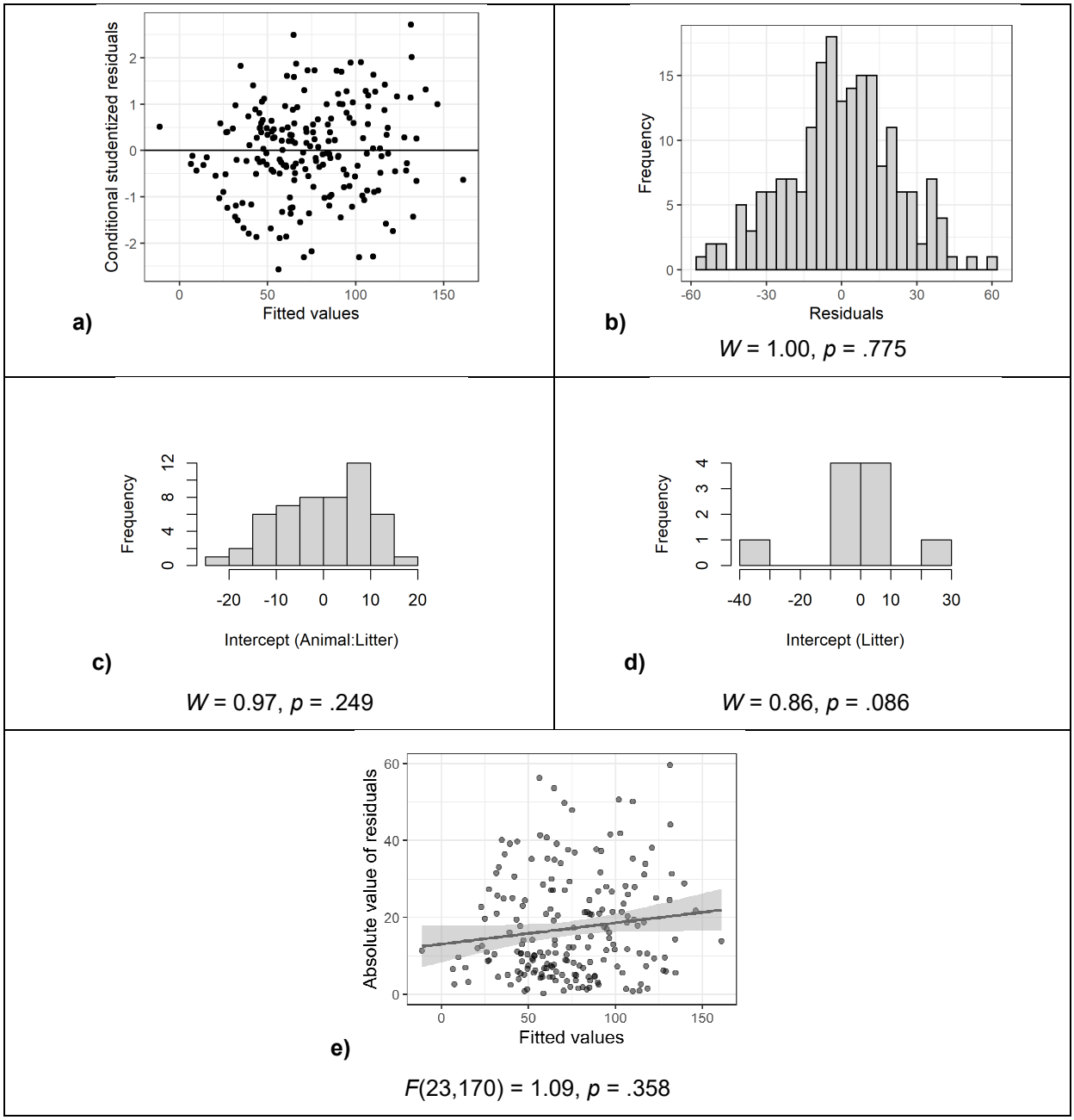

Figure 59: Inspection of model assumptions – EPM Test – Time in Open Arms excluding outliers

a) *Conditional (internally) studentized residuals*: All residuals fall within ±3 SD of the mean. **b)** *Histogram and Shapiro Wilk test of residuals*: The histogram appears approximately symmetric, and the Shapiro Wilk test is not significant (p=.775). **c)** *Histogram and Shapiro Wilk test of random intercepts for animal (nested under litter)*: The histogram appears approximately symmetric, and the Shapiro Wilk test is not significant (p=.249). **d)** *Histogram and Shapiro Wilk test of random intercepts for litter*: The histogram appears approximately symmetric, and the Shapiro Wilk test is not significant, with only a trend towards statistical significance (p=.086). **e)** *Spread-Location plot and Levene's test of residuals*: The S-L-plot shows approximately equal variation across the whole range of values, with a slight trend towards higher variation at higher values, and Levene's test is not significant (p=.358).

Model formula: Open_Arm_Time ~ Dose * Age + Scan + (1 | Litter/Animal)

Table 33: ANOVA-like table for random effects of the LMM of the EPM Open Arm Time data after outlier removal
Shown are the number of model parameters (n par), the log-likelihood (logLik), Akaike information criterion (AIC), likelihood ratio test (LRT), degrees of freedom (df) and p-value for single term deletions of the random effects of the LMM of the EPM Open Arm Time data after outlier removal. Both Animal nested under Litter (p = .001) as well as the random effect of Litter (p = .000) are statistically significant.

	n par	*logLik*	*AIC*	*LRT*	*df*	*p*
<none>	16	-878.14	1788.28	NA	NA	NA
(1 | Animal:Litter)	15	-883.60	1797.20	10.92	1.00	**.001** ***
(1 | Litter)	15	-887.65	1805.30	19.01	1.00	**.000** ***

Table 34: Post hoc multiple comparisons of EPM Open Arm Time data - simple pair-wise t-tests for 'Dose' after outlier removal
Shown are the estimates and standard error (SE) of simple pair-wise t-tests for the contrast LPS dose [µg/kg], including degrees of freedom (df), t ratio, p-values corrected for multiple comparisons using the Tukey method (p) as well as uncorrected p-values (p uncorr) and 95% confidence intervals. Both before and after Tukey adjustment, no contrast shows statistical significance.

Contrast LPS dose [µg/kg]	Age [PD]	*Estimate*	*SE*	*df*	*t ratio*	*p*	*p uncorr*	*95% Confidence Interval*	
								Lower CL	*Upper CL*
0 - 20	~30	22.68	16.05	10.63	1.41	.369	*.186*	-12.79	58.16
0 - 100	~30	3.45	25.04	8.94	0.14	.990	*.893*	-53.26	60.16
20 - 100	~30	-19.23	25.72	9.15	-0.75	.742	*.473*	-77.28	38.81
0 - 20	~45	11.12	16.05	10.63	0.69	.772	*.503*	-24.35	46.59
0 - 100	~45	-15.40	25.04	8.94	-0.62	.816	*.554*	-72.11	41.30
20 - 100	~45	-26.52	25.72	9.15	-1.03	.577	*.329*	-84.57	31.52
0 - 20	~66	18.58	16.05	10.63	1.16	.502	*.272*	-16.89	54.05
0 - 100	~66	-20.82	25.04	8.94	-0.83	.694	*.427*	-77.52	35.89
20 - 100	~66	-39.40	25.72	9.15	-1.53	.322	*.159*	-97.44	18.65
0 - 20	~94	7.95	16.71	12.46	0.48	.884	*.643*	-28.32	44.22
0 - 100	~94	5.64	25.45	9.54	0.22	.973	*.829*	-51.44	62.73
20 - 100	~94	-2.31	26.41	10.15	-0.09	.996	*.932*	-61.03	56.42

Table 35: Post hoc multiple comparisons of EPM Open Arm Time data - simple pair-wise t-tests for 'Age' after outlier removal
Shown are the estimates and standard error (SE) of simple pair-wise t-tests for the contrast Age [PD], including degrees of freedom (df), t ratio, p-values corrected for multiple comparisons using the Tukey method (p) as well as uncorrected p-values (p uncorr) and 95% confidence intervals. After Tukey adjustment, in the control group all contrasts are statistically significant (usually p = .000), except the ~30-~66 PD contrast. The same holds true for the 20 µg/kg LPS group, except that in this group the ~45-~66 PD contrast shows no statistical significance in addition to the ~30-~66 PD contrast as well. In the 100 µg/kg LPS group however, only the ~45-~94 PD contrast is statistically significant (p = .005), and the ~45-~66 PD contrast shows a trend towards statistical significance (p = .096). Without Tukey adjustment, the ~30-~94 PD and the ~45-~66 PD contrast are statistically significant in the 100 µg/kg LPS group as well (p = .046 / .021). In the 20 µg/kg LPS group, the 45-~66 PD contrast also gets statistically significant (p = .028), while in the control group the ~30-~66 PD contrast shows a trend towards statistical significance without Tukey adjustment (p = .065).

Contrast Age [PD]	LPS dose [µg/kg]	*Estimate*	*SE*	*df*	*t ratio*	*p*	*p uncorr*	*95% Confidence Interval*	
								Lower CL	*Upper CL*
~30 - ~45	0	37.88	6.91	133.46	5.48	**.000** ***	*.000* ***	24.22	51.55
~30 - ~66	0	12.87	6.91	133.46	1.86	.249	*.065* .	-0.80	26.53
~30 - ~94	0	-29.72	7.19	135.50	-4.14	**.000** ***	*.000* ***	-43.93	-15.51
~45 - ~66	0	-25.02	6.91	133.46	-3.62	**.002** **	*.000* ***	-38.68	-11.35
~45 - ~94	0	-67.60	7.19	135.50	-9.41	**.000** ***	*.000* ***	-81.82	-53.39
~66 - ~94	0	-42.59	7.19	135.50	-5.93	**.000** ***	*.000* ***	-56.80	-28.37
~30 - ~45	20	26.32	7.92	133.46	3.32	**.006** **	*.001* ***	10.65	42.00
~30 - ~66	20	8.76	7.92	133.46	1.11	.687	*.271*	-6.91	24.44
~30 - ~94	20	-44.46	8.93	140.70	-4.98	**.000** ***	*.000* ***	-62.11	-26.80
~45 - ~66	20	-17.56	7.92	133.46	-2.22	.124	*.028* *	-33.24	-1.89
~45 - ~94	20	-70.78	8.93	140.70	-7.93	**.000** ***	*.000* ***	-88.43	-53.12
~66 - ~94	20	-53.22	8.93	140.70	-5.96	**.000** ***	*.000* ***	-70.87	-35.56
~30 - ~45	100	19.03	13.06	133.46	1.46	.466	*.147*	-6.79	44.86
~30 - ~66	100	-11.40	13.06	133.46	-0.87	.819	*.384*	-37.23	14.42
~30 - ~94	100	-27.53	13.68	136.49	-2.01	.188	*.046* *	-54.57	-0.48
~45 - ~66	100	-30.43	13.06	133.46	-2.33	**.096** .	*.021* *	-56.26	-4.61
~45 - ~94	100	-46.56	13.68	136.49	-3.40	**.005** **	*.001* ***	-73.61	-19.51
~66 - ~94	100	-16.13	13.68	136.49	-1.18	.641	*.240*	-43.17	10.92

6.2.1.2. Time in Center

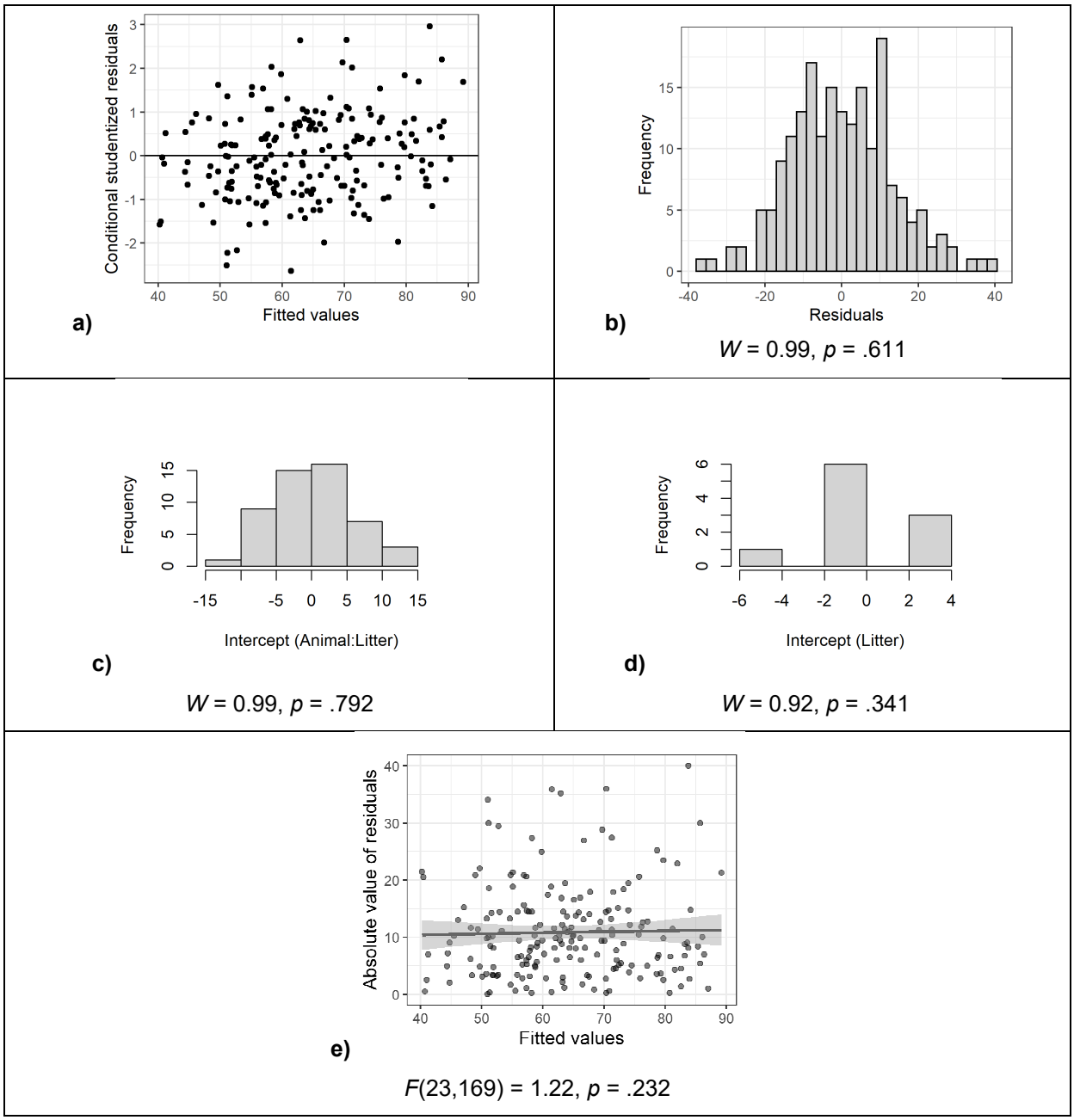

Figure 60: Inspection of model assumptions – EPM Test – Time in Center excluding outliers
a) *Conditional (internally) studentized residuals*: All residuals fall within ±3 SD of the mean. **b)** *Histogram and Shapiro Wilk test of residuals*: The histogram appears approximately symmetric, and the Shapiro Wilk test is not significant (p=.611). **c)** *Histogram and Shapiro Wilk test of random intercepts for animal (nested under litter)*: The histogram appears approximately symmetric, and the Shapiro Wilk test is not significant (p=.792). **d)** *Histogram and Shapiro Wilk test of random intercepts for litter*: The histogram appears approximately symmetric, and the Shapiro Wilk test is not significant (p=.341). **e)** *Spread-Location plot and Levene's test of residuals*: The S-L-plot shows approximately equal variation across the whole range of values, and Levene's test is not significant (p=.232).

Model formula: Center_Square_Time ~ Dose * Age + Scan + (1 | Litter/Animal)

Table 36: ANOVA-like table for random effects of the LMM of the EPM Center Square Time data after outlier removal
Shown are the number of model parameters (n par), the log-likelihood (logLik), Akaike information criterion (AIC), likelihood ratio test (LRT), degrees of freedom (df) and p-value for single term deletions of the random effects of the LMM of the EPM Center Square Time data after outlier removal. Animal nested under Litter is statistically significant (p = .001).

	n par	*logLik*	*AIC*	*LRT*	*df*	*p*
<none>	16	-781.74	1595.49	NA	NA	NA
(1 | Animal:Litter)	15	-787.31	1604.63	11.14	1.00	**.001** ***
(1 | Litter)	15	-782.35	1594.70	1.21	1.00	.270

Table 37: Post hoc multiple comparisons of EPM Center Square Time data - simple pair-wise t-tests for 'Dose' after outlier removal
Shown are the estimates and standard error (SE) of simple pair-wise t-tests for the contrast LPS dose [µg/kg], including degrees of freedom (df), t ratio, p-values corrected for multiple comparisons using the Tukey method (p) as well as uncorrected p-values (p uncorr) and 95% confidence intervals. After Tukey adjustment, the 0-100 and 20-100 contrasts on PD ~45 show statistical significance (p = .022 / .029), and the 20-100 contrast on PD ~30 as well as the 0-100 and 20-100 contrasts on PD ~94 show a trend towards statistical significance (p = .055 / .070 / .067). Without Tukey adjustment, the latter trends turn into statistical significance (p = .022 / .028 / .027).

Contrast LPS dose [µg/kg]	Age [PD]	*Estimate*	*SE*	*df*	*t ratio*	*p*	*p uncorr*	*95% Confidence Interval*	
								Lower CL	*Upper CL*
0 - 20	~30	6.70	6.07	22.56	1.10	.522	*.282*	-5.88	19.27
0 - 100	~30	-16.37	8.82	15.57	-1.86	.184	*.082* .	-35.10	2.36
20 - 100	~30	-23.07	9.13	16.03	-2.53	**.055** .	*.022* *	-42.43	-3.71
0 - 20	~45	-0.46	6.11	23.01	-0.08	.997	*.941*	-13.09	12.18
0 - 100	~45	-26.49	8.85	15.75	-2.99	**.022** *	*.009* **	-45.26	-7.71
20 - 100	~45	-26.03	9.13	16.03	-2.85	**.029** *	*.012* *	-45.39	-6.67
0 - 20	~66	-2.20	6.07	22.56	-0.36	.931	*.721*	-14.77	10.38
0 - 100	~66	-12.97	9.16	18.01	-1.42	.354	*.174*	-32.21	6.27
20 - 100	~66	-10.77	9.46	18.35	-1.14	.503	*.269*	-30.62	9.07
0 - 20	~94	1.32	6.61	29.98	0.20	.978	*.843*	-12.19	14.83
0 - 100	~94	-21.97	9.25	18.69	-2.37	**.070** .	*.028* *	-41.36	-2.59
20 - 100	~94	-23.29	9.78	20.53	-2.38	**.067** .	*.027* *	-43.66	-2.93

Table 38: Post hoc multiple comparisons of EPM Center Square Time data - simple pair-wise t-tests for 'Age' after outlier removal
Shown are the estimates and standard error (SE) of simple pair-wise t-tests for the contrast Age [PD], including degrees of freedom (df), t ratio, p-values corrected for multiple comparisons using the Tukey method (p) as well as uncorrected p-values (p uncorr) and 95% confidence intervals. After Tukey adjustment, in the control group the ~30-~66 PD and ~45-~66 PD contrasts are statistically significant (p = .034 / .023). In the 20 µg/kg LPS group, the same holds true (p = .000 / .022), but in addition the ~30-~94 PD contrast shows a trend towards statistical significance (p = .094). In the 100 µg/kg LPS group no contrast shows statistical significance. Without Tukey adjustment, the ~45-~94 PD contrast in the control group also shows a trend towards statistical significance (p = .078), and the trend from the ~30-~94 PD contrast in the 20 µg/kg LPS group gets statistically significant (p = .021), while in the 100 µg/kg LPS group still no contrast shows statistical significance.

Contrast Age [PD]	LPS dose [µg/kg]	*Estimate*	*SE*	*df*	*t ratio*	*p*	*p uncorr*	*95% Confidence Interval*	
								Lower CL	*Upper CL*
~30 - ~45	0	0.76	4.32	135.07	0.18	.998	*.861*	-7.79	9.31
~30 - ~66	0	-11.74	4.27	134.32	-2.75	**.034** *	*.007* **	-20.19	-3.30
~30 - ~94	0	-7.22	4.44	136.56	-1.63	.368	*.106*	-16.00	1.56
~45 - ~66	0	-12.50	4.32	135.07	-2.89	**.023** *	*.004* **	-21.05	-3.95
~45 - ~94	0	-7.97	4.49	137.33	-1.77	.290	*.078* .	-16.86	0.91
~66 - ~94	0	4.53	4.44	136.56	1.02	.738	*.310*	-4.25	13.31
~30 - ~45	20	-6.40	4.90	134.32	-1.31	.560	*.194*	-16.09	3.29
~30 - ~66	20	-20.64	4.90	134.32	-4.21	**.000** ***	*.000* ***	-30.33	-10.95
~30 - ~94	20	-12.59	5.39	139.93	-2.34	**.094** .	*.021* *	-23.24	-1.94
~45 - ~66	20	-14.24	4.90	134.32	-2.91	**.022** *	*.004* **	-23.93	-4.55
~45 - ~94	20	-6.19	5.39	139.93	-1.15	.659	*.252*	-16.84	4.46
~66 - ~94	20	8.05	5.39	139.93	1.49	.444	*.137*	-2.60	18.70
~30 - ~45	100	-9.36	8.07	134.32	-1.16	.653	*.248*	-25.32	6.60
~30 - ~66	100	-8.34	8.45	137.38	-0.99	.757	*.325*	-25.06	8.37
~30 - ~94	100	-12.82	8.45	137.34	-1.52	.431	*.132*	-29.53	3.90
~45 - ~66	100	1.01	8.45	137.38	0.12	.999	*.905*	-15.70	17.73
~45 - ~94	100	-3.46	8.45	137.34	-0.41	.977	*.683*	-20.17	13.26
~66 - ~94	100	-4.47	8.84	140.97	-0.51	.958	*.614*	-21.95	13.01

6.2.1.3. Head Dips

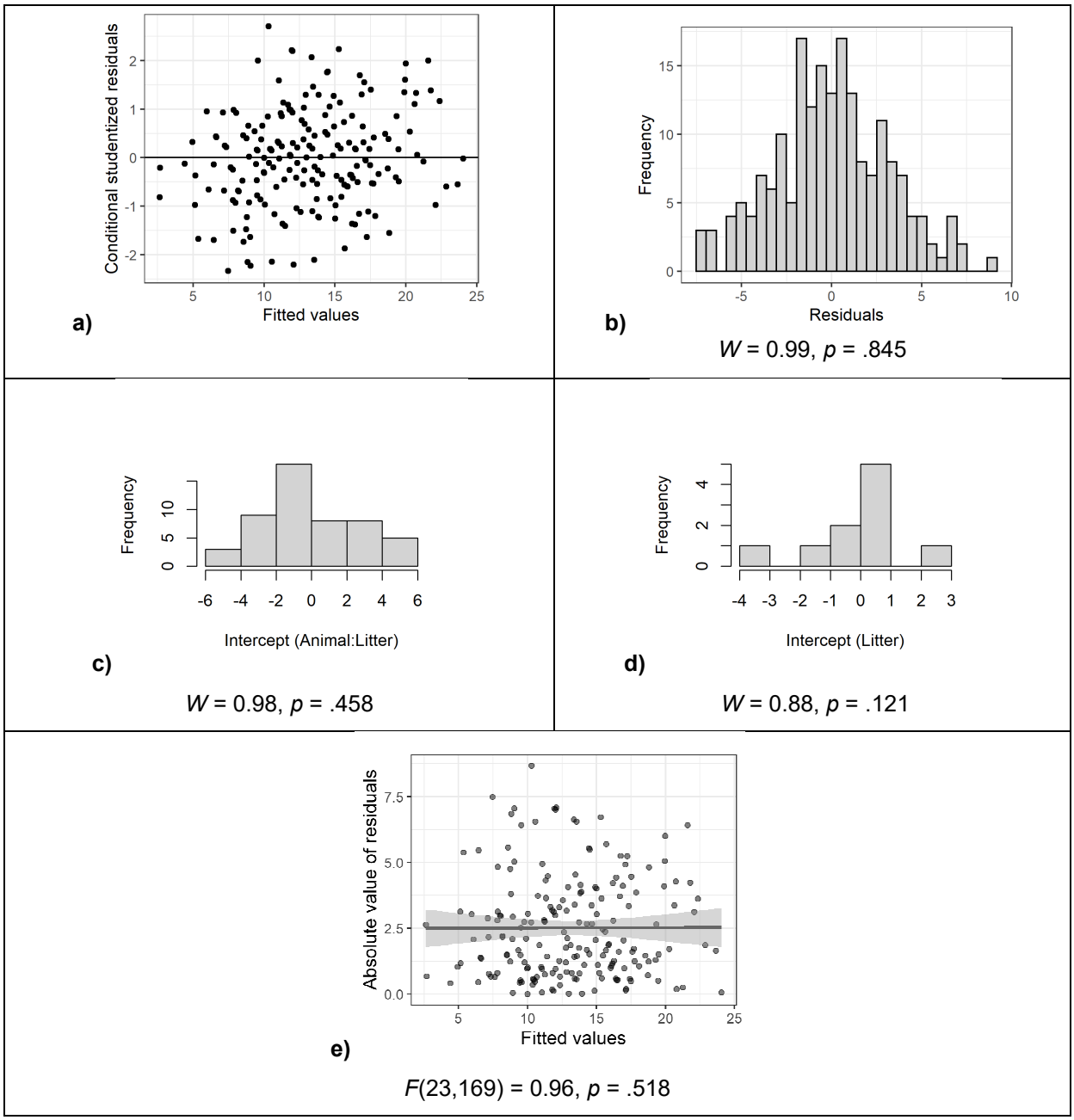

Figure 61: Inspection of model assumptions – EPM Test – Head Dips excluding outliers
a) *Conditional (internally) studentized residuals*: All residuals fall within ±3 SD of the mean. **b)** *Histogram and Shapiro Wilk test of residuals*: The histogram appears approximately symmetric, and the Shapiro Wilk test is not significant (p=.845). **c)** *Histogram and Shapiro Wilk test of random intercepts for animal (nested under litter)*: The histogram appears slightly skewed to the right, but the Shapiro Wilk test is not significant (p=.458). **d)** *Histogram and Shapiro Wilk test of random intercepts for litter*: The histogram appears slightly skewed to the left, but the Shapiro Wilk test is not significant (p=.121). **e)** *Spread-Location plot and Levene's test of residuals*: The S-L-plot shows approximately equal variation across the whole range of values, and Levene's test is not significant (p=.518).

Model formula: Head_Dips ~ Dose * Age + Scan + (1 | Litter/Animal)

Table 39: ANOVA-like table for random effects of the LMM of the EPM Head Dips data after outlier removal
Shown are the number of model parameters (n par), the log-likelihood (logLik), Akaike information criterion (AIC), likelihood ratio test (LRT), degrees of freedom (df) and p-value for single term deletions of the random effects of the LMM of the EPM Head Dips data after outlier removal. Animal nested under Litter as well as litter are statistically significant (p = .000 / .032).

	n par	*logLik*	*AIC*	*LRT*	*df*	*p*
<none>	16	-543.13	1118.26	NA	NA	NA
(1 | Animal:Litter)	15	-561.99	1153.98	37.73	1.00	**.000** ***
(1 | Litter)	15	-545.43	1120.85	4.60	1.00	**.032** *

Table 40: Post hoc multiple comparisons of EPM Head Dips data - simple pair-wise t-tests for 'Dose' after outlier removal
Shown are the estimates and standard error (SE) of simple pair-wise t-tests for the contrast LPS dose [µg/kg], including degrees of freedom (df), t ratio, p-values corrected for multiple comparisons using the Tukey method (p) as well as uncorrected p-values (p uncorr) and 95% confidence intervals. After Tukey adjustment, only the 0-20 contrast on PD ~30 shows a trend towards statistical significance (p = .092). Without Tukey adjustment, the latter trend turns into statistical significance (p = .040), and the 20-100 contrast on PD ~66 is statistically significant as well (p = .044).

Contrast LPS dose [µg/kg]	Age [PD]	*Estimate*	*SE*	*df*	*t ratio*	*p*	*p uncorr*	*95% Confidence Interval*	
								Lower CL	*Upper CL*
0 - 20	~30	4.89	2.13	12.54	2.30	**.093** .	*.040* *	0.27	9.51
0 - 100	~30	0.04	3.21	9.47	0.01	1.000	*.991*	-7.16	7.23
20 - 100	~30	-4.85	3.31	9.80	-1.47	.348	*.174*	-12.25	2.55
0 - 20	~45	1.74	2.13	12.54	0.82	.700	*.429*	-2.88	6.36
0 - 100	~45	-4.18	3.21	9.47	-1.30	.426	*.223*	-11.38	3.02
20 - 100	~45	-5.92	3.31	9.80	-1.79	.224	*.105*	-13.32	1.48
0 - 20	~66	2.55	2.15	12.87	1.19	.481	*.257*	-2.09	7.19
0 - 100	~66	-5.12	3.22	9.57	-1.59	.295	*.144*	-12.32	2.09
20 - 100	~66	-7.66	3.31	9.80	-2.31	.101	*.044* *	-15.06	-0.27
0 - 20	~94	3.54	2.23	14.89	1.59	.281	*.133*	-1.22	8.29
0 - 100	~94	-1.31	3.28	10.39	-0.40	.917	*.698*	-8.59	5.96
20 - 100	~94	-4.85	3.43	11.16	-1.42	.366	*.184*	-12.38	2.68

Table 41: Post hoc multiple comparisons of EPM Head Dips data - simple pair-wise t-tests for 'Age' after outlier removal
Shown are the estimates and standard error (SE) of simple pair-wise t-tests for the contrast Age [PD], including degrees of freedom (df), t ratio, p-values corrected for multiple comparisons using the Tukey method (p) as well as uncorrected p-values (p uncorr) and 95% confidence intervals. After Tukey adjustment, in the control group all contrasts are statistically significant (p < .050) or at least show a trend, except the ~30-~94 contrast. In the 20 µg/kg LPS group, only the ~45-~94 contrast is statistically significant (p = .012), while in the 100 µg/kg LPS group no contrast shows statistical significance. Without Tukey adjustment, the former trend in the control group ~turns into statistical significance (p = .021), and the ~30-~45 as well as the ~66-~94 contrast in the 20 µg/kh LPS group and the ~45-~66 contras in the 100 µg/kg LPS group show a trend towards statistical significance (p = .065 / .070 / .083).

Contrast Age [PD]	LPS dose [µg/kg]	*Estimate*	*SE*	*df*	*t ratio*	*p*	*p uncorr*	*95% Confidence Interval*	
								Lower CL	*Upper CL*
~30 - ~45	0	5.36	1.04	133.28	5.17	**.000** ***	*.000* ***	3.31	7.41
~30 - ~66	0	2.87	1.07	134.01	2.69	**.040** *	*.008* **	0.76	4.97
~30 - ~94	0	-0.53	1.08	134.54	-0.49	.961	*.625*	-2.67	1.61
~45 - ~66	0	-2.49	1.07	134.01	-2.34	**.094** .	*.021* *	-4.60	-0.39
~45 - ~94	0	-5.89	1.08	134.54	-5.45	**.000** ***	*.000* ***	-8.03	-3.75
~66 - ~94	0	-3.40	1.11	135.47	-3.06	**.014** *	*.003* **	-5.59	-1.20
~30 - ~45	20	2.21	1.19	133.28	1.86	.251	*.065* .	-0.14	4.56
~30 - ~66	20	0.53	1.19	133.28	0.44	.971	*.659*	-1.83	2.88
~30 - ~94	20	-1.88	1.32	136.55	-1.43	.484	*.155*	-4.48	0.72
~45 - ~66	20	-1.68	1.19	133.28	-1.42	.492	*.159*	-4.04	0.67
~45 - ~94	20	-4.09	1.32	136.55	-3.11	**.012** *	*.002* **	-6.69	-1.49
~66 - ~94	20	-2.41	1.32	136.55	-1.83	.264	*.070* .	-5.01	0.20
~30 - ~45	100	1.14	1.96	133.28	0.58	.937	*.561*	-2.73	5.02
~30 - ~66	100	-2.29	1.96	133.28	-1.17	.649	*.246*	-6.16	1.59
~30 - ~94	100	-1.88	2.06	135.05	-0.91	.799	*.364*	-5.95	2.20
~45 - ~66	100	-3.43	1.96	133.28	-1.75	.303	*.083* .	-7.31	0.45
~45 - ~94	100	-3.02	2.06	135.05	-1.47	.461	*.145*	-7.09	1.05
~66 - ~94	100	0.41	2.06	135.05	0.20	.997	*.843*	-3.66	4.48

6.2.1.4. Rearings

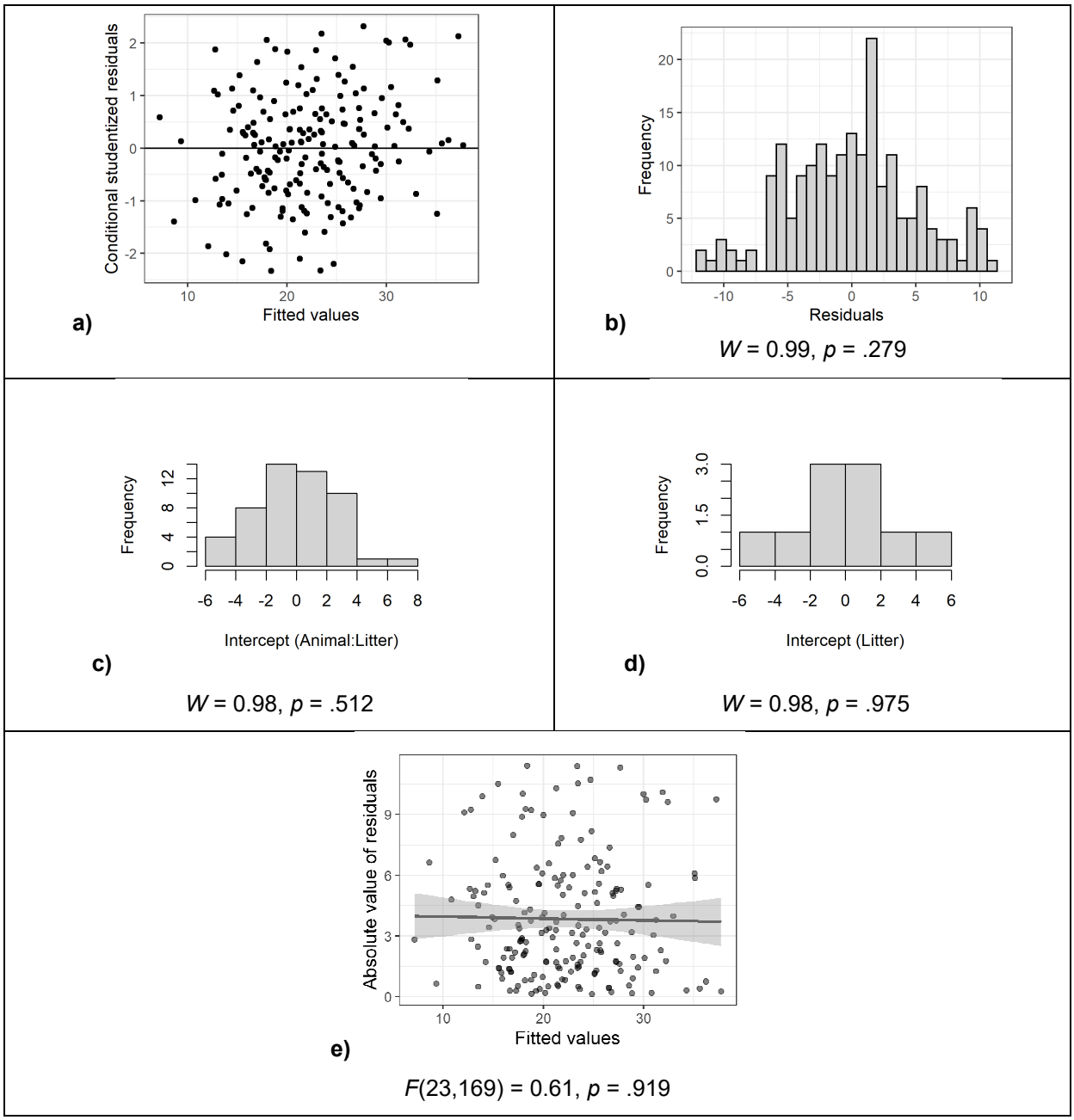

Figure 62: Inspection of model assumptions – EPM Test – Rearings excluding outliers
a) *Conditional (internally) studentized residuals*: All residuals fall within ±3 SD of the mean. **b)** *Histogram and Shapiro Wilk test of residuals*: The histogram appears approximately symmetric, and the Shapiro Wilk test is not significant (p=.279). **c)** *Histogram and Shapiro Wilk test of random intercepts for animal (nested under litter)*: The histogram appears slightly skewed to the right, but the Shapiro Wilk test is not significant (p=.512). **d)** *Histogram and Shapiro Wilk test of random intercepts for litter*: The histogram appears approximately symmetric, and the Shapiro Wilk test is not significant (p=.975). **e)** *Spread-Location plot and Levene's test of residuals*: The S-L-plot shows approximately equal variation across the whole range of values, and Levene's test is not significant (p=.919).

Model formula: Rearings ~ Dose * Age + Scan + (1 | Litter/Animal)

Table 42: ANOVA-like table for random effects of the LMM of the EPM Rearings data after outlier removal
Shown are the number of model parameters (n par), the log-likelihood (logLik), Akaike information criterion (AIC), likelihood ratio test (LRT), degrees of freedom (df) and p-value for single term deletions of the random effects of the LMM of the EPM Rearings data after outlier removal. Animal nested under Litter as well as litter are statistically significant (p = .000 / .010).

	n par	*logLik*	*AIC*	*LRT*	*df*	*p*
<none>	16	-607.15	1246.31	NA	NA	NA
(1 | Animal:Litter)	15	-615.50	1261.01	16.70	1.00	**.000** ***
(1 | Litter)	15	-610.50	1251.01	6.70	1.00	**.010** **

Table 43: Post hoc multiple comparisons of EPM Rearings data - simple pair-wise t-tests for 'Dose' after outlier removal
Shown are the estimates and standard error (SE) of simple pair-wise t-tests for the contrast LPS dose [µg/kg], including degrees of freedom (df), t ratio, p-values corrected for multiple comparisons using the Tukey method (p) as well as uncorrected p-values (p uncorr) and 95% confidence intervals. After Tukey adjustment, only the 20-100 contrast on PD ~45 shows a trend towards statistical significance (p = .072). Without Tukey adjustment, the latter trend turns into statistical significance (p = .031), and the 0-100 contrast on PD ~45 is statistically significant as well (p = .049).

Contrast LPS dose [µg/kg]	Age [PD]	*Estimate*	*SE*	*df*	*t ratio*	*p*	*p uncorr*	*95% Confidence Interval*	
								Lower CL	*Upper CL*
0 - 20	~30	2.02	3.08	11.43	0.66	.793	*.525*	-4.74	8.78
0 - 100	~30	0.32	4.70	8.89	0.07	.997	*.947*	-10.34	10.98
20 - 100	~30	-1.70	4.85	9.17	-0.35	.935	*.733*	-12.63	9.23
0 - 20	~45	1.69	3.11	11.83	0.54	.853	*.598*	-5.11	8.48
0 - 100	~45	-10.71	4.71	8.94	-2.27	.112	*.049* *	-21.37	-0.04
20 - 100	~45	-12.39	4.86	9.26	-2.55	**.072** .	*.031* *	-23.34	-1.45
0 - 20	~66	1.75	3.08	11.43	0.57	.839	*.581*	-5.00	8.51
0 - 100	~66	-1.16	4.70	8.89	-0.25	.967	*.811*	-11.82	9.50
20 - 100	~66	-2.91	4.85	9.17	-0.60	.823	*.562*	-13.84	8.02
0 - 20	~94	1.47	3.23	13.70	0.46	.893	*.656*	-5.48	8.42
0 - 100	~94	-6.67	4.81	9.76	-1.38	.385	*.197*	-17.43	4.10
20 - 100	~94	-8.14	5.02	10.48	-1.62	.279	*.134*	-19.24	2.97

Table 44: Post hoc multiple comparisons of EPM Rearings data - simple pair-wise t-tests for 'Age' after outlier removal
Shown are the estimates and standard error (SE) of simple pair-wise t-tests for the contrast Age [PD], including degrees of freedom (df), t ratio, p-values corrected for multiple comparisons using the Tukey method (p) as well as uncorrected p-values (p uncorr) and 95% confidence intervals. After Tukey adjustment, in the control group the ~30-~66, ~30-~94 and ~45-~66 contrasts are statistically significant (p < .023) and the ~66-~94 contrast shows a trend towards statistical significance (p = .087). In the 20 µg/kg LPS group, the ~30-~66, ~30-~94 and ~45-~66 contrasts are statistically significant as well (p < .043). In the 100 µg/kg LPS group, the first three time points show statistical significance (p < .005). Without Tukey adjustment, all except the first time points are statistically significant in the control group (p < .031), while in the 20 µg/kg LPS group all contrasts except for the first time point at least show a trend towards statistical significance (p < .072). In the 100 µg/kg LPS group, the first three time points show statistical significance (p < .001).

Contrast Age [PD]	LPS dose [µg/kg]	*Estimate*	*SE*	*df*	*t ratio*	*p*	*p uncorr*	*95% Confidence Interval*	
								Lower CL	*Upper CL*
~30 - ~45	0	-1.12	1.57	133.19	-0.71	.893	*.479*	-4.23	2.00
~30 - ~66	0	-8.52	1.55	132.57	-5.48	**.000** ***	*.000* ***	-11.59	-5.45
~30 - ~94	0	-4.68	1.62	134.36	-2.89	**.023** *	*.004* **	-7.88	-1.48
~45 - ~66	0	-7.40	1.57	133.19	-4.71	**.000** ***	*.000* ***	-10.52	-4.29
~45 - ~94	0	-3.56	1.64	135.13	-2.18	.135	*.031* *	-6.80	-0.33
~66 - ~94	0	3.84	1.62	134.36	2.38	**.087** .	*.019* *	0.64	7.04
~30 - ~45	20	-1.45	1.81	133.36	-0.80	.854	*.424*	-5.04	2.13
~30 - ~66	20	-8.79	1.78	132.57	-4.93	**.000** ***	*.000* ***	-12.31	-5.26
~30 - ~94	20	-5.23	1.96	137.40	-2.66	**.043** *	*.009* **	-9.11	-1.34
~45 - ~66	20	-7.34	1.81	133.36	-4.05	**.000** ***	*.000* ***	-10.92	-3.75
~45 - ~94	20	-3.78	1.99	138.72	-1.89	.236	*.060* .	-7.72	0.17
~66 - ~94	20	3.56	1.96	137.40	1.81	.272	*.072* .	-0.32	7.45
~30 - ~45	100	-12.14	2.94	132.57	-4.14	**.000** ***	*.000* ***	-17.95	-6.34
~30 - ~66	100	-10.00	2.94	132.57	-3.41	**.005** **	*.001* ***	-15.81	-4.19
~30 - ~94	100	-11.66	3.08	135.16	-3.79	**.001** ***	*.000* ***	-17.75	-5.58
~45 - ~66	100	2.14	2.94	132.57	0.73	.885	*.467*	-3.66	7.95
~45 - ~94	100	0.48	3.08	135.16	0.16	.999	*.877*	-5.61	6.57
~66 - ~94	100	-1.66	3.08	135.16	-0.54	.949	*.590*	-7.75	4.42

6.2.2. Sensitivity Analysis EPM

6.2.2.1. Time in Open Arms

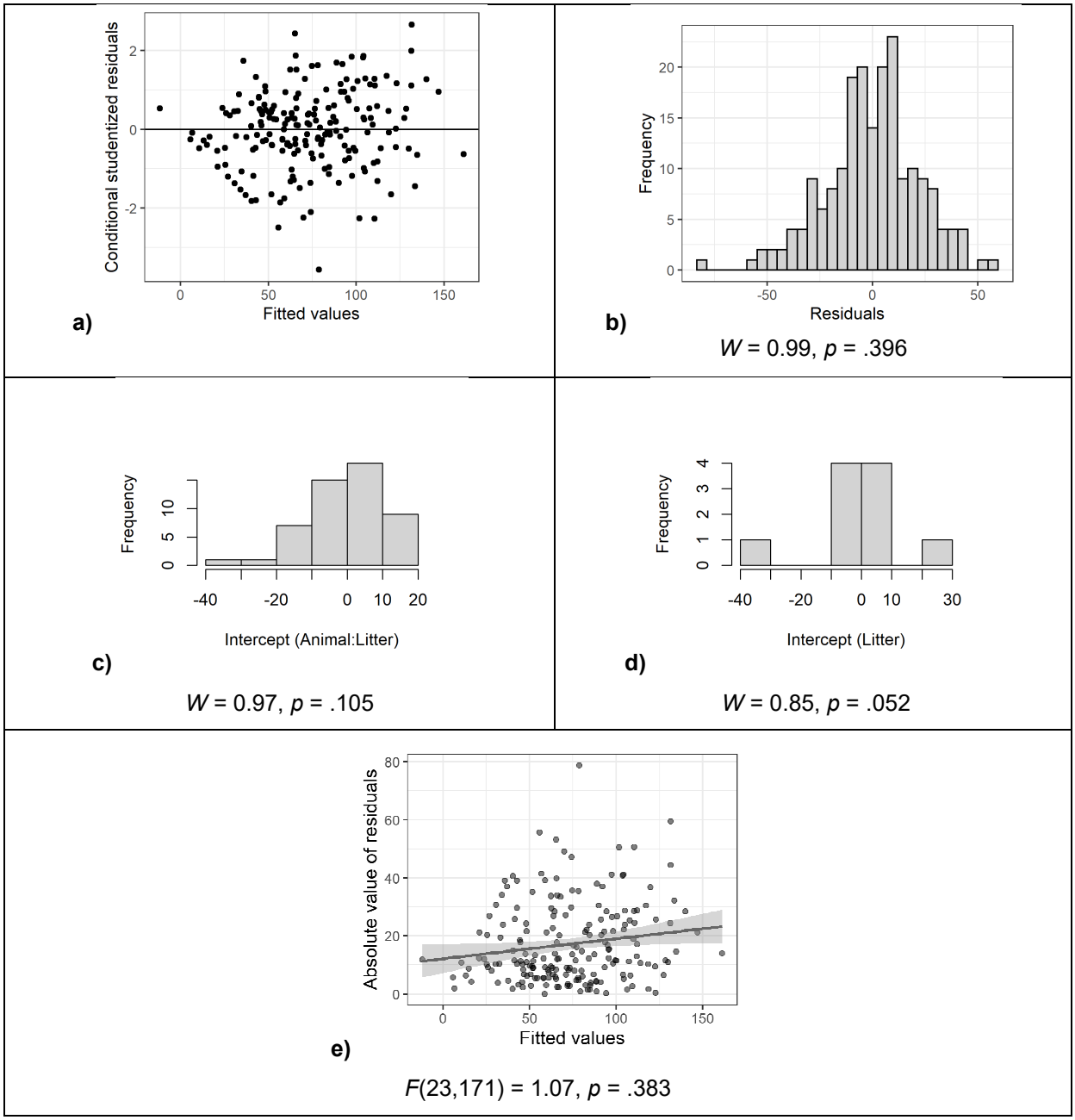

Figure 63: Inspection of model assumptions – EPM Test – Open Arm Time <u>including outliers</u>
a) *Conditional (internally) studentized residuals*: There are outlier residuals exceeding ±3 SD of the mean. **b)** *Histogram and Shapiro Wilk test of residuals:* The histogram appears approximately symmetric, and the Shapiro Wilk test is not significant (p=.396). **c)** *Histogram and Shapiro Wilk test of random intercepts for animal (nested under litter)*: The histogram appears skewed top the left, but the Shapiro Wilk test is not significant (p=.105). **d)** *Histogram and Shapiro Wilk test of random intercepts for litter*: The histogram appears approximately symmetric, and the Shapiro Wilk test is not significant, with only a trend towards statistical significance (p=.052). **e)** *Spread-Location plot and Levene's test of residuals*: The S-L-plot shows approximately equal variation across the whole range of values, with a slight trend towards higher variation at higher values, and Levene's test is not significant (p=.383).

Table 45: ANOVA table of the linear mixed model of the EPM Open Arm Time data including outliers

Shown are the sums of squares (*SS*), mean squares (*MS*), numerator (df_{Num}) and denominator (df_{Den}) degrees of freedom, F- and p-value for each simple factor as well as for the Dose:Age interaction term. The simple effects for Age (p = .000) and Scan (p = .012) show statistical significance.

	SS	*MS*	df_{Num}	df_{Den}	*F*	*p*	
Dose	999.51	499.76	2	7.18	0.80	.486	
Age	60038.72	20012.91	3	136.84	32.01	**.000**	***
Scan	4282.90	4282.90	1	42.17	6.85	**.012**	**
Dose:Age	3552.82	592.14	6	136.80	0.95	.464	

Table 46: ANOVA-like table for random effects of the LMM of the EPM Open Arm Time data including outliers

Shown are the number of model parameters (n par), the log-likelihood (logLik), Akaike information criterion (AIC), likelihood ratio test (LRT), degrees of freedom (df) and p-value for single term deletions of the random effects of the LMM of the EPM Open Arm Time data including outliers. Both Animal nested under Litter as well as the random effect of Litter are statistically significant (p = .000).

	n par	*logLik*	*AIC*	*LRT*	*df*	*p*	
<none>	16	-889.04	1810.09	NA	NA	NA	
(1 | Animal:Litter)	15	-896.54	1823.07	14.98	1.00	**.000**	***
(1 | Litter)	15	-897.03	1824.05	15.96	1.00	**.000**	***

Table 47: Estimated marginal means of the LMM of the EPM Open Arm Time data including outliers

Shown are the estimated marginal mean, standard error (SE), degrees of freedom (df) and 95% confidence interval for each LPS dose and Age combination.

LPS dose [µg/kg]	Age [PD]	*Mean*	*SE*	*df*	*95% Confidence Interval*	
					Lower CL	*Upper CL*
0	~30	85.24	10.62	10.61	61.76	108.73
0	~45	47.36	10.62	10.61	23.88	70.84
0	~66	72.38	10.62	10.61	48.89	95.86
0	~94	114.92	10.81	11.36	91.23	138.62
20	~30	63.13	12.14	11.38	36.53	89.73
20	~45	36.81	12.14	11.38	10.20	63.41
20	~66	54.37	12.14	11.38	27.76	80.97
20	~94	100.49	12.76	13.79	73.10	127.89
100	~30	81.74	22.59	8.73	30.39	133.10
100	~45	62.71	22.59	8.73	11.35	114.07
100	~66	93.14	22.59	8.73	41.79	144.50
100	~94	109.15	22.98	9.34	57.45	160.86

Table 48: Post hoc multiple comparisons of EPM Open Arm Time data - simple pair-wise t-tests for 'Dose' <u>including outliers</u>
Shown are the estimates and standard error (SE) of simple pair-wise t-tests for the contrast LPS dose [µg/kg], including degrees of freedom (df), t ratio, p-values corrected for multiple comparisons using the Tukey method (p) as well as uncorrected p-values (p uncorr) and 95% confidence intervals. Both before and after Tukey adjustment, no contrast shows statistical significance.

Contrast LPS dose [µg/kg]	Age [PD]	*Estimate*	*SE*	*df*	*t ratio*	*p*	*p uncorr*	*95% Confidence Interval*	
								Lower CL	*Upper CL*
0 - 20	~30	22.12	16.08	10.91	1.38	.386	*.197*	-13.31	57.54
0 - 100	~30	3.50	24.97	9.04	0.14	.989	*.892*	-52.96	59.96
20 - 100	~30	-18.62	25.67	9.27	-0.73	.755	*.486*	-76.43	39.20
0 - 20	~45	10.55	16.08	10.91	0.66	.793	*.525*	-24.87	45.97
0 - 100	~45	-15.35	24.97	9.04	-0.61	.816	*.554*	-71.81	41.10
20 - 100	~45	-25.90	25.67	9.27	-1.01	.589	*.339*	-83.72	31.91
0 - 20	~66	18.01	16.08	10.91	1.12	.522	*.287*	-17.41	53.43
0 - 100	~66	-20.77	24.97	9.04	-0.83	.694	*.427*	-77.23	35.69
20 - 100	~66	-38.78	25.67	9.27	-1.51	.330	*.164*	-96.60	19.04
0 - 20	~94	14.43	16.68	12.58	0.86	.671	*.403*	-21.73	50.58
0 - 100	~94	5.77	25.41	9.68	0.23	.972	*.825*	-51.10	62.64
20 - 100	~94	-8.66	26.34	10.24	-0.33	.942	*.749*	-67.15	49.83

Table 49: Post hoc multiple comparisons of EPM Open Arm Time data - simple pair-wise t-tests for 'Age' <u>including outliers</u>

Shown are the estimates and standard error (SE) of simple pair-wise t-tests for the contrast Age [PD], including degrees of freedom (df), t ratio, p-values corrected for multiple comparisons using the Tukey method (p) as well as uncorrected p-values (p uncorr) and 95% confidence intervals. After Tukey adjustment, in the control group all contrasts are statistically significant (usually p = .000), except the ~30-~66 PD contrast. The same holds true for the 20 µg/kg LPS group, except that in this group the ~45-~66 PD contrast shows no statistical significance in addition to the ~30-~66 PD contrast as well. In the 100 µg/kg LPS group however, only the ~45-~94 PD contrast is statistically significant (p = .006). Without Tukey adjustment, the ~45-~66 PD contrast is statistically significant in the 100 µg/kg LPS group as well (p = .024), while the ~30-~94 PD contrast shows a trend towards statistical significance (p = .052). In the 20 µg/kg LPS group, the 45-~66 PD contrast also gets statistically significant (p = .032), while in the control group the ~30-~66 PD contrast shows a trend towards statistical significance without Tukey adjustment (p = .071).

Contrast Age [PD]	LPS dose [µg/kg]	*Estimate*	*SE*	*df*	*t ratio*	*p*	*p uncorr*	*95% Confidence Interval*	
								Lower CL	*Upper CL*
~30 - ~45	0	37.88	7.07	135.31	5.36	**.000** ***	*.000* ***	23.90	51.87
~30 - ~66	0	12.87	7.07	135.31	1.82	.269	*.071* .	-1.12	26.85
~30 - ~94	0	-29.68	7.36	137.17	-4.03	**.001** ***	*.000* ***	-44.23	-15.13
~45 - ~66	0	-25.02	7.07	135.31	-3.54	**.003** **	*.001* ***	-39.00	-11.03
~45 - ~94	0	-67.56	7.36	137.17	-9.18	**.000** ***	*.000* ***	-82.11	-53.01
~66 - ~94	0	-42.55	7.36	137.17	-5.78	**.000** ***	*.000* ***	-57.10	-27.99
~30 - ~45	20	26.32	8.11	135.31	3.24	**.008** **	*.001* ***	10.28	42.36
~30 - ~66	20	8.76	8.11	135.31	1.08	.702	*.282*	-7.28	24.80
~30 - ~94	20	-37.37	8.93	140.37	-4.18	**.000** ***	*.000* ***	-55.03	-19.70
~45 - ~66	20	-17.56	8.11	135.31	-2.16	.138	*.032* *	-33.60	-1.52
~45 - ~94	20	-63.69	8.93	140.37	-7.13	**.000** ***	*.000* ***	-81.35	-46.03
~66 - ~94	20	-46.13	8.93	140.37	-5.16	**.000** ***	*.000* ***	-63.79	-28.47
~30 - ~45	100	19.03	13.36	135.31	1.42	.487	*.157*	-7.40	45.46
~30 - ~66	100	-11.40	13.36	135.31	-0.85	.829	*.395*	-37.83	15.03
~30 - ~94	100	-27.41	14.01	138.06	-1.96	.210	*.052* .	-55.11	0.29
~45 - ~66	100	-30.43	13.36	135.31	-2.28	.109	*.024* *	-56.87	-4.00
~45 - ~94	100	-46.44	14.01	138.06	-3.32	**.006** **	*.001* ***	-74.14	-18.74
~66 - ~94	100	-16.01	14.01	138.06	-1.14	.664	*.255*	-43.71	11.69

6.2.2.2. Time in Center

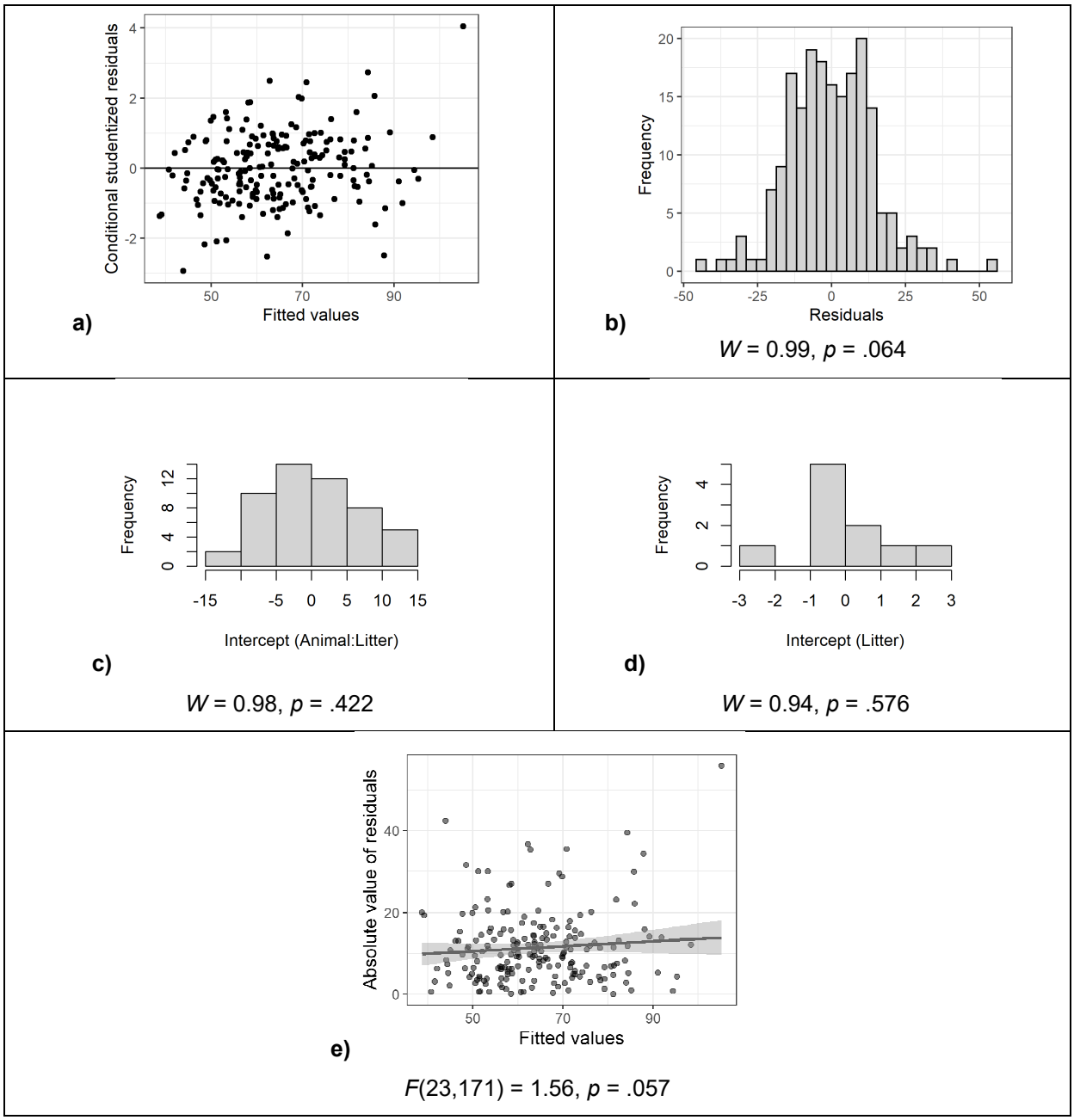

Figure 64: Inspection of model assumptions – EPM Test – Center Square Time <u>including outliers</u>

a) *Conditional (internally) studentized residuals*: There are outlier residuals exceeding ±3 SD of the mean. **b)** *Histogram and Shapiro Wilk test of residuals:* The histogram appears approximately symmetric, and the Shapiro Wilk test only shows a trend towards statistical significance (p=.064). **c)** *Histogram and Shapiro Wilk test of random intercepts for animal (nested under litter)*: The histogram appears approximately symmetric, and the Shapiro Wilk test is not significant (p=.422). **d)** *Histogram and Shapiro Wilk test of random intercepts for litter*: The histogram appears approximately symmetric, and the Shapiro Wilk test is not significant (p=.576). **e)** *Spread-Location plot and Levene's test of residuals*: The S-L-plot shows approximately equal variation across the whole range of values, and Levene's test is not significant, only showing a trend towards statistical significance (p=.057).

Table 50: ANOVA table of the linear mixed model of the EPM Center Square Time data including outliers

Shown are the sums of squares (*SS*), mean squares (*MS*), numerator (df_{Num}) and denominator (df_{Den}) degrees of freedom, F- and p-value for each simple factor as well as for the Dose:Age interaction term. The simple effects for Dose (p = .025) and Age (p = .000) show statistical significance.

	SS	*MS*	df_{Num}	df_{Den}	*F*	*p*	
Dose	3525.84	1762.92	2	6.60	6.76	**.025**	*
Age	6452.21	2150.74	3	137.94	8.24	**.000**	***
Scan	144.31	144.31	1	46.33	0.55	.461	
Dose:Age	805.39	134.23	6	137.93	0.51	.797	

Table 51: ANOVA-like table for random effects of the LMM of the EPM Center Square Time data including outliers

Shown are the number of model parameters (n par), the log-likelihood (logLik), Akaike information criterion (AIC), likelihood ratio test (LRT), degrees of freedom (df) and p-value for single term deletions of the random effects of the LMM of the EPM Center Square Time data including outliers. Only Animal nested under Litter is statistically significant (p = .000).

	n par	*logLik*	*AIC*	*LRT*	*df*	*p*	
<none>	16	-802.65	1637.30	NA	NA	NA	
(1 | Animal:Litter)	15	-808.98	1647.95	12.66	1.00	**.000**	***
(1 | Litter)	15	-802.85	1635.69	0.40	1.00	.530	

Table 52: Estimated marginal means of the LMM of the EPM Center Square Time data including outliers

Shown are the estimated marginal mean, standard error (SE), degrees of freedom (df) and 95% confidence interval for each LPS dose and Age combination.

LPS dose [µg/kg]	Age [PD]	*Mean*	*SE*	*df*	*95% Confidence Interval*	
					Lower CL	*Upper CL*
0	~30	56.99	4.04	28.01	48.71	65.28
0	~45	54.14	4.04	28.01	45.85	62.42
0	~66	68.74	4.04	28.01	60.45	77.02
0	~94	64.22	4.24	32.77	55.59	72.85
20	~30	50.66	4.69	27.24	41.05	60.27
20	~45	57.06	4.69	27.24	47.45	66.67
20	~66	71.30	4.69	27.24	61.69	80.91
20	~94	63.30	5.30	39.93	52.59	74.01
100	~30	73.49	7.81	16.69	57.00	89.99
100	~45	82.85	7.81	16.69	66.36	99.35
100	~66	92.74	7.81	16.69	76.25	109.24
100	~94	86.01	8.27	20.68	68.80	103.21

Table 53: Post hoc multiple comparisons of EPM Center Square Time data - simple pair-wise t-tests for 'Dose' <u>including outliers</u>
Shown are the estimates and standard error (SE) of simple pair-wise t-tests for the contrast LPS dose [µg/kg], including degrees of freedom (df), t ratio, p-values corrected for multiple comparisons using the Tukey method (p) as well as uncorrected p-values (p uncorr) and 95% confidence intervals. After Tukey adjustment, the 0-100 and 20-100 contrasts on PD ~45 as well as the 0-100 contrast on PD ~66 show statistical significance (p = .011 / .028 / .035), and the 20-100 contrast on PD ~30, PD ~66 and PD ~94 as well as the 0-100 contrasts on PD ~94 show a trend towards statistical significance (p = .054 / .073 / .074 / .070). Without Tukey adjustment, the latter trends turn into statistical significance (p = .022 / .030 / .030 / .028).

Contrast LPS dose [µg/kg]	Age [PD]	*Estimate*	*SE*	*df*	*t ratio*	*p*	*p uncorr*	*95% Confidence Interval*	
								Lower CL	*Upper CL*
0 - 20	~30	6.34	6.15	27.09	1.03	.564	*.312*	-6.28	18.95
0 - 100	~30	-16.50	8.80	18.55	-1.87	.174	*.077* .	-34.96	1.96
20 - 100	~30	-22.84	9.13	18.92	-2.50	**.054** .	*.022* *	-41.95	-3.72
0 - 20	~45	-2.92	6.15	27.09	-0.48	.883	*.638*	-15.53	9.69
0 - 100	~45	-28.72	8.80	18.55	-3.26	**.011** *	*.004* **	-47.17	-10.26
20 - 100	~45	-25.79	9.13	18.92	-2.83	**.028** *	*.011* *	-44.91	-6.68
0 - 20	~66	-2.56	6.15	27.09	-0.42	.909	*.680*	-15.17	10.05
0 - 100	~66	-24.01	8.80	18.55	-2.73	**.035** *	*.014* *	-42.46	-5.55
20 - 100	~66	-21.45	9.13	18.92	-2.35	**.073** .	*.030* *	-40.56	-2.33
0 - 20	~94	0.92	6.75	36.32	0.14	.990	*.892*	-12.77	14.61
0 - 100	~94	-21.78	9.30	22.75	-2.34	**.070** .	*.028* *	-41.04	-2.53
20 - 100	~94	-22.71	9.86	24.81	-2.30	**.074** .	*.030* *	-43.02	-2.39

Table 54: Post hoc multiple comparisons of EPM Center Square Time data - simple pair-wise t-tests for 'Age' <u>including outliers</u>
Shown are the estimates and standard error (SE) of simple pair-wise t-tests for the contrast Age [PD], including degrees of freedom (df), t ratio, p-values corrected for multiple comparisons using the Tukey method (p) as well as uncorrected p-values (p uncorr) and 95% confidence intervals. After Tukey adjustment, in the control group the ~45-~66 PD contrasts shows statistical significance (p = .009), while the ~30-~66 PD contrast shows a trend towards statistical significance (p = .054). In the 20 µg/kg LPS group, the same two contrasts both show statistical significance (p = .001 / .037). In the 100 µg/kg LPS group no contrast shows statistical significance. Without Tukey adjustment, the ~45-~94 PD contrast in the control group also shows statistical significance (p = .035) and the trend of the ~30-~66 PD contrast turns into statistical significance (p = .011). Furthermore, the ~30-~94 PD contrast in the 20 µg/kg LPS group also gets statistically significant (p = .030), while in the 100 µg/kg LPS group the ~30-~66 PD contrast shows statistical significance (p = .027).

Contrast Age [PD]	LPS dose [µg/kg]	*Estimate*	*SE*	*df*	*t ratio*	*p*	*p uncorr*	*95% Confidence Interval*	
								Lower CL	*Upper CL*
~30 - ~45	0	2.86	4.57	136.28	0.63	.924	*.533*	-6.18	11.89
~30 - ~66	0	-11.74	4.57	136.28	-2.57	**.054** **.**	*.011* *	-20.78	-2.71
~30 - ~94	0	-7.23	4.75	138.55	-1.52	.427	*.130*	-16.62	2.16
~45 - ~66	0	-14.60	4.57	136.28	-3.20	**.009** **	*.002* **	-23.64	-5.57
~45 - ~94	0	-10.09	4.75	138.55	-2.12	.151	*.035* *	-19.48	-0.69
~66 - ~94	0	4.52	4.75	138.55	0.95	.777	*.343*	-4.88	13.91
~30 - ~45	20	-6.40	5.24	136.28	-1.22	.615	*.224*	-16.76	3.97
~30 - ~66	20	-20.64	5.24	136.28	-3.94	**.001** ***	*.000* ***	-31.00	-10.28
~30 - ~94	20	-12.64	5.77	141.82	-2.19	.130	*.030* *	-24.04	-1.24
~45 - ~66	20	-14.24	5.24	136.28	-2.72	**.037** *	*.007* **	-24.61	-3.88
~45 - ~94	20	-6.24	5.77	141.82	-1.08	.701	*.281*	-17.64	5.16
~66 - ~94	20	8.00	5.77	141.82	1.39	.509	*.167*	-3.40	19.40
~30 - ~45	100	-9.36	8.64	136.28	-1.08	.700	*.280*	-26.43	7.72
~30 - ~66	100	-19.25	8.64	136.28	-2.23	.121	*.027* *	-36.33	-2.17
~30 - ~94	100	-12.51	9.05	139.21	-1.38	.512	*.169*	-30.40	5.38
~45 - ~66	100	-9.89	8.64	136.28	-1.15	.662	*.254*	-26.97	7.18
~45 - ~94	100	-3.15	9.05	139.21	-0.35	.985	*.728*	-21.04	14.73
~66 - ~94	100	6.74	9.05	139.21	0.74	.879	*.458*	-11.15	24.63

6.2.2.3. Head Dips

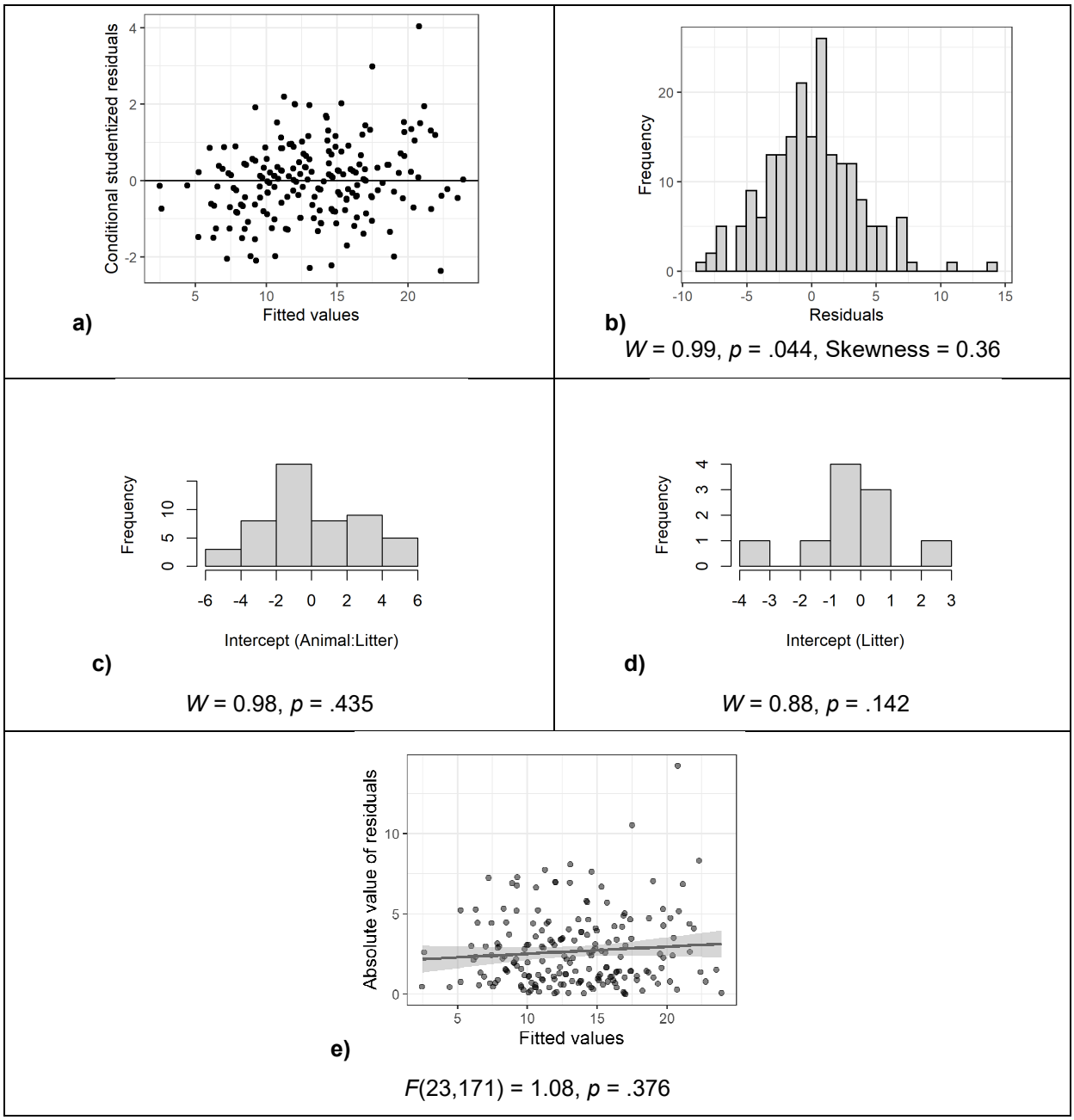

Figure 65: Inspection of model assumptions – EPM Test – Head Dips <u>including outliers</u>
a) *Conditional (internally) studentized residuals*: There are outlier residuals exceeding ±3 SD of the mean. **b)** *Histogram and Shapiro Wilk test of residuals:* The histogram appears slightly skewed to the right, and the Shapiro Wilk test is statistically significant (p=.044). The skewness of 0.36 however suggests the distribution is still fairly symmetrical (Bulmer, 1979). **c)** *Histogram and Shapiro Wilk test of random intercepts for animal (nested under litter)*: The histogram appears slightly skewed to the right, but the Shapiro Wilk test is not significant (p=.435). **d)** *Histogram and Shapiro Wilk test of random intercepts for litter*: The histogram appears approximately symmetric, and the Shapiro Wilk test is not significant (p=.142). **e)** *Spread-Location plot and Levene's test of residuals*: The S-L-plot shows approximately equal variation across the whole range of values, with a slight trend towards higher variation at higher values, and Levene's test is not significant (p=.376).

Table 55: ANOVA table of the linear mixed model of the EPM Head Dips data including outliers
Shown are the sums of squares (*SS*), mean squares (*MS*), numerator (df_{Num}) and denominator (df_{Den}) degrees of freedom, F- and p-value for each simple factor as well as for the Dose:Age interaction term. The simple effects of Age (p = .000) and Scan (p = .032) show statistical significance.

	SS	*MS*	df_{Num}	df_{Den}	*F*	*p*	
Dose	83.69	41.85	2	7.20	2.60	.141	
Age	353.85	117.95	3	136.32	7.33	**.000**	***
Scan	78.66	78.66	1	43.74	4.89	**.032**	*
Dose:Age	102.02	17.00	6	136.29	1.06	.392	

Table 56: ANOVA-like table for random effects of the LMM of the EPM Head Dips data including outliers
Shown are the number of model parameters (n par), the log-likelihood (logLik), Akaike information criterion (AIC), likelihood ratio test (LRT), degrees of freedom (df) and p-value for single term deletions of the random effects of the LMM of the EPM Head Dips data including outliers. Animal nested under Litter as well as litter are statistically significant (p = .000 / .032).

	n par	*logLik*	*AIC*	*LRT*	*df*	*p*	
<none>	16	-562.26	1156.53	NA	NA	NA	
(1 | Animal:Litter)	15	-577.96	1185.92	31.39	1.00	**.000**	***
(1 | Litter)	15	-564.57	1159.15	4.62	1.00	**.032**	*

Table 57: Estimated marginal means of the LMM of the EPM Head Dips data including outliers
Shown are the estimated marginal mean, standard error (SE), degrees of freedom (df) and 95% confidence interval for each LPS dose and Age combination.

LPS dose [µg/kg]	Age [PD]	*Mean*	*SE*	*df*	*95% Confidence Interval*	
					Lower CL	*Upper CL*
0	~30	15.93	1.46	13.08	12.79	19.07
0	~45	10.57	1.46	13.08	7.43	13.71
0	~66	14.41	1.46	13.08	11.27	17.55
0	~94	16.41	1.49	14.36	13.21	19.60
20	~30	10.94	1.68	14.04	7.33	14.55
20	~45	8.73	1.68	14.04	5.12	12.34
20	~66	10.42	1.68	14.04	6.80	14.03
20	~94	12.79	1.80	17.98	9.01	16.57
100	~30	15.90	2.99	9.42	9.19	22.61
100	~45	14.76	2.99	9.42	8.04	21.47
100	~66	18.18	2.99	9.42	11.47	24.90
100	~94	17.79	3.07	10.43	11.00	24.59

Table 58: Post hoc multiple comparisons of EPM Head Dips data - simple pair-wise t-tests for 'Dose' <u>including outliers</u>
Shown are the estimates and standard error (SE) of simple pair-wise t-tests for the contrast LPS dose [µg/kg], including degrees of freedom (df), t ratio, p-values corrected for multiple comparisons using the Tukey method (p) as well as uncorrected p-values (p uncorr) and 95% confidence intervals. After Tukey adjustment, only the 0-20 contrast on PD ~30 shows a trend towards statistical significance (p = .098). Without Tukey adjustment, the latter trend turns into statistical significance (p = .042), and the 20-100 contrast on PD ~66 is statistically significant as well (p = .046). Furthermore, the 0-20 contrast on PD ~66 shows a trend towards statistical significance (p = .094).

Contrast LPS dose [µg/kg]	Age [PD]	*Estimate*	*SE*	*df*	*t ratio*	*p*	*p uncorr*	*95% Confidence Interval*	
								Lower CL	*Upper CL*
0 - 20	~30	4.99	2.21	13.36	2.25	**.098** **.**	*.042* *	0.22	9.76
0 - 100	~30	0.03	3.33	10.03	0.01	1.000	*.993*	-7.38	7.44
20 - 100	~30	-4.96	3.44	10.37	-1.44	.356	*.179*	-12.58	2.66
0 - 20	~45	1.84	2.21	13.36	0.83	.691	*.421*	-2.93	6.61
0 - 100	~45	-4.19	3.33	10.03	-1.26	.448	*.237*	-11.59	3.22
20 - 100	~45	-6.02	3.44	10.37	-1.75	.232	*.109*	-13.64	1.60
0 - 20	~66	3.99	2.21	13.36	1.80	.206	*.094* .	-0.78	8.76
0 - 100	~66	-3.77	3.33	10.03	-1.13	.516	*.283*	-11.18	3.63
20 - 100	~66	-7.77	3.44	10.37	-2.26	.107	*.046* *	-15.39	-0.15
0 - 20	~94	3.62	2.33	16.10	1.55	.293	*.140*	-1.32	8.55
0 - 100	~94	-1.39	3.41	11.09	-0.41	.914	*.692*	-8.89	6.12
20 - 100	~94	-5.00	3.57	11.96	-1.40	.370	*.186*	-12.78	2.77

Table 59: Post hoc multiple comparisons of EPM Head Dips data data - simple pair-wise t-tests for 'Age' <u>including outliers</u>

Shown are the estimates and standard error (SE) of simple pair-wise t-tests for the contrast Age [PD], including degrees of freedom (df), t ratio, p-values corrected for multiple comparisons using the Tukey method (p) as well as uncorrected p-values (p uncorr) and 95% confidence intervals. After Tukey adjustment, in the control group, the ~30-~45, ~45-~66 and ~45-~94 contrasts are statistically significant (p < .005). In the 20 µg/kg LPS group, only the ~45-~94 contrast is statistically significant (p = .028), while in the 100 µg/kg LPS group no contrast shows statistical significance. Without Tukey adjustment, additionally there is a trend towards statistical significance in the control group for the ~66-~94 contrast (p = .094), and in the 20µg/kg group for the ~30-~45 (p = .092).

Contrast Age [PD]	LPS dose [µg/kg]	*Estimate*	*SE*	*df*	*t ratio*	*p*	*p uncorr*	*95% Confidence Interval*	
								Lower CL	*Upper CL*
~30 - ~45	0	5.36	1.13	135.19	4.72	**.000** ***	*.000* ***	3.12	7.60
~30 - ~66	0	1.52	1.13	135.19	1.34	.539	*.183*	-0.72	3.76
~30 - ~94	0	-0.47	1.18	136.61	-0.40	.978	*.689*	-2.81	1.86
~45 - ~66	0	-3.84	1.13	135.19	-3.38	**.005** **	*.001* ***	-6.08	-1.60
~45 - ~94	0	-5.83	1.18	136.61	-4.94	**.000** ***	*.000* ***	-8.17	-3.50
~66 - ~94	0	-1.99	1.18	136.61	-1.69	.334	*.094* .	-4.33	0.34
~30 - ~45	20	2.21	1.30	135.19	1.70	.329	*.092* .	-0.36	4.78
~30 - ~66	20	0.53	1.30	135.19	0.40	.978	*.687*	-2.05	3.10
~30 - ~94	20	-1.85	1.44	138.89	-1.28	.574	*.201*	-4.69	1.00
~45 - ~66	20	-1.68	1.30	135.19	-1.29	.568	*.198*	-4.26	0.89
~45 - ~94	20	-4.06	1.44	138.89	-2.82	**.028** *	*.005* **	-6.90	-1.21
~66 - ~94	20	-2.37	1.44	138.89	-1.65	.354	*.101*	-5.22	0.47
~30 - ~45	100	1.14	2.14	135.19	0.53	.951	*.595*	-3.10	5.38
~30 - ~66	100	-2.29	2.14	135.19	-1.07	.711	*.288*	-6.53	1.95
~30 - ~94	100	-1.89	2.25	137.19	-0.84	.835	*.402*	-6.34	2.56
~45 - ~66	100	-3.43	2.14	135.19	-1.60	.383	*.112*	-7.67	0.81
~45 - ~94	100	-3.04	2.25	137.19	-1.35	.534	*.180*	-7.49	1.42
~66 - ~94	100	0.39	2.25	137.19	0.17	.998	*.862*	-4.06	4.84

6.2.2.4. Rearings

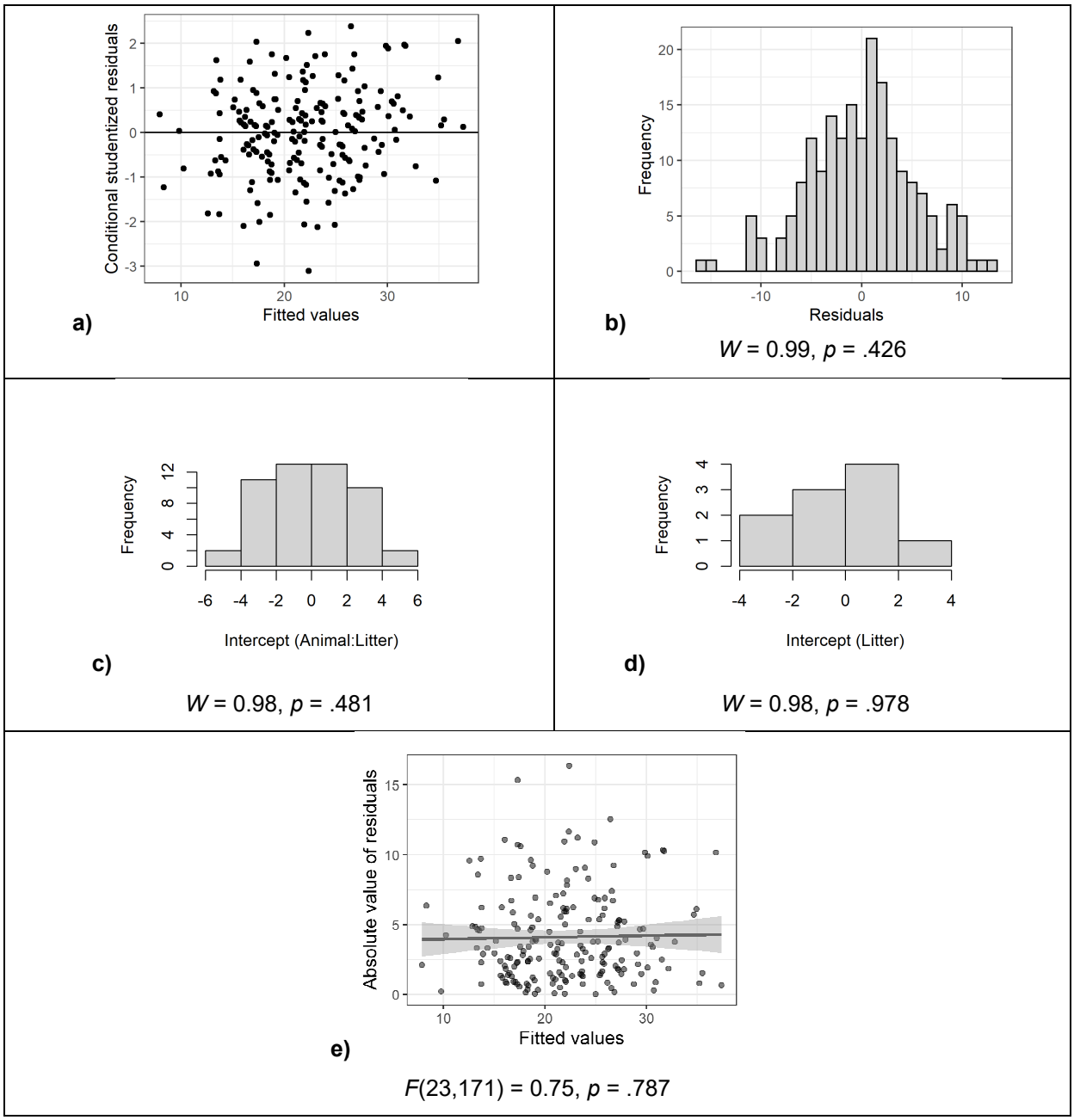

Figure 66: Inspection of model assumptions – EPM Test – Rearings <u>including outliers</u>
a) *Conditional (internally) studentized residuals*: There are outlier residuals exceeding ±3 SD of the mean. **b)** *Histogram and Shapiro Wilk test of residuals:* The histogram appears approximately symmetric, and the Shapiro Wilk test is not significant (p=426). **c)** *Histogram and Shapiro Wilk test of random intercepts for animal (nested under litter)*: The histogram appears approximately symmetric, and the Shapiro Wilk test is not significant (p=.481). **d)** *Histogram and Shapiro Wilk test of random intercepts for litter*: The histogram appears slightly skewed to the right, but the Shapiro Wilk test is not significant (p=.978). **e)** *Spread-Location plot and Levene's test of residuals*: The S-L-plot shows approximately equal variation across the whole range of values, and Levene's test is not significant (p=.787).

Table 60: ANOVA table of the linear mixed model of the EPM Rearings data including outliers
Shown are the sums of squares (*SS*), mean squares (*MS*), numerator (df_{Num}) and denominator (df_{Den}) degrees of freedom, F- and p-value for each simple factor as well as for the Dose:Age interaction term. The Dose:Age interaction shows statistical significance (p = .024), and the simple effect of Scan shows a trend towards statistical significance (p = .091).

	SS	*MS*	df_{Num}	df_{Den}	*F*	*p*	
Dose	107.46	53.73	2	6.48	1.55	.282	
Age	1766.15	588.72	3	136.18	16.99	**.000**	***
Scan	103.46	103.46	1	42.05	2.99	**.091**	.
Dose:Age	526.25	87.71	6	136.15	2.53	**.024**	*

Table 61: ANOVA-like table for random effects of the LMM of the EPM Rearings data including outliers
Shown are the number of model parameters (n par), the log-likelihood (logLik), Akaike information criterion (AIC), likelihood ratio test (LRT), degrees of freedom (df) and p-value for single term deletions of the random effects of the LMM of the EPM Rearings data including outliers. Animal nested under Litter as well as litter are statistically significant (p = .000 / .034).

	n par	*logLik*	*AIC*	*LRT*	*df*	*p*	
<none>	16	-622.57	1277.14	NA	NA	NA	
(1 | Animal:Litter)	15	-629.04	1288.08	12.93	1.00	**.000**	***
(1 | Litter)	15	-624.81	1279.62	4.47	1.00	**.034**	*

Table 62: Estimated marginal means of the LMM of the EPM Rearings data including outliers
Shown are the estimated marginal mean, standard error (SE), degrees of freedom (df) and 95% confidence interval for each LPS dose and Age combination.

LPS dose [µg/kg]	Age [PD]	*Mean*	*SE*	*df*	*95% Confidence Interval*	
					Lower CL	*Upper CL*
0	~30	18.72	1.90	13.65	14.65	22.80
0	~45	19.00	1.90	13.65	14.93	23.08
0	~66	27.24	1.90	13.65	23.17	31.32
0	~94	23.41	1.95	15.29	19.26	27.57
20	~30	16.50	2.19	14.70	11.82	21.17
20	~45	16.92	2.19	14.70	12.24	21.59
20	~66	25.29	2.19	14.70	20.61	29.96
20	~94	21.75	2.37	19.78	16.80	26.70
100	~30	18.46	3.89	9.73	9.77	27.15
100	~45	30.60	3.89	9.73	21.91	39.29
100	~66	28.46	3.89	9.73	19.77	37.15
100	~94	30.08	4.01	11.01	21.26	38.91

Table 63: Post hoc multiple comparisons of EPM Rearings data - simple pair-wise t-tests for 'Dose' <u>including outliers</u>

Shown are the estimates and standard error (SE) of simple pair-wise t-tests for the contrast LPS dose [µg/kg], including degrees of freedom (df), t ratio, p-values corrected for multiple comparisons using the Tukey method (p) as well as uncorrected p-values (p uncorr) and 95% confidence intervals. After Tukey adjustment, only the 20-100 contrast on PD ~45 is statistically significant (p = .028) and the 0-100 contrast on PD ~45 shows a trend towards statistical significance (p = .054). Without Tukey adjustment, the latter trend turns into statistical significance (p = .022), and the 20-100 contrast on PD ~94 shows a trend towards statistical significance as well (p = .098).

Contrast LPS dose [µg/kg]	Age [PD]	*Estimate*	*SE*	*df*	*t ratio*	*p*	*p uncorr*	*95% Confidence Interval*	
								Lower CL	*Upper CL*
0 - 20	~30	2.23	2.88	14.00	0.77	.725	*.452*	-3.95	8.41
0 - 100	~30	0.27	4.33	10.37	0.06	.998	*.952*	-9.33	9.86
20 - 100	~30	-1.96	4.47	10.73	-0.44	.900	*.669*	-11.82	7.90
0 - 20	~45	2.09	2.88	14.00	0.72	.754	*.481*	-4.09	8.27
0 - 100	~45	-11.60	4.33	10.37	-2.68	**.054** .	*.022* *	-21.19	-2.00
20 - 100	~45	-13.68	4.47	10.73	-3.06	**.028** *	*.011* *	-23.55	-3.82
0 - 20	~66	1.96	2.88	14.00	0.68	.779	*.508*	-4.22	8.14
0 - 100	~66	-1.21	4.33	10.37	-0.28	.958	*.785*	-10.81	8.38
20 - 100	~66	-3.17	4.47	10.73	-0.71	.763	*.493*	-13.03	6.69
0 - 20	~94	1.66	3.06	17.53	0.54	.851	*.594*	-4.78	8.11
0 - 100	~94	-6.67	4.46	11.72	-1.49	.328	*.161*	-16.42	3.08
20 - 100	~94	-8.33	4.67	12.76	-1.78	.214	*.098* .	-18.45	1.78

Table 64: Post hoc multiple comparisons of EPM Rearings data - simple pair-wise t-tests for 'Age' <u>including outliers</u>

Shown are the estimates and standard error (SE) of simple pair-wise t-tests for the contrast Age [PD], including degrees of freedom (df), t ratio, p-values corrected for multiple comparisons using the Tukey method (p) as well as uncorrected p-values (p uncorr) and 95% confidence intervals. After Tukey adjustment, in the control group the ~30-~66, ~30-~94 and ~45-~66 contrasts are statistically significant (p < .038) and the ~45-~94 contrast shows a trend towards statistical significance (p = .058). In the 20 µg/kg LPS group, the ~30-~66 and ~45-~66 contrasts are statistically significant as well (p = .000), while the ~30-~94 contrast only shows a trend towards statistical significance (p = .064). In the 100 µg/kg LPS group, the first three time points show statistical significance (p < .010). Without Tukey adjustment, the former trends turn into statistical significance as well (p = .012 / .014).

Contrast Age [PD]	LPS dose [µg/kg]	*Estimate*	*SE*	*df*	*t ratio*	*p*	*p uncorr*	*95% Confidence Interval*	
								Lower CL	*Upper CL*
~30 - ~45	0	-0.28	1.66	134.56	-0.17	.998	*.867*	-3.57	3.01
~30 - ~66	0	-8.52	1.66	134.56	-5.12	**.000** ***	*.000* ***	-11.81	-5.23
~30 - ~94	0	-4.69	1.73	136.60	-2.71	**.038** *	*.008* **	-8.11	-1.26
~45 - ~66	0	-8.24	1.66	134.56	-4.95	**.000** ***	*.000* ***	-11.53	-4.95
~45 - ~94	0	-4.41	1.73	136.60	-2.55	**.058** .	*.012* *	-7.83	-0.98
~66 - ~94	0	3.83	1.73	136.60	2.21	.125	*.029*	0.41	7.26
~30 - ~45	20	-0.42	1.91	134.56	-0.22	.996	*.826*	-4.20	3.36
~30 - ~66	20	-8.79	1.91	134.56	-4.60	**.000** ***	*.000* ***	-12.57	-5.01
~30 - ~94	20	-5.25	2.10	139.93	-2.50	**.064** .	*.014* *	-9.41	-1.10
~45 - ~66	20	-8.37	1.91	134.56	-4.38	**.000** ***	*.000* ***	-12.15	-4.59
~45 - ~94	20	-4.83	2.10	139.93	-2.30	.103	*.023*	-8.99	-0.68
~66 - ~94	20	3.54	2.10	139.93	1.68	.337	*.095*	-0.62	7.69
~30 - ~45	100	-12.14	3.15	134.56	-3.86	**.001** ***	*.000* ***	-18.37	-5.92
~30 - ~66	100	-10.00	3.15	134.56	-3.18	**.010** **	*.002* **	-16.22	-3.78
~30 - ~94	100	-11.63	3.30	137.45	-3.53	**.003** **	*.001* ***	-18.15	-5.11
~45 - ~66	100	2.14	3.15	134.56	0.68	.904	*.497*	-4.08	8.37
~45 - ~94	100	0.52	3.30	137.45	0.16	.999	*.876*	-6.00	7.04
~66 - ~94	100	-1.63	3.30	137.45	-0.49	.960	*.623*	-8.15	4.89

6.2.3. OF

6.2.3.1. Distance

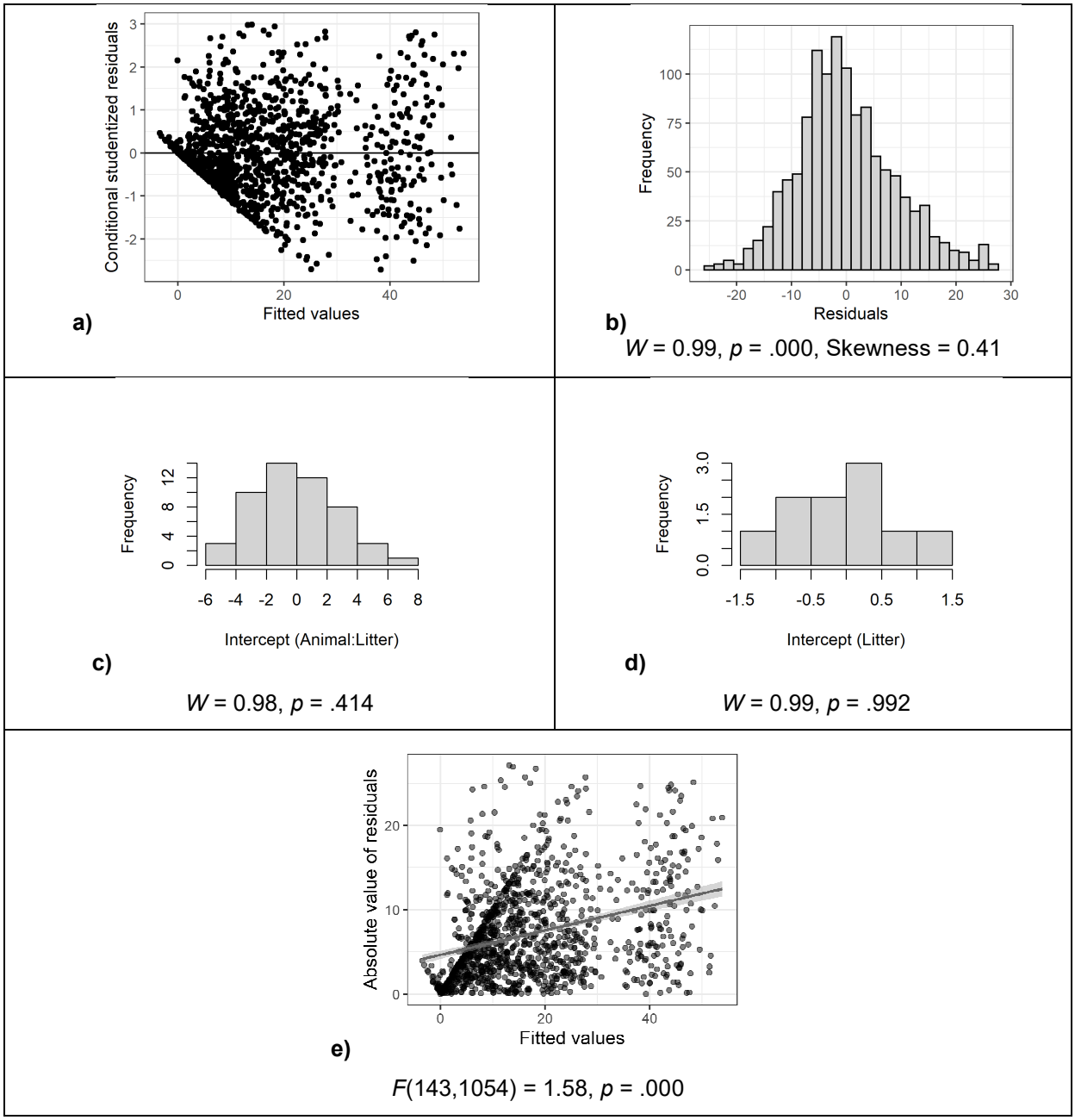

Figure 67: Inspection of model assumptions – OF Test – Distance travelled excluding outliers
a) *Conditional (internally) studentized residuals*: All residuals fall within ±3 SD of the mean, but show a weird pattern. **b)** *Histogram and Shapiro Wilk test of residuals:* The histogram appears approximately symmetric, but the Shapiro Wilk test shows significant difference from a normal distribution (p=.000). The skewness of 0.41 suggests the distribution is still fairly symmetrical (Bulmer, 1979). **c)** *Histogram and Shapiro Wilk test of random intercepts for animal (nested under litter)*: The histogram appears approximately symmetric, and the Shapiro Wilk test is not significant (p=.414). **d)** *Histogram and Shapiro Wilk test of random intercepts for litter*: The histogram appears approximately symmetric, and the Shapiro Wilk test is not significant (p=.992). **e)** *Spread-Location plot and Levene's test of residuals*: The S-L-plot shows a weird pattern and implies heteroscedasticity, which is confirmed by a significant Levene's test (p=.000).

Model formula: Distance ~ Dose * Age * Timeblock + Scan + (1 | Litter/Animal)

Table 65: ANOVA-like table for random effects of the LMM of the OF Distance data after outlier removal

Shown are the number of model parameters (n par), the log-likelihood (logLik), Akaike information criterion (AIC), likelihood ratio test (LRT), degrees of freedom (df) and p-value for single term deletions of the random effects of the LMM of the OF Time in Center data after outlier removal. Animal nested under Litter is statistically significant (p = .000).

	n par	*logLik*	*AIC*	*LRT*	*df*	*p*
<none>	76	-4256.87	8665.75	NA	NA	NA
(1 | Animal:Litter)	75	-4285.50	8720.99	57.24	1.00	**.000** ***
(1 | Litter)	75	-4257.28	8664.55	0.80	1.00	.370

No post-hoc tests were done as the model assumptions were violated.

6.2.3.2. CenterTime

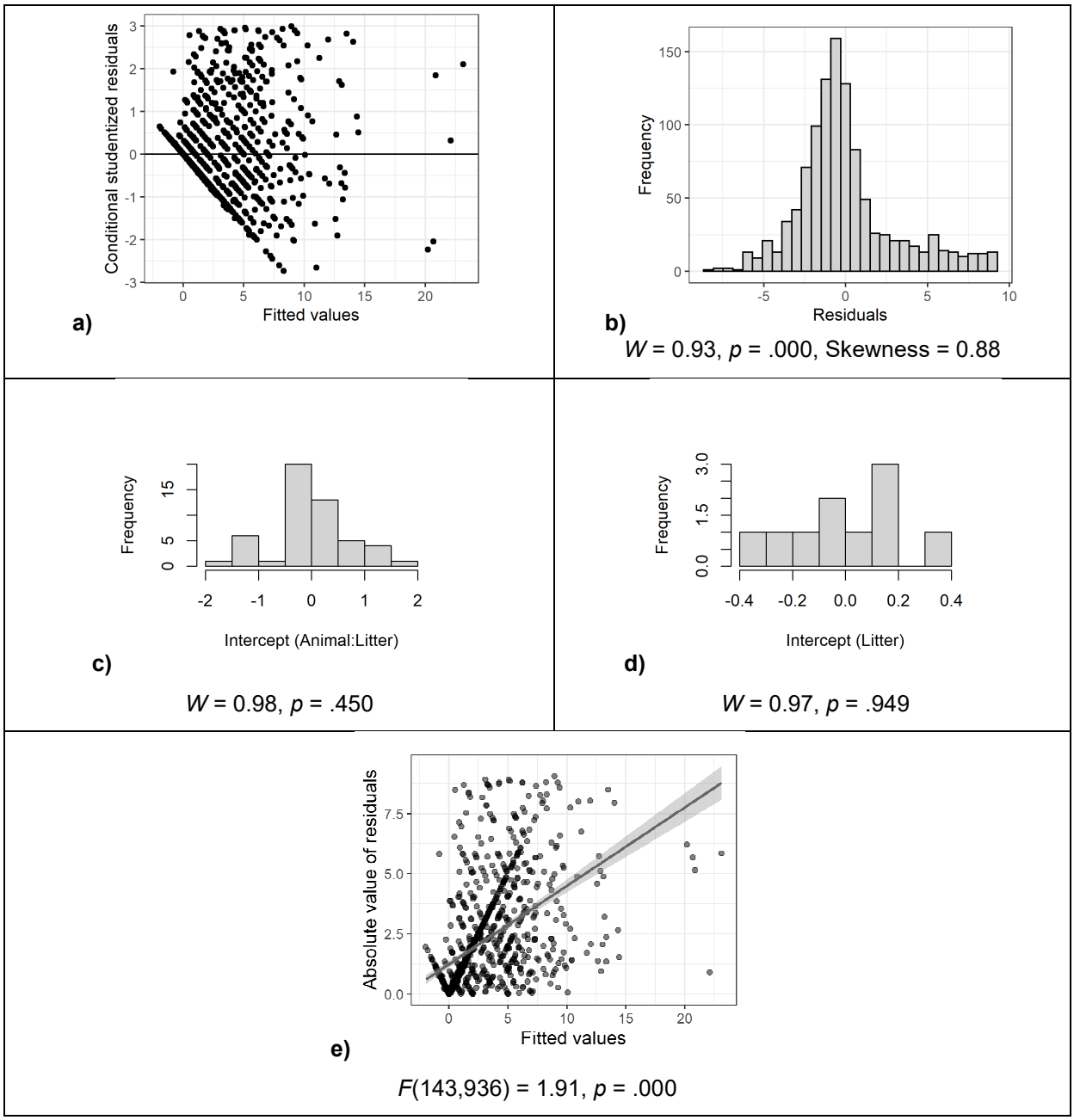

Figure 68: Inspection of model assumptions – OF Test – Time in Center excluding outliers
a) *Conditional (internally) studentized residuals*: All residuals fall within ±3 SD of the mean, but show a weird pattern. **b)** *Histogram and Shapiro Wilk test of residuals*: The histogram appears skewed to the right, the Shapiro Wilk test shows significant difference from a normal distribution (p=.000). The skewness of 0.88 further confirms that the distribution is moderately skewed (Bulmer, 1979). **c)** *Histogram and Shapiro Wilk test of random intercepts for animal (nested under litter)*: The histogram appears approximately symmetric, and the Shapiro Wilk test is not significant (p=.450). **d)** *Histogram and Shapiro Wilk test of random intercepts for litter*: The histogram appears skewed to the left, but the Shapiro Wilk test is not significant (p=.949). **e)** *Spread-Location plot and Levene's test of residuals*: The S-L-plot shows a weird pattern and strongly implies heteroscedasticity, which is confirmed by a significant Levene's test (p=.000).

Model formula: Time_in_Center ~ Dose * Age * Timeblock + Scan + (1 | Litter/Animal)

Table 66: ANOVA-like table for random effects of the LMM of the OF Time in Center data after outlier removal

Shown are the number of model parameters (n par), the log-likelihood (logLik), Akaike information criterion (AIC), likelihood ratio test (LRT), degrees of freedom (df) and p-value for single term deletions of the random effects of the LMM of the OF Time in Center data after outlier removal. Animal nested under Litter is statistically significant (p = .000).

	n par	*logLik*	*AIC*	*LRT*	*df*	*p*
<none>	76	-2710.04	5572.08	NA	NA	NA
(1 | Animal:Litter)	75	-2724.87	5599.74	29.66	1.00	**.000** ***
(1 | Litter)	75	-2710.32	5570.65	0.56	1.00	.452

No post-hoc tests were done as the model assumptions were violated.

6.2.3.3. Rearings

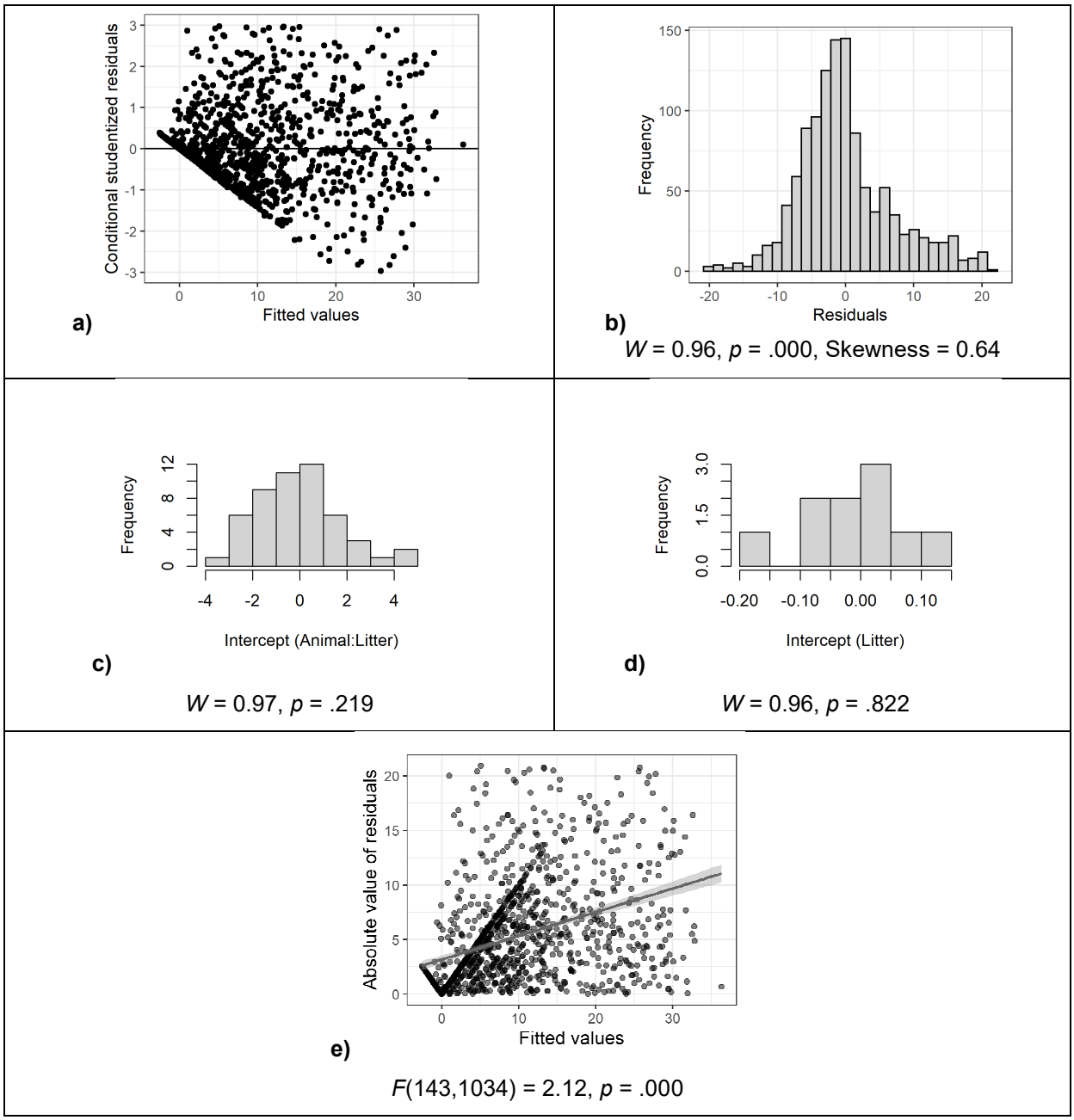

Figure 69: Inspection of model assumptions – OF Test – Rearings excluding outliers
a) *Conditional (internally) studentized residuals*: All residuals fall within ±3 SD of the mean, but show a weird pattern. **b)** *Histogram and Shapiro Wilk test of residuals*: The histogram appears slightly skewed to the right, and the Shapiro Wilk test shows significant difference from a normal distribution (p=.000). The skewness of 0.64 further confirms that the distribution is moderately skewed (Bulmer, 1979). **c)** *Histogram and Shapiro Wilk test of random intercepts for animal (nested under litter)*: The histogram appears slightly skewed to the right, but the Shapiro Wilk test is not significant (p=.219). **d)** *Histogram and Shapiro Wilk test of random intercepts for litter*: The histogram appears approximately symmetric, and the Shapiro Wilk test is not significant (p=.822). **e)** *Spread-Location plot and Levene's test of residuals*: The S-L-plot shows a weird pattern and implies heteroscedasticity, which is confirmed by a significant Levene's test (p=.000).

Model formula: Rearings ~ Dose * Age * Timeblock + Scan + (1 | Litter/Animal)

Table 67: ANOVA-like table for random effects of the LMM of the OF Rearings data after outlier removal

Shown are the number of model parameters (n par), the log-likelihood (logLik), Akaike information criterion (AIC), likelihood ratio test (LRT), degrees of freedom (df) and p-value for single term deletions of the random effects of the LMM of the OF Time in Center data after outlier removal. Animal nested under Litter is statistically significant (p = .000).

	n par	*logLik*	*AIC*	*LRT*	*df*	*p*	
<none>	76	-3891.34	7934.68	NA	NA	NA	
(1 | Animal:Litter)	75	-3908.44	7966.87	34.19	1.00	**.000**	***
(1 | Litter)	75	-3891.34	7932.69	0.01	1.00	.922	

No post-hoc tests were done as the model assumptions were violated.

6.2.4. Sensitivity Analysis OF

6.2.4.1. Distance

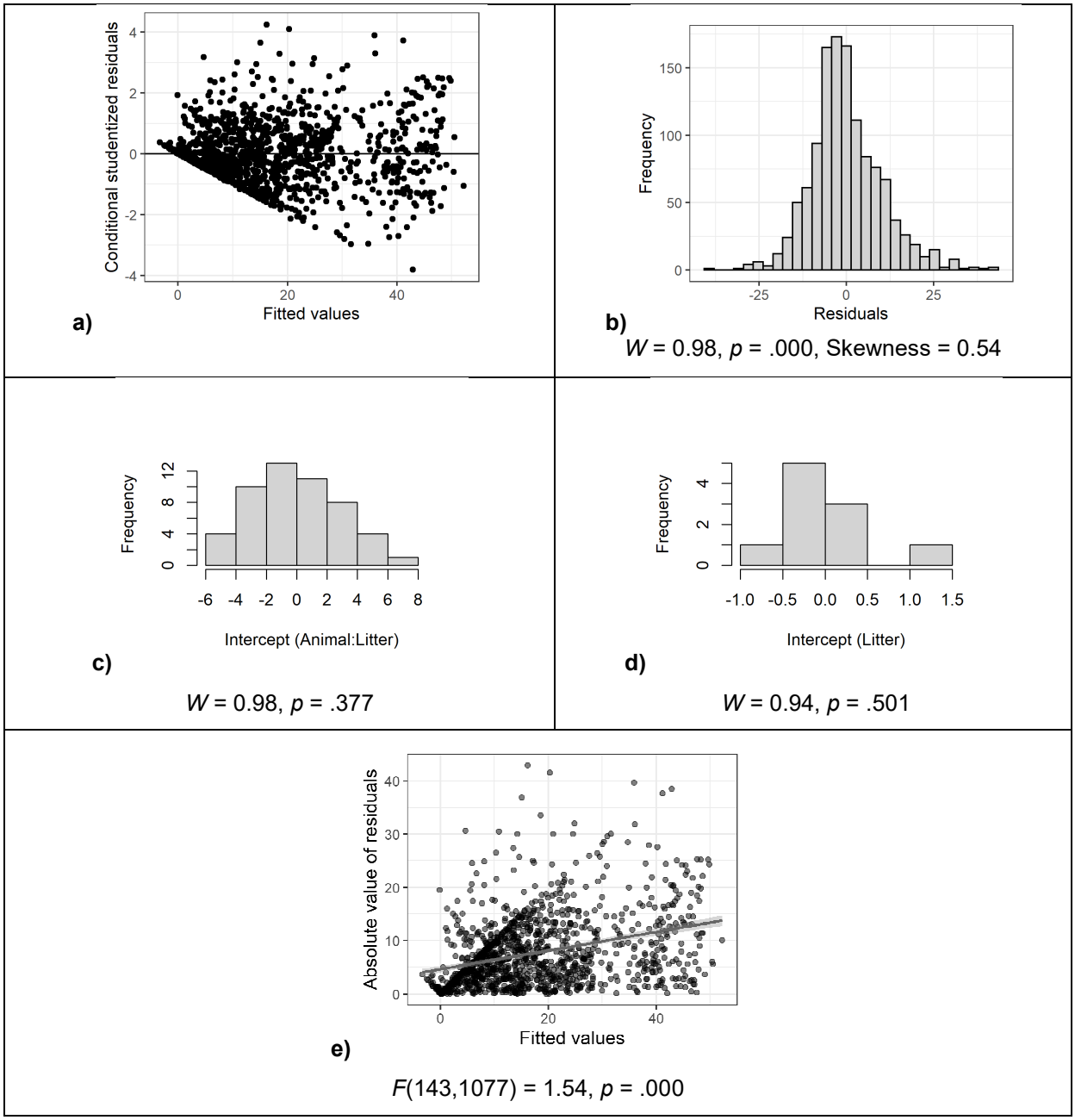

Figure 70: Inspection of model assumptions – OF Test – Time in Center <u>including outliers</u>
a) *Conditional (internally) studentized residuals*: There are outlier residuals exceeding ±3 SD of the mean, and the residuals show a weird pattern. **b)** *Histogram and Shapiro Wilk test of residuals*: The histogram appears approximately symmetric, but the Shapiro Wilk test shows significant difference from a normal distribution (p=.000). The skewness of 0.54 suggests the distribution is moderately skewed (Bulmer, 1979). **c)** *Histogram and Shapiro Wilk test of random intercepts for animal (nested under litter)*: The histogram appears approximately symmetric, and the Shapiro Wilk test is not significant (p=.377). **d)** *Histogram and Shapiro Wilk test of random intercepts for litter*: The histogram appears skewed to the right, but the Shapiro Wilk test is not significant (p=.501). **e)** *Spread-Location plot and Levene's test of residuals*: The S-L-plot implies heteroscedasticity, which is confirmed by a significant Levene's test (p=.000).

Table 68: ANOVA table of the LMM of the OF Distance data <u>including outliers</u>
Shown are the sums of squares (SS), mean squares (MS), numerator (df Num) and denominator (df Den) degrees of freedom, F- and p-value for each simple factor as well as for the Dose:Age, Dose:Timeblock, Age:Timeblock and Dose:Age:Timeblock interaction terms. The Dose:Age, Dose:Timeblock and Age:Timeblock interactions show statistical significance or trend towards statistical significance (p = .029 / .082 / .000).

	SS	*MS*	df_{Num}	df_{Den}	*F*	*p*	
Dose	46.79	23.39	2	4.31	0.21	.819	
Age	3001.69	1000.56	3	1101.08	8.96	**.000**	***
Timeblock	129714.98	25943.00	5	1101.05	232.36	**.000**	***
Scan	56.25	56.25	1	44.32	0.50	.482	
Dose:Age	1578.90	263.15	6	1101.10	2.36	**.029**	*
Dose:Timeblock	1870.85	187.09	10	1101.06	1.68	**.082**	.
Age:Timeblock	4681.32	312.09	15	1101.05	2.80	**.000**	***
Dose:Age:TimeBlock	2181.45	72.72	30	1101.06	0.65	.926	

Table 69: ANOVA-like table for random effects of the LMM of the OF Distance data <u>including outliers</u>
Shown are the number of model parameters (n par), the log-likelihood (logLik), Akaike information criterion (AIC), likelihood ratio test (LRT), degrees of freedom (df) and p-value for single term deletions of the random effects of the LMM of the OF Time in Center data after outlier removal. Animal nested under Litter is statistically significant (p = .000).

	n par	*logLik*	*AIC*	*LRT*	*df*	*p*	
<none>	76	-4468.71	9089.42	NA	NA	NA	
(1 | Animal:Litter)	75	-4496.77	9143.54	56.12	1.00	**.000**	***
(1 | Litter)	75	-4468.81	9087.62	0.20	1.00	.657	

Table 70: Estimated marginal means of the LMM of the OF Distance data <u>including outliers</u>
Shown are the estimated marginal mean, standard error (SE), degrees of freedom (df) and 95% confidence interval for each LPS dose, Age and Timeblock combination. – Table is continued on the next page.

LPS dose [µg/kg]	Age [PD]	Timeblock [min]	*Mean*	*SE*	*df*	*95% Confidence Interval*	
						Lower CL	*Upper CL*
0	~30	0-5	39.88	2.30	141.85	35.34	44.42
0	~45	0-5	28.55	2.30	141.85	24.01	33.10
0	~66	0-5	43.14	2.30	141.85	38.60	47.68
0	~94	0-5	40.63	2.30	141.85	36.09	45.17
20	~30	0-5	44.96	2.65	134.03	39.73	50.19
20	~45	0-5	36.27	2.65	134.03	31.04	41.50
20	~66	0-5	43.41	2.65	134.03	38.18	48.65
20	~94	0-5	45.51	2.65	134.03	40.28	50.74
100	~30	0-5	39.31	4.37	79.65	30.60	48.01
100	~45	0-5	33.79	4.37	79.65	25.09	42.50
100	~66	0-5	45.35	4.37	79.65	36.65	54.05
100	~94	0-5	37.05	4.37	79.65	28.35	45.75
0	~30	5-10	22.63	2.30	141.85	18.09	27.17
0	~45	5-10	22.84	2.30	141.85	18.30	27.38
0	~66	5-10	27.49	2.30	141.85	22.95	32.03
0	~94	5-10	23.51	2.30	141.85	18.97	28.05
20	~30	5-10	23.32	2.65	134.03	18.09	28.55
20	~45	5-10	25.17	2.65	134.03	19.94	30.40
20	~66	5-10	22.18	2.65	134.03	16.95	27.41
20	~94	5-10	16.43	2.65	134.03	11.19	21.66
100	~30	5-10	21.72	4.37	79.65	13.02	30.43
100	~45	5-10	26.79	4.37	79.65	18.09	35.50
100	~66	5-10	28.21	4.37	79.65	19.50	36.91
100	~94	5-10	22.45	4.37	79.65	13.75	31.15
0	~30	10-15	13.29	2.30	141.85	8.75	17.83
0	~45	10-15	13.60	2.30	141.85	9.06	18.14
0	~66	10-15	22.24	2.30	141.85	17.70	26.78
0	~94	10-15	14.29	2.30	141.85	9.75	18.83
20	~30	10-15	10.44	2.65	134.03	5.21	15.67
20	~45	10-15	19.21	2.65	134.03	13.98	24.45
20	~66	10-15	18.01	2.65	134.03	12.78	23.24
20	~94	10-15	12.38	2.65	134.03	7.15	17.62
100	~30	10-15	16.34	4.37	79.65	7.63	25.04
100	~45	10-15	9.85	4.37	79.65	1.15	18.55
100	~66	10-15	16.14	4.37	79.65	7.43	24.84
100	~94	10-15	16.69	4.37	79.65	7.99	25.40

Continuation of Table 70:

0	~30	15-20	5.97	2.30	141.85	1.43	10.51
0	~45	15-20	8.98	2.30	141.85	4.44	13.52
0	~66	15-20	15.17	2.30	141.85	10.63	19.71
0	~94	15-20	17.52	2.30	141.85	12.98	22.06
20	~30	15-20	5.17	2.65	134.03	-0.06	10.40
20	~45	15-20	10.19	2.65	134.03	4.96	15.43
20	~66	15-20	12.16	2.65	134.03	6.92	17.39
20	~94	15-20	9.59	2.65	134.03	4.36	14.83
100	~30	15-20	6.78	4.37	79.65	-1.93	15.48
100	~45	15-20	8.32	4.37	79.65	-0.38	17.03
100	~66	15-20	8.99	4.37	79.65	0.29	17.70
100	~94	15-20	11.28	4.37	79.65	2.57	19.98
0	~30	20-25	4.38	2.30	141.85	-0.16	8.92
0	~45	20-25	5.25	2.30	141.85	0.71	9.79
0	~66	20-25	9.96	2.30	141.85	5.42	14.50
0	~94	20-25	15.51	2.30	141.85	10.97	20.05
20	~30	20-25	3.87	2.65	134.03	-1.36	9.10
20	~45	20-25	5.68	2.71	143.29	0.33	11.04
20	~66	20-25	5.69	2.65	134.03	0.46	10.93
20	~94	20-25	13.02	2.65	134.03	7.79	18.25
100	~30	20-25	4.45	4.37	79.65	-4.25	13.15
100	~45	20-25	2.41	4.37	79.65	-6.30	11.11
100	~66	20-25	4.56	4.37	79.65	-4.14	13.27
100	~94	20-25	7.16	4.37	79.65	-1.54	15.87
0	~30	25-30	4.76	2.30	141.85	0.22	9.30
0	~45	25-30	2.60	2.34	152.22	-2.02	7.22
0	~66	25-30	7.63	2.30	141.85	3.09	12.17
0	~94	25-30	8.92	2.30	141.85	4.38	13.46
20	~30	25-30	5.42	2.65	134.03	0.19	10.65
20	~45	25-30	3.03	2.71	143.29	-2.33	8.38
20	~66	25-30	4.11	2.65	134.03	-1.12	9.35
20	~94	25-30	13.30	2.65	134.03	8.07	18.54
100	~30	25-30	5.81	4.37	79.65	-2.90	14.51
100	~45	25-30	0.85	4.37	79.65	-7.85	9.55
100	~66	25-30	3.29	4.37	79.65	-5.41	12.00

6.2.4.2. CenterTime

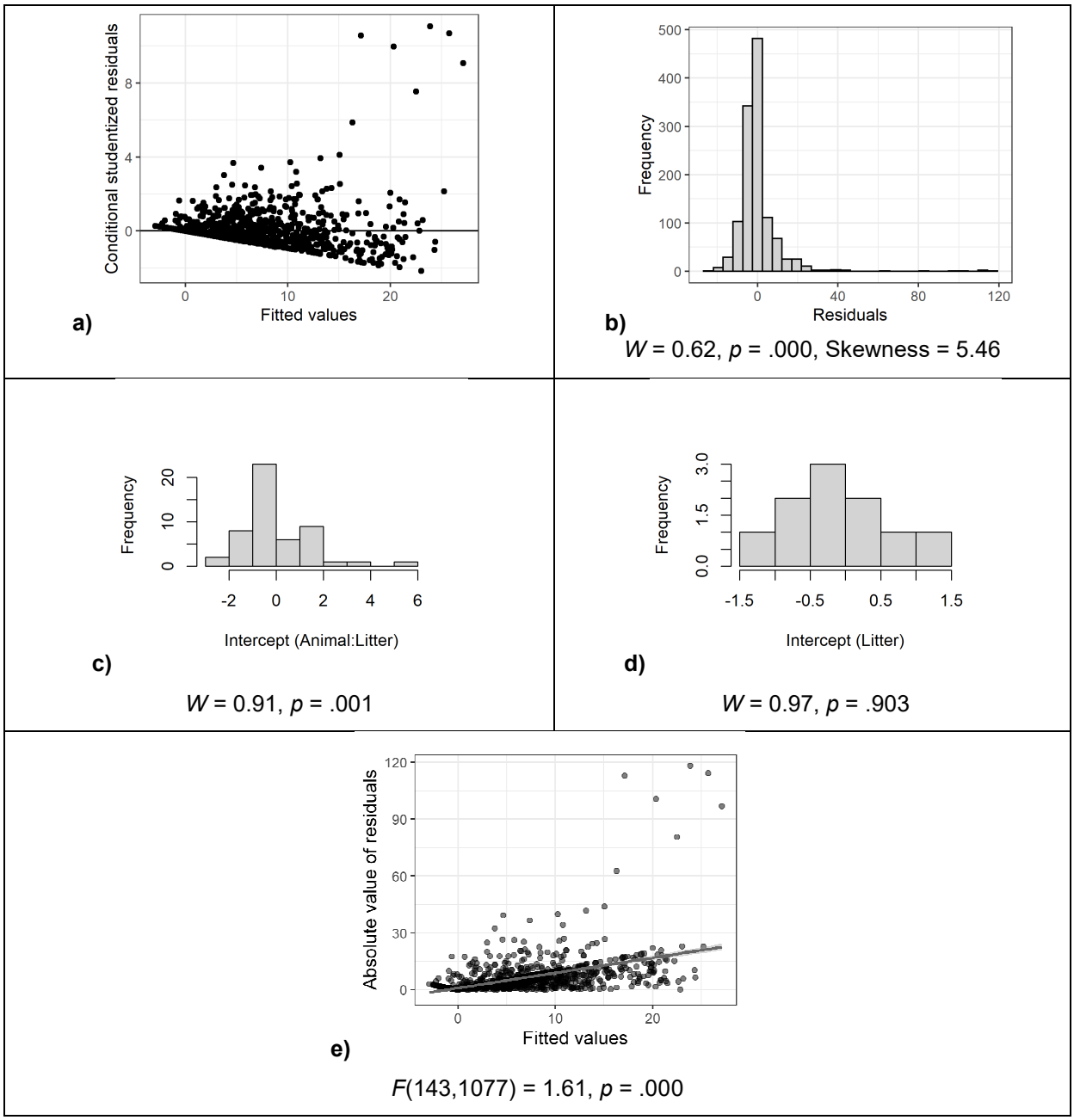

Figure 71: Inspection of model assumptions – OF Test – Time in Center <u>including outliers</u>
a) *Conditional (internally) studentized residuals*: There are outlier residuals exceeding ±3 SD of the mean, and the residuals show a weird pattern. **b)** *Histogram and Shapiro Wilk test of residuals*: The histogram appears skewed to the right, the Shapiro Wilk test shows significant difference from a normal distribution (p=.000). The skewness of 5.46 further confirms that the distribution is highly skewed (Bulmer, 1979). **c)** *Histogram and Shapiro Wilk test of random intercepts for animal (nested under litter)*: The histogram appears skewed to the right, and the Shapiro Wilk test shows significant difference from a normal distribution (p=.001). **d)** *Histogram and Shapiro Wilk test of random intercepts for litter*: The histogram appears approximately symmetric, and the Shapiro Wilk test is not significant (p=.903). **e)** *Spread-Location plot and Levene's test of residuals*: The S-L-plot strongly implies heteroscedasticity, which is confirmed by a significant Levene's test (p=.000).

Table 71: ANOVA table of the LMM of the OF Center Square Time data <u>including outliers</u>
Shown are the sums of squares (SS), mean squares (MS), numerator (df Num) and denominator (df Den) degrees of freedom, F- and p-value for each simple factor as well as for the Dose:Age, Dose:Timeblock, Age:Timeblock and Dose:Age:Timeblock interaction terms. The Age:Timeblock interaction shows statistical significance (p = .000), and the factor scan shows a trend towards statistical significance (p = .075).

	SS	*MS*	df_{Num}	df_{Den}	*F*	*p*	
Dose	262.09	131.04	2	6.44	1.08	.395	
Age	1746.38	582.13	3	1101.10	4.79	**.003**	**
Timeblock	10853.07	2170.61	5	1101.04	17.84	**.000**	***
Scan	403.97	403.97	1	44.15	3.32	**.075**	.
Dose:Age	865.39	144.23	6	1101.14	1.19	.311	
Dose:Timeblock	1581.63	158.16	10	1101.06	1.30	.225	
Age:Timeblock	5459.29	363.95	15	1101.04	2.99	**.000**	***
Dose:Age:TimeBlock	3341.46	111.38	30	1101.06	0.92	.598	

Table 72: ANOVA-like table for random effects of the LMM of the OF Time in Center data <u>including outliers</u>
Shown are the number of model parameters (n par), the log-likelihood (logLik), Akaike information criterion (AIC), likelihood ratio test (LRT), degrees of freedom (df) and p-value for single term deletions of the random effects of the LMM of the OF Time in Center data after outlier removal. Animal nested under Litter is statistically significant (p = .002).

	n par	*logLik*	*AIC*	*LRT*	*df*	*p*	
<none>	76	-4501.92	9155.84	NA	NA	NA	
(1 | Animal:Litter)	75	-4506.77	9163.54	9.70	1.00	**.002**	**
(1 | Litter)	75	-4502.76	9155.53	1.68	1.00	.195	

Table 73: Estimated marginal means of the LMM of the OF Center Square Time data <u>including outliers</u>

Shown are the estimated marginal mean, standard error (SE), degrees of freedom (df) and 95% confidence interval for each LPS dose, Age and Timeblock combination. – Table is continued on the next page.

LPS dose [µg/kg]	Age [PD]	Timeblock [min]	*Mean*	*SE*	*df*	*95% Confidence Interval*	
						Lower CL	*Upper CL*
0	~30	0-5	20.61	2.33	311.10	16.03	25.19
0	~45	0-5	8.77	2.33	311.10	4.19	13.35
0	~66	0-5	11.37	2.33	311.10	6.79	15.95
0	~94	0-5	16.01	2.33	311.10	11.43	20.59
20	~30	0-5	12.68	2.67	312.96	7.42	17.95
20	~45	0-5	5.84	2.67	312.96	0.58	11.10
20	~66	0-5	9.63	2.67	312.96	4.37	14.89
20	~94	0-5	11.53	2.67	312.96	6.26	16.79
100	~30	0-5	22.12	4.45	188.81	13.35	30.89
100	~45	0-5	7.55	4.45	188.81	-1.22	16.32
100	~66	0-5	9.12	4.45	188.81	0.35	17.89
100	~94	0-5	9.55	4.45	188.81	0.78	18.32
0	~30	5-10	19.25	2.33	311.10	14.67	23.83
0	~45	5-10	4.61	2.33	311.10	0.03	9.19
0	~66	5-10	5.97	2.33	311.10	1.39	10.55
0	~94	5-10	6.65	2.33	311.10	2.07	11.23
20	~30	5-10	8.16	2.67	312.96	2.90	13.42
20	~45	5-10	6.58	2.67	312.96	1.32	11.84
20	~66	5-10	5.68	2.67	312.96	0.42	10.95
20	~94	5-10	3.74	2.67	312.96	-1.53	9.00
100	~30	5-10	6.55	4.45	188.81	-2.22	15.32
100	~45	5-10	5.98	4.45	188.81	-2.79	14.75
100	~66	5-10	6.41	4.45	188.81	-2.37	15.18
100	~94	5-10	1.83	4.45	188.81	-6.94	10.60
0	~30	10-15	10.41	2.33	311.10	5.83	14.99
0	~45	10-15	4.09	2.33	311.10	-0.49	8.67
0	~66	10-15	13.37	2.33	311.10	8.79	17.95
0	~94	10-15	3.69	2.33	311.10	-0.89	8.27
20	~30	10-15	4.26	2.67	312.96	-1.00	9.52
20	~45	10-15	4.63	2.67	312.96	-0.63	9.89
20	~66	10-15	12.42	2.67	312.96	7.16	17.68
20	~94	10-15	2.16	2.67	312.96	-3.10	7.42
100	~30	10-15	4.83	4.45	188.81	-3.94	13.60
100	~45	10-15	1.12	4.45	188.81	-7.65	9.89
100	~66	10-15	3.12	4.45	188.81	-5.65	11.89
100	~94	10-15	4.98	4.45	188.81	-3.79	13.75

Continuation of Table 73:

0	~30	15-20	0.69	2.33	311.10	-3.89	5.27
0	~45	15-20	1.29	2.33	311.10	-3.29	5.87
0	~66	15-20	4.05	2.33	311.10	-0.53	8.63
0	~94	15-20	5.49	2.33	311.10	0.91	10.07
20	~30	15-20	0.63	2.67	312.96	-4.63	5.89
20	~45	15-20	1.95	2.67	312.96	-3.31	7.21
20	~66	15-20	4.10	2.67	312.96	-1.16	9.37
20	~94	15-20	1.21	2.67	312.96	-4.05	6.47
100	~30	15-20	1.55	4.45	188.81	-7.22	10.32
100	~45	15-20	0.12	4.45	188.81	-8.65	8.89
100	~66	15-20	5.55	4.45	188.81	-3.22	14.32
100	~94	15-20	1.98	4.45	188.81	-6.79	10.75
0	~30	20-25	1.09	2.33	311.10	-3.49	5.67
0	~45	20-25	1.65	2.33	311.10	-2.93	6.23
0	~66	20-25	3.13	2.33	311.10	-1.45	7.71
0	~94	20-25	8.17	2.33	311.10	3.59	12.75
20	~30	20-25	0.42	2.67	312.96	-4.84	5.68
20	~45	20-25	1.67	2.74	331.37	-3.72	7.07
20	~66	20-25	1.00	2.67	312.96	-4.26	6.26
20	~94	20-25	3.10	2.67	312.96	-2.16	8.37
100	~30	20-25	2.41	4.45	188.81	-6.37	11.18
100	~45	20-25	0.12	4.45	188.81	-8.65	8.89
100	~66	20-25	1.26	4.45	188.81	-7.51	10.03
100	~94	20-25	1.69	4.45	188.81	-7.08	10.46
0	~30	25-30	2.61	2.33	311.10	-1.97	7.19
0	~45	25-30	-0.01	2.37	330.63	-4.68	4.65
0	~66	25-30	1.05	2.33	311.10	-3.53	5.63
0	~94	25-30	1.61	2.33	311.10	-2.97	6.19
20	~30	25-30	0.58	2.67	312.96	-4.68	5.84
20	~45	25-30	0.06	2.74	331.37	-5.33	5.46
20	~66	25-30	0.63	2.67	312.96	-4.63	5.89
20	~94	25-30	7.84	2.67	312.96	2.58	13.10
100	~30	25-30	3.55	4.45	188.81	-5.22	12.32
100	~45	25-30	0.12	4.45	188.81	-8.65	8.89
100	~66	25-30	2.12	4.45	188.81	-6.65	10.89
100	~94	25-30	18.12	4.45	188.81	9.35	26.89

6.2.4.3. Rearings

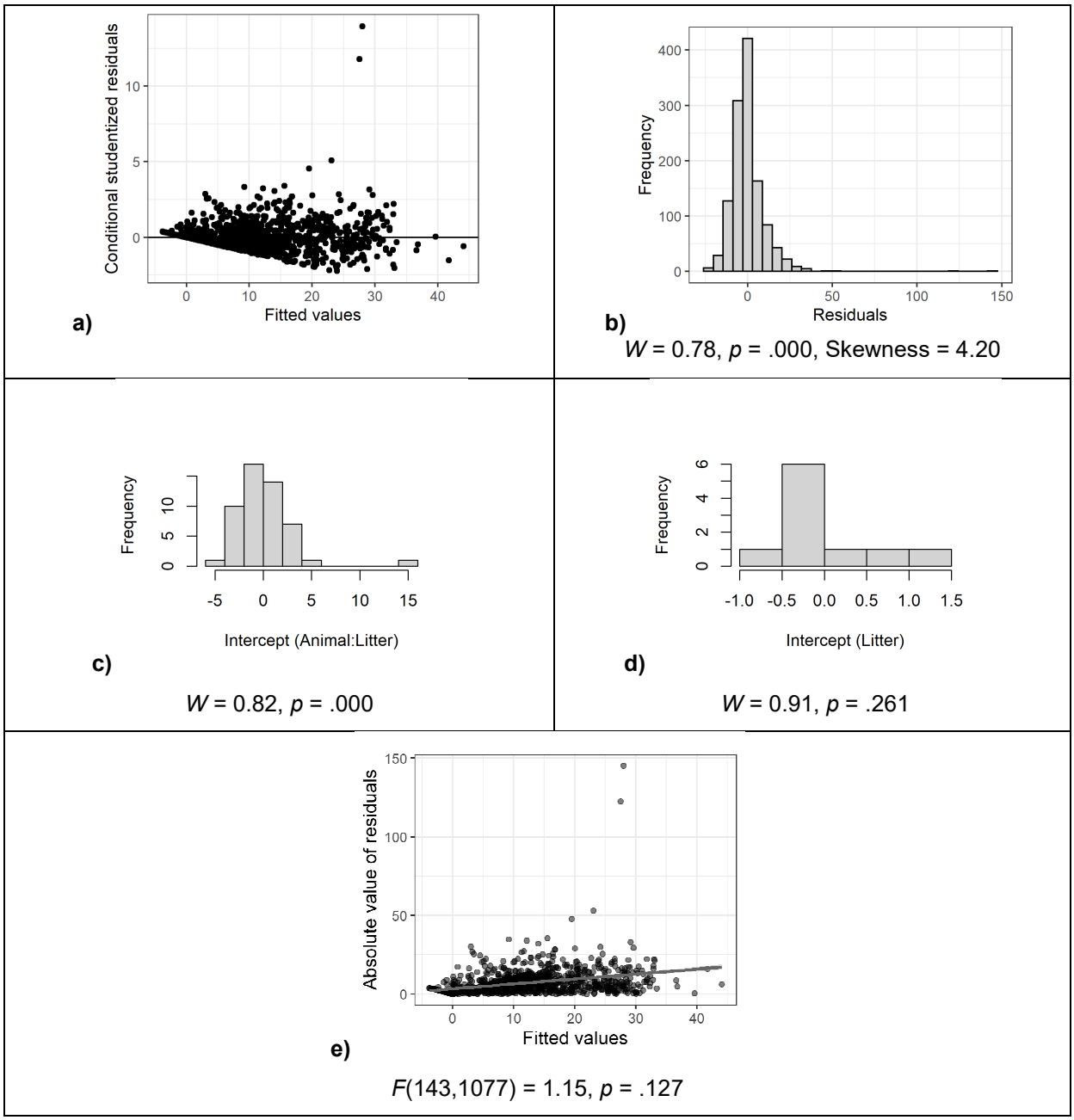

Figure 72: Inspection of model assumptions – OF Test – Rearings <u>including outliers</u>
a) *Conditional (internally) studentized residuals*: There are outlier residuals exceeding ±3 SD of the mean, and the residuals show a weird pattern. **b)** *Histogram and Shapiro Wilk test of residuals*: The histogram appears skewed to the right, the Shapiro Wilk test shows significant difference from a normal distribution (p=.000). The skewness of 4.20 further confirms that the distribution is highly skewed (Bulmer, 1979). **c)** *Histogram and Shapiro Wilk test of random intercepts for animal (nested under litter)*: The histogram appears skewed to the right, and the Shapiro Wilk test shows significant difference from a normal distribution (p=.000). **d)** *Histogram and Shapiro Wilk test of random intercepts for litter*: The histogram appears approximately symmetric, and the Shapiro Wilk test is not significant (p=.261). **e)** *Spread-Location plot and Levene's test of residuals*: The S-L-plot implies heteroscedasticity, but Levene's test is not significant (p=.127)

Table 74: ANOVA table of the LMM of the OF Rearings data <u>including outliers</u>
Shown are the sums of squares (SS), mean squares (MS), numerator (df Num) and denominator (df Den) degrees of freedom, F- and p-value for each simple factor as well as for the Dose:Age, Dose:Timeblock, Age:Timeblock and Dose:Age:Timeblock interaction terms. The effects for Age and Timeblock show statistical significance (p = .000).

	SS	*MS*	df_{Num}	df_{Den}	*F*	*p*
Dose	3.80	1.90	2	2.90	0.02	.984
Age	8031.73	2677.24	3	1099.97	22.63	**.000** ***
Timeblock	52093.16	10418.63	5	1099.93	88.05	**.000** ***
Scan	70.99	70.99	1	42.18	0.60	.443
Dose:Age	904.56	150.76	6	1099.99	1.27	.266
Dose:Timeblock	1754.54	175.45	10	1099.95	1.48	.140
Age:Timeblock	1520.64	101.38	15	1099.93	0.86	.614
Dose:Age:TimeBlock	2479.69	82.66	30	1099.95	0.70	.887

Table 75: ANOVA-like table for random effects of the LMM of the OF Rearings data <u>including outliers</u>
Shown are the number of model parameters (n par), the log-likelihood (logLik), Akaike information criterion (AIC), likelihood ratio test (LRT), degrees of freedom (df) and p-value for single term deletions of the random effects of the LMM of the OF Time in Center data after outlier removal. Animal nested under Litter is statistically significant (p = .000).

	n par	*logLik*	*AIC*	*LRT*	*df*	*p*
<none>	76	-4500.57	9153.15	NA	NA	NA
(1 | Animal:Litter)	75	-4523.55	9197.11	45.96	1.00	**.000** ***
(1 | Litter)	75	-4500.64	9151.28	0.13	1.00	.717

Table 76: Estimated marginal means of the LMM of the OF Rearings data <u>including outliers</u>
Shown are the estimated marginal mean, standard error (SE), degrees of freedom (df) and 95% confidence interval for each LPS dose, Age and Timeblock combination. – Table is continued on the next page.

LPS dose [µg/kg]	Age [PD]	Timeblock [min]	*Mean*	*SE*	*df*	*95% Confidence Interval*	
						Lower CL	*Upper CL*
0	~30	0-5	23.08	2.35	107.73	18.42	27.75
0	~45	0-5	15.96	2.35	107.73	11.30	20.63
0	~66	0-5	29.32	2.35	107.73	24.66	33.99
0	~94	0-5	28.24	2.35	107.73	23.58	32.91
20	~30	0-5	23.55	2.71	101.96	18.18	28.93
20	~45	0-5	20.71	2.71	101.96	15.34	26.09
20	~66	0-5	25.66	2.71	101.96	20.28	31.03
20	~94	0-5	27.97	2.71	101.96	22.60	33.35
100	~30	0-5	25.64	4.48	59.01	16.67	34.61
100	~45	0-5	20.78	4.48	59.01	11.81	29.75
100	~66	0-5	32.07	4.48	59.01	23.10	41.04
100	~94	0-5	27.78	4.48	59.01	18.81	36.75
0	~30	5-10	12.16	2.35	107.73	7.50	16.83
0	~45	5-10	14.00	2.35	107.73	9.34	18.67
0	~66	5-10	19.20	2.35	107.73	14.54	23.87
0	~94	5-10	16.60	2.35	107.73	11.94	21.27
20	~30	5-10	9.45	2.71	101.96	4.07	14.82
20	~45	5-10	12.66	2.71	101.96	7.28	18.03
20	~66	5-10	16.97	2.71	101.96	11.60	22.35
20	~94	5-10	12.24	2.71	101.96	6.86	17.61
100	~30	5-10	12.07	4.48	59.01	3.10	21.04
100	~45	5-10	15.21	4.48	59.01	6.24	24.18
100	~66	5-10	24.50	4.48	59.01	15.53	33.47
100	~94	5-10	19.50	4.48	59.01	10.53	28.47
0	~30	10-15	8.08	2.35	107.73	3.42	12.75
0	~45	10-15	5.88	2.35	107.73	1.22	10.55
0	~66	10-15	16.68	2.35	107.73	12.02	21.35
0	~94	10-15	10.40	2.35	107.73	5.74	15.07
20	~30	10-15	4.34	2.71	101.96	-1.03	9.72
20	~45	10-15	8.66	2.71	101.96	3.28	14.03
20	~66	10-15	14.24	2.71	101.96	8.86	19.61
20	~94	10-15	9.55	2.71	101.96	4.18	14.93
100	~30	10-15	6.50	4.48	59.01	-2.47	15.47
100	~45	10-15	5.21	4.48	59.01	-3.76	14.18
100	~66	10-15	9.07	4.48	59.01	0.10	18.04
100	~94	10-15	15.07	4.48	59.01	6.10	24.04

Continuation of Table 76:

0	~30	15-20	2.28	2.35	107.73	-2.38	6.95
0	~45	15-20	3.68	2.35	107.73	-0.98	8.35
0	~66	15-20	8.44	2.35	107.73	3.78	13.11
0	~94	15-20	12.32	2.35	107.73	7.66	16.99
20	~30	15-20	1.19	2.71	101.96	-4.19	6.56
20	~45	15-20	4.29	2.71	101.96	-1.09	9.67
20	~66	15-20	13.03	2.71	101.96	7.65	18.40
20	~94	15-20	7.45	2.71	101.96	2.07	12.82
100	~30	15-20	1.50	4.48	59.01	-7.47	10.47
100	~45	15-20	0.78	4.48	59.01	-8.19	9.75
100	~66	15-20	4.07	4.48	59.01	-4.90	13.04
100	~94	15-20	10.50	4.48	59.01	1.53	19.47
0	~30	20-25	1.44	2.35	107.73	-3.22	6.11
0	~45	20-25	1.80	2.35	107.73	-2.86	6.47
0	~66	20-25	4.36	2.35	107.73	-0.30	9.03
0	~94	20-25	11.56	2.35	107.73	6.90	16.23
20	~30	20-25	0.97	2.71	101.96	-4.40	6.35
20	~45	20-25	2.98	2.78	109.14	-2.52	8.48
20	~66	20-25	11.45	2.71	101.96	6.07	16.82
20	~94	20-25	8.19	2.71	101.96	2.81	13.56
100	~30	20-25	0.93	4.48	59.01	-8.04	9.90
100	~45	20-25	0.50	4.48	59.01	-8.47	9.47
100	~66	20-25	3.21	4.48	59.01	-5.76	12.18
100	~94	20-25	5.64	4.48	59.01	-3.33	14.61
0	~30	25-30	1.84	2.35	107.73	-2.82	6.51
0	~45	25-30	0.52	2.40	115.98	-4.23	5.27
0	~66	25-30	2.32	2.35	107.73	-2.34	6.99
0	~94	25-30	5.56	2.35	107.73	0.90	10.23
20	~30	25-30	2.61	2.71	101.96	-2.77	7.98
20	~45	25-30	1.48	2.78	109.14	-4.02	6.98
20	~66	25-30	11.92	2.71	101.96	6.55	17.30
20	~94	25-30	8.71	2.71	101.96	3.34	14.09
100	~30	25-30	4.21	4.48	59.01	-4.76	13.18
100	~45	25-30	0.07	4.48	59.01	-8.90	9.04
100	~66	25-30	0.78	4.48	59.01	-8.19	9.75
100	~94	25-30	5.36	4.48	59.01	-3.61	14.32

6.2.5. NOR

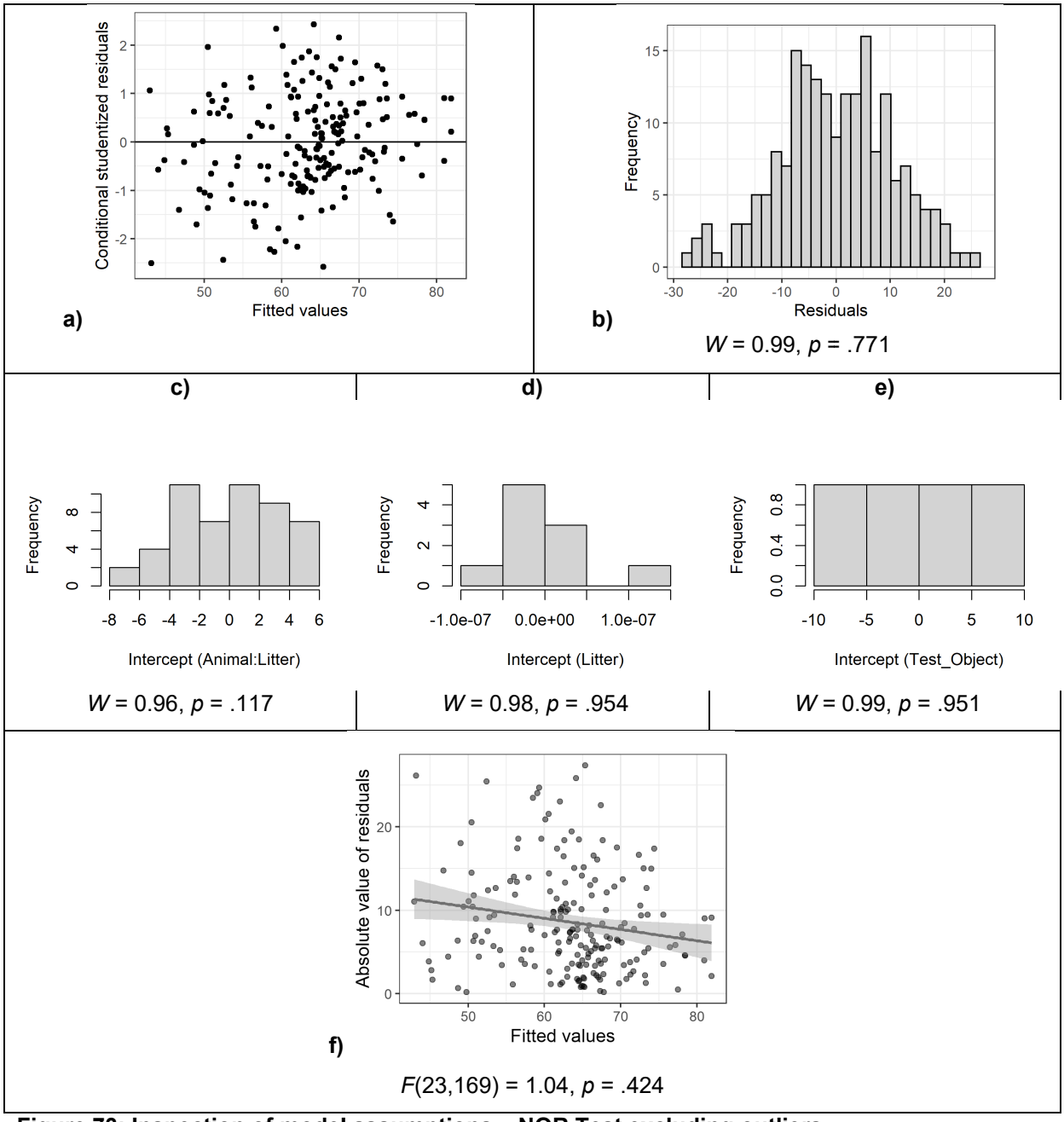

Figure 73: Inspection of model assumptions – NOR Test excluding outliers
a) *Conditional (internally) studentized residuals*: All residuals fall within ±3 SD of the mean. **b)** *Histogram and Shapiro Wilk test of residuals*: The histogram appears approximately symmetric, with a tendency for bimodality, and the Shapiro Wilk test is not significant (p=.771). **c)** *Histogram and Shapiro Wilk test of random intercepts for animal (nested under litter)*: The histogram appears approximately symmetric, and the Shapiro Wilk test is not significant (p=.117). **d)** *Histogram and Shapiro Wilk test of random intercepts for litter*: Considering the low number of intercepts, the histogram appears approximately symmetric, and the Shapiro Wilk test is not significant (p=.954). **e)** *Histogram and Shapiro Wilk test of random intercepts for test object*: The histogram appears symmetric, and the Shapiro Wilk test is not significant (p=.951). **f)** *Spread-Location plot and Levene's test of residuals*: The S-L-plot shows approximately equal variation across the whole range of values, with a slight trend towards lower variation at higher values, and Levene's test is not significant (p=.424).

Model formula: Recognition_Index ~ Dose * Age + Scan + (1 | Litter/Animal)

Table 77: ANOVA-like table for random effects of the LMM of the NOR data after outlier removal
Shown are the number of model parameters (*n par*), the log-likelihood (*logLik*), Akaike information criterion (*AIC*), likelihood ratio test (*LRT*), degrees of freedom (*df*) and p-value for single term deletions of the random effects of the LMM of the NOR data after outlier removal. Animal nested under Litter (p = .019) as well as Test_Object (p = .000) are statistically significant, whereas the random effect of Litter is not.

	n par	*logLik*	*AIC*	*LRT*	*df*	*p*
<none>	17	-731.03	1496.07	NA	NA	NA
(1 | Animal:Litter)	16	-733.78	1499.56	5.49	1.00	**.019** *
(1 | Litter)	16	-731.03	1494.07	-0.00	1.00	1.000
(1 | Test_Object)	16	-739.03	1510.06	15.99	1.00	**.000** ***

Table 78: Post hoc multiple comparisons of NOR data - simple pair-wise t-tests for 'Dose' after outlier removal
Shown are the estimates and standard error (*SE*) of simple pair-wise t-tests for the contrast LPS dose [µg/kg], including degrees of freedom (*df*), t ratio, p-values corrected for multiple comparisons using the Tukey method (*p*) as well as uncorrected p-values (*p uncorr*) and 95% confidence intervals. After Tukey adjustment, only the 0-100 contrast on PD ~45 is statistically significant (p = .018). Without Tukey adjustment, the 20-100 contrast on PD ~30 shows a trend for statistical significance in addition.

Contrast LPS dose [µg/kg]	Age [PD]	*Estimate*	*SE*	*df*	*t ratio*	*p*	*p uncorr*	*95% Confidence Interval*	
								Lower CL	*Upper CL*
0 - 20	~30	-0.69	4.04	168.36	-0.17	.984	*.865*	-8.65	7.28
0 - 100	~30	-11.58	5.79	169.02	-2.00	.116	*.047*	-23.01	-0.14
20 - 100	~30	-10.89	6.09	169.69	-1.79	.177	*.076* .	-22.91	1.14
0 - 20	~45	-6.11	4.00	168.19	-1.53	.280	*.128*	-14.01	1.78
0 - 100	~45	-15.03	5.47	164.59	-2.75	**.018** *	*.007* **	-25.84	-4.23
20 - 100	~45	-8.92	5.74	165.32	-1.55	.269	*.122*	-20.25	2.42
0 - 20	~66	1.86	3.92	166.34	0.47	.884	*.637*	-5.89	9.60
0 - 100	~66	-5.87	5.47	164.65	-1.07	.533	*.285*	-16.68	4.94
20 - 100	~66	-7.73	5.68	164.21	-1.36	.365	*.176*	-18.95	3.50
0 - 20	~94	5.16	4.24	171.67	1.22	.446	*.226*	-3.22	13.53
0 - 100	~94	6.75	5.58	166.24	1.21	.449	*.228*	-4.27	17.77
20 - 100	~94	1.59	5.82	166.31	0.27	.959	*.784*	-9.89	13.08

Table 79: Post hoc multiple comparisons of NOR data - simple pair-wise t-tests for 'Age' after outlier removal

Shown are the estimates and standard error (*SE*) of simple pair-wise t-tests for the contrast Age [PD], including degrees of freedom (*df*), t ratio, p-values corrected for multiple comparisons using the Tukey method (*p*) as well as uncorrected p-values (*p uncorr*) and 95% confidence intervals. After Tukey adjustment, both in the 20 µg/kg and 100 µg/kg LPS group the ~45-~94 PD contrast is statistically significant (p = .030 / 0.003), while in the 100 µg/kg LPS group the ~30-~94 PD contrast shows a trend to statistical significance in addition (p = 0.56). Without Tukey adjustment, this trend is statistically significant (p = .014) and the ~66-~94 PD contrast is statistically significant in the 100 µg/kg LPS group as well (p = .047).

Contrast Age [PD]	LPS dose [µg/kg]	*Estimate*	*SE*	*df*	*t ratio*	*p*	*p uncorr*	*95% Confidence Interval*	
								Lower CL	*Upper CL*
~30 - ~45	0	8.92	6.79	2.92	1.31	.616	*.283*	-13.06	30.89
~30 - ~66	0	1.20	3.35	131.72	0.36	.984	*.722*	-5.44	7.83
~30 - ~94	0	9.10	6.88	3.06	1.32	.609	*.276*	-12.54	30.73
~45 - ~66	0	-7.72	6.80	2.92	-1.14	.698	*.341*	-29.68	14.24
~45 - ~94	0	0.18	3.50	134.92	0.05	1.000	*.959*	-6.74	7.10
~66 - ~94	0	7.90	6.88	3.07	1.15	.691	*.333*	-13.72	29.52
~30 - ~45	20	3.49	7.15	3.57	0.49	.957	*.654*	-17.33	24.31
~30 - ~66	20	3.74	3.93	133.72	0.95	.777	*.343*	-4.04	11.52
~30 - ~94	20	14.94	7.21	3.70	2.07	.309	*.113*	-5.74	35.62
~45 - ~66	20	0.25	7.08	3.44	0.04	1.000	*.973*	-20.74	21.25
~45 - ~94	20	11.45	4.11	137.71	2.79	**.030** *	*.006* **	3.33	19.57
~66 - ~94	20	11.20	7.15	3.58	1.57	.492	*.201*	-9.62	32.01
~30 - ~45	100	5.46	8.83	8.20	0.62	.923	*.553*	-14.82	25.74
~30 - ~66	100	6.90	6.56	134.91	1.05	.719	*.294*	-6.07	19.88
~30 - ~94	100	27.42	8.83	8.20	3.10	**.056** .	*.014* *	7.14	47.70
~45 - ~66	100	1.44	8.61	7.45	0.17	.998	*.871*	-18.68	21.57
~45 - ~94	100	21.96	6.26	130.73	3.51	**.003** **	*.001* ***	9.59	34.34
~66 - ~94	100	20.52	8.61	7.45	2.38	.164	*.047* *	0.39	40.64

Table 80: Post hoc multiple comparisons of NOR data - simple one-sided t-tests vs. chance level (RI of 50 %) after outlier removal
Shown are the estimated marginal means and standard error (*SE*), degrees of freedom (*df*), t ratio, p-values corrected for multiple comparisons using the Sidak method (*p*) as well as uncorrected p-values (*p uncorr*) and 95% confidence intervals. After Tukey adjustment, only the means of the three earlier time points (PD ~30 / ~45 / ~66) in the 100 µg/kg LPS group are statistically significant (p = .007 / .030 / .042). Without Tukey adjustment, most means at least show a trend for statistical significance, except from the latest time point (PD ~94) in the two LPS groups (20 / 100 µg/kg).

Age [PD]	LPS dose [µg/kg]	*Mean*	*SE*	*df*	*t ratio*	*p*	*p uncorr*	*95% Confidence Interval*	
								Lower CL	*Upper CL*
~30	0	67.46	4.92	3.20	3.55	.187	*.017* *	56.18	Inf
~45	0	58.54	4.92	3.20	1.74	.667	*.087* .	47.26	Inf
~66	0	66.26	4.92	3.21	3.30	.221	*.021* *	54.98	Inf
~94	0	58.36	5.03	3.51	1.66	.681	*.091* .	47.19	Inf
~30	20	68.15	5.23	4.08	3.47	.139	*.012* *	57.07	Inf
~45	20	64.66	5.19	3.95	2.83	.254	*.024* *	53.56	Inf
~66	20	64.40	5.13	3.80	2.81	.269	*.026* *	53.29	Inf
~94	20	53.21	5.28	4.24	0.61	.983	*.287*	42.14	Inf
~30	100	79.03	6.68	10.69	4.34	**.007** **	*.001* ***	67.00	Inf
~45	100	73.57	6.39	9.01	3.69	**.030** *	*.003* **	61.86	Inf
~66	100	72.13	6.39	9.01	3.46	**.042** *	*.004* **	60.41	Inf
~94	100	51.61	6.39	9.01	0.25	.998	*.403*	39.89	Inf

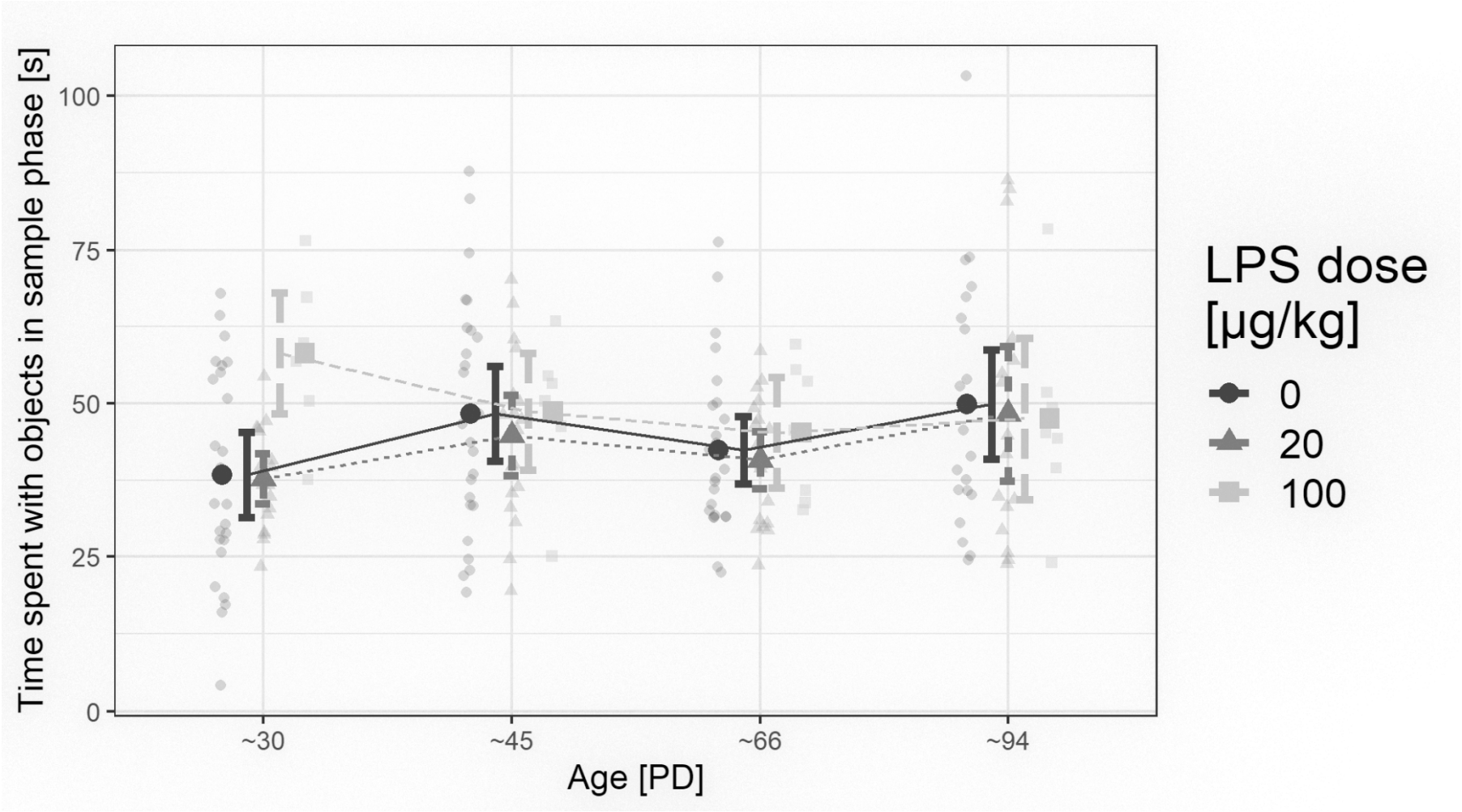

Figure 74: Time spent with objects in sample phase [s] by Age and LPS dose
Shown are means of the time spent with both identical objects in the sample phase ± SEM on top of the jittered raw data. SAL data (0 µg/kg LPS) shown as dark circles, 20 µg/kg LPS as dark grey triangles and 100 µg/kg LPS as light grey squares. The time seems to be similar between groups and time points, with the exception of a possible higher interaction time of the 100 µg/kg LPS group on PD~30.

6.2.6. Sensitivity Analysis NOR

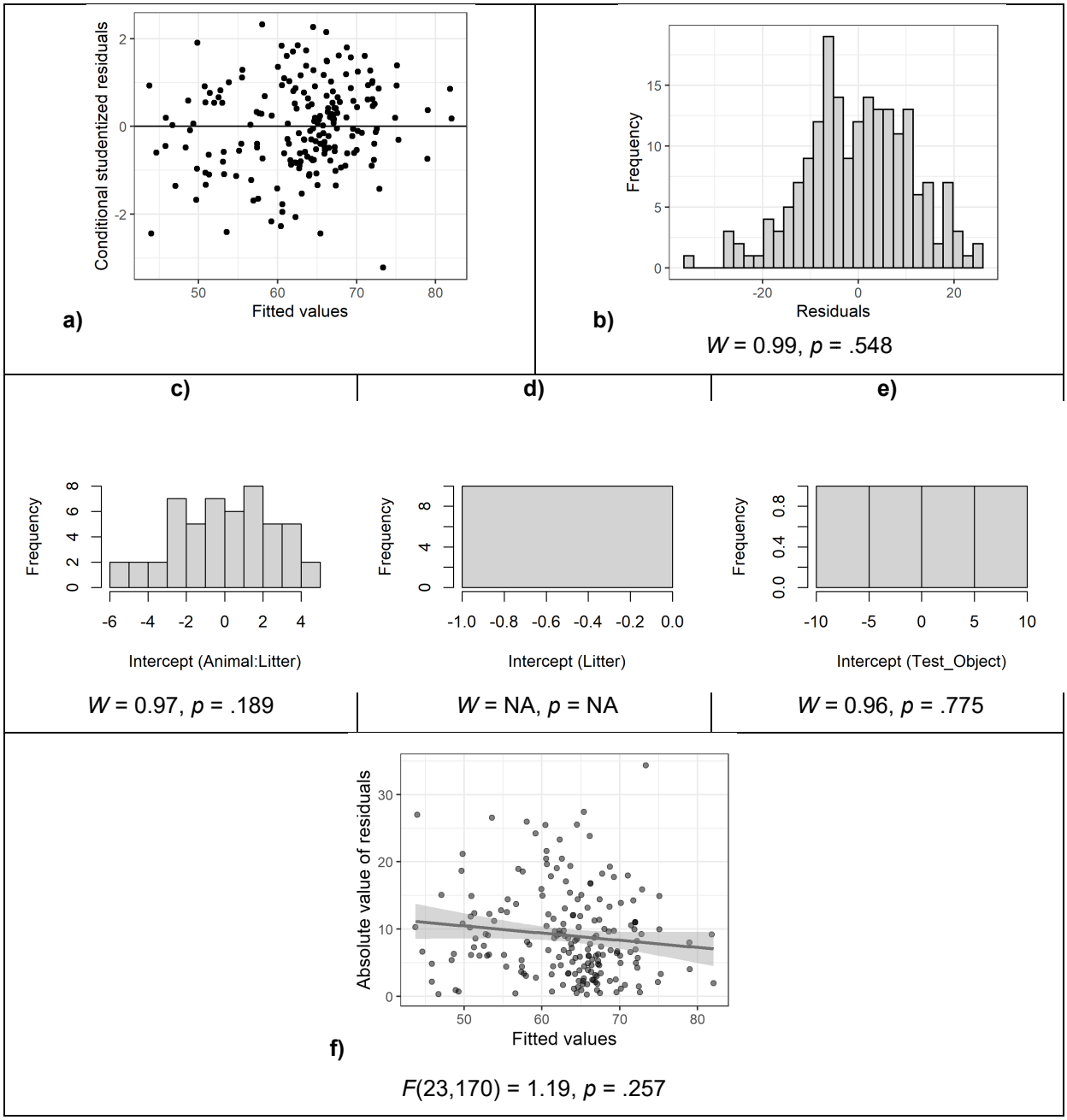

Figure 75: Inspection of model assumptions – NOR Test <u>including outliers</u>
a) *Conditional (internally) studentized residuals*: One residual (Animal 112 on PD~30) is more than 3 SD away from the mean and was thus excluded from the main analysis. **b)** *Histogram and Shapiro Wilk test of residuals*: The histogram appears approximately symmetric, and the Shapiro Wilk test is not significant (p=.548). **c)** *Histogram and Shapiro Wilk test of random intercepts for animal (nested under litter)*: The histogram appears approximately symmetric, and the Shapiro Wilk test is not significant (p=.189). **d)** *Histogram and Shapiro Wilk test of random intercepts for litter*: The histogram is misleading as all random intercepts for litter were estimated as 0.00. Since there is no variation in the intercepts, normality couldn't be assessed. **e)** *Histogram and Shapiro Wilk test of random intercepts for test object*: The histogram appears symmetric, and the Shapiro Wilk test is not significant (p=.775). **f)** *Spread-Location plot and Levene's test of residuals*: The S-L-plot shows approximately equal variation across the whole range of values, with a slight trend towards lower variation at higher values, and Levene's test is not significant (p=.257).

Table 81: ANOVA table of the linear mixed model of the NOR data including outliers
Shown are the sums of squares (*SS*), mean squares (*MS*), numerator (df_{Num}) and denominator (df_{Den}) degrees of freedom, F- and p-value for each simple factor as well as for the Dose:Age interaction term. The factor Age shows a trend for statistical significance (p = .088).

	SS	*MS*	df_{Num}	df_{Den}	*F*	*p*	
Dose	367.63	183.82	2	45.17	1.23	.302	
Age	2628.15	876.05	3	3.05	5.86	**.088**	.
Scan	151.52	151.52	1	45.64	1.01	.319	
Dose:Age	1533.96	255.66	6	134.13	1.71	.123	

Table 82: ANOVA-like table for random effects of the LMM of the NOR data including outliers
Shown are the number of model parameters (*n par*), the log-likelihood (*logLik*), Akaike information criterion (*AIC*), likelihood ratio test (*LRT*), degrees of freedom (*df*) and p-value for single term deletions of the random effects of the LMM of the NOR data including outliers. Test_Object is statistically significant (p = .000), Animal nested under Litter shows a trend for significance (p = .074), whereas the random effect of Litter is not significant.

	n par	*logLik*	*AIC*	*LRT*	*df*	*p*	
<none>	17	-740.02	1514.04	NA	NA	NA	
(1 | Animal:Litter)	16	-741.62	1515.23	3.19	1.00	**.074**	.
(1 | Litter)	16	-740.02	1512.04	-0.00	1.00	1.000	
(1 | Test_Object)	16	-747.07	1526.15	14.11	1.00	**.000**	***

Table 83: Estimated marginal means of the LMM of the NOR data including outliers
Shown are the estimated marginal mean, standard error (*SE*), degrees of freedom (*df*) and 95% confidence interval for each LPS dose and Age combination.

LPS dose [µg/kg]	Age [PD]	*Mean*	*SE*	*df*	*95% Confidence Interval*	
					Lower CL	*Upper CL*
0	~30	67.31	4.90	3.26	52.38	82.23
0	~45	58.51	4.90	3.26	43.59	73.43
0	~66	66.37	4.91	3.27	51.46	81.28
0	~94	58.18	5.03	3.60	43.60	72.77
20	~30	68.07	5.23	4.21	53.84	82.31
20	~45	64.60	5.18	4.06	50.30	78.90
20	~66	64.24	5.12	3.89	49.85	78.63
20	~94	53.16	5.28	4.38	38.98	67.33
100	~30	72.44	6.44	9.54	58.00	86.88
100	~45	73.61	6.44	9.54	59.17	88.05
100	~66	72.24	6.44	9.54	57.80	86.68
100	~94	51.64	6.44	9.54	37.20	66.07

Table 84: Post hoc multiple comparisons of NOR data - simple pair-wise t-tests for 'Dose' <u>including outliers</u>

Shown are the estimates and standard error (*SE*) of simple pair-wise t-tests for the contrast LPS dose [µg/kg], including degrees of freedom (*df*), t ratio, p-values corrected for multiple comparisons using the Tukey method (*p*) as well as uncorrected p-values (*p uncorr*) and 95% confidence intervals. Both before and after Tukey adjustment, only the 0-100 contrast on PD ~45 is statistically significant (p = .021).

Contrast LPS dose [µg/kg]	Age [PD]	*Estimate*	*SE*	*df*	*t ratio*	*p*	*p uncorr*	*95% Confidence Interval*	
								Lower CL	*Upper CL*
0 - 20	~30	-0.77	4.12	173.74	-0.19	.981	*.853*	-8.90	7.37
0 - 100	~30	-5.13	5.59	171.05	-0.92	.629	*.360*	-16.16	5.89
20 - 100	~30	-4.37	5.89	171.72	-0.74	.740	*.460*	-16.00	7.27
0 - 20	~45	-6.09	4.08	173.85	-1.49	.298	*.138*	-14.15	1.97
0 - 100	~45	-15.10	5.59	171.05	-2.70	**.021** *	*.008* **	-26.13	-4.08
20 - 100	~45	-9.01	5.86	171.62	-1.54	.276	*.126*	-20.58	2.56
0 - 20	~66	2.14	4.01	172.53	0.53	.855	*.595*	-5.77	10.04
0 - 100	~66	-5.87	5.59	171.11	-1.05	.547	*.295*	-16.90	5.16
20 - 100	~66	-8.00	5.80	170.77	-1.38	.354	*.170*	-19.45	3.45
0 - 20	~94	5.03	4.34	175.78	1.16	.480	*.248*	-3.54	13.59
0 - 100	~94	6.55	5.70	172.10	1.15	.485	*.252*	-4.70	17.80
20 - 100	~94	1.52	5.94	172.21	0.26	.964	*.798*	-10.20	13.25

Table 85: Post hoc multiple comparisons of NOR data - simple pair-wise t-tests for 'Age' after <u>including outliers</u>

Shown are the estimates and standard error (*SE*) of simple pair-wise t-tests for the contrast Age [PD], including degrees of freedom (*df*), t ratio, p-values corrected for multiple comparisons using the Tukey method (*p*) as well as uncorrected p-values (*p uncorr*) and 95% confidence intervals. After Tukey adjustment, both in the 20 µg/kg and 100 µg/kg LPS group the ~45-~94 PD contrast is statistically significant (p = .042 / 0.006). Without Tukey adjustment, the ~30-~94 PD and the ~66-~94 PD contrast are statistically significant in the 100 µg/kg LPS group as well (p = .044 / .046).

Contrast Age [PD]	LPS dose [µg/kg]	*Estimate*	*SE*	*df*	*t ratio*	*p*	*p uncorr*	*95% Confidence Interval*	
								Lower CL	*Upper CL*
~30 - ~45	0	8.80	6.81	3.03	1.29	.623	*.286*	-12.75	30.34
~30 - ~66	0	0.93	3.51	132.98	0.27	.993	*.791*	-6.00	7.87
~30 - ~94	0	9.12	6.89	3.19	1.32	.607	*.273*	-12.10	30.35
~45 - ~66	0	-7.86	6.81	3.03	-1.15	.688	*.331*	-29.40	13.67
~45 - ~94	0	0.33	3.66	136.59	0.09	1.000	*.929*	-6.91	7.56
~66 - ~94	0	8.19	6.90	3.20	1.19	.671	*.316*	-13.02	29.40
~30 - ~45	20	3.47	7.19	3.77	0.48	.959	*.656*	-16.99	23.93
~30 - ~66	20	3.83	4.11	135.16	0.93	.787	*.353*	-4.30	11.96
~30 - ~94	20	14.91	7.26	3.91	2.05	.308	*.111*	-5.42	35.25
~45 - ~66	20	0.36	7.12	3.62	0.05	1.000	*.962*	-20.25	20.98
~45 - ~94	20	11.44	4.29	139.53	2.67	**.042** *	*.009* **	2.97	19.92
~66 - ~94	20	11.08	7.19	3.77	1.54	.499	*.203*	-9.38	31.53
~30 - ~45	100	-1.17	8.77	8.24	-0.13	.999	*.897*	-21.31	18.96
~30 - ~66	100	0.20	6.54	132.00	0.03	1.000	*.976*	-12.74	13.14
~30 - ~94	100	20.80	8.77	8.24	2.37	.159	*.044* *	0.67	40.93
~45 - ~66	100	1.37	8.77	8.24	0.16	.999	*.879*	-18.76	21.50
~45 - ~94	100	21.98	6.54	131.97	3.36	**.006** **	*.001* ***	9.03	34.92
~66 - ~94	100	20.60	8.77	8.24	2.35	.164	*.046* *	0.47	40.73

Table 86: Post hoc multiple comparisons of NOR data - simple one-sided t-tests vs. chance level (RI of 50 %) after <u>including outliers</u>
Shown are the estimated marginal means and standard error (*SE*), degrees of freedom (*df*), t ratio, p-values corrected for multiple comparisons using the Sidak method (*p*) as well as uncorrected p-values (*p uncorr*) and 95% confidence intervals. After Tukey adjustment, only the means of the three earlier time points (PD ~30 / ~45 / ~66) in the 100 µg/kg LPS group are statistically significant (p = .037 / .028 / .039). Without Tukey adjustment, most means at least show a trend for statistical significance, except from the latest time point (PD ~94) in the two LPS groups (20 / 100 µg/kg).

Age [PD]	LPS dose [µg/kg]	*Mean*	*SE*	*df*	*t ratio*	*p*	*p uncorr*	*95% Confidence Interval*	
								Lower CL	*Upper CL*
~30	0	67.31	4.90	3.26	3.53	.185	*.017* *	56.13	Inf
~45	0	58.51	4.90	3.26	1.74	.664	*.087* .	47.34	Inf
~66	0	66.37	4.91	3.27	3.34	.211	*.020* *	55.20	Inf
~94	0	58.18	5.03	3.60	1.63	.691	*.093* .	47.12	Inf
~30	20	68.07	5.23	4.21	3.46	.134	*.012* *	57.08	Inf
~45	20	64.60	5.18	4.06	2.82	.249	*.024* *	53.60	Inf
~66	20	64.24	5.12	3.89	2.78	.269	*.026* *	53.22	Inf
~94	20	53.16	5.28	4.38	0.60	.983	*.290*	42.18	Inf
~30	100	72.44	6.44	9.54	3.49	**.037** *	*.003* **	60.71	Inf
~45	100	73.61	6.44	9.54	3.67	**.028** *	*.002* **	61.89	Inf
~66	100	72.24	6.44	9.54	3.45	**.039** *	*.003* **	60.51	Inf
~94	100	51.64	6.44	9.54	0.25	.998	*.402*	39.91	Inf

6.2.7. PPI

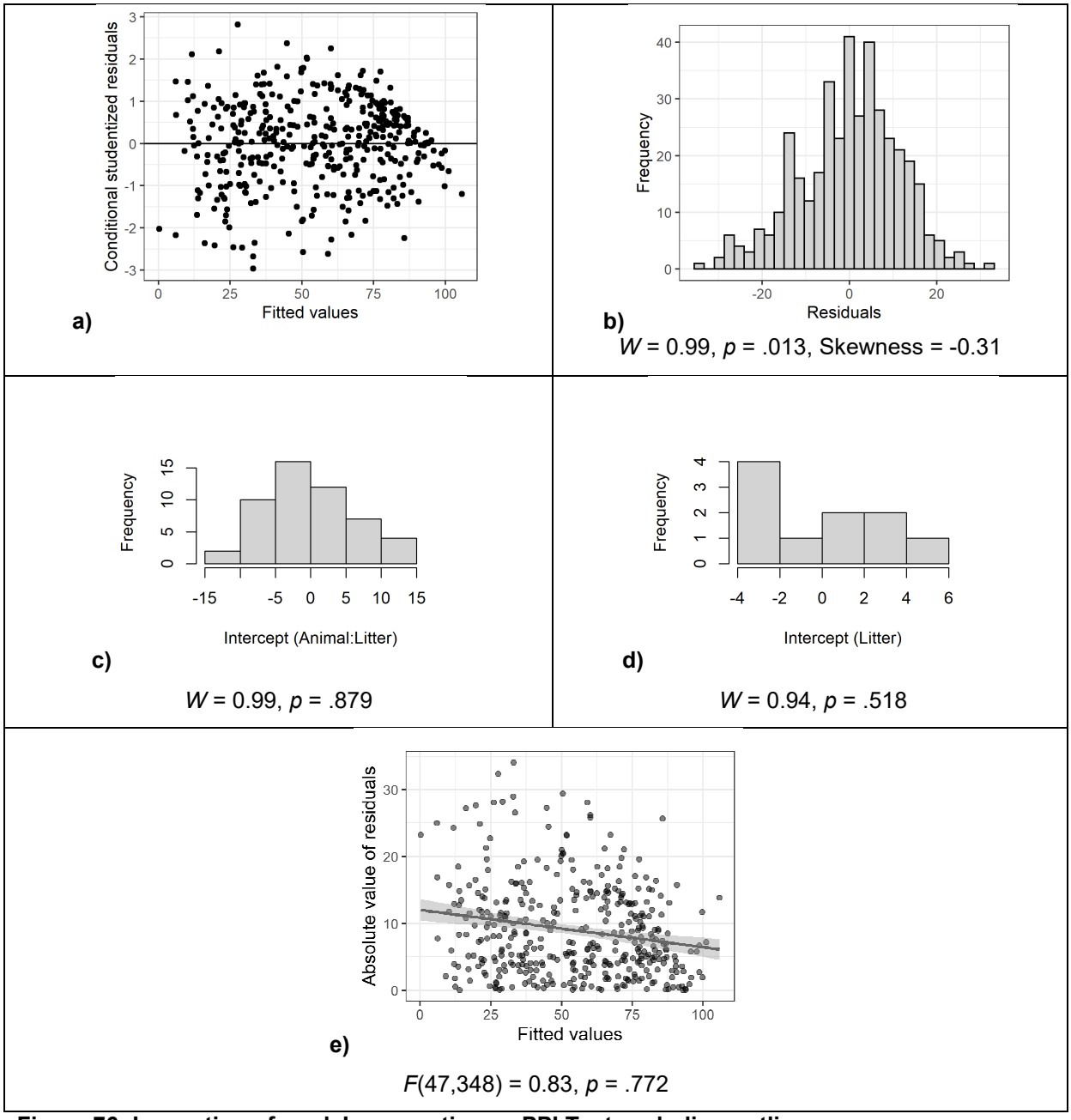

Figure 76: Inspection of model assumptions – PPI Test excluding outliers
a) *Conditional (internally) studentized residuals*: All residuals fall within ±3 SD of the mean. **b)** *Histogram and Shapiro Wilk test of residuals*: The histogram appears approximately symmetric, but the Shapiro Wilk test shows significant difference from a normal distribution (p=.013). However, as the skewness of -0.31 is smaller than -0.5, it can still be considered fairly symmetrical (Bulmer, 1979). **c)** *Histogram and Shapiro Wilk test of random intercepts for animal (nested under litter)*: The histogram appears approximately symmetric, and the Shapiro Wilk test is not significant (p=.879). **d)** *Histogram and Shapiro Wilk test of random intercepts for litter*: The histogram appears skewed to the right, but the Shapiro Wilk test is not significant (p=.518). **e)** *Spread-Location plot and Levene's test of residuals*: The S-L-plot shows approximately equal variation across the whole range of values, with a slight trend towards lower variation at higher values, and Levene's test is not significant (p=.772).

Model formula: Prepulse_Inhibition ~ Dose * Age + Scan + (1 | Litter/Animal)

Table 87: ANOVA-like table for random effects of the LMM of the NOR data after outlier removal
Shown are the number of model parameters (*n par*), the log-likelihood (*logLik*), Akaike information criterion (*AIC*), likelihood ratio test (*LRT*), degrees of freedom (*df*) and p-value for single term deletions of the random effects of the LMM of the PPI data after outlier removal. Animal nested under Litter (p = .000) is statistically significant, while the random effect of Litter shows a trend towards statistical significance (p = .062).

	n par	*logLik*	*AIC*	*LRT*	*df*	*p*	
<none>	28	-1532.04	3120.09	NA	NA	NA	
(1 | Animal:Litter)	27	-1560.51	3175.01	56.92	1.00	**.000**	***
(1 | Litter)	27	-1533.78	3121.57	3.48	1.00	**.062**	.

Table 88: Post hoc multiple comparisons of PPI data - simple pair-wise t-tests for 'Dose' after outlier removal
Shown are the estimates and standard error (*SE*) of simple pair-wise t-tests for the contrast LPS dose [µg/kg], including degrees of freedom (*df*), t ratio, p-values corrected for multiple comparisons using the Tukey method (*p*) as well as uncorrected p-values (*p uncorr*) and 95% confidence intervals. After Tukey adjustment, only the 0-20 contrast on PD ~66 is statistically significant (p = .027).

Contrast LPS dose [µg/kg]	Age [PD]	ISI [ms]	*Estimate*	*SE*	*df*	*t ratio*	*p*	*p uncorr*	*95% Confidence Interval*	
									Lower CL	*Upper CL*
0 - 20	~30	50	-3.05	5.69	19.97	-0.54	.855	*.598*	-14.91	8.81
0 - 100	~30	50	-8.19	8.41	14.12	-0.97	.604	*.346*	-26.21	9.82
20 - 100	~30	50	-5.15	8.69	14.61	-0.59	.826	*.563*	-23.71	13.42
0 - 20	~45	50	3.17	5.75	20.93	0.55	.848	*.588*	-8.80	15.13
0 - 100	~45	50	7.56	8.42	14.23	0.90	.651	*.384*	-10.48	25.60
20 - 100	~45	50	4.39	8.72	14.80	0.50	.870	*.622*	-14.21	22.99
0 - 20	~66	50	8.42	5.69	19.97	1.48	.321	*.154*	-3.44	20.28
0 - 100	~66	50	-1.21	8.41	14.12	-0.14	.989	*.888*	-19.22	16.80
20 - 100	~66	50	-9.63	8.69	14.61	-1.11	.524	*.285*	-28.20	8.93
0 - 20	~94	50	2.84	5.71	20.32	0.50	.873	*.624*	-9.05	14.74
0 - 100	~94	50	-0.53	8.42	14.23	-0.06	.998	*.950*	-18.57	17.50
20 - 100	~94	50	-3.38	8.69	14.61	-0.39	.921	*.703*	-21.94	15.19
0 - 20	~30	140	-8.11	5.69	19.97	-1.43	.347	*.169*	-19.97	3.75
0 - 100	~30	140	-1.44	8.41	14.12	-0.17	.984	*.867*	-19.45	16.58
20 - 100	~30	140	6.67	8.69	14.61	0.77	.728	*.455*	-11.89	25.24
0 - 20	~45	140	-3.90	5.75	20.94	-0.68	.779	*.505*	-15.86	8.06
0 - 100	~45	140	0.75	8.67	15.92	0.09	.996	*.932*	-17.63	19.12
20 - 100	~45	140	4.65	8.95	16.45	0.52	.863	*.611*	-14.30	23.59
0 - 20	~66	140	16.14	5.71	20.30	2.83	**.027** *	*.010* **	4.24	28.04
0 - 100	~66	140	6.23	8.66	15.87	0.72	.756	*.482*	-12.14	24.60
20 - 100	~66	140	-9.91	8.91	16.17	-1.11	.521	*.283*	-28.79	8.97
0 - 20	~94	140	-5.89	5.81	21.55	-1.01	.577	*.322*	-17.95	6.18
0 - 100	~94	140	7.58	8.67	15.92	0.87	.664	*.395*	-10.80	25.96
20 - 100	~94	140	13.46	8.99	16.65	1.50	.317	*.153*	-5.54	32.46

Table 89: Post hoc multiple comparisons of PPI data - simple pair-wise t-tests for 'Age' after outlier removal – 50 ms ISI
Shown are the estimates and standard error (*SE*) of simple pair-wise t-tests for the contrast Age [PD], including degrees of freedom (*df*), t ratio, p-values corrected for multiple comparisons using the Tukey method (*p*) as well as uncorrected p-values (*p uncorr*) and 95% confidence intervals. After Tukey adjustment, all contrasts are statistically significant (p usually <.000, see below), except the PD~66-~94 contrast in the control group (trend to statistical significance without Tukey adjustment) and the PD~30-~45 as well as PD~66-~94 contrast in the 100 µg/kg LPS group.

Contrast Age [PD]	LPS dose [µg/kg]	ISI [ms]	*Estimate*	*SE*	*df*	*t ratio*	*p*	*p uncorr*	*95% Confidence Interval*	
									Lower CL	*Upper CL*
~30 - ~45	0	50	-26.47	3.55	324.75	-7.46	**.000** ***	*.000* ***	-33.44	-19.49
~30 - ~66	0	50	-47.84	3.51	324.36	-13.65	**.000** ***	*.000* ***	-54.74	-40.94
~30 - ~94	0	50	-53.94	3.55	324.78	-15.21	**.000** ***	*.000* ***	-60.92	-46.97
~45 - ~66	0	50	-21.37	3.55	324.75	-6.03	**.000** ***	*.000* ***	-28.35	-14.40
~45 - ~94	0	50	-27.48	3.59	325.18	-7.66	**.000** ***	*.000* ***	-34.53	-20.42
~66 - ~94	0	50	-6.10	3.55	324.78	-1.72	.314	*.086* .	-13.08	0.87
~30 - ~45	20	50	-20.25	4.08	325.05	-4.96	**.000** ***	*.000* ***	-28.29	-12.22
~30 - ~66	20	50	-36.37	4.02	324.36	-9.05	**.000** ***	*.000* ***	-44.28	-28.46
~30 - ~94	20	50	-48.05	4.02	324.36	-11.95	**.000** ***	*.000* ***	-55.96	-40.14
~45 - ~66	20	50	-16.12	4.08	325.05	-3.95	**.001** ***	*.000* ***	-24.15	-8.08
~45 - ~94	20	50	-27.80	4.08	325.05	-6.81	**.000** ***	*.000* ***	-35.83	-19.77
~66 - ~94	20	50	-11.68	4.02	324.36	-2.91	**.020** *	*.004* **	-19.59	-3.77
~30 - ~45	100	50	-10.71	6.62	324.36	-1.62	.370	*.107*	-23.75	2.32
~30 - ~66	100	50	-40.86	6.62	324.36	-6.17	**.000** ***	*.000* ***	-53.89	-27.83
~30 - ~94	100	50	-46.29	6.62	324.36	-6.99	**.000** ***	*.000* ***	-59.32	-33.25
~45 - ~66	100	50	-30.14	6.62	324.36	-4.55	**.000** ***	*.000* ***	-43.17	-17.11
~45 - ~94	100	50	-35.57	6.62	324.36	-5.37	**.000** ***	*.000* ***	-48.60	-22.54
~66 - ~94	100	50	-5.43	6.62	324.36	-0.82	.845	*.413*	-18.46	7.60

Table 90: Post hoc multiple comparisons of PPI data - simple pair-wise t-tests for 'Age' after outlier removal – 140 ms ISI

Shown are the estimates and standard error (*SE*) of simple pair-wise t-tests for the contrast Age [PD], including degrees of freedom (*df*), t ratio, p-values corrected for multiple comparisons using the Tukey method (*p*) as well as uncorrected p-values (*p uncorr*) and 95% confidence intervals. After Tukey adjustment, all contrasts are statistically significant (p usually <.000, see below), except the PD~66-~94 contrast in the control group (trend to statistical significance without Tukey adjustment), the PD~30-~45 contrast in the 20 µg/kg LPS group and the PD~30-~45 as well as PD~66-~94 contrasts in the 100 µg/kg LPS group.

Contrast Age [PD]	LPS dose [µg/kg]	ISI [ms]	*Estimate*	*SE*	*df*	*t ratio*	*p*	*p uncorr*	*95% Confidence Interval*	
									Lower CL	*Upper CL*
~30 - ~45	0	140	-11.47	3.55	324.78	-3.24	**.007** **	*.001* ***	-18.45	-4.50
~30 - ~66	0	140	-48.04	3.55	324.75	-13.55	**.000** ***	*.000* ***	-55.02	-41.07
~30 - ~94	0	140	-54.14	3.55	324.76	-15.27	**.000** ***	*.000* ***	-61.11	-47.16
~45 - ~66	0	140	-36.57	3.59	325.15	-10.20	**.000** ***	*.000* ***	-43.62	-29.52
~45 - ~94	0	140	-42.66	3.59	325.19	-11.90	**.000** ***	*.000* ***	-49.72	-35.61
~66 - ~94	0	140	-6.09	3.59	325.14	-1.70	.326	*.090*	-13.15	0.96
~30 - ~45	20	140	-7.26	4.08	325.05	-1.78	.286	*.076* .	-15.29	0.77
~30 - ~66	20	140	-23.79	4.02	324.36	-5.92	**.000** ***	*.000* ***	-31.70	-15.88
~30 - ~94	20	140	-51.91	4.15	325.42	-12.51	**.000** ***	*.000* ***	-60.07	-43.74
~45 - ~66	20	140	-16.53	4.08	325.05	-4.05	**.000** ***	*.000* ***	-24.56	-8.50
~45 - ~94	20	140	-44.65	4.21	326.17	-10.60	**.000** ***	*.000* ***	-52.94	-36.36
~66 - ~94	20	140	-28.12	4.15	325.42	-6.78	**.000** ***	*.000* ***	-36.28	-19.95
~30 - ~45	100	140	-9.29	6.93	326.43	-1.34	.538	*.181*	-22.92	4.34
~30 - ~66	100	140	-40.37	6.92	326.04	-5.83	**.000** ***	*.000* ***	-54.00	-26.75
~30 - ~94	100	140	-45.12	6.93	326.43	-6.51	**.000** ***	*.000* ***	-58.75	-31.49
~45 - ~66	100	140	-31.09	7.23	328.46	-4.30	**.000** ***	*.000* ***	-45.30	-16.87
~45 - ~94	100	140	-35.83	7.16	324.36	-5.01	**.000** ***	*.000* ***	-49.91	-21.76
~66 - ~94	100	140	-4.75	7.23	328.46	-0.66	.913	*.512*	-18.96	9.47

Table 91: Post hoc multiple comparisons of PPI data - simple pair-wise t-tests for 'Inter Stimulus Interval (ISI)' after outlier removal
Shown are the estimates and standard error (*SE*) of simple pair-wise t-tests for the contrast ISI [ms], including degrees of freedom (*df*), t ratio, p-values corrected for multiple comparisons using the Tukey method (*p*) as well as uncorrected p-values (*p uncorr*) and 95% confidence intervals. After Tukey adjustment, all contrasts are statistically significant (p usually ≤.001, see below), except the 50-140 ms contrast in the 20 µg/kg LPS group on PD~94, which only shows a trend to statistical significance (p = .091).

Contrast ISI [ms]	Age [PD]	LPS dose [µg/kg]	*Estimate*	*SE*	*df*	*t ratio*	*p*		*p uncorr*		*95% Confidence Interval*	
											Lower CL	*Upper CL*
50 - 140	~30	0	15.96	3.51	324.36	4.55	**.000**	***	*.000*	***	9.06	22.86
50 - 140	~45	0	30.95	3.59	325.18	8.63	**.000**	***	*.000*	***	23.90	38.01
50 - 140	~66	0	15.76	3.55	324.75	4.44	**.000**	***	*.000*	***	8.78	22.73
50 - 140	~94	0	15.77	3.59	325.19	4.40	**.000**	***	*.000*	***	8.71	22.82
50 - 140	~30	20	10.89	4.02	324.36	2.71	**.007**	**	*.007*	**	2.98	18.80
50 - 140	~45	20	23.89	4.13	324.36	5.78	**.000**	***	*.000*	***	15.76	32.02
50 - 140	~66	20	23.47	4.02	324.36	5.84	**.000**	***	*.000*	***	15.56	31.38
50 - 140	~94	20	7.04	4.15	325.42	1.70	**.091**	.	*.091*	.	-1.13	15.20
50 - 140	~30	100	22.71	6.62	324.36	3.43	**.001**	***	*.001*	***	9.68	35.75
50 - 140	~45	100	24.14	6.93	326.43	3.48	**.001**	***	*.001*	***	10.51	37.77
50 - 140	~66	100	23.20	6.92	326.04	3.35	**.001**	***	*.001*	***	9.58	36.82
50 - 140	~94	100	23.88	6.93	326.43	3.45	**.001**	***	*.001*	***	10.25	37.51

6.2.8. PPI Sensitivity Analysis

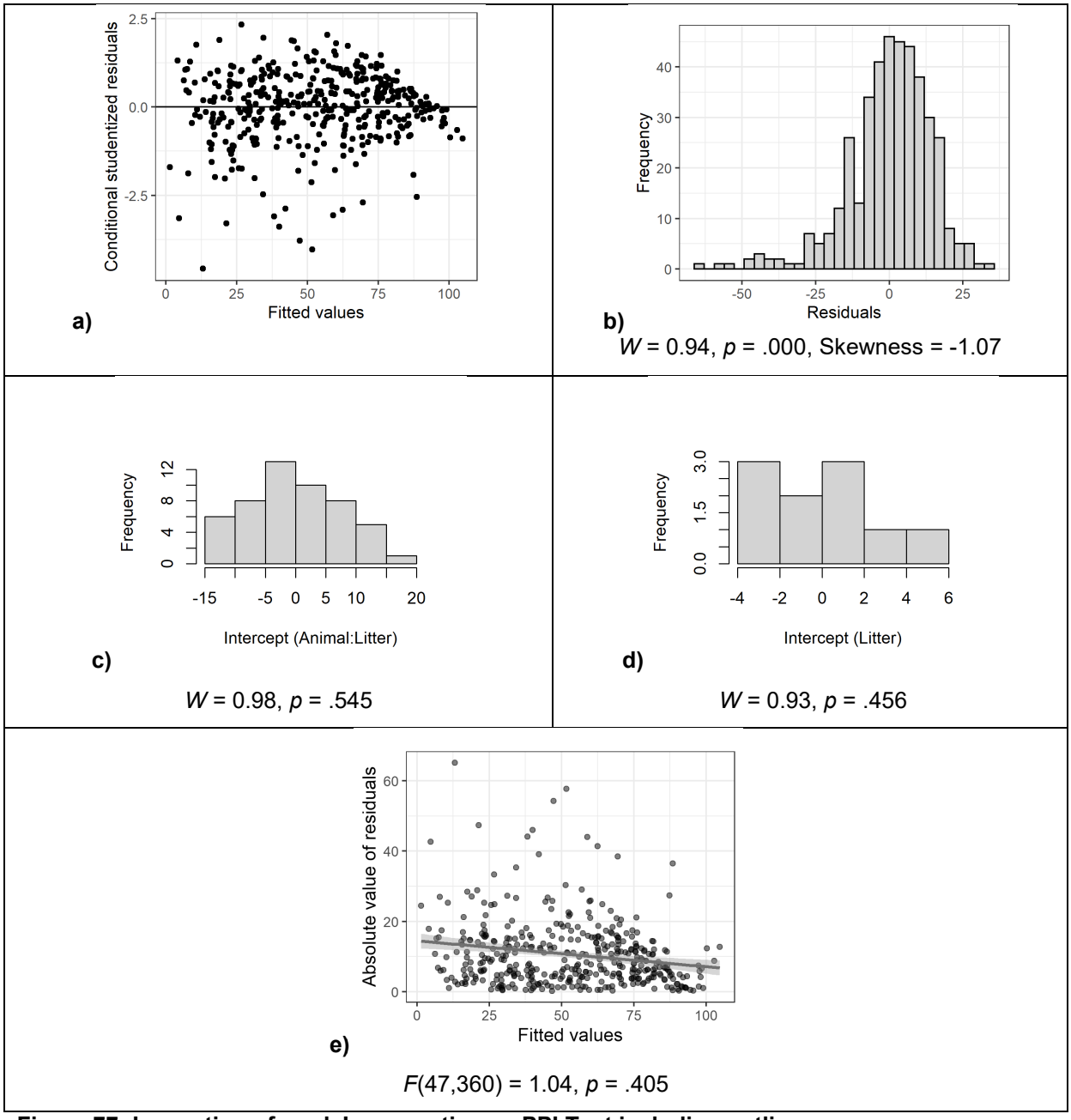

Figure 77: Inspection of model assumptions – PPI Test <u>including outliers</u>
a) *Conditional (internally) studentized residuals*: There are outlier residuals exceeding ±3 SD of the mean. **b)** *Histogram and Shapiro Wilk test of residuals*: The histogram appears skewed to the left, the Shapiro Wilk test shows significant difference from a normal distribution (p=.000). The skewness of -1.07 further confirms that the distribution is highly skewed (Bulmer, 1979). **c)** *Histogram and Shapiro Wilk test of random intercepts for animal (nested under litter)*: The histogram appears approximately symmetric, and the Shapiro Wilk test is not significant (p=.545). **d)** *Histogram and Shapiro Wilk test of random intercepts for litter*: The histogram appears skewed to the right, but the Shapiro Wilk test is not significant (p=.456). **e)** *Spread-Location plot and Levene's test of residuals*: The S-L-plot shows approximately equal variation across the whole range of values, with a slight trend towards lower variation at higher values, and Levene's test is not significant (p=.405).

Table 92: ANOVA table of the linear mixed model of the PPI data <u>including outliers</u>
Shown are the sums of squares (*SS*), mean squares (*MS*), numerator (df_{Num}) and denominator (df_{Den}) degrees of freedom, F- and p-value for each simple factor as well as for the Dose:Age interaction term. The Dose:Age (p = .014) and Dose:ISI (p = .050) interactions are statistically significant, and the Age:ISI interaction shows a trend for statistical significance (p = .064).

	SS	*MS*	df_{Num}	df_{Den}	*F*	*p*	
Dose	72.74	36.37	2	6.18	0.15	.861	
Age	112424.19	37474.73	3	336.00	157.90	**.000**	***
ISI	39079.22	39079.22	1	336.00	164.66	**.000**	***
Scan	360.31	360.31	1	44.24	1.52	.224	
Dose:Age	3850.85	641.81	6	336.00	2.70	**.014**	*
Dose:ISI	1437.25	718.62	2	336.00	3.03	**.050**	*
Age:ISI	1741.90	580.63	3	336.00	2.45	**.064**	.
Dose:Age:ISI	731.02	121.84	6	336.00	0.51	.798	

Table 93: ANOVA-like table for random effects of the LMM of the PPI data <u>including outliers</u>
Shown are the number of model parameters (*n par*), the log-likelihood (*logLik*), Akaike information criterion (*AIC*), likelihood ratio test (*LRT*), degrees of freedom (*df*) and p-value for single term deletions of the random effects of the LMM of the PPI data <u>including outliers</u>. Animal nested under Litter is statistically significant (p = .000), whereas the random effect of Litter is not significant.

	n par	*logLik*	*AIC*	*LRT*	*df*	*p*	
<none>	28	-1660.24	3376.48	NA	NA	NA	
(1 | Animal:Litter)	27	-1685.14	3424.29	49.81	1.00	**.000**	***
(1 | Litter)	27	-1660.88	3375.76	1.28	1.00	.257	

Table 94: Estimated marginal means of the LMM of the PPI data <u>including outliers</u>
Shown are the estimated marginal mean, standard error (*SE*), degrees of freedom (*df*) and 95% confidence interval for each LPS dose, Age and ISI combination.

LPS dose [µg/kg]	Age [PD]	ISI [ms]	*Mean*	*SE*	*df*	*95% Confidence Interval*	
						Lower CL	*Upper CL*
0	~30	50	33.32	4.13	27.22	24.84	41.79
0	~45	50	57.32	4.13	27.22	48.84	65.79
0	~66	50	81.16	4.13	27.22	72.68	89.63
0	~94	50	85.60	4.13	27.22	77.12	94.07
20	~30	50	36.25	4.78	27.81	26.45	46.04
20	~45	50	53.35	4.78	27.81	43.56	63.15
20	~66	50	72.62	4.78	27.81	62.82	82.41
20	~94	50	84.30	4.78	27.81	74.51	94.09
100	~30	50	41.14	8.11	16.69	24.02	58.27
100	~45	50	51.86	8.11	16.69	34.73	68.98
100	~66	50	82.00	8.11	16.69	64.87	99.13
100	~94	50	87.43	8.11	16.69	70.30	104.56
0	~30	140	17.36	4.13	27.22	8.88	25.83
0	~45	140	26.68	4.13	27.22	18.20	35.15
0	~66	140	62.80	4.13	27.22	54.32	71.27
0	~94	140	69.52	4.13	27.22	61.04	77.99
20	~30	140	25.35	4.78	27.81	15.56	35.15
20	~45	140	28.30	4.78	27.81	18.51	38.09
20	~66	140	49.14	4.78	27.81	39.35	58.94
20	~94	140	72.14	4.78	27.81	62.35	81.94
100	~30	140	18.43	8.11	16.69	1.30	35.56
100	~45	140	19.00	8.11	16.69	1.87	36.13
100	~66	140	52.00	8.11	16.69	34.87	69.13
100	~94	140	54.29	8.11	16.69	37.16	71.41

Table 95: Post hoc multiple comparisons of PPI data - simple pair-wise t-tests for 'Dose' including outliers

Shown are the estimates and standard error (*SE*) of simple pair-wise t-tests for the contrast LPS dose [µg/kg], including degrees of freedom (*df*), t ratio, p-values corrected for multiple comparisons using the Tukey method (*p*) as well as uncorrected p-values (*p uncorr*) and 95% confidence intervals. After Tukey adjustment, only the 0-20 contrast on PD ~66 shows a trend for statistical significance (p = .094). Before Tukey adjustment, this trend is statistically significant (p = .039) and the 20-100 contrast on PD ~94 shows a trend for statistical significance as well (p = .074).

Contrast LPS dose [µg/kg]	Age [PD]	ISI [ms]	*Estimate*	*SE*	*df*	*t ratio*	*p*	*p uncorr*	*95% Confidence Interval*	
									Lower CL	*Upper CL*
0 - 20	~30	50	-2.93	6.28	27.16	-0.47	.887	*.644*	-15.82	9.96
0 - 100	~30	50	-7.83	9.11	18.37	-0.86	.672	*.401*	-26.93	11.27
20 - 100	~30	50	-4.90	9.43	18.92	-0.52	.863	*.610*	-24.63	14.84
0 - 20	~45	50	3.96	6.28	27.16	0.63	.805	*.534*	-8.93	16.85
0 - 100	~45	50	5.46	9.11	18.37	0.60	.822	*.556*	-13.64	24.56
20 - 100	~45	50	1.49	9.43	18.92	0.16	.986	*.876*	-18.24	21.23
0 - 20	~66	50	8.54	6.28	27.16	1.36	.376	*.185*	-4.35	21.43
0 - 100	~66	50	-0.85	9.11	18.37	-0.09	.995	*.927*	-19.95	18.26
20 - 100	~66	50	-9.38	9.43	18.92	-1.00	.589	*.332*	-29.12	10.35
0 - 20	~94	50	1.30	6.28	27.16	0.21	.977	*.838*	-11.59	14.18
0 - 100	~94	50	-1.83	9.11	18.37	-0.20	.978	*.843*	-20.94	17.27
20 - 100	~94	50	-3.13	9.43	18.92	-0.33	.941	*.744*	-22.87	16.61
0 - 20	~30	140	-8.00	6.28	27.16	-1.27	.422	*.214*	-20.89	4.89
0 - 100	~30	140	-1.07	9.11	18.37	-0.12	.992	*.907*	-20.18	18.03
20 - 100	~30	140	6.92	9.43	18.92	0.73	.746	*.472*	-12.81	26.66
0 - 20	~45	140	-1.62	6.28	27.16	-0.26	.964	*.798*	-14.51	11.26
0 - 100	~45	140	7.67	9.11	18.37	0.84	.682	*.410*	-11.43	26.78
20 - 100	~45	140	9.30	9.43	18.92	0.99	.594	*.336*	-10.44	29.04
0 - 20	~66	140	13.65	6.28	27.16	2.17	**.094** .	*.039* *	0.76	26.54
0 - 100	~66	140	10.79	9.11	18.37	1.19	.476	*.251*	-8.31	29.90
20 - 100	~66	140	-2.86	9.43	18.92	-0.30	.951	*.765*	-22.60	16.88
0 - 20	~94	140	-2.63	6.28	27.16	-0.42	.908	*.679*	-15.52	10.26
0 - 100	~94	140	15.23	9.11	18.37	1.67	.242	*.111*	-3.87	34.33
20 - 100	~94	140	17.86	9.43	18.92	1.89	.168	*.074* .	-1.88	37.59

Table 96: Post hoc multiple comparisons of PPI data - simple pair-wise t-tests for 'Age' <u>including outliers</u> – 50 ms ISI

Shown are the estimates and standard error (*SE*) of simple pair-wise t-tests for the contrast Age [PD], including degrees of freedom (*df*), t ratio, p-values corrected for multiple comparisons using the Tukey method (*p*) as well as uncorrected p-values (*p uncorr*) and 95% confidence intervals. After Tukey adjustment, all contrasts are statistically significant (p usually <.000, see below), except the PD~66-~94 contrast in the control group and the PD~66-~94 contrast in the 100 µg/kg LPS group. Also, the PD~66-~95 contrast in the 20 µg/kg LPS group only shows a trend for statistical significance after Tukey adjustment (p = .092).

Contrast Age [PD]	LPS dose [µg/kg]	ISI [ms]	*Estimate*	*SE*	*df*	*t ratio*	*p*	*p uncorr*	*95% Confidence Interval*	
									Lower CL	*Upper CL*
~30 - ~45	0	50	-24.00	4.36	336.00	-5.51	**.000** ***	*.000* ***	-32.57	-15.43
~30 - ~66	0	50	-47.84	4.36	336.00	-10.98	**.000** ***	*.000* ***	-56.41	-39.27
~30 - ~94	0	50	-52.28	4.36	336.00	-12.00	**.000** ***	*.000* ***	-60.85	-43.71
~45 - ~66	0	50	-23.84	4.36	336.00	-5.47	**.000** ***	*.000* ***	-32.41	-15.27
~45 - ~94	0	50	-28.28	4.36	336.00	-6.49	**.000** ***	*.000* ***	-36.85	-19.71
~66 - ~94	0	50	-4.44	4.36	336.00	-1.02	.738	*.309*	-13.01	4.13
~30 - ~45	20	50	-17.11	5.00	336.00	-3.42	**.004** **	*.001* ***	-26.94	-7.27
~30 - ~66	20	50	-36.37	5.00	336.00	-7.28	**.000** ***	*.000* ***	-46.20	-26.54
~30 - ~94	20	50	-48.05	5.00	336.00	-9.61	**.000** ***	*.000* ***	-57.88	-38.22
~45 - ~66	20	50	-19.26	5.00	336.00	-3.85	**.001** ***	*.000* ***	-29.09	-9.43
~45 - ~94	20	50	-30.95	5.00	336.00	-6.19	**.000** ***	*.000* ***	-40.78	-21.12
~66 - ~94	20	50	-11.68	5.00	336.00	-2.34	**.092** .	*.020* *	-21.52	-1.85
~30 - ~45	100	50	-10.71	8.23	336.00	-1.30	.563	*.194*	-26.91	5.48
~30 - ~66	100	50	-40.86	8.23	336.00	-4.96	**.000** ***	*.000* ***	-57.06	-24.66
~30 - ~94	100	50	-46.29	8.23	336.00	-5.62	**.000** ***	*.000* ***	-62.48	-30.09
~45 - ~66	100	50	-30.14	8.23	336.00	-3.66	**.002** **	*.000* ***	-46.34	-13.94
~45 - ~94	100	50	-35.57	8.23	336.00	-4.32	**.000** ***	*.000* ***	-51.77	-19.37
~66 - ~94	100	50	-5.43	8.23	336.00	-0.66	.912	*.510*	-21.63	10.77

Table 97: Post hoc multiple comparisons of PPI data - simple pair-wise t-tests for 'Age' <u>including outliers</u> – 140 ms ISI

Shown are the estimates and standard error (*SE*) of simple pair-wise t-tests for the contrast Age [PD], including degrees of freedom (*df*), t ratio, p-values corrected for multiple comparisons using the Tukey method (*p*) as well as uncorrected p-values (*p uncorr*) and 95% confidence intervals. After Tukey adjustment, all contrasts are statistically significant (p usually <.000, see below), except the PD~30-~45 contrast in all 3 groups, and the PD~66-~94 contrast in the 100 µg/kg LPS group.

Contrast Age [PD]	LPS dose [µg/kg]	ISI [ms]	*Estimate*	*SE*	*df*	*t ratio*	*p*	*p uncorr*	*95% Confidence Interval*	
									Lower CL	*Upper CL*
~30 - ~45	0	140	-9.32	4.36	336.00	-2.14	.143	*.033* *	-17.89	-0.75
~30 - ~66	0	140	-45.44	4.36	336.00	-10.43	**.000** ***	*.000* ***	-54.01	-36.87
~30 - ~94	0	140	-52.16	4.36	336.00	-11.97	**.000** ***	*.000* ***	-60.73	-43.59
~45 - ~66	0	140	-36.12	4.36	336.00	-8.29	**.000** ***	*.000* ***	-44.69	-27.55
~45 - ~94	0	140	-42.84	4.36	336.00	-9.83	**.000** ***	*.000* ***	-51.41	-34.27
~66 - ~94	0	140	-6.72	4.36	336.00	-1.54	.413	*.124*	-15.29	1.85
~30 - ~45	20	140	-2.95	5.00	336.00	-0.59	.935	*.556*	-12.78	6.88
~30 - ~66	20	140	-23.79	5.00	336.00	-4.76	**.000** ***	*.000* ***	-33.62	-13.96
~30 - ~94	20	140	-46.79	5.00	336.00	-9.36	**.000** ***	*.000* ***	-56.62	-36.96
~45 - ~66	20	140	-20.84	5.00	336.00	-4.17	**.000** ***	*.000* ***	-30.67	-11.01
~45 - ~94	20	140	-43.84	5.00	336.00	-8.77	**.000** ***	*.000* ***	-53.67	-34.01
~66 - ~94	20	140	-23.00	5.00	336.00	-4.60	**.000** ***	*.000* ***	-32.83	-13.17
~30 - ~45	100	140	-0.57	8.23	336.00	-0.07	1.000	*.945*	-16.77	15.63
~30 - ~66	100	140	-33.57	8.23	336.00	-4.08	**.000** ***	*.000* ***	-49.77	-17.37
~30 - ~94	100	140	-35.86	8.23	336.00	-4.35	**.000** ***	*.000* ***	-52.06	-19.66
~45 - ~66	100	140	-33.00	8.23	336.00	-4.01	**.000** ***	*.000* ***	-49.20	-16.80
~45 - ~94	100	140	-35.29	8.23	336.00	-4.29	**.000** ***	*.000* ***	-51.48	-19.09
~66 - ~94	100	140	-2.29	8.23	336.00	-0.28	.993	*.782*	-18.48	13.91

Table 98: Post hoc multiple comparisons of PPI data - simple pair-wise t-tests for 'Inter Stimulus Interval (ISI)' <u>including outliers</u>
Shown are the estimates and standard error (*SE*) of simple pair-wise t-tests for the contrast ISI [ms], including degrees of freedom (*df*), t ratio, p-values corrected for multiple comparisons using the Tukey method (*p*) as well as uncorrected p-values (*p uncorr*) and 95% confidence intervals. After Tukey adjustment, all contrasts are statistically significant (p usually ≤.000, see below).

Contrast ISI [ms]	Age [PD]	LPS dose [µg/kg]	*Estimate*	*SE*	*df*	*t ratio*	*p*		*p uncorr*		*95% Confidence Interval*	
											Lower CL	*Upper CL*
50 - 140	~30	0	15.96	4.36	336.00	3.66	**.000**	***	*.000*	***	7.39	24.53
50 - 140	~45	0	30.64	4.36	336.00	7.03	**.000**	***	*.000*	***	22.07	39.21
50 - 140	~66	0	18.36	4.36	336.00	4.21	**.000**	***	*.000*	***	9.79	26.93
50 - 140	~94	0	16.08	4.36	336.00	3.69	**.000**	***	*.000*	***	7.51	24.65
50 - 140	~30	20	10.89	5.00	336.00	2.18	**.030**	*	*.030*	*	1.06	20.73
50 - 140	~45	20	25.05	5.00	336.00	5.01	**.000**	***	*.000*	***	15.22	34.88
50 - 140	~66	20	23.47	5.00	336.00	4.70	**.000**	***	*.000*	***	13.64	33.31
50 - 140	~94	20	12.16	5.00	336.00	2.43	**.016**	*	*.016*	*	2.33	21.99
50 - 140	~30	100	22.71	8.23	336.00	2.76	**.006**	**	*.006*	**	6.52	38.91
50 - 140	~45	100	32.86	8.23	336.00	3.99	**.000**	***	*.000*	***	16.66	49.06
50 - 140	~66	100	30.00	8.23	336.00	3.64	**.000**	***	*.000*	***	13.80	46.20
50 - 140	~94	100	33.14	8.23	336.00	4.02	**.000**	***	*.000*	***	16.94	49.34

6.3. Resting state fMRI

6.3.1. Signal Dropout in rs-fMRI Data Animal 815

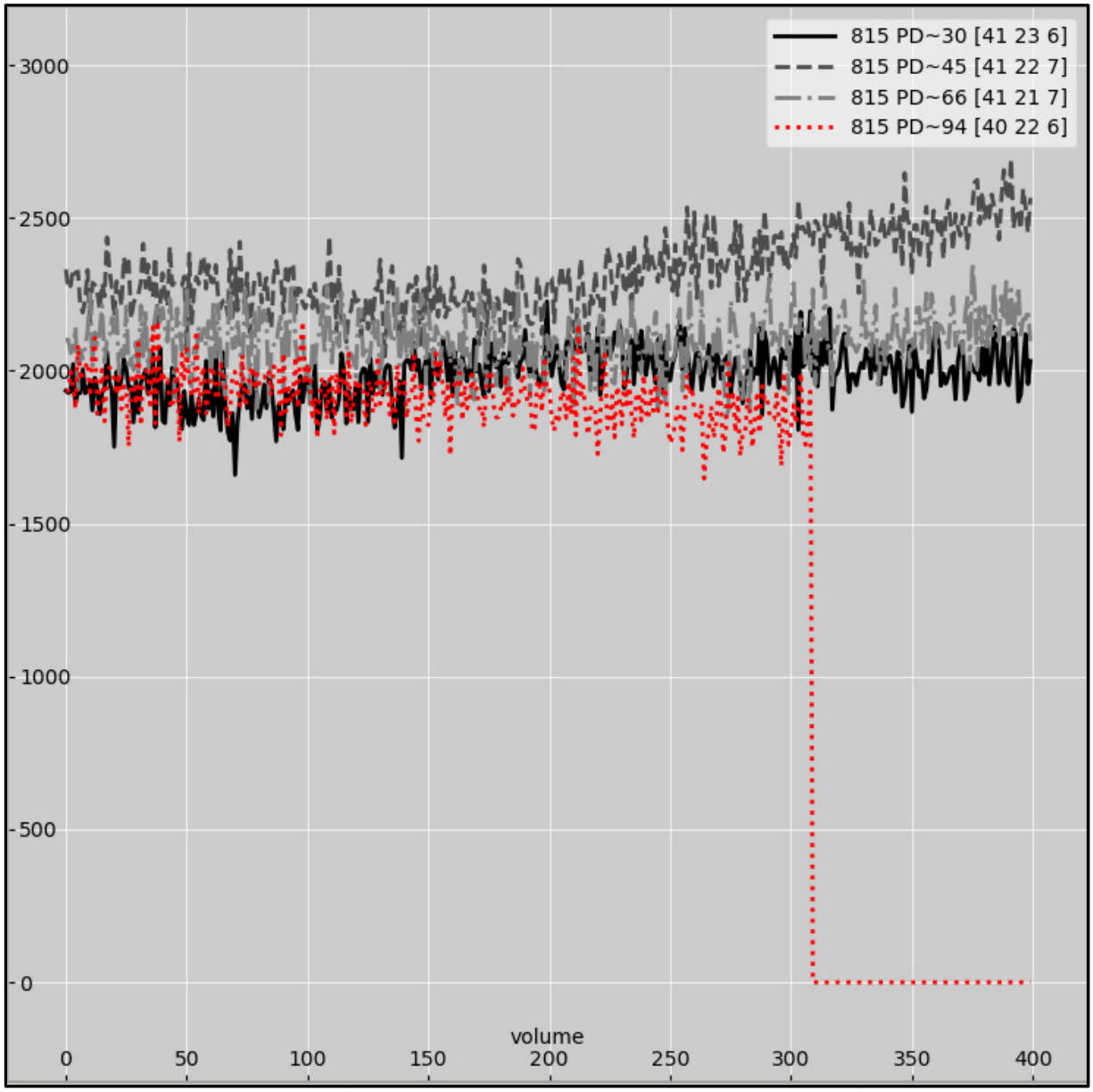

Figure 78: Signal dropout in rs-fMRI data of animal 815
Shown is the signal intensity time series (400 volumes) of a representative voxel of the rs-fMRI raw data for all four measured time points of animal 815. PD~30 is shown as a solid black line, PD~45 is shown as a dashed dark grey line, PD~66 is shown as a dashed-dotted grey line and PD~94 is shown as a dotted red line. Compared to all other time points, the time series shows a strong rapid signal drop after three quarters of the measurement, which led to abnormally high z-scores for this animal in the further analysis steps. Thus, as the MRM model used for the statistical comparison (see section 2.6.2) is not able to handle single missing values, the data from all four time points of this animal were excluded in the analysis.

6.3.2. ICs Classified as Noise

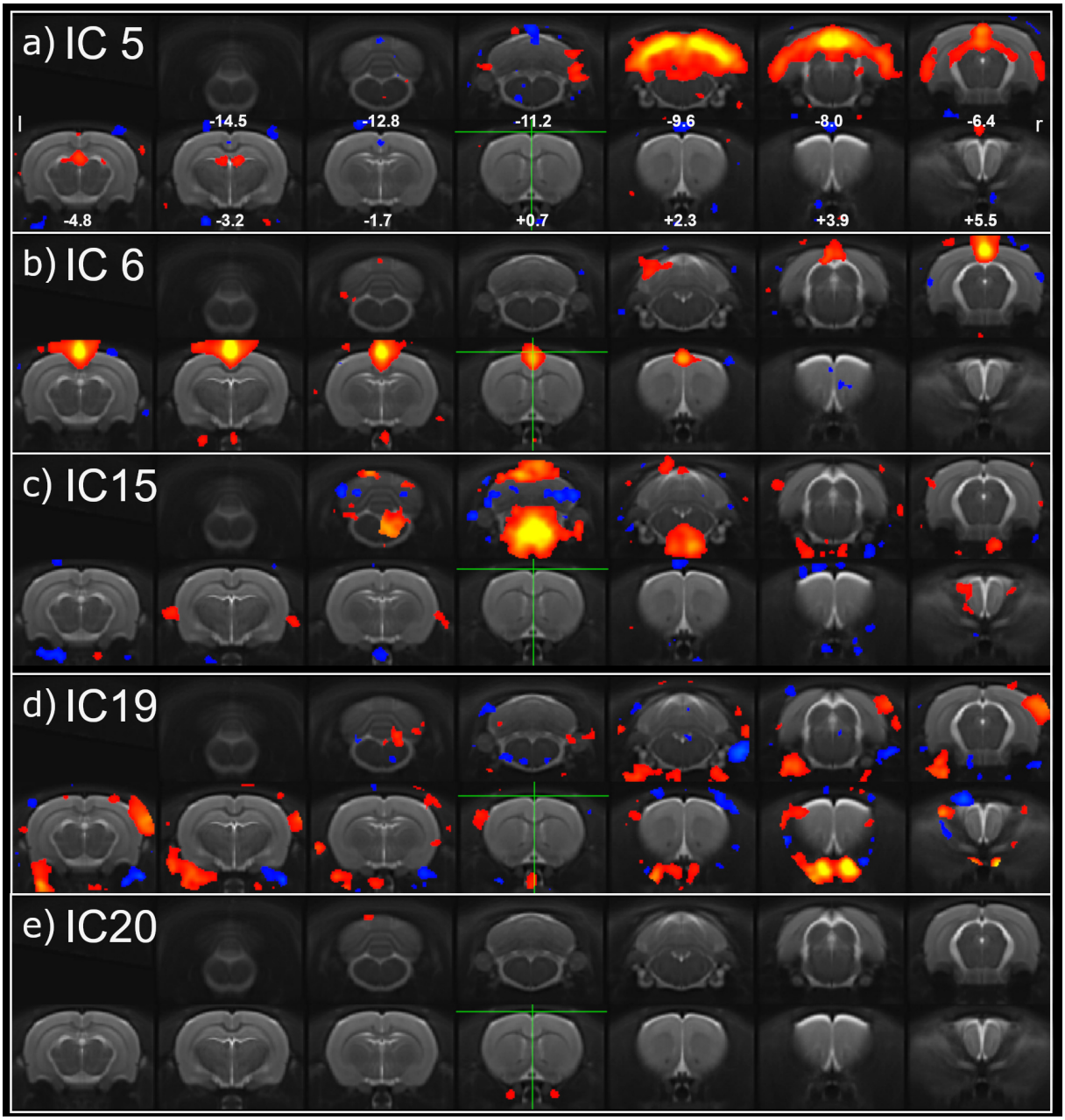

Figure 79: ICs classified as noise/unidentifiable – Blood Vessels, Brainstem, Nerves
Shown are **a)** IC 5 and **b)** IC 6, representing the large brain vessels, the transverse sinus and the superior saggital sinus, with IC 5 also including the lateral and dorsal ventricles, **c)** IC 15 representing noise stemming from the brainstem **d)** IC 19 and **e)** IC 20 representing (optic) nerves. All images are thresholded for z-scores between ±3 and ±15 (positive values in red-yellow, negative values in blue) overlaid on the structural template brain. Distances to Bregma (mm) are labeled at the bottom of the images. Images are displayed in neurological convention (l = left, r = right).

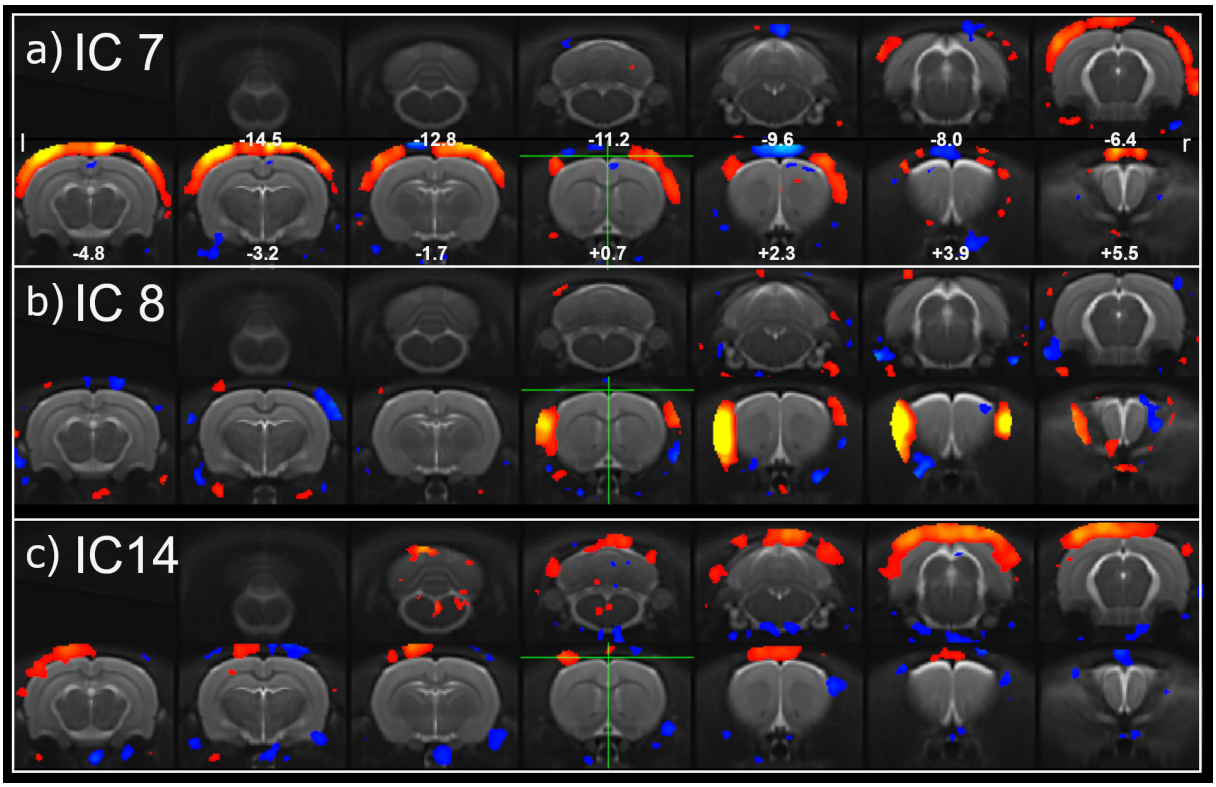

Figure 80: ICs classified as noise/unidentifiable – Movement
Shown are **a)** IC 7, **b)** IC 8 and **c)** IC 14, representing noise stemming from movement. All images are thresholded for z-scores between ±3 and ±15 (positive values in red-yellow, negative values in blue) overlaid on the structural template brain. Distances to Bregma (mm) are labeled at the bottom of the images. Images are displayed in neurological convention (l = left, r = right).

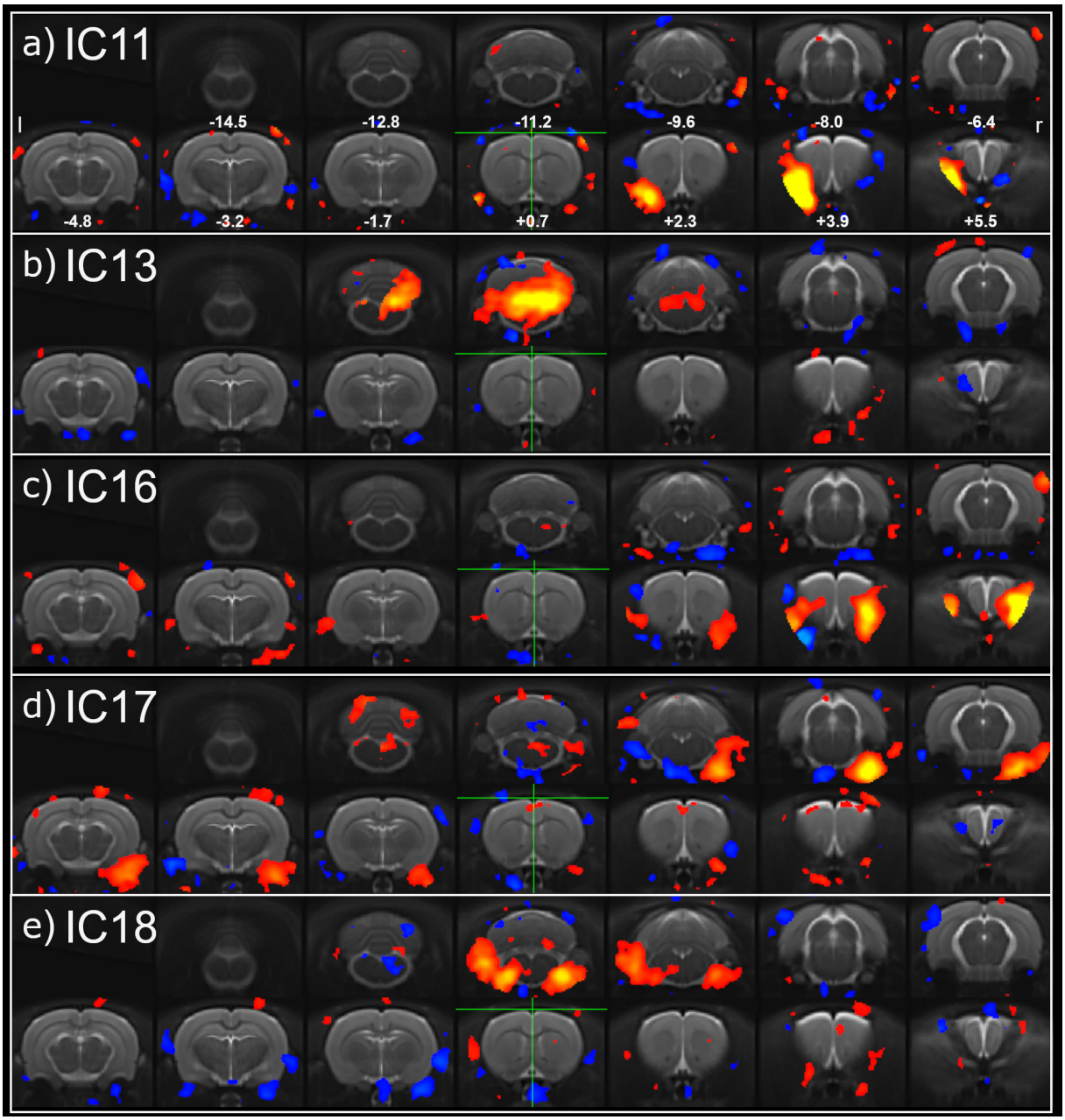

Figure 81: ICs classified as noise/unidentifiable – Unclassified Noise
Shown are **a)** IC 11, **b)** IC 13 **c)** IC 16, **d)** IC 17 and **e)** IC18, all representing noise which was simply classified as noise/unidentifiable. All images are thresholded for z-scores between ±3 and ±15 (positive values in red-yellow, negative values in blue) overlaid on the structural template brain. Distances to Bregma (mm) are labeled at the bottom of the images. Images are displayed in neurological convention (l = left, r = right).

6.4. Miscellaneous

6.4.1. List of Experimental Animals

Table 99: Experimental animals
In total 51 animals (25 SAL, 26 LPS) were used for the behavioral experiments. Ten animals from the LPS and SAL group were also used for rs-fMRI experiments. The change in weight of the animal's respective mothers after the first injection (from GD 15 to 16) was noted either as weight gain or loss. The treatment of each mother fostering the offspring until PD 21 is noted as either SAL or LPS.

Animal	Litter	Mother's weight after treatment		Scanned for rs-fMRI experiments		LPS dose [µg/kg]	Age [PD] on experimental block				Cross-Fostering mother	
							1	2	3	4		
111	LPS 1		Loss	Yes		100	29	43	64	92		LPS
112	LPS 1		Loss	Yes		100	29	43	64	92		LPS
115	LPS 1		Loss		No	100	29	43	64	92		LPS
123	LPS 1		Loss		No	100	29	43	64	92	SAL	
124	LPS 1		Loss		No	100	29	43	64	92	SAL	
125	LPS 1		Loss	Yes		100	29	43	64	92	SAL	
126	LPS 1		Loss	Yes		100	29	43	64	92	SAL	
611	LPS 2	Gain			No	20	29	43	64	92		LPS
612	LPS 2	Gain			No	20	29	43	64	92		LPS
613	LPS 2	Gain			No	20	29	43	64	92		LPS
711	LPS 3		Loss		No	20	33	47	68	96	SAL	
713	LPS 3		Loss		No	20	33	47	68	96	SAL	
722	LPS 3		Loss	Yes		20	33	47	68	96		LPS
724	LPS 3		Loss	Yes		20	33	47	68	96		LPS
725	LPS 3		Loss	Yes		20	33	47	68	96		LPS
732	LPS 3		Loss		No	20	33	47	68	96	SAL	
734	LPS 3		Loss		No	20	33	47	68	96	SAL	
811	LPS 4	Gain		Yes		20	33	47	68	96	SAL	
813	LPS 4	Gain		Yes		20	33	47	68	96	SAL	
815	LPS 4	Gain		Yes		20	33	47	68	96	SAL	
821	LPS 4	Gain			No	20	33	47	68	96		LPS
822	LPS 4	Gain			No	20	33	47	68	96		LPS
823	LPS 4	Gain			No	20	33	47	68	96		LPS
832	LPS 5	Gain			No	20	34	48	69	97		LPS
833	LPS 5	Gain			No	20	34	48	69	97		LPS
834	LPS 5	Gain			No	20	34	48	69	97		LPS
113	SAL 1	Gain		Yes		0	29	43	64	92		LPS
114	SAL 1	Gain			No	0	29	43	64	92		LPS
121	SAL 1	Gain		Yes		0	29	43	64	92	SAL	
122	SAL 1	Gain			No	0	29	43	64	92	SAL	
211	SAL 2	Gain			No	0	29	43	64	92	SAL	
212	SAL 2	Gain		Yes		0	29	43	64	92	SAL	
213	SAL 2	Gain			No	0	29	43	64	92	SAL	
214	SAL 2	Gain		Yes		0	29	43	64	92	SAL	
215	SAL 2	Gain			No	0	29	43	64	92	SAL	

Continuation of table 99:

411	SAL 3	Gain		Yes		0	29	43	64	92	SAL	
412	SAL 3	Gain			No	0	29	43	64	92	SAL	
413	SAL 3	Gain			No	0	29	43	64	92	SAL	
414	SAL 3	Gain			No	0	29	43	64	92	SAL	
415	SAL 3	Gain		Yes		0	29	43	64	92	SAL	
712	SAL 4	Gain			No	0	31	45	66	94	SAL	
714	SAL 4	Gain			No	0	31	45	66	94	SAL	
715	SAL 4	Gain			No	0	31	45	66	94	SAL	
721	SAL 4	Gain		Yes		0	31	45	66	94		LPS
723	SAL 4	Gain		Yes		0	31	45	66	94		LPS
731	SAL 4	Gain			No	0	31	45	66	94	SAL	
733	SAL 4	Gain			No	0	31	45	66	94	SAL	
812	SAL 5		Loss	Yes		0	32	46	67	95	SAL	
814	SAL 5		Loss	Yes		0	32	46	67	95	SAL	
824	SAL 5		Loss		No	0	32	46	67	95		LPS
831	SAL 5		Loss		No	0	32	46	67	95		LPS

Table 100: Additional experimental animals for Histology on PD 30
In total 20 animals (10 SAL, 10 LPS) were euthanized and perfused (see section 2.5) on PD 30 for planned histological experiments. The change in weight of the animal's respective mothers after the first injection (i.e. from GD 15 to 16) was noted either as weight gain or weight loss. The treatment of each respective mother which fostered the animal until PD 21 is noted as either SAL or LPS.

Animal	Litter	Mother's weight after treatment		LPS dose [µg/kg]	Cross-Fostering mother	
744	LPS 6		Loss	20		LPS
745	LPS 6		Loss	20		LPS
746	LPS 6		Loss	20		LPS
747	LPS 6		Loss	20		LPS
841	LPS 5	Gain		20		LPS
842	LPS 5	Gain		20		LPS
843	LPS 5	Gain		20		LPS
844	LPS 5	Gain		20		LPS
845	LPS 4	Gain		20		LPS
846	LPS 4	Gain		20		LPS
311	SAL 6		Loss	0	SAL	
312	SAL 6		Loss	0	SAL	
313	SAL 6		Loss	0	SAL	
314	SAL 6		Loss	0	SAL	
315	SAL 6		Loss	0	SAL	
316	SAL 6		Loss	0	SAL	
317	SAL 6		Loss	0	SAL	
741	SAL 4	Gain		0		LPS
742	SAL 4	Gain		0		LPS
743	SAL 4	Gain		0		LPS

6.4.2. Maternal Immune Activation Model Reporting Guidelines Checklist according to Kentner et al., 2019

Table 101: Maternal Immune Activation Model Reporting Guidelines Checklist according to (Kentner et al., 2019)**.**

ARRIVE Reporting Guideline & Recommendation	Arrive Item	MIA Model Specific Reporting Recommendation Please complete this chart for each point outlined below. If not applicable, write N/A
Study design *➢ Overview of immune activation issues* *For each experiment, give brief details of the study design including:* *a. The number of experimental and control groups.* *b. Any steps taken to minimize the effects of subjective bias when allocating animals to treatment (e.g. randomization procedure) and when assessing results (e.g. if done, describe who was blinded and when).* *c. The experimental unit (e.g. a single animal, group or cage of animals).* *A time-line diagram or flow chart can be useful to illustrate how complex study designs were carried out.*	6	*MIA Specific Reporting:* *a. General need for improved reporting in MIA model methods + reporting pilot data* o Details on pilot data: **25 control animals from 5 saline treated dams** **26 experimental animals from 5 LPS treated dams (1 dam treated with 100µg/kg, 4 with 20 µg/kg)** **No special steps undertaken when allocating LPS or SAL treatment to experimental dams.** **Offspring was cross-fostered with surrogate mothers, whereby roughly 50% of animals were exchanged between one SAL and one LPS treated mother (i.e. ~50% of animals remained with their mother, whereas ~50% were fostered by surrogate mothers of the opposite treatment).** **For the allocation into groups of 5-6 animals per cage after weaning at PD 21, a 50/50 distribution inside of each cage was pursued.** **The animal was seen as experimental unit, but for the behavioral experiments, the dependencies between animals from one litter were respected by including animal nested under litter as a random factor in the mixed model statistical analysis.** **Due to the more complex statistics this would have involved, these dependencies were not included in the analyis of the rs-fMRI experiments though.**
Experimental procedures *➢ Compounds* *➢ Validation measures* *For each experiment and each experimental group, including controls, provide precise details of all procedures carried out. For example:* *a. How (e.g. drug formulation and dose, site and route of administration, anaesthesia and analgesia used [including monitoring], surgical procedure, method of euthanasia). Provide details of*	7	*Provide details of:* *a. Compounds – source, vehicle, preparation/storage, administration route, volume administered, whether anesthetics were used at time of immune challenge.* o Name of compound: **Lipopolysaccharides from Escherichia coli 0111:B4, γ-irradiated, purified by gel-filtration chromatography** o Catalogue number: **L4391** o Lot number: **036M4070V** o Vehicle control used: **Saline** o Route of administration: **Intraperitoneal** o Volume administered: **1 ml/kg bodyweight** o Storage conditions: **Aliquots of 0.5 ml in standard Eppendorf tubes at -20°C** o Anesthetic (type, dose, duration) used: **N/A** *b. Housing variables at injection - temperature of room at injection time, cage change at time of injection or not*

any specialist equipment used, including supplier(s). *b. When (e.g. time of day).* *c. Where (e.g. home cage, laboratory, water maze).* d. *Why (e.g. rationale for choice of specific anaesthetic, route of administration, drug dose used).*		o Light cycle of animal housing room: **12h dark/light cycle, lights onat 7 a.m.** o Time of day of injection: **~10:00-12:00** o Room temperature at injection time: **~22°C** o Did a cage change occur at time of injection: **NO** *c.Validation of immune activation – behavior, physiological indices and/or cytokine data, including pilot dosing data* o Method used to verify immune activation: **An observer not blind to treatment observed sickness behaviors of the dams, i.e. measures of ptosis (droopy eyelids), piloerection (ruffled coat) and lethargy. However, the observations made were declared unsuitable for a clear confirmation of sickness behavior. There was no additional validation of the immune activation in the dams.** *d. Validation of gestational timing – vaginal plug, estrous cycle, weight gain* o Method of validating gestational timing: **The estrous cycle of the female rats was controlled routinely as described by (Howland et al., 2012), using cytological methods (Hubscher et al., 2005; Marcondes et al., 2002). Animals were bred together when the female rats were in the phase of estrus. Pregnancy was verified by the existence of sperm in the vaginal smear the day after breeding, defined as gestational day 0.** Additional comments: **N/A**
Experimental animals ➢ *Species/strain/vendor* *a. Provide details of the animals used, including species, strain, sex, developmental stage (e.g. mean or median age plus age range) and weight (e.g. mean or median weight plus weight range).* b. *Provide further relevant information such as the source of animals, international strain nomenclature, genetic modification status (e.g. knock-out or transgenic), genotype, health/immune status, drug or test naïve, previous procedures, etc.*	8	*Provide details of:* *a. Species – considerations for appropriate species (mouse, rat, non human primate, other)* o Species: **Rat** *b. Strain – variability in strain can influence model* o Strain: **Wistar** *c. Maternal/Offspring Physiological Variables at time of immune challenge – age, body weight* o Maternal Age at challenge: **~PD 100** o Maternal Body weight: **~230-300 g** o Offspring Age at challenge: **N/A** o Offspring Sex: **Males only tested** o Offspring Body weight: **~100-350g (longitudinal study, offspring measured at PD~30 - PD~90** *d. Vendor – even within the same strain, vendor can influence endpoints* o Vendor: **Charles River** o Location of Vendor: **Sulzfeld, Germany** o Room/area where animals originated from: **unknown** Additional comments: **N/A**
Housing and husbandry	9	*Provide details of:* *a. Caging systems*

➢ *Cage, ventilation, bedding, enrichment* *Provide details of:* a. *Housing (type of facility e.g. specific pathogen free [SPF]; type of cage or housing; bedding material; number of cage companions; tank shape and material etc. for fish).* b. *Husbandry conditions (e.g. breeding program, light/dark cycle, temperature, quality of water etc for fish, type of food, access to food and water, environmental enrichment).* c. *Welfare-related assessments and interventions that were carried out prior to, during, or after the experiment.*		o At breeding Material of cage: **polycarbonate (Type IV Makrolon cages)** Cage dimensions: **59 x 38 x 20 cm** o After parturition Material of cage: **polycarbonate (Type IV Makrolon cages)** Cage dimensions: **59 x 38 x 20 cm** o At weaning Material of cage: **polycarbonate (Type IV Makrolon cages)** Cage dimensions: **59 x 38 x 20 cm** *b. Animal Holding room o Temperature in room:* o Humidity in room: **~22°C** o Ventilation system: **YES, room ventilation** o Specific pathogen free [SPF]: **NO** o Are males & females housed in the same or separate rooms: **Housed in separate rooms after weaning** *c. Bedding exchanges/bedding type* o Type of cage bedding used: **softwood chavings** o Frequency of cage changes per week during gestation: **1 / once** during neonatal period: **1 / once** following weaning: **2 / twice** *d. Breeding - bred on site or timed pregnant, how many different sires (are the same fathers breeding with both experimental and control dams)* Breeding location: **bread on site: University of Bremen Faculty 2 Biology / Chemistry Neuropharmacology Department Hochschulring 18 28359 Bremen, Germany** o Gestational age at shipping: **N/A** o Biological age of dams (if not listed in Section 8c):**~PD 100** o Number of Dams bred: **16** o How many times have dams been mated previously: **0** o How many times did the dams mate and not become pregnant: **0** o Are the dams primiparous or multiparous? **Dams are a mix of primi- & multiparous** o What was the frequency of maternal handling during the gestational/neonatal period (e.g. cage cleanings, weighing, blood collection manipulations):**cage change once a week, twice handling (weighing + injection on GD 15/16)** o Biological age of sires: **~PD 100 - ~PD 400** o Number of sires bred: **4** o How many times have sires been mated previously: **0**

		o How many times did the sires mate successfully (e.g. mating resulted in pregnancy, full term birth): **13** o If bred previously, what was the interval between mating times: **N/A** o Are sires matched to experimental and control dams: **NO** o Describe the mating design (1:1, 1:2 etc): **1:4** *e. Social enrichment – number of cage companions* o Number of cage companions prior to breeding: **4-6** o Gestational age when dam separated for parturition: **GD 0** o Number of cage companions at weaning**: after weaning groups of 4-6** *f. Physical enrichment – describe enrichment devices, and when enrichment is in the cage (removed when pups born? Or present throughout study), does the enrichment type change? How frequently?* o Describe what type of enrichment devices (and how many) are included in cage/housing room: **Wooden houses + paper towels present all the time;** **Wooden houses were cleaned once a week using water and mild soap;** **Paper towels were replaced twice a week when changing cages / bedding (Beginning of a week full cage was changed, mid of a week only bedding was exchanged)** o Does enrichment type/access change across study? **NO** o If so, when does enrichment type/access change (e.g. enrichment removed prior to parturition and replaced in late neonatal period): **N/A** Additional comments: **N/A**
Sample size ➢ *Litter versus offspring* *a. Specify the total number of animals used in each experiment, and the number of animals in each experimental group.* *b. Explain how the number of animals was arrived at. Provide details of any sample size calculation used.* **c.** *Indicate the number of independent replications of each experiment, if relevant.*	10	*Provide details of:* *a. Maternal N vs offspring N* o What is the total number of dams/litters included in the study: **16/10** o What is the total number of offspring per litter included the study: **3-7** *b. Litter size and sex distribution* o What size was each litter maintained at: **4-8** o What age did culling take place at: **PD 1-3** o How many males and females were maintained in each litter: **4-8 males; all females culled** *c. Cross fostering* o Did cross fostering occur: **YES** o If so, at what age did cross fostering occur: **PD 1-3** Additional comments: **N/A**
Allocating animals to experimental groups	11	*a. How many offspring per litter were used in each measure*: **3-7**

a. *Give full details of how animals were allocated to experimental groups, including randomization or matching if done.* b. *Describe the order in which the animals in the different experimental groups were treated and assessed.*		*b. Randomization/Matching procedures* o What procedures were used to assign animals to groups: **Regarding LPS treatment, dams were mated in pairs, and assignment to LPS or saline treated was done in an alternating fashion.** **Regarding assignment of offspring into mixed cages, LPS and Saline offspring were picked in an alternating fashion and assigned to one of the mixed cages in a way creating overall counterbalanced mixed cages (mixed LPS and SAL, with mixed origin from LPS and SAL dams from cross-fostering).** *c. Sex as a biological variable (behavioral and physiological outcomes)* o Were both males and females evaluated in each behavioral and physiological outcome: **NO** Additional comments: **N/A**
Experimental outcomes ➢ *Behavioral testing* ➢ *Physiological endpoints* *Clearly define the primary and secondary experimental outcomes assessed (e.g. cell death, molecular markers, behavioral changes).*	12	*a. Maternal behavior and pup interactions* o If maternal care was evaluated, were there differences following immunogen challenge (if so, please briefly describe): **not evaluated** *b. Age(s) of offspring at behavioral testing/physiological evaluation endpoints:* **~PD30, ~PD45, ~PD66, ~PD94** *c. Order of testing (e.g. behavioral test order)* o Were animals evaluated in a counter-balanced order in terms of: presentation of tests to each animal: **YES/NO** **All animals did the same tests in the same order** order of experimental/control groups run through each test:**YES** o What was the inter-test interval if a single animal underwent a battery of tests: **Within each test block:** **Between EPM and OF test 2.5 h** **Between OF and NOR test 1 day** **Between NOR and 1st PPI session 2.5h** **Between 1st PPI and 2nd PPI session 1 day** **Between 2nd PPI session and fMRI 1-2 days** **Between the test blocks:** **15, 21 and 28 days** **(i.e. tested on PD~30, PD~45, PD~66, PD~94)** Additional comments: **N/A**
Statistical methods a. *Provide details of the statistical methods used for each analysis.* b. *Specify the unit of*	**13**	*a. Unit of analysis for each data set* o Is the unit (n) of each analysis based on number of litters, or number of animals used per group: **number of animals, with (number of) litters used as random factor in mixed-model analysis for behavioral**

analysis for each dataset (e.g. single animal, group of animals, single neuron). *c. Describe any methods used to assess whether the data met the assumptions of the statistical approach.*		**experiments;** **n for rs-fMRI data is based on number of animals only**
Other Disclosures		*Please make note of any other extraneous variables that you would like to report (e.g. fire alarms, construction, temporary relocations, other variables that you think we should be considering in our studies etc.):* **N/A**

6.4.3. List of abbreviations

- ACC — Anterior cingulate cortex
- activated B cells
- ANOVA — Analysis of Variance
- ASR — Acoustic startle response
- Au1 — Primary auditory cortex
- BOLD — Blood oxygenation level-dependent
- BSS — Blind source separation
- CA1 — Dorsal hippocampus
- CBF — Cerebral blood flow
- CBV — Cerebral blood volume
- Cg — Cingulate cortex
- CoA — Certificate of analysis
- COVID-19 — Coronavirus disease 2019
- DAN — Dorsal attention network
- Decomposition into Independent Components
- df — Degrees of freedom
- DMN — Default mode network
- dmPFC — Dorsal medial prefrontal cortex
- ECN — Executive control network
- EPI — Echo planar imaging
- EPM — Elevated plus maze
- EZM — Elevated zero maze

- FDR False discovery rate
- FID Free induction decay
- fMRI Functional magnetic resonance imaging
- FSL FMRIB Software Library
- FWHM Full width at half maximum
- GD Gestational day(s)
- GEE Generalized Estimating Equations
- GIFT Group ICA Toolbox
- GLM General Linear Model
- GSH Glutathione
- IC Independent component
- ICA Independent component analysis
- IFN Interferon
- IL Interleukin / Infralimbic cortex
  inducing interferon β
- IRF Interferon Regulatory Factor
- ISI Interstimulus interval
- ISI Inter-Stimulus-Interval
- ITI Inter-trial interval
- LMM Linear mixed model(s)
- LO Lateral orbital frontal cortex
- LPS Lipopolysaccharides
- MANOVA Multivariate Analysis of Variance

- MELODIC Multivariate Exploratory Linear Optimized
- MIA Maternal immune activation
- mPFC medial prefrontal cortex
- MRI Magnetic resonance Imaging
- MRM Multivariate and repeated measures (toolbox)
- MS Mean squares
- MW Molecular weight
- MyD88 Myeloid differentiation primary response protein 88
- NF-κB Nuclear factor kappa-light-chain-enhancer of
- NMR Nuclear magnetic resonance
- NOR Novel object recognition
- OF Open field
- OFC Orbital frontal cortex
- OMPFC Orbital medial prefrontal cortex
- PCA Principal component analysis
- PCC Posterior cingulate cortex
- PD Postnatal day
- PET Positron emission tomography
- PFC Prefrontal cortex
- Poly(I:C) Polyribosinic:polyribocytidylic acid
- PPC Posterior parietal cortex
- PPI Prepulse inhibition
- PrL Prelimbic cortex

- PtPD Dorsal posterior parietal cortex
- PtPR Rostral posterior parietal cortex
- RF Radiofrequency
- RI Recognition index
- rMO rostral medial orbital frontal cortex
- ROI Region(s) of interest
- ROS Reactive oxygen species
- RSD Dysgranular retrosplenial cortex
- rs-fMRI resting-state functional magnetic resonance imaging
- RSG Granular retrosplenial cortex
- RSN Resting-state network(s)
- SAL Saline (0.9%)
- SD Standard deviation
- SE(M) Standard error (mean)
- SLN Salience network
- SOR Spontaneous object recognition
- SPL Sound pressure level
- SPM Statistical Parametric Mapping
- SS Sums of squares
- TE Echo time
- TeA Temporal association cortex
- TFCE Threshold-Free Cluster Enhancement
- TLR Toll-like receptor

- TNF-α Tumor necrosis factor α
- TR Repetition time
- TRIF Toll-IL-1 receptor domain-containing adapter-
- V2M Medial secondary visual cortex
- vmPFC Ventral medial prefrontal cortex
- VO Ventral orbital frontal cortex